

INFORMATION TO USERS

The most advanced technology has been used to photograph and reproduce this manuscript from the microfilm master. UMI films the original text directly from the copy submitted. Thus, some dissertation copies are in typewriter face, while others may be from a computer printer.

In the unlikely event that the author did not send UMI a complete manuscript and there are missing pages, these will be noted. Also, if unauthorized copyrighted material had to be removed, a note will indicate the deletion.

Oversize materials (e.g., maps, drawings, charts) are reproduced by sectioning the original, beginning at the upper left-hand corner and continuing from left to right in equal sections with small overlaps. Each oversize page is available as one exposure on a standard 35 mm slide or as a 17" × 23" black and white photographic print for an additional charge.

Photographs included in the original manuscript have been reproduced xerographically in this copy. 35 mm slides or 6" × 9" black and white photographic prints are available for any photographs or illustrations appearing in this copy for an additional charge. Contact UMI directly to order.



300 North Zeeb Road, Ann Arbor, MI 48106-1346 USA

Order Number 8900293

The origin and evolution of lavas from Haleakala Crater, Hawaii

West, Howard Bruce, Ph.D.

Rice University, 1988

U·M·I
300 N. Zeeb Rd.
Ann Arbor, MI 48106

RICE UNIVERSITY

THE ORIGIN AND EVOLUTION OF LAVAS FROM HALEAKALA CRATER,
HAWAII

by

HOWARD BRUCE WEST

A THESIS SUBMITTED
IN PARTIAL FULFILLMENT OF THE
REQUIREMENTS FOR THE DEGREE

DOCTOR OF PHILOSOPHY

APPROVED, THESIS COMMITTEE:

William P. Leeman

William P. Leeman, Professor (Chairman)

John C. Stormer

John C. Stormer, Professor

Dieter Heymann

Dieter Heymann, Professor

Mason Tomson

Mason Tomson, Professor

Houston, Texas

April, 1988

ABSTRACT

The Origin and Evolution of Lavas from Haleakala Crater, Hawaii

by

Howard Bruce West

Sr, Nd and Pb isotope systematics of lavas from the Maui Volcanic Complex [MVC] are consistent with a three-component petrogenetic mixing model. MVC shield-building [SB] lavas define linear trends on isotope-isotope plots, consistent with two-component mixing between primitive [PM] and enriched [EM] mantle components. The two-component (PM-EM) Hawaiian plume source is variable in composition during production of tholeiite magmas even within a single shield. Sr and Pb isotopic ratios of Haleakala post shield-building [PSB] lavas define a strong positively correlated array that deviates from the SB array towards an unradiogenic end-member. The PSB array may therefore result from time- and volume-dependent binary mixing between Hawaiian plume melts and a depleted [DM] mantle (i.e. MORB source) component.

Several trace element ratios in Haleakala PSB lavas are correlated with isotopic compositions but not with major and trace element contents, and therefore appear to reflect changes in source composition. Trace element mixing systematics for these lavas indicate that the DM component must be a melt. The inferred PM component has chondritic ratios for several trace elements, consistent with it representing primitive mantle. The EM component may represent a part of the Hawaiian plume source that was either metasomatized or metasomatically scavenged.

Alkalic cap lavas exposed in the northwest wall of Haleakala Crater display systematic, upsection geochemical variations indicative of the repetitive intrusion of discrete magma batches. Magma batches are separated by geochemical discontinuities characterized by abrupt upsection increases in incompatible element contents and commensurate drops in compatible element contents. In contrast, lava compositions within magma batches vary upsection progressively, and geochemical variations are opposite to

those observed for interbatch discontinuities. Together, these geochemical variations are interpreted as resulting from the cyclic operation of a dynamic, evolving, open system magma chamber. Interbatch transitions appear to reflect periods of eruptive quiescence characterized by low magma recharge rates and relatively high degrees of crystal fractionation. Intrabatch variations appear to represent eruptive periods characterized by relatively high recharge rates, low degrees of crystal fractionation, and progressive mixing of evolved rest magma with more primitive recharge magma.

Acknowledgements

I would like to dedicate this thesis to the great *Akua Mo'o* who watches over all of us on the screen behind our beds. Ever so often, as we meander along life's often branching path, the time arrives when tribute must be paid to those who worked so hard to pave that golden surface. Indeed, one's personal QIE can often be measured by the quality and number of our companions.

First, mahalo nui loa to my friend and advisor, Bill Leeman, who has helped maintain my child's sense of *verlorenheit* throughout the years. Some of the finest acronyms I've had the privilege to be associated with have been developed in collaboration with Bill. GITFOO, NEMO, SQUID, MO'O, and HAIKU are among my personal favorites.

Thanks also to Jay Stormer, my committee member. I will always remember his words of wisdom concerning Ph.D. theses, "Well, I'll read the damn thing." Dieter Heymann, committee member, provided a host of intriguing answers to questions this thesis couldn't even begin to ask. I would very much like to thank Mason Tomson for consenting to be my outside committee member.

Aloha no to my friends at Rice. Marian "Superstar" Allen, Amy "Amy's World" Leventer, Normbo Read (Jr.), Clinton "The Lumpster" Lum, Steffi Ann Minnis (aka "The Stef Monster"), Andy "Big Guy" Mirkin, Nova Pestana, Rick Gottschalk, Donna Weideman ("The Dominating Executive Wench"), and Marge Herron, the one and only *Blonde Mound of Rebound*. A special aloha to my oldest friend at Rice, Chingju Liu (S.N.C.). Pack your bags.

Words are pitifully inadequate to express the contributions made by my office mate, Norio Honjo, aka "The Doctor". His unique brand of wisdom will be remembered. "What?"

A big mahalo to Marc Norman and Dave "Sweet Mate" Reid. When the cry of "Dog" drifted out of a black sky, Dave's resounding echo of "Don't make me tie-up my shoes" always followed. A special aloha to Marc for the interchange of intuitive realiza-

tions on this harmony we so often call life. No doubt, we have travelled much common ground on many planes since that time called *chulfa burung ra*. In this context, Darryl & Wanda Kennedy deserve a significant proportion of the credit.

Mahalo to Dave Gerlach (you bad boy!) for his insistence on maintaining an atmosphere of unrelenting discipline even in the midst of mighty temptations. I will always remember Dave's hospitality and demand for regular scorpion-bowl treatments during my stay in Cambridge.

Thanks to A. W. Bally for his encouragement and support throughout my tenure at Rice. I would also like to thank Dr. Hans Ave Lallemand from whom I have learned much, and whose project I am still, to my embarrassment, in the process of finishing.

Mahalo to Mike Garcia for initially suggesting that I consider attending Rice and working with "Big Bill". I would like to thank Fred Frey for his much appreciated support during my visit to Cambridge.

Mahalo to Theresa Atwill for her hospitality, and a big aloha to Nancy Riggs (M.F.J.), Else Neumann, and Bobbi John for making my stay at Santa Barbara a warm one. Thanks also to George Tilton for his patient and always friendly help in the lab.

Thanks to Slimy's (aka "Sammy's") Cafeteria at Rice for providing the kind of nutritional support so essential to continued physical and intellectual growth. Their efforts towards imbuing every meal with at least three of the four basic food groups (i.e. sugar, grease, caffeine, and alcohol) are much appreciated. The sacred *Slime Altar* would have been a sham without their offerings.

Mahalo nui loa to my good friend, Fred Mullins, without whose kokua this project would have been infinitely more difficult. Aloha no to my friends, Darryl Lee, Duane Morita, Glen Shiraki, and Duke Wise for their scientific insights and support.

Aloha nui loa and mahalo to my wife, Sophie, for her support through the long years in Houston.

Finally, aloha nui loa to my parents and my brother, Glenn, for their unending kokua and aloha and for their ability to say, even under the most demanding circumstances, "What? I owe you money?"

TABLE OF CONTENTS

Abstract	
Acknowledgements	
Table of Contents	
List of Tables	
Introduction	1
Chapter 1. Petrology and Geochemistry of Lavas from Haleakala Crater, Hawaii: An Overview	2
Introduction	3
Geologic History and Distribution of Rock Types	6
Previous Petrologic and Geochemical Studies of Haleakala	7
Geochemistry	7
Honomanu Formation	7
Kumuilihi Formation	8
Kula Formation	9
Hana Formation	10
Magma Batches	11
Isotopic Evolution: Implications for Magma Sources	12
Conclusions	14
References	15
Figure Captions	18
Figures	20
Chapter 2. Isotopic Evolution of Lavas from Haleakala Crater, Hawaii	31
Abstract	32
Introduction	33
Previous Isotopic Studies of Hawaiian Volcanoes	35
Geologic Setting and Sampling	35
Analytical Procedures	38
Results	38
Pb	38
Sr	39
Pb-Sr Relationships	40
Constraints on Mixing End-Members	41
Mixing Model	43
Shield-building Volcanism: PM-EM Mixing	43
Alkalic Cap Volcanism	45
Plume Composition	46
Plume-DM Mixing	47
A Possible Mixing Scenario	47
Loa and Kea Trends	48
Conclusions	49
Acknowledgements	51
References	52
Tables	55
Figure Captions	57
Figures	59
Chapter 3. Isotopic Constraints on the Origin of Hawaiian Lavas from the Maui Volcanic Complex, Hawaii	65
Abstract	66
Introduction	67
New Sr, Nd and Pb Isotopic Results	69

Hawaiian Magma Source Mixing Systematics	70
Implications for Hawaiian Mantle Components	73
Scale of Mantle Heterogeneity	76
Acknowledgements	77
References	78
Tables	81
Figure Captions	83
Figures	85
Chapter 4. The Origin and Geochemical Evolution of Lavas from Haleakala Crater, Hawaii	89
Abstract	90
Introduction	91
Geologic Setting	93
Sampling and Analytical Information	95
Petrography	97
Analytical Procedures	99
Results	99
Shield-Building Stage: Honomanu Formation	100
Alkalic Cap Stage	102
Kumuiliahi Formation	102
Kula Formation	104
Post-Erosional Stage: Hana Formation	106
Temporal Compositional Variations	108
Isotopic Ratios	108
Trace Element Ratios	110
The Role of Fractional Crystallization	110
Honomanu Formation	111
Kumuiliahi Formation	112
Kula Formation	113
Origin of Holua Trachyte	116
Hana Formation	117
Magma Mixing Effects in Hana Lavas	118
Trace Element Constraints on Mantle Source Components	118
Depleted Mantle [DM] Component	119
Primitive Mantle [PM] Component	120
Enriched Mantle [EM] Component	122
Implications for Plume Models	124
Depth of Plume Penetration	125
The Parasitic Plume Model	125
Effects Related to the Reduction of Melt Volume with Time	127
Post-Erosional Volcanism	128
Implications for Eruptive Hiatuses	128
Conclusions	129
Acknowledgements	131
References	132
Tables	138
Figure Captions	149
Figures	155
Chapter 5. Open System Geochemical Evolution of Alkalic Cap Lavas from Haleakala Crater, Hawaii	209
Abstract	210
Introduction	212
General Geologic Setting and Sampling	213
Previous Investigations of Haleakala Alkalic Cap Lavas	214
Petrography	216

Analytical Techniques	217
Geochemistry	217
Magma Batches	218
Variations in Isotopic Compositions and Trace Element Ratios	220
Interbatch Transitions	220
General Compositional Variations and Evidence for Crystal Fractionation	221
Detailed Evaluation of Interbatch Transitions	223
Batch 3 to 4 / Batch 7 to 8	224
Batch 5 to 6	224
Batch 8 to 9	225
Batch 9 to 10	226
Batch 12 to 13	226
Quantitative Evaluation of Fractional Crystallization	227
Mineral Compositions	227
Results	228
Batch 12 to 13	228
Batch 9 to 10	228
Batch 7 to 8	229
Evidence for High Pressure Clinopyroxene Fractionation	230
Possible Causes for Comparable Enrichments in Highly and Slightly Incompatible Trace Elements	230
Phenocryst Accumulation	230
Mixing	231
Resorption	232
Intrabatch Variations	233
Batch 7	234
Batch 9	235
Batch 12	236
Modeling Closed and Open System Fractionation	237
Parental Magma Compositions	237
Results of Calculations	239
Open System Recharge Models	239
Closed System Fractionation Models	240
Combined Recharge and Assimilation	240
Magma Chamber Model	242
Low Magma Flux Regime	242
High Magma Flux Regime	244
Implications for Closed System Magma Chambers	245
Eruption Rate Estimates Based on Magma Batches	246
Changes in Parental Magma Composition with Time	247
Changes in Source Mixing Systematics	248
Conclusions	249
Acknowledgements	251
References	252
Tables	256
Figure Captions	276
Figures	282
Appendix 1. Raw major element data - University of Houston	335
Appendix 2. Raw major element data - University of Massachusetts	342
Appendix 3. Normalizing values	346
Appendix 4. List of Samples	348
Appendix 5. Rock Standard and Duplicate Analyses	351

LIST OF TABLES

Chapter 2:

1.	Pb and Sr isotopic compositions of lavas from Haleakala	55
2.	Sr isotope and trace element composition of Holua Trachyte	56

Chapter 3:

1.	Ages and rock types of the Maui Volcanic Complex	81
2.	Isotopic compositions of Maui Volcanic Complex lavas	82

Chapter 4:

1.	Distribution of rock types at Haleakala	138
2.	Major and trace element data for lavas from Haleakala	139
3.	Compositions of trachytes and other differentiated Hawaiian lavas	148

Chapter 5:

1.	Mineral modes for Kula Formation lavas from Haleakala Crater	256
2.	Major and trace element data for lavas from the Halemau section	257
3.	Range in rock compositions for magma batches	263
4.	Compositions of components used in least-squares mixing model for batch 12 to 13 transition	264
5.	Results of least-squares modeling for batch 12 to 13 transition	265
6.	Compositions of components used in least-squares mixing model for batch 9 to 10 transition	266
7.	Results of least-squares modeling for batch 9 to 10 transition	267
8.	Compositions of components used in least-squares mixing model for batch 7 to 8 transition	268
9.	Results of least-squares modeling for batch 7 to 8 transition	269
10.	Results of open and closed system fractionation calculations using the method of Nielsen (1988)	270
11.	Results of combined recharge and assimilation calculations using the method of Nielsen (1988)	274
12.	Comparison of selected major and trace element ranges for older and younger batch lavas from Haleakala Crater	275

Introduction

The purpose of this study is to examine, geochemically and isotopically, lavas collected from Haleakala Crater, an erosional caldera located at the summit of Haleakala volcano on the island of Maui, Hawaii. Haleakala is one of six large shield volcanoes that together compose the Maui Volcanic Complex. The results from this study are presented in the form of five chapters. Each chapter was written as a separate, self-contained work, designed as an individual paper for publication. The first three chapters have undergone peer review and are published in scientific journals. The last two chapters will be submitted separately for publication in the near future. Because each chapter was written to stand alone, there is some unavoidable duplication between chapters.

The first chapter presents an overview of the project and a brief summary of some of the results. The second chapter presents the Sr and Pb isotope systematics of lavas from Haleakala Crater and a general model for the origin of Hawaiian lavas. The third chapter integrates the isotope systematics of lavas from Haleakala with isotopic data for other volcanoes of the Maui Volcanic Complex and presents a more detailed and comprehensive model of Hawaiian volcanism. The fourth chapter combines major and trace element geochemical data with isotopic data to describe geochemical evolution within the four principal rock formations exposed at Haleakala. These data are then used to further constrain the nature of source of Hawaiian lavas. The fifth chapter is a detailed study of alkalic cap lavas collected from a stratigraphic section of lavas exposed on the northwest wall of Haleakala Crater along the Halemau Trail.

Chapter 1

**PETROLOGY AND GEOCHEMISTRY OF LAVAS FROM HALEAKALA
CRATER, HAWAII: AN OVERVIEW**

INTRODUCTION

The islands of Maui, Molokai, Lanai, and Kahoolawe form a large volcanic complex (the Maui Volcanic Complex) consisting of six major shield volcanoes that are either extinct or in the last stages of their evolution. At one time, these volcanoes formed a single island that was about half the present area of the island of Hawaii (Stearns and Macdonald, 1942; Macdonald et al., 1983). Maui itself comprises two large shield volcanoes: West Maui and the younger Haleakala, which forms the eastern half of the island (Fig. 1). At the summit of Haleakala lies its most distinctive geologic feature, Haleakala Crater, which is an erosional caldera roughly 7 miles long and 2 miles wide.

In this overview, we briefly outline the general geology and geologic history of Haleakala volcano as well as the results of previous petrologic and geochemical investigations. We then summarize new major element, trace element, and isotopic data for lavas from Haleakala Crater, and focus on a detailed study of samples collected along the Halemauu trail from a continuous section of the northwest wall (West and Leeman, 1987a, 1987b).

GEOLOGIC HISTORY AND DISTRIBUTION OF ROCK TYPES

Much of the following discussion is based on the extensive geologic work and mapping of Stearns and Macdonald (1942) and on the detailed map of the Crater area by Macdonald (1978).

Haleakala was built by eruptions emanating principally from three rift zones, all presently well delineated by numerous cinder cones. This activity culminated in the formation of a large volcanic shield which in late Pliocene or early Pleistocene time may have reached an elevation up to 1000 meters above the present summit at 3055 meters above sea level (Macdonald et al., 1983). The volcano has been subdivided into four formations on the basis of stratigraphy and rock type (Stearns and Macdonald, 1942; Macdonald, 1978).

The lowermost exposed lavas of the Honomanu Formation (Macdonald, 1978) out-

crop only along the northern coast of Haleakala and in some deep gulches on its lower flanks. The duration of Honomanu activity is not known, but a sample collected from the type section at Honomanu Valley (Stearns and Macdonald, 1942) has been dated at 0.83 ± 0.17 Ma (Naughton et al., 1980). Because the Honomanu Formation consists of interbedded tholeiitic and alkalic basalts, it appears to record a period of transition between the shield-building stage and the alkalic cap stage. Honomanu lavas are typically highly vesicular and contain abundant plagioclase phenocrysts along with olivine.

The Kumuiliahia Formation is stratigraphically higher than the Honomanu Formation, but is exposed only in Haleakala Crater (Macdonald, 1978). The type section is located on the south wall of the Crater, where Kumuiliahia lavas are separated from the overlying Kula Formation by an angular unconformity that may be a fault scarp (Stearns, 1942; Macdonald, 1978). Four samples dated by Naughton et al. (1980) range from 0.70 ± 0.03 to 0.91 ± 0.07 Ma. These lavas consist of interbedded alkalic basalts and hawaiites and resemble those of the Honomanu Formation in that they are highly vesicular and contain abundant plagioclase phenocrysts. Their chemistry, however, suggests that they belong to the alkalic cap stage of the volcano.

The Kula Formation (Macdonald, 1978) represents the alkalic cap stage of Haleakala and comprises the majority of subaerially exposed lavas. Age determinations on six samples collected from both the Crater and the flanks of the volcano range from 0.88 to 0.36 Ma (McDougall, 1964; Naughton et al., 1980). At Honomanu Valley, the Kula Formation is separated from the underlying Honomanu Formation by an ashy soil layer, and a significant change in the style of magmatism is evident. Kula lavas consist of thick-bedded, non-vesicular a'a flows and are aphyric to sparsely phyric, with clinopyroxene now appearing as a phenocryst phase. These features appear to reflect changes in both magma rheology (e.g. increased magma viscosity) and fractionating mineral assemblage.

In Haleakala Crater, Kula lavas form thick exposures (up to 670 meters) along the Crater walls. On the northwest wall of the Crater, these lavas are traversed by the

Halemauu trail which affords good access to the entire stratigraphic section. Compositions of Kula lavas typically range from alkalic basalt to mugearite; rock types spanning this range occur throughout the section. Olivine, clinopyroxene and plagioclase are the dominant phenocryst phases. In the alkalic basalts, all three of these phases may be present, but in the more differentiated rock types, olivine is rare and the lavas tend to be aphyric. Among the more unusual Kula lavas are (1) a single occurrence of trachyte, exposed as a dike below the northwest wall, just south of Holua Cabin; (2) small intrusive bodies of olivine-clinopyroxene microdiorite, exposed in the west wall of the Crater (Macdonald, 1978); and (3) a mugearite flow containing the only documented occurrence of amphibole at Haleakala, located at Pakaoao (White Hill), next to the Crater lookout.

Kula volcanism was followed by a period of eruptive quiescence during which deep valleys were cut by stream erosion along the north (Keanae Valley) and southeast (Kaupo and Kipahulu Valleys) flanks of the volcano. Haleakala Crater was formed by the merging and expansion of the heads of Keanae and Kaupo valleys as they receded to the summit region (Stearns, 1942). Kipahulu Valley, to the east, fell just short of merging with Kaupo Valley and is separated from Haleakala Crater by a narrow ridge. After an extended erosional period, renewed volcanism, primarily from the southwest and east rift zones, produced lavas ranging in composition from basanitoid to hawaiiite. These post-erosional lavas are designated the Hana Formation (Macdonald, 1978). It is unknown when this renewed volcanism began, but the most recent eruption occurred around 1790 (Oostdam, 1965) on the southwest rift. Hana lava flows, cinder cones, and pyroclastic products blanket the floor of Haleakala Crater. These lavas typically are much glassier than their Kula counterparts and contain variable amounts of olivine and clinopyroxene phenocrysts along with much less abundant plagioclase. Some of the cinder cones contain pyroclastic bombs with inclusions of small gabbroic xenoliths.

PREVIOUS PETROLOGIC AND GEOCHEMICAL STUDIES OF HALEAKALA

The first concerted petrologic study of the volcano was that of Macdonald (1942) who concluded that the diversity of observed rock compositions was created by varying degrees of fractional crystallization of a common basaltic parental magma and that coexisting basaltic and "andesitic" (hawaiites, mugearites, and trachytes) lavas were tapped from different levels of the same magma chamber. Macdonald and Powers (1946, 1968) presented new major element analyses, including several from Haleakala Crater, and suggested that Hana Formation lavas could have been derived from greater depths in the Haleakala magma reservoir than were Kula lavas. Composite ankaramite and alkalic olivine basalt flows exposed near the rim of Haleakala Crater were also interpreted as products from a zoned magma body (Macdonald, 1972). The mineralogy of lavas studied by Macdonald has been discussed in some detail in a series of papers by Fodor and others (Fodor et al., 1972, 1975, 1977; Keil et al., 1972; Fodor and Keil, 1979).

Chen and Frey (1983, 1985) presented trace element and Sr and Nd isotopic data on Honomanu lavas collected along the beach at Honomanu Bay and on drill core samples of Kula and Hana lavas (down to a depth of 300 feet) from the northern flank of Haleakala. They observed systematic isotopic differences between Honomanu, Kula and Hana lavas that precluded a simple cogenetic relationship between these magmas, and suggested that their petrogenesis involved two isotopically distinct mantle sources (relatively undepleted or "primitive" mantle and depleted MORB-source mantle). He isotopic studies of these lavas (Kurz et al., 1985; Kurz, 1986) added support to Chen and Frey's (1983, 1985) proposition that the tholeiites were derived from a relatively undepleted mantle source (i.e. highest $^3\text{He}/^4\text{He}$ ratios) and that alkalic cap and post-erosional lavas reflect interaction with depleted mantle (i.e. lower ratios, similar to those of MORB). Chen and Frey (1985) further concluded that variations in trace element abundances were consistent with fractional crystallization, but that variations in the ratios of some highly incompatible elements (e.g. La/Ce) required mixing between

magmas with distinct trace element compositions. The later conclusion was based on the supposition that such incompatible elements are not significantly fractionated from each other during crystal fractionation.

Our recent and ongoing studies focus on major element, trace element, and isotopic variations primarily in the well-exposed crater area where there is a more continuous and longer duration record of eruptive activity than available elsewhere on the volcano. Results of this work are summarized below.

GEOCHEMISTRY

Honomanu Formation

Major and trace element compositions of Honomanu tholeiites (see Figs. 2-6) are typical of tholeiites from other Hawaiian volcanoes (e.g. Kilauea, see Fig. 2). They resemble Kilauea tholeiites in that these lavas have chondrite/primitive mantle-normalized trace element abundances that show a slight enrichment of highly incompatible elements over moderately incompatible elements (Fig. 3). The relative depletion of Rb and K apparent in figure 3 probably reflects alteration, which is a problem in rocks exposed on the rainy flanks of the volcano. Honomanu lavas contain relatively low abundances of incompatible elements (e.g. Th < 1.0 ppm, La < 20 ppm, Ba < 200 ppm, Nb < 15 ppm; e.g. Fig. 4) and relatively high abundances of Sc (> 25 ppm), Ni (> 100 ppm), and Cr (> 226 ppm) (e.g. Figs. 4-5). Interbedded alkalic basalts extend the Honomanu field into the alkalic field of the silica-alkalies diagram (Fig. 2), and thus form a transitional sequence.

Decreases in Ni and Cr with increasing Nb abundance are consistent with olivine and Cr-spinel fractionation. The lack of such a correlation for Sc or $\text{Al}_2\text{O}_3/\text{CaO}$ suggests that clinopyroxene was not a major fractionating phase in Honomanu magmas. The incompatible behavior of V, TiO_2 , and P_2O_5 (e.g. Figs. 5-6) indicates that fractionation of Fe-Ti oxides or apatite was insignificant. The lack of Sr and Eu depletions coupled with the presence of plagioclase phenocrysts in Honomanu lavas suggests that feldspar

was not efficiently separated from the parental magmas.

Isotopic data for Honomanu tholeiites fall within the general range of Hawaiian tholeiites. $^{87}\text{Sr}/^{86}\text{Sr}$ ratios range from 0.70368 to 0.70387 (Chen and Frey, 1985; West and Leeman, 1987b), $^{143}\text{Nd}/^{144}\text{Nd}$ from 0.51291 to 0.51298 (Chen and Frey, 1985; Hegner et al., 1986), $^{206}\text{Pb}/^{204}\text{Pb}$ from 18.264 to 18.303, $^{207}\text{Pb}/^{204}\text{Pb}$ from 15.452 to 15.482, and $^{208}\text{Pb}/^{204}\text{Pb}$ from 37.919 to 38.038 (Hegner et al., 1986; West and Leeman, 1987b). Isotopic data for Hawaiian tholeiites define coherent negatively correlated arrays on Sr-Nd (e.g. see Chen and Frey, 1985) and Sr-Pb (Stille et al., 1986; West and Leeman, 1987b; West et al., 1987) diagrams; these trends have been interpreted to reflect binary mixing between isotopically distinct materials (e.g. Chen and Frey, 1985).

Kumuilihi Formation

Kumuilihi lavas have higher abundances of incompatible elements (e.g. Th: 1.8-2.7 ppm, La: 25-33.4 ppm, Ba: 310-445 ppm, Nb: 25-36 ppm) and lower Ni and Cr contents than do Honomanu lavas (see Figs. 3-5). Major and trace element compositions overlap those of the Kula Formation (Figs. 2-6). Ni and Cr variations are consistent with olivine and Cr-spinel fractionation. Weak correlations of Sc, Sr, and $\text{Al}_2\text{O}_3/\text{CaO}$ with increasing Nb (e.g. Figs. 4,6) suggest there may have been minor clinopyroxene and plagioclase fractionation. Positive correlations of V, TiO_2 , and P_2O_5 with Nb (e.g. Figs. 5-6) indicate that fractionation of Fe-Ti oxides or apatite was insignificant.

$^{87}\text{Sr}/^{86}\text{Sr}$ ratios (0.70345-0.70355) are intermediate between those of the Honomanu and Kula Formations (Fig. 7). Pb isotope ratios (e.g. $^{206}\text{Pb}/^{204}\text{Pb} = 18.344\text{-}18.383$) are slightly more radiogenic than Honomanu Pb, and overlap with some Kula compositions (Fig. 7). Their distinct isotopic compositions indicate that Kumuilihi lavas cannot be simple differentiates of parental Honomanu magmas.

Kula Formation

Kula lavas have major element compositions similar to those from other Hawaiian alkalic suites and form a distinctive alkalic trend on a silica-alkalies diagram (Fig. 2). Lavas collected from the Halemauu trail section of Haleakala Crater span a large range in both major and trace element composition (Figs. 2-6). With increasing incompatible element abundance, Kula lavas display decreasing Ni, Cr, and Sc (Fig. 4-5). V, TiO₂, Sr, and P₂O₅ are initially positively correlated with incompatible elements, but then decrease at higher incompatible element contents (Fig. 5-6). Ratios of highly versus moderately incompatible elements (H/M ratios; e.g. La/Sm, La/Yb, Zr/Y) also increase with incompatible elements, but La/Sm and La/Yb ratios decrease in the most evolved lavas (Fig. 8). Some ratios of highly incompatible elements (H/H ratios) and of elements of close geochemical affinity systematically change with increasing abundance of such elements (e.g. Zr/Hf, La/Ce and Ba/Rb) (Fig. 8). Neither major element compositions nor trace element abundances change systematically with relative stratigraphic position (Fig. 11). This is not surprising since there is also no correlation between rock type and stratigraphic position.

Olivine, clinopyroxene, and Cr-spinel were probably the dominant fractionating phases in the alkalic basalts. At slightly more evolved compositions (i.e. mafic hawaiites and the more differentiated alkalic basalts), oxide fractionation also became important. Clinopyroxene and oxide fractionation were dominant in the hawaiites. The general absence of clinopyroxene phenocrysts in hawaiites, despite geochemical evidence for such fractionation, has also been noted for Mauna Kea (West and Garcia, 1982), and may be related to a combination of high pressure fractionation and the mechanisms of fractionation (e.g. dynamic flow crystallization, filter pressing, etc.). At very evolved compositions (i.e. mugearites and highly differentiated hawaiites), plagioclase and apatite fractionation also became important, suggesting increased residence of these magmas at high levels.

When plotted against relative stratigraphic position, geochemical data of lavas from

the Halemau trail section exhibit distinct breaks which delineate coherent subsets in the data (West and Leeman, 1987a). Such breaks suggest the operation of complex open system magma chamber processes (e.g. recharge and mixing coupled with crystallization and eruption; c.f. O'Hara and Matthews, 1981). These processes will be discussed in a later section.

Kula lavas have less radiogenic Sr (0.70308–0.70353; Chen and Frey, 1985; West and Leeman, 1987b) and more radiogenic Nd (0.51299–0.51309; Chen and Frey, 1985) than those of the Honomanu Formation. Pb isotopic compositions of Kula lavas from Haleakala Crater overlap Honomanu and Kumuilihi compositions but span a larger range (e.g. $^{206}\text{Pb}/^{204}\text{Pb} = 18.132\text{--}18.398$). Pb and Sr isotope ratios of these lavas are positively correlated, form a trend distinct from that of Hawaiian tholeiites (Fig. 7), and appear to vary systematically with age. Specifically, Sr and Pb isotopic ratios become less radiogenic upsection (Fig. 10), with the exception of the oldest exposed lava in the Crater which has relatively unradiogenic $^{87}\text{Sr}/^{86}\text{Sr}$ (0.70320). Isotopic compositions are not correlated with rock type (as expressed, for example, in terms of silica; see Fig. 9), trace element abundances, or with H/H ratios. However, some H/M ratios (e.g. La/Yb, Ba/La) are correlated with isotopic ratios.

Hana Formation

Hana major element, trace element, and isotopic compositions generally overlap those of Kula lavas (Figs. 2–7). Compared to the Kula Formation, Hana lavas tend to be more silica undersaturated, have higher Ni, Cr, and Sc abundances, and lower $\text{Al}_2\text{O}_3/\text{CaO}$, P_2O_5 , and Zr at comparable incompatible element abundances. The decrease in Ni, Cr, Sc, and V with increasing Nb (e.g. Figs. 4–5) probably reflects fractionation of olivine, clinopyroxene, and Fe–Ti oxide/spinel. In contrast to the Kula Formation, P_2O_5 and Sr contents of Hana lavas do not decrease at high Nb abundances (Fig. 6) and indicate that plagioclase and apatite fractionation were insignificant.

Isotopically, Hana lavas overlap the least radiogenic and youngest Kula lavas and

resemble post-erosional lavas from Kauai (Koloa Formation) (Fig. 7). These results indicate that Hana and Kula lavas were derived from isotopically similar sources.

MAGMA BATCHES

The geochemical discontinuities observed within the Halemau Trail stratigraphic sequence (Fig. 12) reflect what appears to be a succession of individual magma batches (West and Leeman, 1987a). The discontinuities *between* magma batches, are characterized by significant upsection increases in incompatible element abundances (e.g. K_2O , Th, La, Nb, Zr, and Y) and in some ratios (e.g. Al_2O_3/CaO , La/Sm, Zr/Hf), and concomitant decreases in compatible elements (e.g. Sc, Cr, V). *Within* batches, incompatible element abundances progressively decrease and compatible element abundances progressively increase (Fig. 11). Although the full spectrum of compositions are not represented in every batch, the first eruptive products in an individual batch tend to be either highly evolved hawaiites or mugearites; the final products tend to be alkalic basalts. Interbatch and intrabatch isotopic variations do not appear to be systematic and are generally within analytical error.

The observed geochemical variations and changes in rock type are consistent with the successive emplacement of discrete magma batches into an evolving open system magma chamber. Interbatch geochemical variations could reflect periods of low magma recharge and little or no discharge combined with significant fractional crystallization. Intrabatch patterns likely reflect eruptive periods during which recharge rate was high, the amount of crystal fractionation small, and mixing of evolved rest magma in the chamber with more primitive recharge magma was a dominant process.

Individual magma batches were likely created under unique petrogenetic conditions, as suggested by variable compositional ranges both within and between batches. Compositional controls include (1) variations in the composition of recharge magmas, (2) recharge rates (which includes frequency of recharge), and (3) total recharge volumes. However, it is probably recharge rate that exerts the strongest influence on geochemical

evolution. For example, prolonged periods of little or no recharge ultimately lead to extensive fractionation and the formation of highly evolved magmas (e.g. hawaiites and mugearites). Conversely, extended periods of high recharge ultimately results in increased eruption rates and may result in lavas approaching the composition of the recharge magma.

Regardless of uncertainties in the details of the open system magmatic evolution recorded at Haleakala, it is notable that the processes operating there significantly modify ratios of incompatible elements, many of which are not normally expected to change during fractional crystallization (e.g. Zr/Hf, La/Ce, Ba/Rb). Ratios like Zr/Hf are correlated with compatible element (e.g. Sc) and incompatible element (e.g. Nb) abundances and with other ratios (e.g. $\text{Al}_2\text{O}_3/\text{CaO}$); therefore, variations are unlikely to result from simple contamination. For example, if the potential contaminant is a melt, it must have paradoxically high abundances of both compatible (e.g. Sc) and incompatible (e.g. Nb) elements. The fact that clinopyroxene appears to be the only common fractionating mineral phase in all Kula magma compositions (alkalic basalt and more evolved hawaiites and mugearites) suggests that variations in these incompatible element ratios are the result of clinopyroxene removal. Because of their resistance to change by partial melting or fractional crystallization, such ratios are often used to constrain the composition of the mantle sources of magmas. Control of these ratios by magmatic processes precludes their direct use in inferring the compositions of magma sources.

ISOTOPIC EVOLUTION: IMPLICATIONS FOR MAGMA SOURCES

Isotope systematics of Hawaiian lavas reveal two significant observations. (1) Collectively, Hawaiian tholeiites form coherent isotope-isotope arrays that are consistent with binary mixing between isotopically distinct end members. Nd-Pb (see Staudigel et al., 1984) and Sr-Pb (West and Leeman, 1987b; West et al., 1987) relations suggest these end members are represented by Koolau/Lanai and Kilauea. (2) Alkalic lavas from Haleakala form a distinct array that appears to reflect mixing between an end member

lying on the tholeiite array and another end member approximated by Hawaiian post-erosional lavas (e.g. Koloa, Lahaina, and Honolulu) (West and Leeman, 1987b). This dichotomy can be explained in terms of mixing between three isotopically distinct end members whose compositions lie in the direction of the Koolau, Kilauea, and Koloa fields. The physical significance of these components can be constrained both by the isotopic data and by the change in isotopic compositions as a function of time.

Koolau has Sr, Nd, and Pb isotopic compositions similar to those estimated for bulk silicate Earth or "primitive mantle" (see White, 1985). Post-erosional lavas have isotopic compositions similar to those of MORB, which suggests these lavas may have been derived from or have interacted with a MORB signature component (e.g. depleted asthenosphere, lithosphere). To account for the compositions of Kilauea tholeiites, the third end member must contain relatively radiogenic Pb and have a Sr and Nd isotopic composition intermediate to that of the primitive mantle and depleted mantle components. Because such a composition requires this component to have relatively high U/Pb ratios for a significant time period, this end member can be thought of as an "enriched" mantle component.

Hawaiian tholeiites could represent melts derived from mantle plumes containing both primitive and enriched components that are mixed in various proportions. The relatively tight arrays formed by Hawaiian tholeiites and Hawaiian alkalic lavas, respectively, suggests end members of relatively restricted composition. It is thus unlikely that altered oceanic crust, which is isotopically quite heterogeneous, is a significant contaminant for either of these two lava suites. Alkalic lavas may reflect mixing between plume melts (themselves two-component mixtures) and depleted asthenosphere and/or lithosphere, in which case the trend towards less radiogenic Sr and Pb with time suggests a progressive increase in interaction with this depleted component. For example, the observed trend could result from increasing residence times of plume magmas within the lithosphere or upper asthenosphere.

CONCLUSIONS

Haleakala contains a diverse range of lava compositions which represent the shield-building, alkalic cap, and post-erosional stages of the volcano. The geochemistry of lavas collected from the Halemau trail section of the Crater wall clearly indicates that compositions of alkalic cap lavas are controlled by the evolution of an open system magma chamber. Compositional variations between and within individual magma batches are consistent with alternating periods of (1) low recharge rates, relatively large amounts of fractional crystallization, and little or no magma discharge, and (2) high recharge rates, small amounts of fractional crystallization, and high magma discharge rates. The isotopic systematics of Hawaiian lavas in general appear to reflect variable mixing between three isotopically distinct mantle components (primitive, depleted, and enriched). Hawaiian tholeiites could represent melts derived from a binary plume source composed of primitive and enriched components, whereas isotopic variations within alkalic lavas from Haleakala Crater suggest these lavas represent plume melts that experienced progressive contamination by depleted (MORB composition) mantle.

REFERENCES

- Chen, C.-Y., 1982, Geochemical and Petrologic Systematics in Lavas from Haleakala Volcano, East Maui: Implications for the Evolution of Hawaiian Mantle: Ph.D. Thesis, M.I.T., 344 p.
- Chen, C.-Y. and Frey, F. A., 1983, Origin of Hawaiian Tholeiite and Alkalic Basalt: *Nature*, v. 302, p. 785-789.
- Chen, C.-Y. and Frey, F. A., 1985, Trace Element and Isotopic Geochemistry of Lavas from Haleakala Volcano, East Maui, Hawaii: Implications for the Origin of Hawaiian Basalts: *J. Geophys. Res.*, v. 90, p. 8743-8768.
- Cross, W., 1915, Lavas of Hawaii and their Relation: U.S.G.S. Prof. Paper 99, 97 p.
- Daly, R. A., 1933, *Igneous Rocks and Their Origin*, New York, 563 p.
- Fodor, R. V. and Keil, K., 1979, Review of the Mineral Chemistry of Volcanic Rocks from Maui, Hawaii: in *Field Trip Guide to the Hawaiian Islands*, H.I.G. Spec. Pub., p. 93-106.
- Fodor, R. V., Keil, K. and Bunch, T. E., 1972, Mineral Chemistry of Volcanic Rocks from Maui, Hawaii: Fe-Ti Oxides: *G.S.A. Abstr. w/Progr.* 4, p. 507.
- Fodor, R. V., Keil, K. and Bunch, T. E. 1975, Contributions to the Mineral Chemistry of Hawaiian Rocks IV. Pyroxenes in Rocks from Haleakala and West Maui volcanoes, Maui, Hawaii: *Contrib. Mineral. Petrol.* 50, p. 173-195.
- Fodor, R. V., Keil, K. and Bunch, T. E., 1977, Contributions to the Mineral Chemistry of Hawaiian Rocks. VI. Olivines in Rocks from Haleakala and West Maui Volcanoes, Maui, Hawaii: *Pac. Sci.* 31, p. 299-308.
- Hegner, E., Unruh, D. and Tatsumoto, M., 1986, Nd-Sr-Pb Isotope Constraints on the Sources of West Maui Volcano, Hawaii: *Nature*, v. 319, p. 478-480.
- Hinds, N. E. A., 1931, The Relative Ages of the Hawaiian Landscapes: *Univ. Calif. Publ. Bull.*, v. 20, p. 143-260.
- Keil, K., Fodor, R. V. and Bunch, T. E., 1972, Contributions to the Mineral Chemistry of Hawaiian Rocks. II. Feldspars and Interstitial Material in Rocks from Haleakala and West Maui Volcanoes, Maui, Hawaii: *Contrib. Mineral. Petrol.* 37, p. 253-275.
- Kurz, M. D., 1986, Cosmogenic Helium in a Terrestrial Igneous Rock: *Nature*, v. 320, p. 435-439.
- Kurz, M. D., O'Brien, P. A., Garcia, M. O. and Frey, F. A., Isotopic Evolution of Haleakala Volcano: Primordial, Radiogenic and Cosmogenic Helium: *EOS*, v. 66, p. 1120.
- Macdonald, G. A., 1942, Petrography of Maui: *Hawaii Div. Hydrogr. Bull.*, v. 7, p. 275-334.
- Macdonald, G. A., 1972, Composite Lava Flows on Haleakala Volcano, Hawaii: *G.S.A. Bull.*, v. 83, p. 2971-2974.

- Macdonald, G. A., 1978, Geologic Map of the Crater Section of Haleakala National Park, Maui, Hawaii: U.S.G.S. Misc. Inv. Ser. Map I-1088.
- Macdonald, G. A. and Powers, H. A., 1946, Contribution to the Petrography of Haleakala Volcano, Hawaii: G.S.A. Bull., v. 57, p. 115-124.
- Macdonald, G. A. and Powers, H. A., 1968, A Further Contribution to the Petrology of Haleakala Volcano, Hawaii: G.S.A. Bull., v. 79, p. 877-888.
- Macdonald, G. A. and Katsura, T., 1964, Chemical Composition of Hawaiian Lavas: J. Petrol., v. 5, p. 82-133.
- Macdonald, G. A., Abbott, A. T. and Peterson, F. L., 1983, *Volcanoes in the Sea*, Univ. of Hawaii Press, 517 p.
- McDougall, I., 1964, Potassium-Argon Ages from Lavas of the Hawaiian Islands: G.S.A. Bull., v. 75, p. 107-128.
- Naughton, J. J., Macdonald, G. A. and Greenberg, V. A., 1980, Some Additional Potassium-Argon Ages of Hawaiian Rocks: The Maui Volcanic Complex of Molokai, Maui, Lanai and Kahoolawe: J. Volc. Geoth. Res., v. 7, p. 339-355.
- O'Hara, M. J. and Mathews, R. E., 1981, Geochemical Evolution in an Advancing, Periodically Replenished, Periodically Tapped, Continuously Fractionating Magma Chamber: J. Geol. Soc. Lond., v. 138, p. 237-277.
- Oostdam, B. L., 1965, Age of Lava Flows on Haleakala, Maui, Hawaii: G.S.A. Bull., v. 76, p. 393-394.
- Powers, S., 1917, Tectonic Lines in the Hawaiian Islands: G.S.A. Bull., v. 28, p. 501-514.
- Staudigel, H. Zindler, A., Hart, S. R., Leslie, T., Chen, C.-Y. and Clague, D., 1984, The Isotope Systematics of a Juvenile Intraplate Volcano: Pb, Nd, and Sr Isotope Ratios of Basalts from Loihi Seamount, Hawaii: Earth Planet. Sci. Lett., v. 69, p. 13-29.
- Stearns, H. T., 1942, Origin of Haleakala Crater, Island of Maui, Hawaii: G.S.A. Bull., v. 53, p. 1-14.
- Stearns, H. T. and Macdonald, G. A., 1942, Geology and Ground-Water Resources of the Island of Maui, Hawaii: Hawaii Div. Hydrogr. Bull. 7, 344 p.
- Stille, P., Unruh, D. M. and Tatsumoto, M., 1986, Pb, Sr, Nd, and Hf Isotopic Constraints on the Origin of Hawaiian Basalts and Evidence for a Unique Mantle Source: Geochim. Cosmochim. Acta, v. 50, p. 2303-2319.
- Washington, H. S. and Keyes, M. G., 1928, Petrology of the Hawaiian Islands: IV. Maui: Am. J. Sci., v. 15, p. 199-220.
- West, H. B. and Garcia, M. O., 1982, Composition and Evolution of Alkalic Cap Stage Lavas from Mauna Kea Volcano, Hawaii: EOS, v. 63, p. 1138.
- West, H. B. and Leeman, W. P., 1987a, Open System Magma Chamber Processes: Trace Element Systematics of Alkalic Cap Lavas from Haleakala Crater, Hawaii: Hawaii Symp. on How Volcanoes Work, Jan. 1987, p. 266.

- West, H. B. and Leeman, W. P., 1987b, Isotopic Evolution of Lavas from Haleakala Crater, Hawaii: *Earth Planet. Sci. Lett.*, in press.
- West, H. B., Gerlach, D. C., Leeman, W. P. and Garcia, M. O., 1987, Isotopic Evolution of Hawaiian Magma Sources: Evidence from the Maui Volcanic Complex: submitted to *Nature*.
- White, W. M., 1985, Sources of Oceanic Basalts, Radiogenic Isotopic Evidence: *Geology*, v. 13, p. 115-118.

FIGURE CAPTIONS

Figure 1. Simplified map of Haleakala Crater (after Macdonald, 1978) with inset map showing general location relative to the island of Maui. Shaded areas are as follows: black (south wall of Crater) - Kumuilihi Formation, dots - Kula Formation flank lavas, shading - Kula Formation lavas exposed on the Crater walls, hachured - Hana Formation cinder cones and other vents.

Figure 2. Silica-alkalies diagram for lavas from Haleakala. Field for Honomanu Formation lavas based on data from this study and from the study of Chen (1982). Cross denotes the Holua trachyte (Kula Formation). Shaded field for Kilauea tholeiites shown for comparison (data from the literature). Solid diagonal line separates the alkalic and tholeiitic fields of Macdonald and Katsura (1964).

Figure 3. Log plot of ranges in trace element abundances for lavas from Haleakala normalized to C1 chondritic or estimated primitive mantle (Rb, K, Sr, P) abundances. Shaded area = Honomanu Formation, vertical striped field = Kumuilihi Formation, field between solid lines = Kula Formation, field between dashed lines = Hana Formation. Elements on horizontal axis are in order of increasing compatibility (i.e. higher bulk distribution coefficient values) from left to right.

Figure 4. Rb and Sc vs. Nb for lavas from Haleakala. Symbols are as follows: open squares - Honomanu Formation, X - Kumuilihi Formation, solid diamonds - Kula Formation, open circles - Hana Formation.

Figure 5. TiO₂ and Cr vs. Nb for lavas from Haleakala. Symbols as in Fig. 4.

Figure 6. P₂O₅ and Sr vs. Nb for lavas from Haleakala. Symbols as in Fig. 4.

Figure 7. $^{208}\text{Pb}/^{204}\text{Pb}$, $^{207}\text{Pb}/^{204}\text{Pb}$ and $^{87}\text{Sr}/^{86}\text{Sr}$ vs. $^{206}\text{Pb}/^{204}\text{Pb}$ for lavas from Haleakala (from West and Leeman, 1987b). Data for fields of other Hawaiian volcanoes taken from the literature. Additional unpublished data for Mauna Kea field from Kwon and Tilton (Pb) and Kennedy and Frey (Sr and Nd). Symbols as follows: solid squares - Honomanu Formation, X - Kumuilihi Formation, solid diamonds - Kula Formation, cross - Holua trachyte (Kula Formation), solid circles - Hana Formation.

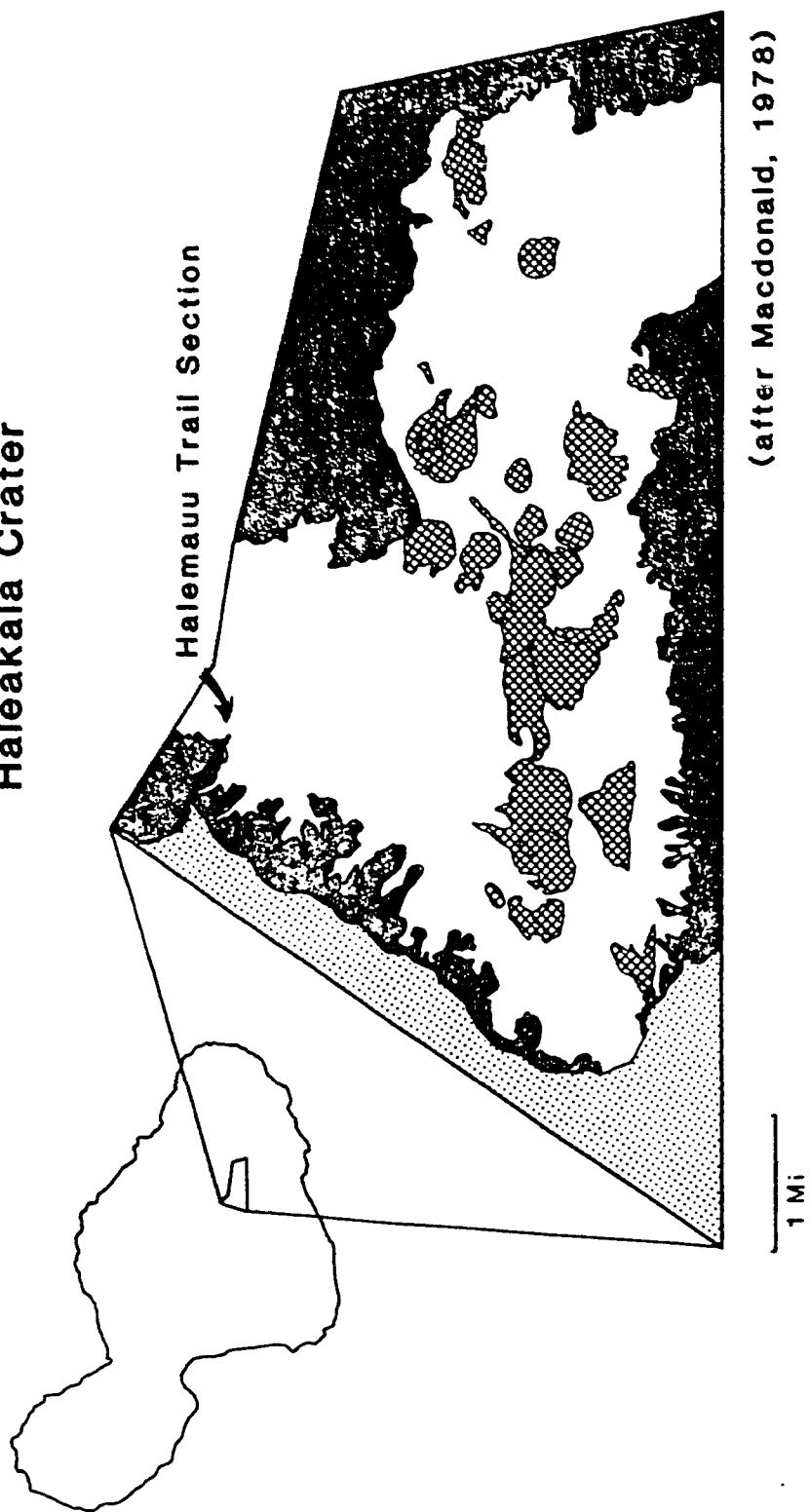
Figure 8. La/Ce, La/Yb and Zr/Hf vs. Nb for lavas from Haleakala. Symbols as in Fig. 4.

Figure 9. La, $^{206}\text{Pb}/^{204}\text{Pb}$ and $^{87}\text{Sr}/^{86}\text{Sr}$ vs. SiO_2 for lavas from Haleakala (from West and Leeman, 1987b). Symbols as in Fig. 7. Additional data shown as open symbols and from the following sources: La and $^{87}\text{Sr}/^{86}\text{Sr}$ (Chen and Frey, 1985), SiO_2 (Chen, 1982), and $^{206}\text{Pb}/^{204}\text{Pb}$ (Hegner et al., 1986).

Figure 10. $^{87}\text{Sr}/^{86}\text{Sr}$ and $^{206}\text{Pb}/^{204}\text{Pb}$ vs. relative stratigraphic position for lavas from Haleakala (from West and Leeman, 1987b). Symbols as in Fig. 7. Breaks between formations are indicated with vertical lines.

Figure 11. Upsection variations in K_2O , Sc and $\text{Al}_2\text{O}_3/\text{CaO}$ for Kula Formation lavas from the Halemauu trail section, northwest wall of Haleakala Crater. Vertical lines indicate geochemical discontinuities which reflect individual magma batches.

Haleakala Crater



(after Macdonald, 1978)

FIG. 1

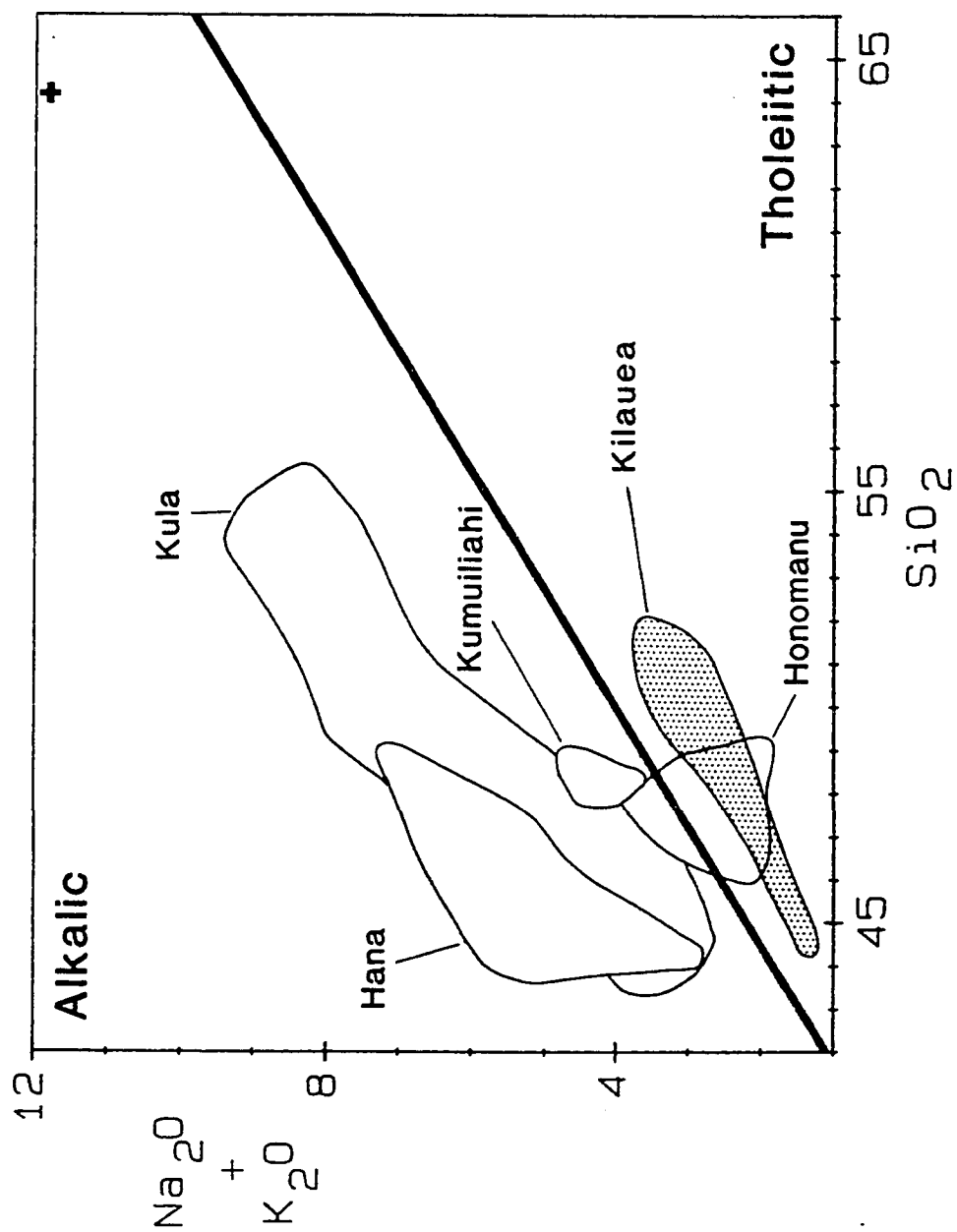


FIG. 2

FIG. 3

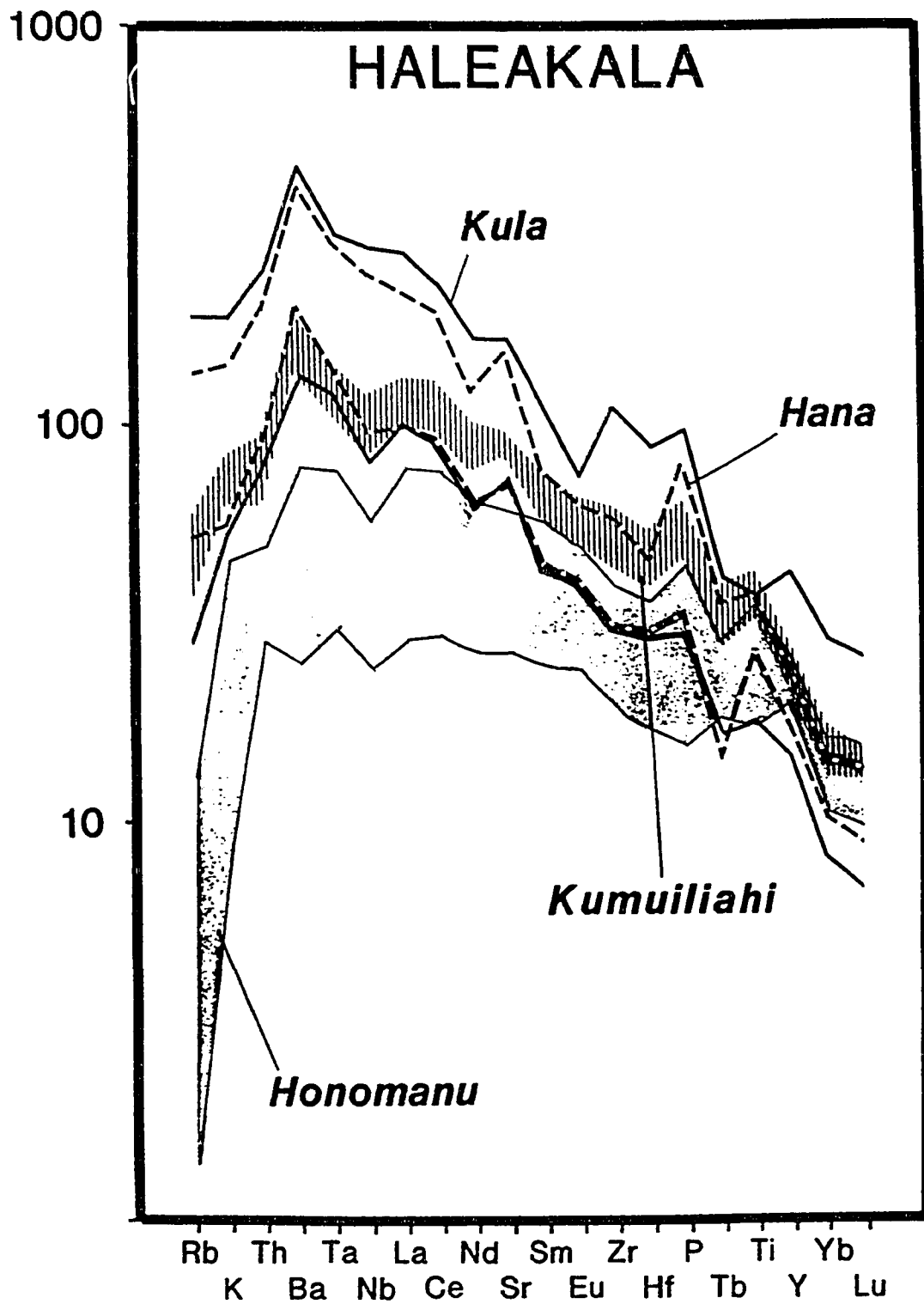


FIG. 4

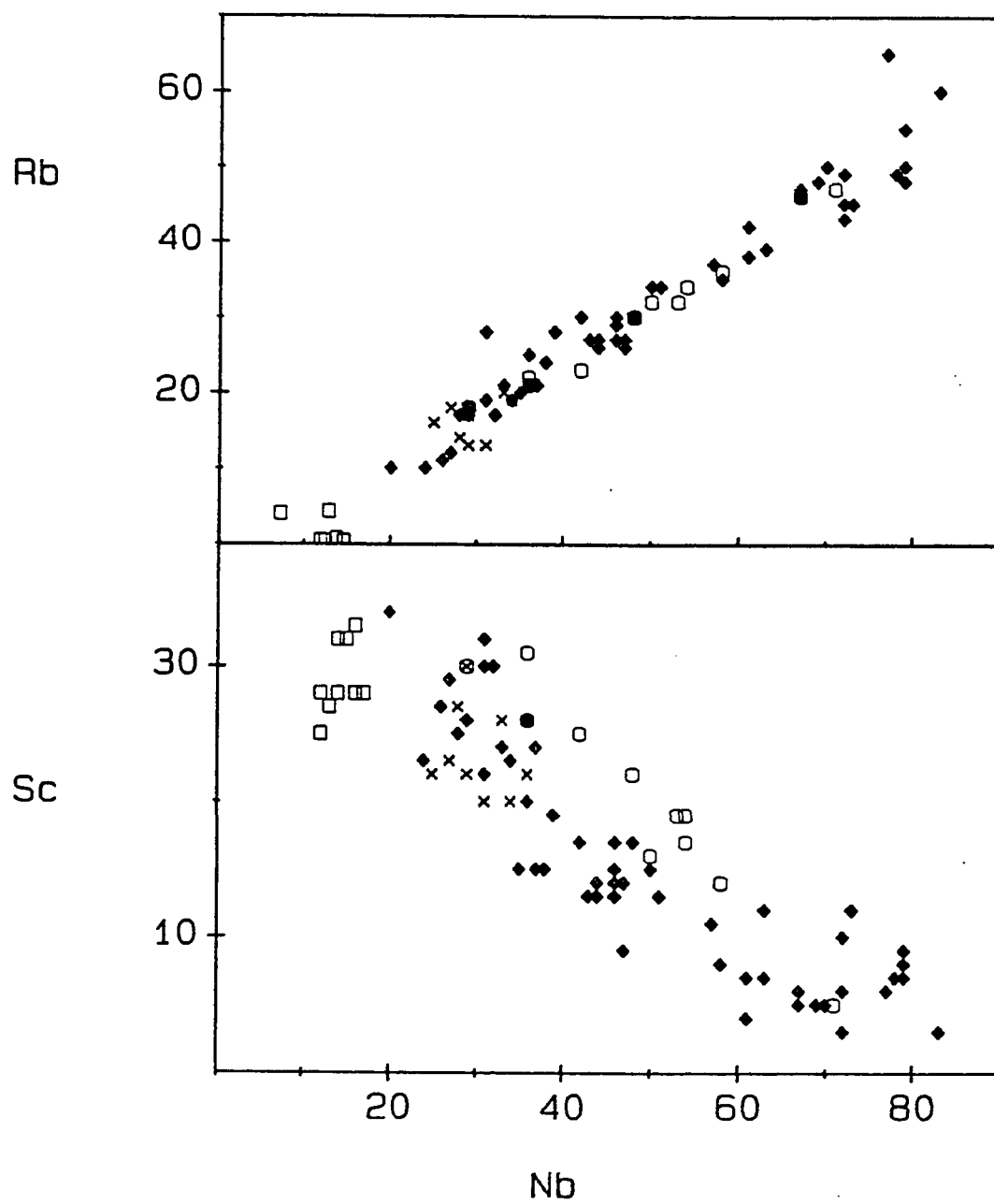


FIG. 5

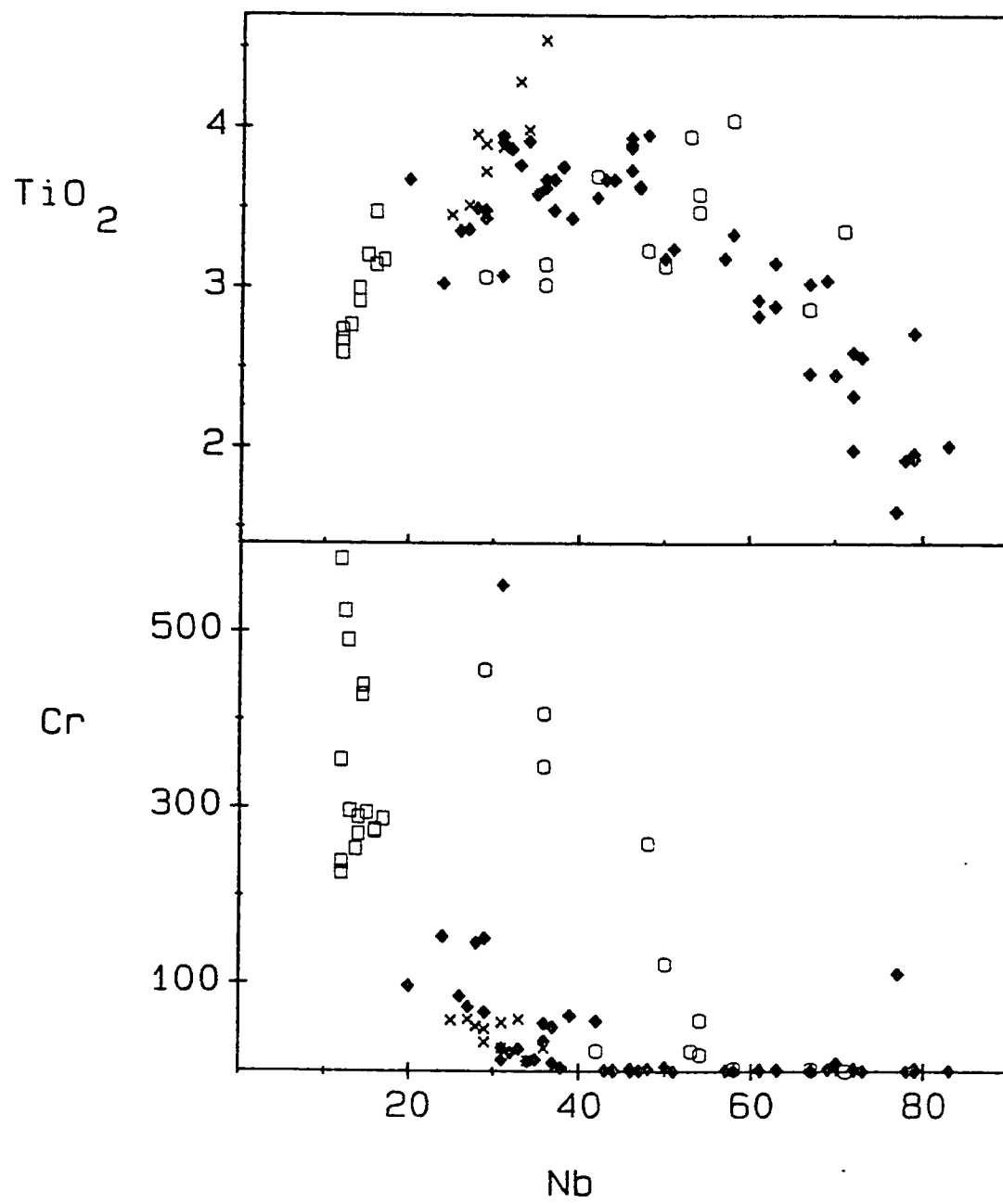
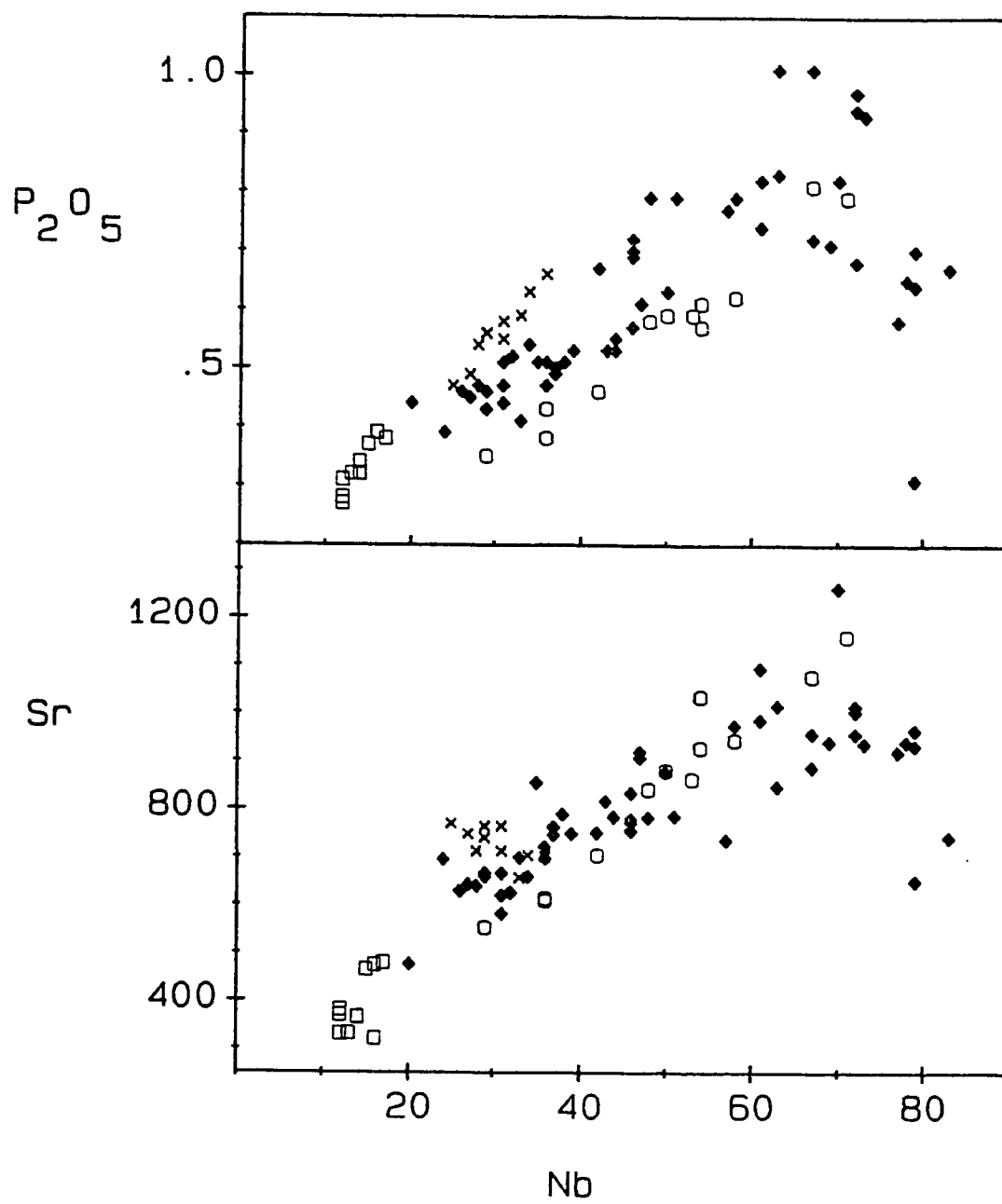


FIG. 6



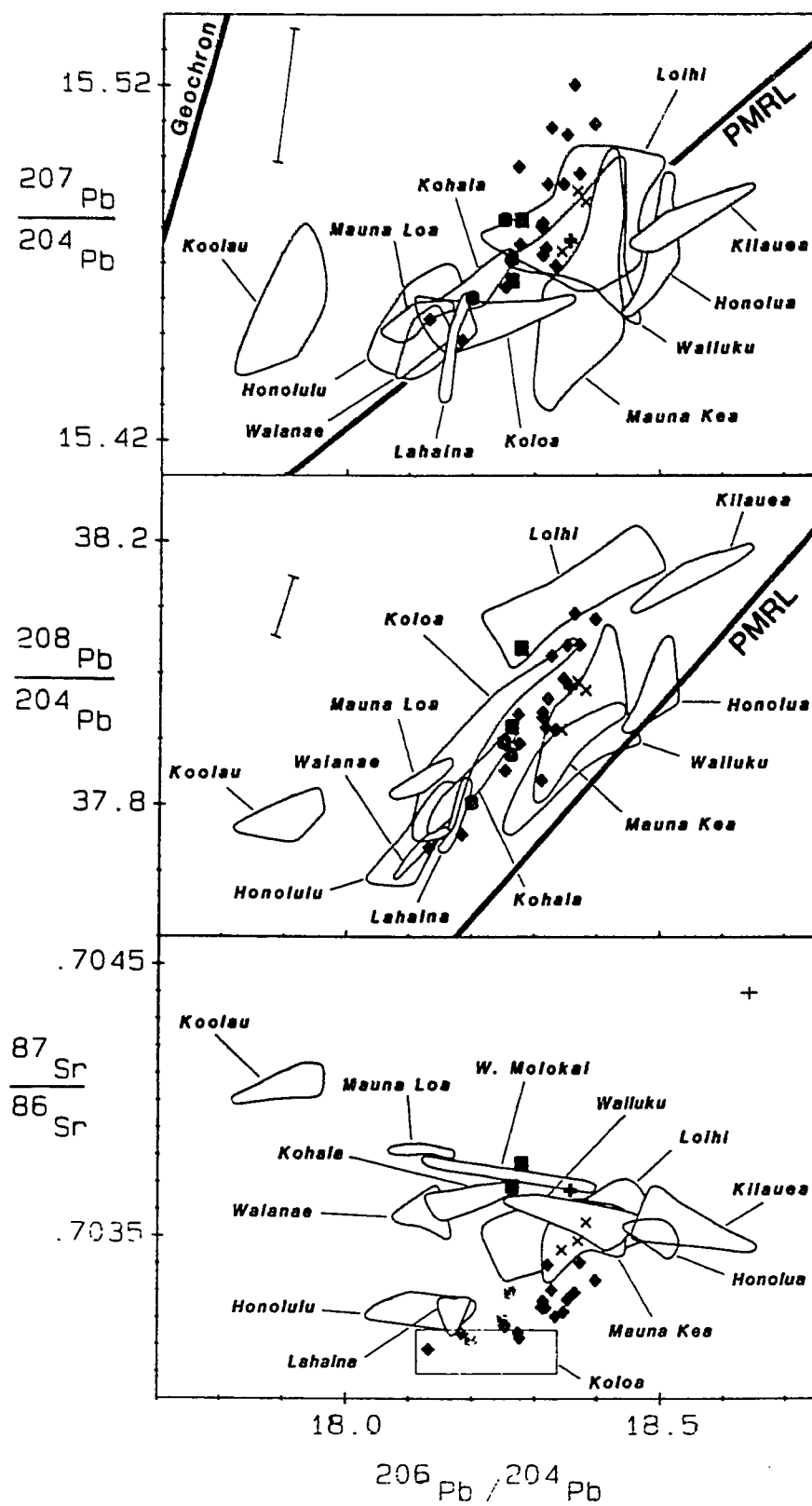


FIG. 7

FIG. 8

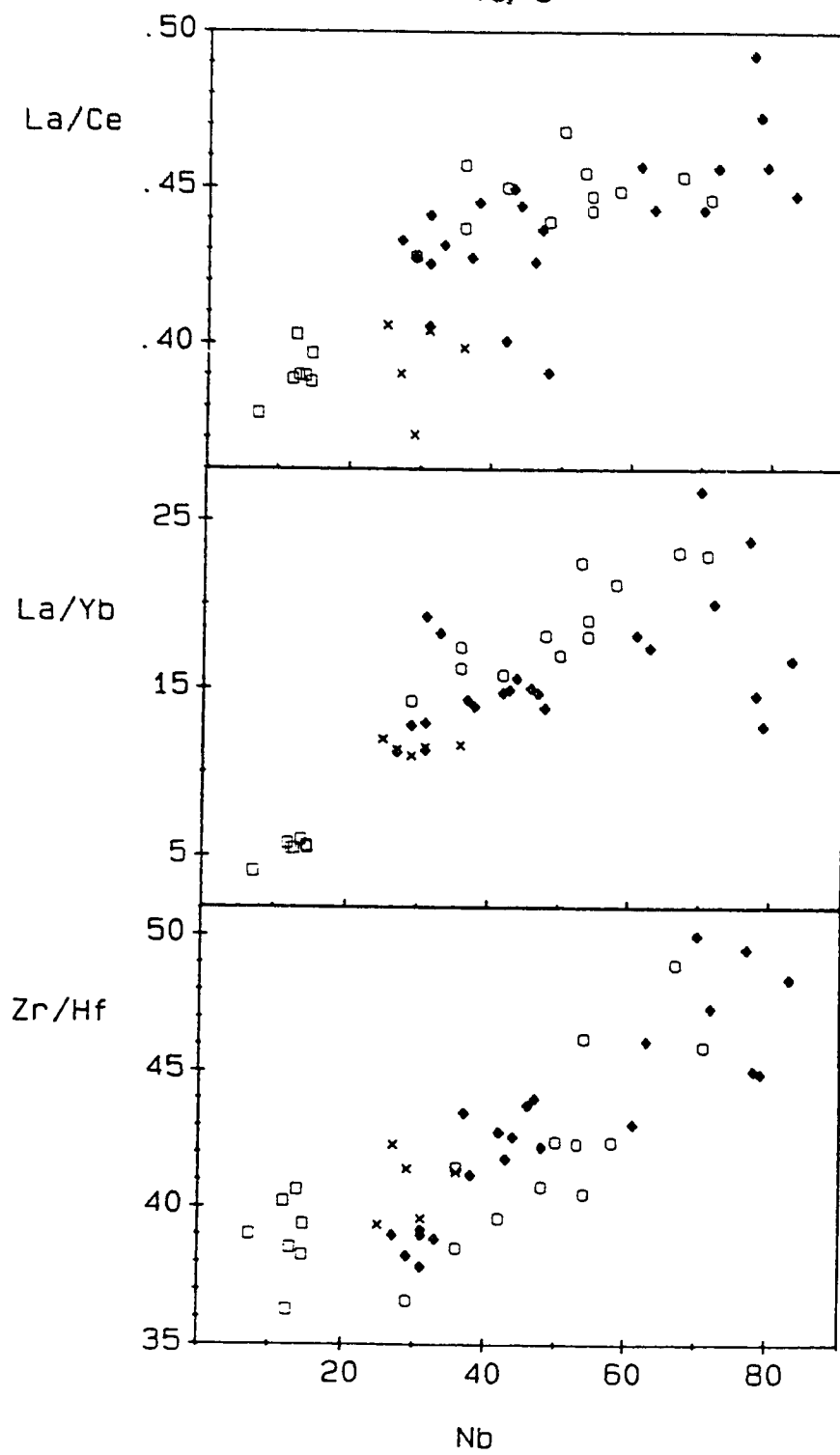


FIG. 9

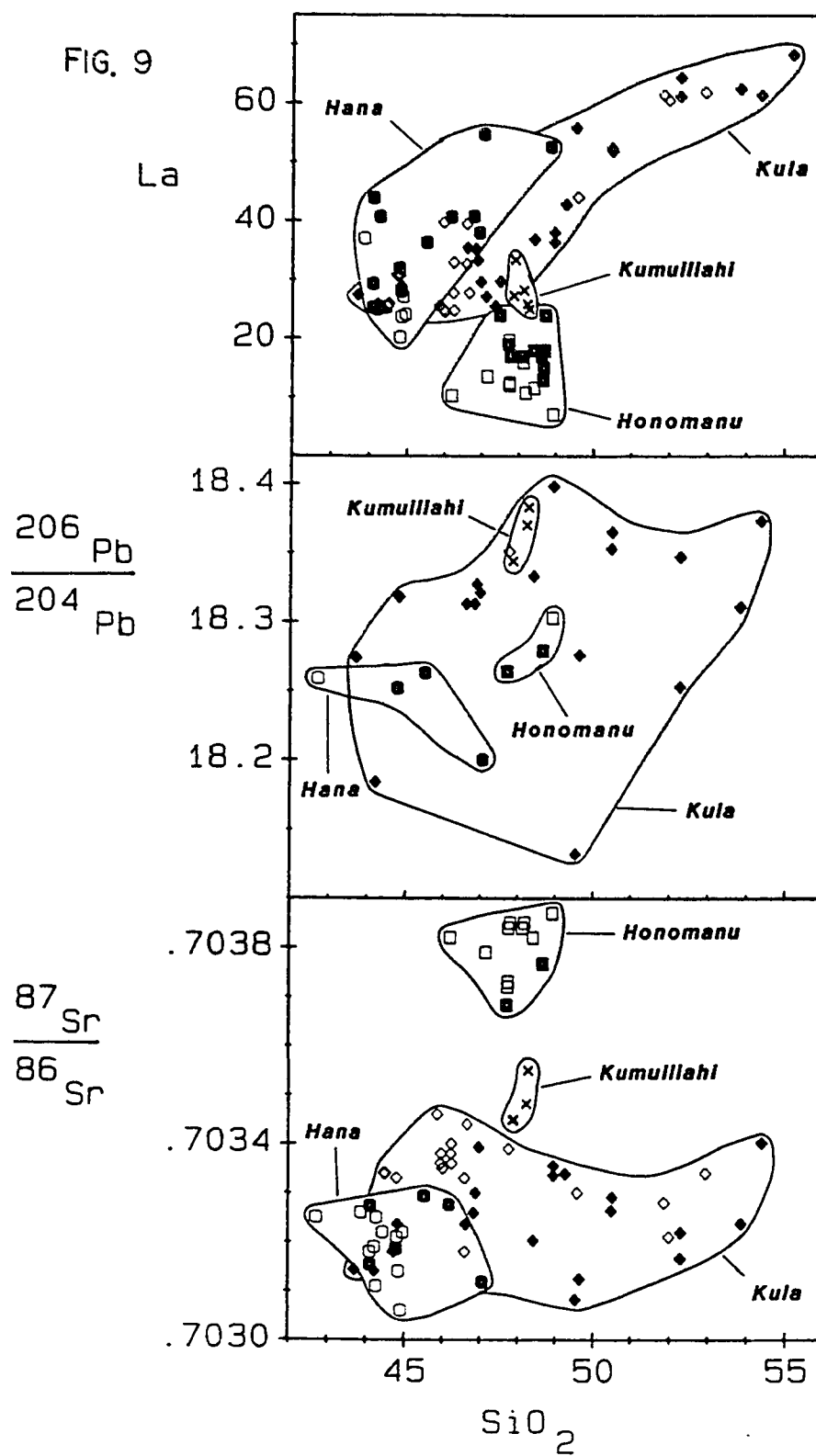
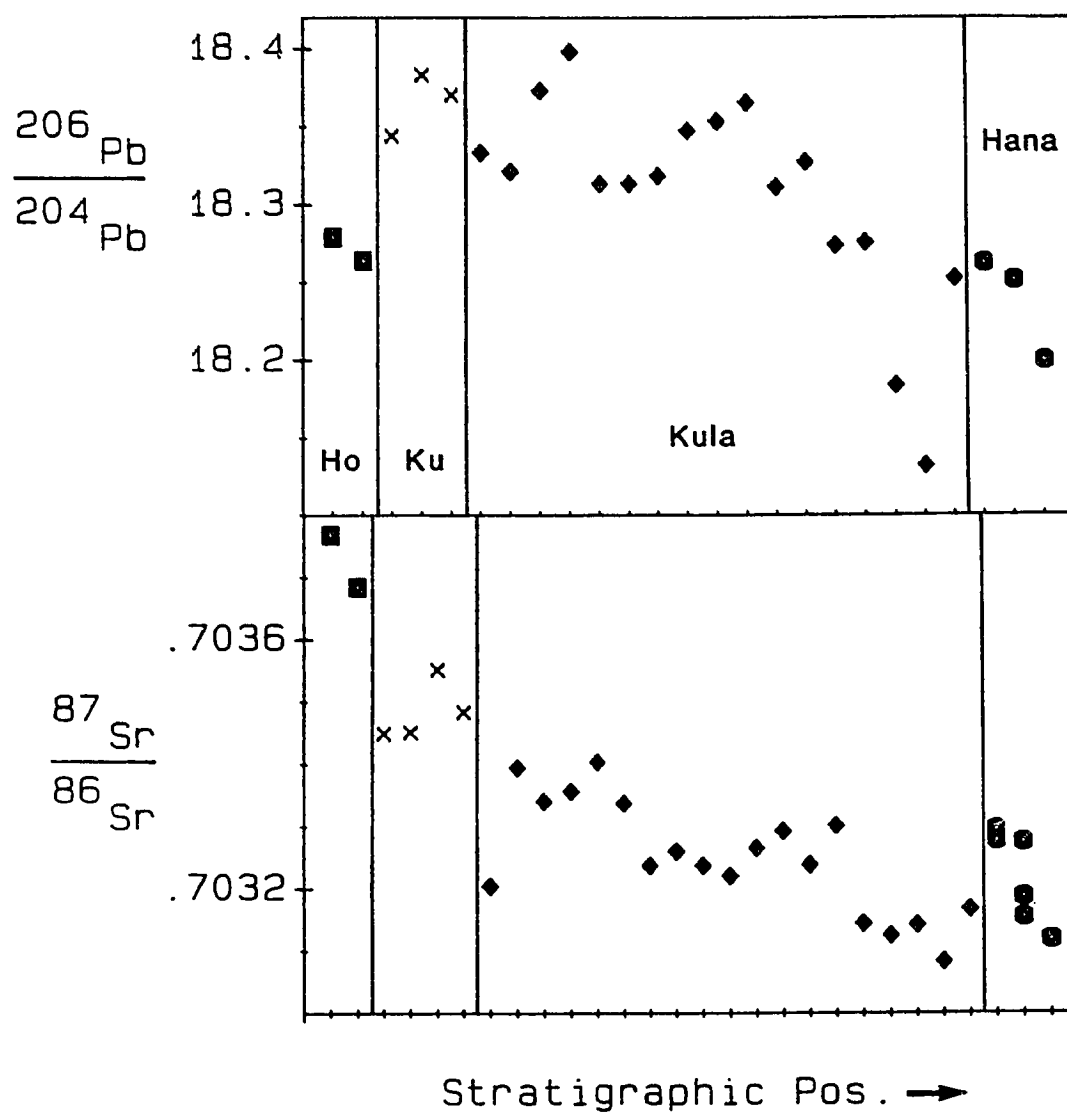
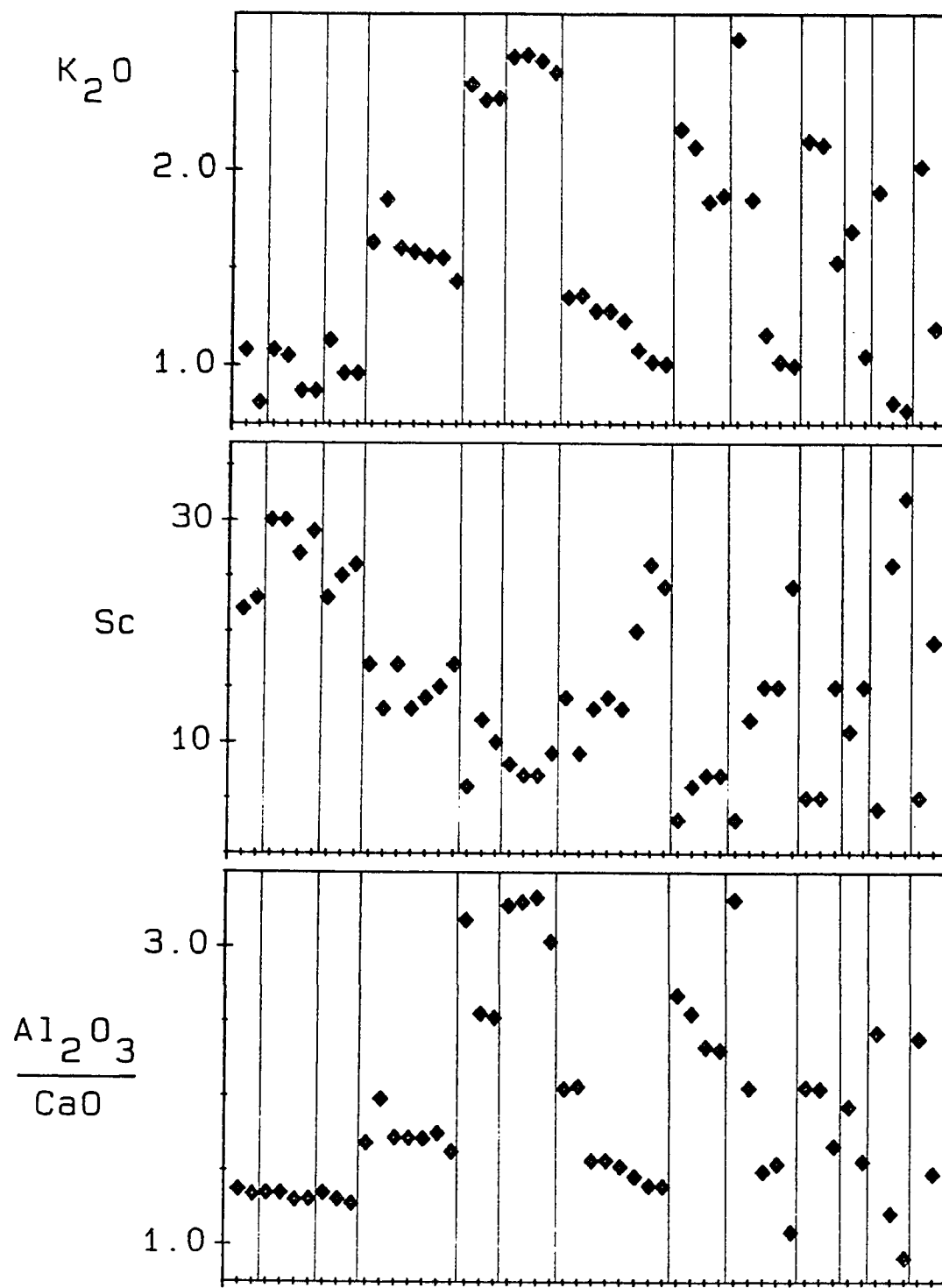


FIG. 10





Stratigraphic Position · FIG. 11

Chapter 2

ISOTOPIC EVOLUTION OF LAVAS FROM HALEAKALA CRATER, HAWAII

Abstract

Pb and Sr isotopic ratios have been determined for tholeiitic shield-building, alkalic cap, and post-erosional stage lavas from Haleakala Crater. Pb isotopic compositions of the tholeiites overlap those of the alkalic cap lavas, although $^{87}\text{Sr}/^{86}\text{Sr}$ ratios of these two suites are distinct. Alkalic cap and post-erosional lavas appear to be indistinguishable on the basis of Sr and Pb isotopic composition.

Sr and Pb isotopic ratios of Haleakala post shield-building lavas are positively correlated. Such a trend is previously undocumented for any suite of Hawaiian lavas and contrasts with the general negative correlation observed for data from Hawaiian tholeiites. These relations are consistent with a three-component petrogenetic mixing model. Specifically, it is proposed that magma batches at individual Hawaiian volcanoes formed by: (1) mixing of melts generated from mantle plumes containing two isotopically distinct mantle components (primitive vs. enriched), and (2) subsequent variable degrees of interaction between these plume melts and a third (MORB signature) mantle reservoir prior to their emplacement in a crustal magma chamber. These observations and inferences provide new constraints on physical models of Hawaiian magmatism. Based on observed temporal isotopic variations of Haleakala lavas, it is suggested that the ratio of enriched:primitive mantle components in the Hawaiian plume source decreases during the waning stages of alkalic volcanism. Over the same time interval, both decreasing melt production and protracted residence of ascending melts within the upper mantle contribute to a systematic increase in the ratio of depleted vs. plume component.

1. Introduction

Geochemical studies of oceanic basalts serve as a primary means of evaluating the composition and evolution of the Earth's mantle because it can be reasonably argued that these lavas have not interacted with continental crust or lithosphere. Systematic geochemical and isotopic differences between mid-ocean ridge basalts (MORB) and oceanic island basalts (OIB) [1,2] indicate that the mantle is geochemically heterogeneous. In the "standard" two-reservoir model [3], MORB melts are derived from depleted upper mantle (formed as a result of continental crust extraction), whereas OIB melts are produced from comparatively primitive material upwelling as plumes [4] from the lower mantle.

Since 1980, a multitude of new isotopic data for MORB and OIB has revealed the sub-oceanic mantle to be heterogeneous on scales ranging from thousands of kilometers (the spacing between island groups) to a few kilometers (individual volcanoes). This complex isotopic spectrum requires the preservation of multiple geochemically distinct mantle domains [e.g. 5]. Because the existence of these mantle domains has strong bearing on petrochemical evolution and convection within the mantle, their origin, composition, scale, distribution, and interaction are topics presently under vigorous debate by both geochemists and geophysicists.

A major problem in attempting to resolve the nature of mantle heterogeneity is that sampling is typically reconnaissance in nature and insufficient to evaluate in detail evolutionary processes on the scale of individual eruptive centers. In principle, detailed geochemical studies of single, long-lived volcanic centers may provide the clearest means of evaluating the evolution of underlying mantle. Specifically, magmas from hotspot-related oceanic island volcanoes should provide a relatively detailed record of the evolution of deep-seated mantle plumes and their interaction with geochemically and isotopically distinct wall rock materials during ascent through the mantle. Here, we present the isotopic results of such a study, focusing on Haleakala, one of the larger Hawaiian volcanoes.

The consistent age progression of its volcanoes and compositional similarity of erupted magma suites over some 70 m.y. firmly establish the Hawaiian-Emperor Chain of islands and seamounts as a paradigm for the hotspot model. These volcanoes serve as a well documented natural laboratory for investigations into the dynamics of magma formation, segregation, transport, and modification. Despite the relatively large volume of work on Hawaii, the evolutionary interaction of possible mantle reservoirs remains poorly constrained because little systematic work has been done on older volcanoes along the Hawaiian Chain. To further document the temporal evolution of the Hawaiian Chain, we have carried out a detailed Sr and Pb isotopic study of a spatially and temporally well-constrained set of lavas from Haleakala volcano (East Maui). Nearly the full spectrum of recognized Hawaiian magmatic activity is represented, and because of the unique presence of a large erosional caldera at its summit it was possible to obtain a detailed sampling of well-exposed fresh samples.

The results from our isotopic study reveal for the first time systematic, time-dependent isotopic variations in alkalic cap lavas and a decoupling of the alkalic cap trend from that of shield-building lavas. These variations appear to reflect mixing between three isotopically distinct mantle reservoirs: depleted (MORB) upper mantle and a Hawaiian mantle plume containing both a primitive and an enriched component. Previous Hawaiian studies [6-10] proposing multi-component mixing models presented insufficient data to document fully the evolutionary and systematic nature of the interaction between proposed mantle components during the alkalic cap stage. The model we present has additional implications for plume dynamics and is consistent with recently developed plume models [11-13]. Major and trace element results from this study will be presented elsewhere.

2. Previous Isotopic Studies of Hawaiian Volcanoes

The evolution of Hawaiian volcanoes is accompanied by changes in the isotopic composition of Pb, Sr and Nd. Where data are available within a single volcano, shield-building tholeiites appear to have more radiogenic Sr and less radiogenic Nd compositions than associated alkalic cap lavas [e.g. 9,14]. Post-erosional nephelinites from Honolulu (Oahu) and Koloa (Kauai) volcanics have the least radiogenic Sr and most radiogenic Nd compositions observed for Hawaiian volcanoes and approach MORB values. Koolau (Oahu) tholeiites have isotopic compositions similar to those postulated for the bulk Earth ($^{87}\text{Sr}/^{86}\text{Sr} = 0.7045$, $^{143}\text{Nd}/^{144}\text{Nd} = 0.51262$, $^{206}\text{Pb}/^{204}\text{Pb} = 17.7$, $^{207}\text{Pb}/^{204}\text{Pb} = 15.43$, $^{208}\text{Pb}/^{204}\text{Pb} = 37.6$; [15]).

Chen and Frey [14] found that shield-building and alkalic cap lavas from Haleakala are isotopically distinct in terms of Sr and Nd. Most significantly, although post-erosional lavas from Haleakala fall entirely within the range of associated alkalic cap lavas [22], Sr isotopic compositions appear to be correlated with age [14]. The time-dependent correlation between incompatible trace element ratios (La/Ce) and $^{87}\text{Sr}/^{86}\text{Sr}$ ratios lead Chen and Frey [14] to propose that lavas from Haleakala were the result of mixing between a Hawaiian plume having primitive mantle geochemical characteristics and partial melts of depleted (MORB) mantle. However, further Hawaiian studies [6-10] incorporating Pb isotopes appear to preclude simple two-component mixing.

3. Geologic Setting and Sampling

Haleakala forms the eastern half of The island of Maui (Fig. 1). Four volcanic formations have been recognized [23,24]; these are briefly discussed in sequence from oldest to youngest.

The Honomanu Formation comprises the lowermost exposed lavas and consists primarily of shield-building tholeiites with some interbedded alkalic basalts. These rocks are exposed along the northern coast and in deep valleys on the northern and southern flanks of the volcano. It is unknown when volcanism began but a sample col-

lected from the type section at Honomanu Valley has been dated at 0.83 ± 0.17 Ma [25]. We analyzed two tholeiitic basalts from the type section, including the uppermost exposed flow (HHM-1) and a flow exposed near the base of the section (HHM-9).

The stratigraphically higher Kumuilihi Formation consists of interbedded alkalic basalts and hawaiites and is exposed only in Haleakala Crater [24]. Kumuilihi lavas are separated from overlying Kula Formation lavas by a pronounced angular unconformity. Samples dated by Naughton [25] have a mean age of 0.75 ± 0.04 Ma. Samples from this study span the exposed type section on the south wall of Haleakala Crater.

The Kula Formation unconformably overlies the Kumuilihi Formation in Haleakala Crater and represents the alkalic cap stage of Haleakala, comprising the majority of subaerially exposed lavas. The presence of an ashy soil layer at the Honomanu-Kula contact in Honomanu Valley [23], the change in petrographic character of the lavas from strongly phyrlic to sparsely phyrlic, and the change from thin-bedded pahoehoe to thick-bedded a'a all indicate that a significant change in the style of magmatism occurred at this break. Rock types include alkalic basalt, hawaiite, mugearite, basanitoid and a single occurrence of trachyte; hawaiite and alkalic basalt are the dominant lithologies. K-Ar age determinations range from 0.36 to 0.86 Ma [25,26]. Kula samples from this study were collected primarily from a continuous 1000 foot section (the Halemau Trail Section) on the northeast wall of Haleakala Crater (Fig. 1), although one sample (HK-46) was collected from just above the Kumuilihi Formation. We consider HK-46 to be the oldest Kula lava exposed in Haleakala Crater primarily because the underlying Kumuilihi Formation is not exposed beneath sections of Kula lavas elsewhere in the Crater. The most evolved sample collected is from a trachyte dike (the Holua trachyte), exposed on the northeast wall of the Crater and mapped as part of the Kula Formation [24]. The Holua trachyte was dated at 0.49 ± 0.15 Ma [25].

The Hana Formation represents the youngest period of volcanism and forms the post-erosional stage of Haleakala. Rock types include basanitoid, hawaiite, alkalic basalt and ankaramite. Hana lavas were primarily erupted from vents along the southwest and

east rift zones of Haleakala and are separated from underlying Kula Formation lavas by a major erosional unconformity, representing perhaps 400,000 years of inactivity. The most recent known Hana eruption occurred around the year 1790 [27]. Hana Formation samples were collected from cinder cones and lava flows on the floor of Haleakala Crater.

Honomanu tholeiites have major and trace element compositions typical of Hawaiian tholeiites. On a silica-alkalies diagram (Fig. 2), Honomanu tholeiites and alkalic basalts form a trend extending from the Kilauea field to slightly into the alkalic field. Despite their petrographic similarity to Honomanu lavas [23,24], Kumuilihi lavas have higher incompatible element contents at similar silica contents (Fig. 2). Kula lavas fall entirely within the alkalic field and form a trend similar to other Hawaiian alkalic cap suites. Hana post-erosional lavas have major and trace element compositions which generally fall within the compositional range of the Kula Formation, although critically silica-undersaturated compositions (e.g. basanitoids) are more common and evolved lavas (e.g. hawaiiite) less common.

The presence of three of the four known stages of Hawaiian volcanism at Haleakala (early alkalic, shield-building, alkalic cap, and post-erosional stages; only the early alkalic stage appears not to be exposed) makes it possible to document in detail variations in the isotopic composition of an individual Hawaiian volcano over a significant portion of its lifetime. We have specifically concentrated on the section of alkalic cap lavas exposed in Haleakala Crater which provide a more continuous and complete record of eruptive activity than do the thinner and less complete stratigraphic sections from the distal flank of the volcano that have been previously studied [14].

4. Analytical Procedures

Pb: The majority of measurements were performed at the University of California at Santa Barbara. All chemical processing was carried out in laminar flow hoods. Samples were dissolved in HF-HClO₄ and Pb was separated by standard anion exchange techniques [29]. Pb concentrations were determined by spiking with ²⁰³Pb. Isotope ratios were measured on a Finnegan MAT 261 fixed multiple collector mass spectrometer. Samples were run on single filaments using the phosphoric acid-silica gel method. Precision based on replicate analyses of NBS SRM 981 is $\pm 0.08\%$ (²⁰⁴Pb/²⁰⁶Pb) to 0.04% (²⁰⁷Pb/²⁰⁶Pb and ²⁰⁸Pb/²⁰⁶Pb). To correct for isotopic fractionation, Pb isotopic ratios were normalized to an SRM 981 value for ²⁰⁸Pb/²⁰⁶Pb of 2.1671 [30]. Five samples were analyzed for Pb isotopic composition at M.I.T. using standard chemical and mass spectrometric techniques [31]. Pb isotope compositions determined at M.I.T. are precise to better than $\pm 0.05\%$ per a.m.u. based on replicate analyses of NBS 981. For the four samples analyzed in both labs, results agree closely (0.029% for ²⁰⁶Pb/²⁰⁴Pb; 0.031% for ²⁰⁷Pb/²⁰⁴Pb; 0.041% for ²⁰⁸Pb/²⁰⁴Pb).

Sr: Sample dissolutions, chemical processing and isotopic measurements were carried out at M.I.T. and U.C.S.B.. In addition, six samples were analyzed by D. C. Gerlach at Leeds University. Techniques are described in [32]. Average in-run precision (± 0.000027) for M.I.T. data is comparable to that for complete chemistry duplicate analyses; in-run precision obtained at U.C.S.B. and Leeds is better. ⁸⁷Sr/⁸⁶Sr ratios have been adjusted to a value of 0.70800 for the Eimer and Amend SrCO₃ standard.

5. Results

5.1. Pb

Haleakala ²⁰⁶Pb/²⁰⁴Pb and ²⁰⁸Pb/²⁰⁴Pb ratios (Table 1) fall within the relatively broad range for other Hawaiian volcanoes, but ²⁰⁷Pb/²⁰⁴Pb ratios extend to higher values and define a greater range than for other Hawaiian volcanoes. Only Koolau, Hualalai and Kilauea data appear to have compositional ranges distinct from the Haleakala field

(Fig. 3). It is likely the comparatively large range of Haleakala Pb isotopic compositions at least partly reflects the paucity of data for most other Hawaiian volcanoes. The Kula Formation encompasses the total observed range in Pb isotope ratios for Haleakala; the Honomanu, Kumuiliahi and Hana Formations display more restricted ranges (Fig. 3). The Holua trachyte has a composition similar to that of Kumuiliahi and older Kula Formation lavas, but is distinctly more radiogenic than Honomanu or Hana Formation lavas. Pb isotopic compositions are not correlated with major or trace element contents (Fig. 4). Within the Halemauu Trail section (Kula Formation), there appears to be a general upsection decrease in $^{206}\text{Pb}/^{204}\text{Pb}$ (Fig. 5).

5.2. Sr

Haleakala $^{87}\text{Sr}/^{86}\text{Sr}$ ratios (Table 1) fall within the range of data for other Hawaiian volcanoes. Honomanu $^{87}\text{Sr}/^{86}\text{Sr}$ ratios (0.70368–0.70387 [14, this study]) are typical of Hawaiian tholeiites in general. Kumuiliahi $^{87}\text{Sr}/^{86}\text{Sr}$ ratios (0.70345–0.70355) are lower than Honomanu values but overlap Kula Formation ratios. New data for Kula lavas collected from Haleakala Crater extend to lower values the range in $^{87}\text{Sr}/^{86}\text{Sr}$ ratios found in flank lavas [14]. $^{87}\text{Sr}/^{86}\text{Sr}$ ratios of all analyzed Kula lavas collectively span a considerable range (0.70308–0.70353) but are distinct from Honomanu alkalic basalts (0.70372 [14]). Hana lavas from this study (0.70312–0.70329) are compositionally similar to Hana flank lavas (0.70306–0.70328 [14]). Altogether, Hana $^{87}\text{Sr}/^{86}\text{Sr}$ ratios overlap the range observed for Kula lavas and are among the lowest found in Hawaii; only leucite-normative alkalic lavas from Kauai [19] have lower $^{87}\text{Sr}/^{86}\text{Sr}$ ratios (i.e. 0.70299).

The Holua trachyte (Table 2) whole rock has an unusually radiogenic initial $^{87}\text{Sr}/^{86}\text{Sr}$ ratio (duplicate analyses average 0.70426) which contrasts strongly with the ratio measured on fresh feldspar separates (0.70367). This discrepancy could reflect prolonged interaction of the trachyte magma with migrating ground waters that had experienced mixing with seawater. The feldspar $^{87}\text{Sr}/^{86}\text{Sr}$ ratio is higher than observed Kula or Kumuiliahi ratios and falls within the range of Honomanu ratios. However, the

Holua trachyte is clearly younger than the Honomanu Formation, as it intrudes the Kula section.

Consistent with the findings of Chen and Frey [14], $^{87}\text{Sr}/^{86}\text{Sr}$ ratios of lavas from this study appear to be correlated with stratigraphic position (Fig. 5), but with a notable exception. The oldest Kula lava exposed in Haleakala Crater has a low $^{87}\text{Sr}/^{86}\text{Sr}$ ratio (0.70320), similar to those found for the youngest exposed Kula lavas.

Stratigraphic relations for the Hana Formation in Haleakala Crater are poorly defined; from Macdonald's [24] study, it is possible to distinguish only three stratigraphically distinct groups in the collected samples. Although the youngest Hana lava exposed in the Crater has the lowest $^{87}\text{Sr}/^{86}\text{Sr}$ ratio and lavas from the oldest group have the highest $^{87}\text{Sr}/^{86}\text{Sr}$ ratios, it is not possible to demonstrate conclusively the existence of temporal correlations. In comparison, Hana flank lavas [14] show no systematic variation in $^{87}\text{Sr}/^{86}\text{Sr}$ ratios with stratigraphic position.

In general, $^{87}\text{Sr}/^{86}\text{Sr}$ ratios of Haleakala lavas do not correlate with major or trace element contents; there is also no correlation within individual formations (Fig. 4). Honomanu and Kumuilahi lavas have intermediate silica contents and high $^{87}\text{Sr}/^{86}\text{Sr}$ ratios relative to Kula and Hana lavas.

5.3. Pb-Sr Relationships

Covariations between Hawaiian Pb and Sr isotope data (Fig. 3c) are more complex than Sr-Nd [e.g. 6-10] or Pb-Pb (Figs. 3a-3b) relations. Hawaiian data form an approximately triangular field, the apices defined by Koolau, Kilauea, and Koloa/Honolulu. Viewed separately, Hawaiian tholeiites appear to form a general negative Sr-Pb array extending from Koolau to Kilauea (Fig. 3c). There is no systematic relationship between the position of a particular Hawaiian volcano within this field and its age nor with its location along the Hawaiian Chain.

Stratigraphic breaks separating the Honomanu, Kumuilahi, and Kula Formations are accompanied by shifts in the isotopic compositions of these lavas (Fig. 3c).

Honomanu lavas form a distinct high $^{87}\text{Sr}/^{86}\text{Sr}$, intermediate $^{206}\text{Pb}/^{204}\text{Pb}$ field relative to post shield-building lavas (Kumuiliahi, Kula, Hana). The latter exhibit a strong, positive Sr-Pb correlation that appears to have temporal significance: Kumuiliahi lavas define the radiogenic end of the trend, whereas Hana lavas and the youngest Kula lavas contain the least radiogenic Pb and Sr. This Sr-Pb trend is unique and has not been previously observed for lavas from other Hawaiian volcanoes. The Sr-Pb isotope correlation for Haleakala post shield-building lavas is consistent with a binary mixing curve. Main points to be addressed concern: (1) the nature of the two mixing end-members, and (2) the mechanisms or processes that produce the distinct Sr-Pb trends for shield-building tholeiites and post shield-building alkalic and post-erosional lavas.

6. Constraints on Mixing End-Members

The overall isotopic variability of oceanic island basalts is very large and deviations from linear arrays on isotope-isotope plots [see 5,16] require the existence of multiple isotopically distinct mantle reservoirs. The intersection of most OIB isotope data with some point along the Sr-Pb MORB array [see 16] implies that individual islands (e.g. St. Helena) and island groups (e.g. Hawaii, Marquesas) represent interactions between a depleted mantle (DM) reservoir and a second or third mantle component. Non-depleted mantle reservoirs from which OIB's derive their relatively radiogenic Pb and Sr and unradiogenic Nd signatures could include a primitive mantle (PM) reservoir possibly residing in the lower mantle, an enriched mantle reservoir (EM) possibly related to subducted materials, or migratory mantle fluids having enriched trace element compositions. Of course, these hypothetical reservoirs are likely variable in composition and all may be involved in OIB genesis. Because ancient subducted materials of various age and composition must form a significant portion of the mantle [33], it is unlikely that the present sub-oceanic mantle consists of a small number (e.g. six [5]) of enriched domains from which all oceanic magmatism derives. A likely explanation for the isotopic diversity of OIB groups is that mantle not involved in MORB genesis must have

undergone numerous depletion and enrichment events both spatially and temporally, thus producing a spectrum of mantle domains which have evolved independently.

In the following discussion, we cite specific compositions of hypothetical mantle components for illustrative purposes. It is not suggested that these components have global significance.

The divergence of Hawaiian Island isotope data from linear arrays (Fig. 3) and the general triangular nature of the Hawaiian field are consistent with mixing between at least three distinct end-members [e.g. 8]. The compositions of these end-members must lie somewhere in the vicinity of or beyond the apices of the Hawaiian field. For example, the similarity of Koolau Pb-Sr-Nd isotopic compositions to those estimated for primitive mantle [see 15] suggests that such material could be involved in the genesis of Hawaiian magmas and shield-building tholeiites in particular.

Sr and Nd isotopic compositions of Honolulu/Koloa post-erosional lavas are similar to MORB compositions and suggest that an end-member with MORB characteristics (e.g. depleted asthenosphere, lithosphere, or melts thereof) was involved in their genesis. Shallow-level interaction between Hawaiian magmas and altered oceanic crust is not considered to be significant in the petrogenesis of Haleakala magmas because such material is generally distinct from isotopic fields for Hawaii (i.e. relatively radiogenic Sr and intermediate Pb isotopic compositions). For purposes of modeling, we use as the composition of DM the least radiogenic Pacific MORB composition observed ($^{206}\text{Pb}/^{204}\text{Pb}$ 17.721, $^{207}\text{Pb}/^{204}\text{Pb}$ = 15.369, $^{208}\text{Pb}/^{204}\text{Pb}$ = 37.039, $^{87}\text{Sr}/^{86}\text{Sr}$ = 0.70217; [34]); these values are similar to those suggested by Davies [38] for depleted mantle.

The Kilauea end-member must have relatively radiogenic Pb ($^{206}\text{Pb}/^{204}\text{Pb}$ > 18.65) and a Sr composition intermediate between DM and PM. This implies an enriched reservoir (EM) with high U/Pb and Th/Pb relative to both PM and DM; higher $^{87}\text{Sr}/^{86}\text{Sr}$ than DM is also consistent with an enriched Rb/Sr source. EM compositions could be produced by relatively recent trace element enrichment of previously depleted mantle (e.g. subducted oceanic lithosphere or depleted asthenosphere). Enrichment may have

been in the form of intrusion of partial melts [35], mantle metasomatic events [36], or subduction of sediments [37] or oceanic crust [17] into the DM reservoir. The relatively low $^{87}\text{Sr}/^{86}\text{Sr}$ ratio inferred for the EM component relative to its radiogenic Pb composition could result from the buffering effect of high Sr abundances in the mantle relative to Pb. For the purposes of modeling, we have used the EM composition suggested by Davies [38], which is consistent with the Kilauea apex of the Hawaiian field.

Assumptions concerning the physical nature of EM are important in constructing a consistent mixing model. If EM is a volatile-rich component [39] and/or has a composition similar to a basaltic melt [40], then it should have a lower melting temperature than surrounding (primitive or depleted) mantle peridotite. Melting of a mixture of EM and either depleted or primitive mantle will therefore produce magmas which have compositional characteristics indicative of two-component mixing [40]. Under such conditions, isotopic variations will be controlled by the degree of melting and the proportions of each end-member in the melt phase.

7. Mixing Model

The mantle plume/hotspot model [4] provides a viable explanation for the systematic age progression along the Hawaiian Chain and the consistency of magmatic evolution at individual volcanoes. We therefore consider the results of recent experiments concerning plume dynamics [11–13] as they pertain to the interaction of various mantle reservoirs. In the following sections, we discuss some constraints imposed by the isotopic data and several possible physical scenarios for the evolution of Hawaiian shield-building and post shield-building magmatism.

7.1. Shield-Building Volcanism: PM-EM Mixing

The large volumes of magma associated with the shield-building stage (e.g. Haleakala: 293,000 km³, Mauna Loa: 425,000 km³, Kilauea: 194,000 km³; [41]) are erupted within a geologically short time span (< 1 My; [41]) and indicate high magma

production rates [42]. Seismic evidence indicates that Kilauea and Mauna Loa shield-building lavas originate at depths in excess of 60 km [43]. Other seismic studies [44,45] are inconsistent with the presence of deep-crustal intrusive complexes beneath young Hawaiian volcanoes in the shield-building stage (e.g. Kilauea and Mauna Loa), and preclude storage of significant volumes of magma at the base of the oceanic (MORB) crust. It appears likely that these magmas ascended more or less directly from a sublithospheric source to high-level reservoirs within the shield edifice. Thus, it is unlikely these magmas are contaminated by MORB composition lithosphere or crust and we assume their compositions are representative of the plume source.

The negative Sr-Pb correlation (Koolau-Kilauea) of Hawaiian tholeiites is consistent with shield-building melts being two-component mixtures [46] of EM and PM (see Fig. 6). This presents two possibilities concerning the nature of the plume source: (1) the plume itself is a two-component mixture of PM and EM, or (2) PM and EM are physically isolated reservoirs whose melts subsequently mix.

The two-component plume hypothesis suggests several possible scenarios. The plume might consist of two isotopically distinct solid materials which upon melting produce magmas that are a two-component (PM-EM) mixture. For example, a plume consisting primarily of PM material might also contain streaks or blobs of an EM component.

The isolated PM and EM reservoir hypothesis is consistent with rise of a PM-type plume through (or emplacement within) some part of the mantle containing EM-type material. Heat from the plume may induce melting of EM-rich material and these melts may then mix with melts of the plume itself. Alternatively, physical mixing of PM and EM solids might occur to form a two-component mixed plume source.

The above scenarios could account for the observed PM-EM Hawaiian shield-building array (Fig. 6). Source mixing calculations (Fig. 6) suggest that the proportion of the EM component in Hawaiian lavas is small relative to PM. However, if the EM end-member is a melt rather than a solid, then the Sr/Pb ratio of EM will likely be dif-

ferent than that used in our calculations. For example, if Pb has a smaller bulk distribution coefficient than Sr in the EM source, then a partial melt of EM will most likely have a smaller Sr/Pb ratio than the solid source. Accordingly, the specifics of the mixing systematics will differ somewhat from those depicted in figure 6.

Although shield-building lavas from individual Hawaiian volcanoes appear to have restricted isotopic ranges compared to the total observed range for Hawaii, this may simply reflect the relatively limited time span represented by exposed lavas. Any of the previously mentioned scenarios could result in tholeiites from a single volcano being isotopically heterogeneous as a result of several factors, including: (1) inherent differences in EM:PM ratios of the plume source of these magmas, (2) variations in the mixing proportions of the end-members during partial melting, (3) a heterogeneous EM component, or (4) variations in mixing proportions related to the physical mixing of melts.

7.2. Alkalic Cap Volcanism

A consistent model for alkalic cap magmatism at Haleakala must satisfy the following constraints: (1) there is a progressive decrease in the rate of magma production [42,48], (2) early post shield-building lavas (Kumuilihi Formation) contain more radiogenic Pb and less radiogenic Sr than Honomanu shield-building tholeiites, and (3) post shield-building lavas form a positively correlated Sr-Pb array which deviates from the general negative Hawaiian shield-building trend and within which Sr and Pb compositions become increasingly less radiogenic with time.

7.2.1. Plume Composition

The Hawaiian alkalic cap stage is a period of drastically decreased effusive volume, eruptive frequency, and reduced magma production rates [48]. Qualitatively, these observations could be satisfied by models invoking either a dying single plume or compositionally distinct primary and secondary plumes. If it is assumed that shield-building and alkalic cap magmas were ultimately derived from a common plume, a decrease in magma supply could reflect progressive exhaustion of fusible material in the plume source due to long-term shield-building magmatism and to heat loss from the plume. Alternatively, alkalic cap magmas may have been derived from a separate, relatively undepleted subsidiary plume. In support of this concept, experimental studies [11–12] reveal that plumes ascending through a non-stationary medium (e.g. convecting mantle) develop smaller, subsidiary (i.e. parasitic [11–12]) plumes which ascend independently.

Isotopic constraints imply that at Haleakala the genesis of early post shield-building lavas somehow involved an increase in EM:PM ratio relative to shield-building lavas (Fig. 6). If the EM component has a lower temperature solidus than PM, then long-term shield-building magmatism related to a single plume would presumably consume the EM component or at least reduce the EM:PM ratio with time. Because the opposite trend is observed at Haleakala, a two-component single plume model appears to have serious drawbacks. Single plume models or multiple plume/separate EM reservoir models require either a relatively large EM reservoir that would not be exhausted during shield-building magmatism, or replenishment of consumed EM components possibly by metasomatism [36]. The mechanics of a replenishment process are problematic. Specifically, such a process must be temporally reproducible (i.e. occur at the same evolutionary stage) for each volcano concerned, and must create similarly reproducible geochemical changes. The source of replenishing material is also difficult to constrain.

It seems more attractive to derive alkalic cap magmas from a subsidiary plume which was not involved in the formation of shield-building tholeiites, and which

retained a relatively undepleted EM:PM ratio. This hypothesis is less complex than the scenarios discussed above in that it does not necessarily require an inexhaustible EM reservoir nor metasomatic replenishment.

7.2.2. Plume-DM Mixing

Sr-Pb isotopic variations are consistent with two-component mixing of plume magmas (containing both PM and EM components) with a third (DM) component. Plume-DM mixing could occur within depleted asthenosphere, at the base of the lithosphere, or within the lithosphere as plume magmas ascend.

The ascent of a plume through depleted asthenosphere might generate a partially molten zone around the plume due both to heat exchange from the hotter plume and to stresses exerted by the ascending plume [49]. Alternatively, the plume may flatten out at the base of the lithosphere during emplacement [13] and partially melt portions of the uppermost asthenosphere and/or lower lithosphere. In either case, these melts could then mix with plume melts. In addition, decreasing melt production with time as the Pacific plate migrates past the hotspot focus could result in a decrease in the efficiency of magma ascent and increased stagnation of ascending magmas within the lithosphere. Such conditions could result in increased interaction with surrounding MORB composition wall-rock.

The Sr-Pb trend for post shield-building lavas appears to indicate a progressively decreasing EM:PM ratio in these magmas. This trend could reflect: (1) progressive exhaustion of a more fusible EM component residing within a two-component plume, (2) progressive exhaustion of a separate EM reservoir, or (3) a reduction in the rate of replenishment (metasomatism?) of the plume.

7.3. A Possible Mixing Scenario

Plumes initially generated in a PM (lower mantle?) reservoir may contain variable amounts of an EM component. Incorporation of EM in the plume could occur either

during incipient plume formation or during ascent. Melting of the two-component plume during ascent and/or emplacement at the base of the lithosphere presumably produces tholeiitic magmas which reflect two-component mixing (see PM-EM mixing curve, Fig. 6).

Variations in the isotopic composition of shield-building lavas within individual volcanoes might reflect variations in the partial melting processes (e.g. temporal depletion or enrichment of the EM component). Inter-volcano isotopic differences may reflect temporal and/or spatial variations in plume EM:PM ratios (e.g. the plume source for Kilauea magmas apparently contains a relatively high proportion of EM compared to that for Koolau magmas).

Alkalic cap stage magmas could represent partial melts of a subsidiary plume that was not involved in the production of tholeiitic magmas and thus retained a relatively undepleted EM signature compared to the plume source for shield-building lavas.

Decreased plume melt production during the alkalic cap stage could result in increased magma residence times at depths where interaction with MORB composition material could occur. Such a scenario can explain the apparent two-component mixing trend (see Plume-DM mixing curve, Fig. 6) as well as the observed temporal relationship between volume of magma produced. Based on the observed Sr-Pb trend of post shield-building lavas, the apparent decrease in EM:PM ratio could indicate a progressive exhaustion of the EM component in the plume source of these magmas.

8. Loa and Kea Trends

The scale of Hawaiian mantle source heterogeneities is a critical factor in petrogenetic models. The summits of Kilauea and Mauna Loa are roughly 30 km apart and yet these volcanoes appear to be distinct both isotopically [9,16] and in terms of trace element composition [50]. A possible isotopic distinction between the western (Kea) and eastern (Loa) trends of volcanoes on the island of Hawaii is illustrated on a plot of $^{208}\text{Pb}/^{204}\text{Pb}$ vs. $^{206}\text{Pb}/^{204}\text{Pb}$ (Fig. 3b). Hualalai, Mauna Loa and Loihi (Loa

trend) have higher $^{208}\text{Pb}/^{204}\text{Pb}$ for a given $^{206}\text{Pb}/^{204}\text{Pb}$ than do Kohala, Mauna Kea and Kilauea (Kea trend). This apparent isotopic contrast has led to the proposition [e.g. 8] that the loci of Loa and Kea trend volcanoes are controlled by separate tectonic lineaments and that they tap two isotopically distinct plume sources. However, no Loa/Kea distinction is observed for these volcanoes on plots of $^{207}\text{Pb}/^{204}\text{Pb}$ vs. $^{206}\text{Pb}/^{204}\text{Pb}$ or $^{87}\text{Sr}/^{86}\text{Sr}$ vs. $^{206}\text{Pb}/^{204}\text{Pb}$ (Fig. 3). The fact that Haleakala data overlap both Loa and Kea trends on Pb-Pb and Sr-Pb isotope plots suggests that the apparent existence of these trends may be an artifact of insufficient data for other volcanoes. We conclude that if the concept of two isotopically distinct tectonic lines has validity, it cannot be extended beyond the island of Hawaii.

9. Conclusions

Lavas from Haleakala Crater span a greater range in Sr and Pb isotopic compositions than is observed at other studied Hawaiian volcanoes. Post shield-building lavas (Kumuilihi, Kula, and Hana Formations) appear to be isotopically distinct from shield-building tholeiites (Honomanu Formation). There is, however, no consistent isotopic distinction between the youngest alkalic cap (Kula Formation) lavas and post-erosional (Hana Formation) lavas.

Sr-Pb isotope variations for Haleakala and other Hawaiian volcanoes require interaction between a minimum of three isotopically distinct end-members. These data are consistent with varied degrees of mixing between two components (primitive + enriched) residing within the Hawaiian mantle plume, and between this plume material and a MORB signature (depleted mantle) reservoir. It is proposed that shield-building lavas represent plume-derived magmas having a larger primitive:enriched mantle ratio compared to associated alkalic cap lavas. Alkalic cap lavas may have been derived from a separate, parasitic plume or possibly by replenishment of the tholeiitic plume source. Isotopic evolution of alkalic cap lavas appears to be controlled primarily by progressively increasing amounts of interaction between plume melts and a MORB signature com-

ponent (possibly melts of depleted mantle). Decreasing melt supply combined with an increase in the residence times of plume magmas within isotopically distinct MORB material (depleted asthenosphere, lithosphere) could result in progressively increasing amounts of contamination of these magmas.

Acknowledgements

Samples for this study were collected with the expert assistance of F. T. Mullins. Special thanks to G. R. Tilton, S. R. Hart, and F. A. Frey for access to their laboratory facilities and to D. C. Gerlach, G. R. Tilton, and S.-T. Kwon for their laboratory assistance. We are grateful to G. R. Tilton, S.-T. Kwon, F. A. Frey, and A. Kennedy for permission to show fields of their unpublished Mauna Kea data. Thanks also to Dean Yoshimura for additional field-map work. A special mahalo to Ranger Ron Nagata, Superintendent Hugo Huntzinger, and other personnel of the Haleakala National Park Service for their kokua and enthusiastic support. We thank C. J. Hawkesworth, F. A. Frey, D. C. Gerlach, Z. A. Palacz, and an anonymous reviewer for providing critical comments which greatly improved this manuscript. This work was sponsored in part through National Science Foundation Grants EAR85-12167 and EAR83-20358, G.S.A. Penrose Grant 3515-85, and the Rice University Department of Geology and Geophysics; in particular, funding assistance from A. W. Bally is gratefully acknowledged.

References

- 1 Gast, P. W., Tilton, G. R. and Hedge, C., Isotopic Composition of Lead and Strontium from Ascension and Gough Islands, *Science* 145, 1181-1185, 1964.
- 2 Engel, A. E. J., Engel, C. G. and Havens, R. G., Chemical Characteristics of Oceanic Basalts and the Upper Mantle, *G.S.A. Bull.* 76, 719-734, 1965.
- 3 Hofmann, A. W., Geochemical Mantle Models, *Terra Cognita* 4, 157-165, 1984.
- 4 Morgan, W. J., Convection Plumes in the Lower Mantle, *Nature* 230, 42-43, 1971.
- 5 Zindler, A. and Hart, S., Chemical Geodynamics, *Ann. Rev. Earth Planet Sci.* 14, 493-571, 1986.
- 6 Stille, P., Unruh, D. M. and Tatsumoto, M., Pb, Sr, Nd and Hf Isotopic Evidence of Multiple Sources for Oahu, Hawaii Basalts, *Nature* 304, 25-29, 1983.
- 7 Roden, M. F., Frey, F. A. and Clague, D. A., Geochemistry of Tholeiitic and Alkalic Lavas from the Koolau Range, Oahu, Hawaii, Implications for Hawaiian Volcanism, *Earth Planet. Sci. Lett.* 69, 141-158, 1984.
- 8 Staudigel, H., Zindler, A., Hart, S. R., Leslie, T., Chen, C.-Y. and Clague, D. A., The Isotope Systematics of a Juvenile Intraplate Volcano, Pb, Nd, and Sr Isotope ratios of Basalts from Loihi Seamount, Hawaii, *Earth Planet. Sci. Lett.* 69, 13-29, 1984.
- 9 Hegner, E., Unruh, D. and Tatsumoto, M., Nd-Sr-Pb Isotope Constraints on the Sources of West Maui Volcano, Hawaii, *Nature* 319, 478-480, 1986.
- 10 Stille, P., Unruh, D. M. and Tatsumoto, M., Pb, Sr, Nd, and Hf Isotopic Constraints on the Origin of Hawaiian Basalts and Evidence for a Unique Mantle Source, *Geochim. Cosmochim. Acta* 50, 2303-2319, 1986.
- 11 Whitehead, J. A., Instabilities of Fluid Conduits in a Flowing Earth - Are Plates Lubricated by the Asthenosphere?, *Geophys. J. R. Astron. Soc.* 70, 415-433, 1982.
- 12 Olson, P. and Singer, H. A., Creeping Plumes, *J. Fluid Mech.* 158, 511-531, 1985.
- 13 Olson, P. and Nam, I. S., Formation of Seafloor Swells by Mantle Plumes, *J. Geophys. Res.* 91, 7181-7191, 1986.
- 14 Chen, C.-Y. and Frey, F. A., Trace Element and Isotopic Geochemistry of Lavas from Haleakala Volcano, East Maui, Hawaii, Implications for the Origin of Hawaiian Basalts, *J. Geophys. Res.* 90, 8743-8768, 1985.
- 15 White, W. M., Sources of Oceanic Basalts, Radiogenic Isotopic Evidence, *Geology* 13, 115-118, 1985.
- 16 Herzberg, C. T., Chemical Stratification in the Silicate Earth, *Earth Planet. Sci. Lett.* 67, 249-260, 1984.
- 17 Hofmann, A. W. and White, W. M., Mantle Plumes from Ancient Oceanic Crust, *Earth Planet. Sci. Lett.* 57, 421-436, 1982.

- 18 Presnall, D. C. and Helsley, C. E., 1982, Diapirism of Depleted Peridotite - A Model for the Origin of Hot Spots, *Phys. Earth Planet. Int.* 29, 148-160, 1982.
- 19 Feigenson, M. D., Geochemistry of Kauai Volcanics and a Mixing Model for the Origin of Hawaiian Alkali Basalts, *Contrib. Mineral. Petrol.* 87, 109-119, 1984.
- 20 Clague, D. A. and Frey, F. A., Petrology and Trace Element Geochemistry of the Honolulu Volcanics, Oahu, Implications for the Oceanic Mantle Below Hawaii, *J. Petrol.* 23, 447-504, 1982.
- 21 Wright, T. L., Origin of Hawaiian Tholeiite: A Metasomatic Model, *J. Geophys. Res.* 89, 3233-3252, 1984.
- 22 West, H. B. and Leeman, W. P., Composition and Evolution of Lavas from Haleakala Crater, Hawaii, *EOS* 65, 1131-1132, 1984.
- 23 Stearns, H. T. and Macdonald, G. A., Geology and Ground-Water Resources of the Island of Maui, Hawaii, *Hawaii Div. Hydrogr. Bull.* 7, 344 p., 1942.
- 24 Macdonald, G. A., Geologic Map of the Crater Section of Haleakala National Park, Maui, Hawaii, U.S.G.S. Misc. Inv. Ser. Map I-1088, 1978.
- 25 Naughton, J. J., Macdonald, G. A. and Greenberg, V. A., Some Additional Potassium-Argon Ages of Hawaiian Rocks: The Maui Volcanic Complex of Molokai, Maui, Lanai and Kahoolawe, *J. Volc. Geoth. Res.* 7, 339-355, 1980.
- 26 McDougall, I., Potassium-Argon Ages from Lavas of the Hawaiian Islands, *G.S.A. Bull.* 75, 107-128, 1964.
- 27 Oostdam, B. L., Age of Lava Flows on Haleakala, Maui, Hawaii, *G.S.A. Bull.* 76, 393-394, 1965.
- 28 Macdonald, G. A. and Katsura, T., Chemical Composition of Hawaiian Lavas, *J. Petrol.* 5, 82-133, 1964.
- 29 Grunefelder, M. H., Tilton, G. R., Bell, K. and Blenkinsop, J., Lead and Strontium Isotope Relationships in the Oka Carbonatite Complex, Quebec, *Geochim. Cosmochim. Acta.* 50, 461-468, 1986.
- 30 Todt, W., Cliff, R. A., Hanser, A. and Hofmann, A. W., ^{202}Pb + ^{205}Pb Double Spike for Lead Isotopic Analyses, *Terra Cognita* 4, 209, 1984.
- 31 Manhès, G., Minster, J. F. and Allegre, C. J., Comparative Uranium-Thorium-Lead and Rubidium-Strontium of St. Severin Amphoterite: Consequences for Early Solar System Chronology, *Earth Planet. Sci. Lett.* 39, 14-24, 1978.
- 32 Zindler, A., Geochemical Processes in the Earth's Mantle and the Nature of Crustal-Mantle Interactions: Evidence from Studies of Nd and Sr Isotopic Ratios in Mantle Derived Igneous Rocks and Lherzolite Nodules, Ph.D. Thesis, M.I.T., 263 p., 1980.
- 33 Olson, P., Yuen, D. A. and Balsinger, D., Mixing of Passive Heterogeneities by Mantle Convection, *J. Geophys. Res.* 89, 425-436, 1984.

- 34 Hamelin, B., Dupre, B. and Allegre, C. J., Lead-Strontium Isotopic Variations Along the East Pacific Rise and the Mid-Atlantic Ridge: A Comparative Study, *Earth Planet. Sci. Lett.* 67, 340-350, 1984.
- 35 Wilshire, H. G., Mantle Metasomatism: The REE Story, *Geology* 12, 395-398, 1984.
- 36 Menzies, M. A. and Murthy, V. R., Mantle Metasomatism as a Precursor to the Genesis of Alkaline Magmas - Isotopic Evidence, *Am. J. Sci.* 280-A, 622-638, 1980.
- 37 Weaver B. L., Wood, D. A., Tarney, J. and Joron J. L., Role of Subducted Sediment in the Genesis of Ocean-Island Basalts: Geochemical Evidence from South Atlantic Ocean Islands, *Geology* 14, 275-278, 1986.
- 38 Davies, G. F., Geophysical and Isotopic Constraints on Mantle Convection: An Interim Synthesis, *J. Geophys. Res.* 89, 6017-6040, 1984.
- 39 Sleep, N. H., Tapping of Magmas from Ubiquitous Mantle Heterogeneities: An Alternative to Mantle Plumes?, *J. Geophys. Res.* 89, 10029-10041, 1984.
- 40 Hanson, G. N., Geochemical Evolution of the Suboceanic Mantle, *J. Geol. Soc. Lond.* 134, 235-253, 1977.
- 41 Bargar, K. E. and Jackson, E. D., Calculated Volumes of Individual Shield Volcanoes Along the Hawaiian-Emperor Chain, *U.S.G.S. J. Res.* 2, 545-550, 1974.
- 42 Wise, W. S., A Volume-Time Framework for the Evolution of Mauna Kea Volcano, Hawaii, *EOS* 62, 1137, 1982.
- 43 Eaton, J. P. and Murata, K. J., How Volcanoes Grow, *Science* 132, 925-938, 1960.
- 44 Ryan, M. P., Koyanagi, R. Y. and Fiske, R. S., Modeling the Three-Dimensional Structure of Macroscopic Magma Transport Systems: Application to Kilauea volcano, Hawaii, *J. Geophys. Res.* 86, 7111-7129, 1981.
- 45 Dzurisin, D. Koyanagi, R. Y. and English, T. T., Magma Supply and Storage at Kilauea Volcano, Hawaii, 1956-1983, *J. Volc. Geoth. Res.* 21, 177-206, 1984.
- 46 West, H. B., Pb Isotopic Variations in Lavas from Haleakala Crater, Hawaii, *EOS* 66, 1133, 1985.
- 47 Vollmer, R., Rb-Sr and U-Th-Pb Systematics of Alkaline Rocks: The Alkaline Rocks from Italy, *Geochim. Cosmochim. Acta* 40., 283-295, 1976.
- 48 Macdonald, G. A., Composition and Origin of Hawaiian Lavas, *G.S.A. Mem.* 116, 477-522, 1968.
- 49 Anderson, D. L., Rise of Deep Diapirs, *Geology* 9, 7-9, 1981.
- 50 Leeman, W. P., Budahn, J. R., Gerlach, D. C., Smith, D. R. and Powell, B. N., Origin of Hawaiian Tholeiites: Trace Element Constraints, *Am. J. Sci.* 280-A, 794-819, 1980.

TABLE 1

Lead and Strontium isotopic compositions of Haleakala lavas.

Formation	Sample	Rock type	$^{87}\text{Sr}/^{86}\text{Sr}^a$	$\frac{^{206}\text{Pb}}{^{204}\text{Pb}}$	$\frac{^{207}\text{Pb}}{^{204}\text{Pb}}$	$\frac{^{208}\text{Pb}}{^{204}\text{Pb}}$
Hana	HH-18	hawaiite	0.70312 ± 2	18.200	15.460	37.804
	HH-20	alkalic basalt	0.70319 ± 3	18.252	15.482	37.895
	HH-11	basanitoid	0.70327 ± 3			
	HH-19	basanitoid	0.70315 ± 3			
	HH-3	basanitoid	0.70329 ± 3	18.279 18.263 ^b	15.471 15.456 ^b	37.876 37.838 ^b
Kula	HK-26	basanitoid	0.70328 ± 3			
	HK-48	mugearite	0.70317 ± 3	18.253 18.244 ^b	15.463 15.450 ^b	37.852 37.812 ^b
	HK-59	hawaiite	0.70308 ± 2	18.132	15.454	37.735
	HK-58	ankaramite	0.70314 ± 2^c	18.184	15.448	37.755
	HK-51	hawaiite	0.70312 ± 1^c	18.276	15.475	37.893
	HK-50	basanitoid	0.70314 ± 2	18.274	15.497	37.937
	HK-45	mafic hawaiite	0.70330 ± 2	18.327	15.508	38.026
	HK-43	mugearite	0.70324 ± 1	18.311	15.480	37.837
	HK-40	hawaiite	0.70329 ± 3	18.365	15.520	38.090
	HK-39	hawaiite	0.70326 ± 2	18.353	15.506	38.042
	HK-37	mugearite	0.70322 ± 3	18.347	15.492	37.991
	HK-36	alkalic basalt	0.70324 ± 1^c	18.318	15.474	37.917
	HK-33	mafic hawaiite	0.70326 ± 3	18.313	15.481	37.940
	HK-31	hawaiite	0.70324 ± 3	18.313	15.472	37.932
	HK-29	hawaiite	0.70334 ± 3	18.398	15.509	38.082
	HK-28	mugearite	0.70340 ± 3	18.373	15.495	38.043
	HK-19	hawaiite	0.70336 ± 2			
	HK-13	hawaiite	0.70334 ± 3			
	HK-1	mafic hawaiite	0.70339 ± 3	18.321	15.492	37.961
	HK-46	hawaiite	0.70320 ± 3	18.333 18.340 ^b	15.469 15.477 ^b	37.914 37.944 ^b
Kumailiahi	HKU-1	alkalic basalt	0.70348 ± 1^c	18.370	15.490	37.987
	HKU-2	alkalic basalt	0.70355 ± 3	18.383 ^b	15.487 ^b	37.974 ^b
	HKU-7	hawaiite	0.70345 ± 3			
	HKU-10	mafic hawaiite	0.70345 ± 2	18.344	15.473	37.914
Honomanu	HHM-1	tholeiite	0.70345 ± 3			
	HHM-9	tholeiite	0.70368 ± 1^c	18.264	15.465	37.919
Holua Trachyte			0.70377 ± 1^c	18.279	15.482	38.038
	HOLUA	trachyte	0.70495 ± 3	18.358	15.476	37.969
			0.70502 ± 2	18.359 18.369 ^b	15.479 15.476 ^b	37.988 37.983 ^b
		feldspar	0.70375 ± 3			

^a Measured $^{87}\text{Sr}/^{86}\text{Sr}$ ratios. Errors are given in parentheses and represent 2 σ of the mean based on in-run statistics.

^b Pb isotopic composition determined at MIT.

^c Determined by D. C. Gerlach at Leeds University.

TABLE 2

Strontium isotope and selected trace element data for Holua trachyte.

	Rb ^a	Sr ^a	Rb/Sr	⁸⁷ Sr/ ⁸⁶ Sr	⁸⁷ Sr/ ⁸⁶ Sr ₀ ^b
whole rock	159.20	4.40	36.18	0.704951	
		4.39		0.705015	
avg.	159.20	4.40	36.18	0.704983	0.70426
feldspar ^c	46.79	11.11	4.21	0.703753	0.70367

a Sr and Rb concentrations in ppm as determined by isotope dilution.

b Initial ⁸⁷Sr/⁸⁶Sr ratios calculated using an age of 0.49 Ma [21].

c Leached in HCl.

Figure Captions

Figure 1. Relative position of Haleakala Crater on the island of Maui and simplified map of Haleakala Crater after [24]. Shaded areas represent Kula Formation lavas. Solid areas represent exposures of Kumuiliahi Formation lavas. Hachured areas represent Hana Formation cinder cones and lava flows. The Halemauu Trail section is indicated by the thick, solid line on the northwest wall of the Crater.

Figure 2. Silica vs. total alkalis diagram indicating fields for Honomanu, Kumuiliahi, Kula, and Hana Formation lavas from this study. Honomanu field includes data from [14]. Cross indicates Holua trachyte. Field for Kilauea based on data from the literature. Solid line divides figure into alkalic and tholeiitic fields as previously defined [31].

Figure 3. $^{207}\text{Pb}/^{204}\text{Pb}$, $^{208}\text{Pb}/^{204}\text{Pb}$, and $^{87}\text{Sr}/^{86}\text{Sr}$ vs. $^{206}\text{Pb}/^{204}\text{Pb}$ for Haleakala lavas from this study. Data for other Hawaiian volcanoes from the literature; additional unpublished data for Mauna Kea courtesy of S.-T. Kwon, G. R. Tilton (Pb), A. Kennedy, and F. A. Frey (Sr). Symbols: squares - Honomanu Formation; X - Kumuiliahi Formation; diamonds - Kula Formation; circles - Hana Formation; cross - Holua trachyte. In (c), the range of values from published data are shown as fields for Sr and Pb data from the same sample set and as boxes for Sr and Pb data from different sample sets.

Figure 4. La, $^{206}\text{Pb}/^{204}\text{Pb}$, and $^{87}\text{Sr}/^{86}\text{Sr}$ vs. silica content for Haleakala lavas. Symbols for data from this study are shown as solid symbols as in Fig. 3; additional data from the literature are shown as open symbols. Neither $^{87}\text{Sr}/^{86}\text{Sr}$ nor $^{206}\text{Pb}/^{204}\text{Pb}$ correlates with silica; silica and La are positively correlated (correlation coefficient = 0.919; confidence level > 99.9 %). Sr and Pb isotopic compositions of Kula lavas are not correlated with rock type.

Figure 5. $^{206}\text{Pb}/^{204}\text{Pb}$ and $^{87}\text{Sr}/^{86}\text{Sr}$ vs. relative stratigraphic position for Haleakala lavas (all samples from this study). Symbols as in figure 3.

Figure 6. Proposed three component mixing model depicted for $^{87}\text{Sr}/^{86}\text{Sr}$ vs. $^{206}\text{Pb}/^{204}\text{Pb}$. Fields and boxes for Hawaiian volcanoes and symbols for Haleakala as in figure 3a. Shaded field represents published data for Pacific MORB. End-member compositions for PM, EM, and MORB are as follows. Sr (ppm): 17.8, 100, 130; Pb (ppm): 0.12, 1.6, 0.496; $^{87}\text{Sr}/^{86}\text{Sr}$: 0.7045, 0.7035, 0.70217; $^{206}\text{Pb}/^{204}\text{Pb}$: 17.7, 19.0, 17.72. Mixing calculations are after Vollmer [47]. The upper curve (labeled % Primitive Mantle) represents various proportions of a Primitive Mantle (PM)/Enriched Mantle (EM) mixture; compositions of Hawaiian plume melts associated with the shield-building stage lie along this curve. Subvertical mixing curves represent various proportions of mixing between Hawaiian plume melt and a MORB signature component. Haleakala post shield-building lavas (Kumuiliahi, Kula, and Hana Formations) illustrate two-component (Plume + MORB) mixing.

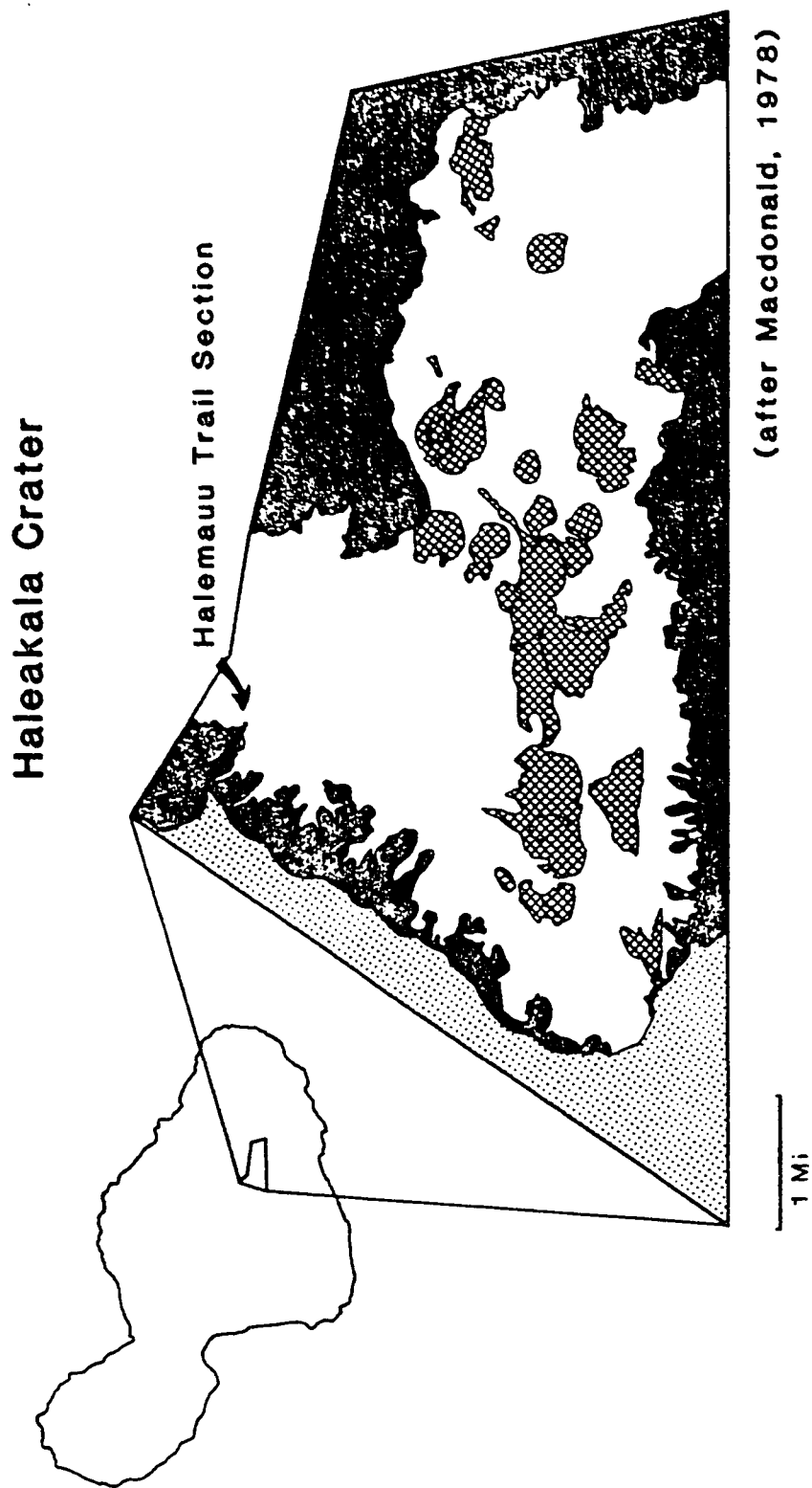


FIG. 1

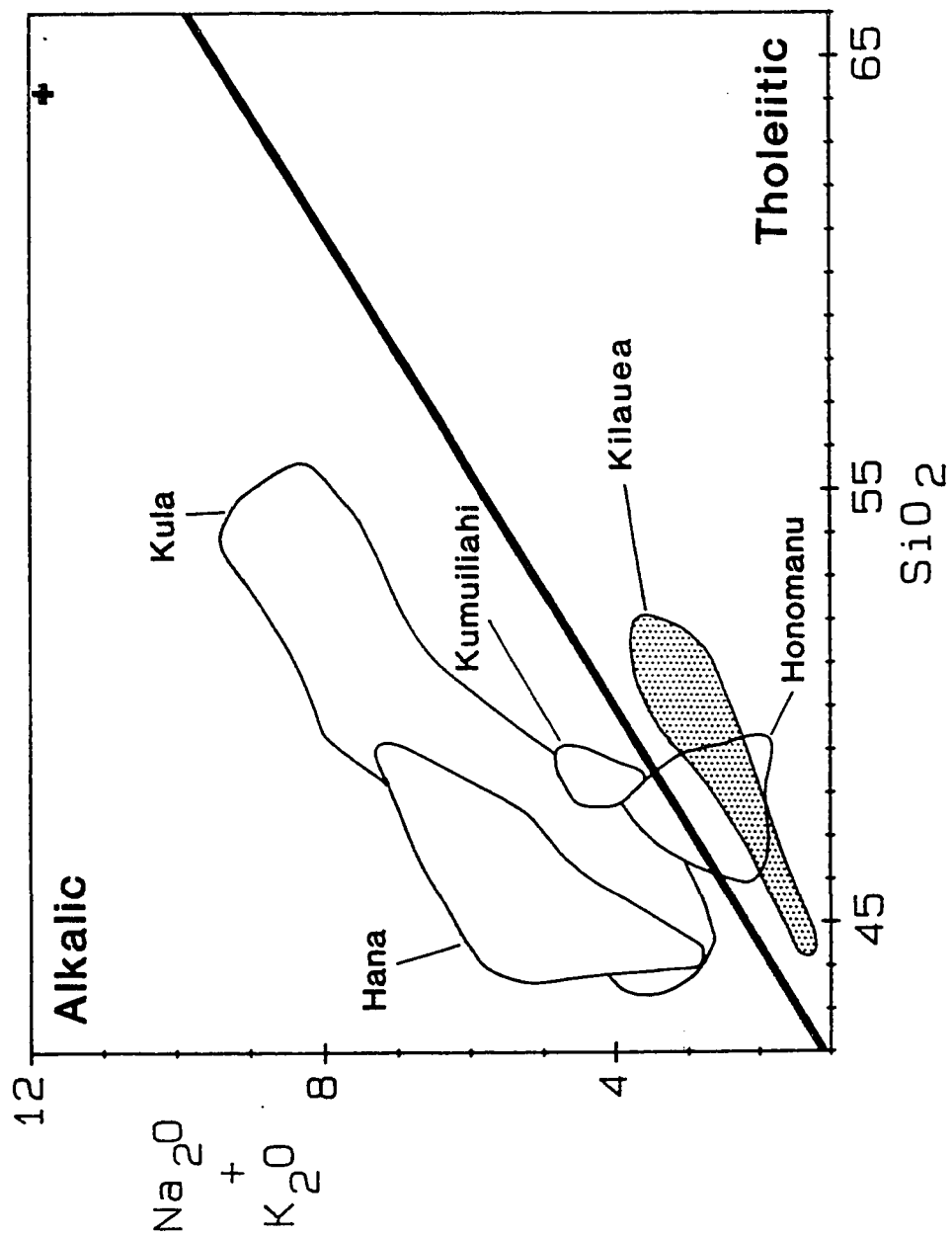


FIG. 2

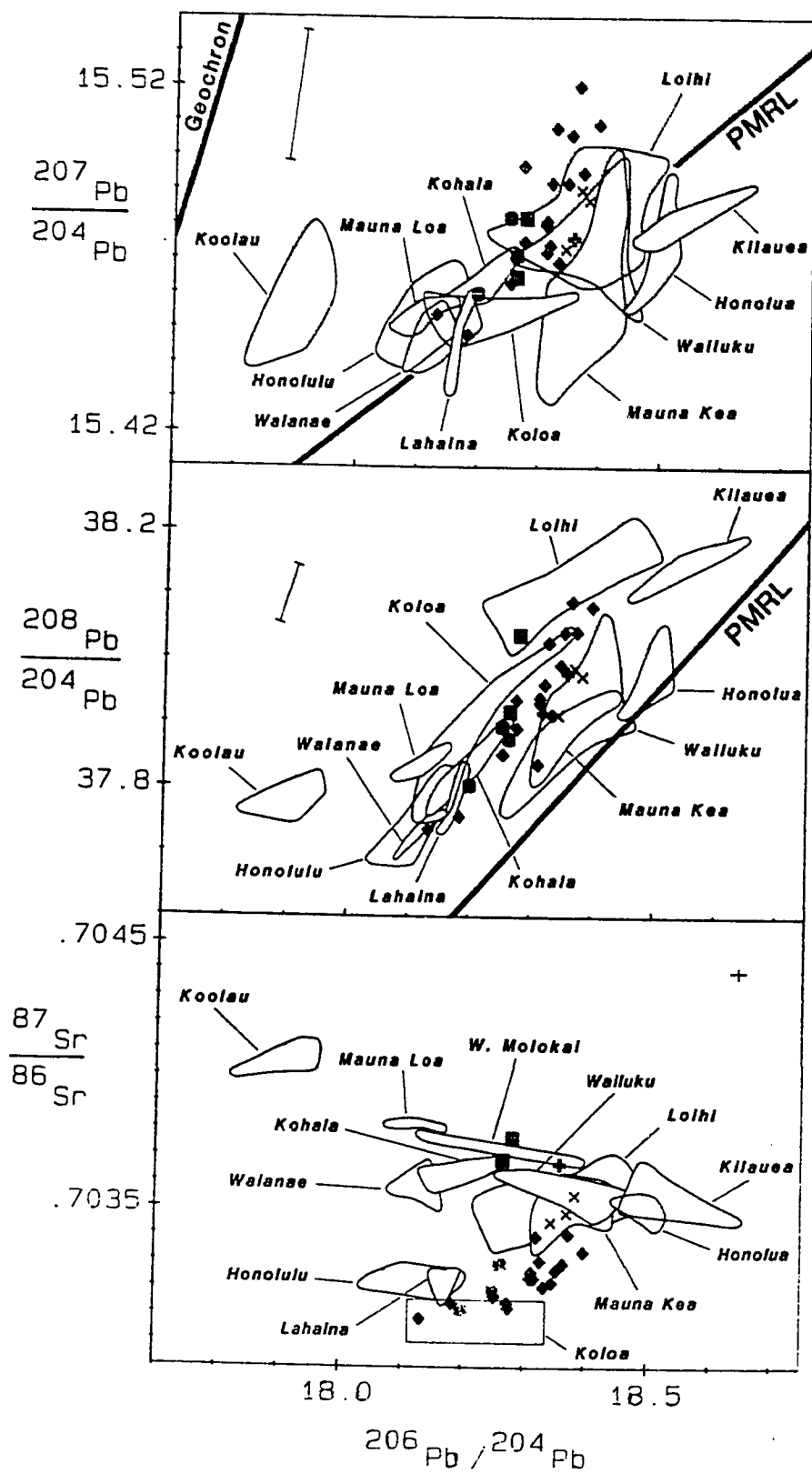


FIG. 3

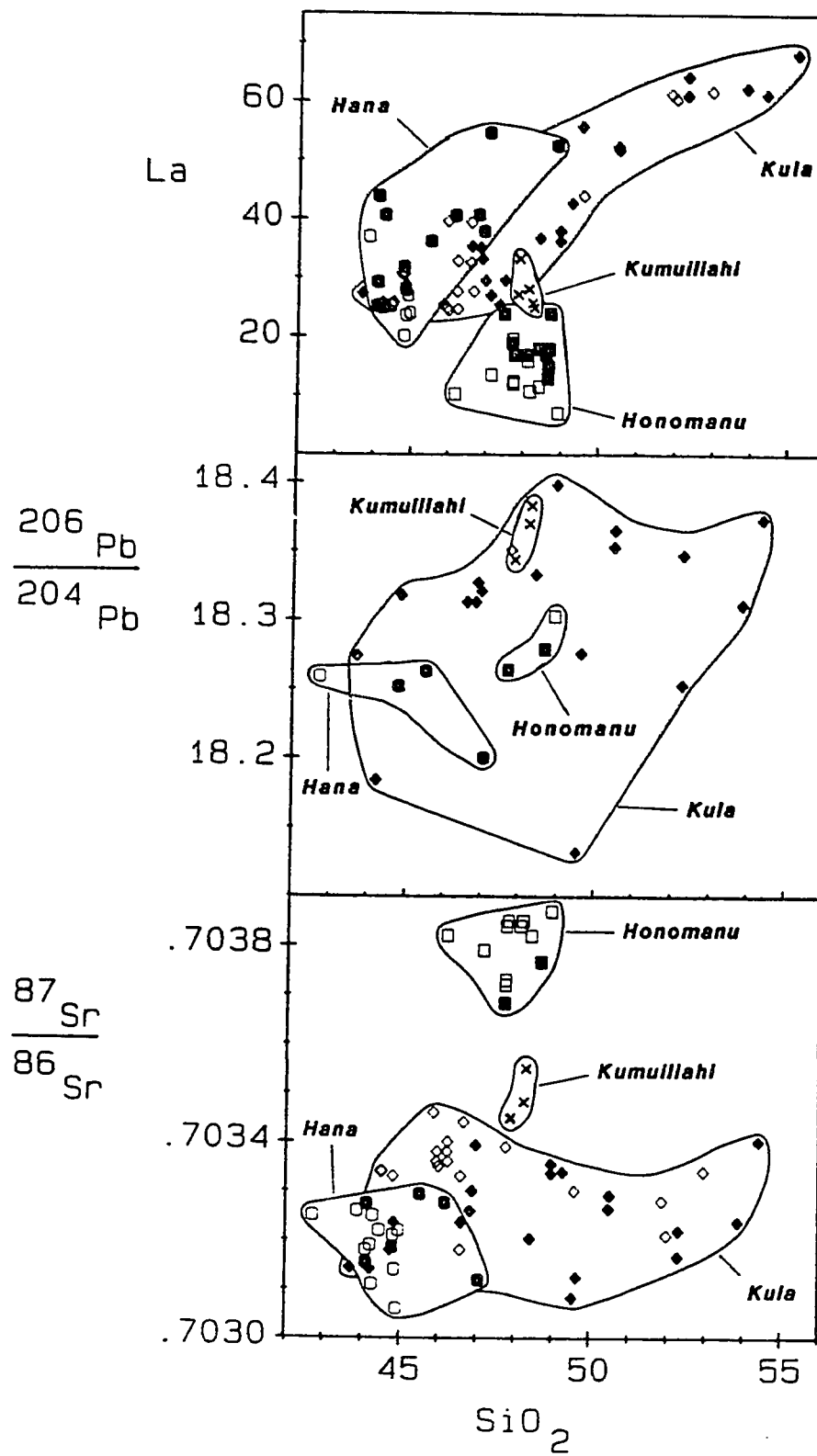


FIG. 4

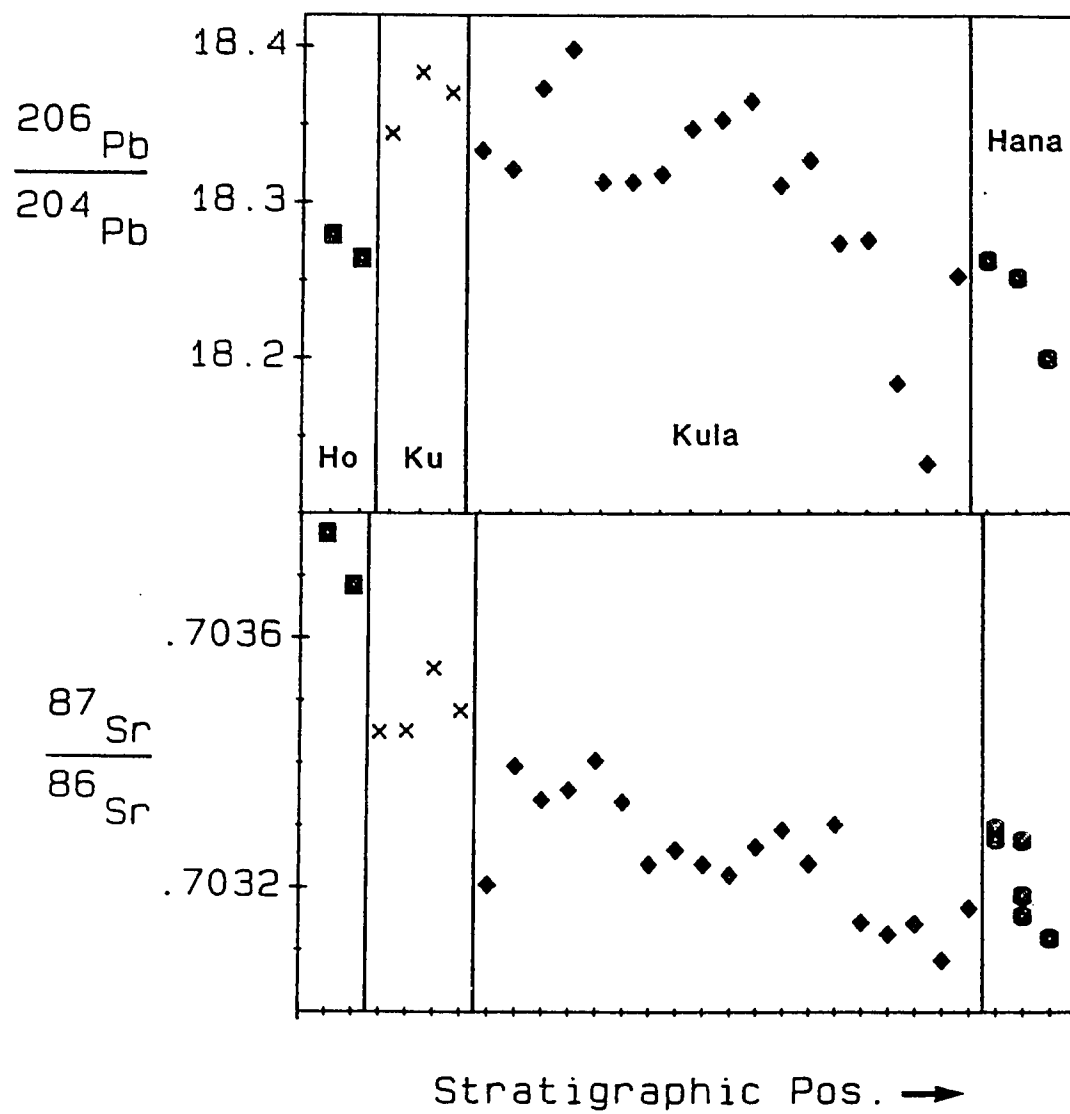


FIG. 5

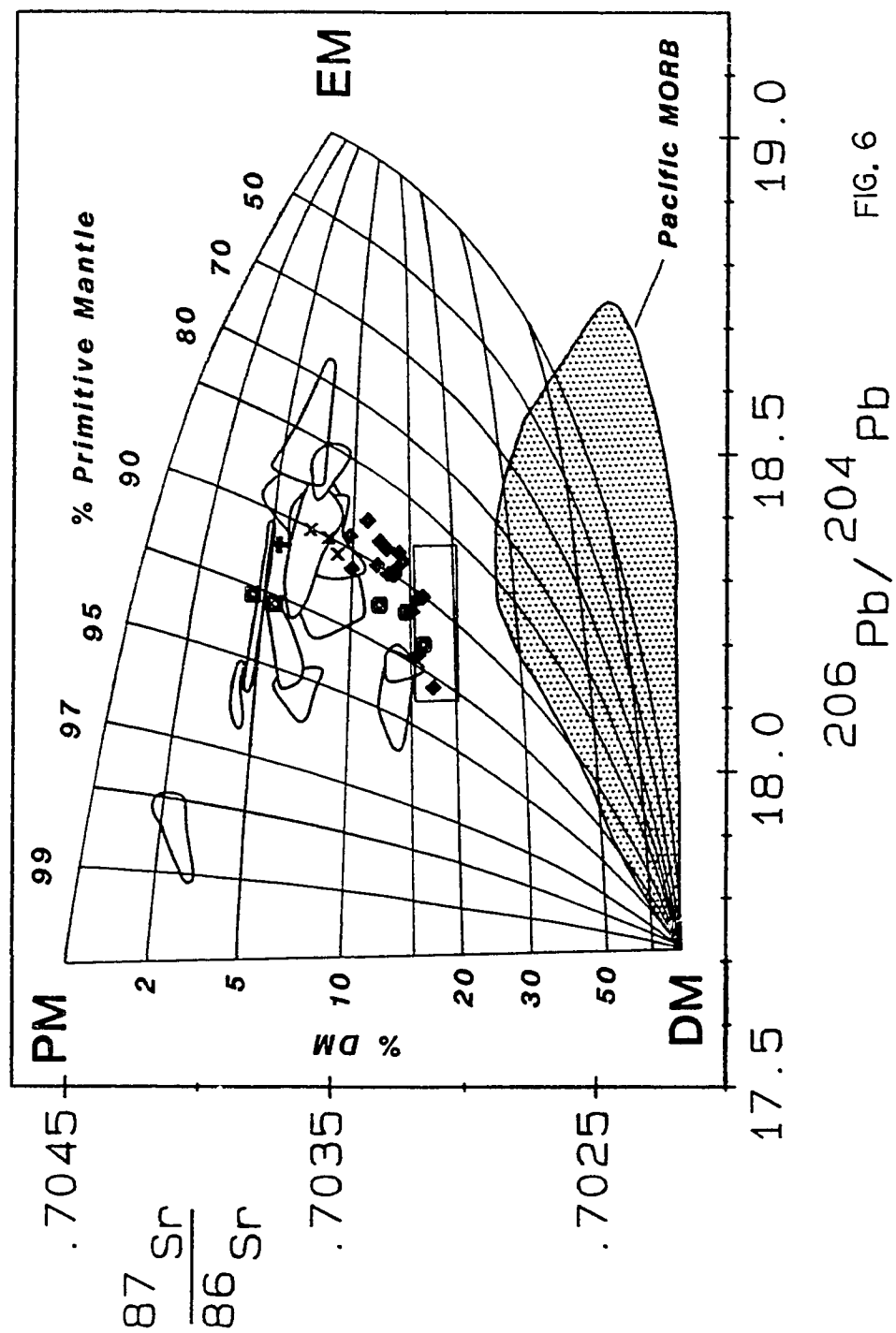


FIG. 6

Chapter 3

**ISOTOPIC CONSTRAINTS ON THE ORIGIN OF HAWAIIAN LAVAS FROM THE
MAUI VOLCANIC COMPLEX, HAWAII**

Abstract

Sr, Nd, and Pb isotopic data for samples from five volcanoes of the Maui Volcanic Complex, Hawaii, span nearly the total compositional range previously recognized for the Hawaiian Islands. These data reveal a systematic compositional continuum for Hawaiian tholeiites which is interpreted to result from partial melting of a variably mixed two-component mantle plume source. In contrast, post shield-building alkalic cap lavas define distinct compositional trends which appear to result from time- and volume-dependent binary mixing between Hawaiian plume melts and a depleted mantle component.

Introduction

Petrological studies of Hawaiian volcanic rocks have been dominated by research on the island of Hawaii where there are six major shield volcanoes in various stages of development, including presently active Kilauea and Mauna Loa and the developing Loihi Seamount. Because of the relative youthfulness of this island, only three of these volcanoes have reached the alkalic cap stage and none has erupted lavas characteristic of the post-erosional stage [1]. Thus, these young volcanoes provide a limited perspective on the chemical evolution of Hawaiian volcanoes. Here, we examine spatial and temporal isotopic variations in associated tholeiites, alkalic cap, and post-erosional lavas for individual volcanoes from an older part of the Hawaiian volcanic chain.

The present study concerns the Maui Volcanic Complex (MVC), which comprises six major shield volcanoes that are now extinct (West Molokai, East Molokai, Lanai, Kahoolawe, and West Maui) or in their final evolutionary stage (Haleakala). These six volcanoes once formed a single island (Fig. 1) that was about half the present area of the Island of Hawaii [1]. The oldest dated lavas of the MVC are from West Molokai (1.9-2.0 Ma [2,3]). Ages of shield-building stage lavas (Table 1) decrease to the southeast [3], and the most recent (post-erosional stage) eruption occurred at Haleakala in approximately 1790 [4]. The oldest exposed lavas at each of the MVC volcanoes are tholeiites; alkalic cap lavas occur on all but Lanai, and silica-undersaturated post-erosional lavas are found on three (East Molokai, West Maui, and Haleakala).

New Sr, Nd, and Pb isotopic data are presented here for 18 samples from Kahoolawe, Lanai, and West Molokai. Comparable data are available for East and West Molokai, West Maui, and Haleakala [5-10], and the temporal isotopic evolution of lavas from Haleakala has previously been examined in detail [9,10]. Brief descriptions of the volcanoes considered in this study are given below; Table 1 gives a summary of ages and rock types exposed at each volcano.

Kahoolawe is subdivided into pre-caldera, caldera-filling, and post-caldera lava sequences [11]. Pre-caldera and caldera-filling lavas are typical Hawaiian tholeiites,

similar to those from Kilauea. Alkalic series lavas are interbedded in the upper caldera-filling section and are found in the post-caldera eruptive sequence [11]. The thirteen samples analyzed span the range from lowermost exposed pre-caldera tholeiites to young post-caldera hawaiiites (Table 2).

Lanai lavas are tholeiitic in composition [11,12]. Field relations, petrography, K-Ar ages, and major element analyses of the four samples in this study were reported by Bonhommet et al. [13], and trace element analyses have been given by Budahn and Schmitt [14].

West Molokai has received little attention owing to its poorly dissected condition and extensive soil cover; its geology is discussed by Stearns and Macdonald [15]. In general, the volcano is constructed primarily of typical Hawaiian tholeiites with a thin, discontinuous cap of alkalic basalt and hawaiiite. We present isotopic data for one tholeiite for which a major element analysis is available [16].

West Maui consists of shield-building (Wailuku Formation), alkalic cap (Honolua Formation), and post-erosional (Lahaina Formation) stage lavas [1,17]. Wailuku lavas are predominantly tholeiitic with interbedded alkalic basalts in the uppermost part of the section [18], Honolua lavas range in composition from alkalic basalt to trachyte [16-18], and Lahaina lavas consist solely of basanitoids [16]. Isotopic and major element compositions of lavas from each of these stages have been published [6-8,16-18].

Haleakala is deeply dissected and lavas from the shield-building, alkalic cap, and post-erosional stages are well exposed. It is, thus, ideal for evaluating in detail the petrologic and geochemical evolution of a single Hawaiian volcano over a period of at least 0.8 Ma [3]. Previous publications have presented the general geology of Haleakala [17,19] and compositions of its lavas [9,10,18,20,21]. Four formations are recognized, including (with decreasing age) Honomanu Formation shield-building tholeiites and minor intercalated alkalic basalts, Kumuilihi Formation transitional alkalic basalts and hawaiiites (exposed only in Haleakala Crater), Kula Formation alkalic series lavas (alkalic basalt to trachyte), and Hana Formation post-erosional lavas (basanitoid, alkalic basalt,

and hawaiiite).

New Sr, Nd, and Pb Isotopic Results

The lavas of the MVC exhibit substantial ranges in $^{87}\text{Sr}/^{86}\text{Sr}$ (0.70376–0.70442), $^{206}\text{Pb}/^{204}\text{Pb}$ (17.712–18.367), $^{208}\text{Pb}/^{204}\text{Pb}$ (37.701–38.023), and $^{143}\text{Nd}/^{144}\text{Nd}$ (0.51272–0.51298) [Table 2]. In fact, ranges in $^{87}\text{Sr}/^{86}\text{Sr}$ and $^{143}\text{Nd}/^{144}\text{Nd}$ ratios (Fig. 2) are twice those for tholeiites from the island of Hawaii and span virtually the entire compositional spectrum observed for the Hawaiian Islands. The overlap of Lanai and Kahoolawe data with those for Koolau (Oahu) tholeiites clearly demonstrates that the latter volcano is not "anomalous" with respect to other Hawaiian volcanoes [22]. Despite the wide compositional range observed for Kahoolawe lavas, there is no obvious systematic temporal variation, and pre-caldera lavas alone encompass the entire compositional range. This observation contrasts with the systematic temporal Sr–Nd–Pb isotopic variations characteristic of both shield-building and alkalic cap lavas from Haleakala [9,10]. It is worth noting that at Haleakala, isotopic compositions of post-erosional lavas fall entirely within the field for alkalic cap lavas.

Figure 3 shows the Pb isotope systematics of MVC and other Hawaiian volcanoes. Kahoolawe lavas display a wide range in $^{206}\text{Pb}/^{204}\text{Pb}$, but relatively narrow ranges in $^{207}\text{Pb}/^{204}\text{Pb}$ and $^{208}\text{Pb}/^{204}\text{Pb}$. Kahoolawe Pb isotopic compositions overlap those of Koolau lavas, and Lanai tholeiites contain the least radiogenic Pb yet reported for Hawaiian lavas. The Pb isotopic composition of the West Molokai tholeiite is similar to those determined for post-erosional Honolulu Series (Oahu) lavas, but it has distinctly higher $^{87}\text{Sr}/^{86}\text{Sr}$ and lower $^{143}\text{Nd}/^{144}\text{Nd}$ ratios.

Hawaiian Magma Source Mixing Systematics

Combined Sr–Pb systematics for Hawaiian lavas define an approximately triangular field with apices represented by tholeiites from Koolau–Lanai–Kahoolawe and Kilauea, respectively, and by Koloa post-erosional lavas from Kauai (Fig. 3). These data are

consistent with mixing between a minimum of three compositionally distinct end-members, each represented potentially by the compositional extremes of the Hawaiian field. Within the Hawaiian field, two distinct trends are recognized (Fig. 3): a shield-building (primarily tholeiite) trend, characterized by a negative Sr-Pb correlation, that is best exemplified by Kahoolawe, and a post shield-building (alkalic cap/post-erosional) trend, characterized by a positive Sr-Pb correlation, represented by Haleakala (shaded field in Fig. 3) and (to a lesser extent) West Maui.

The Sr-Pb array for shield-building lavas ("SB" in Fig. 4) is consistent with binary mixing between an end-member with relatively radiogenic Sr and unradiogenic Pb and another with relatively unradiogenic Sr and radiogenic Pb. The post shield-building array is also consistent with binary mixing, but differs in that one end-member must lie along the shield-building array whereas the other must have relatively unradiogenic Sr and Pb. These mixing arrays are distinct and have opposite slopes, and therefore provide strong evidence that shield-building and post shield-building lavas cannot have been generated from a common heterogeneous source by different degrees of mixing between source components. Instead, tholeiites and alkalic cap lavas appear to have been generated from separate, two-component sources. In addition, the strong correlation of data within these two arrays is consistent with binary mixing between end-members of relatively restricted isotopic composition, although curvatures of the arrays suggest these end-members likely have different Sr/Pb ratios.

The three isotopically distinct end-members suggested by the Hawaiian Sr-Pb data can be construed as the following: (1) a component with a "primitive mantle" signature (PM, essentially equivalent to "bulk silicate Earth"); (2) "enriched mantle" (EM); and (3) "depleted mantle" (DM, essentially a MORB [Mid-Ocean Ridge Basalt] signature component, possibly representing depleted mantle). These end-members are similar to the Koolau, Kea, and PE end-members of Stille et al. [7] and correspond, at least in spirit, to the PUM (or BSE), HIMU, and DMM components of Zindler and Hart [23]. If end-member compositions remained relatively constant beneath the MVC during the last 2.3

Ma, then isotopic compositions of MVC lavas must reflect variations in mixing proportions between these end-members. Figure 4 shows a mixing grid constructed to examine the mixing systematics of MVC lavas in the context of these hypothetical end-members.

Data for Kahoolawe, which span half the shield-building Sr-Pb array, reveal that tholeiites from individual Hawaiian volcanoes are isotopically diverse and therefore cannot represent homogenized melts (as suggested by Chen [24]). The shield-building array could result from mixing within a two-component (PM-EM) "mantle plume" source, which upon melting produces tholeiitic magmas. Mixing between isotopically distinct magmas cannot be ruled out, but this would not alleviate the requirement of at least two distinct tholeiite magma sources beneath Hawaii. The absence of systematic temporal isotopic variations in Kahoolawe tholeiites rules out progressive introduction or exhaustion of one component and implies that the proportions of PM and EM in these plume melts are variable even over relatively short time spans. This effect could result from inherent source variations in PM:EM ratio, differences in solidus temperatures for EM versus PM components (as would result from enriched blobs [25] or streaks [26] in the Hawaiian plume source), or possibly from short-term variations in the volume or composition of an introduced enriched metasomatic component [e.g. 27]. There is no correlation between the age of tholeiites from a particular MVC volcano and position along the Hawaiian Sr-Pb (Fig. 3) or Sr-Nd (Fig. 2) array; therefore, Hawaiian shield-building lavas as a whole cannot have been generated by progressive mixing between PM and EM components over a larger time framework (such as the age of the Hawaiian Islands).

Minimal involvement of DM-type material in the genesis of Hawaiian tholeiites is inferred from the absence of trends toward that component (Fig. 4). This inference is consistent with high melt production rates during the shield-building stage, with consequent rapid magma ascent and eruption, and with limited residence times in depleted upper mantle and MORB crust, all of which would tend to minimize contamination by MORB composition wall-rock.

The transition for MVC volcanoes (specifically, West Maui and Haleakala) from

shield-building to alkalic cap activity appears to be accompanied by a shift to lower $^{87}\text{Sr}/^{86}\text{Sr}$ and higher $^{143}\text{Nd}/^{144}\text{Nd}$ and $^{206}\text{Pb}/^{204}\text{Pb}$ [8-10]. The cause for this shift is not clear; if it reflects an increase in the EM:PM ratio of the post shield-building source, then the shift could result either from a decrease in melt production coupled with relatively enhanced proportions of more readily fusible EM streaks or blobs, or from an increase in involvement of an enriched metasomatic component. Alternatively, alkalic cap lavas may be derived from separate, subsidiary plumes that were not involved previously in generation of shield-building magmas [10]. The latter scenario obviates the need to explain production of incompatible trace element-enriched alkalic cap lavas from a source which should be depleted in those elements following extraction of voluminous shield-building magmas.

The post shield-building array ("PSB" in Fig. 4) is consistent with mixing between Hawaiian plume magmas, with compositions that lie along the shield-building array, and a DM component. Also, because the post shield-building array has temporal significance, a progressive incorporation of the DM component is inferred [9,10]. Increasing involvement of this component could reflect progressive contamination of either the plume source or plume-derived magmas by depleted uppermost asthenosphere. For example, decreased melt production in the plume during the waning stages of magmatic activity could promote increased melt stagnation and wall-rock interaction (e.g. at the lithosphere-asthenosphere boundary). In addition, relatively small-volume, subsidiary plumes might be more susceptible to contamination than would larger-volume plumes associated with primary shield-building activity.

Haleakala post shield-building lavas also display an apparent systematic temporal decrease in EM:PM ratio (Fig. 4) [10]. This trend could result from progressive exhaustion of available EM material in the post shield-building magma source if a finite mantle volume is involved in melt production, and/or may reflect the influence of small compositional heterogeneities in the DM reservoir.

Implications for Hawaiian Mantle Components

Sr, Nd and Pb isotope systematics of oceanic island basalts (OIB) imply that the sub-oceanic mantle sources of these lavas have retained isotopic heterogeneities on the order of 10^9 years [e.g. 29,30]. It is, however, uncertain whether the isotopic variability observed in OIB reflects the existence of a broad spectrum of end-member compositions or, alternatively, varied mixing proportions between relatively few distinct end-members. It is unlikely that diverse, time-dependent processes such as convective source mixing, extraction or intrusion of silicate melts, or infiltration of non-silicate metasomatic fluids would uniformly affect large mantle domains, and it is reasonable to expect the existence of isotopic heterogeneities on a variety of scales. Although there is considerable leeway regarding the compositions and spatial distribution of the mantle reservoirs inferred for Hawaii, our above interpretations are not dependent upon the exact choice of end-member compositions.

There has been considerable debate over the possible existence of primitive mantle [e.g. 23,31-34]. In this paper, the PM component is taken to represent a mantle reservoir possessing the inferred isotopic composition of primitive mantle [c.f. 25]. It has been proposed [32-34] that this PM component cannot actually be primitive (chondritic) mantle because oceanic basalts (MORB and OIB), including those from Koolau which have PM-like isotopic compositions, possess non-chondritic and constant Nb/U, Nb/Th, and Pb/Ce ratios [32-34]. However, elemental ratios measured in lavas may not be representative of their source mantle, particularly if a multi-component source is involved or complex melting [35] and fractionation [36] processes modify these ratios. For example, negative correlations between Nb/Th and elemental abundances (e.g. rare-earth elements) in Kahoolawe tholeiites imply that this ratio was controlled by magmatic processes. Furthermore, Kahoolawe Nb/Th ratios span a considerably greater range (9.6-23.5) than that proposed for Hawaiian volcanoes (15.2 ± 1.7 [34]) and approach chondritic values (7.9-8.8). Although trace element ratios cannot at present rule out the involvement of primitive mantle, debate over the origin of the PM component in

Hawaiian lavas is by no means resolved.

Similarly, there is uncertainty concerning the origin of a Hawaiian EM component. It could represent previously depleted (possibly MORB source) mantle that was subsequently re-enriched via recycling of oceanic crust and lithosphere [32-34] or sediment [37], magma injection, or metasomatic processes resulting in increased U/Pb, and to a lesser extent Rb/Sr and Nd/Sm. In fact, the range in isotopic compositions for Pacific MORB may reflect addition of an EM-like component to a DM reservoir [see ref. 38].

The EM composition assumed here is constrained only to the extent that it cannot have less radiogenic Pb than that in the most radiogenic Hawaiian lavas. Lavas from certain oceanic islands (e.g. St. Helena, Tubuai, and Mangaia [39,40]) are characterized by even more radiogenic $^{206}\text{Pb}/^{204}\text{Pb}$ (> 21.6 [40]) and have Sr and Nd isotopic compositions intermediate to our PM and DM end-members. Presumably, these lavas were generated, at least in part, from mantle domains that underwent more extreme U/Pb enrichment than our postulated EM end-member. If such extreme EM compositions are more appropriate for Hawaii than the example used here, then Kilauea tholeiites could contain a commensurately smaller proportion of EM component than shown in Fig. 4. Comparable enrichments in Rb and Nd would be less effective in accelerating isotopic evolution than would additions of U, owing to the buffering effect of larger Sr and Nd abundances in the mantle relative to that of Pb [37], and to more rapid decay of ^{235}U and ^{238}U compared to ^{87}Rb and ^{147}Sm . If these enrichments occurred sufficiently long ago, it would have been possible to generate a component with relatively radiogenic Pb but with Sr and Nd compositions intermediate between DM and PM. However, because the age, degree, and nature of enrichment are likely to vary throughout the mantle, a compositional continuum of EM reservoirs probably exists on a global scale.

It is unlikely that EM represents an enriched portion of heterogeneous MORB lithosphere, nor can Hawaiian isotope systematics represent simple two-component mixing of PM-type material with such lithosphere [28]. In order to reproduce the oppositely correlated Sr-Pb shield-building and post shield-building arrays, such a model

requires that shield-building magmas interact primarily with enriched-type lithosphere whereas post shield-building magmas interact primarily with strongly depleted lithosphere. There is, however, no compelling explanation why tholeiites and alkalic cap magmas should interact exclusively with the compositional extremes of this lithosphere (avoiding lithosphere of intermediate Sr-Pb isotopic composition), nor why one magma suite should interact with only one compositional end-member and not the other. Mixing between a relatively fixed end-member (PM) and a heterogeneous end-member (MORB lithosphere) would not likely produce the observed binary mixing trends; rather, such interaction would produce a fan-shaped field [as in ref. 28] which is not observed (see Fig. 4).

For several reasons, we consider it improbable that contamination of magmas at shallow depths by altered oceanic crust was significant in producing the shield-building Sr-Pb array (Fig. 3). First, although uptake of U from seawater [41] could result in old, altered oceanic having radiogenic Pb compositions similar to our postulated EM component, such material would also possess excessively radiogenic Sr [42]. Second, the low Nd content of seawater [41] makes it unlikely that seawater alteration would produce significant Nd heterogeneities in oceanic crust. Thus, strong correlations between Nd and the other isotopic systems in Hawaiian basalts suggest that neither their Sr nor their Pb compositions have been affected significantly by interaction of these magmas with altered oceanic crust. In addition, the relatively restricted EM composition inferred is inconsistent with isotopically heterogeneous [43] oceanic crust. Finally, seismicity associated with recent eruptions at Kilauea and Mauna Loa [44,45] indicates that Hawaiian tholeiites ascend rapidly from upper mantle depths (> 60 km [46]) with only short residence times (< 100 years [46]) at crustal depths. Under these conditions, crustal contamination appears to have been negligible, as evidenced by insignificant Sr and Nd isotopic variations during the 1969–1973 Mauna Ulu (Kilauea) eruptions [47].

Scale of Mantle Heterogeneity

A possible inverse relationship between magma production rates and isotopic diversity in oceanic basalts (MORB and OIB) has led to the proposal [48–50] that basalt compositions are controlled by variable degrees of melting of mantle sources that are heterogeneous on a small scale. In this model, MORB is generated by large and OIB by small degrees of melting of a common heterogeneous mantle; homogeneous melts would be produced in cases where the scale of melting is larger than the scale of heterogeneity. If small-scale heterogeneities are responsible for the isotopic diversity of Hawaiian lavas, and if tholeiites are generated by larger degrees of melting than are associated alkalic lavas, then it follows that tholeiites should be comparatively homogeneous. Because they clearly are not, we infer that the scale of mantle heterogeneity in the shield-building plume source (PM+EM) is larger than the scale of melting. Thus, the data for MVC shield-building lavas imply large-scale heterogeneities in the Hawaiian plume source, and the isotopic heterogeneity of post shield-building lavas requires a distinct petrogenesis involving interaction between shield-building type magmas and a DM (MORB signature) component [see ref. 10].

Acknowledgements

We thank W. M. White, A. W. Hofmann, and an anonymous reviewer for their thoughtful and constructive reviews. In particular, we would like to thank AWH for his detailed and incisive comments. DCG acknowledges a post-doctoral fellowship from the University of Leeds and thanks R. Cliff, P. Guise, and R. Green for technical support, and Buffy, Fossil, and Scram for general support. HBW and WPL are indebted to D. & W. Kennedy for invaluable contributions to our personal QIE. We thank the U. S. Navy for providing access and transportation to the island of Kahoolawe, a U. S. bombing target (Auwe no ka ho'i e), and M. Manghnani for providing the West Molokai sample from the Macdonald collection. This research was partly supported by National Science Foundation Grants EAR85-12167 and EAR83-20358 to WPL and Grant OCE84-16216 to MOG. Hawaii Institute of Geophysics Contribution 1910.

References

- 1 Macdonald, G. A., Abbott, A. T. & Peterson, F. L., in *Volcanoes in the Sea* (University of Hawaii Press, Honolulu, 1983).
- 2 McDougall, I., G.S.A. Bull. 75, 107-128 (1964).
- 3 Naughton, J. J., Macdonald, G. A. & Greenberg, V. A., J. Volc. Geoth. Res. 7, 339-355 (1980).
- 4 Oostdam, B. L., G.S.A. Bull. 76, 393-394 (1965).
- 5 Clague, D. A. et al., Pac. Sci. 36, 411-420 (1982).
- 6 Stille, P., Unruh, D. M. & Tatsumoto, M., Nature 304, 25-29 (1983).
- 7 Stille, P., Unruh, D. M. & Tatsumoto, M., Geochim. Cosmochim. Acta 50, 2303-2319 (1986).
- 8 Hegner, E., Unruh, D. M. & Tatsumoto, M., Nature 319, 478-480 (1986).
- 9 Chen, C.-Y. & Frey, F. A., J. Geophys. Res. 90, 8743-8768 (1985).
- 10 West, H. B. & Leeman, W. P., Earth Planet. Sci. Lett. 84, 211-225 (1987).
- 11 Stearns, H. T., Hawaii Div. Hydrogr. Bull. 6, 177 p. (1940).
- 12 Wentworth, C. K., B. P. Bishop Museum Bull. 24, 72 p. (1925).
- 13 Bonhommet, N., Beeson, M. H. & Dalrymple, G. B., G.S.A. Bull. 88, 1282-1286 (1977).
- 14 Budahn, J. R. & Schmitt, R. A., Geochim. Cosmochim. Acta 49, 67-87 (1985).
- 15 Stearns, H. T. & Macdonald, G. A., Hawaii Div. Hydrogr. Bull. 11, 113 p. (1947).
- 16 Macdonald, G. A., G.S.A. Mem. 116, 477-522 (1968).
- 17 Stearns, H. T. & Macdonald, G. A., Hawaii Div. Hydrogr. Bull. 7, 344 p. (1942).
- 18 Macdonald, G. A. & Katsura, T., J. Petrol. 5, 82-133 (1964).
- 19 Macdonald, G. A., U.S.G.S. Misc. Inv. Ser. Map I-1088 (1978).
- 20 Macdonald, G. A. & Powers, H. A., G.S.A. Bull. 57, 115-124 (1946).
- 21 Macdonald, G. A. & Powers, H. A., G.S.A. Bull. 79, 877-888 (1968).
- 22 Roden, M. F., Frey, F. A. & Clague, D. A., Earth Planet. Sci. Lett. 69, 141-158 (1984).
- 23 Zindler, A. & Hart, S. R., Ann. Rev. Earth Planet. Sci. 14, 493-571 (1986).
- 24 Staudigel, H. et al., Earth Planet. Sci. 69, 13-29 (1984).

- 25 Allegre, C. J., Hamelin, B. & Dupre, B., *Earth Planet. Sci. Lett.* 71, 71-84 (1984).
- 26 Olsen, P., Yuen, D. A. & Balsiger, D., *Phys. Earth Planet. Int.* 36, 291-304 (1984).
- 27 Menzies, M. A. & Murthy, V. R., *Am. J. Sci.* 280-A, 622-638 (1980).
- 28 Chen, C.-Y., *Nature* 327, 49-52 (1987).
- 29 Sun, S.-S. & Hanson, G. N., *Geology* 3, 297-302 (1975).
- 30 Tatsumoto, M., *Earth Planet. Sci. Lett.* 38, 62-87 (1978).
- 31 White, W. M., *Geology* 13, 115-118 (1985).
- 32 Hofmann, A. W., Jochum, K. P., Seifert, M. & White, W. M., *Earth Planet. Sci. Lett.* 79, 33-45 (1986).
- 33 Newsom, H. E., White, W. M., Jochum, K. P. & Hofmann, A. W., *Earth Planet. Sci. Lett.* 80, 299-313 (1986).
- 34 Hofmann, A. W., *Chem. Geol.* 57, 17-30 (1986).
- 35 O'Hara, M. J., *Nature* 314, 58-62 (1985).
- 36 O'Hara, M. J., *Nature* 266, 503-507 (1977).
- 37 Armstrong, R. L., *Trans. R. Soc. Lond. A-301*, 443-472 (1981).
- 38 LeRoex, A. P., in *Mantle Metasomatism* (eds. Menzies, M. A. & Hawkesworth, C. J.), 389-422 (1987).
- 39 Sun, S.-S., *Trans. R. Soc. Lond. A-297*, 409-445 (1980).
- 40 Palacz, Z. A. & Saunders, A. D., *Earth Planet. Sci. Lett.* 79, 270-280 (1986).
- 41 Michard, A., Albarede, F., Michard, G., Minster, J. F. & Charlou, J. L., *Nature* 303, 795-797 (1983).
- 42 Menzies, M. A. & Seyfried, W. E., *Earth Planet. Sci. Lett.* 44, 463-472 (1979).
- 43 Hart, S. R. & Staudigel, H., *Earth Planet. Sci. Lett.* 58, 202-212 (1982).
- 44 Ryan, M. P., Koyanagi, R. Y. & Fiske, R. S., *J. Geophys. Res.* 86, 7111-7129 (1981).
- 45 Dzurisin, D., Koyanagi, R. Y. & English, T. T., *J. Volc. Geoth. Res.* 21, 177-206 (1984).
- 46 Wright, T. L., *J. Geophys. Res.* 89, 3233-3252 (1984).
- 47 Hofmann, A. W., Feigenson, M. D. & Raczek, I., *Contrib. Mineral. Petrol.* 88, 24-35 (1984).
- 48 Batiza, R., *Geophys. Res. Lett.* 8, 853-856 (1981).

- 49 Batiza, R., Nature 309, 440-441 (1984).
- 50 McDougall, J. D. & Lugmair, G. W., Nature 313, 209-211 (1985).

Table 1. Ages and rock types represented at individual MVC volcanoes.

<u>Volcano/Formation</u>	<u>Age (Myr)</u>	<u>Stage</u>	<u>Rock Types*</u>
West Molokai:			
Lower Member	1.52-1.99 ^{2,3}	Shield-building	Thol
Upper Member	?	Alkalic cap	AB, Haw
East Molokai:			
Lower Member	1.51-2.00 ^{2,3}	Shield-building	Thol, AB
Upper Member	1.31-1.46 ³	Alkalic cap	Haw → Tr
Kalaupapa	0.34-1.24 ^{3,13}	Post-erosional	AB, Bas
Lanai:			
Lanai Volc Ser	1.20-1.46 ⁵	Shield-building	Thol
Kahoolawe:			
Pre-Caldera	?	Shield-building	Thol
Caldera-Filling	?	Shield-building	Thol, AB
Post-Caldera	1.02-1.05 ³	Alkalic cap	Haw
West Maui:			
Wailuku	1.31-1.97 ^{2,3}	Shield-building	Thol, AB
Honolua	1.20-1.50 ^{2,3}	Alkalic cap	AB → Tr
Lahaina	1.30 ³	Post-erosional	Bas
Haleakala:			
Honomanu	0.83 ³	Shield-building	Thol, AB
Kumuiliahi	0.70-0.91 ³	Transitional	AB, Haw
Kula	0.36-0.88 ^{2,3}	Alkalic cap	AB → Tr, Bas
Hana	0 - ? ⁴	Post-erosional	Bas, AB, Haw

* Rock types abbreviated as follows: tholeiite (Thol), alkalic basalt (AB), hawaiite (Haw), trachyte (Tr), basanitoid (Bas).

Table 2 Isotopic compositions of lavas from the Maui Volcanic Complex

Sample	Rock type*	$^{87}\text{Sr}/^{86}\text{Sr} \dagger$	$^{143}\text{Nd}/^{144}\text{Nd} \ddagger$	$^{206}\text{Pb}/^{204}\text{Pb} \S$	$^{207}\text{Pb}/^{204}\text{Pb} \P$	$^{208}\text{Pb}/^{204}\text{Pb}$
Kahoolawe						
Pre-caldera						
KW-24	Thol	0.704131 (8)	0.512868 (20)	18.025	15.429	37.759
KW-25	Thol	0.704162 (8)	0.512848 (14)	18.047	15.428	37.786
KW-1	Thol	0.704136 (8)	0.512809 (20)	17.954	15.445	37.805
KW-2	Thol	0.704211 (10)	0.512784 (20)	17.921	15.439	37.733
KW-7	Thol	0.703833 (10)	0.512975 (10)	18.337	15.450	37.990
KW-6	Thol	0.704039 (11)¶	0.512887 (18)¶	18.125¶	15.433¶	37.849¶
		0.704223 (10)	0.512902 (20)	18.120	15.431	37.842
KW-5	Thol	0.703785 (12)¶	0.512929 (20)¶	18.369¶	15.458¶	38.030¶
		0.704609 (8)	0.512928 (20)	18.364	15.451	38.016
Caldera-filling						
KW-23	Thol	0.704090 (8)	0.512901 (16)	18.036	15.430	37.800
KW-19	Thol	0.704399 (12)¶	0.512731 (15)¶	17.939¶	15.453¶	37.842¶
KW-16	Thol	0.704419 (12)	0.512741 (14)	17.946	15.454	37.836
KW-18	Thol	0.704149 (12)	0.512897 (16)	18.149	15.445	37.845
		0.704159 (10)	0.512900 (12)	18.092	15.439	37.866
Post-caldera						
H1440	Haw	0.704257 (10)	0.512864 (18)	18.005	15.447	37.817
KW-14	Haw	0.704032 (10)	0.512924 (16)	18.027	15.466	37.770
			0.512917 (13)			
Lanai						
OX067	Thol	0.704249 (8)	0.512729 (20)	17.854	15.435	37.727
OX068	Thol	0.704111 (8)	0.512784 (17)	17.853	15.420	37.702
OX069	Thol	0.704352 (8)	0.512721 (18)	17.871	15.436	37.701
OX078	Thol	0.704239 (10)	0.512768 (20)	17.886	15.431	37.742
				17.712	15.428	37.738
				17.713	15.424	37.745
West Molokai (lower member)						
C-162	Thol	0.703758 (10)	0.512910 (18)	18.071	15.444	37.731

* Abbreviations as in Table 1.

† Normalized to $^{86}\text{Sr}/^{88}\text{Sr} = 0.1194$; E&A standard = 0.70800.‡ Normalized to $^{142}\text{Nd}/^{144}\text{Nd} = 0.7219$; BCR-1 standard = 0.512640.

§ Normalized and corrected for mass discrimination based on results for NBS981. Uncertainty ~0.05% per a.m.u.

¶ Analysis of leached sample (2.5 N HCl decanted several times until colourless).

Figure Captions

Figure 1. Map of the Maui Volcanic Complex after Macdonald et al. [1]. Solid line around the islands is the 180 meter submarine contour. Molokai comprises two volcanoes: West (W) and East (E). Maui comprises West Maui (W) and Haleakala (H) volcanoes.

Figure 2. $^{87}\text{Sr}/^{86}\text{Sr}$ vs $^{143}\text{Nd}/^{144}\text{Nd}$ for Hawaiian tholeiites, including Kahoolawe (tholeiites - open squares; hawaiiites - solid squares), Lanai (open triangles), and West Molokai (cross). Fields for other MVC tholeiites are shaded as follows: Wailuku (West Maui) - diagonal stripes, East Molokai - hachured, Honomanu (Haleakala) - heavy stippling, and West Molokai - light shading. A field representing Pacific MORB is shown for comparison. Additional Hawaiian and MORB data are from the literature (see [7] for listing of Hawaiian isotope data references). Other Hawaiian shield-building formations and respective volcanoes are as follows: Hamakua (Mauna Kea), Pololu (Kohala), and Waimea (Kauai). Fields for Waimea and Hamakua are based on unpublished data from D. C. Gerlach and W. P. Leeman, and Frey et al. (in preparation), respectively.

Figure 3. Pb-Pb and Sr-Pb isotope plots for lavas from Kahoolawe (squares), Lanai (diamonds) and West Molokai (cross). Shaded area denotes the field for Haleakala post shield-building (Kumuilihi, Kula, and Hana Formations) lavas which become progressively less radiogenic with age [10]. Diagonally striped field in Sr-Pb figure represents field for Haleakala shield-building (Honomanu Formation) lavas [9,10]. Indicated formations and their respective volcanoes as in figure 2, with the following additions: Honolua (alkalic cap) and Lahaina (post-erosional) - West Maui; Koloa (post-erosional) - Kauai; Honolulu (post-erosional) - Koolau. Data sources as in Fig. 2. Geochron and Pacific MORB regression line [PMRL, ref. 10] are shown for reference.

Figure 4. Sr-Pb isotopic mixing model for the Maui Volcanic Complex (MVC). SB and PSB fields denote MVC shield-building and post shield-building lavas, respectively. Data sources as in Fig. 2. End-member compositions from [10]. EM = enriched mantle, PM = primitive mantle, DM = depleted mantle. Upper scale refers to the percentage of PM in a PM-EM mix (i.e. the Hawaiian Plume Composition); vertical scale refers to the percentage of DM in a DM-Plume mix. See text for discussion.

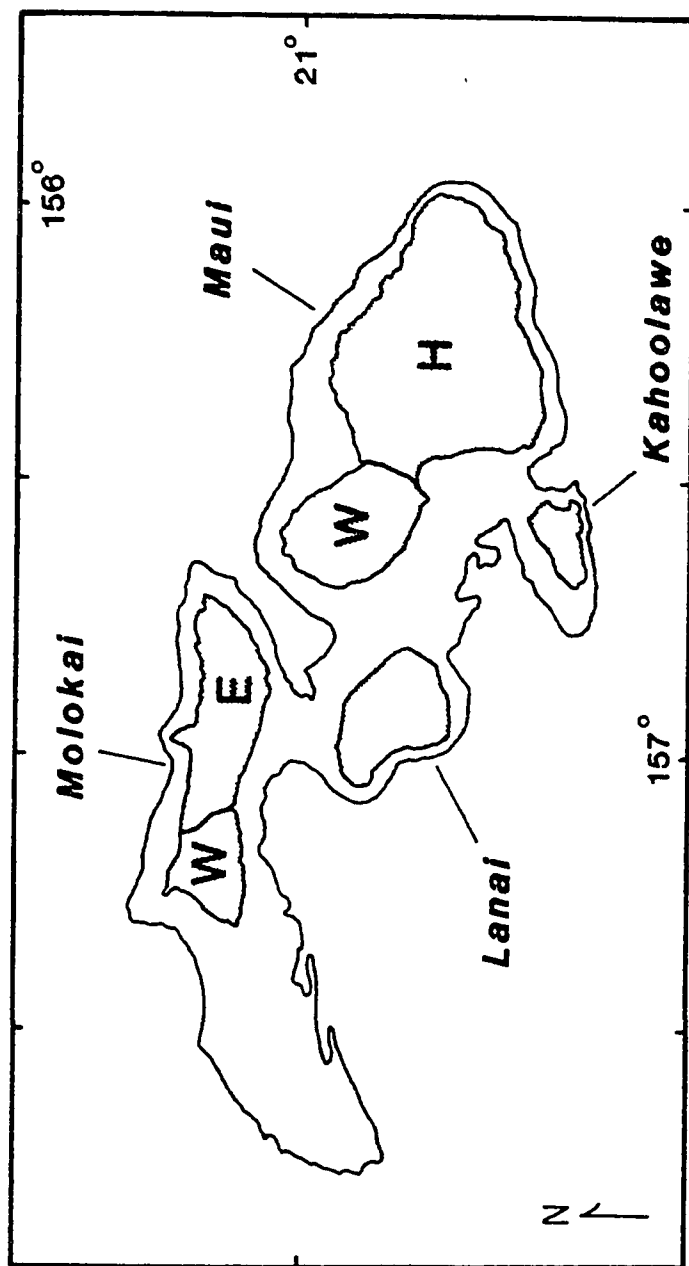


FIG. 1

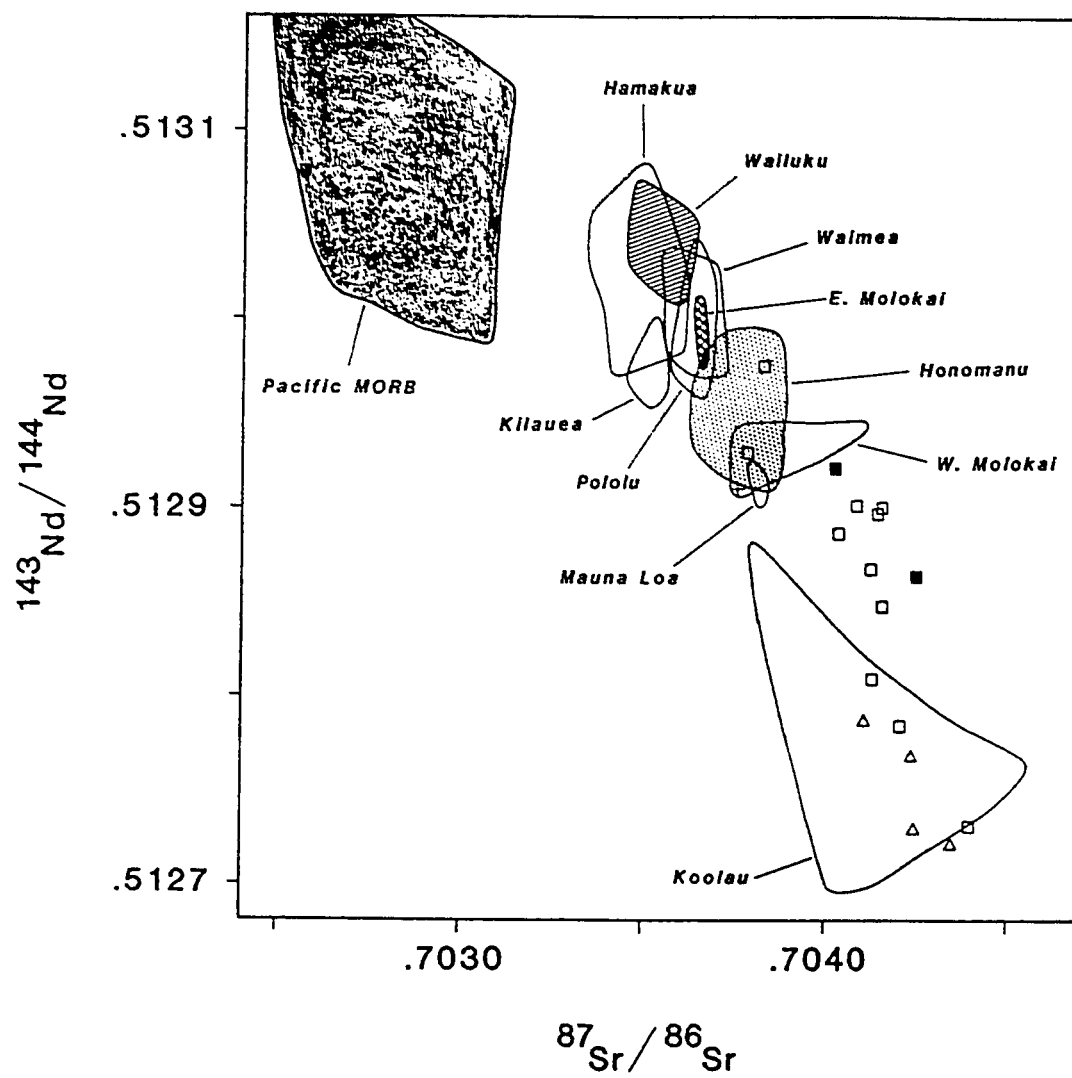


FIG. 2

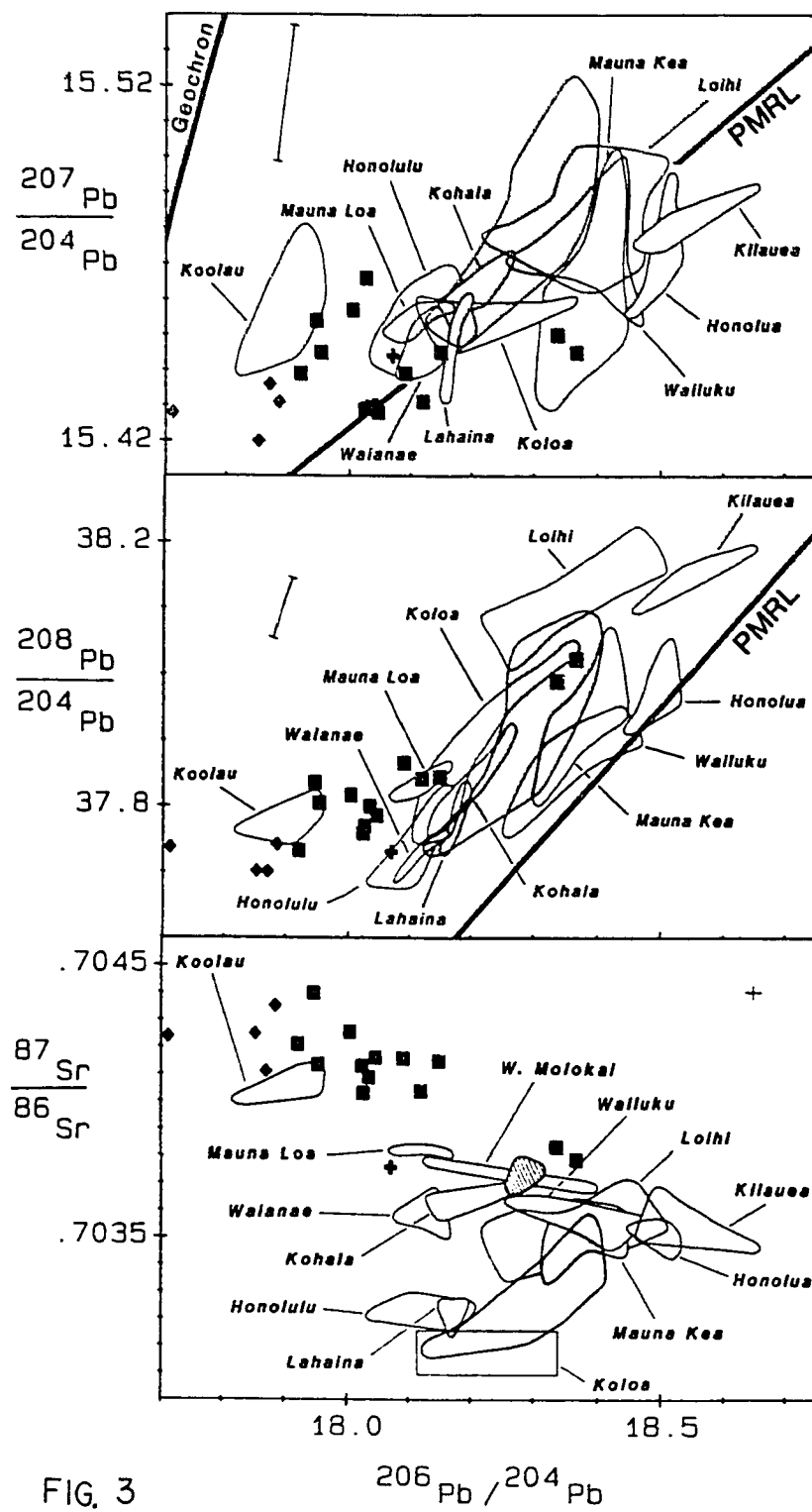


FIG. 3

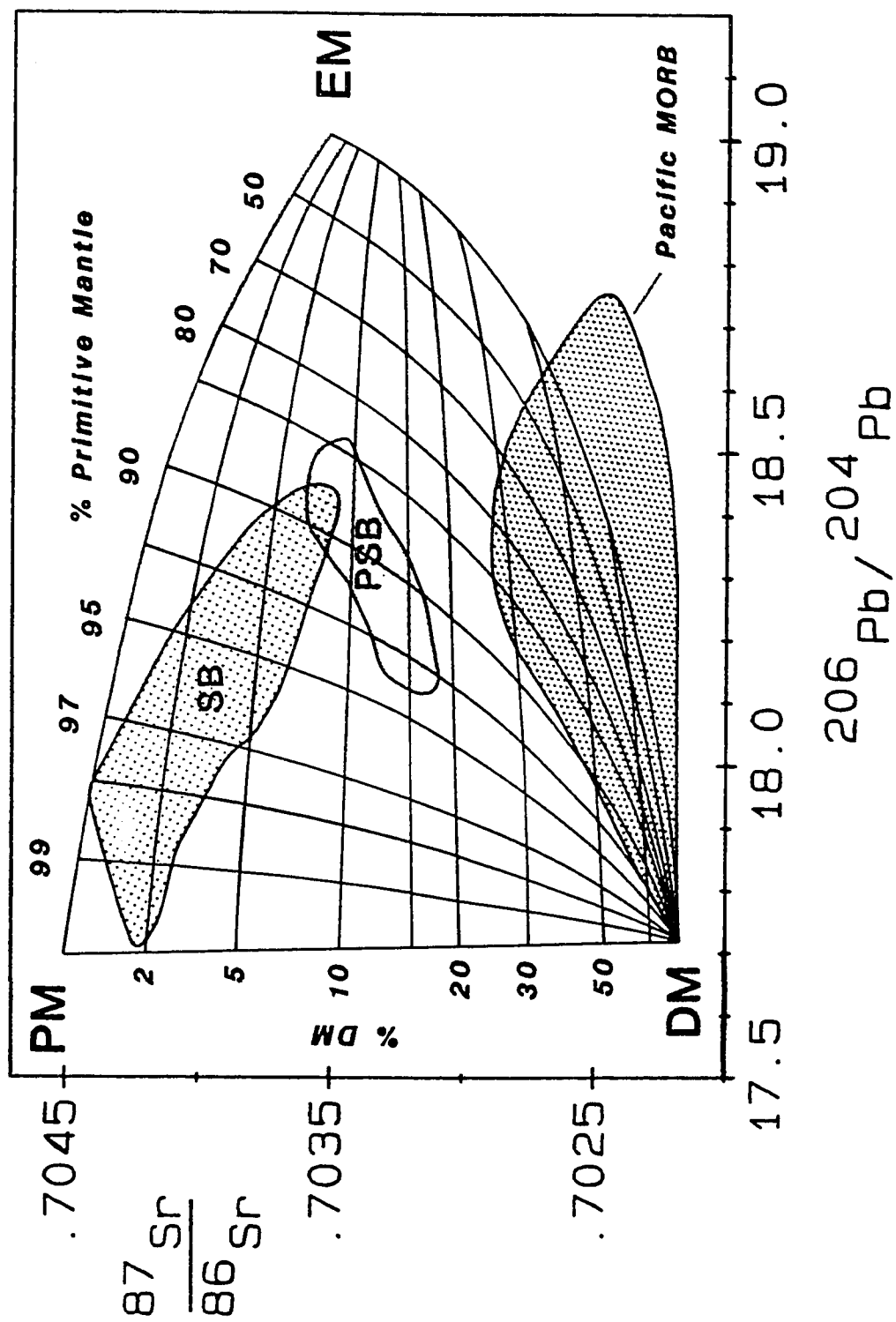


FIG. 4

Chapter 4

**THE ORIGIN AND GEOCHEMICAL EVOLUTION OF LAVAS FROM HALEAKALA
CRATER, HAWAII**

Abstract

Haleakala Crater consists of post shield-building [PSB] lavas representing the early alkalic cap, principal alkalic cap, and post-erosional periods of volcanism on Haleakala. Although major and trace element contents of these lavas are not correlated with isotopic composition, several trace element ratios reveal significant correlations. Paradoxically, ratios of highly incompatible trace elements (H/H ratios) are not significantly correlated with isotopic composition, whereas ratios of highly versus moderately incompatible trace elements (H/M ratios) tend to be strongly correlated with $^{87}\text{Sr}/^{86}\text{Sr}$. H/M ratios such as Zr/Nb and Ba/Y covary with both isotopic composition and with relative stratigraphic position (i.e. age), and are not significantly correlated with major and trace element compositions, implying that variations in these ratios reflect changes in source composition. Mixing relations indicated by trace element systematics are consistent with Haleakala PSB lavas having evolved by mixing between a plume source similar in composition to Haleakala shield-building [SB] lavas and an isotopically-depleted but trace element-enriched (e.g. high Ba/Y, low Zr/Nb) component. The inferred trace element composition of the depleted component requires that it be a melt, possibly of depleted uppermost asthenosphere. Similar trace element systematics for shield-building lavas from the Maui Volcanic Complex are consistent with mixing between primitive and enriched components. The inferred primitive component has chondritic ratios for several trace elements (e.g. Ba/Y, Zr/Nb), as well as a Sr and Pb isotopic composition similar to that estimated for primitive mantle. The enriched component possibly represents a part of the Hawaiian plume source that was either metasomatized or metasomatically scavenged.

INTRODUCTION

The development of modern concepts concerning hot spot volcanism has been greatly influenced by geophysical, geochemical, and petrological studies of Hawaiian volcanoes. As these studies evolved from reconnaissance type investigations to detailed examinations of individual volcanoes, insights into the origin and evolution of hot spot magmatism have increased markedly. For example, early Sr and Nd isotope studies of Hawaiian lavas (O'Nions et al., 1977) supported a two component mixing model in which isotopically primitive material (e.g. plumes from the lower mantle [Morgan, 1971]) interacted with isotopically depleted material (e.g. depleted [MORB source] upper mantle) to produce the spectrum of observed lava compositions. Later studies by Chen and Frey (1983, 1985) on lavas from Haleakala further refined this model and showed that mixing between primitive and depleted components was time-progressive.

Recently, more detailed isotopic studies of lavas from Haleakala Crater (West and Leeman, 1987a) and from other volcanoes of the Maui Volcanic Complex [MVC] (West et al., 1987), demonstrate that: (1) the mixing systematics of Hawaiian shield-building lavas are decoupled from those of the younger alkalic cap lavas, and (2) at least three isotopically distinct components are required in the source of Hawaiian lavas. Multiple components in the Hawaiian source have been similarly advocated by Stille et al. (1983, 1987), Staudigel et al. (1984), and Tatsumoto et al. (1987). Their data and the results of West and Leeman (1987a) and West et al. (1987) are consistent with a model in which Hawaiian shield-building (SB) lavas represent relatively uncontaminated melts derived from a Hawaiian mantle plume containing both an isotopically primitive mantle [PM] component and an enriched mantle [EM] component. In terms of $^{87}\text{Sr}/^{86}\text{Sr}$ - $^{206}\text{Pb}/^{204}\text{Pb}$ systematics, these lavas form a well-defined negative array (the Hawaiian SB array; cf. West et al., 1987). In contrast, Hawaiian post shield-building (PSB) lavas (alkalic cap + post-erosional stages) appear to represent plume melts that underwent increasing amounts of contamination with time by an isotopically depleted [DM] component (e.g. depleted upper asthenosphere). A well-defined positive correlation of $^{87}\text{Sr}/^{86}\text{Sr}$ and $^{206}\text{Pb}/^{204}\text{Pb}$

is exhibited by MVC PSB lavas.

An important conclusion inferred from the strong isotopic correlations is that the three distinct components in the source of Hawaiian magmas must be relatively homogeneous isotopically (West and Leeman, 1987a; West et al., 1987). Nevertheless, the exact nature and composition of these components remain speculative. For example, although some Hawaiian lavas possess primitive mantle-type isotopic compositions (e.g. Kahoolawe and Lanai [West et al., 1987], and Koolau [Stille et al., 1983; Roden et al., 1984]), they have non-chondritic ratios of certain trace elements (e.g. Nb/U, Ce/Pb; see Hofmann, 1987). However, trace element ratios of Hawaiian lavas may reflect interaction between diverse mantle components. It is unlikely that melts derived from a mixed, multi-component source possess trace element ratios indicative of any one single component.

In this paper, we examine the major and trace element compositions of lavas from Haleakala Crater in order to: (1) further define the petrogenetic [mixing] relationship between the shield-building, alkalic cap, and post-erosional stages of Haleakala, and (2) better constrain the nature and composition of components present in the source of Hawaiian lavas, in light of the isotope mixing systematics already established for these rocks. Because Haleakala Crater PSB lavas essentially define the Hawaiian PSB array (West et al., 1987), integration of trace element with isotopic data can potentially provide insights into the behavior of these elements during complex mixing processes. Importantly, PSB Kula Formation lavas, which represent the vast bulk of the exposed alkalic cap stage of Haleakala, were collected from a nearly continuous stratigraphic section and thus allow a more detailed assessment of the geochemical evolution of the Hawaiian alkalic cap stage than has previously been possible.

Our results indicate that lavas from each of the four known volcanic formations of Haleakala were derived from distinct sources and followed distinct evolutionary paths. Although Kula alkalic cap and Hana post-erosional lavas overlap in isotopic compositions for Sr, Pb, and Nd, major and trace element systematics indicate that the geochemical

evolution of Kula lavas was controlled by a combination of fractional crystallization, magma mixing and source mixing, whereas the geochemical evolution of Hana lavas was dominated by both magma and source mixing. Kumuilihi Formation transitional alkalic cap lavas also have major and trace element compositions that fall within the range for Kula Formation alkalic cap lavas, but they evolved primarily by plagioclase + clinopyroxene fractionation from parental magmas that contained isotopically less radiogenic Sr and Pb. Here we investigate combined isotopic and trace element systematics for these lavas in terms of the three component mixing model discussed earlier. In particular, the inferred trace element composition of the depleted [DM] component indicates that it must represent a low degree of partial melt of such a source. The inferred trace element composition of the enriched [EM] component is inconsistent with it representing subducted sediment, subducted oceanic crust, or melts of either material.

GEOLOGIC SETTING

The general geology of Haleakala and distribution of rock types have been extensively covered by Stearns and Macdonald (1942), Macdonald and Powers (1946, 1968), and Macdonald (1978), and are summarized in West and Leeman (1987a). Figure 1 depicts the relative aerial distribution of lavas from the four formations that compose Haleakala. These formations are briefly discussed below, and the general distribution of rock types is given in Table 1.

Honomanu Formation. The Honomanu Formation consists primarily of tholeiites with subordinate, interbedded alkalic basalts and thus represents a transitional period marking the waning stages of primary shield-building activity at Haleakala. Due to burial by lavas during extensive post shield-building activity, Honomanu lavas are exposed only along cliffs and in valleys on the north flank and at the bases of some deep valleys on the south flank. A sample collected from the type section at Honomanu Valley has been dated at 0.83 ± 0.17 Ma (Naughton et al., 1980; see West et al., 1987 for a

summary of ages of MVC volcanoes).

Kumuilihi Formation. Lavas of the Kumuilihi Formation are exposed only in Haleakala Crater and, at the type section located at the Crater's south wall (Macdonald, 1978), are separated from overlying lavas of the Kula Formation by an angular unconformity (Macdonald et al., 1983). These lavas consist of intercalated alkalic basalts and hawaiites and thus appear to represent an early period in the alkalic cap stage of Haleakala. Ages determined for these lavas range from 0.70 to 0.91 Ma (Naughton et al., 1980). Although the age distribution for these rocks overlaps ages determined for the Honomanu Formation, the Kumuilihi Formation is thought to be stratigraphically higher (Macdonald, 1978). Paleomagnetic data (R. Coe, personal communication) indicate that all Kumuilihi lava flows from the type section have reversed polarity and therefore must have been emplaced above the Brunhes-Matuyama boundary (see Harland et al., 1982), thus making the Kumuilihi Formation < 0.73 Ma.

Kula Formation. Kula Formation lavas constitute the vast bulk of the alkalic cap stage at Haleakala and represent the majority of all subaerially exposed lavas. Compositions of Kula lavas range from alkalic basalt and basanitoid to trachyte, although hawaiites and alkalic basalts are the dominant rock types exposed (Table 1). A K-Ar date of 0.82-0.86 Ma was determined for a Kula hawaiite overlying the Honomanu Formation at Honomanu Valley (McDougall, 1964). Dated lavas from Haleakala Crater and from the flanks of Haleakala range from 0.36 to 0.49 Ma (McDougall, 1964; Naughton et al., 1980). Like the underlying Kumuilihi Formation, exposed lava flows have reversed polarity (R. Coe, personal communication) and are therefore younger than 0.73 Ma. The lack of geochronological information on the oldest Kula lavas exposed in Haleakala Crater makes it difficult to estimate the lower age limit for Kula volcanism in the Crater.

Hana Formation. In general, Hana lavas form a relatively thin carapace over Kula lavas and were erupted primarily along a continuous arcuate line of cinder cones and vents formed by the union of the southwest and southeast rift zones of Haleakala

(Stearns and Macdonald, 1942). Because an extended period of volcanic quiescence lasting perhaps 400,000 years (Macdonald et al., 1983) separates Hana and Kula activity, the Hana Formation represents the post-erosional stage of Haleakala. These lavas consist primarily of basanitoids and hawaiites with subordinate alkalic basalts (Table 1). The age of the initiation of Hana volcanism is largely unknown; the most recent eruption took place in historical times (≈ 1790 ; Oostdam, 1965). There is a lava flow located in Haleakala Crater which, despite being located towards the rainy side of the crater, is extremely fresh and may represent an undocumented historical eruption (Macdonald, 1978).

SAMPLING AND ANALYTICAL INFORMATION

Ten stratigraphically-controlled Honomanu lavas were collected from the type section at Honomanu Valley and analyzed for major and XRF trace elements. Isotopic data for the uppermost exposed flow (HHM-1) and a flow collected near the bottom of the section (HHM-9) are given in West and Leeman (1987a). Ten Kumuiliahi Formation lavas were collected from the type stratigraphic section below Kumuiliahi Peak on the south wall of Haleakala Crater and analyzed for major and XRF trace elements. Five of these samples were analyzed for INAA trace elements, and isotopic data for three of these samples are given in West and Leeman (1987a).

Kula Formation samples were collected from three localities. Two samples (HK-61 and HK-62) were collected from flows directly overlying the Honomanu Formation in Honomanu Valley. Two samples (HK-46 and HK-47) were collected from flows directly overlying the Kumuiliahi Formation on the south wall of Haleakala. Fifty samples were collected from a continuous 1000 foot section exposed along the northwest wall of Haleakala Crater and traversed by Halemauu Trail. Additional samples include the Holua trachyte (HOLUA) which is exposed as a dike on the northwest crater wall and an amphibole-bearing mugearite flow located on the upper southwest rim of Haleakala Crater. Major and trace element data for samples collected from the

Halemauu Section of Haleakala Crater are presented in West and Leeman (in prep). Major and trace element data for the other Kula samples are given in Table 2. Sr and Pb isotopic data for twenty Kula samples (including HK-46 and HK-48) are given in West and Leeman (1987a).

Twenty-nine Hana Formation samples were collected from cinder cones and lava flows exposed on the floor of Haleakala Crater and analyzed for major and XRF trace elements. Twelve of these samples were analyzed for INAA trace elements and six for Sr and Pb isotopic ratios (isotopic data presented in West and Leeman, 1987).

The possible effects of late-stage, subaerial alteration on the compositions of drill-core samples of Haleakala lavas have been discussed at length by Chen and Frey (1985). Similar to their findings, Honomanu samples from this study display the effects of minor weathering (i.e. olivine rims are slightly altered to iddingsite). Distinctly lower K_2O/P_2O_5 ratios in Honomanu lavas (0.44-1.63) relative to those in other Haleakala lavas (1.7-8.1) and lack of a correlation between K_2O and Nb may reflect loss of alkalis due to alteration. Although some Kumuilahi lavas contain reddish oxidized olivines, the groundmass and other phenocryst phases (e.g. plagioclase) of these lavas are fresh. Also, K_2O/P_2O_5 ratios in Kumuilahi lavas are relatively constant and essentially identical to fresh Kula lavas of equivalent composition, and K_2O and Nb in these lavas are strongly correlated. We conclude that alteration of Kumuilahi lavas was slight and that their compositions were not affected significantly.

Kula lavas collected from the northwest wall of Haleakala Crater (Halemauu Section) are extremely fresh and show no petrographic or geochemical evidence of late stage alteration. Similarly, Hana lavas were collected from the dry, high-altitude (> 6600 feet elevation) floor of Haleakala Crater and are extremely fresh.

PETROGRAPHY

The petrography and mineral chemistry of lavas from Haleakala have been discussed in detail by Macdonald (1942, 1978), Macdonald and Powers (1946, 1968), Fodor et al. (1972, 1975, 1977), Keil et al. (1972), and Fodor and Keil (1979), and only brief descriptions are presented here. The general petrography of Kula lavas collected from the Halemau Section is also discussed in West and Leeman (in prep).

Honomanu lavas are typically porphyritic and contain abundant olivine and plagioclase phenocrysts. Many of the olivines show the effects of oxidation and weathering and have rims altered to iddingsite. Clinopyroxene occurs in the groundmass but is not a phenocryst phase in any of the lavas examined.

Kumuilihi lavas are porphyritic and contain abundant plagioclase phenocrysts, with subordinate olivine and minor clinopyroxene. Plagioclase phenocrysts commonly are strongly zoned. The olivines have slightly altered rims, but other phenocryst phases and the groundmass are quite fresh. The groundmass of these lavas is dominated by plagioclase and Fe-Ti oxides with subordinate clinopyroxene and olivine.

Kula basalts are fresh and typically contain olivine, clinopyroxene, and plagioclase as their dominant phenocryst/microphenocryst phases with significantly less abundant magnetite microphenocrysts and rare magnetite phenocrysts. The lavas range from seriate to strongly porphyritic; some are glomeroporphyritic. The weakly trachytic groundmass is generally coarse and consists of plagioclase, Fe-Ti oxides, clinopyroxene, and olivine. Plagioclase phenocrysts commonly are zoned and some are partially resorbed. Some olivine phenocrysts contain subgrain boundaries and may also be partially resorbed. Some samples contain clinopyroxene-rich clots of varying mineralogy, but generally: (1) clinopyroxene, (2) clinopyroxene + magnetite, and (3) clinopyroxene + magnetite + olivine.

Kula hawaiites and mugearites commonly are nearly aphyric and tend to be strongly trachytic. Typically, plagioclase and magnetite are the dominant phenocryst/microphenocryst phases with less abundant olivine and clinopyroxene. In

some of the most evolved samples (e.g. HK-25), clinopyroxene is absent. These phenocrysts and microphenocrysts are usually partially resorbed and strongly zoned. In addition, clots of various mineral assemblage are present in some samples and commonly consist of clinopyroxene + magnetite \pm olivine. Samples HK-48, HK-21, and HK-63 (not analyzed) contain small phenocrysts of brown amphibole many of which are strongly resorbed, leaving rims of granular magnetite surrounding a fresh core. Commonly, only pseudomorphs of granular magnetite remain to mark former amphibole grains. Other samples from the HK-48 locality at Pakaoao (located on the upper west rim of Haleakala Crater) have been described by Macdonald (1942) and Macdonald and Powers (1946). The groundmass is dominated by plagioclase and Fe-Ti oxides with subordinate clinopyroxene, olivine, and apatite. Apatite is also present as inclusions (typically in plagioclase) in the most evolved lavas, but rarely occurs as a microphenocryst phase (e.g. HK-28). As noted by Macdonald (1942), biotite is found rarely in the groundmass of some lavas.

The trachyte sample (HOLUA) contains scattered plagioclase phenocrysts up to 6 mm in length and monomineralic plagioclase clots, some containing green diopsidic clinopyroxene. Scattered magnetite microphenocrysts and rare microphenocrysts of partially resorbed greenish diopsidic clinopyroxene and brown amphibole are also present. Apatite is present in the groundmass.

Hana basanitoids and alkalic basalts generally contain sparse phenocrysts and microphenocrysts of olivine with subordinate Fe-oxide, plagioclase, and clinopyroxene microphenocrysts set in a fine-grained or glassy groundmass dominated by magnetite and subordinate plagioclase. Hana hawaiites are petrographically identical to Kula hawaiites of equivalent major element composition and contain plagioclase as the dominant phenocryst phase with subordinate olivine, clinopyroxene, and magnetite.

ANALYTICAL PROCEDURES

Major and trace element data are listed in Table 2. Major oxides were determined by XRF at the University of Massachusetts at Amherst and the University of Houston. Major elements are plotted after setting $\text{Fe}^{2+}/(\text{Fe}^{2+}+\text{Fe}^{3+})$ to 0.90 and recalculating to 100 % on an anhydrous basis. Rb, Sr, Ba, Y, Zr, Nb, Ni, V, Cr, Sc, Cu, and Zn were determined by XRF at the University of Edinburgh. Rare Earth Elements (REE), Th, Ta, Hf, Cr, and Sc were determined by instrumental neutron activation analysis (INAA) at M.I.T. using techniques described by Ila and Frey (1984); additional INAA data was obtained from the University of Oregon.

RESULTS

The following sections describe geochemical variations observed for Haleakala lavas and emphasize those elements and elemental ratios that are most diagnostic of particular magmatic and/or source processes. Elements with geochemical affinities for specific mineral phases (e.g. Mg, Ni, Cr, Sc, V, Ti, Sr, P) and ratios of these elements (e.g. $\text{Al}_2\text{O}_3/\text{CaO}$, $\text{Al}_2\text{O}_3/\text{TiO}_2$, V/Ni, Sc/Ni) can be used to monitor the specifics of fractional crystallization. For example, olivine fractionation should result in decreasing Mg and Ni, clinopyroxene fractionation in decreasing Sc and increasing $\text{Al}_2\text{O}_3/\text{CaO}$, plagioclase fractionation in decreasing Sr, Fe-Ti oxide fractionation in decreasing Cr, V, and Ti, and apatite fractionation in decreasing P.

Highly incompatible elements (HITE; e.g. Rb, K, Th, Nb, La, Ce, Nb) are useful for determining the degree of magmatic differentiation because the bulk partition coefficients for these lavas are significantly less than unity. Figures 3-6 and 10-13 illustrate compositional variations in Haleakala lavas as a function of the highly incompatible trace element, Nb. Nb was chosen because it exhibits the best correlation with other highly incompatible elements (e.g. Th, La, Ce, Rb, Ba, K_2O).

Ratios of highly versus moderately [MITE] incompatible elements (H/M ratios) or of highly versus slightly incompatible (SITE; e.g. Y, Yb) elements can be used to assess

the role of fractional crystallization or partial melting variations, because variations in these ratios are a direct function of the difference in bulk partition coefficients. Ratios of light [LREE] versus middle [MREE] (e.g. La/Sm) and light versus heavy [HREE] (e.g. La/Yb) rare-earth elements fall into this category, as do Zr/Nb and Ba/Y ratios.

Ratios of highly incompatible elements (H/H ratios; e.g. La/Ce, Ba/Rb, Ba/La, Nb/Ta), because they are excluded from most common mineral phases, are typically used to evaluate changes in magma source composition. In theory, H/H ratios and ratios of elements with presumably identical geochemical affinity (e.g. Zr/Hf, Y/Ho) should be unaffected by magmatic processes such as fractional crystallization.

Shield-Building Stage: Honomanu Formation

Although the Honomanu Formation consists of interbedded tholeiites and alkalic basalts (cf. Macdonald and Katsura, 1964; Chen and Frey, 1985), all ten samples from our study are tholeiites having major and trace element compositions similar to those for other Hawaiian tholeiites. Based on the silica-alkalies diagram (Macdonald and Katsura, 1964), Honomanu lavas form a transitional sequence extending from the tholeiite field (overlapping the field for Kilauea) into the alkalic field (Fig. 2). Transitional sequences such as this also characterize the upper shield-building stages of Mauna Kea (West et al., 1988), Kohala (Lanphere and Frey, 1987), East Molokai (Beeson, 1976), and Waianae (Macdonald and Katsura, 1964).

Al_2O_3 , FeO, TiO_2 , and P_2O_5 systematically increase with increasing Nb, whereas MgO and CaO decrease. SiO_2 and K_2O show little systematic variation. In the case of K_2O , this likely reflects post-emplacement alteration and alkali mobility. Ni and Cr abundances decrease, V increases, and Sc roughly increases with increasing Nb (Fig. 4). Sr, Ba, Rb, REE, Th, Ta, Hf, Zr, and Y all behave incompatibly and increase with increasing Nb abundance (Figs. 5-6). Chondrite-normalized relative trace element abundance patterns of Honomanu basalts are similar to those of Kilauea tholeiites (Fig. 7a); apparent depletions in Rb and K are likely a result of alkali loss due to alteration.

Based on enrichment factors for Honomanu lavas (i.e. rock/lowest observed abundance), the apparent order of incompatibility (i.e. increasing bulk distribution coefficient [D]) for the incompatible trace elements is:

$$\text{Rb} < \text{K} < \text{Ba} < \text{P} < \text{La} < \text{Ce} < \text{Ta} < \text{Sm} < \text{Nd} < \text{Nb} < \text{Sr} < \text{Zr} < \text{Hf} < \text{Eu} < \text{Ti} < \text{Th} < \text{Yb} < \text{Y}$$

Honomanu lavas have low La/Sm (< 2.3), La/Yb (< 6.0), Ba/Y (< 6), and Ba/La (< 8.8) ratios and high Zr/Nb (> 11.2) relative to Haleakala PSB lavas (Fig. 10). La/Ce (< 0.405), Zr/Hf (< 41), and $\text{Al}_2\text{O}_3/\text{CaO}$ (1.27–1.63) ratios of these lavas, although relatively low, fall within the range for Haleakala PSB lavas. La/Ce ratios (0.378–0.407) are near-chondritic (0.381–0.392), although most ratios (e.g. La/Sm, La/Yb, Zr/Hf) deviate significantly from chondrites. Excessively high Ba/Rb ratios for many Honomanu lavas (up to 209; Chen and Frey, 1985) likely result from Rb loss during post-depositional weathering (Fig. 10e). Although there are limited data, La/Ce, La/Sm, La/Yb, and Ba/Y ratios appear to be positively correlated with increasing Nb abundance (Figs. 10a–d). In contrast, there appears to be no systematic variation in Zr/Hf or $\text{Al}_2\text{O}_3/\text{CaO}$ ratios with Nb abundance (Figs. 10f–g). Honomanu $\text{Al}_2\text{O}_3/\text{TiO}_2$ ratios fall within the range of Haleakala PSB lavas and are negatively correlated with Nb abundance (Fig. 11). V/Ni (< 4 ; Fig. 12) and Sc/Ni (< 0.4 ; Fig. 13) ratios are low and positively correlated with Nb.

The Sr, Nd, and Pb isotopic compositions of Honomanu lavas have been discussed by Chen and Frey (1985) and West and Leeman (1987a). In terms of $^{87}\text{Sr}/^{86}\text{Sr}$ – $^{206}\text{Pb}/^{204}\text{Pb}$, these lavas occupy an intermediate position on the Hawaiian SB array (West et al., 1987). Honomanu $^{87}\text{Sr}/^{86}\text{Sr}$ ratios are distinctly higher than those for Haleakala PSB lavas, but Pb isotopic compositions fall within the PSB range. Although isotopic compositions of Honomanu lavas do not appear to be correlated with either rock type or major element composition (Fig. 14a; cf. West and Leeman, 1987a), some incompatible

trace element abundances (e.g. Nb, Zr, Th, LREE) appear to be negatively correlated with isotopic composition (Fig. 14b). With the exception of La/Yb (Fig. 14f) and Sm/Yb (not shown) ratios, which appear to be negatively correlated, neither major nor trace element ratios are correlated with isotopic composition (Fig. 14c-j).

Alkalic Cap Stage:

Kumuiliahi Formation:

Kumuiliahi lava compositions fall entirely within the alkalic field of the silica-alkalies diagram but tend to have higher silica at a given alkali content than do Kula lavas (Fig. 2a). Although the range in major and trace element compositions of these lavas falls within the range for Kula lavas, the Kumuiliahi Formation forms distinct compositional fields and/or trends (Figs. 3-6). SiO_2 and MgO contents remain constant with increasing Nb abundance, whereas Al_2O_3 , CaO and Mg#s decrease, and FeO, Na_2O , K_2O , P_2O_5 and TiO_2 increase (Fig. 3). Trends for Na_2O , P_2O_5 , and TiO_2 are similar to those observed for the Honomanu Formation but are offset to higher Nb abundance. In contrast, correlations for Al_2O_3 and CaO are opposite to those observed for Honomanu lavas. Ni contents do not vary systematically with increasing Nb abundance, whereas V shows a scattered increase, and Sc a scattered decrease (Fig. 4). Data for Sr scatters somewhat but in general appear to decrease with increasing Nb (Fig. 6c).

The incompatible elements, Ba, Rb, REE, Th, Ta, Hf, Zr, and Y systematically increase with increasing Nb (Figs. 5-6). Chondrite-normalized trace element abundance patterns for Kumuiliahi lavas indicate they are enriched in highly incompatible trace elements over moderately incompatible trace elements compared to Honomanu tholeiites and fall within the range for Kula lavas (Fig. 7b). From enrichment factors, the apparent order of incompatibility is:

Rb < Th < Nb \approx Zr < Ba < P < Hf < Ta < Yb < K < Ce < Sm < Nd < La < Y < Eu < Ti

Because Sr abundances appear to decrease with increasing Nb (from 768 to 655 ppm; Fig. 6c), the calculated enrichment factor is less than unity (E.F. = 0.85).

Al₂O₃/CaO ratios of Kumuilahi lavas are similar to those for Honomanu lavas (1.40–1.60) and, like Sr, data are somewhat scattered but appear to decrease with increasing Nb (Fig. 10g). Most incompatible trace element ratios for Kumuilahi lavas are similar to those for Kula lavas, but do not appear to be correlated significantly with Nb abundances (Fig. 10). La/Sm ratios are slightly lower (2.82–2.93) and Zr/Nb ratios slightly higher (> 9.2) in these lavas than in Kula lavas (> 3.0 and \leq 9.1, respectively). Other trace element ratios simply fall at the low end (e.g. La/Ce, La/Yb, Ba/Y, Ba/Zr, La/Hf, Nb/La) or high end (e.g. Zr/La, Zr/Th) of the range for PSB lavas from Haleakala Crater. There is a strong negative correlation between Al₂O₃/TiO₂ ratios and Nb abundance (Fig. 11), and Kumuilahi lavas form a sub-parallel trend to Honomanu lavas. V/Ni ratios are positively correlated with Nb (Fig. 12), but Sc/Ni ratios show poor correlation (Fig. 13).

Sr and Pb isotopic compositions of Kumuilahi lavas fall at the radiogenic end of the Hawaiian PSB array and contain distinctly less radiogenic Sr and more radiogenic Pb than do Honomanu lavas (West and Leeman, 1987a; West et al., 1987). Based on limited data, neither major nor trace element ratios are correlated with isotopic composition (Fig. 14), although some incompatible element abundances (e.g. Nb; Fig. 14b) appear to be negatively correlated with ⁸⁷Sr/⁸⁶Sr for the five samples analyzed.

Kula Formation:

Kula lavas span a considerable range in both major and trace element composition; for example, SiO_2 ranges from 43.5 (basanitoid) to 64.2 (trachyte). On a silica-alkalies plot, the Kula Formation defines a trend (Fig. 2a), similar to other Hawaiian alkalic cap suites (Figs. 2b-c). With increasing Nb abundance, SiO_2 , Al_2O_3 , Na_2O , and K_2O increase, whereas MgO , CaO , and FeO decrease (Fig. 3). TiO_2 increases from roughly 3.0 wt.% to nearly 4.0 wt.% at 30-45 ppm Nb and then strongly decreases down to 1.6 wt.% at 80-85 ppm Nb (Fig. 3i). Similarly, P_2O_5 increases from roughly 0.40 wt.% to 1.00 wt.% at 65 ± 2 ppm Nb and then decreases to 0.31 wt.% (Fig. 3h). V behaves similar to TiO_2 , whereas Sc, Ni and Cr abundances decrease systematically with increasing Nb (Fig. 4). Sr abundances increase with increasing Nb, from 580 to 700 ppm Sr (at 24-31 ppm Nb) up to 1240 ppm Sr (at 70 ppm Nb), and then decrease down to < 750 ppm Sr (at 79-83 ppm Nb) in the most evolved mugearites (Fig. 6c). Rb, Th, Ta, Ba, and LREE are positively correlated with Nb abundance (Figs. 5-6). Zr, Hf, Y, MREE, and HREE are also positively correlated with Nb abundance, but the data are somewhat scattered (Figs. 5-6).

Chondrite-normalized trace element abundance patterns of Kula lavas indicate they are enriched relative to Honomanu lavas and have greater H/M relative enrichments than either Honomanu or Kumuiliahi lavas (Fig. 7). Compositions of alkalic cap lavas from Mauna Kea in general fall within the Kula field, but Mauna Kea lavas appear to have lower H/M enrichments and greater enrichments in MITE over SITE [e.g. Y, HREE] (Fig. 8b). Compared to Kula lavas, alkalic cap lavas from Kohala are more enriched and display strong negative Th and Ti anomalies (Fig. 8b). In fact, relative to Kohala and Mauna Kea, Haleakala alkalic cap lavas are depleted in P, judging from the apparent positive P anomalies for those two volcanoes (Fig. 8b). Kula lavas are significantly more enriched than alkalic lavas from Hualalai, particularly for elements Ba→Hf (Fig. 8c). Based on greater relative depletions in Ba, Sr, and P, the Holua trachyte is more fractionated than the Puu Waawaa trachyte of Hualalai (Fig. 8c).

Based on enrichment factors for Kula Formation lavas from Haleakala Crater, the apparent order of incompatibility is:

$$\text{Rb} < \text{Th} < \text{Lu} < \text{Zr} \approx \text{Yb} < \text{K} \approx \text{Nb} < \text{Ba} < \text{P} < \text{Hf} < \text{Y} < \text{La} < \text{Nd} < \text{Ta} < \text{Sm} \approx \text{Ce} < \text{Sr} < \text{Eu}$$

The apparent relative enrichment of HREE over LREE and other trace elements generally assumed to be more incompatible (e.g. K, Nb, Ba) reflected in this order is unusual and must reflect the operation of processes more complex than simple crystal fractionation of observed phenocryst phases or a combination of processes. This is discussed in full in West and Leeman (in prep).

$\text{Al}_2\text{O}_3/\text{CaO}$ ratios of Kula lavas from Haleakala Crater span a considerable range (0.91-3.33) and are positively correlated with Nb abundance (Fig. 10g). Ratios of highly vs. moderately incompatible elements (H/M ratios) also span relatively large ranges and several vary systematically with Nb abundance (Fig. 10). La/Sm range from 3.02 to 6.40 and increase up to approximately 77 ppm Nb but then level off or even decrease at higher Nb abundance (Fig. 10b). An exception to this is the amphibole-bearing mugearite sample from Pakaoao (HK-48) which has the highest La/Sm ratio). La/Yb ratios of Kula lavas from Haleakala Crater span a much larger range (11.2-27.0) than do flank lavas (10.3-18.9; Chen and Frey, 1985). Similar to La/Sm, both La/Yb and Ba/Y ratios increase to a maximum (Ba/Y from 10.3 to ≈ 31) and then decrease (Fig. 10c), but there is much more scatter in the data.

Some ratios of geochemically similar elements span relatively large ranges and are correlated with incompatible element abundances. For example, La/Ce ratios range from 0.391 to 0.493 and appear to increase with increasing Nb abundance (fig. 10a). Similarly, Zr/Hf (37.8-52.1) and Ba/Rb (13.4-31.6) ratios span considerable ranges and are correlated with Nb abundance (Fig. 10). $\text{Al}_2\text{O}_3/\text{TiO}_2$ ratios of Kula basalts and mafic hawaiites are not correlated with Nb abundance (up to ≈ 50 ppm Nb), but show a

strong positive correlation for the more evolved hawaiiites and mugearites (Fig. 11). V/Ni and Sc/Ni ratios increase with Nb abundance in the basalts and mafic hawaiiites, but decrease in the more evolved hawaiiites and mugearites (Figs. 12-13).

Sr and Pb isotopic compositions of Kula lavas fall within the Hawaiian PSB array (West et al., 1987) and are correlated with stratigraphic position such that with decreasing age, lavas become less radiogenic (West and Leeman, 1987). This isotopic composition-age relationship was previously found for Haleakala by Chen and Frey (1983) on the basis of Sr-Nd isotope ratios. Isotopic compositions of these lavas are not correlated with rock type, major element composition, $\text{Al}_2\text{O}_3/\text{CaO}$ ratios, or trace element abundances (West and Leeman, 1987a) (e.g. Figs. 14a-c). Both Sr and Pb isotopic ratios are correlated with several H/M ratios (e.g. Zr/Nb, Ba/Y, La/Yb, La/Sm, Ba/Zr, Hf/Th) (Figs. 14e-h). In contrast, isotopic ratios are not correlated significantly with H/H ratios (e.g. La/Ce, Nb/Th, Nb/La, Ba/Rb, Nb/Ta; see Figs. 14d, i) or with ratios of elements of close geochemical affinity (e.g. Zr/Hf; Fig. 14j).

Post-Erosional Stage: Hana Formation

Major and trace element compositions of Hana lavas generally fall within the compositional range of the Kula Formation, but Hana lavas tend to be more silica-undersaturated than do Kula lavas of equivalent alkali content (Fig. 2a). Hana lavas are similar to post-erosional basanitoids from West Maui, but are considerably more silica-saturated than post-erosional nephelinites and melilitites from Oahu and Kaula (Fig. 2d). With increasing Nb abundance, SiO_2 , Al_2O_3 , Na_2O , K_2O , P_2O_5 , and Al_2O_3 increase, FeO, MgO, CaO and Mg# decrease, and TiO_2 appears to increase at lower Nb abundances and decrease at higher Nb abundances (Fig. 3). At a given Nb content, Hana lavas have distinctly lower SiO_2 , Al_2O_3 , Na_2O , and P_2O_5 contents and distinctly higher Mg#'s than Kula lavas. V, Sc, Cr, and Ni abundances of Hana lavas decrease with increasing Nb abundance (Fig. 4). Hana lavas contain higher absolute abundances of these compatible elements than do Kula lavas of comparable Nb content (Fig. 4). Similar to the Kula

Formation, Rb, Ba, Sr, Th, Ta, Zr, Hf, Y, and REE abundances in Hana lavas increase with Nb abundance, however data for Hana lavas tend to lie along higher Nb/MITE trends than do Kula lavas (Figs. 5-6). In contrast to Kula lavas, Sr abundances do not tail off or decrease at higher Nb abundances (Fig. 6c).

Chondrite-normalized data for the Hana Formation fall within the field for Kula lavas, but Hana lavas are less enriched in MITE [e.g. Sm, Eu, Zr, Hf] and SITE [e.g. Y, HREE] (Fig. 7d). In general, Hana lavas fall within the field for Honolulu post-erosional lavas, but contain conspicuously lower relative P abundances (Fig. 9b). A post-erosional basanitoid from West Maui contains relative trace element abundances that are virtually identical to those of Hana lavas (Fig. 9c). Kaula post-erosional nephelinites, although similar in trace element composition to Hana lavas, display extreme relative enrichments in Sr and P and relative depletions in Zr and Hf (Fig. 9c).

In contrast to the Kula Formation, the order of incompatible trace element incompatibility for the Hana Formation as a whole is more typical of geochemical behavior observed for basaltic suites, i.e. LREE are more incompatible than are MREE or HREE. Based on enrichment factors, the apparent order of incompatibility is:

$$\text{Rb} < \text{K} < \text{Nb} < \text{P} < \text{Th} < \text{La} < \text{Sr} < \text{Ta} < \text{Ce} < \text{Ba} < \text{Nd} < \text{Zr} < \text{Sm} < \text{Eu} < \text{Hf} < \text{Yb} < \text{Y}$$

Most major and trace element ratios fall within the range defined by Kula lavas from Haleakala Crater and, like Kula lavas, many of these ratios (e.g. $\text{Al}_2\text{O}_3/\text{CaO}$, La/Sm , La/Yb , Ba/Y , Zr/Hf , Ba/Rb) are correlated with Nb abundance (Fig. 10). La/Ce ratios appear to be an exception and are not strongly correlated with Nb (Fig. 10a). For several incompatible trace element ratios, Hana lavas fall at either the low end (e.g. Zr/Nb , Zr/La , Zr/Th) or high end (e.g. Ba/Y , Ba/Zr) of the range for Haleakala PSB lavas. However, the contention that Hana lavas are more enriched in highly incompatible trace elements than Kula lavas (Chen and Frey, 1985) is not supported by samples collected from Haleakala Crater. For example, when both Crater and flank

lavas are considered, Hana lavas do *not* have consistently higher Nb/La, Ba/La, Ba/K, La/Ce, or Rb/La ratios (cf. Chen and Frey, 1985, p. 8753). $\text{Al}_2\text{O}_3/\text{TiO}_2$ ratios scatter slightly but appear to increase with increasing Nb abundance (Fig. 11). Both V/Ni and Sc/Ni ratios of Hana lavas are positively correlated with Nb, but unlike Kula lavas, this ratio does not decrease at higher Nb abundances (Figs. 12-13).

Sr and Pb isotopic compositions of Hana lavas fall at the unradiogenic end of the PSB array (West et al., 1987) and are not correlated with rock type (West and Leeman, 1987), trace element abundances, or $\text{Al}_2\text{O}_3/\text{CaO}$ ratios (Figs. 14b-c). For Hana lavas from Haleakala Crater, correlations between trace element and isotope ratios generally follow those defined by Kula lavas (Fig. 14). For Hana lavas from the flank of Haleakala, there is no significant correlation between some of these trace element ratios (e.g. La/Yb, La/Sm) and $^{87}\text{Sr}/^{86}\text{Sr}$ (Figs. 14e-f). Zr/Nb ratios are poorly correlated with $^{87}\text{Sr}/^{86}\text{Sr}$ (Fig. 14g).

TEMPORAL COMPOSITIONAL VARIATIONS

Isotopic Ratios

Chen and Frey (1983, 1985) found that drill-core samples of Kula and Hana lavas from the north flank of Haleakala and Honomanu samples from Honomanu Valley display a progressive upsection change in Sr and Nd isotopic composition. Isotopic compositions change from $^{87}\text{Sr}/^{86}\text{Sr} = 0.70372\text{--}0.70387$ and $^{143}\text{Nd}/^{144}\text{Nd} = 0.51291\text{--}0.51298$ in the Honomanu Formation, to $0.70318\text{--}0.70353$ and $0.51299\text{--}0.51309$ in the Kula Formation, to $0.70306\text{--}0.70328$ and $0.51306\text{--}0.51313$ in the Hana Formation (Chen & Frey, 1985). Although isotopic compositions of these flank lavas progressively vary upsection *within* the Kula Formation, there is no significant systematic change in isotopic composition within either the Honomanu or Hana Formations.

In a study of lavas from Haleakala Crater, West and Leeman (1987a) found that, although Sr and Pb isotopic compositions are broadly correlated with relative stratigraphic position, the range for the Hana Formation ($^{87}\text{Sr}/^{86}\text{Sr} = 0.70312\text{--}0.70329$,

$^{206}\text{Pb}/^{204}\text{Pb} = 18.200\text{--}18.263$) falls within that of the Kula Formation ($^{87}\text{Sr}/^{86}\text{Sr} = 0.70308\text{--}0.70340$, $^{206}\text{Pb}/^{204}\text{Pb} = 18.132\text{--}18.398$). It is apparent that, for Haleakala, there is no clear isotopic distinction between the youngest lavas erupted during the alkalic cap stage and those erupted during the post-erosional stage. Within the Kula Formation, both Sr and Pb isotopic ratios of Kula lavas from Haleakala Crater decrease upsection, with the exception of the lowermost exposed lava, which has relatively low $^{87}\text{Sr}/^{86}\text{Sr}$ (0.70320; West and Leeman, 1987a). Because of poor stratigraphic control over lavas erupted on the floor of Haleakala Crater (Macdonald, 1978), it is difficult to determine whether isotopic compositions varied systematically during Hana volcanism (West and Leeman, 1987a). Based on available data, however, an isotope-age correlation is not supported. The oldest Hana lavas exposed in Haleakala Crater ($^{87}\text{Sr}/^{86}\text{Sr} = 0.70328\text{--}0.70329$, $^{206}\text{Pb}/^{204}\text{Pb} = 18.271$; West and Leeman, 1987a) are comparable isotopically to the historic eruption of 1790 ($^{87}\text{Sr}/^{86}\text{Sr} = 0.70325$, $^{206}\text{Pb}/^{204}\text{Pb} = 18.259$; Tatsumoto et al., 1987)

Kumuilihi lavas (0.70345–0.70355) have more radiogenic Sr than do Kula lavas, but less radiogenic Sr than Honomanu lavas (0.70368–0.70387; based on data in West and Leeman [1987a] and Chen and Frey [1985]). Although data for the Kumuilihi Formation are limited, neither Sr nor Pb isotopic compositions appear to be correlated with relative stratigraphic position (West and Leeman, 1987a). In contrast to the case for Sr, Pb isotopic compositions for Honomanu, Kumuilihi, Kula, and Hana Formation lavas are not distinct. Together, Sr and Pb isotopic compositions of Haleakala PSB lavas define a temporally significant positive array (the PSB array) within which Kumuilihi lavas lie at one [radiogenic] end, and younger Kula lavas and Hana lavas lie at the other [unradiogenic] end (West and Leeman, 1987a).

Trace Element Ratios

Although neither major element contents nor trace element abundances of lavas from Haleakala change systematically with relative stratigraphic position [Figs. 15a-b] (see Chen and Frey, 1985; West and Leeman, 1987b,c), several trace element ratios show significant temporal correlations. Details concerning temporal variations in trace element ratios for Haleakala flank lavas have been presented by Chen and Frey (1985) and the reader is referred to that work for more detailed information on those lavas.

In general, trace element ratios for Kula lavas from Haleakala Crater fall into two distinct classes: (1) those ratios that are correlated with both relative stratigraphic position and isotopic composition, and (2) those ratios that are correlated with trace element or major element contents but not with stratigraphic position. Trace element ratios belonging to the former group are apparently independent of the systematic geochemical variations associated with Kula magma batches (West and Leeman, 1987b, 1987c, in prep) and include several H/M ratios [e.g. Zr/Nb, Ba/Y, Ba/Zr, Zr/Th, Hf/Th, Zr/La] (Figs. 15c-d). In contrast, the later group consists of ratios sensitive to fractional crystallization (e.g. $\text{Al}_2\text{O}_3/\text{CaO}$, $\text{Al}_2\text{O}_3/\text{TiO}_2$; see West and Leeman, in prep), as well as H/H ratios (e.g. Ba/Rb and to a lesser extent, La/Ce), and ratios of elements of similar geochemical affinity (e.g. Zr/Hf) which should remain relatively unaffected by fractional crystallization (Figs. 15e-g).

THE ROLE OF FRACTIONAL CRYSTALLIZATION

From the isotope systematics of lavas from Haleakala it is apparent that the source composition changed as a function of time. The correlation of several trace element ratios with isotopic composition indicates that the trace element composition of the source of these lavas also varied with time. Before using ratios of these incompatible elements to further constrain the nature and composition of geochemically distinct components in the source, it is important to assess the effects of fractional crystallization. A detailed investigation of the role of fractional crystallization in controlling major and

trace element variations of Honomanu, Kula, and Hana Formation flank lavas has been presented by Chen (1982). The effects of magmatic [magma chamber] processes on Kula lavas from Haleakala Crater, and the formation of magma batches are detailed in West and Leeman (in prep). The following sections briefly outline the geochemical variations within each of the four principal formations of Haleakala consistent with fractional crystallization.

Honomanu Formation

Systematic decreases in MgO and Ni contents with increasing Nb (Figs. 3d, 4a) are consistent with extensive fractionation of olivine. This is supported by the presence of olivine as the dominant phenocryst phase in these lavas. An attendant decrease in Cr abundances (Fig. 4b) is consistent with significant Cr-spinel fractionation. The positive correlation between Sc and Nb (Fig. 4c) and lack of a negative correlation for $\text{Al}_2\text{O}_3/\text{CaO}$ (Fig. 10g) indicates that clinopyroxene was probably not a significant fractionating phase. Positive correlations of V and TiO_2 with Nb (Figs. 3i, 4d) suggest that fractionation of Fe-Ti oxides was not significant and is supported by a concomitant decrease in $\text{Al}_2\text{O}_3/\text{TiO}_2$ and V/Ni ratios (Figs. 11-12). Although plagioclase is present in Honomanu lavas as a phenocryst phase, the incompatible behavior of Sr (Fig. 6c), the lack of Eu anomalies (also, see Chen and Frey, 1985, p. 8752), and the absence of any systematic decrease in $\text{Al}_2\text{O}_3/\text{CaO}$ ratios suggest that precipitated plagioclase phenocrysts were not separated from surrounding magma. The lack of efficient plagioclase separation could be due to flotation resulting from phenocrysts being less dense than magma (cf. Elthon, 1984). These conclusions are similar to those reached by Chen (1982) who suggested that major and trace element variations are largely the result of olivine \pm clinopyroxene fractionation

Kumuilihi Formation

Although Kumuilihi lavas are petrographically similar to Honomanu lavas, their distinct geochemistry indicates that they followed a separate evolutionary path. Because MgO and Ni contents are buffered in these lavas (Figs. 3d, 4a), olivine was probably not a dominant fractionating phase. However, that olivine fractionation did occur is implied by the positive correlation between V/Ni and Nb (Fig. 12). Al_2O_3 and Sr are negatively correlated with Nb (Figs. 3b, 6c) which suggests that plagioclase removal was important. This is consistent with plagioclase being the dominant phenocryst phase in these lavas. Increasing TiO_2 , V, and FeO contents and decreasing $\text{Al}_2\text{O}_3/\text{TiO}_2$ ratios with increasing Nb abundance (Figs. 3c, 3i, 3d, 11b) indicate that fractionation of Fe-Ti oxides was probably not significant.

Decreasing Sc abundances (Fig. 4c) indicate that clinopyroxene fractionation also occurred, although the lack of any significant correlation between Sc/Ni and Nb (Fig. 13b) suggests that dominance of clinopyroxene over olivine was not great. Olivine fractionation should increase Sc/Ni ratios because, for olivine, $D^{\text{Ni}} \gg D^{\text{Sc}}$ (e.g. Lindstrom, 1976; Villemant et al., 1981). Conversely, in alkaline series rocks, $D^{\text{Ni}} < D^{\text{Sc}}$ for clinopyroxene (Villemant et al., 1981; Lemarchand et al., 1987), therefore clinopyroxene-dominated fractionation should decrease Sc/Ni ratios in the melt. Because $D^{\text{Sc}} \gg D^{\text{Ni}}$ for hedenbergite (Lemarchand et al., 1987) and because D^{Ni} increases with decreasing Fo-content in olivine, the decrease in Sc/Ni ratios should become increasingly pronounced as magmas continue to evolve. This can be seen in the steep negative Sc/Ni-Nb slope (Fig. 13b) for lavas with Nb contents greater than ≈ 50 ppm.

Geochemical variations within the Kumuilihi Formation would appear to indicate that these lavas evolved primarily by plagioclase \pm clinopyroxene \pm olivine fractionation. Experimental results on alkalic basalts and hawaiites (Thompson, 1974; Knutsen and Green, 1975; Mahood and Baker, 1986) indicate that at lower temperatures and at low to moderate pressures, plagioclase is the dominant liquidus phase. The implied dominance of plagioclase and generally low MgO, Ni, Cr, and Sc contents suggest that

Kumuilihi lavas may be low pressure derivatives of olivine- and clinopyroxene-depleted parental magmas.

Kula Formation

Lavas from the Halemauu section of Haleakala Crater reveal a systematic upsection series of geochemical discontinuities consistent with the emplacement of discrete magma batches. The details of this process are presented in West and Leeman (in prep). Briefly, a combination of processes are responsible for the observed compositional variations, including fractionation, magma mixing, recharge by mafic magma, and possibly phenocryst resorption. Despite the obvious complexities of open system magma chamber processes, overall geochemical variations for many elements and elemental ratios illustrate the control exerted by fractional crystallization over the compositions of Kula lavas.

Decreasing MgO, Ni, and Cr contents with increasing Nb abundance (Figs. 3d, 4a-b) are consistent with significant fractionation of olivine and Cr-spinel. Decreasing Sc and increasing $\text{Al}_2\text{O}_3/\text{CaO}$ ratios (Figs. 4c, 10g) reflect a strong role of clinopyroxene fractionation in the evolution of these lavas. In the less evolved Kula lavas (alkalic basalts and mafic hawaiites), increasing Sc/Ni ratios suggest that clinopyroxene is subordinate to olivine, whereas in the more evolved hawaiites and mugearites, clinopyroxene dominates (Fig. 13). Variations in MgO, Ni, and Cr reveal the possibility of two distinct trends within the Kula Formation: (1) a high-Mg, high-Ni trend similar to that exhibited by Hana lavas, and (2) a low-Mg, low-Ni trend within which the vast majority of Kula lavas fall. The high-Mg trend may simply be an artifact of the relatively anomalous composition of one sample (HK-58), which contains elevated MgO (11.44 wt.%), Ni (217 ppm), and Cr (610 ppm) contents compared to other Kula lavas; this sample compositionally resembles the least evolved lavas of the Hana Formation (e.g. sample HH-11). It is possible that this sample is related petrogenetically to the Hana Formation rather than the Kula Formation and may simply represent an early precursor

to Hana volcanism, erupted during the waning stages of the alkalic cap stage of Haleakala. However, two distinct Kula trends, one including HK-58 as well as other Kula lavas, are also evident in the plot of SiO_2 versus Nb (Fig. 3a).

FeO, TiO_2 , and V contents of Kula basalts increase with increasing Nb (Figs. 3e, 3i, 4d), suggesting that Fe-Ti oxide fractionation was not significant in these lavas. For more evolved lavas (hawaiites and mugearites), FeO, TiO_2 , V, and V/Ni are negatively correlated with Nb, indicating significant Ti-Fe oxide fractionation. For the hawaiites and mugearites, plagioclase and apatite fractionation became important, as indicated by decreases in Sr and P_2O_5 contents (Figs. 3h, 6c).

Trace element ratios such as La/Sm, La/Ce, Ba/Rb, and Zr/Hf are apparently affected by fractional crystallization. Increasing La/Sm with increasing Nb (Fig. 10b) is consistent with fractionation of a clinopyroxene-rich phase assemblage ($D^{\text{La}}[\text{cpx}] < D^{\text{Sm}}[\text{cpx}]$; e.g. Frey et al., 1978). This is supported by the general negative correlation between La/Sm and Sc (Fig. 16b). The slight leveling off of La/Sm ratios in the evolved hawaiites and mugearites could be due in part to plagioclase fractionation ($D^{\text{La}} > D^{\text{Sm}}$; e.g. Higuchi and Nagasawa, 1969; Henderson, 1984). The tight positive correlation between La/Sm and Ba (Fig. 16a), which is only slightly incompatible for plagioclase ($D^{\text{Ba}} \approx 0.15$ to 0.60 ; cf. LeRoex and Erlank, 1982), may also be a function of plagioclase fractionation. It is unlikely that any leveling off of La/Sm ratios could be due to fractionation of apatite, because for apatite, $D^{\text{La}} < D^{\text{Sm}}$ (Watson and Green, 1981).

For olivine, clinopyroxene, and Fe-Ti oxides, $D^{\text{La}} > D^{\text{Yb}}$, therefore a positive correlation between La/Yb ratios and incompatible trace element abundances is expected for Kula lavas having undergone fractionation of these phases (see Fig. 10c). Although data are somewhat scattered, there does appear to be a general negative correlation between La/Yb and Sc (Fig. 16c). Because REE partition coefficients are significantly larger for clinopyroxene than for olivine, Fe-Ti oxides, or spinel, clinopyroxene fractionation probably exerts the greatest effect on La/Yb ratios, at least for the

basalt→hawaiite sequence. The drop in La/Yb ratios in the most evolved hawaiites and mugearites (Figs. 10b-c) could be related to the onset of apatite fractionation, combined with the increased role of plagioclase, because for these two mineral phases, $D^{La} > D^{Yb}$ (e.g. Higuchi and Nagasawa, 1969; Henderson, 1984; Irving and Frey, 1984).

La/Ce, Ba/Rb, and Zr/Hf are positively correlated with Nb abundance (Figs. 10a, e-f). Because $D^{La} < D^{Ce}$ for clinopyroxene (e.g. Frey et al., 1978; Fujimaki et al., 1984), segregation of a clinopyroxene-rich phase assemblage could account for the observed increase in La/Ce ratios. In addition, fractionation of La/Ce ratios would be enhanced in an open system magma chamber characterized by repetitive recharge and continuous fractionation of clinopyroxene. For apatite and amphibole, $D^{Ce} > D^{La}$ (Irving and Frey, 1984), therefore fractionation of these phases would contribute to the increase in La/Ce ratios. In fact, the sample with the highest La/Ce ratio (0.493) is the amphibole-bearing mugearite lava from Pakaoao (HK-48), which also contains comparatively low P_2O_5 .

Ba/Rb ratios of Kula lavas are negatively correlated with Nb abundance, indicating that bulk $D^{Ba} > D^{Rb}$. Because Ba/Rb ratios decrease from basalts through mugearites and plagioclase fractionation is significant only for the more evolved hawaiites and mugearites, it is unlikely that variations in this ratio are due to plagioclase fractionation alone. Although relatively high values have been reported (e.g. ≈ 0.44 ; Shimizu, 1980), D^{Ba} [clinopyroxene] is typically ≈ 0.1 [Griffin and Murthy, 1969]), therefore clinopyroxene-dominated fractionation could significantly decrease Ba/Rb ratios in the basalts and mafic hawaiites, particularly in an open system magma chamber.

Because Zr and Hf have virtually identical ionic radii and occur in the same valance state (Whittaker and Muntus, 1970), they are generally assumed to be inseparable by simple fractionation processes, although Zr/Hf fractionation has been reported for some lunar rocks (Hughes and Schmitt, 1984). Zr/Hf ratios of Kula Formation lavas are positively correlated with Nb and Al_2O_3/CaO and negatively correlated with Sc (Figs. 10f, 17) for the entire sequence of compositions, from alkalic basalt to mugearite. This

strongly suggests that clinopyroxene fractionation controlled Zr/Hf variations and that $D^{\text{Zr}} [\text{cpx}] < D^{\text{Hf}} [\text{cpx}]$. Although $D^{\text{Zr}} < D^{\text{Hf}}$ has been reported for ilmenites in high-Ti mare basalts (Nakamura et al., 1986; McKay et al., 1986), it is unlikely that Fe-Ti oxide fractionation provided the principal control over Zr/Hf ratios because this ratio systematically changes throughout the basalt→mafic hawaiite sequence where oxide fractionation was not significant.

Origin of Holua Trachyte

The Holua trachyte contains extremely low MgO (0.12 wt.%; $\text{Mg\#} \approx 3.9$), Ni (3 ppm), Cr (2 ppm), Sc (1.1 ppm), Sr (4.4 ppm), P_2O_5 (0.02 wt.%), and TiO_2 (0.34 wt.%) suggesting that this magma evolved through extensive fractionation of olivine, Cr-spinel, clinopyroxene, plagioclase, apatite, and Fe-Ti oxides. In addition, petrographic evidence indicates that amphibole may also have been a significant fractionating phase. These strong depletions in major and compatible element contents and the accompanying enrichments in incompatible elements (e.g. Nb = 229 ppm, Zr = 1916 ppm, Rb = 159 ppm) indicate that the Holua trachyte is one of the most highly differentiated lavas found in the Hawaiian islands (Table 3).

If the Holua trachyte evolved by closed system fractional crystallization of an alkalic basalt parental magma and it is assumed that $D^{\text{Nb}} \approx 0$ (based on chondrite-normalized relative abundance [Fig. 7c]), then the total extent of crystallization can be approximated by $F \approx C_o/C_l$. Assuming that $C_o \approx 24$ ppm Nb (the Nb content of HK-2, lowest among Kula lavas from Haleakala Crater), a minimum of 89.5 % crystallization is indicated. The relatively high $^{87}\text{Sr}/^{86}\text{Sr}$ ratio (0.70367) of the Holua trachyte resembles those of Honomanu basalts and may therefore be related petrogenetically to the Honomanu Formation. If a parental magma composition of 7.2 ppm Nb (C-122, the lowest Nb Honomanu basalt; Chen and Frey, 1985) is assumed, the Holua trachyte represents a minimum of ≈ 97 % crystallization.

Hana Formation

Systematic decreases in MgO, Ni, Cr, Sc, and $\text{Al}_2\text{O}_3/\text{CaO}$ with increasing Nb abundance (Figs. 3d, 4a-c) are consistent with fractional crystallization of olivine, Cr-spinel, and clinopyroxene. The positive correlation between Sc/Ni ratios and Nb (Fig. 13), along with petrographic observations, suggest that olivine is dominant over clinopyroxene in the fractionating phase assemblage. In the less evolved Hana lavas, TiO_2 contents appear to increase with increasing Nb (Fig. 3i), which suggests that fractionation of Fe-Ti oxides was not significant. At more evolved compositions, TiO_2 , FeO, and V decrease strongly and $\text{Al}_2\text{O}_3/\text{TiO}_2$ ratios increase (Figs. 3c, 3i, 4d, 11), indicating that oxide fractionation became more important. Sr and P_2O_5 behave incompatibly (Figs. 3h, 6c), therefore neither plagioclase nor apatite fractionation appears to have been significant.

La/Sm and La/Yb ratios of Hana lavas increase throughout the observed compositional range and, unlike Kula lavas, these ratios do not level off or decrease in the more evolved lavas. This possibly reflects the lack of significant apatite or plagioclase fractionation in these lavas. Negative correlations of La/Sm and La/Yb ratios with Sc abundance (Figs. 16b-c) suggest that increases in these ratios are primarily the result of clinopyroxene fractionation. The lack of any strong positive correlation between La/Ce and Nb may, in part, be due to the lack of significant apatite (or amphibole) fractionation.

The role of clinopyroxene in lowering Ba/Rb ratios is supported by data for the Hana Formation, because plagioclase fractionation in these lavas was probably not sufficient to affect this ratio to the extent observed. Similarly, Zr/Hf ratios increase with increasing Nb and $\text{Al}_2\text{O}_3/\text{CaO}$ and decreasing Sc (Figs. 10f, 17) even for the least evolved Hana lava compositions where Fe-Ti oxide fractionation was not significant. Thus, clinopyroxene fractionation may have been the major control over Zr/Hf ratios for Hana as well as Kula lavas.

Magma Mixing Effects in Hana Lavas

Unlike the Kula Formation, compatible element-incompatible element correlations tend to be linear rather than curved (e.g. Figs. 4a-b), suggesting that the compositions of Hana lavas have been strongly influenced by magma mixing. Fractional crystallization should produce a curved fractionation trend. Based on the restriction of mantle xenoliths to Hawaiian post-erosional lavas and their absence from alkalic cap and shield-building lavas, Clague (1987) has suggested that post-erosional lavas may have ascended from deep source regions without residence in shallow- or intermediate-depth magma chambers. However, evidence for magma mixing in Hana lavas and the presence of more differentiated hawaiite compositions indicates that these magmas have experienced some degree of storage.

TRACE ELEMENT CONSTRAINTS ON MANTLE SOURCE COMPONENTS

By using the constraints imposed by isotopic compositions, incompatible trace element ratios that can demonstrably be shown to be unaffected by magmatic processes can be utilized to further constrain the nature of these source components and their mutual interaction. Trace element-isotope correlations for Haleakala PSB lavas, which define a mixing array between plume and DM end members [i.e. the MVC PSB array], can be used to estimate trace element ratios in the DM component. Similar correlations for Kilauea and MVC shield-building, which span the Hawaiian SB array, can be used to estimate trace element ratios in both the PM and EM components.

Assuming that isotopic ratios vary in proportion to degrees of mixing between the postulated mantle end members, it is appropriate to examine isotope-trace element ratio or trace element ratio-ratio correlations to help constrain further the compositions of these end members. For example, both Ba/Y and Zr/Nb ratios are correlated with $^{87}\text{Sr}/^{86}\text{Sr}$ ratios. In addition, neither of these trace element ratios appears to have been significantly affected by magmatic processes. $^{87}\text{Sr}/^{86}\text{Sr}$ and Ba/Y ratios of Haleakala PSB lavas are negatively correlated, with older PSB [Kumuilihi] lavas (low Ba/Y-high

$^{87}\text{Sr}/^{86}\text{Sr}$) and young PSB [Hana + young Kula] lavas (high Ba/Y-low $^{87}\text{Sr}/^{86}\text{Sr}$) falling at the ends of a well-defined array (Fig. 18a). Post-erosional lavas from other Hawaiian volcanoes (Honolulu Volcanic Series and Lahaina Formation) also fall at the high Ba/Y-low $^{87}\text{Sr}/^{86}\text{Sr}$ end of the PSB array. In contrast, Hawaiian shield-building lavas form a low Ba/Y array with Kilauea at the low $^{87}\text{Sr}/^{86}\text{Sr}$ end and MVC SB lavas at the high $^{87}\text{Sr}/^{86}\text{Sr}$ end.

Zr/Nb- $^{87}\text{Sr}/^{86}\text{Sr}$ relations for these lavas indicate that Haleakala PSB lavas form an array of positive slope, with older PSB lavas at the low Zr/Nb end and younger PSB lavas at the high Zr/Nb end (Fig. 18b). Limited Zr/Nb- $^{87}\text{Sr}/^{86}\text{Sr}$ data for other Hawaiian post-erosional lavas are consistent with relations at Haleakala. MVC SB lavas form a separate, triangular field at high Zr/Nb-high $^{87}\text{Sr}/^{86}\text{Sr}$, whereas Kilauea lavas fall within the high Zr/Nb end of the PSB field.

Plotted against each other, Ba/Y and Zr/Nb ratios of lavas from Haleakala reveal a strong, temporally significant, negative correlation (Fig. 19a), virtually identical to Sr-Pb isotope relations. Combined Ba/Y-Zr/Nb and $^{87}\text{Sr}/^{86}\text{Sr}$ relations for Haleakala PSB lavas and other Hawaiian post-erosional lavas suggest that the DM component of the Hawaiian PSB array has high Ba/Y ($>\approx 50$) and low Zr/Nb (≈ 3) [Fig. 19b]. The PM component, represented by MVC SB lavas must have low Ba/Y (< 5) and high Zr/Nb (> 21). The EM component, represented by Kilauea, appears to require low Ba/Y and low Zr/Nb (Fig. 19b).

Depleted Mantle (DM) Component

Because depleted MORB's typically have low Ba/Y (≈ 0.35) and high Zr/Nb (≈ 34) [based on data for normal MORB from 22°N, Mid-Atlantic Ridge] and estimated MORB source mantle has Ba/Y ≈ 0.29 and Zr/Nb ≈ 37.4 (Tarney et al., 1980), the DM component cannot represent MORB-source material or MORB magmas.

If Zr/Nb and Ba/Y ratios of MORB are representative of their DM source, then Ba/Y ratios must be enriched approximately 172 fold, from 0.29 in the source to ≈ 50 in

the melt (i.e. the contaminant). If, in the DM source, bulk D^{Ba} is assumed to be 0, then the percent partial melt can be calculated for a given bulk D^Y value from the equation for equilibrium melting.

$$F = \frac{D^Y}{(R_l/R_o) - 1 + D^Y}$$

R_l = Ba/Y ratio of the melt, R_o = Ba/Y ratio in the source, F = melt fraction. For $R_l/R_o = 172$, and assuming $D^Y = 0.10$, the percent partial melt is restricted to less than ≈ 0.06 %. An enrichment of approximately 12.5 % in Nb over Zr is required to produce a DM Zr/Nb ratio of 3 from a MORB source Zr/Nb ratio of 37.4. For a reasonable bulk D^{Zr} value (≈ 0.01 ; cf. Frey et al., 1978) and assuming that $D^{Nb} = 0$, then the percent partial melt is restricted to less than ≈ 0.09 %, similar to the result obtained for Ba/Y. Because Zr/Nb and Ba/Y ratios in observed depleted MORB are virtually identical to those estimated for MORB source mantle and because F is independent of the absolute concentrations of these elements, the calculated % melt required for MORB itself is also comparable (Ba/Y ≈ 0.06 %, Zr/Nb ≈ 0.10 %). Given the uncertainties in partition coefficients for incompatible trace elements in mantle source minerals, the consistency between these calculations suggests that the DM component could be a very small degree (< 0.1 %) melt of MORB source material, as suggested by Chen and Frey (1983, 1985).

Primitive Mantle (PM) Component

The existence of a primitive, unprocessed reservoir in the Earth's mantle and the possible role of such a reservoir in the production of basaltic magmas are still major unresolved points in modern geochemistry. Correlations between the three isotopic systems, Nd, Sr, and Pb, have led to a more or less agreed upon *range* of possible compositions for a primitive reservoir, assuming it remained a closed system subsequent to

core segregation (see White [1985] for a discussion of the rationale behind such estimations). White (1985) listed the isotopic composition of primitive mantle as: $^{87}\text{Sr}/^{86}\text{Sr} = 0.7045$, $^{206}\text{Pb}/^{204}\text{Pb} = 17.7$, $^{207}\text{Pb}/^{204}\text{Pb} = 15.43$, $^{208}\text{Pb}/^{204}\text{Pb} = 37.6$. The primitive mantle $^{143}\text{Nd}/^{144}\text{Nd}$ composition, based on chondritic Sm/Nd for the bulk earth, is estimated to be ≈ 0.51262 - 0.51263 (DePaolo and Wasserburg, 1979; Dupre and Allegre, 1980).

The isotopic compositions of lavas from Kahoolawe and Lanai (both part of the MVC) fall within these ranges and define one end of the Hawaiian SB array (West et al., 1987). This is consistent with the existence of a primitive mantle component, or at least a component with a primitive mantle-like isotopic composition in the source of Hawaiian lavas (i.e. the PM component). On the other hand, Hofmann et al. (1986) and Hofmann (1987) suggest that because these lavas do not possess chondritic ratios of certain trace elements (e.g. Nb/Th, Nb/U, Ce/Pb), that this component cannot be primitive mantle, but rather must be a form of enriched mantle (e.g. subducted oceanic lithosphere). However, as pointed out by West et al. (1987), it is unlikely that lavas derived from a multi-component source will have trace element ratios representing any *single* component. Instead, trace element ratios will reflect the relative contributions of each component in the source of these lavas.

Trace element systematics indicate that Kula lavas are unlikely to have been derived from parental magmas having chondritic (i.e. primitive mantle) trace element ratios. For example, Kula lavas must have been derived from parental magmas with relatively high Ba/Rb ratios (> 32) and then evolved to lower Ba/Rb ratios (down to 13.4); in contrast, estimated primitive mantle Ba/Rb ratios range from as low as ≈ 6.6 (compilation, this study) to ≈ 11.3 (Hofmann and White, 1983). However, combined trace element-isotope data suggest that these lavas were derived from a mixed source containing a primitive component. In particular, the low Ba/Y-high Zr/Nb PM composition inferred by MVC shield-building lavas (Fig. 19b) is very close to chondritic (Ba/Y ≈ 1.5 , Zr/Nb ≈ 19), and suggests that this component could represent a primitive mantle reser-

voir.

Enriched Mantle (EM) Component

The relatively radiogenic Pb composition and intermediate $^{87}\text{Sr}/^{86}\text{Sr}$ composition (≈ 0.7035) of the Hawaiian EM component inferred by Sr-Pb mixing systematics implies a preferential enrichment in U/Pb over Rb/Sr (West and Leeman, 1987a; West et al., 1987). Extreme examples of this kind of source enrichment has been documented for several oceanic islands, such as St. Helena (Sun, 1980; Cohen and O'Nions, 1982; White and Hofmann, 1982), Mangaia (Palacz and Saunders, 1987), and Tubuaii (Vidal et al., 1984). Several possible sources for an EM component have been proposed, representing various mechanisms of enrichment: (1) contamination by oceanic lithosphere [e.g. Tatsumoto, 1978; Stille et al., 1983, 1987; Hegner et al., 1986], (2) incorporation of melts derived from subducted oceanic crust and lithosphere [e.g. Hofmann and White, 1980], (3) incorporation of a subducted sediment component [e.g. White and Hofmann, 1982; Weaver et al., 1986], (4) infiltration of migrating mantle melts [e.g. Anderson, 1981], and (5) mantle metasomatism involving volatile-rich fluids (as opposed to silicate melts) [e.g. Tatsumoto et al., 1984].

Using the compositional constraints imposed by Kilauea, Ba/Y-Zr/Nb systematics (Fig. 19b) suggest that the Hawaiian EM component has low Ba/Y and Zr/Nb. Such a composition virtually rules out the possibility that EM represents a melt-enriched mantle reservoir. Melting of either depleted or primitive mantle compositions or even lithospheric materials would increase Ba/Y ratios because Y is less incompatible than Ba. Furthermore, if such enrichment occurred sufficiently long ago, a silicate melt of typical mantle materials would substantially increase Rb/Sr and U/Pb and therefore produce elevated $^{87}\text{Sr}/^{86}\text{Sr}$ and $^{206}\text{Pb}/^{204}\text{Pb}$ ratios.

Sr-Pb isotope systematics indicate that subducted sediments are highly unlikely to have been significantly involved in the genesis of Hawaiian lavas (West et al., 1987). In support of that conclusion, sediments also have trace element compositions that are

inappropriate for any Hawaiian source component, including the EM component. For example, average oceanic pelagic clay (Li, 1982) has relatively high Ba/Y (≈ 25) and intermediate Zr/Nb (Fig. 20), and oceanic sediments in general have high Ba/Y and high Zr/Nb (Hole et al., 1984). Thus, subducted sediments or melts of such sediments could not have contributed significantly to the Hawaiian EM component.

Sr-Pb isotopic compositions are consistent with the Hawaiian plume being essentially a binary mixture of primitive and enriched components (West and Leeman, 1987a; West et al., 1987). If the EM component resides within the plume itself, then this enriched component could possibly represent volatile-enriched areas of the plume that were metasomatized by a kimberlite-type fluid or possibly scavenged by such fluids. Because Zr, Nb, and Y are comparatively immobile in the presence of a fluid phase (Pearce and Norry, 1979), the relative abundances of these elements would not change significantly during metasomatism. In contrast, Ba could be preferentially removed by a migrating, volatile-rich fluid phase, resulting in low Ba/Y. If minor melting occurred in the mantle region as the result of the intrusion of such a fluid phase, then those melts would have lower Zr/Nb. It is possible that retention of small degree partial melts in this source could result in decreased Zr/Nb.

The composition of a mantle metasomatic component is difficult to constrain, but it is possible that such a component could be kimberlitic. Experimental evidence favors the generation of kimberlites by melting of volatile-enriched mantle (see Wyllie [1980] and Pasteris [1984] for reviews), although controversy still rages as to whether kimberlites *result in* or are the *result of* mantle metasomatism (Wyllie, 1980). If a part of the Hawaiian mantle plume underwent volatile-induced melting, then melts resembling kimberlites could possibly have been generated. It has been suggested that kimberlitic melts may have played a role in the genesis of some continental alkalic basalts (Feigenson, 1986b). In that study, Feigenson (1986b) found that the grain surfaces of minerals contained in mantle-derived xenoliths from New Mexico contained a kimberlitic component highly enriched in incompatible trace elements. Feigenson suggested that the host alkalic

basalts could represent mixtures between a kimberlite melt and depleted mantle material (as represented by the xenoliths). Of course, it remains to be shown whether or not a kimberlitic melt might have a composition appropriate for the Hawaiian EM component. Although kimberlites vary greatly in trace element composition, a kimberlite collected from the East Griqualand Field (Nixon et al., 1983) has low Ba/Y (1.92) and Zr/Nb (1.85) ratios comparable to the inferred composition of the Hawaiian EM component. Although the U/Pb ratio of this kimberlite was not determined, it does have low Rb/Sr and therefore would not cause a significant increase in $^{87}\text{Sr}/^{86}\text{Sr}$ over time.

IMPLICATIONS FOR PLUME MODELS

There many basic questions pertaining to the nature of mantle plumes and their role in producing Hawaiian volcanism. For example, does each volcano represent a distinct mantle plume or are clusters of volcanic centers (e.g. Maui Volcanic Complex [MVC], island of Hawaii) fed via a single large plume? Is the observed temporal evolution within a single volcano, evolving from tholeiitic shield-building volcanism through alkalic cap and post-erosional volcanism, the expression of the evolution of a single plume or of the successive emplacement of multiple plumes?

Because the general compositional evolution of volcanoes that make up the Hawaiian-Emperor Chain has been reproducible over roughly 70 Ma, it is reasonable to infer that these volcanoes were formed by the emplacement of many distinct, individual plumes. Although single plumes are generally assumed by most workers to ultimately have produced the entire spectrum of eruptive products for each volcano, isotopic and geochemical data are also consistent with multiple plume scenarios. It is possible that the principal stages of Hawaiian volcanism each reflect the emplacement of a separate mantle plume, or that, even within a single stage, multiple plumes may be involved.

Depth of Plume Penetration

The depth of seismicity beneath the island of Hawaii begins at least 60 km depth (Eaton and Murata, 1960) and intense earthquake swarms occur at 50–60 km depth (Eissler and Kanamori, 1986). These observations suggest that plume penetration/lithospheric thinning occurs to these depths relative to a normal lithospheric thickness of 60 km (interpolated after Leeds, 1975) expected for 80 Ma (Watts, 1978) oceanic crust. This 50–60 km depth is thus interpreted as the initial depth of melt segregation from the plume and depth of plume penetration into the oceanic lithosphere. These depths are consistent with work on the Hawaiian swell (Detrick and Crough, 1978; Crough, 1978) which suggest that compensation is within the lower lithosphere (50–100 km depth). Heat flow modeling (Von Herzen et al., 1982) also suggests a 50 km depth. Experimental (Olson and Nam, 1986) and numerical (Daly and Raefsky, 1985) results suggest that plumes do not penetrate but rather are plastered at the base of the lithosphere, and Olson and Singer (1985) conclude that only a small fraction of the total plume mass is ever erupted.

The Parasitic Plume Model

Perhaps one of the most significant conclusions drawn from the isotopic mixing model presented by West and Leeman (1987a) and West et al. (1987) is that Hawaiian tholeiite sources or melts of these sources do not undergo significant interaction with isotopically depleted (MORB composition) materials. The lack of apparent contamination of these melts by either depleted asthenosphere or depleted lithosphere implies that the (asthenospheric) plume material flux into the lithosphere must be large enough that tapped magmas do not stagnate prior to emplacement within the volcanic edifice.

Although a single plume can account for the Hawaiian shield-building stage, there are significant problems in trying to generate alkalic cap and post-erosional stage lavas from the same plume. Alkalic cap lavas are both volumetrically less significant and appreciably more enriched in incompatible trace elements than associated tholeiites. In

order that the enriched mantle end-member, postulated to be dispersed enriched material resident in the plume, not be depleted during long-term tholeiite production, a replenishment process must be at work. Progressive extraction of melt from a single plume over prolonged periods would likely result in depletion of enriched (and presumably more fusible) material, thereby making the plume incapable of producing primitive (high Mg#) alkalic basalts having enriched trace element signatures. A similar problem exists in trying to derive highly enriched, high Mg# post-erosional lavas from the same plume that produced the tholeiites. Metasomatism has been proposed to account for the incompatible trace element enrichments (e.g. Menzies and Murthy, 1980), but such models imply enrichment of previously scavenged mantle material which is inconsistent with the primitive major element compositions of these lavas.

The apparent discrepancies evident in the single plume model may be resolved at least in part by recent plume models based on dynamical and experimental results (e.g., Olson and Nam, 1986; Olson and Singer, 1985). Dynamical treatments (Olson and Nam, 1986; Olson and Singer, 1985) have shown that plumes rising through non-stationary media develop parasitic instabilities (i.e. parasitic plumes). Based on the model developed for the MVC (West et al., 1987) and assuming that parasitic plumes are compositionally similar, if not equivalent, to the principal (shield-building) plume, a model for post shield-building magmatism can be inferred. Like the primary shield-building plume, parasitic plumes contain both primitive and enriched components but, in contrast, preferentially incorporate enriched, fusible material due to smaller amounts of melting. The intrusion of these volumetrically smaller, parasitic plumes provides a means of generating primitive (i.e. undepleted by previous melting events) magmas with enriched trace element signatures. The small volume of such plumes could result in increased stagnation of melts at the base of the lithosphere, resulting in increased contamination by either depleted lower lithosphere or depleted upper asthenosphere. As the parasitic plume material becomes exhausted, isotopic compositions shift more strongly towards the DM end-member.

Effects Related to the Reduction of Melt Volume with Time

The ascent of volumetrically smaller parasitic plumes in the asthenosphere would tend to be inhibited because the scale height of a rising diapir is a function of its radius (Ribe, 1983). If the observed relative volumes of volcanic output during shield-building, alkalic cap, and post-erosional volcanism are an accurate indication of relative plume size, then parasitic plumes may have order of magnitude (or less) smaller volumes. These smaller volumes might make such plumes more prone to stagnation in the asthenosphere. A particular plume train (i.e. primary plume plus associated parasitic plumes) must traverse a non-uniform and (at least) bi-directional velocity gradient in the asthenosphere due to large-scale mantle convection. Under such conditions smaller plumes will be more subject to break-up and separation from the trailing conduit of the main plume body primarily because of the higher susceptibility of small mass flux plumes to shear (Whitehead, 1982). Thus, magmatism related to the emplacement of parasitic plumes will in general be inhibited.

Because volumetrically smaller parasitic plumes will be more susceptible to stagnation, these plumes will also, by implication, be more susceptible to contamination by surrounding wall-rock. The smaller melt volumes associated with parasitic plumes also have implications for the storage of these melts in magma chambers. As suggested by Clague (1987), smaller volumes of melts may lead to stagnation at deeper levels and the solidification of shallow and intermediate depth magma chambers. In addition, magmatic pressure exerted by the small volumes of magma that do reach shallow or intermediate level magma chambers may be insufficient to overcome lithostatic pressure.

Post-Erosional Volcanism

Because small-volume post-erosional melts will tend to stagnate both at the point of plume emplacement and in any existing magma chambers, this results in post-erosional volcanics being volumetrically insignificant or absent altogether. The smaller volume of post-erosional lavas relative to that of alkalic cap lavas and the similarity of alkalic cap and post-erosional isotopic compositions suggest that there is a physical limit to the degree of stagnation and contamination that plume melts can undergo if they are to be erupted. Parasitic plumes associated with the post-erosional volcanism, may be significantly smaller in volume than those associated with alkalic cap volcanism, and may therefore be capable of producing magmas throughout its lifetime that have undergone appreciably more interaction with depleted materials. Thus, isotopic compositions will overlap only the non-radiogenic end of the Sr-Pb PSB array. The lack of even less radiogenic (more MORB-like in terms of Pb) post-erosional lavas probably reflects a lower volume limit below which magmas or the plume itself wholly stagnant.

Implications for Eruptive Hiatuses

The previous analysis suggests that plume dynamics may be a controlling factor in the occurrence of erosional breaks which characterize Hawaiian volcanic evolution. Several Hawaiian volcanoes have significant time breaks between shield-building and alkalic cap volcanism and between the cessation of alkalic cap volcanism and the onset of post-erosional volcanism. Plume dynamics (Olson and Nam, 1986) suggests that these breaks could be related to the intervals between arrivals of parasitic plumes. The absence of alkalic cap and/or post-erosional activity at certain Hawaiian volcanoes implies that either parasitic instabilities do not always form, or that the volume of these instabilities is variable and smaller volume plumes may be incapable of producing eruptive activity. The latter is consistent with the suggestion (Olson and Singer, 1985) that only a small fraction of the total plume mass is ever erupted.

CONCLUSIONS

Honomanu, Kumuiliah, Kula, and Hana Formation lavas are isotopically and compositionally distinct and therefore require distinct petrogeneses. Each of these formations appears to have been derived from parental magmas having distinct trace element and major element compositions. Kumuiliah lavas were derived from parental magmas compositionally distinct from those that produced either Honomanu shield-building lavas or Kula Formation alkalic cap lavas. The Kumuiliah Formation appears to represent an early phase of post shield-building activity at Haleakala, dominated by fractionation primarily of plagioclase possibly at low pressure.

Hana Formation and younger Kula Formation lavas are isotopically indistinguishable and therefore appear to have been derived by mixing between plume and DM source components in similar proportions. Differences in major and trace element compositions for these two lava suites are due in part to differences in fractionating phase assemblage; specifically, Kula lavas are characterized by more dominant role for clinopyroxene fractionation and by fractionation of amphibole and apatite, whereas Hana lavas are dominated by olivine fractionation. The compatible trace element contents of Hana lavas also reflect the effects of magma mixing which may, be due to these magmas having undergone minimal residence in small-volume magma chambers compared to the relatively protracted storage experienced by Kula lavas. Because Kula and Hana lavas have similar H/M ratios and thus represent similar degrees of incompatible trace element enrichment, differences in major element composition and in some trace element ratios are unlikely to be the result of differences in the degree of partial melting of a compositionally uniform source.

Trace element compositions of Haleakala and other MVC lavas are consistent with Sr-Pb isotope systematics and support the existence of three distinct components in the source of these magmas. Based on trace element-isotope covariations, a primitive mantle component in the Hawaiian source cannot be ruled out. Trace element systematics for Hawaiian shield-building lavas are consistent with the Hawaiian SB having formed by

mixing between a primitive component and an enriched component. The inferred trace element composition of this enriched component suggests that it does not represent a subducted sediment component, nor is it a melt of either mantle or lithospheric material. It is possible that this enriched component reflects a metasomatized or metasomatically scavenged portion of the Hawaiian plume component.

The various stages of Hawaiian magmatism may reflect the emplacement of a large, deep-mantle plume followed by smaller associated parasitic plumes. Such a model can account for the production of primitive magmas within each of the principal stages of Hawaiian volcanism and provides a mechanism for incompatible trace element enrichment in the post shield-building stages without having to invoke transient processes such as mantle metasomatism. The parasitic/multiple plume model can also theoretically account for the periods of volcanic quiescence which separate these stages on several Hawaiian volcanoes.

ACKNOWLEDGEMENTS

We wish to thank the amazing F. T. Mullins for his expertise in the field and F. A. Frey, J. M. Rhodes, and D. Elthon for access to their laboratory facilities. Thanks also to the Oregon State University Reactor Facility for providing additional INAA Data. We are especially grateful to G. Fitton for high quality, holistic XRF trace element data. We thank D. C. Gerlach for laboratory assistance. Mahalo to Dean Yoshimura and to Ron Nagata, Hugo Huntzinger, and other personnel of the Haleakala National Park Service for their assistance and general aloha 'aina. Special thanks to D. and W. Kennedy for continuing to provide us with a holistic perspective towards the complexities of geochemical acronyms. This work was sponsored in part through National Science Foundation Grants EAR85-12167 and EAR83-20358, G.S.A. Penrose grant 3515-85, and the Rice University Department of Geology and Geophysics.

REFERENCES

- Anderson, D. L., 1981, Hotspots, Basalts and the Evolution of the Mantle: *Science* 213, p. 82-89.
- Beeson, M. H., 1976, Petrology, Mineralogy and Geochemistry of the East Molokai Volcanic Series, Hawaii: U.S.G.S. Prof. Paper 961, 55 p.
- Chen, C.-Y., 1982, Geochemical and Petrologic Systematics in Lavas from Haleakala Volcano, East Maui: Implications for the Evolution of Hawaiian Mantle: Ph.D. Thesis, M.I.T., 344 p.
- Chen, C.-Y., 1987, Lead Isotope Constraints on the Origin of Hawaiian Basalts: *Nature* 327, p. 49-52.
- Chen, C.-Y. and Frey, F. A., 1983, Origin of Hawaiian Tholeiites and Alkalic Basalt: *Nature* 302, p. 785-789.
- Chen, C.-Y. and Frey, F. A., 1985, Trace Element and Isotopic Geochemistry of Lavas from Haleakala Volcano, East Maui, Hawaii: Implications for the Origin of Hawaiian Basalts: *J. Geophys. Res.* 90, p. 8743-8768.
- Clague, D. A., 1987, Hawaiian Xenolith Populations, Magma Supply Rates, and Development of Magma Chambers: *Bull. Volcanol.* 49, p. 577-587.
- Cohen, R. S. and O'Nions, R. K., 1982, Identification of Recycled Continental Material in the Mantle from Sr, Nd and Pb Isotope Investigations: *Earth Planet. Sci. Lett.* 61, p. 73-84.
- Crough, S. T., 1978, Thermal Origin of Mid-Plate Hot Spot Swells: *Geophys. J. R. Astr. Soc.* 55, p. 451-469.
- Daly, S. F. and Raefsky, A., 1985, On the Penetration of a Hot Diapir Through a Strongly Temperature-Dependent Viscosity Medium: *Geophys. J. R. Astr. Soc.* 83, p. 657-681.
- DePaolo, D. J. and Wasserburg, G. J., 1979, Petrogenetic Mixing Models and Nd-Sr Isotopic Patterns: *Geochim. Cosmochim. Acta* 43, p. 615-627.
- Detrick, R. S. and Crough, S. T., 1978, Island Subsidence, Hot Spots, and Lithospheric Thinning: *J. Geophys. Res.* 83, p. 1236-1244.
- Dupre, B. and Allegre, C. J., 1980, Pb-Sr-Nd Isotopic Correlation and the Chemistry of the North Atlantic Mantle: *Nature* 286, p. 17-22.
- Eaton, J. P. and Murata, K. J., 1960, How Volcanoes Grow: *Science* 132, p. 925-938.
- Eissler, H. K. and Kanamori, H., 1986, Depth Estimates of Large Earthquakes on the Island of Hawaii Since 1940: *J. Geophys. Res.* 91, p. 2063-2076.
- Elthon, D., 1984, Plagioclase Buoyancy in Oceanic Basalts: Chemical Effects: *Geochim. Cosmochim. Acta* 48, p. 753-768.
- Feigenson, M. D., 1986a, Constraints on the Origin of Hawaiian Lavas: *J. Geophys. Res.* 91, p. 9383-9393.

- Feigenson, M. D., 1986b, Continental Alkali Basalts as Mixtures of Kimberlite and Depleted Mantle: Evidence from Kilbourne Hole Maar, New Mexico: *Geophys. Res. Lett.* 13, p. 965-968.
- Fodor, R. V. and Keil, K., 1979, Review of the Mineral Chemistry of Volcanic Rocks from Maui, Hawaii: in *Field Trip Guide to the Hawaiian Islands*, H.I.G. Spec. Pub., p. 93-106.
- Fodor, R. V., Keil, K. and Bunch, T. E., 1972, Mineral Chemistry of Volcanic Rocks from Maui, Hawaii: Fe-Ti Oxides: *G.S.A. Abstr. w/Progr.* 4, p. 507.
- Fodor, R. V., Keil, K. and Bunch, T. E. 1975, Contributions to the Mineral Chemistry of Hawaiian Rocks IV. Pyroxenes in Rocks from Haleakala and West Maui volcanoes, Maui, Hawaii: *Contrib. Mineral. Petrol.* 50, p. 173-195.
- Fodor, R. V., Keil, K. and Bunch, T. E., 1977, Contributions to the Mineral Chemistry of Hawaiian Rocks. VI. Olivines in Rocks from Haleakala and West Maui Volcanoes, Maui, Hawaii: *Pac. Sci.* 31, p. 299-308.
- Frey, F. A., Green, D. H., and Roy, S. D., 1978, Integrated Models of Basalt Petrogenesis: A Study of Quartz Tholeiites to Olivine Melilitites from South Eastern Australia Utilizing Geochemical and Experimental Petrological Data: *J. Petrol.* 19, p. 463-513.
- Griffin, W. L. and Murthy, V. R., 1969, Distribution of K, Rb, Sr and Ba in Some Minerals Relevant to Basalt Genesis: *Geochim. Cosmochim. Acta* 33, p. 1389-1414.
- Harland, W. B., Cox, A. V., Llewellyn, P. G., Pickton, C. A. G., Smith, A. G. and Walters, R., 1982, *A Geologic Time Scale*, Cambridge University Press, 131 p.
- Hegner, E., Unruh, D. and Tatsumoto, M., 1986, Nd-Sr-Pb Isotope Constraints on the Sources of West Maui Volcano, Hawaii: *Nature* 319, p. 478-480.
- Henderson, P. 1984, General Geochemical Properties and Abundances of the Rare Earth Elements: in *Rare Earth Element Geochemistry* (P. Henderson, ed.), p. 1-32.
- Higuchi, H. and Nagasawa, H., 1969, Partition of Trace Elements Between Rock Forming Minerals and the Host Volcanic Rocks: *Earth Planet. Sci. Lett.* 7, p. 281-287.
- Hofmann, A. W., 1987, Nb in Hawaiian Magmas: Constraints on Source Composition and Evolution: *Chem. Geol.* 57, p. 17-30.
- Hofmann, A. W. and White, W. M., 1980, The Role of Subducted Oceanic Crust in Mantle Evolution: *Carn. Inst. Wash. Ybook* 79, p. 477-483.
- Hofmann, A. W. and White, W. M., 1983, Ba, Rb and Cs in the Earth's Mantle: *Z. Naturforsch.* 38a, p. 256-266.
- Hofmann, A. W., Jochum, K.P., Seufert, M. and White, W. M., 1986, Nb and Pb in Oceanic Basalts: New Constraints on Mantle Evolution: *Earth Planet. Sci. Lett.* 79, p. 33-45.
- Hole, M. J., Saunders, A. D., Marriner, G. F. and Tarney, J., 1984, Subduction of Pelagic Sediments: Implications for the Origin of Ce-Anomalous Basalts from the Mariana Islands: *J. Geol. Soc. London* 141, p. 453-472.

- Hughes, S. S. and Schmitt, R. A., Confirmation of Zr-Hf Fractionation in Lunar Petrogenesis--An Interim Report: *Lunar Planet. Sci.* 15, p. 385-386.
- Ila, P. and Frey, F. A., 1984, Utilization of Neutron Activation Analysis in the Study of Geologic Materials: *Atomkernenergie Kerntechnik* 44, p. 710-716.
- Irving, A. J. and Frey, F. A., 1984, Trace Element Abundance in Megacrysts and their Host Basalts: Constraints on Partition Coefficients and Megacryst Genesis: *Geochim. Cosmochim. Acta* 48, p. 1201-1221.
- Keil, K., Fodor, R. V. and Bunch, T. E., 1972, Contributions to the Mineral Chemistry of Hawaiian Rocks. II. Feldspars and Interstitial Material in Rocks from Haleakala and West Maui Volcanoes, Maui, Hawaii: *Contrib. Mineral. Petrol.* 37, p. 253-275.
- Knutson, J. and Green, T. H., 1975, Experimental Duplication of a High-Pressure Megacryst/Cumulate Assemblage in a Near-Saturated Hawaiiite: *Contrib. Mineral. Petrol.* 52, p. 121-132.
- Lanphere, M. A. and Frey, F. A., 1987, Geochemical Evolution of Kohala Volcano, Hawaii: *Contrib. Mineral. Petrol.* 95, p. 100-113.
- Leeds, A. R., 1975, Lithospheric thickness in the Western Pacific: *Phys. Earth Planet. Int.* 11, p. 61-64.
- Lemarchand, F. Villemant, B. and Calas, G., 1987, Trace Element Distribution Coefficients in Alkaline Series: *Geochim. Cosmochim. Acta* 51, p. 1071-1081.
- LeRoex, A. P. and Erlank, A. J., 1982, Quantitative Evaluation of Fractional Crystallization in Bouvet Island Lavas: *J. Volc. Geoth. Res.* 13, p. 309-338.
- Li, Y.-H., 1982, A Brief Discussion on the Mean Oceanic Residence Time of Elements: *Geochim. Cosmochim. Acta* 46, p. 2671-2675.
- Lindstrom, D. J., 1976, Experimental Study of the Partitioning of the Transition Metals Between Clinopyroxene and Coexisting Silicate Liquids: Ph.D. Thesis, University of Oregon.
- Macdonald, G. A., 1942, Petrography of Maui: *Hawaii Div. Hydrogr. Bull.* 7, p. 275-334.
- Macdonald, G. A., 1978, Geologic Map of the Crater Section of Haleakala National Park, Maui, Hawaii: *U.S.G.S. Misc. Inv. Ser. Map* I-1088.
- Macdonald, G. A. and Katsura, T., 1964, Chemical Composition of Hawaiian Lavas: *J. Petrol.* 5, p. 82-133.
- Macdonald, G. A. and Powers, H. A., 1946, Contribution to the Petrography of Haleakala Volcano, Hawaii: *G.S.A. Bull.* 57, p. 115-124.
- Macdonald, G. A. and Powers, H. A., 1968, A Further Contribution to the Petrology of Haleakala Volcano, Hawaii: *G.S.A. Bull.* 79, p. 877-888.
- Macdonald, G. A., Abbott, A. T. and Peterson, F. L., 1983, *Volcanoes in the Sea: The Geology of Hawaii* (2nd Edition), University of Hawaii Press, 517 p.

- Mahood, G. A. and Baker, D. R., 1986, Experimental Constraints on Depths of Fractionation of Mildly Alkalic Basalts and Associated Felsic Rocks: Pantelleria, Strait of Sicily: *Contrib. Mineral. Petrol.* 93, p. 251-264.
- McDougall, I., 1964, Potassium-Argon Ages from Lavas of the Hawaiian Islands: *Geol. Soc. Am. Bull.* 75, p. 107-128.
- McKay, G., Wagstaff, J. and Yang, S.-R., 1986, Zirconium, Hafnium, and Rare Earth Element Partition Coefficients for Ilmenite and Other Minerals in High-Ti Lunar Mare Basalts: An Experimental Study: *J. Geophys. Res.* 91, p. D229-D237.
- Menzies, M. A. and Murthy, V. R., 1980, Mantle Metasomatism as a Precursor to the Genesis of Alkaline Magmas - Isotopic Evidence: *Am. J. Sci.* 280-A, p. 622-638.
- Morgan, W. J., 1971, Convection Plumes in the Lower Mantle: *Nature* 230, p. 42-43.
- Nakamura, Y. Fujimaki, H., Nakamura, N. and Tatsumoto, M., 1986, Hf, Zr, and REE Partition Coefficients Between Ilmenite and Liquid: Implications for Lunar Petrogenesis: *J. Geophys. Res.* 91, p. D239-D250.
- Naughton, J. J., Macdonald, G. A. and Greenberg, V. A., 1980, Some Additional Potassium-Argon Ages of Hawaiian Rocks: The Maui Volcanic Complex of Molokai, Maui, Lanai and Kahoolawe: *J. Volc. Geoth. Res.* 7, p. 339-355.
- Nixon, P. H., Boyd, F. R. and Bockor, N. Z., 1983, East Griqualand Kimberlites: *Trans. Geol. Soc. S. Africa* 86, p. 221-236.
- Olson, P. and Nam, I. S., 1986, Formation of Seafloor Swells by Mantle Plumes: *J. Geophys. Res.* 91, p. 7181-7191.
- Olson, P. and Singer, H. A., 1985, Creeping Plumes: *J. Fluid Mech.* 158, p. 511-531.
- O'Nions, R. K., Hamilton, P. J. and Evensen, N.M., 1977, Variations in $^{143}\text{Nd}/^{144}\text{Nd}$ and $^{87}\text{Sr}/^{86}\text{Sr}$ Ratios in Oceanic Basalts: *Earth Planet. Sci. Lett.* 34, p. 13-22.
- Oostdam, B. L., 1965, Age of Lava Flows on Haleakala, Maui, Hawaii: *G.S.A. Bull.* 76, p. 393-394.
- Palacz, Z. A. and Saunders, A. D., 1986, Coupled Trace Element and Isotope Enrichment in the Cook-Austral-Samoa Islands, Southwest Pacific: *Earth Planet. Sci. Lett.* 79, p. 270-280.
- Pasteris, J. D., 1984, Kimberlites: Complex Mantle Melts: *Ann. Rev. Earth Planet. Sci.* 12, p. 133-153.
- Pearce, J. A. and Norry, M. J., 1979, Petrogenetic Implications of Ti, Zr, Y, and Nb Variations in Volcanic Rocks: *Contrib. Mineral. Petrol.* 69, p. 33-47.
- Ribe, N. M., 1983, Diapirism in the Earth's Mantle: Experiments on the Motion of a Hot Sphere in a Fluid with Temperature-Dependent Viscosity: *J. Volc. Geoth. Res.* 16, p. 221-245.
- Roden, M. F., Frey, F. A. and Clague, D. A., 1984, Geochemistry of Tholeiitic and Alkalic Lavas from the Koolau Range, Oahu, Hawaii: Implications for Hawaiian Volcanism: *Earth Planet. Sci. Lett.* 69, p. 141-158.

- Roden, M. F. and Murthy, V. R., 1985, Mantle Metasomatism: *Ann. Rev. Earth Planet. Sci.* 13, p. 269-296.
- Shimizu, H., 1980, Experimental Study on Rare-Earth Element Partitioning in Minerals Formed at 20 and 30 Kb for Basaltic Systems: *Geochem. J.* 14, p. 185-202.
- Staudigel, H., Zindler, A., Hart, S. R., Leslie, T., Chen, C.-Y. and Clague, D. A., 1984, The Isotope Systematics of a Juvenile Intraplate Volcano: Pb, Nd, and Sr Isotope ratios of Basalts from Loihi Seamount, Hawaii: *Earth Planet. Sci. Lett.* 69, p. 13-29.
- Stearns, H. T., 1946, Geology of the Hawaiian Islands: *Hawaii Div. Hydrogr. Bull.* 8, 106 p.
- Stearns, H. T. and Macdonald, G. A., 1942, Geology and Ground-Water Resources of the Island of Maui, Hawaii: *Hawaii Div. Hydrogr. Bull.* 7, 344 p.
- Stille, P., Unruh, D. M. and Tatsumoto, M., 1983, Pb, Sr, Nd and Hf Isotopic Evidence of Multiple Sources for Oahu, Hawaii Basalts: *Nature* 304, p. 25-29.
- Stille, P., Unruh, D. M. and Tatsumoto, M., 1986, Pb, Sr, Nd, and Hf Isotopic Constraints on the Origin of Hawaiian Basalts and Evidence for a Unique Mantle Source: *Geochim. Cosmochim. Acta* 50, p. 2303-2319.
- Sun, S.-S., 1980, Lead Isotope Study of Young Volcanic Rocks from Mid-Ocean Ridges, Ocean Islands and Island Arcs: *Phil. Trans. R. Soc. London A*-297, p. 409-445.
- Tarney, J. Wood, D. A., Saunders, A. D., Cann, J. R. and Varet, J., 1980, Nature of Mantle Heterogeneity in the North Atlantic: Evidence from Deep Sea Drilling: *Phil. Trans. R. Soc. London A*297, p. 179-202.
- Tatsumoto, M., 1978, Isotopic Composition of Lead in Oceanic Basalt and Its Implication to Mantle evolution: *Earth Planet. Sci. Lett.* 38, p. 62-87.
- Tatsumoto, M., Hegner, E. and Unruh, D. M., 1987, Origin of the West Maui Volcanic Rocks Inferred from Pb, Sr, and Nd Isotopes and a Multicomponent Model for Oceanic Basalt: *U.S.G.S. Prof. Paper* 1350, p. 723-744.
- Tatsumoto, M., Unruh, D. M., Stille, P. and Fujimaki, H., 1984, Pb, Sr, and Nd Isotopes in Oceanic Island Basalts: *Proc. 27th Int. Geol. Cong.* 11, p. 485-501.
- Thompson, R. N., 1974, Primary Basalts and Magma Genesis. I. Skye, North-West Scotland: *Contrib. Mineral. Petrol.* 45, p. 317-341.
- Vidal, P., Chauvel, C. and Brousse, R., 1984, Large Mantle Heterogeneity Beneath French Polynesia: *Nature* 307, p. 536-538.
- Villemant, B., Jaffrezic, H., Joron, J.-L. and Treuil, M., 1981, Distribution Coefficients of Major and Trace Elements: Fractional Crystallization in the Alkali Basalt Series of Chaîne des Puys (Massif Central, France): *Geochim. Cosmochim. Acta* 45, p. 1997-2016.
- Von Herzen, R. P., Detrick, R. S., Crough, S. T., Epp, D. and Fehn, U., 1982, Thermal Origin of the Hawaiian Swell: Heat Flow Evidence and Thermal Models: *J. Geophys. Res.* 87, p. 6711-6723.

- Watson, E. B. and Green, T. H., 1981, Apatite/Liquid Partition Coefficients for the Rare Earth Elements and Strontium: *Earth Planet. Sci. Lett.* 56, p. 405-421.
- Watts, A. B., 1978, An Analysis of Isostasy in the World's Oceans 1. Hawaiian-Emperor Seamount Chain: *J. Geophys. Res.* 83, p. 5989-6004.
- Weaver B. L., Wood, D. A., Tarney, J. and Joron J. L., 1986, Role of Subducted Sediment in the Genesis of Ocean-Island Basalts: Geochemical Evidence from South Atlantic Ocean Islands: *Geology* 14, p. 275-278.
- West, H. B. and Leeman, W. P., 1987a, Isotopic Evolution of Lavas from Haleakala Crater, Hawaii: *Earth Planet. Sci. Lett.* 84, p. 211-225.
- West, H. B. and Leeman, W. P. 1987b, Petrology and Geochemistry of Lavas from Haleakala Crater, Hawaii: An Overview: in *Field Trip Guide to Maui* (J. S. Sinton, ed.), 83rd G.S.A. Cordilleran Section Meeting, Hilo, p. 45-65.
- West, H. B. and Leeman, W. P., 1987c, Open System Magma Chamber Processes: Trace Element Systematics of Alkalic Cap Lavas from Haleakala Crater, Hawaii: in Abstract Volume, Hawaii Symp. on How Volcanoes Work, Hilo, Hawaii, p. 266.
- West, H. B., Gerlach, D. C., Leeman, W. P. and Garcia, M. O., 1987, Isotopic Constraints on the Origin of Hawaiian Magmas from the Maui Volcanic Complex, Hawaii: *Nature* 330, p. 216-220.
- West, H. B., Garcia, M. O., Frey, F. A. and Kennedy, A., 1988, Evolution of Alkalic Cap Lavas: Mauna Kea Volcano, Hawaii: *Contrib. Mineral. Petrol.*, in press.
- White, W. M., 1985, Sources of Oceanic Basalts: Radiogenic Isotopic Evidence: *Geology* 13, p. 115-118.
- White, W. M. and Hofmann, A. W., 1982, Sr and Nd Isotope Geochemistry of Oceanic Basalts and Mantle Evolution: *Nature* 296, p. 821-825.
- Whitehead, J. A., 1982, Instabilities of Fluid Conduits in a Flowing Earth - Are Plates Lubricated by the Asthenosphere?: *Geophys. J. R. Astron. Soc.* 70, p. 415-433.
- Whittaker, E. J. W. and Muntus, R., 1970, Ionic Radii for Use in Geochemistry: *Geochim. Cosmochim. Acta* 34, p. 945-956.
- Wyllie, P. J., 1980, The Origin of Kimberlite: *J. Geophys. Res.* 85, p. 6902-6910.

Table 1. Distribution of rock types at Haleakala. Numbers refer to % of rock type within each formation. Numbers in parentheses refer to the number of samples. Alk bas = alkalic basalt, ank = ankaramite.

<u>Formation</u>	<u>tholeiite</u>	<u>alk bas</u>	<u>hawaiite</u>	<u>mugearite</u>	<u>trachyte</u>	<u>basanitoid</u>	<u>ank</u>	<u>samples</u>	<u>references</u>
Honomanu	95.0(19)	5.0(1)	-	-	-	-	-	20	1,2
Kumuliiahi	-	50.0(7)	50.0(7)	-	-	-	-	14	1,3
Kula	-	20.2(17)	56.0(47)	13.1(11)	1.2(1)	8.3(7)	1.2(1)	84	1,2,4,5
Hana	-	5.0(3)	21.7(13)	-	-	68.3(41)	5.0(3)	60	1,2,5,6,7

References: (1) this study; (2) Chen, 1982; (3) Macdonald, 1978; (4) Macdonald and Katsura, 1964; (5) Macdonald and Powers, 1968; (6) Brill, 1975; (7) Horton, 1977.

Table 2a. Major and trace element data for Honomanu Formation lavas from Honomanu Valley. Major element data normalized to 100 % on an anhydrous basis with $\text{Fe}^{2+}/(\text{Fe}^{2+}+\text{Fe}^{3+})$ set to 0.90.

	HHM-1	HHM-2	HHM-3	HHM-4A	HHM-4B	HHM-5	HHM-6	HHM-7	HHM-8
SiO ₂	47.71	48.61	47.49	48.72	48.69	47.77	48.40	48.10	48.65
Al ₂ O ₃	14.81	15.10	15.04	13.77	14.77	14.79	13.86	14.19	15.52
FeO*	12.19	12.33	12.51	13.56	12.64	12.18	13.82	12.52	12.34
MgO	8.09	7.39	8.06	6.40	7.81	8.01	10.05	8.04	6.82
CaO	10.48	10.49	10.13	10.77	10.26	10.44	8.95	10.56	10.40
Na ₂ O	2.49	2.34	2.42	2.10	2.03	2.54	2.07	2.55	2.57
K ₂ O	0.31	0.14	0.40	0.40	0.33	0.37	0.16	0.32	0.28
P ₂ O ₅	0.38	0.32	0.37	0.39	0.32	0.39	0.27	0.34	0.31
TiO ₂	3.17	2.91	3.20	3.47	2.76	3.14	2.59	2.99	2.73
MnO	0.17	0.17	0.17	0.20	0.18	0.17	0.16	0.18	0.18
Rb	-	-	-	1	1	-	-	3	-
Sr	478	364	464	320	331	473	330	365	380
Ba	179	119	156	134	110	155	117	87	114
La	19	17	24	24	18	17	18	17	13
Ce	39	45	47	42	34	45	33	37	36
Nd	26	25	29	29	18	26	19	22	26
Y	31	32	31	39	31	31	29	33	30
Nb	17	14	15	16	13	16	12	14	12
Zr	212	185	210	223	174	208	169	196	170
Ni	188	178	190	100	201	183	354	183	130
V	313	324	306	365	302	303	290	317	293
Cr	287	289	294	275	296	273	354	270	226
Sc	28	28	32	33	27	28	25	32	25
Cu	62	81	57	85	70	60	68	79	84
Zn	121	119	156	135	119	119	126	113	110
Pb(ID)	1.394	-	-	-	-	-	-	-	-

Table 2a (cont). Major and trace element data for Honomanu Formation lavas from Honomanu Valley.

	HHM-9
SiO ₂	48.67
Al ₂ O ₃	15.44
FeO*	12.38
MgO	6.76
CaO	10.67
Na ₂ O	2.44
K ₂ O	0.29
P ₂ O ₅	0.28
TiO ₂	2.67
MnO	0.19
Rb	1
Sr	369
Ba	108
La	15
Ce	37
Nd	27
Y	30
Nb	12
Zr	168
Ni	136
V	297
Cr	238
Sc	28
Cu	78
Zn	113
Pb(TD)	-

Table 2b. Major and trace element data for Kumuilihi Formation lavas from Haleakala Crater. Major element data normalized to 100 % on an anhydrous basis with $\text{Fe}^{2+}/(\text{Fe}^{2+}+\text{Fe}^{3+})$ set to 0.90.

	HKU-1	HKU-2	HKU-3	HKU-4	HKU-5	HKU-6	HKU-7	HKU-8	HKU-9
SiO ₂	48.23	48.28	47.90	47.96	48.13	48.29	47.90	48.42	48.82
Al ₂ O ₃	17.13	17.20	14.34	15.23	15.34	16.43	14.61	16.77	14.48
FeO*	11.56	11.34	13.45	12.69	12.49	11.80	13.41	11.49	12.61
MgO	4.04	4.21	4.56	4.45	4.43	3.99	4.05	4.00	4.55
CaO	10.77	11.02	10.25	10.82	10.70	10.54	9.90	10.49	9.80
Na ₂ O	2.95	2.76	3.07	2.95	2.99	3.11	3.26	3.11	3.50
K ₂ O	0.96	0.92	1.13	1.02	1.03	1.03	1.26	1.10	1.22
P ₂ O ₅	0.49	0.47	0.59	0.54	0.55	0.58	0.66	0.56	0.63
TiO ₂	3.51	3.45	4.28	3.95	3.93	3.87	4.54	3.72	3.98
MnO	0.17	0.17	0.20	0.19	0.19	0.17	0.20	0.17	0.20
K	-	7666	-	-	-	-	10274	-	-
Cs	-	0.306	-	-	-	-	0.152	-	-
Rb(ID)	-	17.23	-	-	-	-	23.95	-	-
Rb(XRF)	18	16	20	14	13	13	21	17	19
Sr(ID)	-	762	-	-	-	-	713	-	-
Sr(XRF)	747	768	655	711	711	763	699	763	702
Ba(ID)	-	318	-	-	-	-	373	-	-
Ba(XRF)	310	384	397	366	353	375	445	371	410
La(XRF)	27	27	37	27	29	30	28	29	33
Ce(XRF)	66	79	73	68	76	74	85	67	97
Nd(XRF)	40	40	43	40	46	46	58	41	50
La	25.8	25.0	-	-	28.2	-	33.4	-	-
Ce	66.1	61.6	-	-	69.8	-	83.8	-	-
Nd	38.7	36.3	-	-	40.4	-	48.7	-	-
Sm	8.81	8.71	-	-	9.98	-	11.70	-	-
Eu	2.89	3.16	-	-	3.21	-	3.81	-	-
Tb	1.06	1.22	-	-	1.33	-	1.52	-	-
Ho	1.5	2.1	-	-	1.6	-	2.0	-	-
Yb	2.28	2.09	-	-	2.46	-	2.88	-	-
Lu	0.33	0.31	-	-	0.32	-	0.37	-	-
Y	32	31	37	35	36	35	41	33	39
Th	1.8	1.9	-	-	2.0	-	2.7	-	-
Ta	1.8	2.0	-	-	2.5	-	2.5	-	-
Nb	27	25	33	28	31	31	36	29	34
Zr	258	244	315	275	285	297	351	280	328
Hf	6.1	6.2	-	-	7.2	-	8.5	-	-
Ni	49	49	45	45	45	37	40	41	36
V	311	292	379	347	358	322	356	301	318
Cr(INAA)	61	71	-	-	60	-	29	-	-
Cr(XRF)	59	58	59	51	55	26	26	33	12
Sc(INAA)	23.2	25.7	-	-	25.5	-	24.9	-	-
Sc(XRF)	23	22	26	27	20	20	22	22	20
Co	49.2	50.9	-	-	49.4	-	50.4	-	-
Cu	88	80	120	105	104	91	110	83	79
Zn	112	100	134	111	119	114	139	106	117
Pb(ID)	1.343	-	-	-	-	-	-	-	-

Table 2b (cont). Kumuiliahi Formation major and trace element data.

HKU-10	
SiO ₂	47.86
Al ₂ O ₃	15.65
FeO*	12.33
MgO	4.53
CaO	10.70
Na ₂ O	3.11
K ₂ O	1.00
P ₂ O ₅	0.56
TiO ₂	3.89
MnO	0.17
K	8297
Cs	0.062
Rb(ID)	15.80
Rb(XRF)	13
Sr(ID)	762
Sr(XRF)	739
Ba(ID)	-
Ba(XRF)	349
La(XRF)	26
Ce(XRF)	71
Nd(XRF)	42
La	27.3
Ce	73.6
Nd	43.2
Sm	9.69
Eu	3.37
Tb	1.06
Ho	1.51
Yb	2.49
Lu	0.33
Y	34
Th	2.0
Ta	1.9
Nb	29
Zr	294
Hf	7.1
Ni	47
V	339
Cr(INAA)	47
Cr(XRF)	48
Sc(INAA)	24.0
Sc(XRF)	30
Co	49.1
Cu	98
Zn	124
Pb(ID)	1.839
Density	2.732
Viscosity	259

Table 2c. Major and trace element data for Kula Formation lavas. Major element data normalized to 100 % on an anhydrous basis with $\text{Fe}^{2+}/(\text{Fe}^{2+}+\text{Fe}^{3+})$ set to 0.90.

	HK-46	HK-47	HK-61	HK-62	HK-48
SiO ₂	48.41	50.04	49.76	49.31	52.29
Al ₂ O ₃	16.22	16.37	14.09	14.27	17.53
FeO*	11.96	10.88	12.66	12.74	9.12
MgO	4.71	3.85	5.32	5.41	3.58
CaO	8.31	7.94	10.12	10.32	6.26
Na ₂ O	4.34	4.69	2.80	2.72	6.31
K ₂ O	1.33	1.66	0.76	0.70	2.34
P ₂ O ₅	0.57	0.79	0.44	0.44	0.58
TiO ₂	3.73	3.33	3.67	3.70	1.60
MnO	0.22	0.26	0.18	0.18	0.24
B	3.8	-	-	-	3.1
K	11093	-	-	-	19442
Cs	0.342	-	-	-	0.631
Rb(ID)	30.55	-	-	-	65.46
Rb(XRF)	29	35	10	-	65
Sr(ID)	844	-	-	-	928
Sr(XRF)	833	972	474	-	918
Ba(ID)	488	-	-	-	-
Ba(XRF)	518	683	208	-	1022
La(XRF)	32	48	23	-	60
Ce(XRF)	90	111	51	-	136
Nd(XRF)	49	57	33	-	54
La	36.9	-	-	-	61.2
Ce	85.8	-	-	-	124.2
Nd	43.4	-	-	-	49.9
Sm	9.52	-	-	-	9.56
Eu	3.09	-	-	-	2.97
Tb	1.08	-	-	-	1.27
Ho	1.69	-	-	-	1.60
Yb	2.47	-	-	-	2.57
Lu	0.35	-	-	-	0.37
Y	33	39	37	-	33
Zr	280	325	243	-	401
Hf	6.4	-	-	-	8.1
Nb	46	58	20	-	77
Ta	3.3	-	-	-	5.1
Th	3.3	-	-	-	6.9
Ni	3	3	69	-	45
V	196	145	355	-	64
Cr(INAA)	2	-	-	-	135
Cr(XRF)	1	1	97	-	111
Sc(INAA)	13.1	-	-	-	6.4
Sc(XRF)	13	8	34	-	6
Co	39.8	-	-	-	29.2
Cu	9	7	99	-	13
Zn	109	124	128	-	123
Pb(ID)	-	-	-	-	-

Table 2d. Major and trace element data for Hana Formation lavas from Haleakala Crater. Major element data normalized to 100 % on an anhydrous basis with $\text{Fe}^{2+}/(\text{Fe}^{2+}+\text{Fe}^{3+})$ set to 0.90.

	HH-1	HH-2	HH-3	HH-4	HH-5	HH-6	HH-7	HH-8	HH-9
SiO ₂	44.34	47.03	45.52	46.93	44.82	44.84	44.41	44.39	44.16
Al ₂ O ₃	12.66	15.71	14.42	15.85	13.11	12.97	12.90	13.99	13.74
FeO*	13.49	12.02	12.65	12.13	13.21	13.19	13.71	13.57	13.82
MgO	9.70	5.74	7.32	3.91	9.26	9.65	9.01	6.59	6.70
CaO	11.89	9.47	10.79	9.57	11.78	11.88	11.93	11.45	11.29
Na ₂ O	2.77	4.21	3.71	4.03	2.92	2.67	2.91	3.67	3.83
K ₂ O	0.99	1.58	1.35	1.44	0.96	0.94	0.98	1.48	1.51
P ₂ O ₅	0.41	0.66	0.58	0.59	0.46	0.43	0.49	0.57	0.58
TiO ₂	3.33	3.15	3.23	3.13	3.06	3.01	3.23	3.86	3.92
MnO	0.20	0.22	0.21	0.22	0.20	0.20	0.20	0.21	0.22
B	-	-	3.9	-	-	-	-	-	-
K	-	-	11322	-	-	-	-	-	-
Cs	-	-	0.396	-	-	-	-	-	-
Rb(ID)	-	-	32.53	-	-	-	-	-	-
Rb(XRF)	23	36	30	32	22	22	22	32	32
Sr(ID)	-	-	874	-	-	-	-	-	-
Sr(XRF)	610	888	840	879	621	612	671	849	847
Ba(ID)	-	-	625	-	-	-	-	-	-
Ba(XRF)	487	698	657	666	497	462	483	645	659
La(XRF)	31	41	33	38	30	34	32	39	40
Ce(XRF)	65	94	83	74	65	63	67	93	84
Nd(XRF)	31	50	40	42	35	34	36	44	45
La	-	-	36.3	38.0	-	28.0	-	-	-
Ce	-	-	82.7	81.2	-	64.1	-	-	-
Nd	-	-	40.2	39.1	-	31.8	-	-	-
Sm	-	-	8.35	8.58	-	7.27	-	-	-
Eu	-	-	2.88	2.88	-	2.49	-	-	-
Tb	-	-	1.11	1.01	-	0.55	-	-	-
Ho	-	-	2.30	1.35	-	1.11	-	-	-
Yb	-	-	2.00	2.24	-	1.73	-	-	-
Lu	-	-	0.28	0.31	-	0.25	-	-	-
Y	25	30	28	28	26	26	26	29	27
Th	-	-	3.5	3.4	-	2.8	-	-	-
Ta	-	-	3.6	3.7	-	2.5	-	-	-
Nb	36	53	48	50	37	36	38	51	52
Zr	184	259	216	229	181	181	190	251	252
Hf	-	-	5.3	5.4	-	4.7	-	-	-
Ni	129	44	94	53	102	108	115	59	64
V	377	235	309	255	358	357	406	409	419
Cr(INAA)	-	-	274	136	-	401	-	-	-
Cr(XRF)	384	112	259	122	327	346	305	71	19
Sc(INAA)	-	-	23.1	17.6	-	31.1	-	-	-
Sc(XRF)	30	10	22	16	30	26	24	22	19
Co	-	-	74.4	61.6	-	81.6	-	-	-
Cu	42	27	70	41	31	37	45	72	73
Zn	106	117	108	110	103	103	114	112	122

Table 2d (cont). Major and trace element data for Hana Formation lavas from Haleakala Crater.

	HH-10	HH-11	HH-12	HH-13	HH-14	HH-15	HH-16	HH-17	HH-18
SiO ₂	48.88	44.12	44.52	44.49	48.86	46.66	46.78	47.10	47.06
Al ₂ O ₃	17.58	11.67	13.94	14.03	17.52	16.81	16.86	16.78	17.15
FeO*	10.66	13.77	13.70	13.63	10.73	12.16	11.81	12.14	11.41
MgO	3.66	11.26	6.74	6.56	3.63	5.23	5.23	5.08	4.43
CaO	8.02	12.36	11.08	11.21	8.03	8.92	8.64	8.59	8.64
Na ₂ O	5.17	2.20	3.69	3.74	5.21	4.19	4.65	4.09	4.70
K ₂ O	1.94	0.79	1.49	1.49	1.95	1.55	1.60	1.90	2.04
P ₂ O ₅	0.78	0.35	0.59	0.61	0.81	0.57	0.57	0.59	0.79
TiO ₂	2.88	3.06	3.82	3.80	2.86	3.51	3.47	3.33	3.35
MnO	0.24	0.20	0.21	0.22	0.23	0.21	0.20	0.22	0.24
B	-	-	-	-	-	-	-	-	3.8
K	-	6667	-	-	-	-	-	-	16923
Cs	-	0.230	-	-	-	-	-	-	0.506
Rb(ID)	-	19.56	-	-	-	-	-	-	50.08
Rb(XRF)	47	18	31	32	46	34	34	39	47
Sr(ID)	-	566	-	-	-	-	-	-	1199
Sr(XRF)	1080	551	836	830	1076	1031	1033	987	1159
Ba(ID)	-	-	-	-	-	-	-	-	883
Ba(XRF)	834	457	649	649	851	761	784	775	905
La(XRF)	46	27	37	41	49	38	40	42	51
Ce(XRF)	116	48	81	89	122	84	97	98	121
Nd(XRF)	53	26	43	46	55	43	44	50	57
La	-	25.2	-	-	52.7	-	40.8	-	54.8
Ce	-	58.9	-	-	116.2	-	92.2	-	122.8
Nd	-	29.9	-	-	53.3	-	44.0	-	57.4
Sm	-	6.81	-	-	10.78	-	9.29	-	11.57
Eu	-	2.37	-	-	3.40	-	3.02	-	3.67
Tb	-	0.78	-	-	1.19	-	1.14	-	1.38
Ho	-	0.90	-	-	1.00	-	1.70	-	2.20
Yb	-	1.77	-	-	2.28	-	2.14	-	2.39
Lu	-	0.23	-	-	0.34	-	0.32	-	0.31
Y	33	25	27	27	35	30	31	32	33
Th	-	2.8	-	-	5.6	-	3.9	-	5.3
Ta	-	2.3	-	-	4.4	-	3.7	-	4.8
Nb	66	29	50	51	67	53	54	55	71
Zr	320	172	243	243	323	237	245	250	326
Hf	-	4.7	-	-	6.6	-	5.3	-	7.1
Ni	4	146	64	57	4	14	13	8	3
V	123	404	394	394	124	217	213	211	193
Cr(INAA)	-	512	-	-	-	-	24	-	3
Cr(XRF)	3	456	141	128	2	20	19	4	-
Sc(INAA)	-	33.6	-	-	6.3	-	13.6	-	8.5
Sc(XRF)	7	30	20	20	-	14	17	10	5
Co	-	85.8	-	-	43.1	-	47.7	-	48.7
Cu	10	35	54	56	10	28	24	25	14
Zn	115	102	118	115	124	100	108	111	123

Table 2d (cont). Major and trace element data for Hana Formation lavas from Haleakala Crater.

	HH-19	HH-20	HH-21	HH-22	HH-23	HH-24	HH-25	HH-26	HH-27
SiO ₂	44.11	44.79	47.07	47.19	44.10	45.40	45.77	46.17	44.21
Al ₂ O ₃	14.66	14.40	16.46	15.20	12.87	15.22	15.66	15.29	15.03
FeO*	14.25	14.66	12.31	12.60	13.60	12.44	12.94	13.00	13.42
MgO	5.86	6.55	5.29	5.96	9.77	6.98	5.96	5.91	7.44
CaO	10.28	11.02	9.14	9.62	12.16	10.39	9.99	9.99	11.72
Na ₂ O	4.06	2.93	3.65	3.74	2.41	3.99	3.86	3.47	2.99
K ₂ O	1.64	1.04	1.65	1.48	1.14	1.37	1.51	1.54	1.05
P ₂ O ₅	0.62	0.46	0.58	0.54	0.38	0.53	0.55	0.61	0.48
TiO ₂	4.04	3.69	3.43	3.25	3.14	3.25	3.34	3.58	3.25
MnO	0.23	0.22	0.21	0.21	0.20	0.21	0.21	0.21	0.20
B	-	2.0	-	-	-	-	-	-	-
K	-	8670	-	-	-	-	-	12796	-
Cs	-	0.333	-	-	-	-	-	0.445	-
Rb(ID)	-	25.64	-	-	-	-	-	37.57	-
Rb(XRF)	36	23	34	36	21	31	36	34	27
Sr(ID)	981	731	-	-	-	-	-	955	-
Sr(XRF)	942	702	984	840	607	867	836	926	706
Ba(ID)	-	534	-	-	-	-	-	-	-
Ba(XRF)	726	555	777	724	470	670	770	697	562
La(XRF)	32	28	37	38	28	38	43	36	34
Ce(XRF)	99	74	89	83	65	79	80	90	69
Nd(XRF)	51	35	42	45	36	40	39	51	29
La	43.9	31.9	-	-	29.3	-	-	40.7	-
Ce	97.8	70.9	-	-	64.1	-	-	91.0	-
Nd	47.0	35.3	-	-	32.9	-	-	43.7	-
Sm	10.06	8.16	-	-	7.69	-	-	9.21	-
Eu	3.16	2.84	-	-	2.53	-	-	3.03	-
Tb	1.10	0.97	-	-	1.03	-	-	1.08	-
Ho	1.27	1.22	-	-	0.99	-	-	1.90	-
Yb	2.07	2.02	-	-	1.68	-	-	2.25	-
Lu	0.25	0.28	-	-	0.22	-	-	0.31	-
Y	28	29	32	30	26	28	29	31	28
Th	4.1	3.3	-	-	2.5	-	-	4.3	-
Ta	4.0	2.9	-	-	2.4	-	-	3.5	-
Nb	58	42	54	54	36	49	51	54	42
Zr	267	198	244	231	199	222	228	243	209
Hf	6.3	5.0	-	-	4.8	-	-	6.0	-
Ni	34	56	13	54	128	83	46	42	92
V	388	447	229	330	407	318	292	299	404
Cr(INAA)	4	28	-	-	430	-	-	67	-
Cr(XRF)	3	23	6	74	406	224	49	58	199
Sc(INAA)	16.2	23.1	-	-	30.2	-	-	18.7	-
Sc(XRF)	14	25	18	23	31	24	19	19	25
Co	73.6	71.8	-	-	72.2	-	-	58.4	-
Cu	41	57	34	50	50	70	51	50	76
Zn	129	128	106	109	115	111	96	121	115

Table 2d (cont). Major and trace element data for Hana Formation lavas from Haleakala Crater.

	HH-28	HH-29
SiO ₂	44.28	46.11
Al ₂ O ₃	13.81	16.10
FeO*	14.15	12.78
MgO	6.77	5.59
CaO	11.34	9.47
Na ₂ O	3.64	4.00
K ₂ O	1.50	1.45
P ₂ O ₅	0.59	0.51
TiO ₂	3.94	3.58
MnO	0.22	0.21
B	-	-
K	-	-
Cs	-	-
Rb(ID)	-	-
Rb(XRF)	32	30
Sr(ID)	658	-
Sr(XRF)	861	892
Ba(ID)	-	-
Ba(XRF)	646	712
La(XRF)	41	29
Ce(XRF)	83	85
Nd(XRF)	41	44
La	40.7	-
Ce	89.5	-
Nd	44.5	-
Sm	9.61	-
Eu	3.12	-
Tb	0.82	-
Ho	1.50	-
Yb	1.81	-
Lu	0.24	-
Y	29	28
Th	3.9	-
Ta	4.0	-
Nb	53	48
Zr	254	222
Hf	6.0	-
Ni	66	25
V	416	281
Cr(INAA)	21	-
Cr(XRF)	23	15
Sc(INAA)	21.4	-
Sc(XRF)	19	16
Co	68.8	-
Cu	72	38
Zn	126	106

Table 3. Compositions of trachytes and other differentiated Hawaiian lavas.

	<u>HOLUA</u>	<u>RTH-27</u>	<u>KA-37</u>	<u>KH1</u>	<u>C-116</u>	<u>RTH-7</u>
SiO ₂	64.16	62.26	54.25	59.17	62.90	68.07
Al ₂ O ₃	16.58	17.36	17.86	18.41	18.45	14.94
FeO	5.82	4.17	4.94	6.27	4.56	2.86
MgO	0.12	0.39	1.85	1.73	0.51	2.05
CaO	0.87	1.06	1.29	3.40	1.35	2.90
Na ₂ O	6.69	9.00	7.88	6.08	7.38	4.74
K ₂ O	5.09	4.90	5.09	2.72	3.97	3.62
P ₂ O ₅	0.02	0.15	0.63	0.59	0.13	0.18
TiO ₂	0.34	0.36	0.51	1.39	0.52	0.60
MnO	0.22	0.35	0.28	0.23	0.23	0.07
Zr	1916	935	507	-	-	171
Nb	229	140	115	-	-	46
Rb	159	133	98	49.9	64.5	110
Ba	134	305	628	980	-	247
Sr	4.4	28	406	1075	432	317
La	78.9	78	120	-	-	24
Sm	20.40	9.5	12.50	21.00	20.33	8.0
Yb	7.53	5.70	5.32	5.56	-	1.78
Th	16.9	8.8	7.7	-	-	3.7
Sc	1.1	-	12	7.4	-	-
Mg#	3.92	15.55	42.57	35.37		

HOLUA = Trachyte, Haleakala Crater (this study).

RTH-27 = Trachyte obsidian, Puu Waawaa, Hualalai (Thompson et al., 1974).

KA-37 = Phonolite, Kaula (Garcia et al., 1987).

KH1 = Benmoreite, Kohala (Feigenson, et al., 1983).

C-116 = Trachyte, Ukumehame Dome, West Maui (Macdonald and Katsura, 1964).

RTH-7 = Rhyodacite, Kauaopuu Ridge, Waianae (Thompson et al., 1974).

FIGURE CAPTIONS

Figure 1. Simplified Map of the island of Maui depicting the subaerial distribution of lavas from the Honomanu Formation (shield-building stage), Kula Formation (principal alkalic cap stage), and Hana Formation (post-erosional stage). Not shown is the relative distribution of Kumuilihi Formation lavas (early alkalic cap stage) which are exposed only in Haleakala Crater (Macdonald, 1978). From Macdonald et al. (1983; after Stearns, 1946).

Figure 2. Silica versus total alkalies ($K_2O + Na_2O$) diagrams. (a) Fields for Kumuilihi, Kula, and Hana Formation lavas from Haleakala Crater, and for Honomanu Formation lavas from Honomanu Valley. Open cross represents Holua trachyte (mapped as part of the Kula Formation; Macdonald, 1978). Additional Honomanu data from Macdonald and Katsura (1964), Macdonald and Powers (1968), and Chen (1982). Field for Kilauea tholeiites included for comparison (data from the literature. Figures (b) and (c) compare Kula Formation lavas from Haleakala Crater (shaded field) with alkalic cap lavas from Mauna Kea (Laupahoehoe Group), Kohala (Hawi Formation), West Maui (Honolua Formation), East Molokai, and Hualalai. Figure (d) compares Hana Formation lavas from Haleakala Crater with post-erosional lavas from West Maui (Lahaina Formation), Oahu (Honolulu Volcanic Series), and Kaula. Additional Hawaiian data from the literature. Line dividing tholeiite and alkalic fields from Macdonald and Katsura (1964).

Figure 3. Major element variations versus Nb abundance for lavas from Haleakala Crater and for Honomanu Formation lavas from Honomanu Valley. Symbols as follows: squares - Honomanu Formation, X - Kumuilihi Formation, circles - Kula Formation, triangles - Hana Formation.

Figure 4. Ni, Cr, Sc, and V abundances versus Nb abundance for lavas from Haleakala

Crater. Symbols as in figure 3.

Figure 5. Rare earth element abundances versus Nb abundance for lavas from Haleakala Crater. Symbols as in figure 3.

Figure 6. Incompatible trace element abundances versus Nb abundance for lavas from Haleakala Crater. Symbols as in figure 3.

Figure 7. Mo'o (Mantle Overview Order) diagrams for lavas from Haleakala. Elemental abundances are normalized to CI Chondritic abundances with the exception of Rb, K, and P which are normalized to estimated primitive mantle abundances. (a) Range for Honomanu Formation lavas (additional data from Chen and Frey, 1985). A typical Kilauea tholeiite (U.S.G.S. standard rock, BHVO-1) is shown for comparison. The apparent relative depletions in K and Rb are probably due to alkali loss from weathering (cf. Chen and Frey, 1985). (b) Range for Kumuliahia Formation lavas with the range for Kula Formation lavas from Haleakala Crater shown for comparison. (c) Range for Kula Formation lavas from Haleakala Crater, including Holua trachyte; note that the vertical scale is expanded to portray the extreme Sr depletion in the Holua trachyte. (d) Range for Hana Formation lavas from Haleakala Crater with the range for Kula Formation lavas from Haleakala Crater shown for comparison.

Figure 8. Mo'o diagrams of (a) Kula Formation lavas from Haleakala Crater, (b) alkalic cap lavas from Mauna Kea (Laupahoehoe Group; shaded field) and Kohala (Hawi Formation), and (c) alkalic cap lavas from Hualalai (shaded field), including a trachyte sample (open crosses). Additional Hawaiian data are from the literature.

Figure 9. Mo'o diagrams of (a) Hana Formation lavas from Haleakala Crater (shaded field), with field for Kula lavas shown for comparison, (b) post-erosional lavas from

Oahu (Honolulu Volcanic Series), with field for Hana lavas (shaded field) shown for comparison, and (c) post-erosional lavas from Kaula (shaded field) and a post-erosional basanitoid from West Maui (Lahaina Formation (triangles)). Additional Hawaiian data are from the literature.

Figure 10. Trace element and major element ratios versus Nb abundance for Kumuiliahi, Kula, and Hana Formation lavas from Haleakala Crater and for Honomanu Formation lavas from Honomanu Valley. See figure 3 caption for key to symbols and data sources. Only three Honomanu lavas have been plotted in (e) because excessively high Ba/Rb ratios (up to 209; Chen and Frey, 1985) in the other samples likely reflect Rb loss during subaerial weathering.

Figure 11. $\text{Al}_2\text{O}_3/\text{TiO}_2$ versus Nb abundance for lavas from Haleakala Crater and for Honomanu Formation lavas from Honomanu Valley. Symbols and data sources as in figure 3. (a) all data, (b) Honomanu and Kumuiliahi Formation lavas, (c) Kula Formation lavas, and (d) Hana Formation lavas. Strong negative correlations for Honomanu and Kumuiliahi lavas reflects the dominance of plagioclase over Fe-Ti oxide fractionation in these two suites. Sub-parallel trends for Honomanu and Kumuiliahi lavas indicate that these magmas probably evolved from compositionally distinct parental magmas (and sources). Strong positive correlations for Kula lavas and, to a lesser extent, Hana lavas reflects the importance of Fe-Ti oxide fractionation in the petrogenesis of these magmas.

Figure 12. V/Ni versus Nb abundance for lavas from Haleakala Crater and for Honomanu Formation lavas from Honomanu Valley. Symbols and data sources as in figure 3. (a) all data, (b) Honomanu and Kumuiliahi Formation lavas, (c) Kula Formation lavas, and (d) Hana Formation lavas. Positive correlations for Honomanu, Kumuiliahi, and Hana Formation lavas reflects olivine-dominated fractionation relative to Fe-Ti oxide fractionation. The convex upwards trend for Kula lavas reflects the importance of

olivine fractionation in the less evolved lavas (alkalic basalts and mafic hawaiites), followed by a significantly increased role for Fe-Ti oxide fractionation in the more evolved lavas (hawaiites and mugearites).

Figure 13. Sc/Ni versus Nb abundance for lavas from Haleakala Crater and for Honomanu Formation lavas from Honomanu Valley. Symbols and data sources as in figure 3. (a) all data, (b) Honomanu and Kumuilihi Formation lavas, (c) Kula Formation lavas, and (d) Hana Formation lavas. Positive correlations for Honomanu and Hana Formation lavas reflects olivine-dominated fractionation relative to clinopyroxene fractionation. The scatter in Kumuilihi data probably reflects removal of a olivine-clinopyroxene poor fractionating phase assemblage. The convex upwards trend for Kula lavas reflects the importance of olivine fractionation in the less evolved lavas (alkalic basalts and mafic hawaiites), followed by a significantly increased role for clinopyroxene fractionation in the more evolved lavas (hawaiites and mugearites).

Figure 14. $^{87}\text{Sr}/^{86}\text{Sr}$ versus (a) SiO_2 , (b) Nb, (c) $\text{Al}_2\text{O}_3/\text{CaO}$, (d) La/Ce, (e) La/Sm, (f) La/Yb, (g) Zr/Nb, (h) Ba/Y, (i) Ba/Rb, and (j) Zr/Hf for lavas from Haleakala Crater. Symbols as in figure 3 with the following changes: the large open circles and large solid triangles refer to Kula and Hana Formation lavas from Haleakala Crater (this study), and the small open circles and small solid triangles refer to Kula and Hana flank lavas (data from Macdonald and Katsura, 1964; Macdonald and Powers, 1968; Chen, 1982; Chen and Frey, 1985; Tatsumoto et al., 1987).

Figure 15. Relative stratigraphic position versus (a) SiO_2 , (b) Nb, (c) Zr/Nb, (d) Ba/Y, (e) La/Ce, (f) Zr/Hf, and (g) Ba/Rb for lavas from the Halemau section of Haleakala Crater. Major element contents and trace element abundances are not significantly correlated with stratigraphic position. H/M ratios such as Zr/Nb and Ba/Y are strongly correlated with relative stratigraphic position, but H/H ratios (e.g. Ba/Rb, La/Ce) and

ratios of elements of similar geochemical affinity (e.g. Zr/Hf) do not appear to be correlated significantly.

Figure 16. (a) Ba versus La/Sm, (b) Sc versus La/Sm, (c) Sc versus La/Yb, and (d) Ba versus La/Yb for lavas from Haleakala Crater. Symbols as in figure 3.

Figure 17. Zr/Hf versus (a) Sc and (b) $\text{Al}_2\text{O}_3/\text{CaO}$ for lavas from Haleakala Crater and Honomanu lavas from Honomanu Valley. Symbols and data sources as in figure 3. Negative correlations between Zr/Hf and Sc and positive correlations between Zr/Hf and $\text{Al}_2\text{O}_3/\text{CaO}$ are consistent with variations in Zr/Hf observed for Kula and Hana Formation lavas being controlled primarily by clinopyroxene fractionation.

Figure 18. $^{87}\text{Sr}/^{86}\text{Sr}$ versus (a) Ba/Y and (b) Zr/Nb for Haleakala post shield-building [PSB] lavas, shield-building [SB] lavas from the Maui Volcanic Complex [MVC], Kilauea tholeiites, and Hawaiian post-erosional lavas from the Honolulu Volcanic Series [Oahu] and the Lahaina Formation [West Maui]. The distinct and oppositely correlated arrays in (a) for Haleakala post shield-building [PSB] and MVC SB lavas is equivalent to the separate arrays defined for Sr-Pb isotope systematics. Additional Hawaiian data from the literature.

Figure 19. Ba/Y versus Zr/Nb for (a) Haleakala from Haleakala Crater and Honomanu Formation lavas and (b) for Haleakala post shield-building [PSB] lavas, MVC shield-building [SB] lavas, Kilauea tholeiites, and post-erosional lavas from the Honolulu Volcanic Series [Oahu] and the Lahaina Formation [West Maui]. Symbols and data sources in (a) as in figure 3. The strong negative array formed by Haleakala PSB lavas (i.e. Kumuilahi, Kula, and Hana Formations) is temporally significant and implies progressive, time-dependent mixing between a Honomanu (plume) composition component and a component having high Ba/Y and low Zr/Nb ratios. The later component corresponds,

isotopically, to the Hawaiian depleted mantle [DM] component (West and Leeman, 1987a). In (b), the low Ba/Y Hawaiian shield-building array defined by MVC SB and Kilauea lavas implies end-member mixing components having low Ba/Y-low Zr/Nb and low Ba/Y-high Zr/Nb, respectively. The negative array formed by Haleakala PSB and Hawaiian post-erosional lavas is consistent with mixing between a high Ba/Y-low Zr/Nb component and a component with low Ba/Y and intermediate Zr/Nb. These relations are consistent with those observed for $^{87}\text{Sr}/^{86}\text{Sr}$ and $^{206}\text{Pb}/^{204}\text{Pb}$.

Figure 20. Ba/Y versus Zr/Nb for lavas from Haleakala and selected Hawaiian volcanoes. Symbols as follows: solid circles = Haleakala PSB lavas, open triangles = Honolulu and Lahaina post-erosional lavas, crosses = Kilauea tholeiites, open squares = MVC shield-building lavas from Haleakala, Kahoolawe, Lanai, and West Molokai [data from this study; West and Leeman, in prep; Garcia et al., in prep]. Also indicated are estimated compositions of possible source components: chondrite [or primitive mantle; based on compilation of C1 chondrites] = star, estimated MORB source (depleted) mantle [from Tarney et al., 1980] = sun, average pelagic clay [from Li, 1982] = open circle with embedded cross. The PSB array indicates that the Hawaiian DM (depleted mantle) component must be a melt of such material. The SB array is consistent with mixing between a chondritic (primitive mantle or PM) component and a component with low Ba/Y and Zr/Nb, possibly representing metasomatized or metasomatically scavenged mantle material.

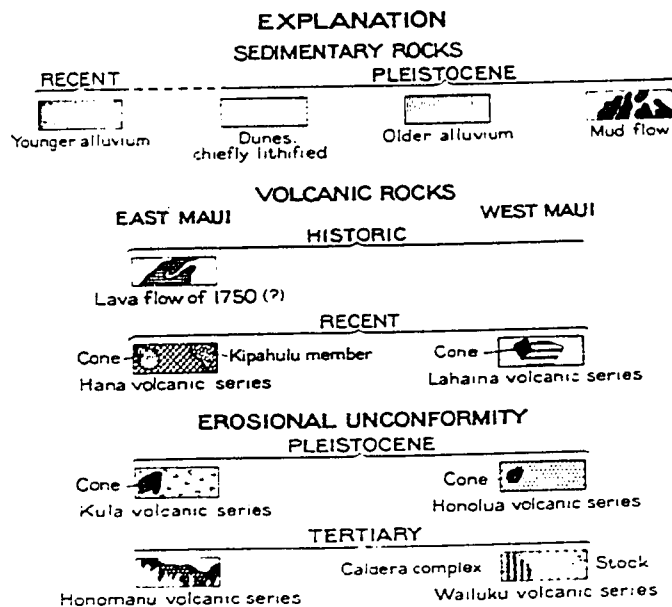
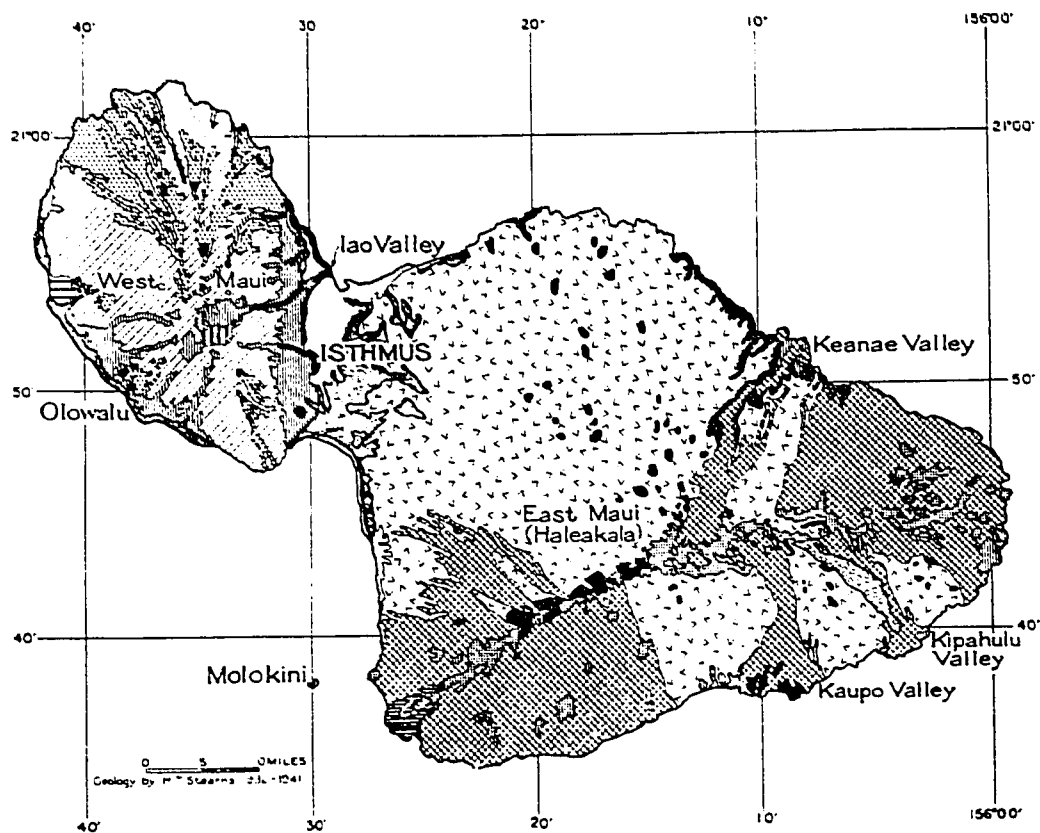
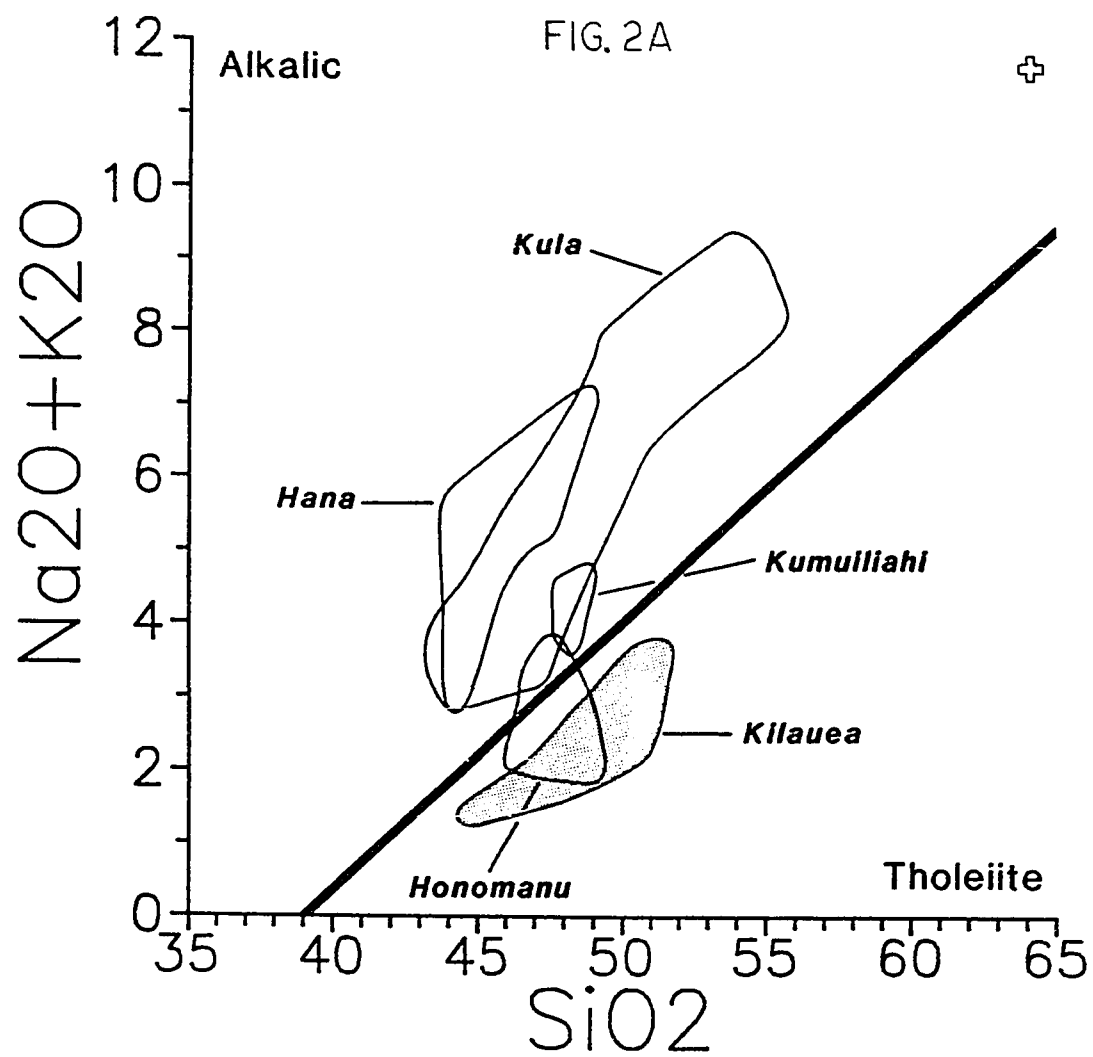
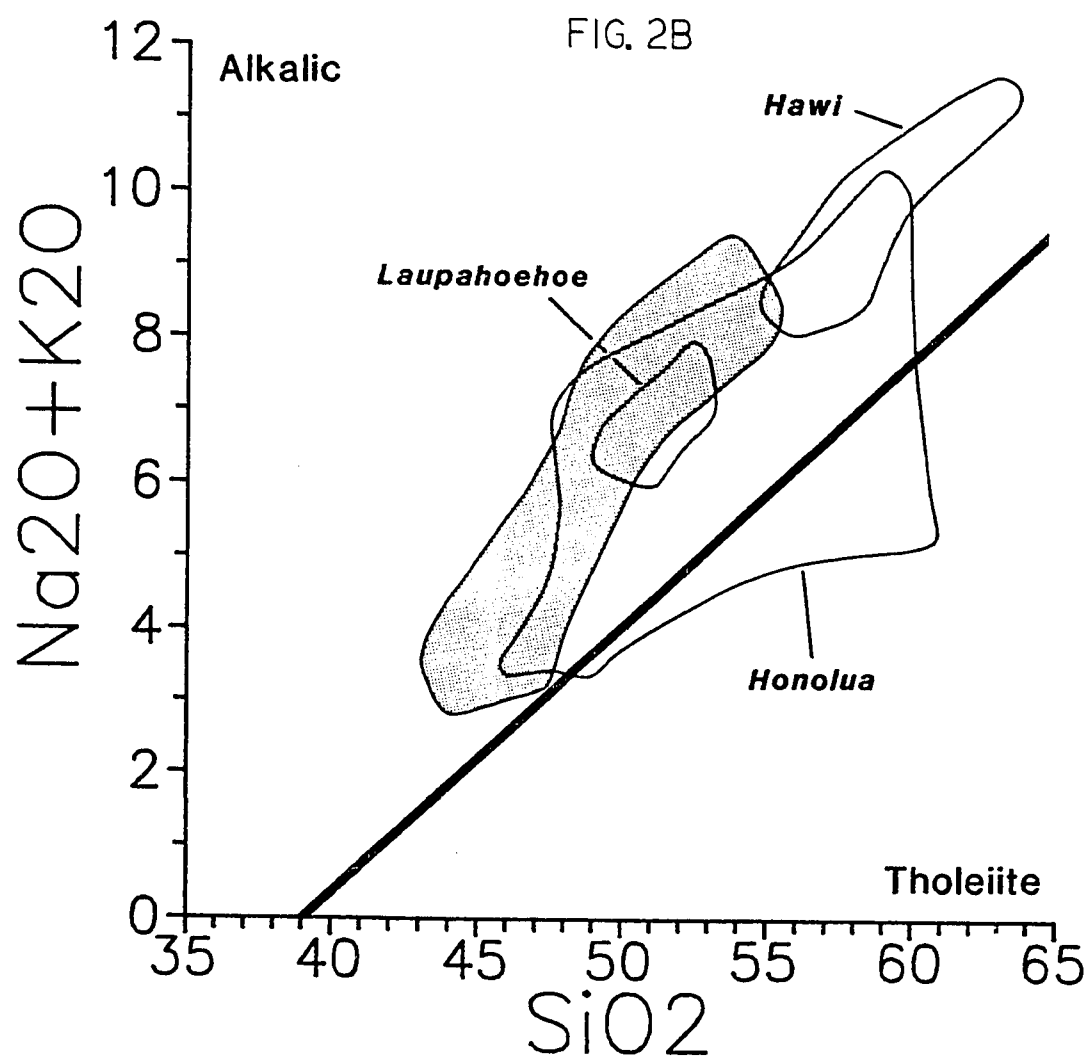
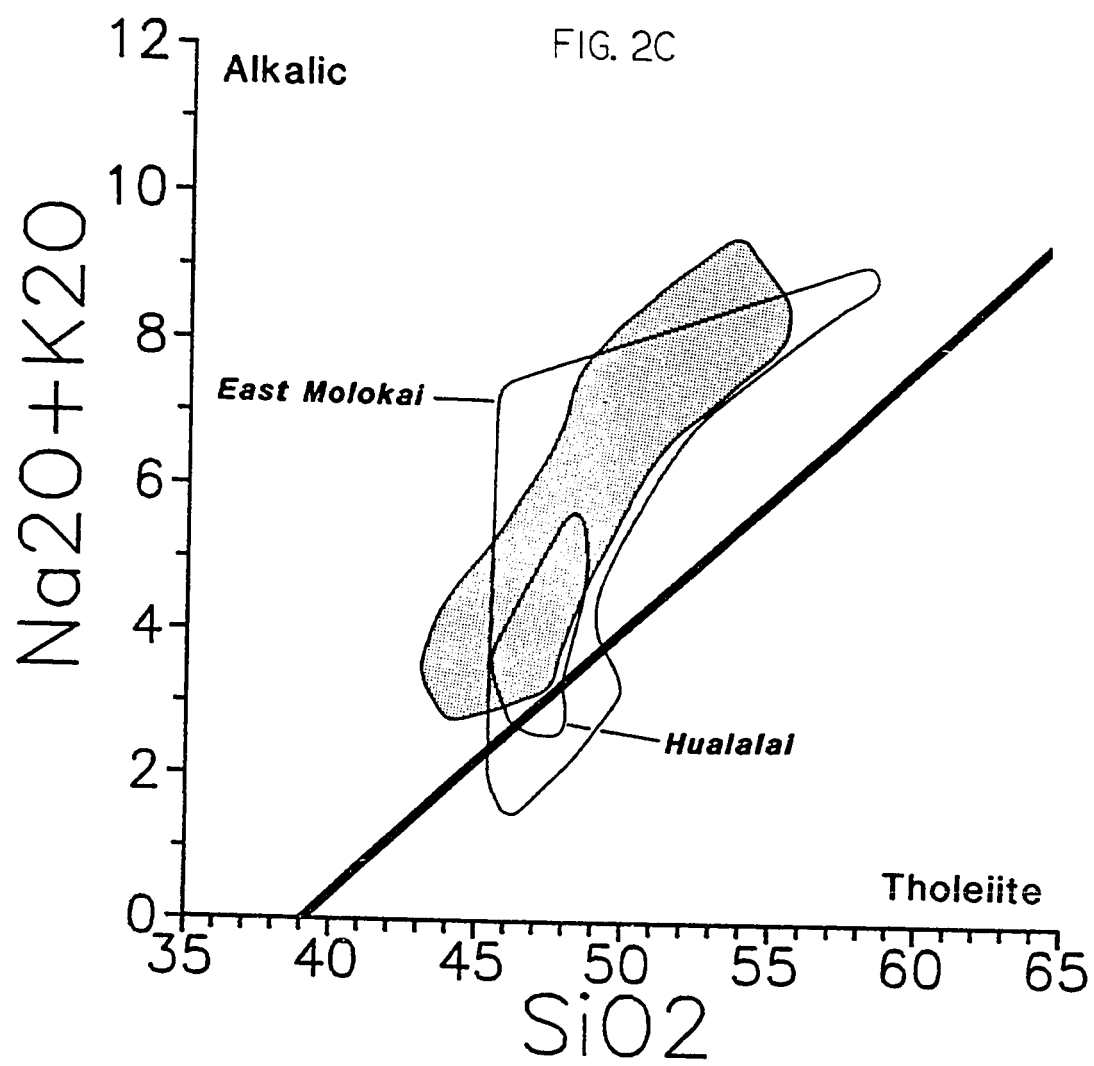
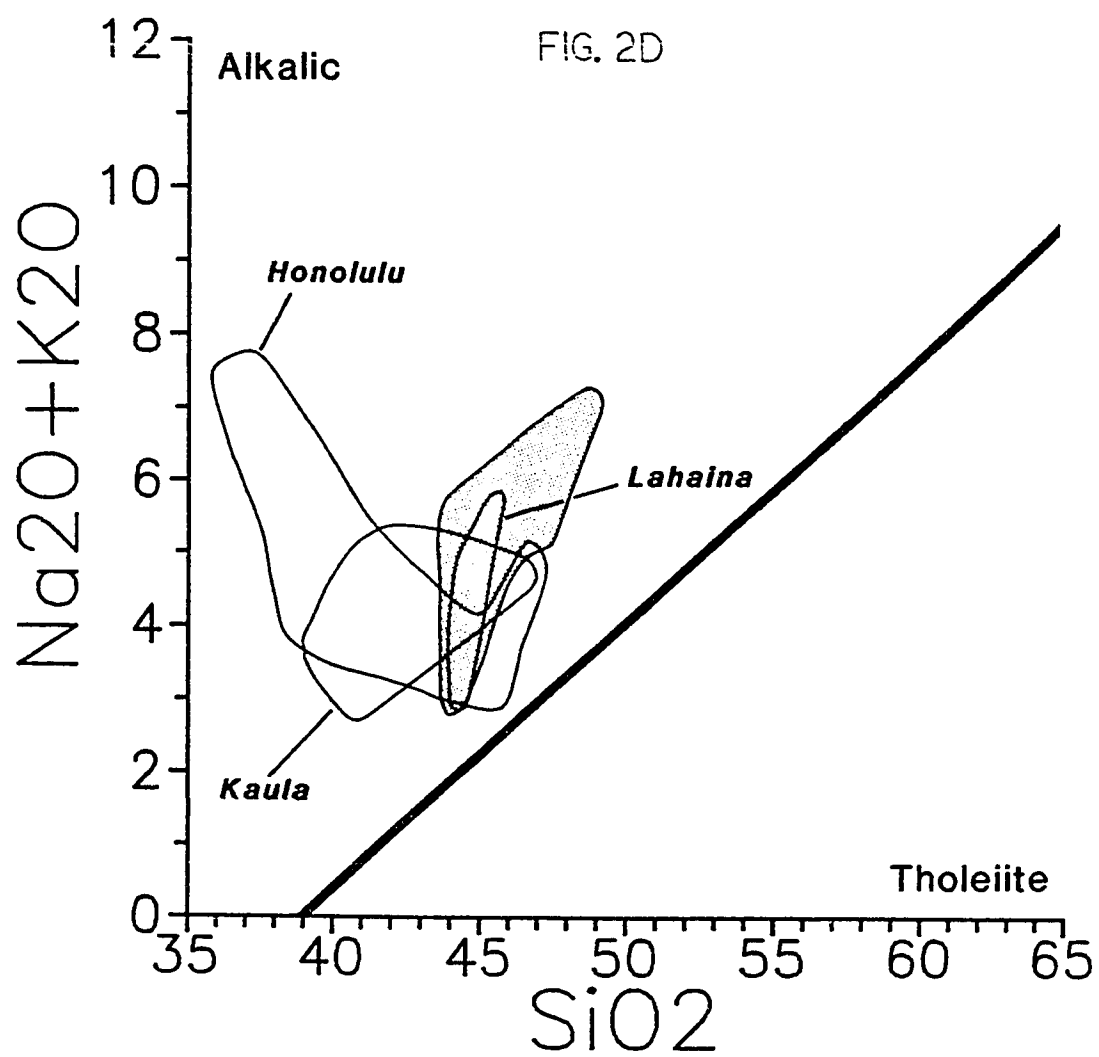


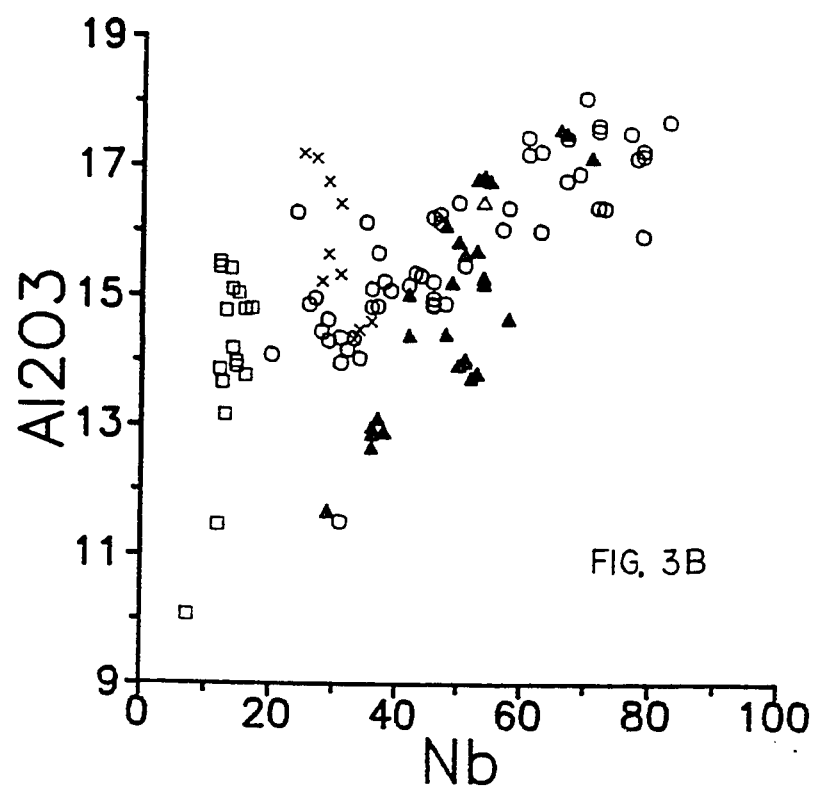
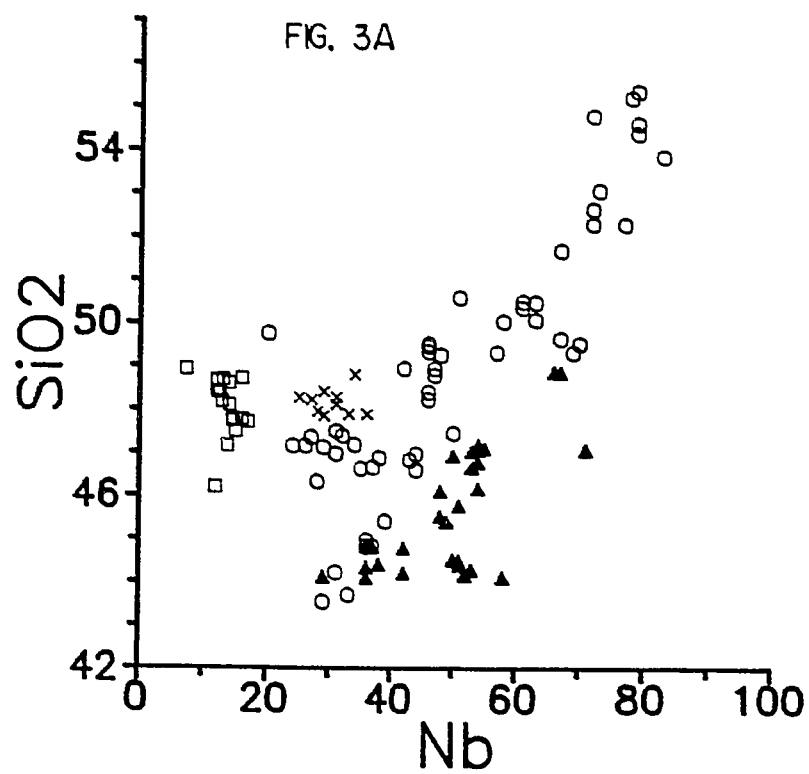
FIG. 1

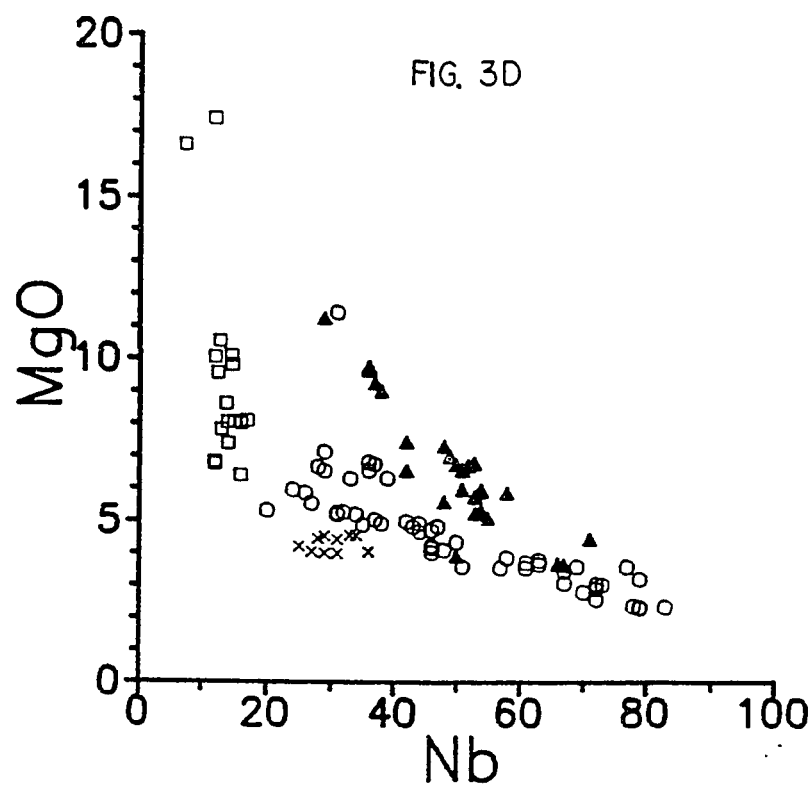
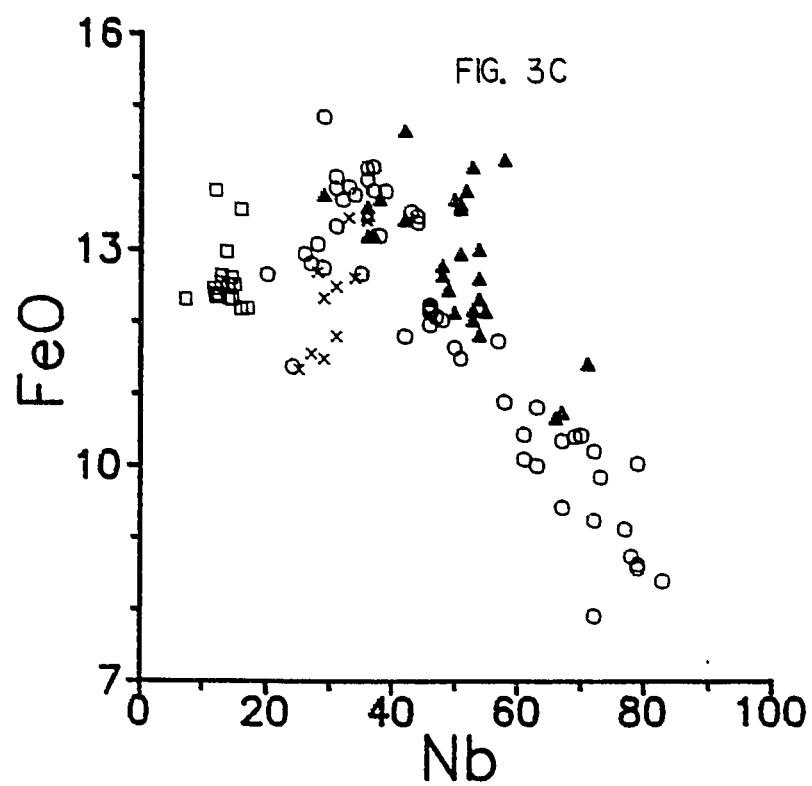


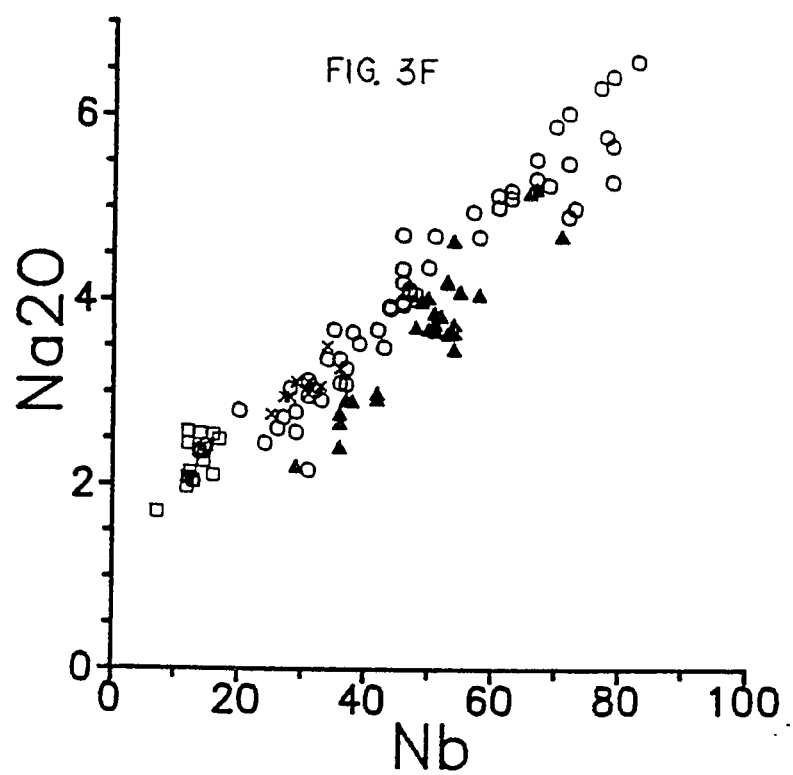
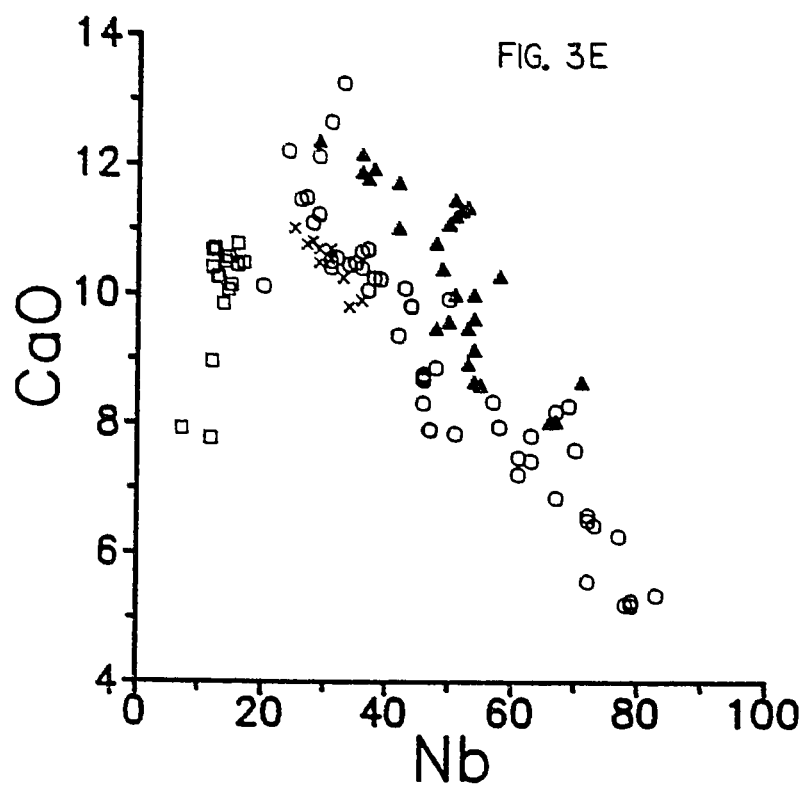


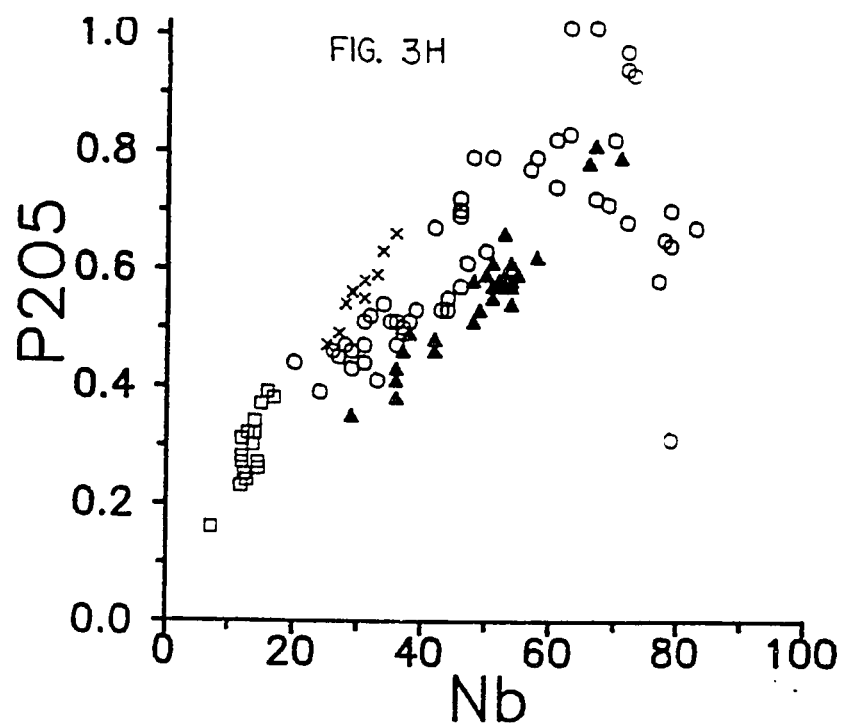
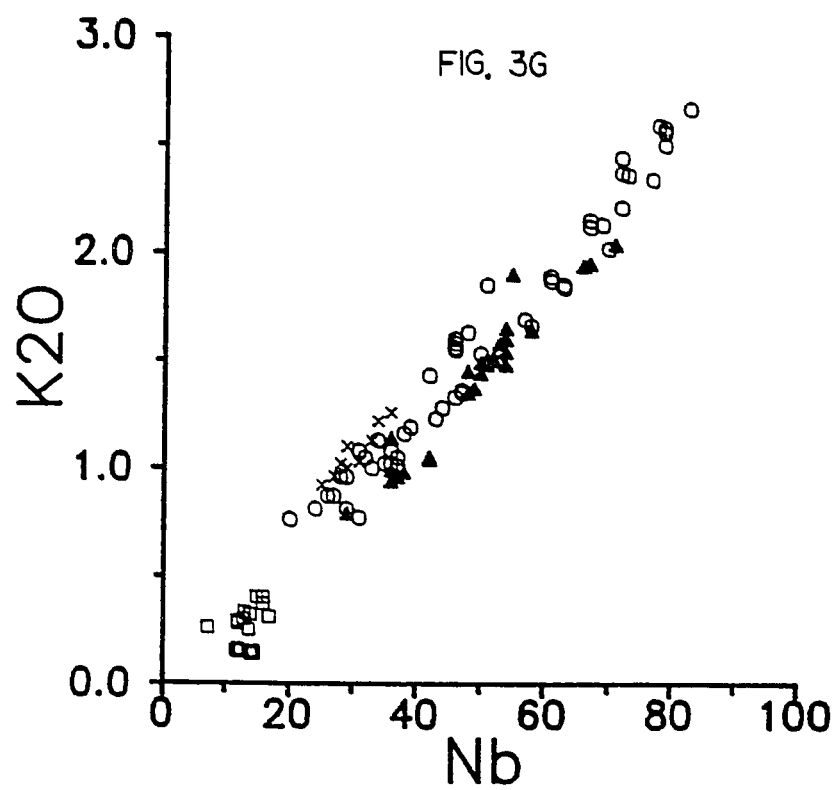


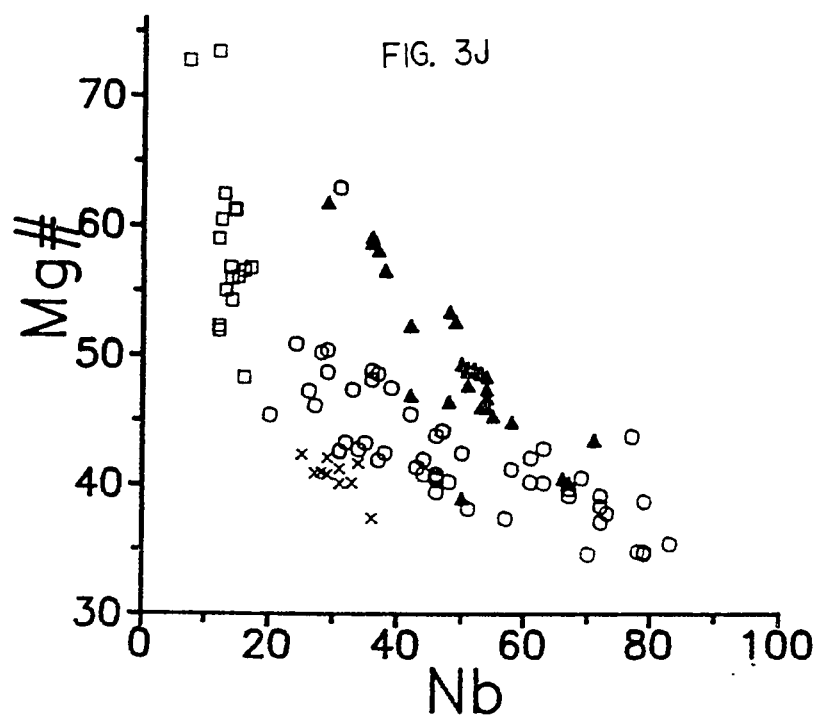
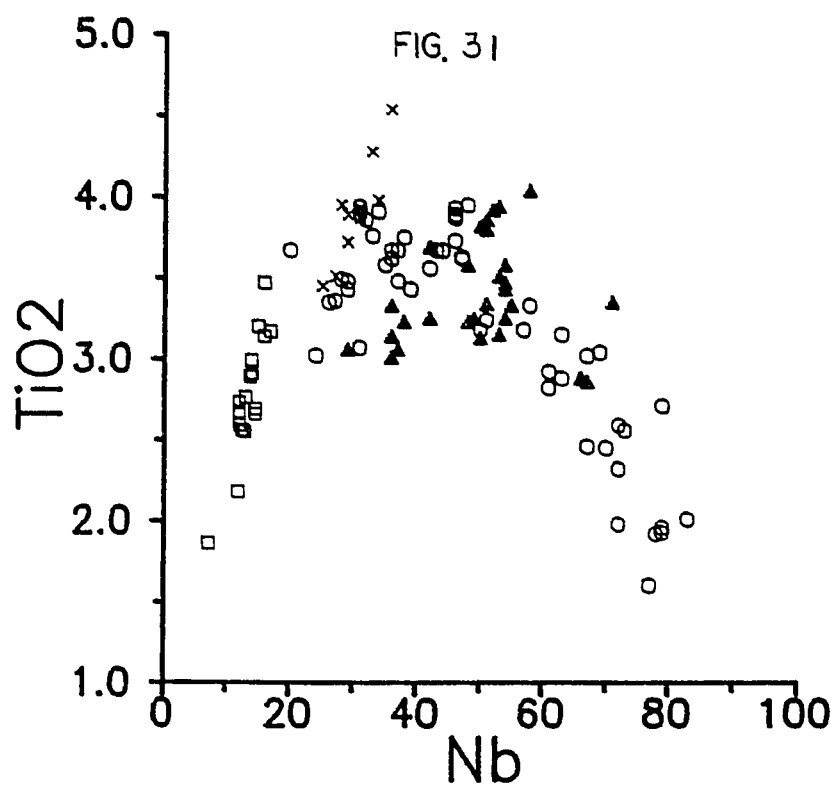


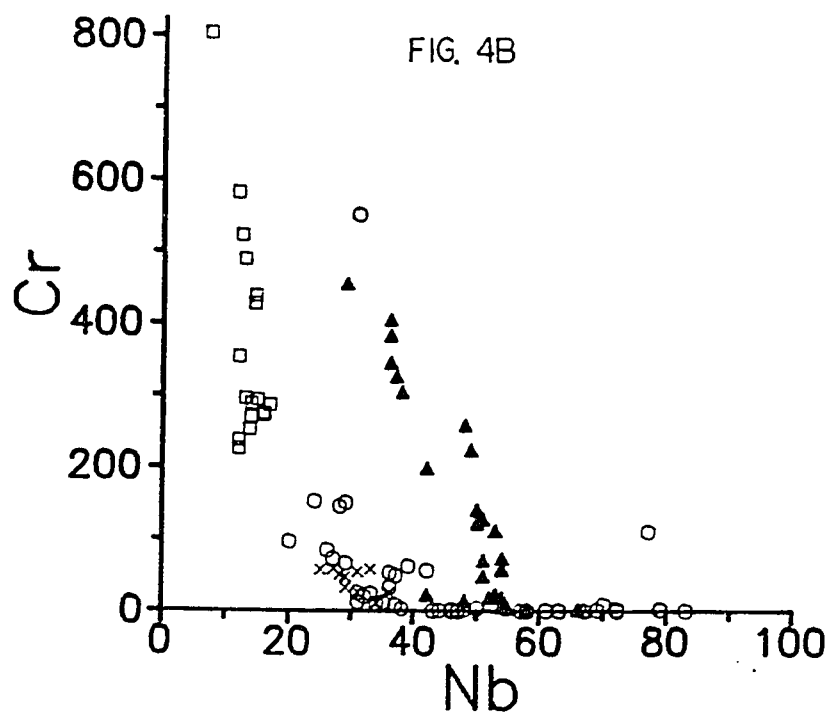
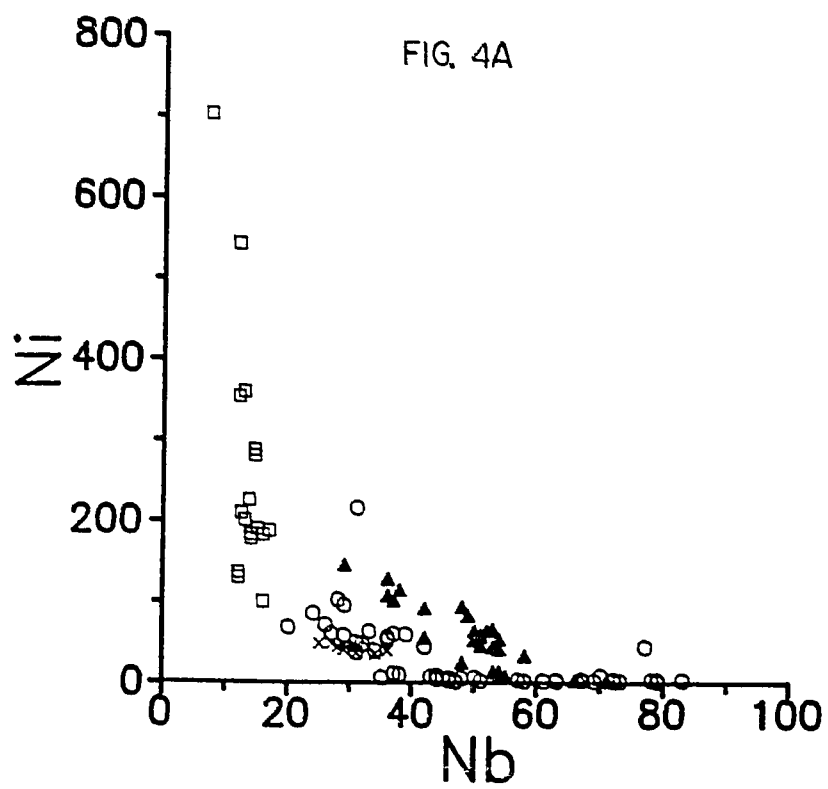


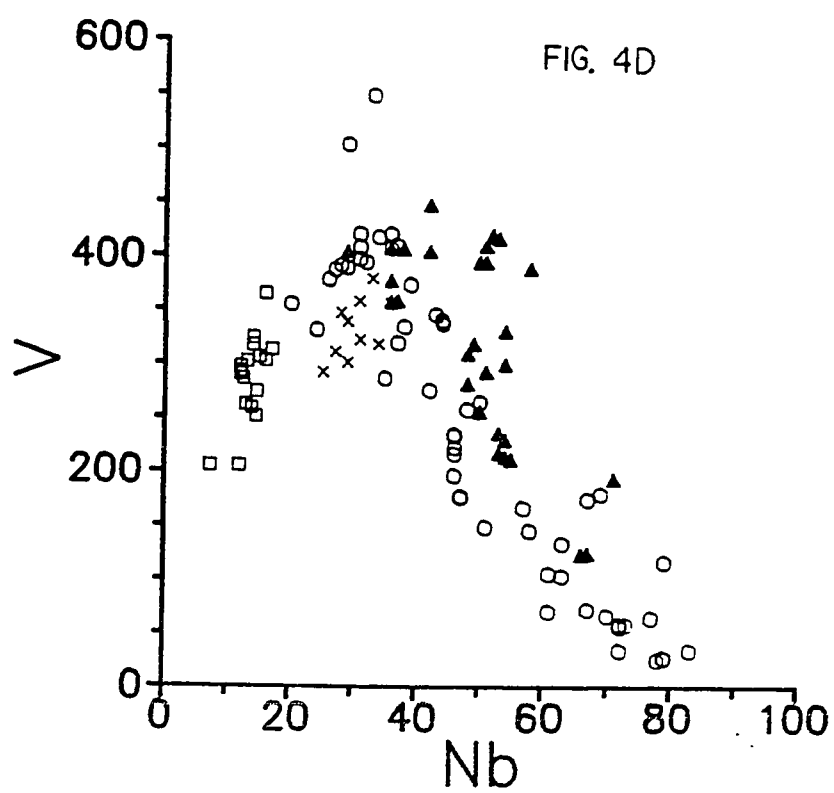
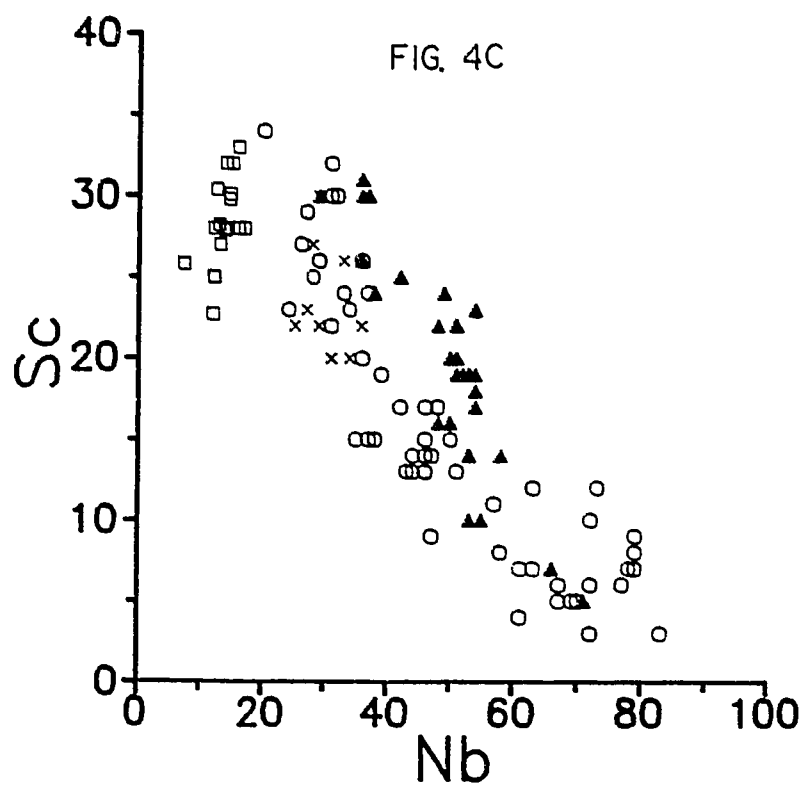


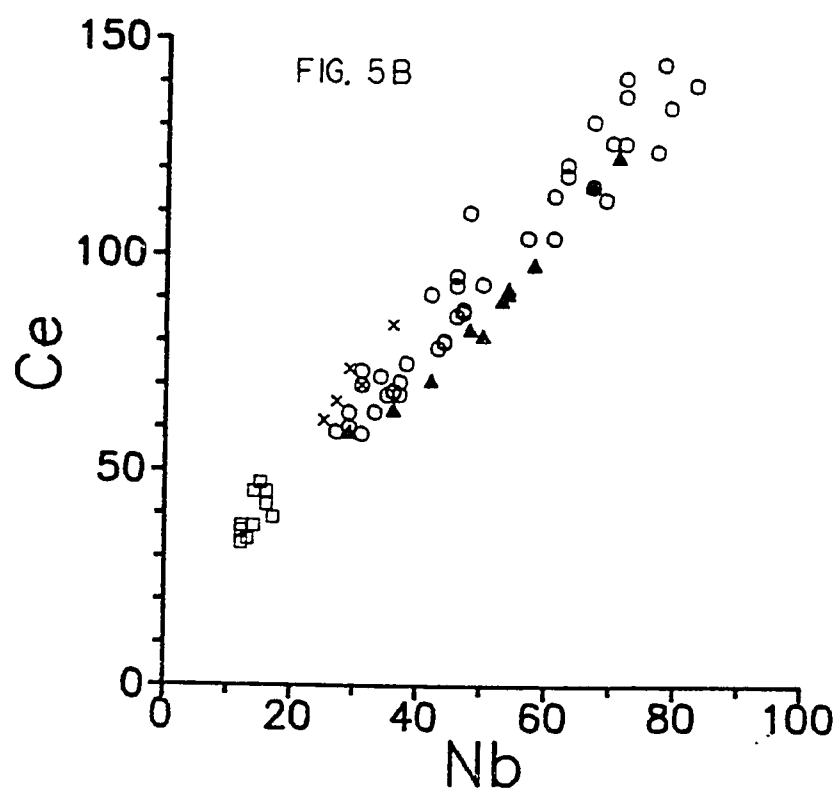
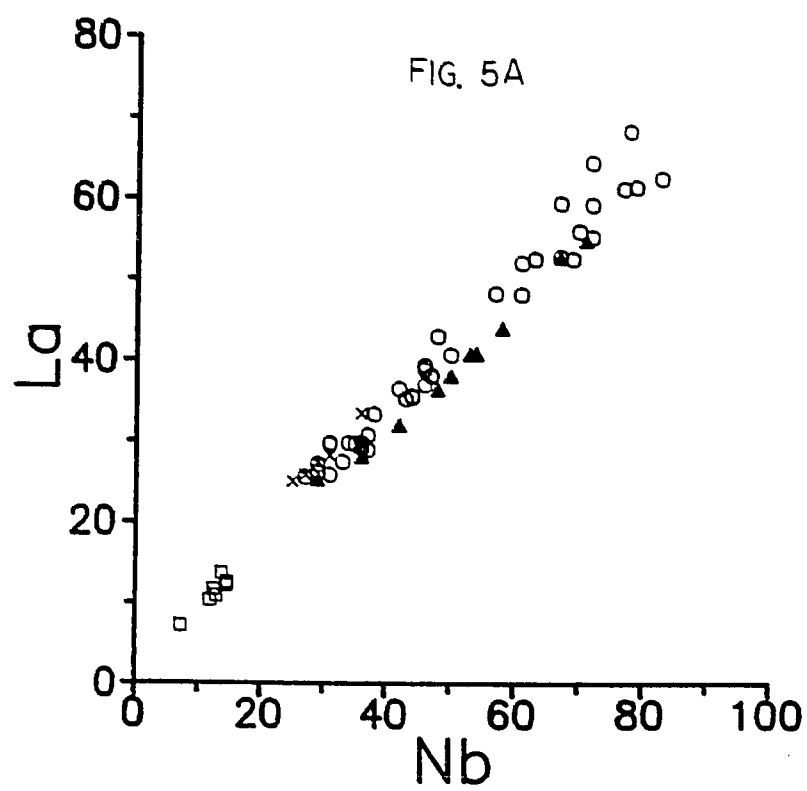


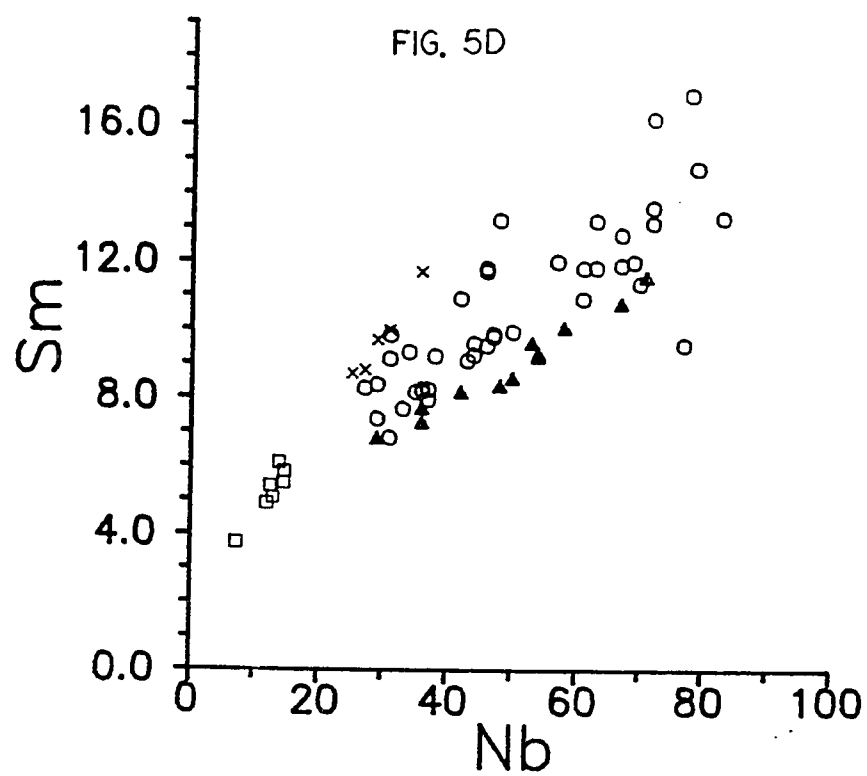
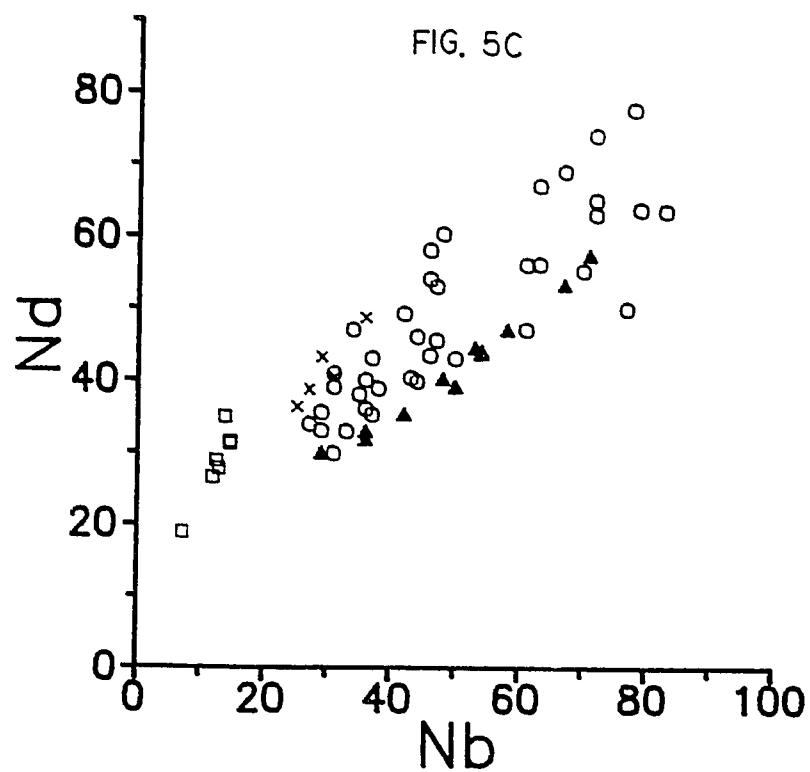


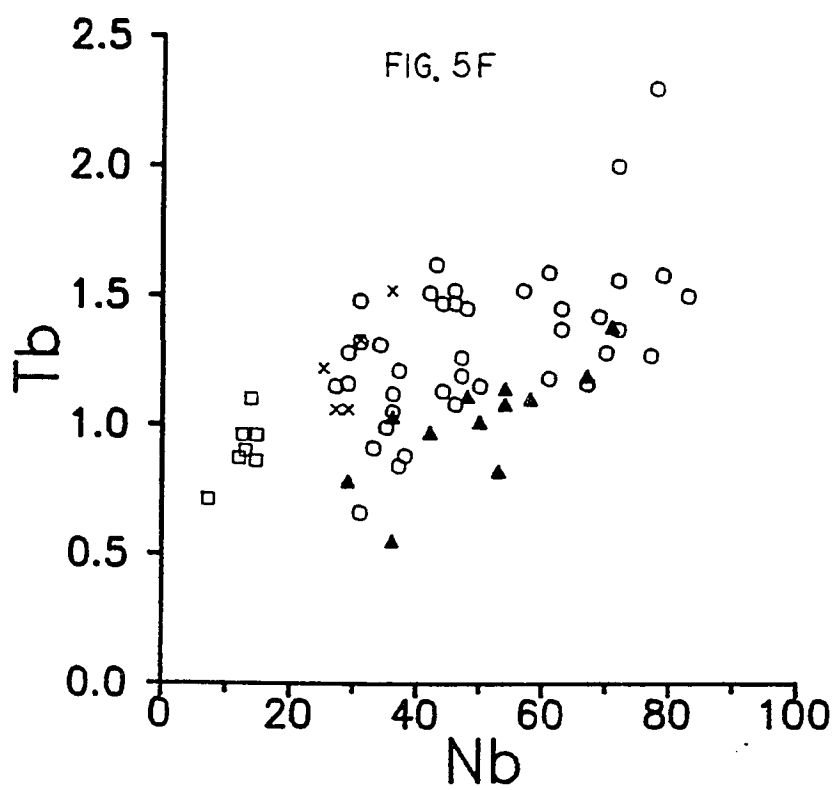
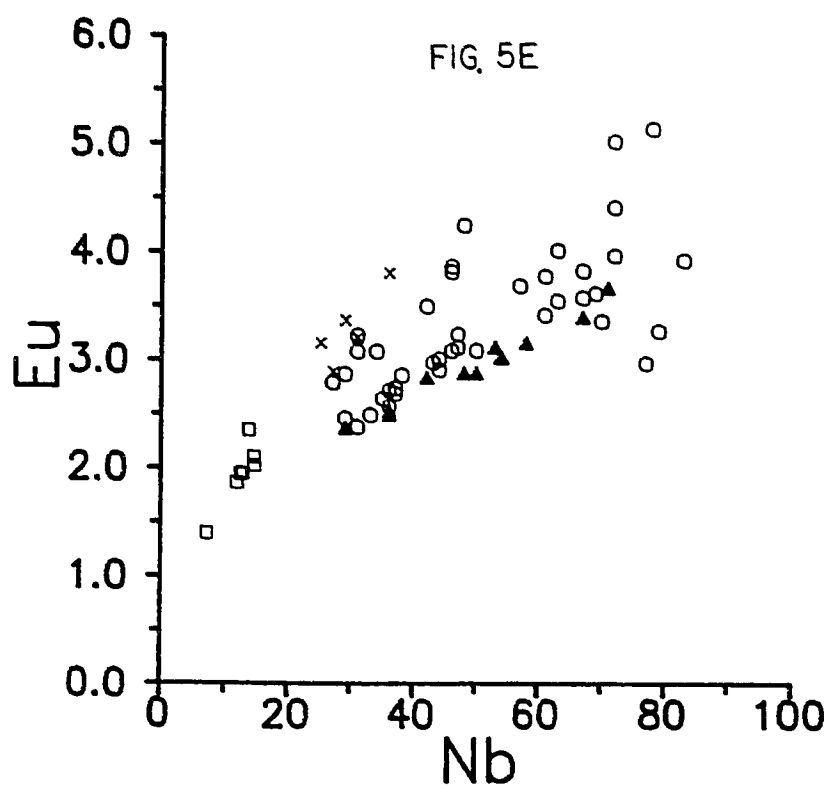


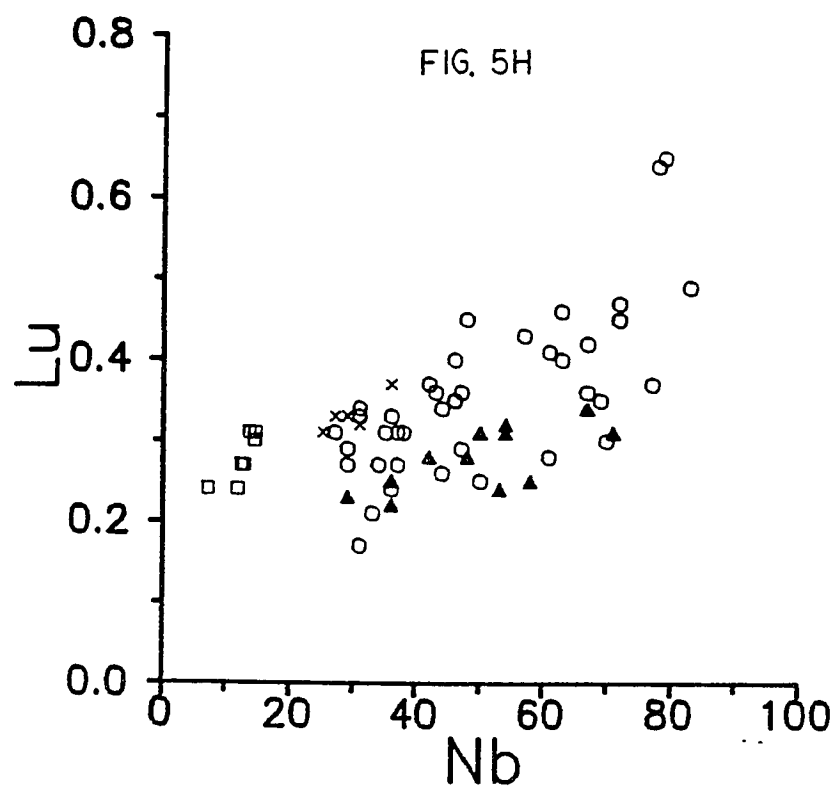
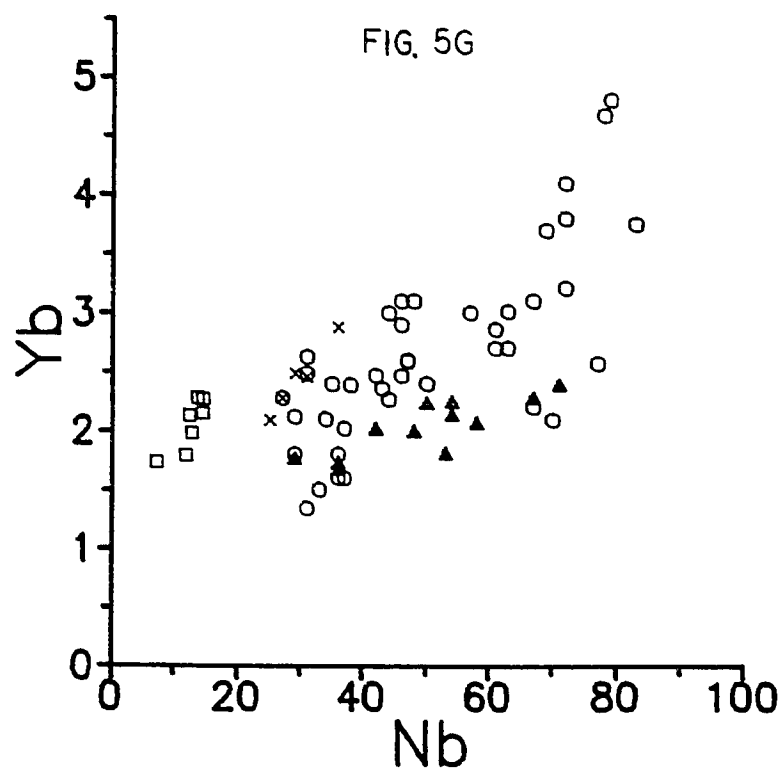


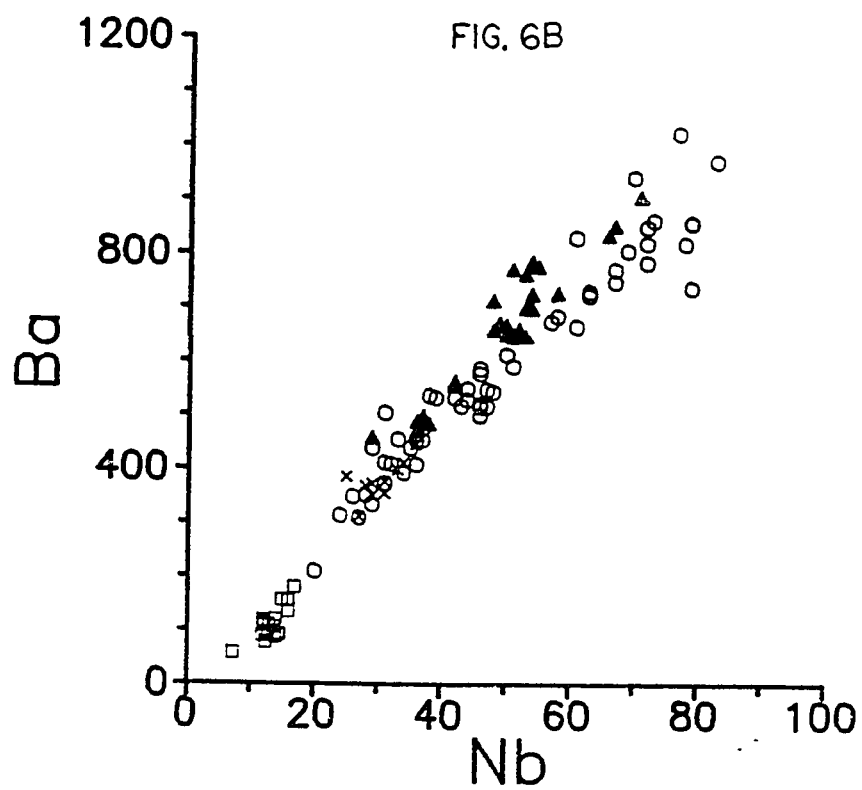
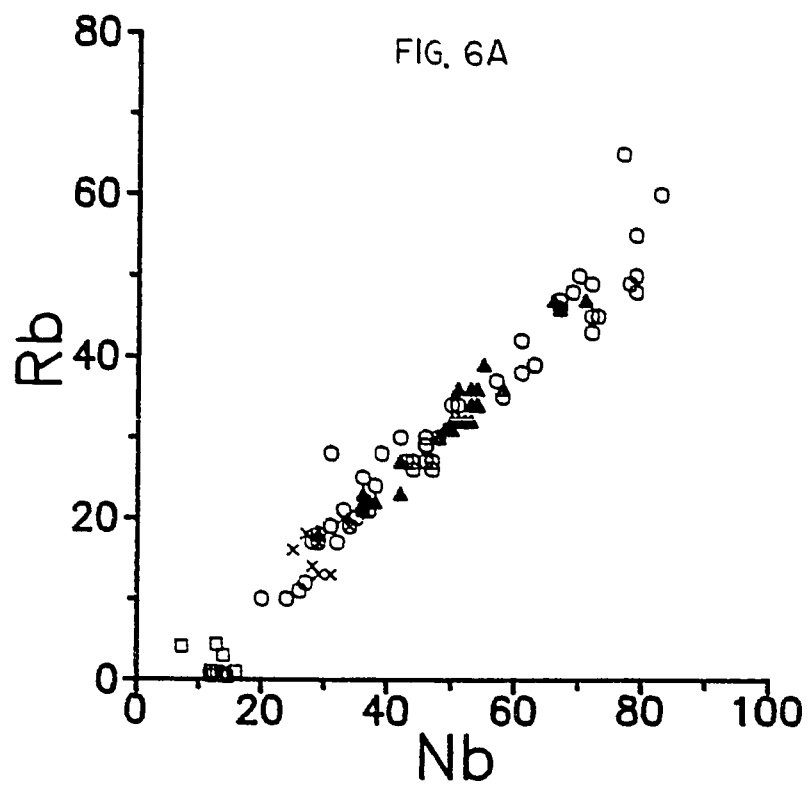


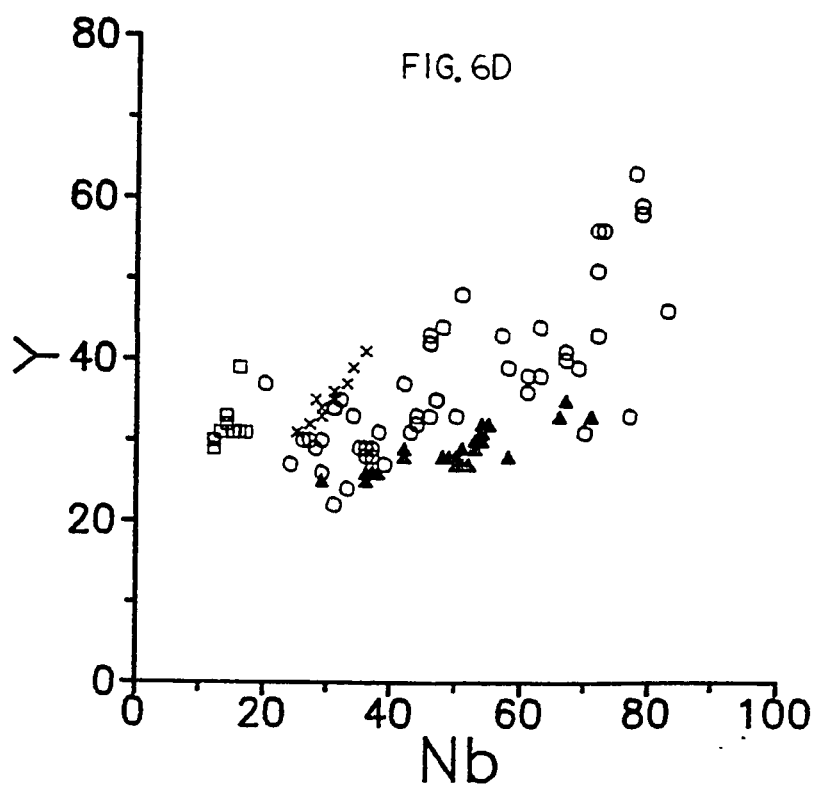
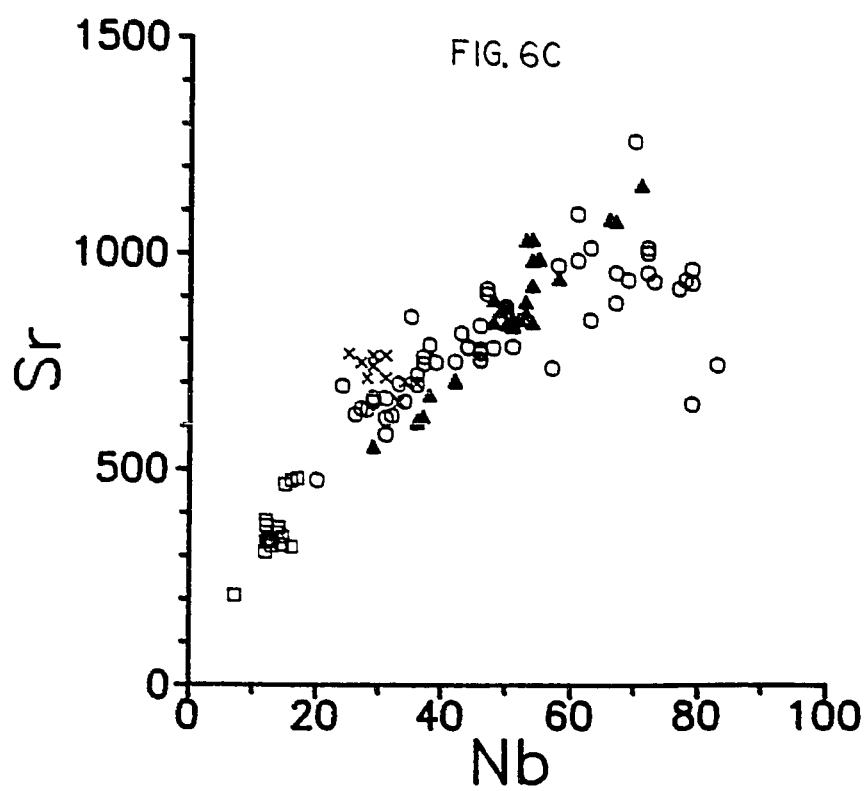


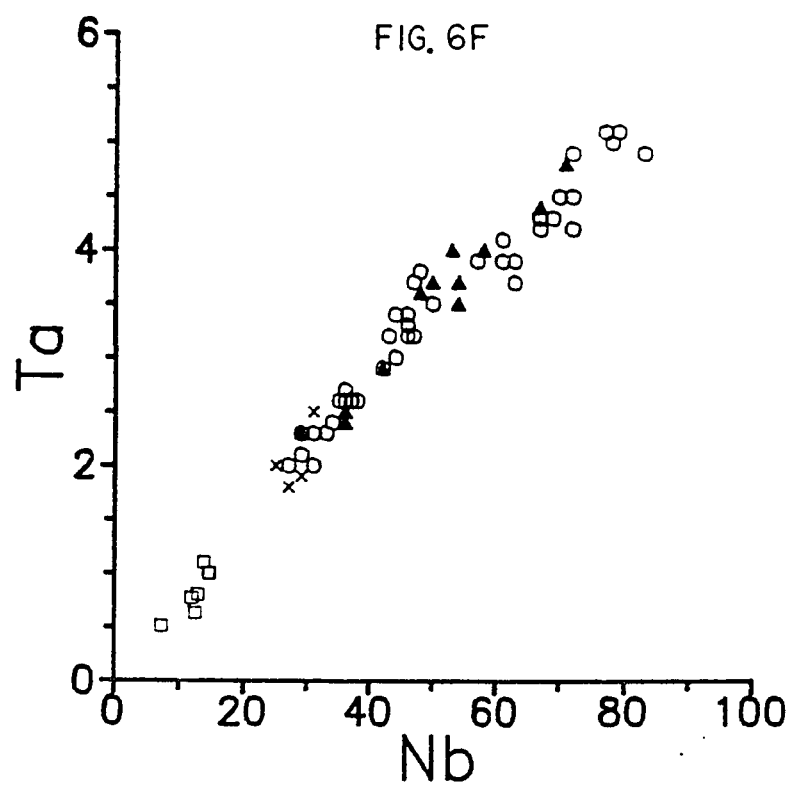
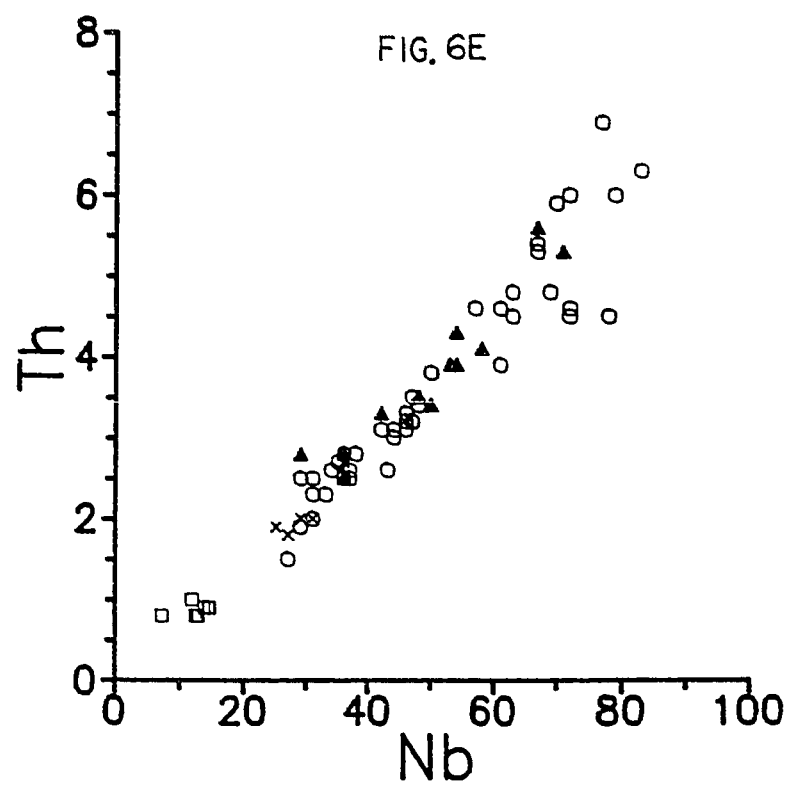


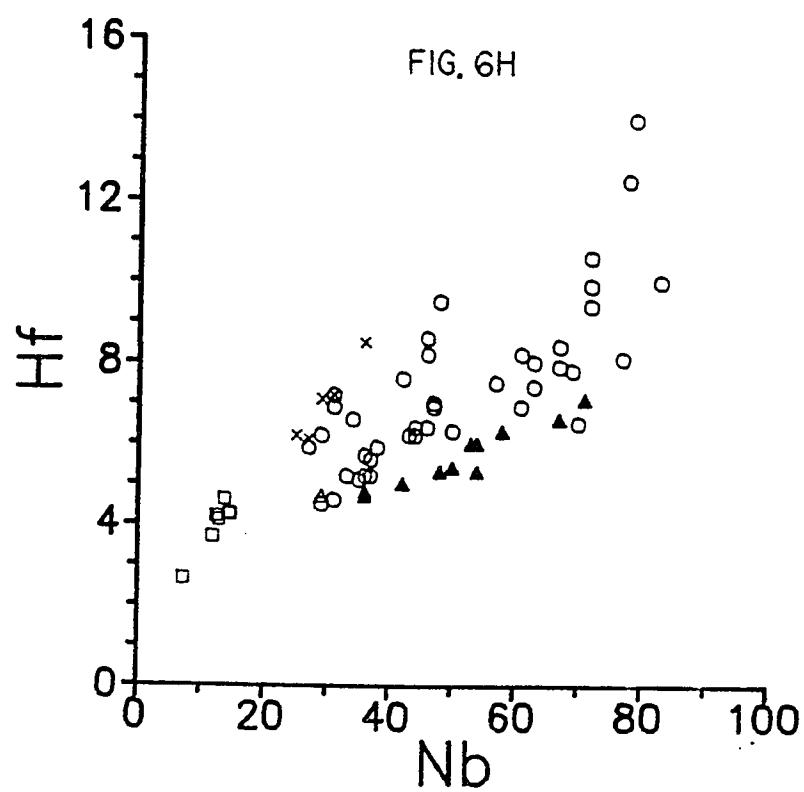
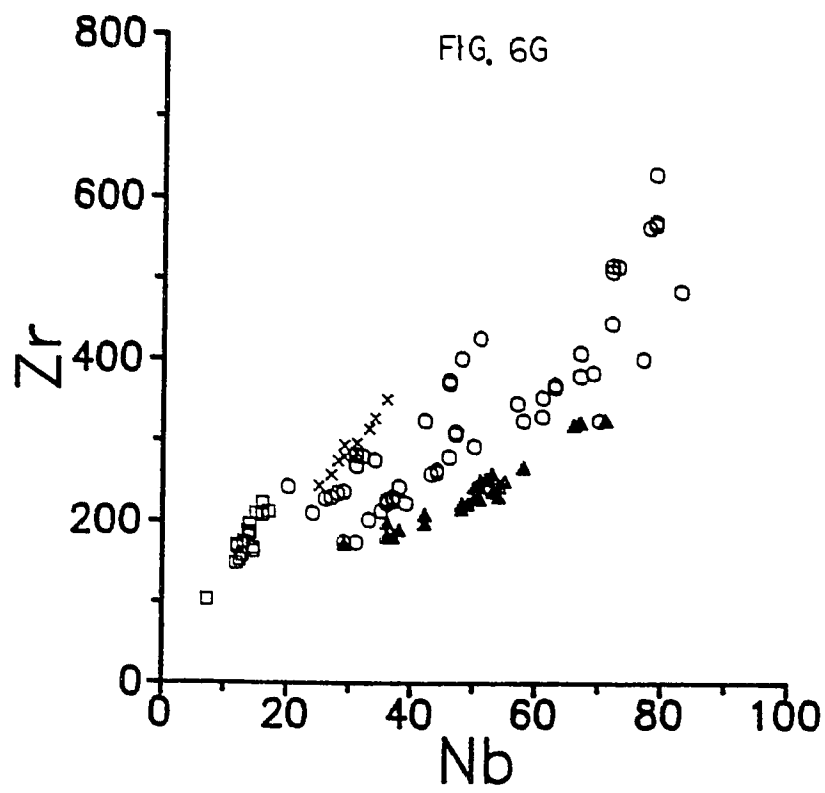


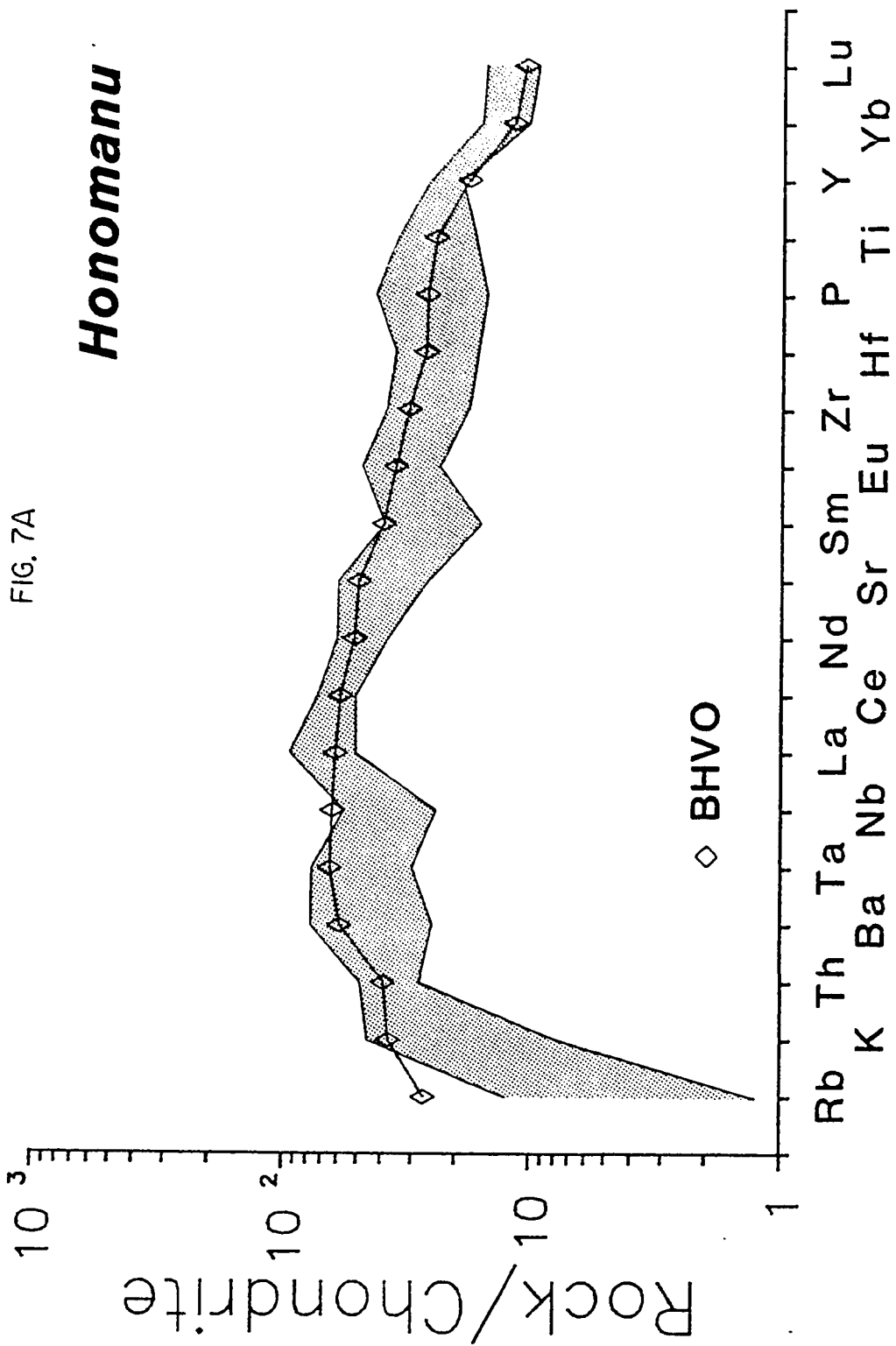












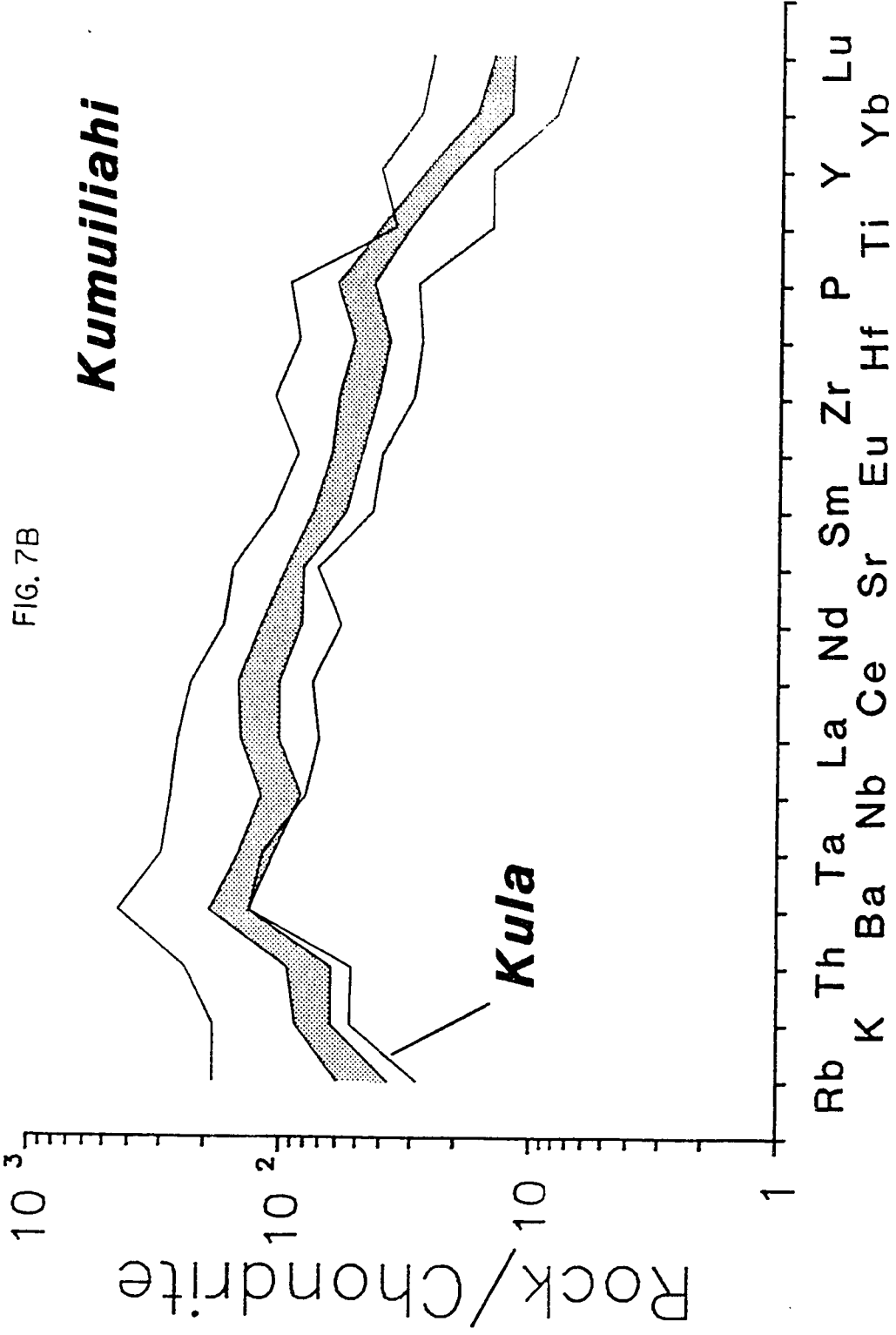


FIG. 7B

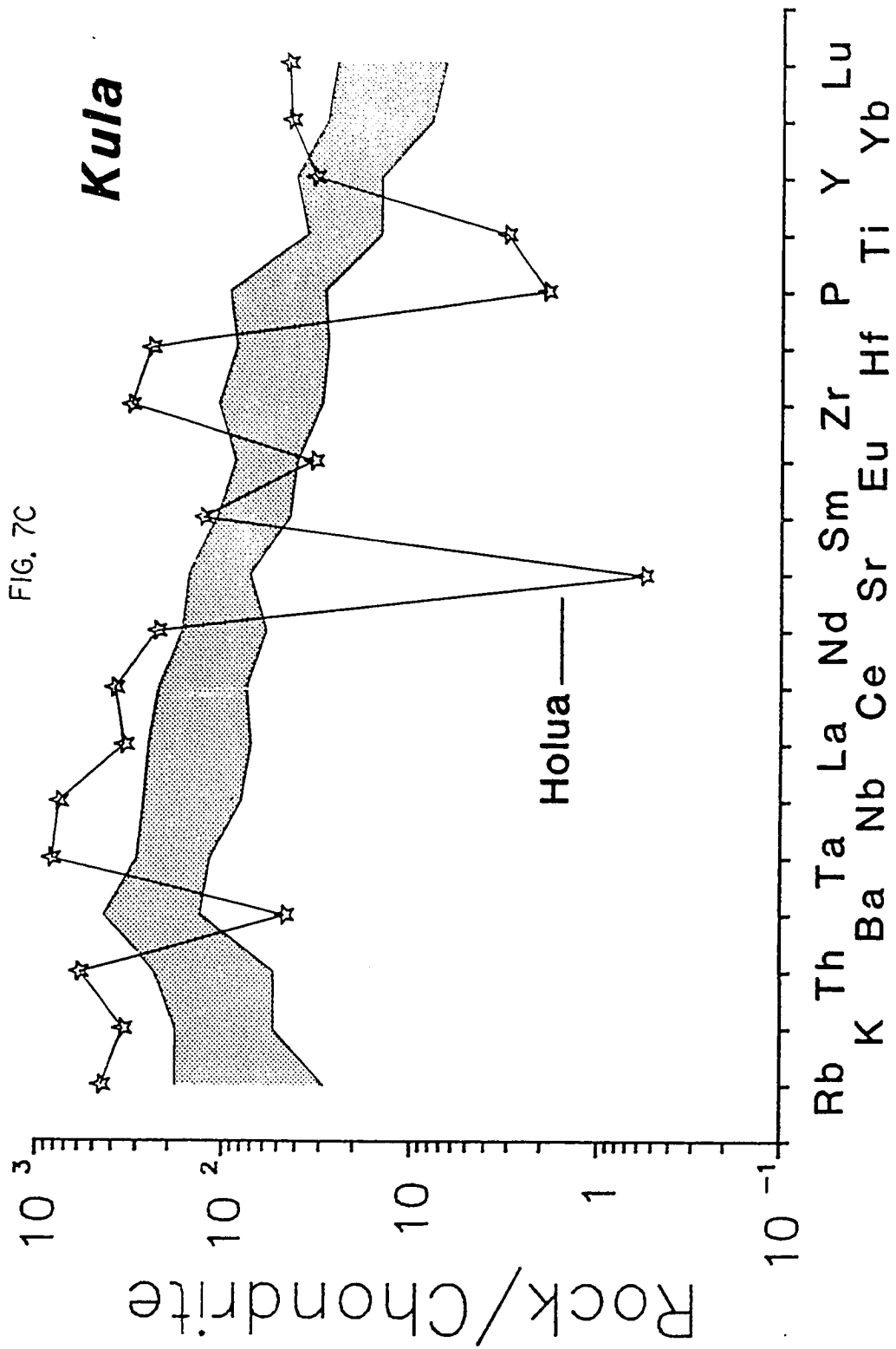
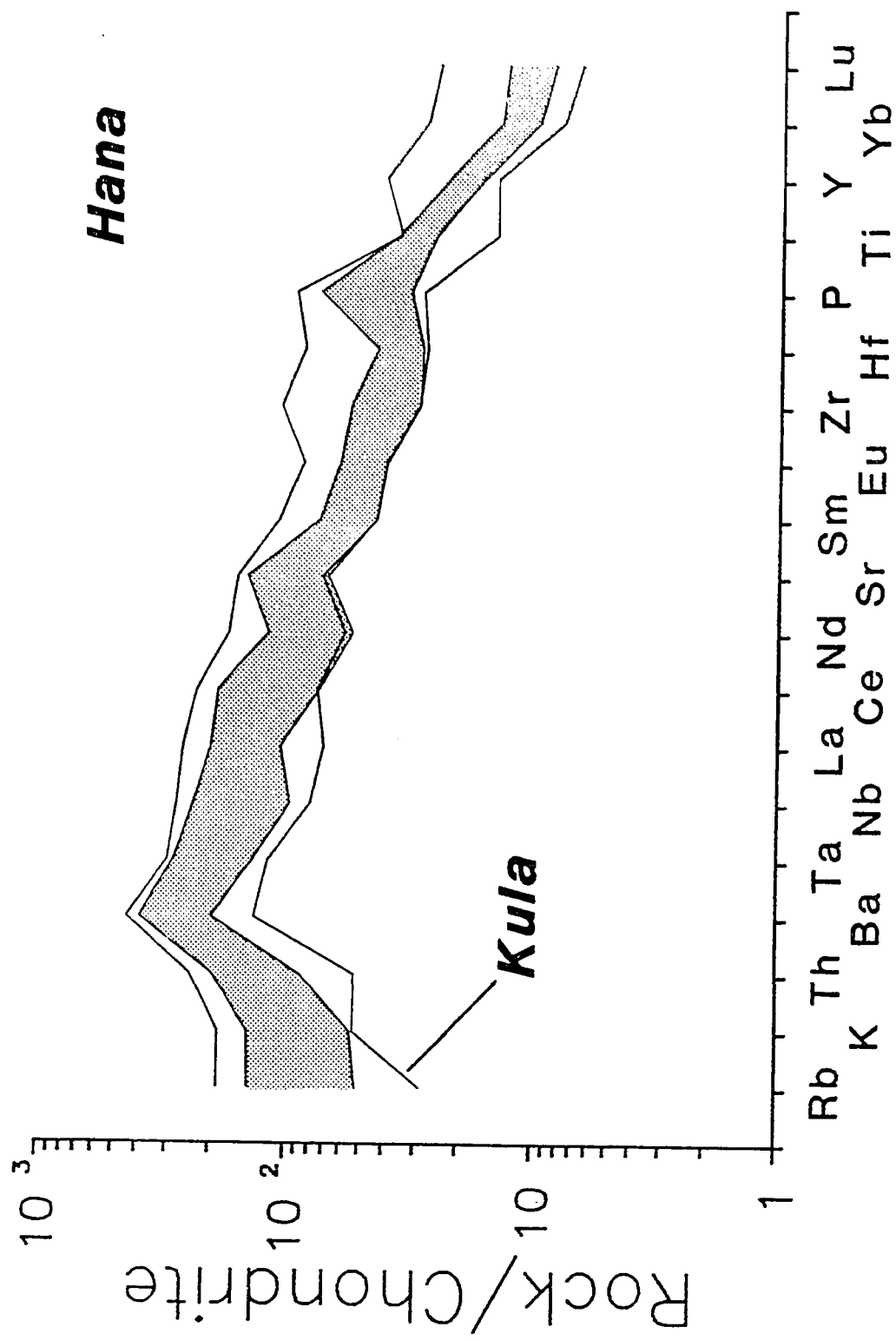


FIG. 7C



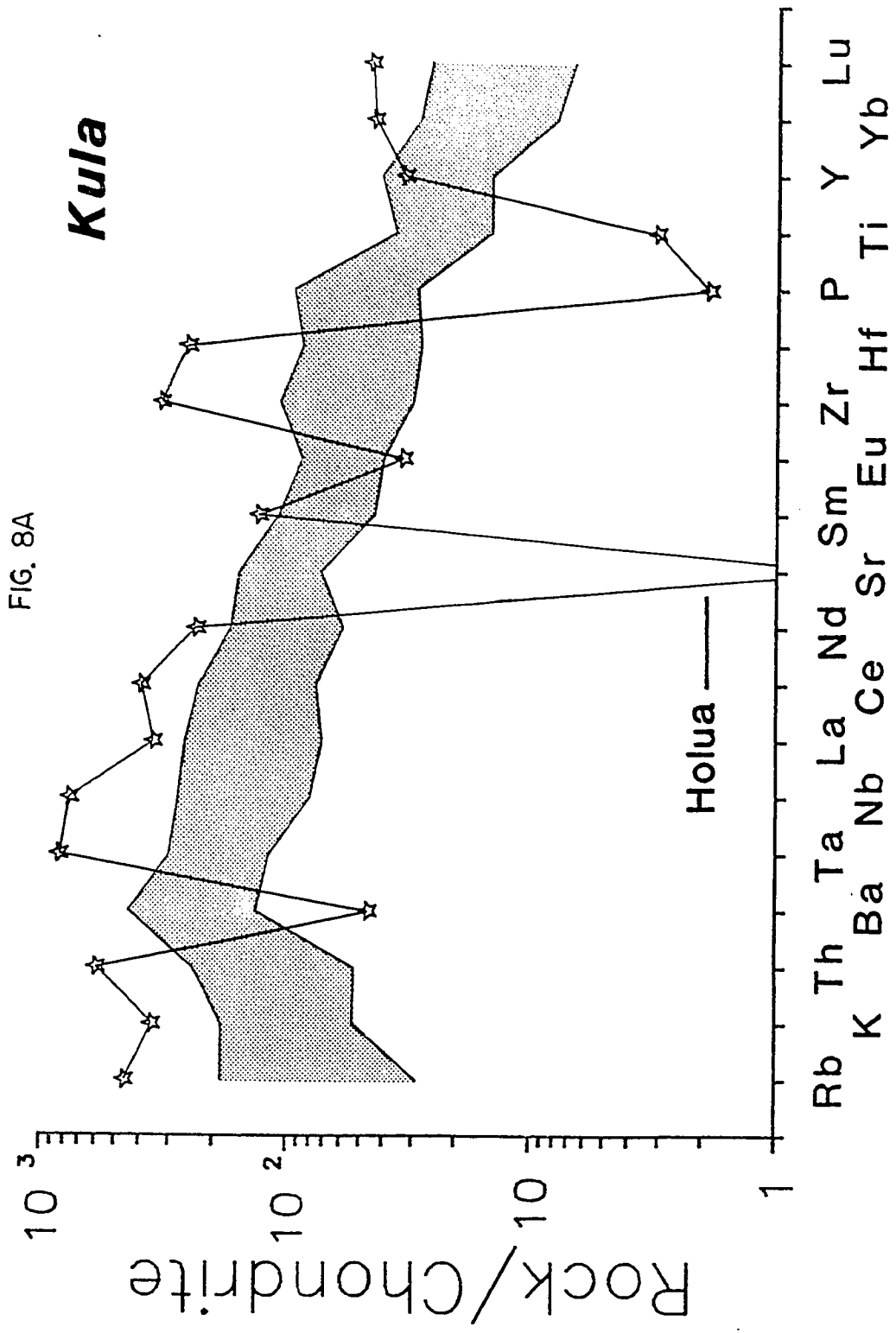
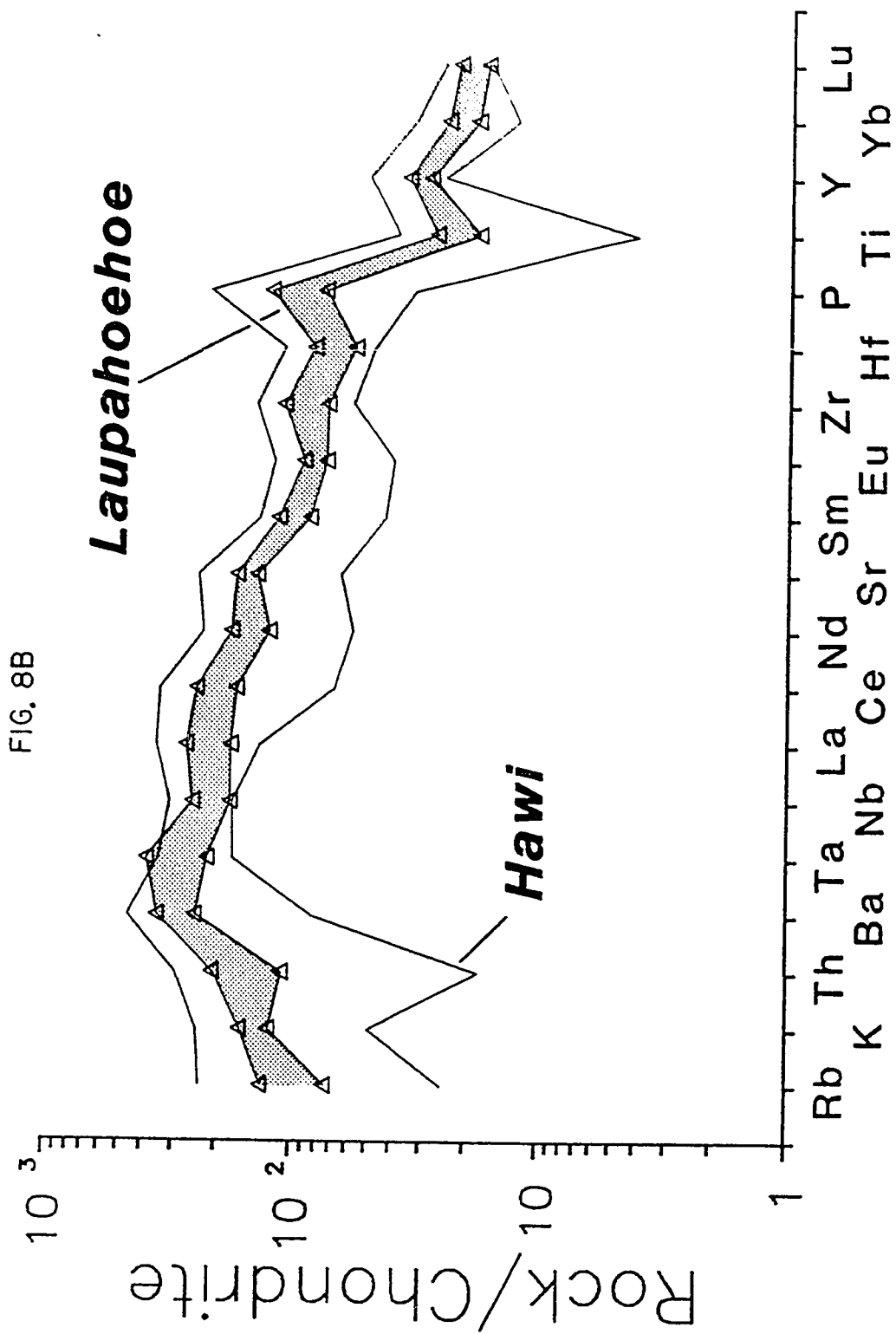
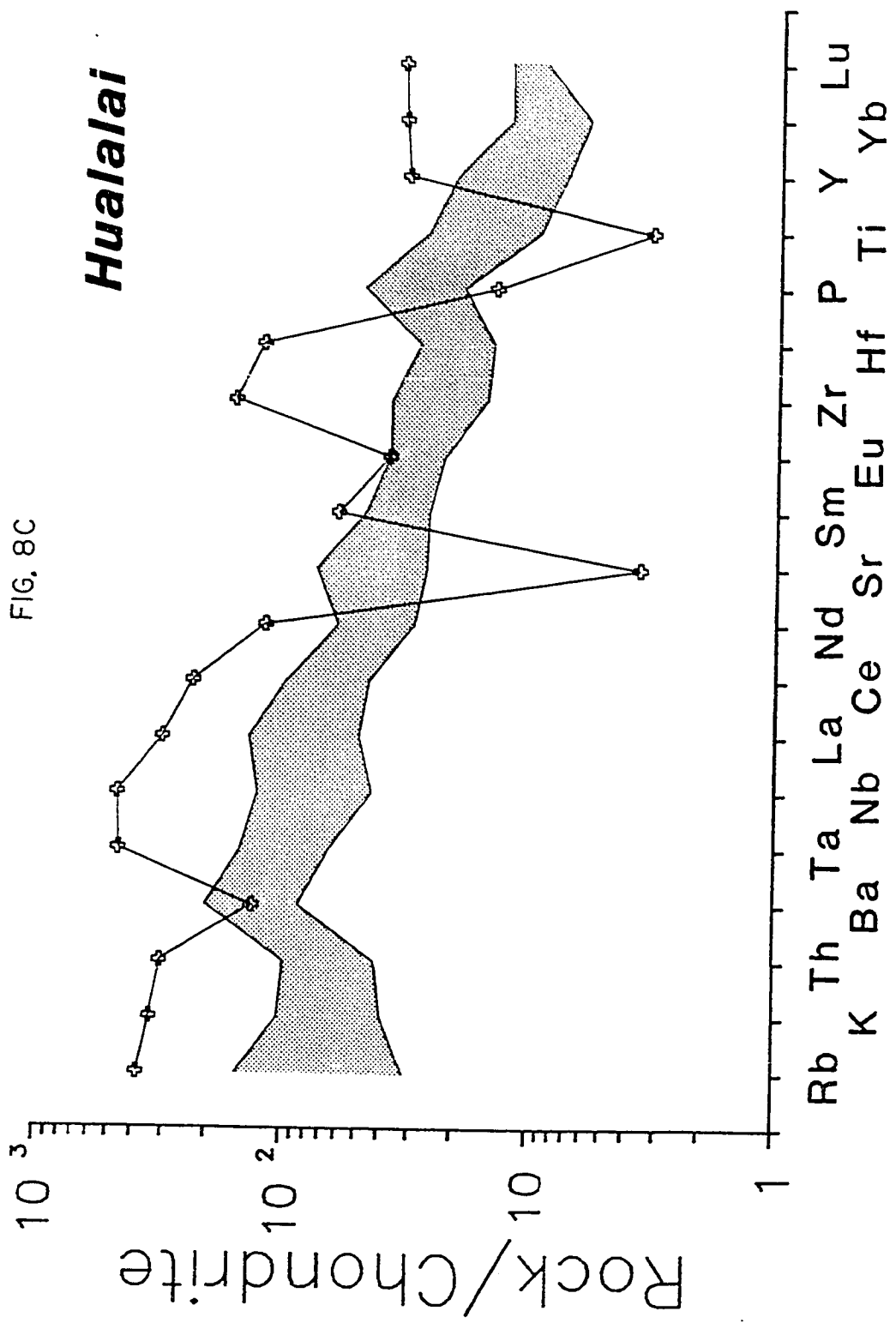
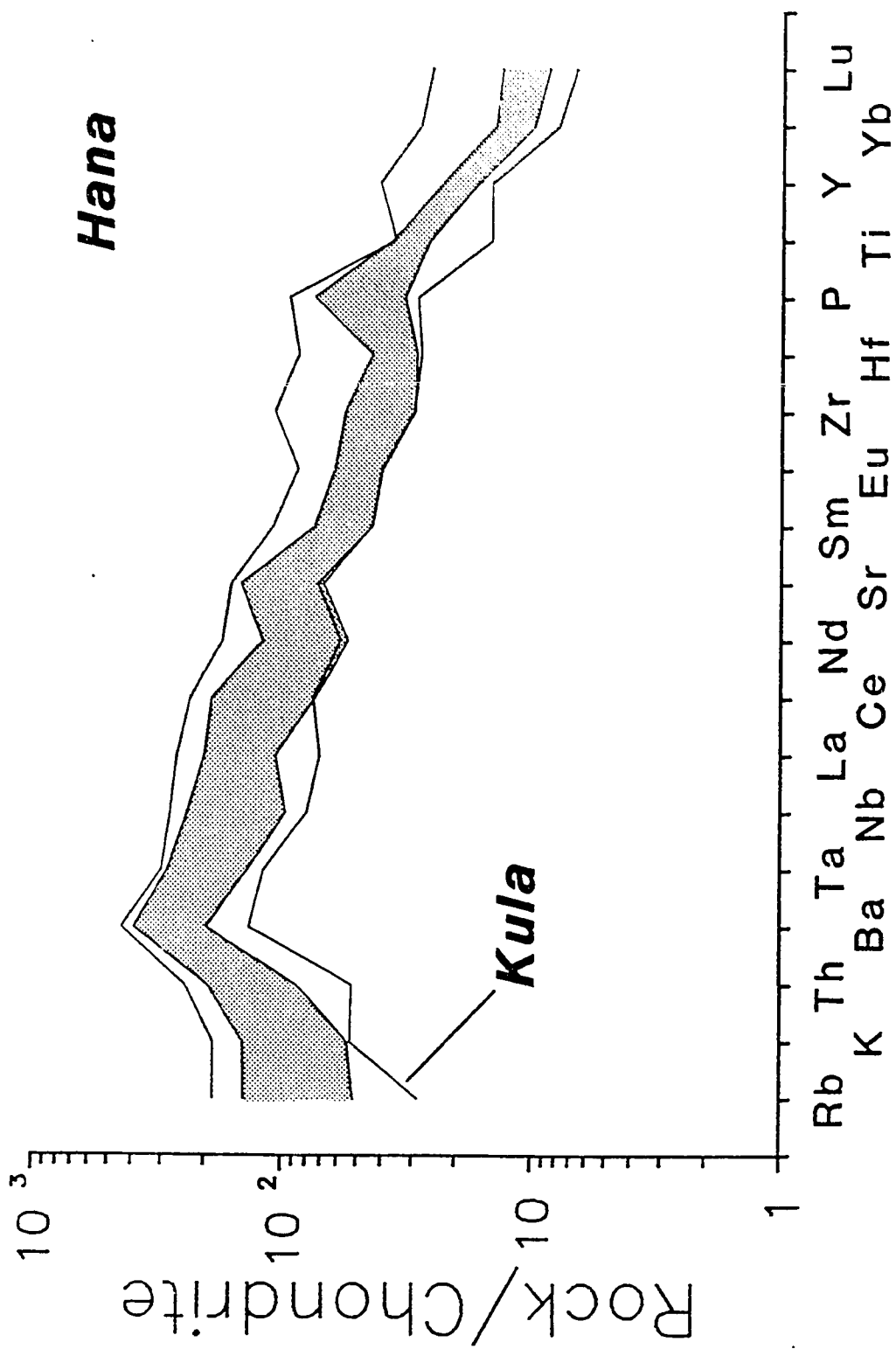


FIG. 8A







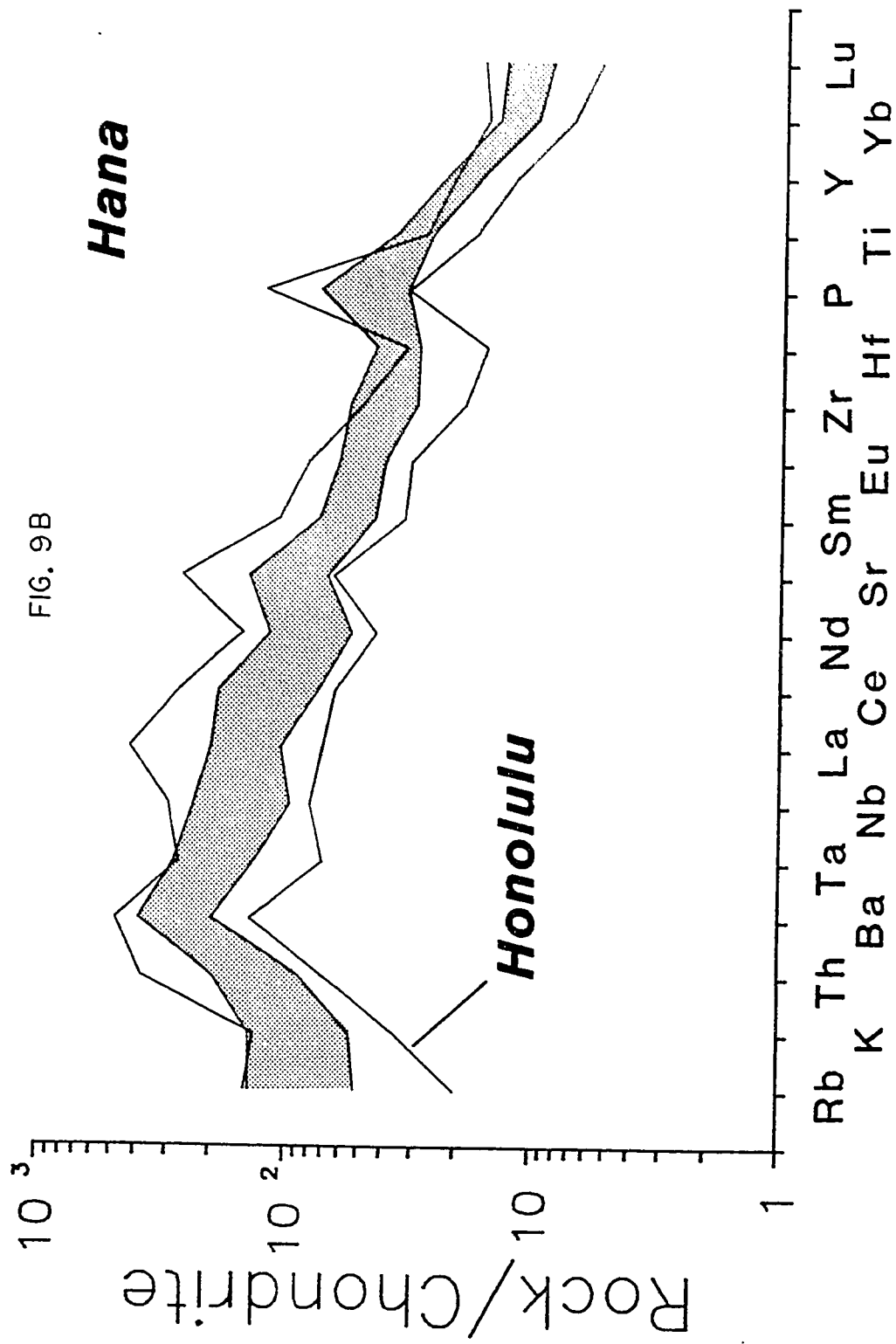
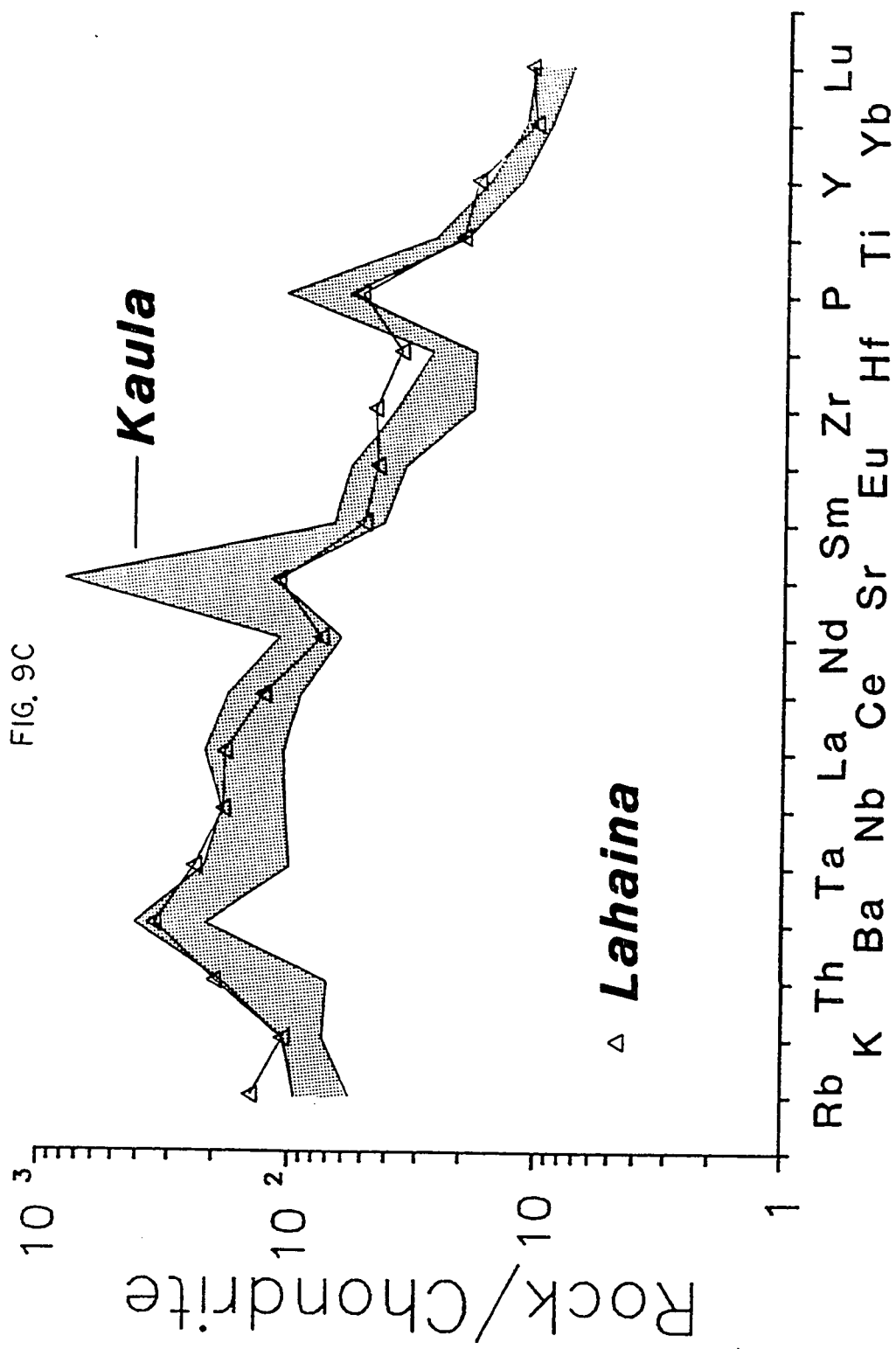
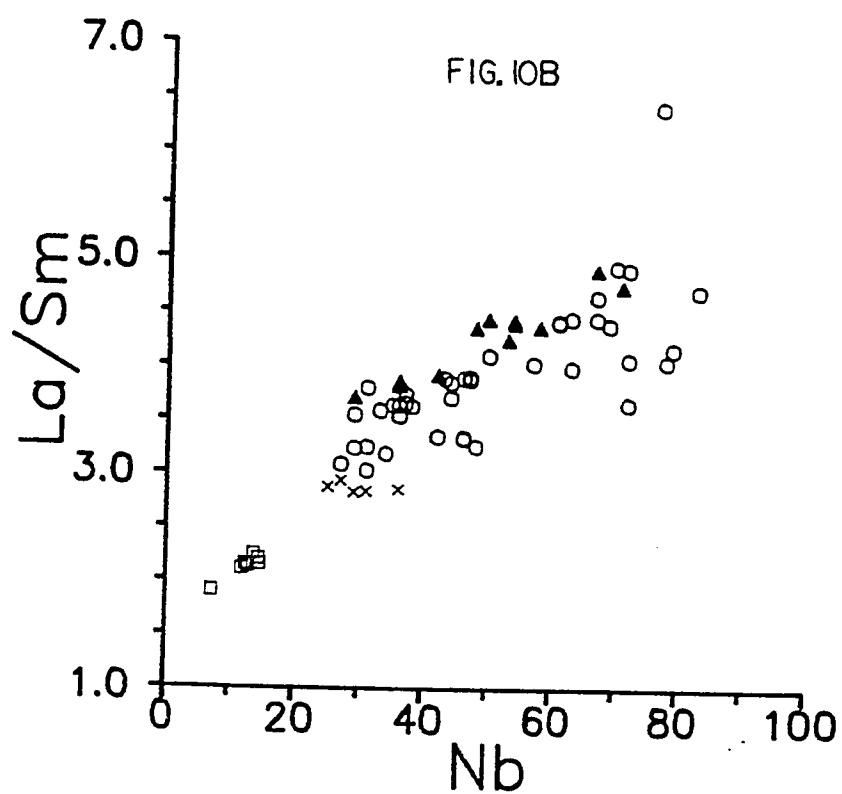
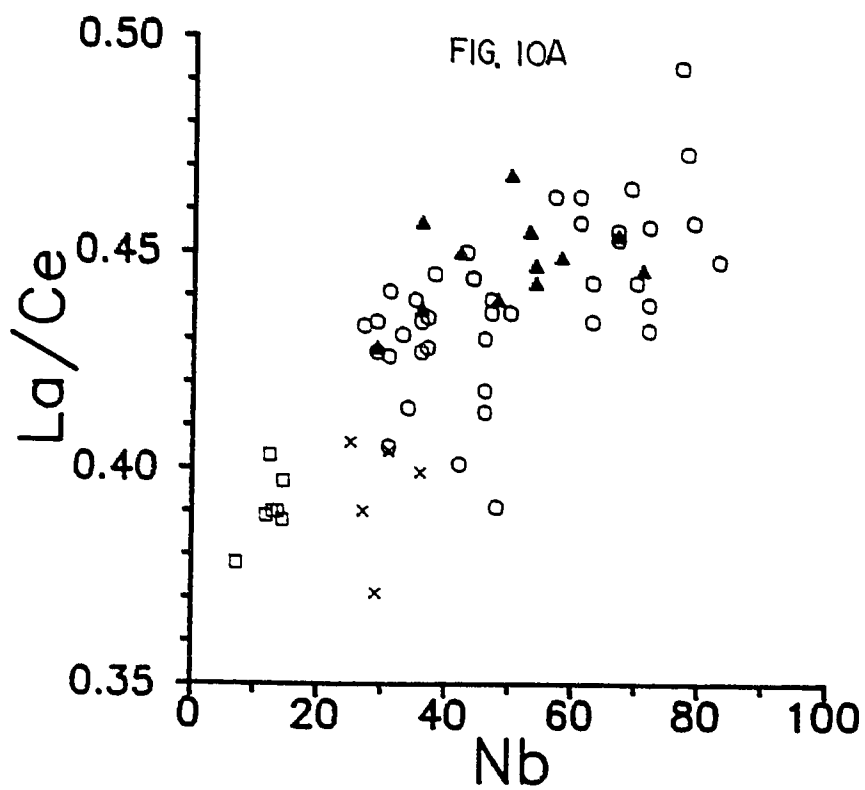
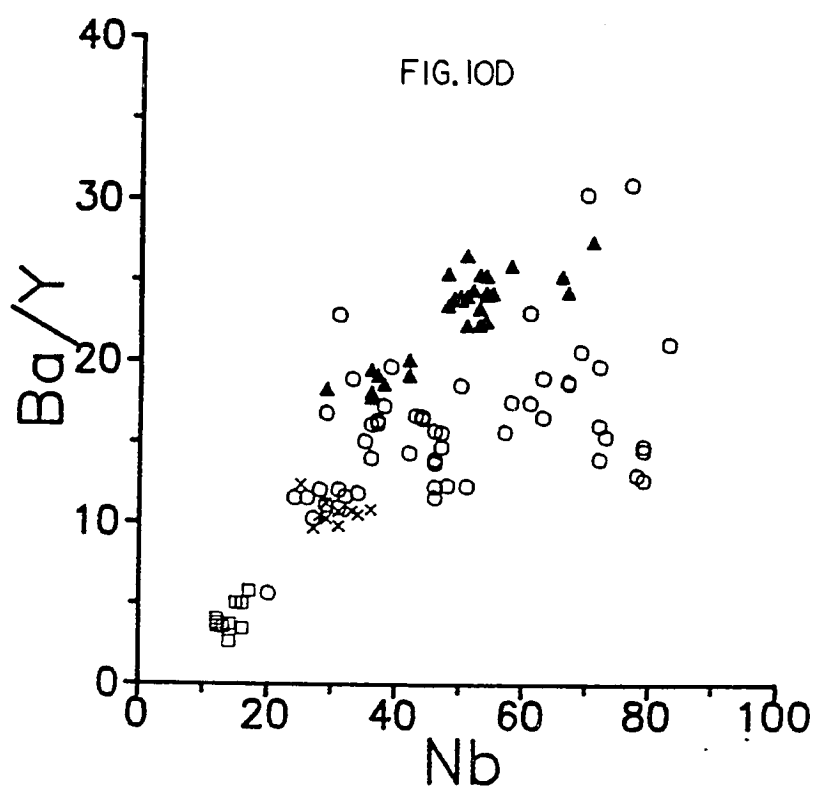
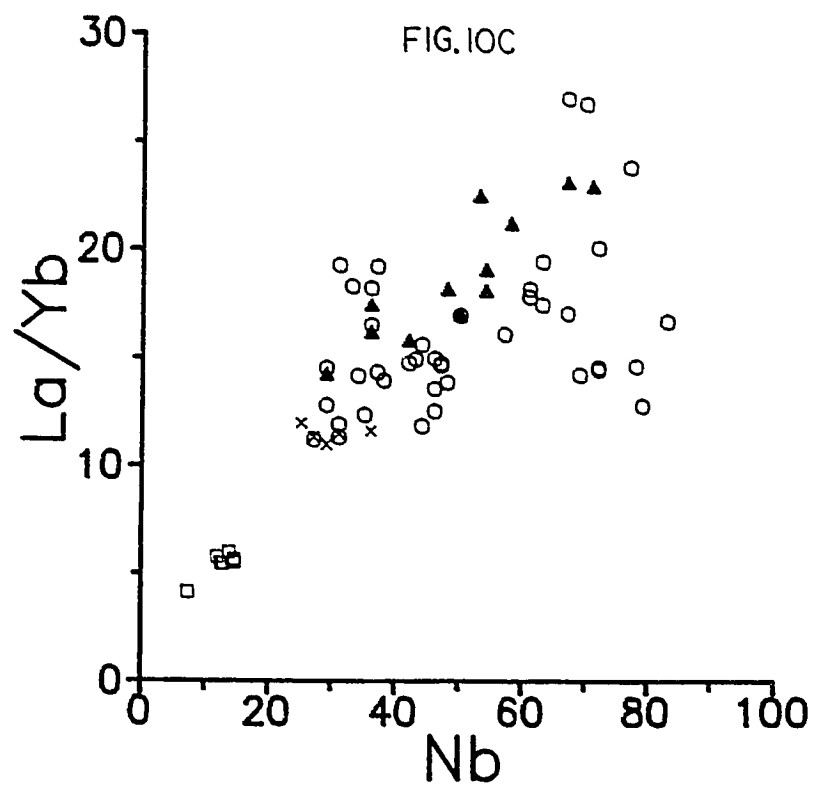
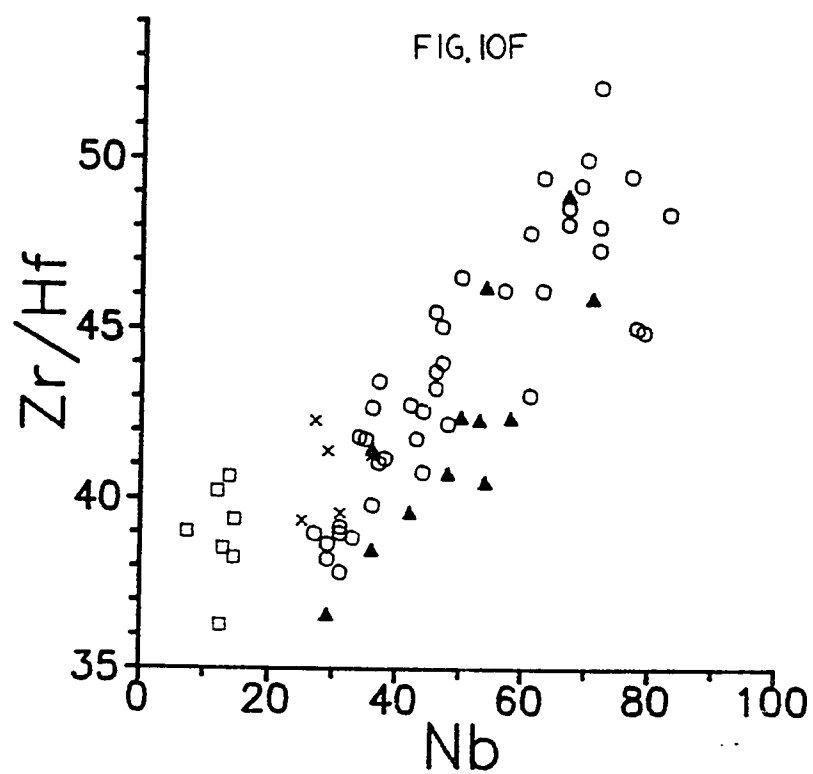
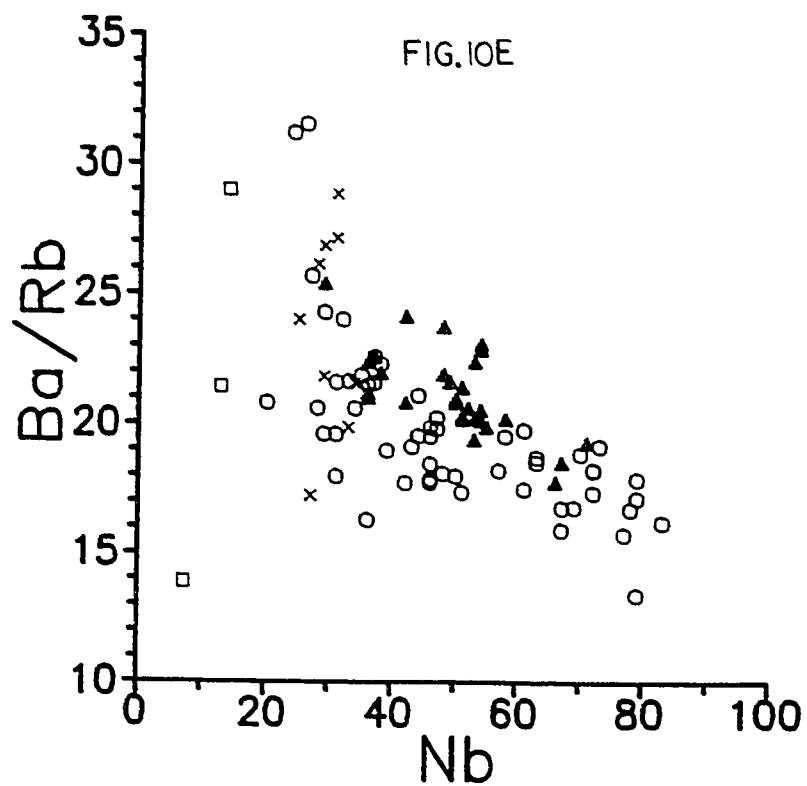


FIG. 9B









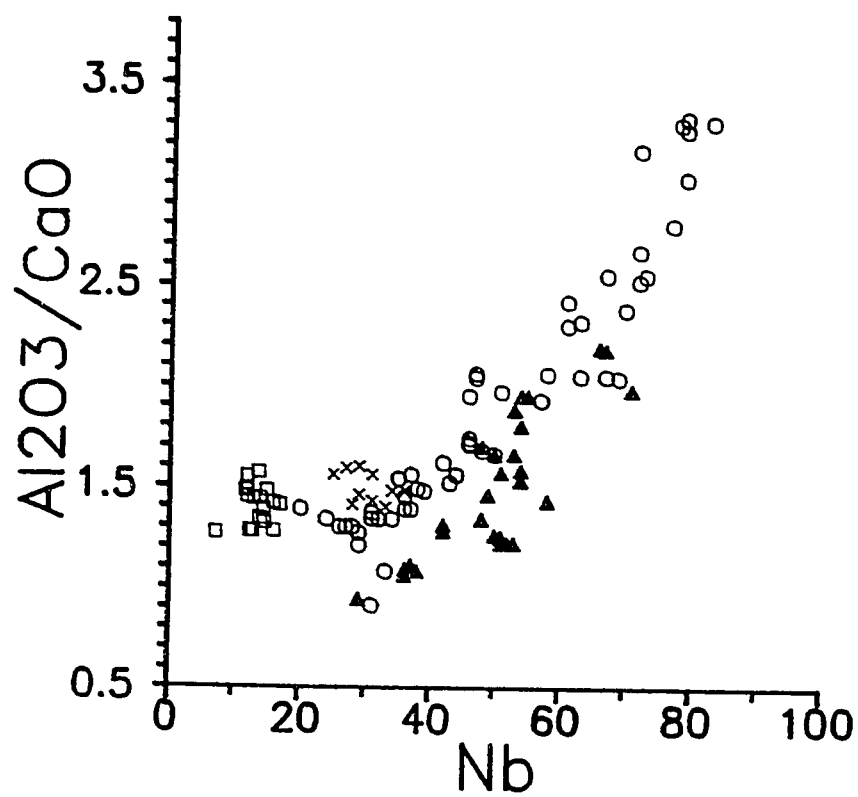


FIG. 10G

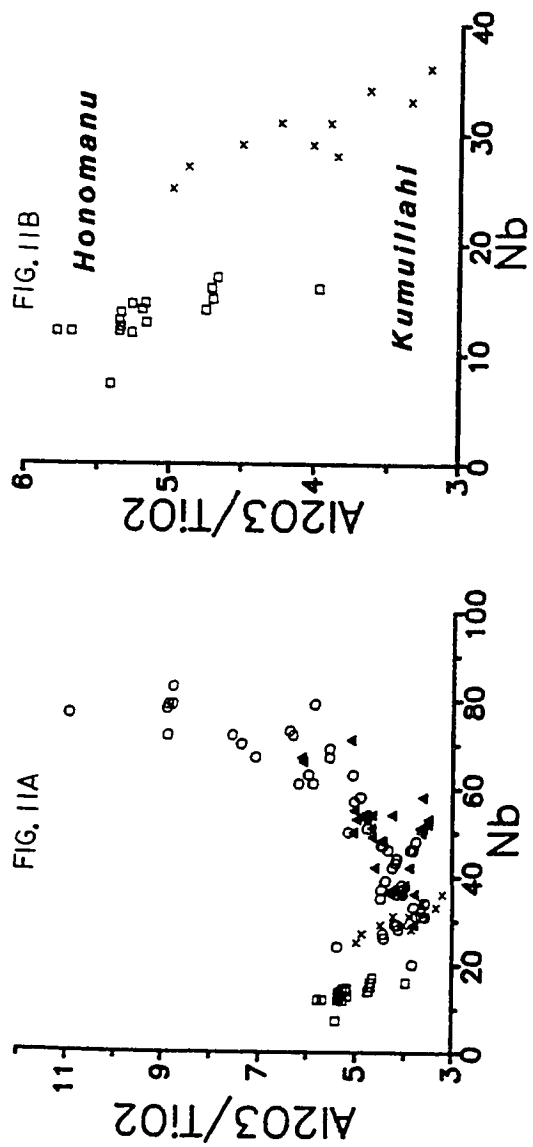
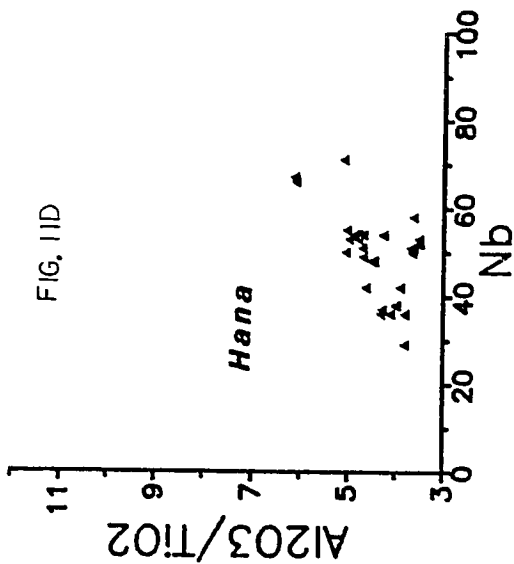
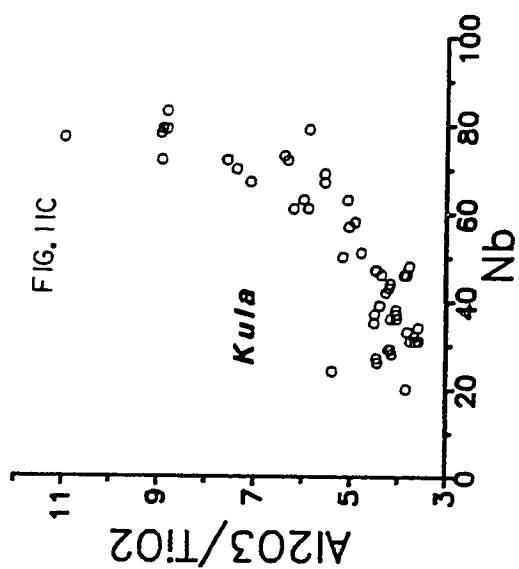
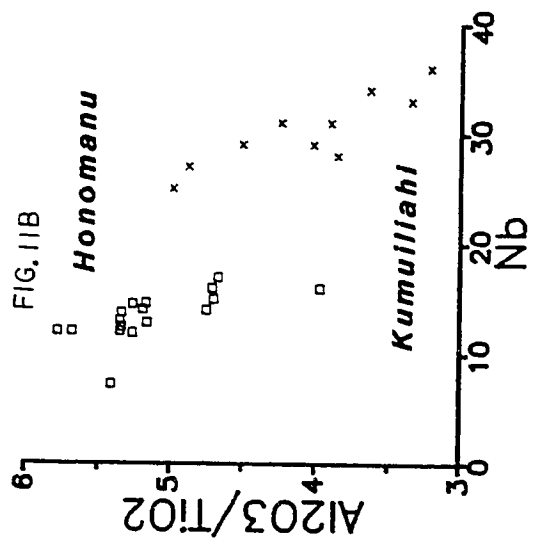
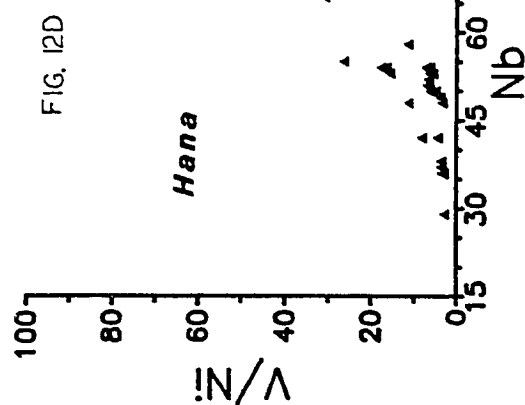
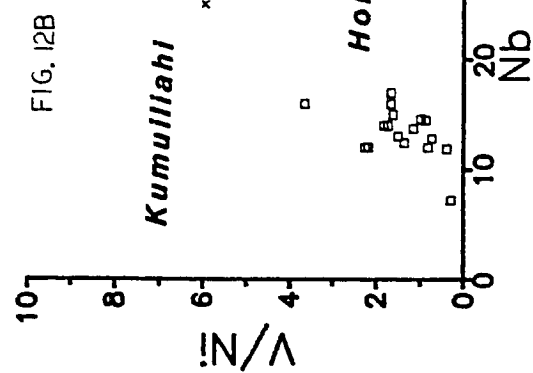
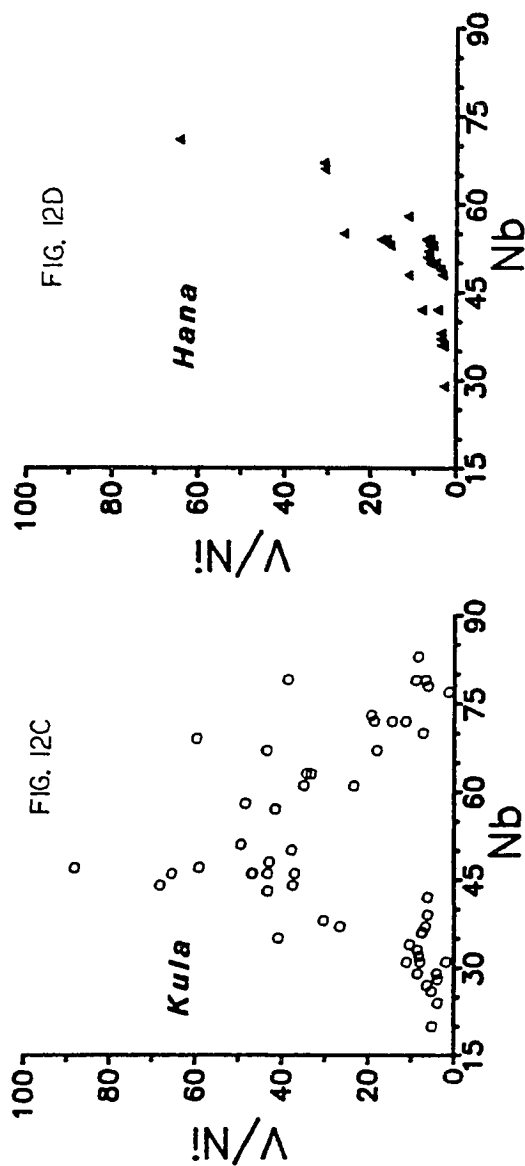
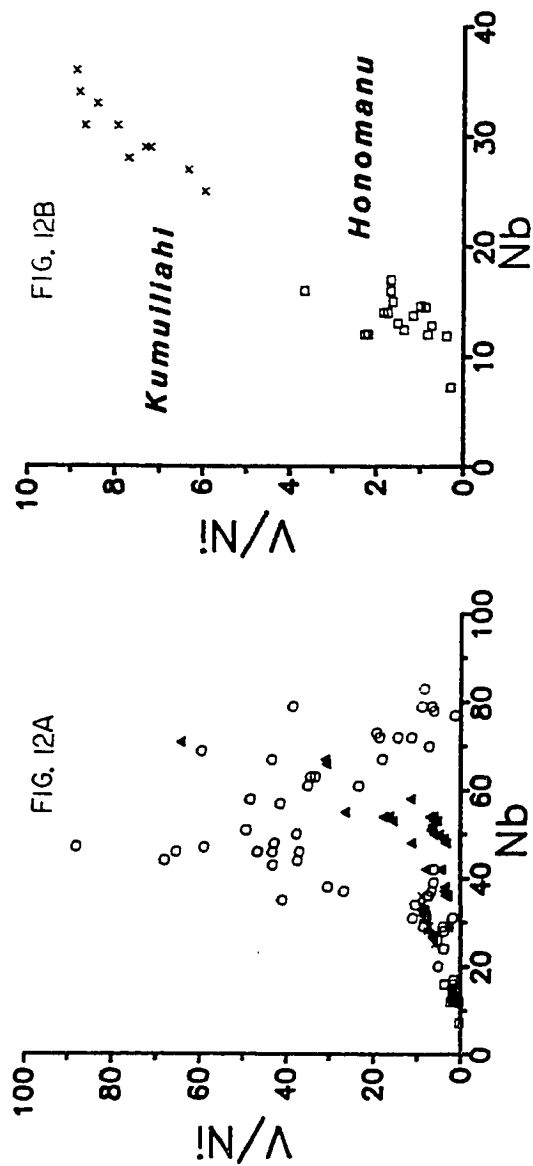
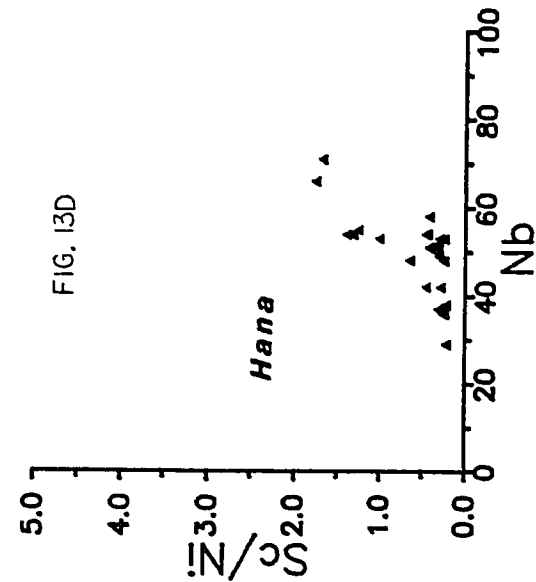
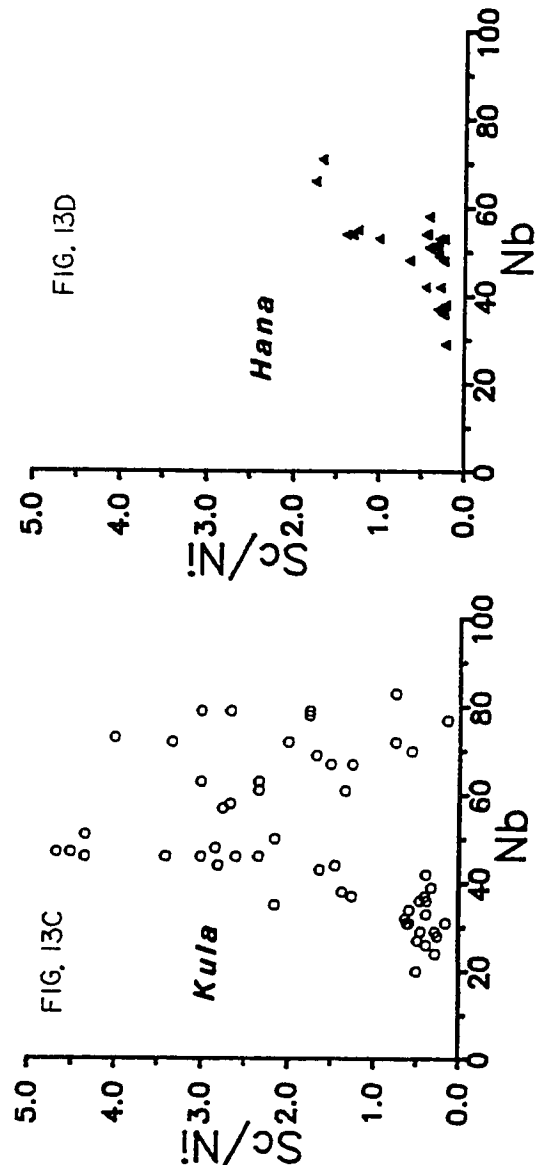
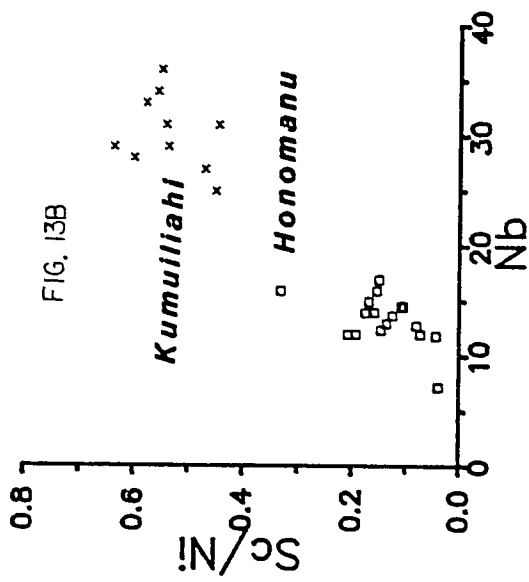
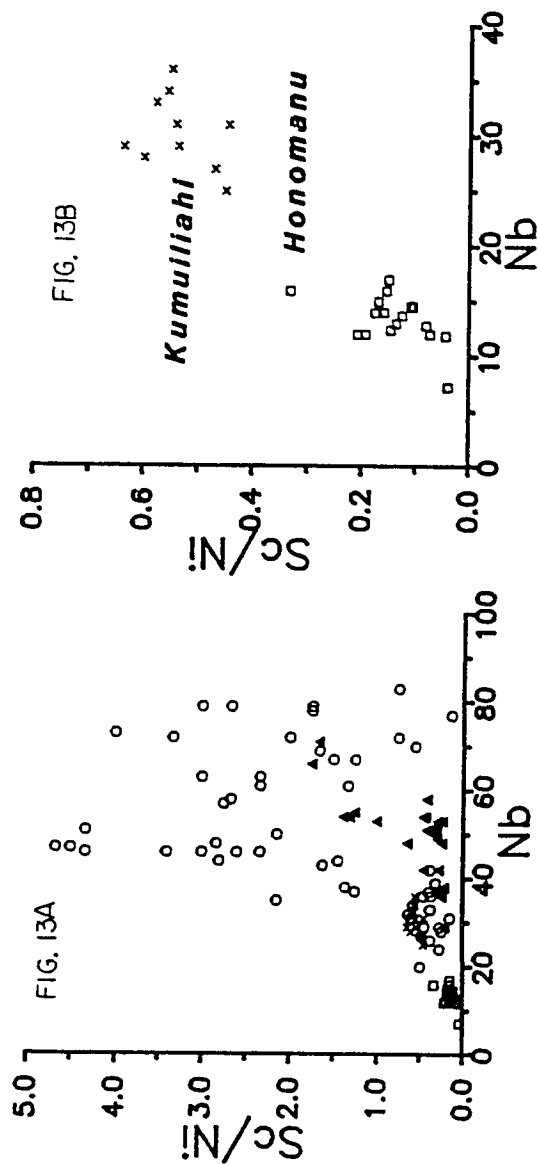
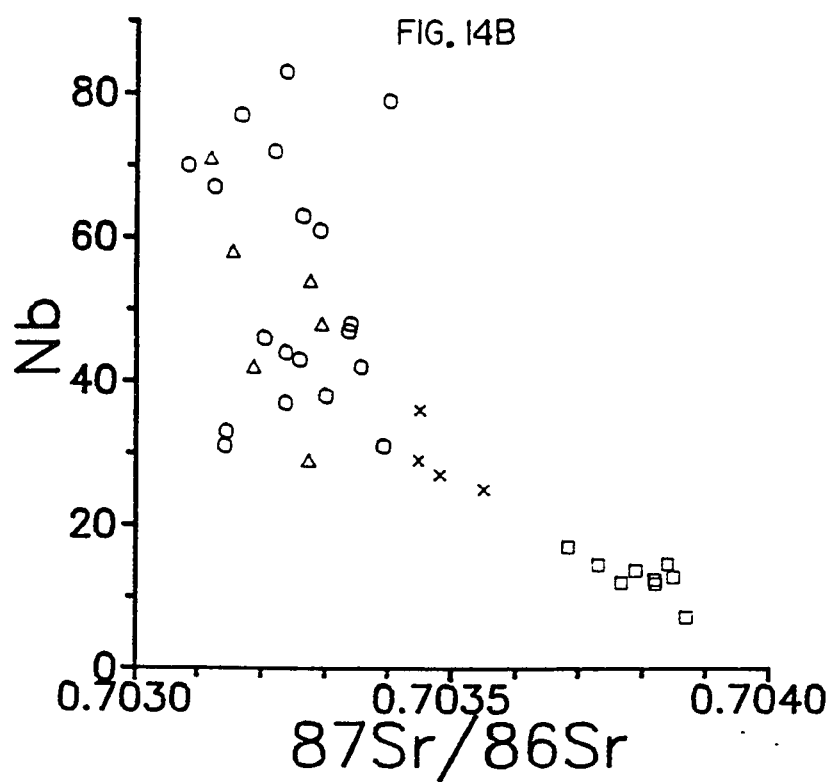
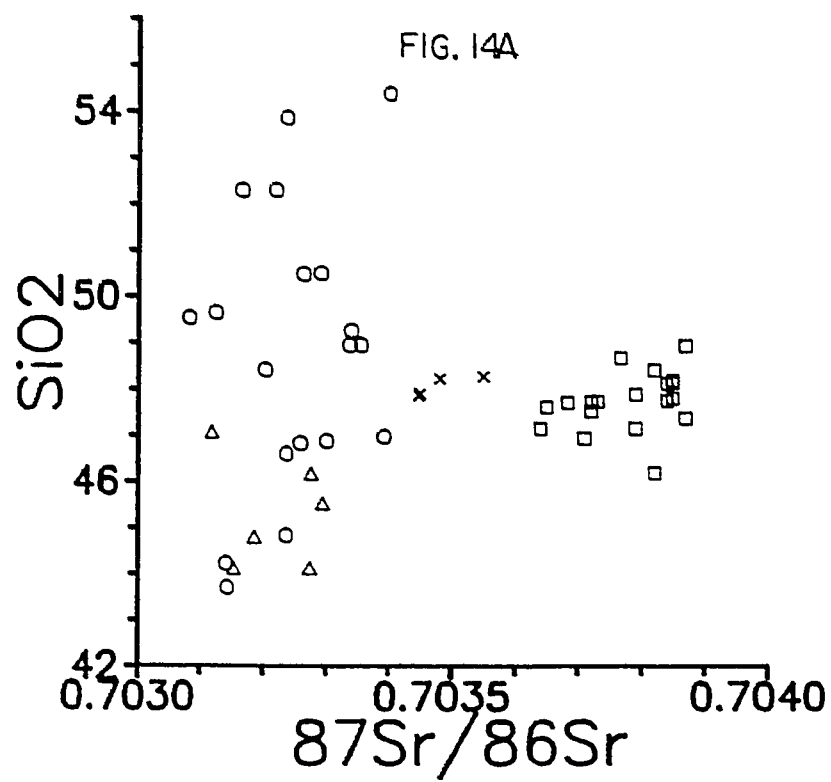


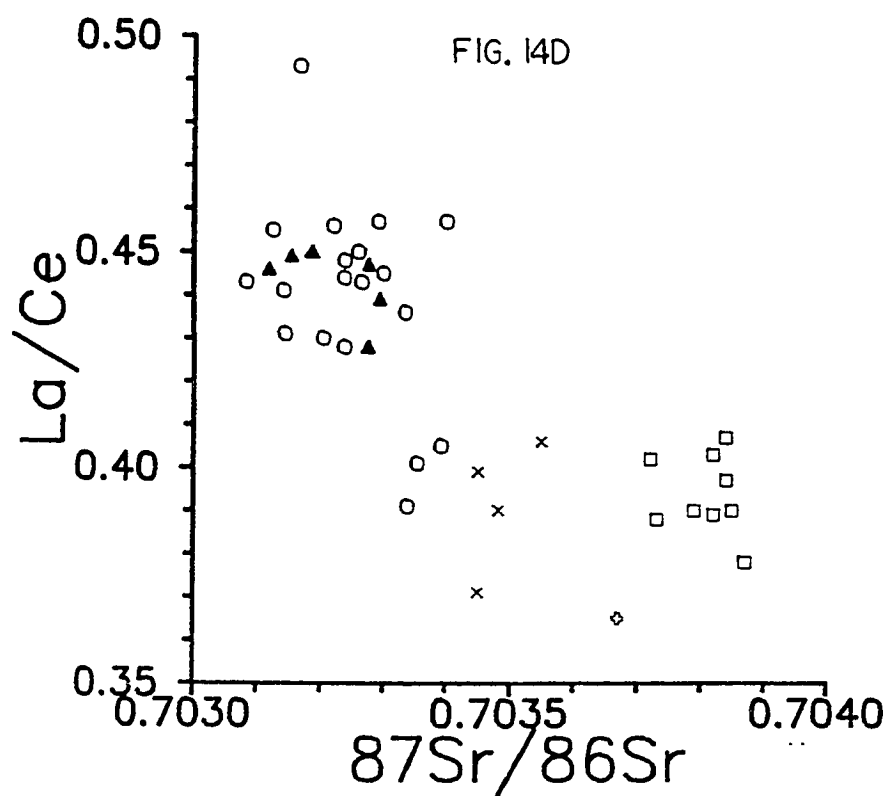
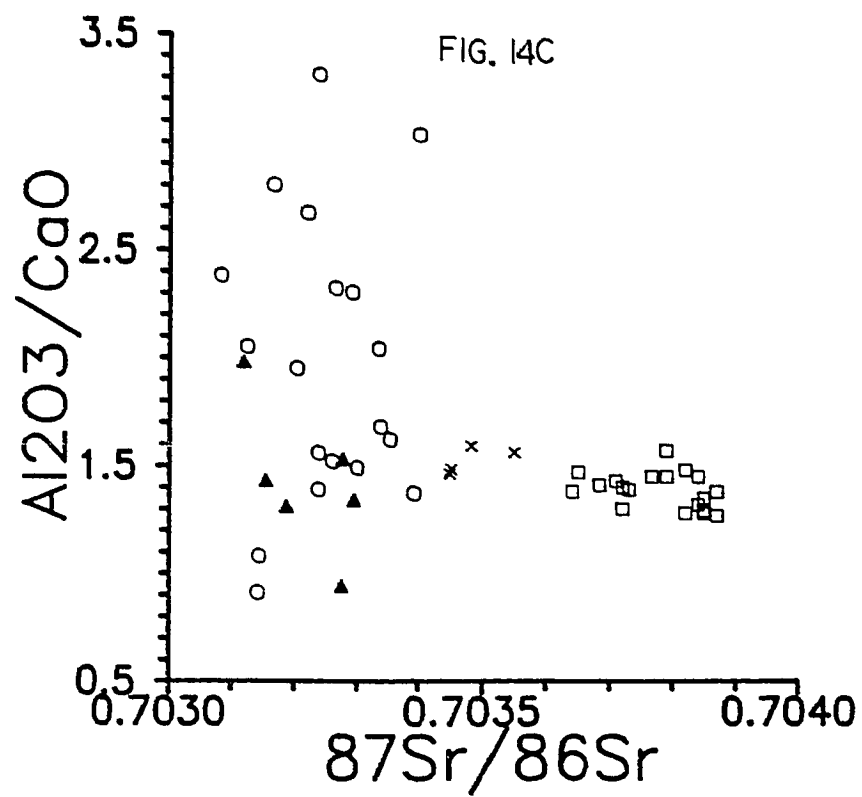
FIG. IIB

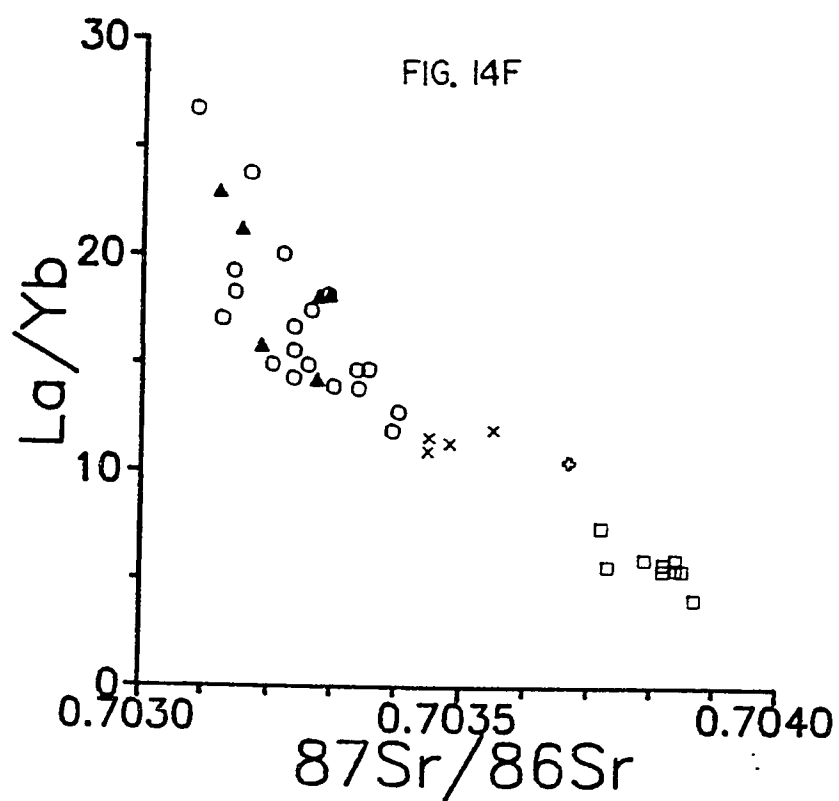
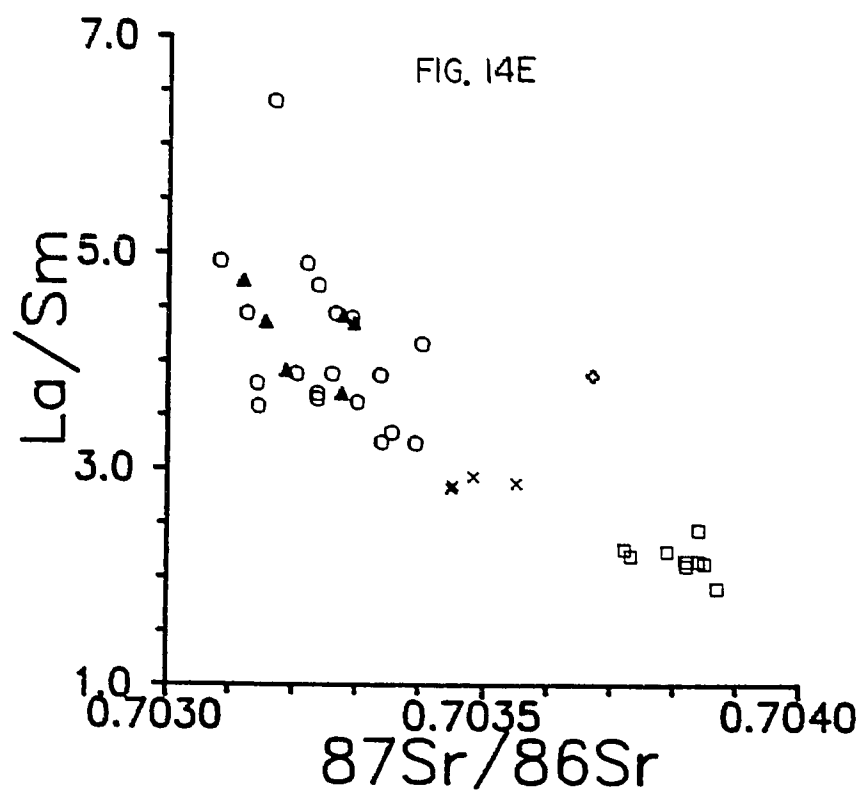


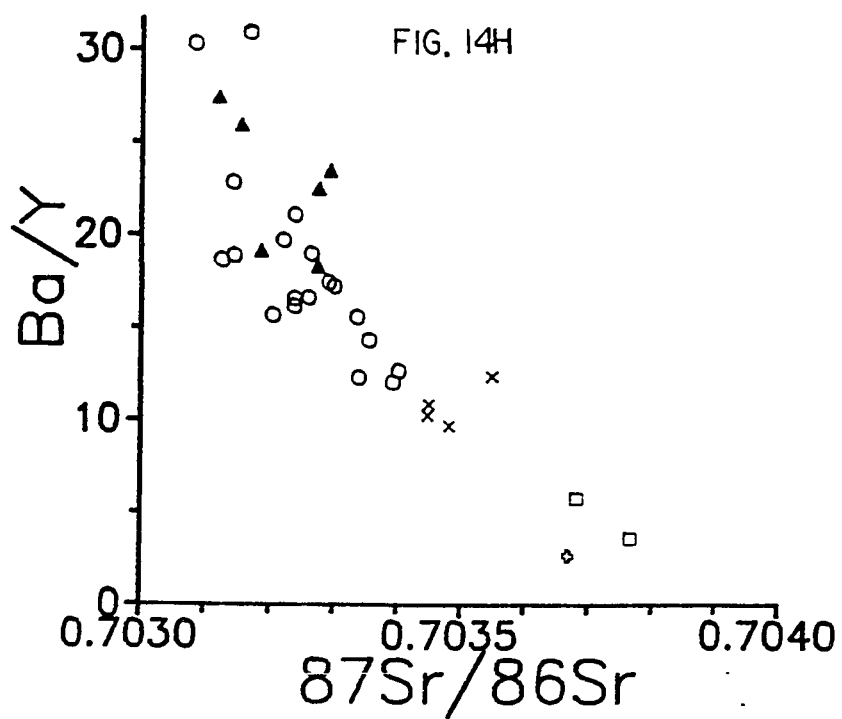
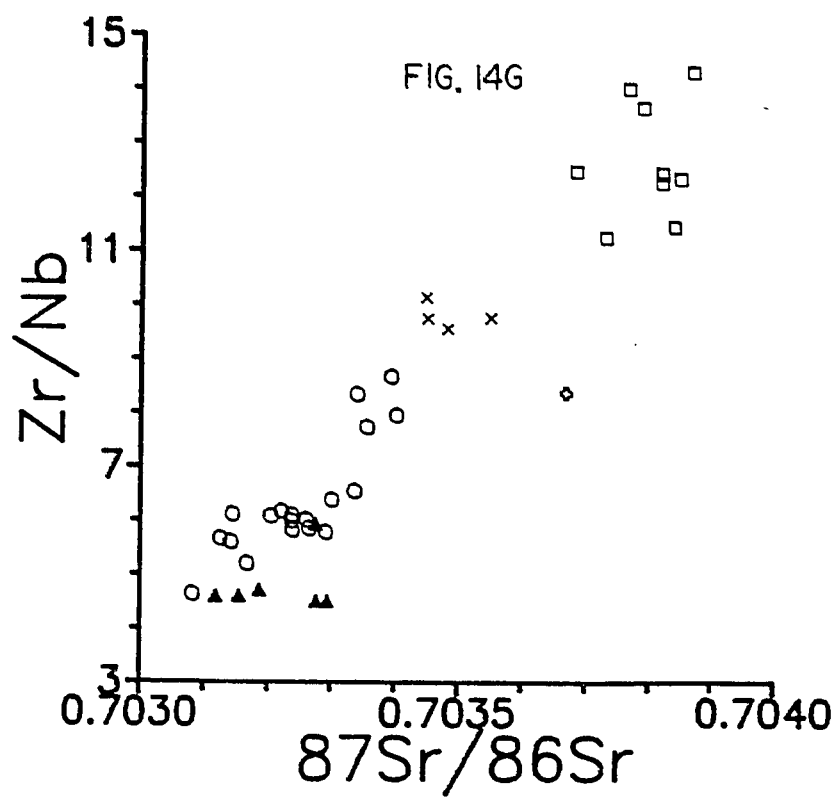


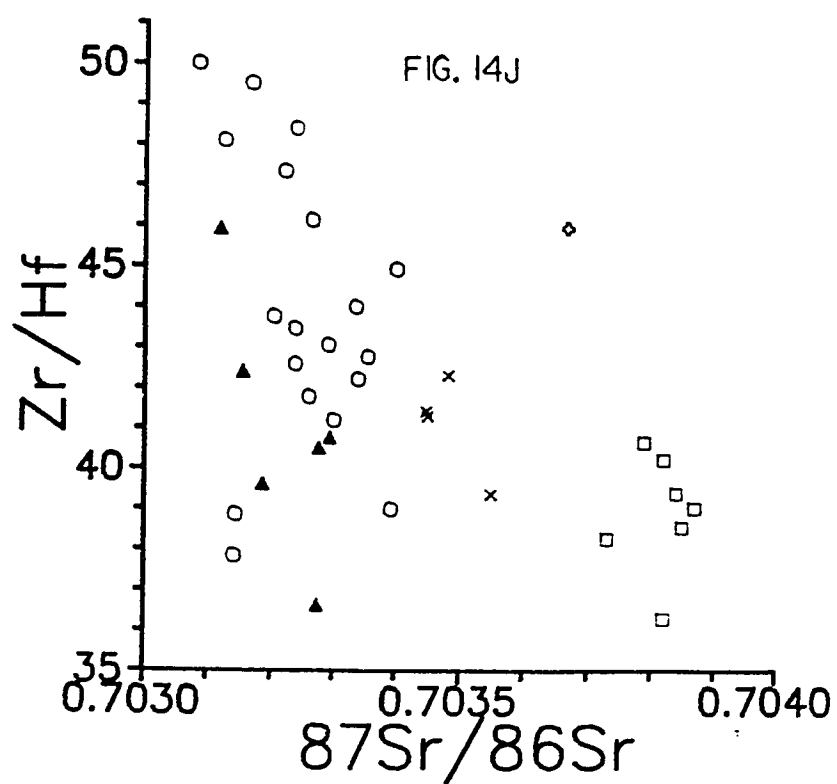
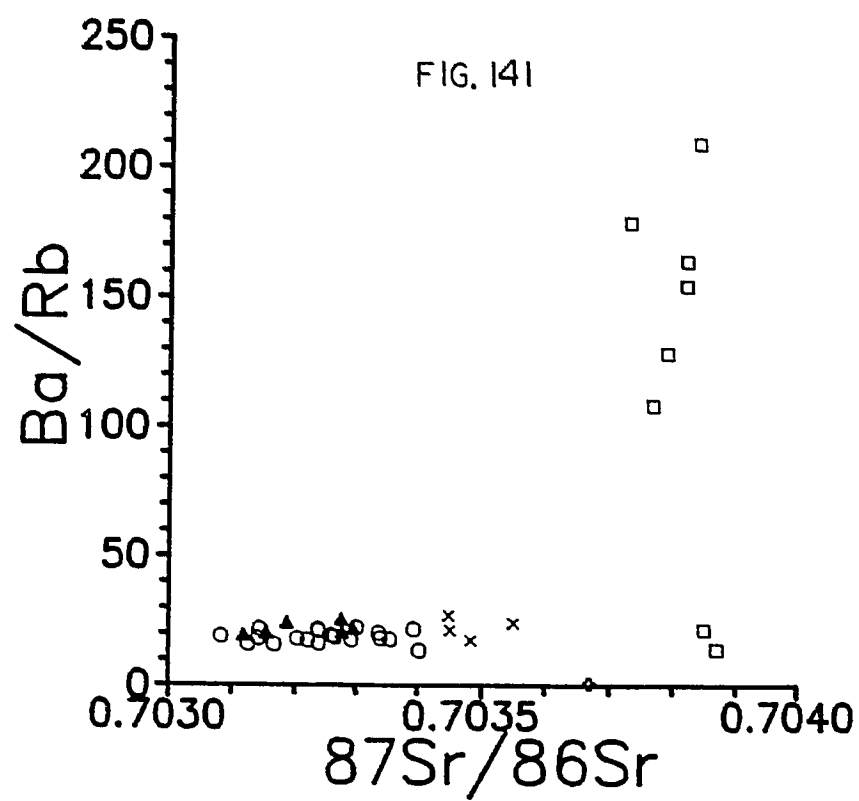












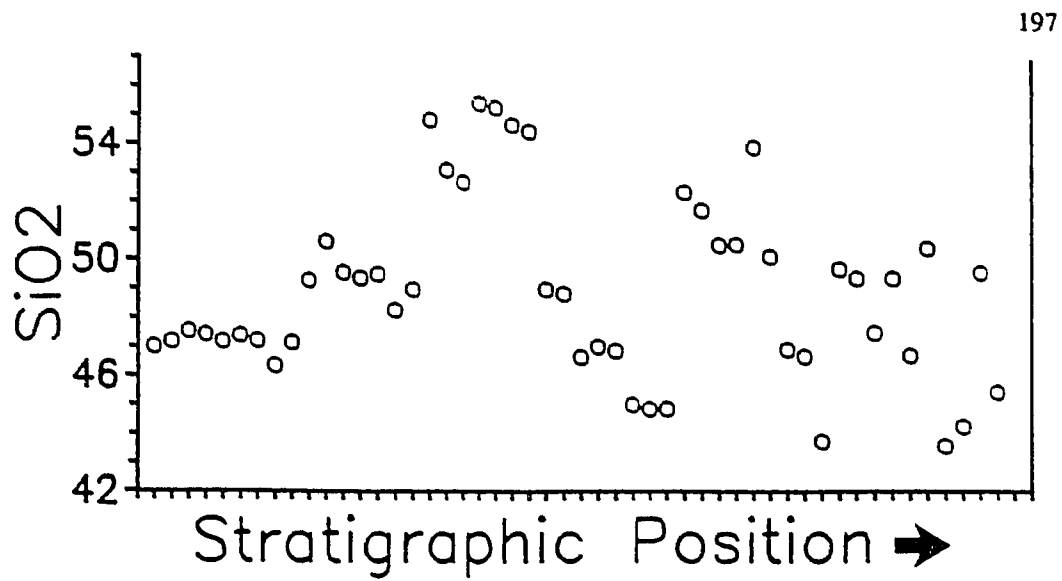


FIG. 15A

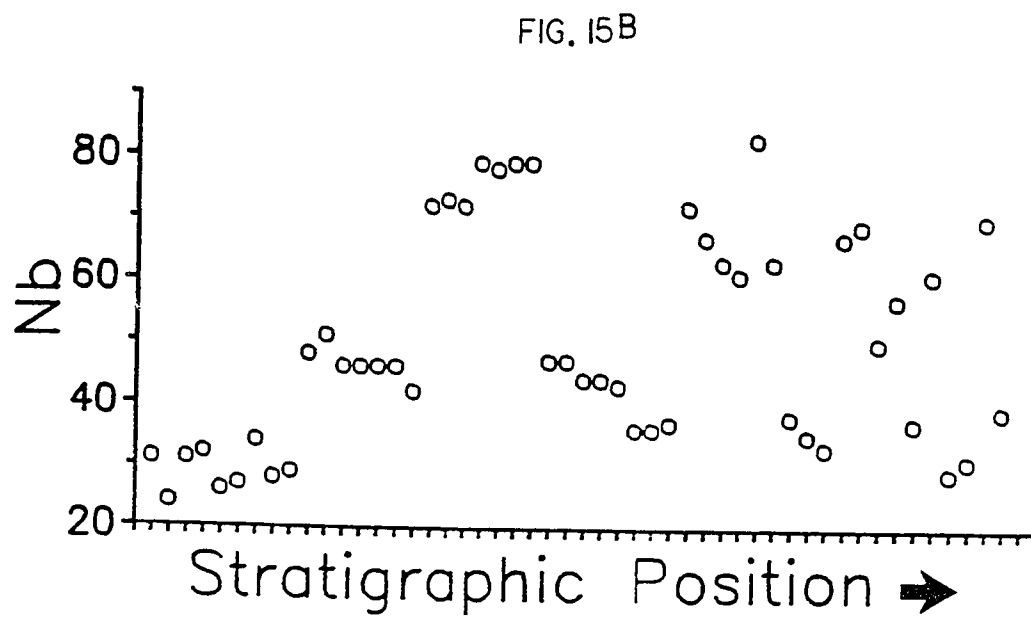
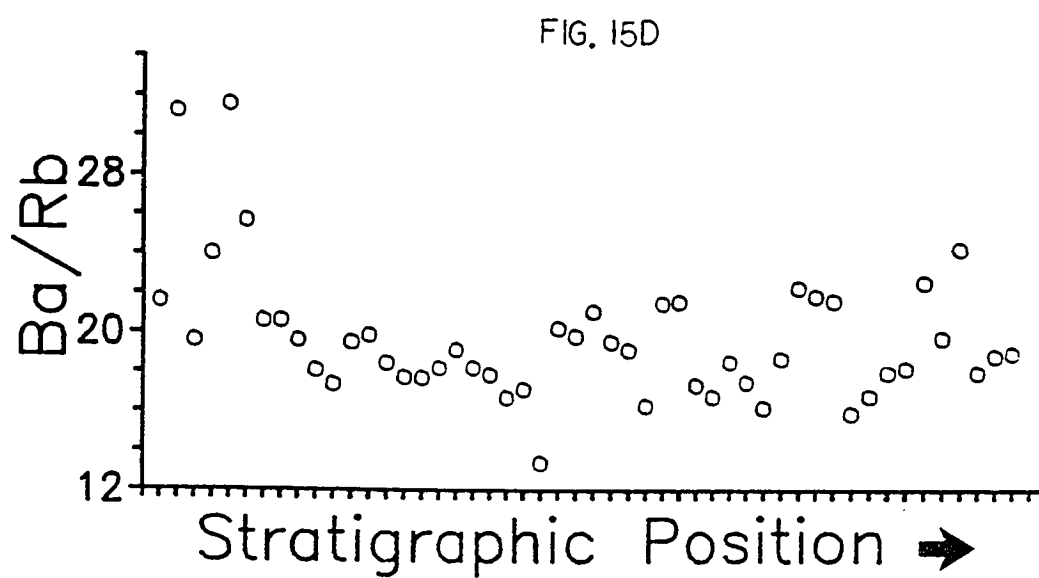
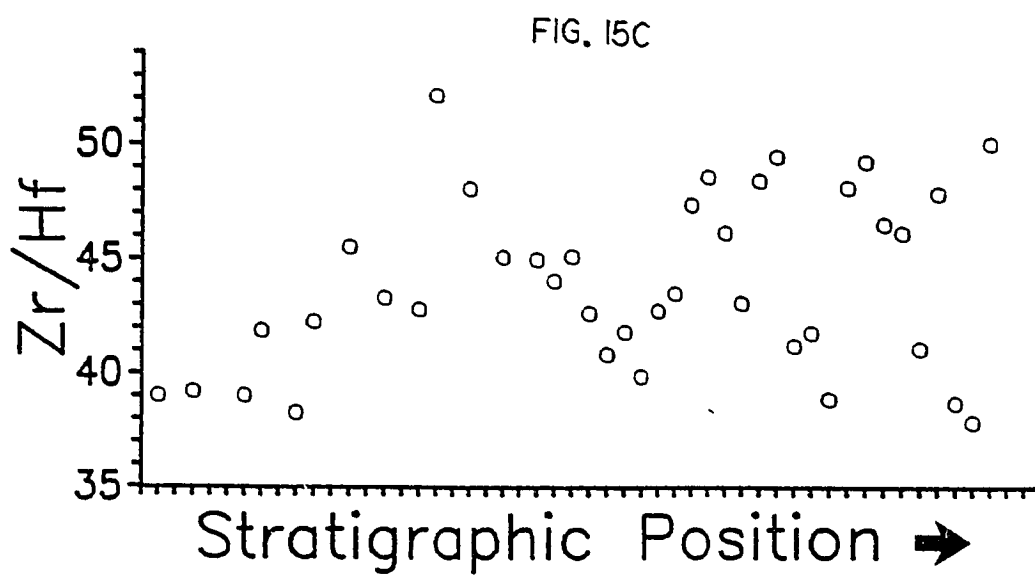


FIG. 15B



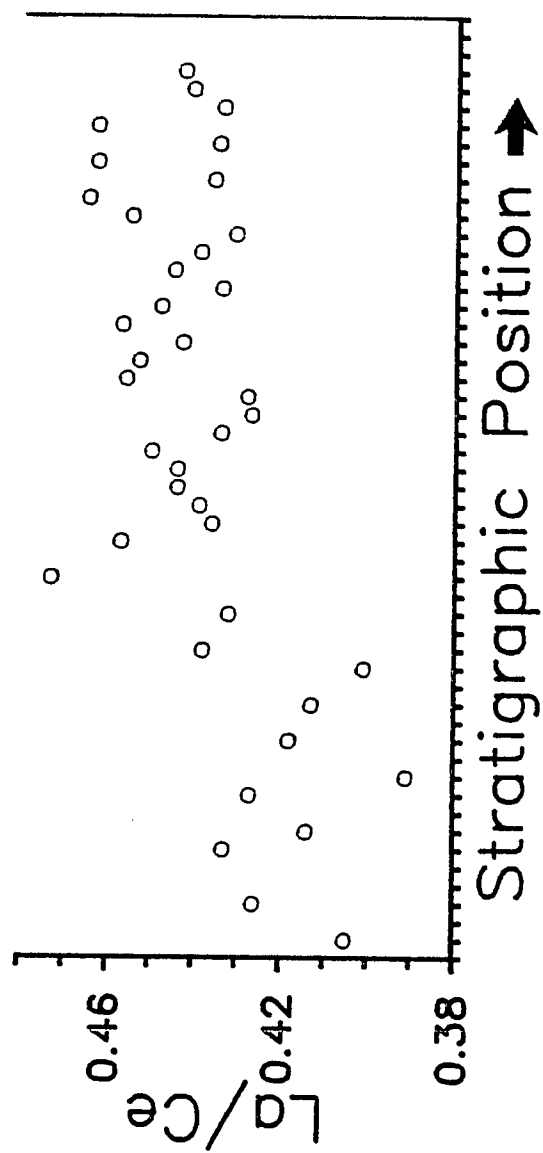


FIG. 15E

FIG. 15F

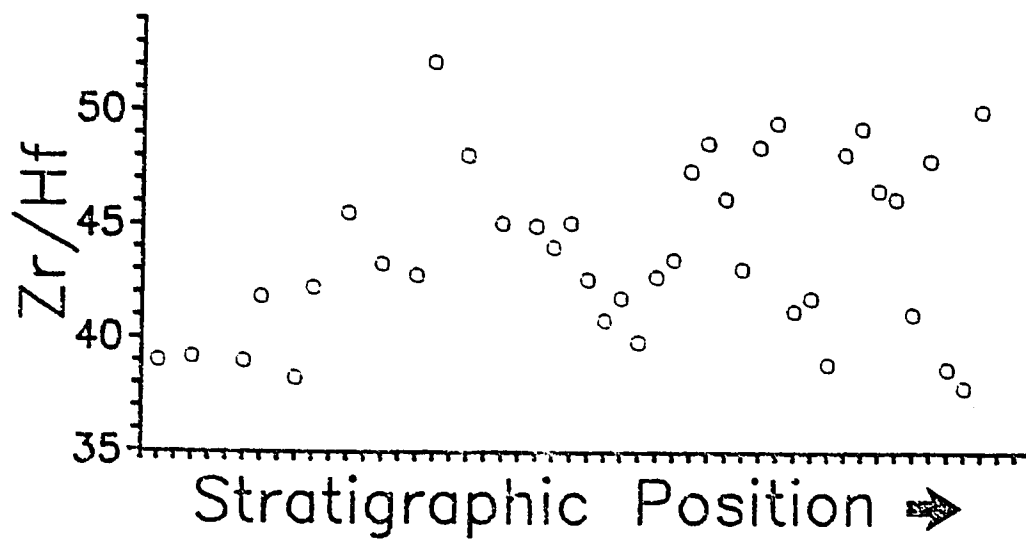
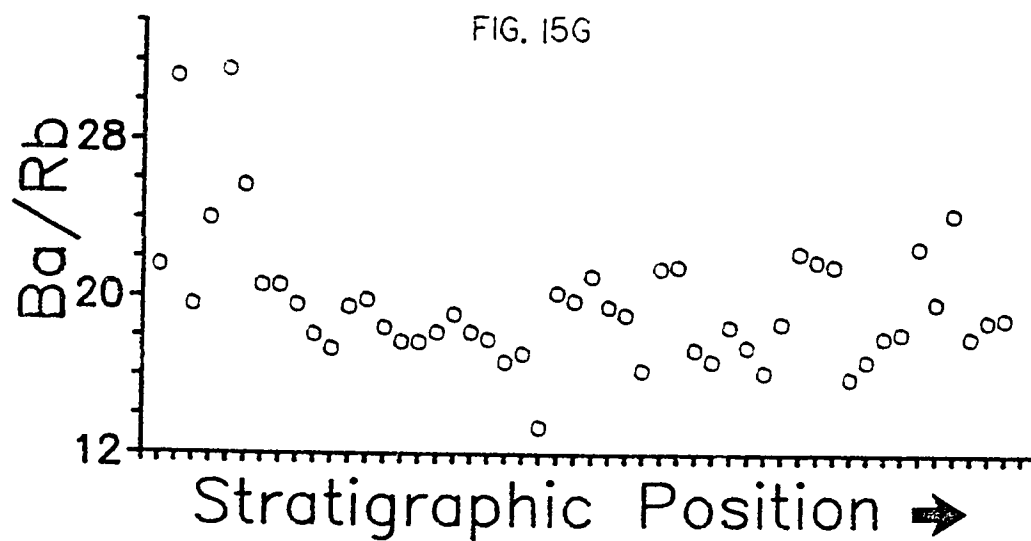
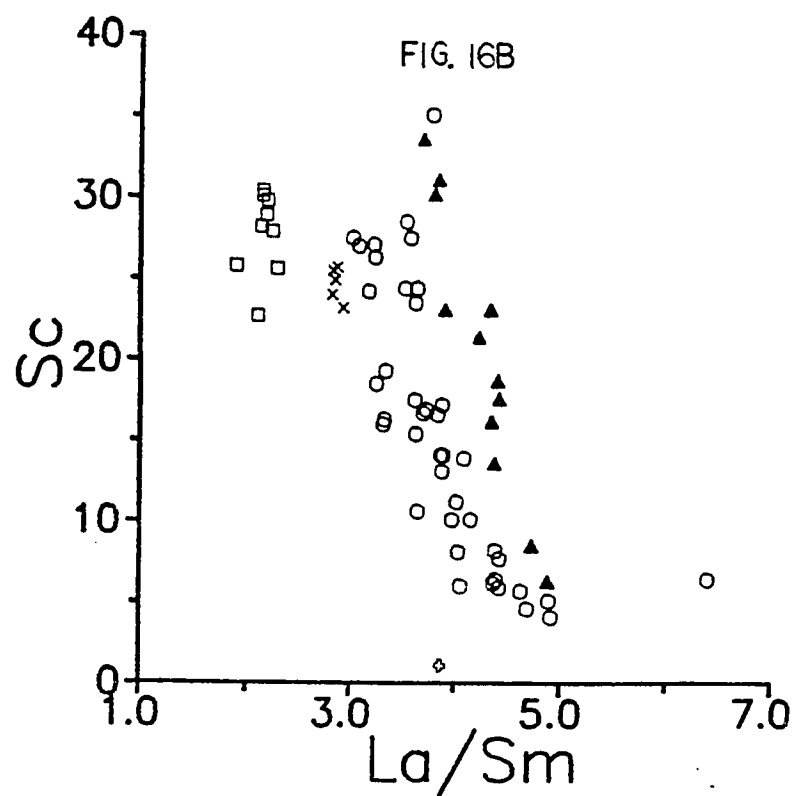
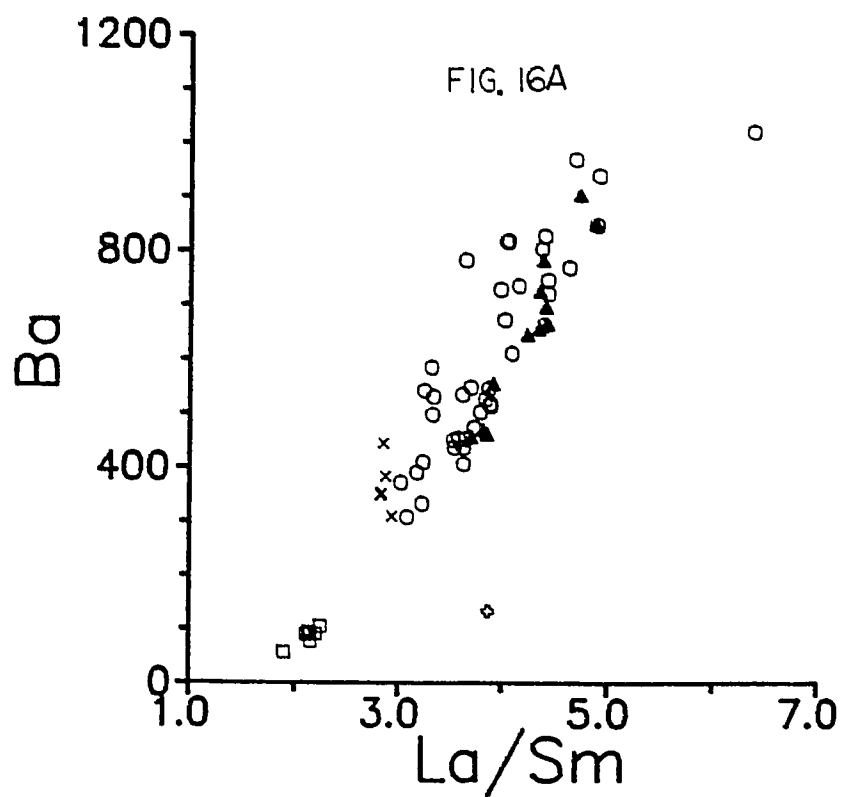
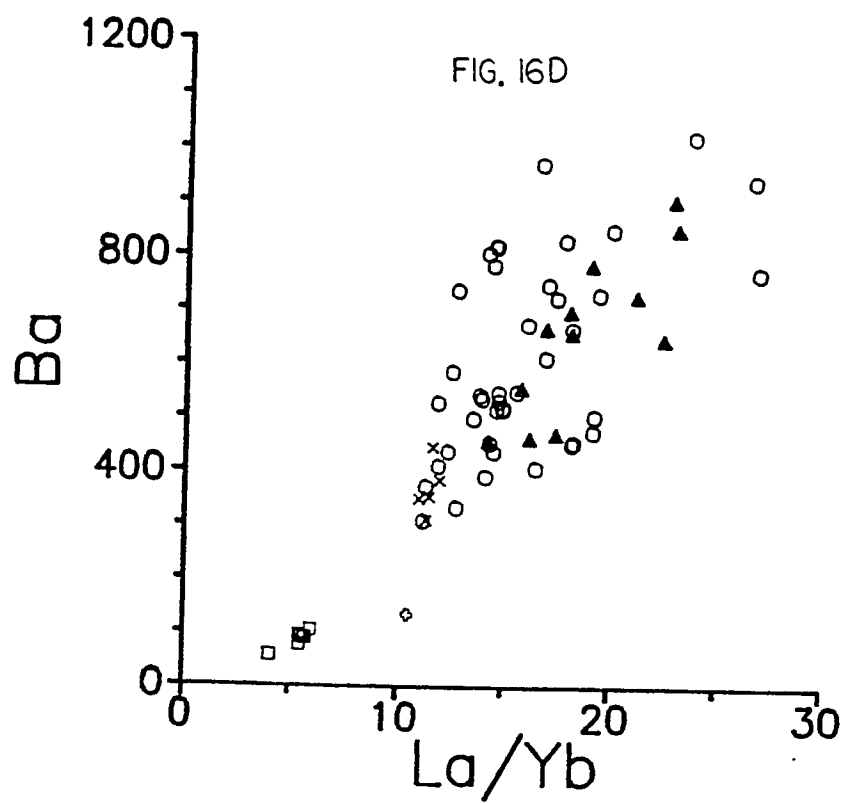
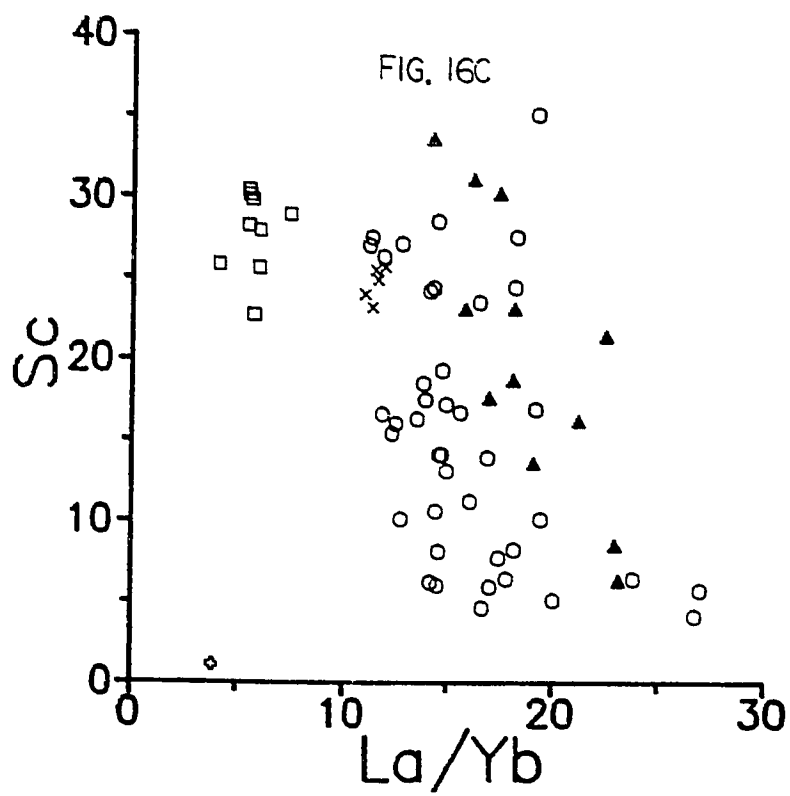


FIG. 15G







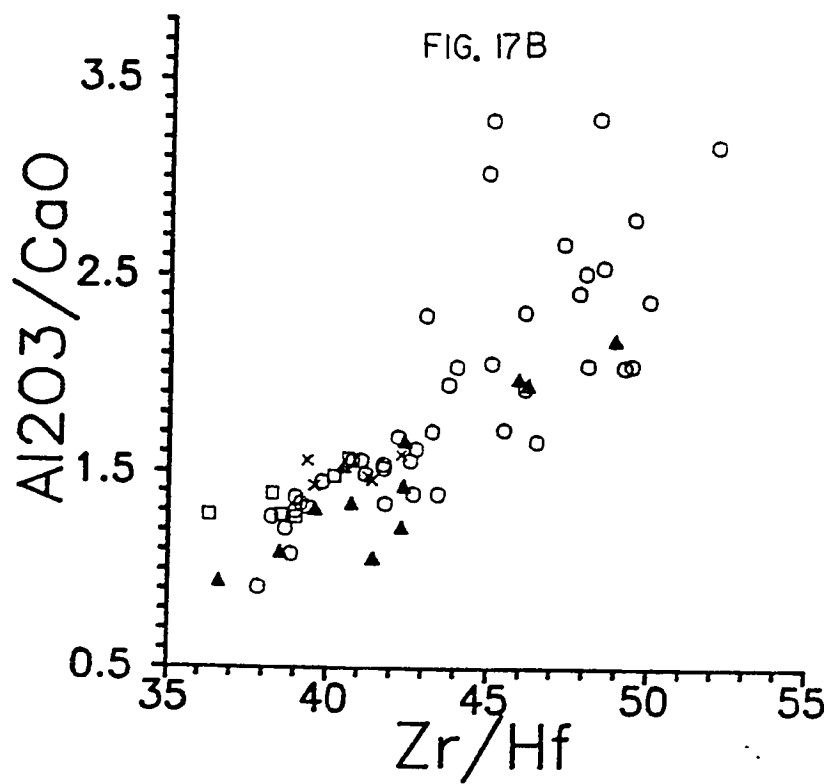
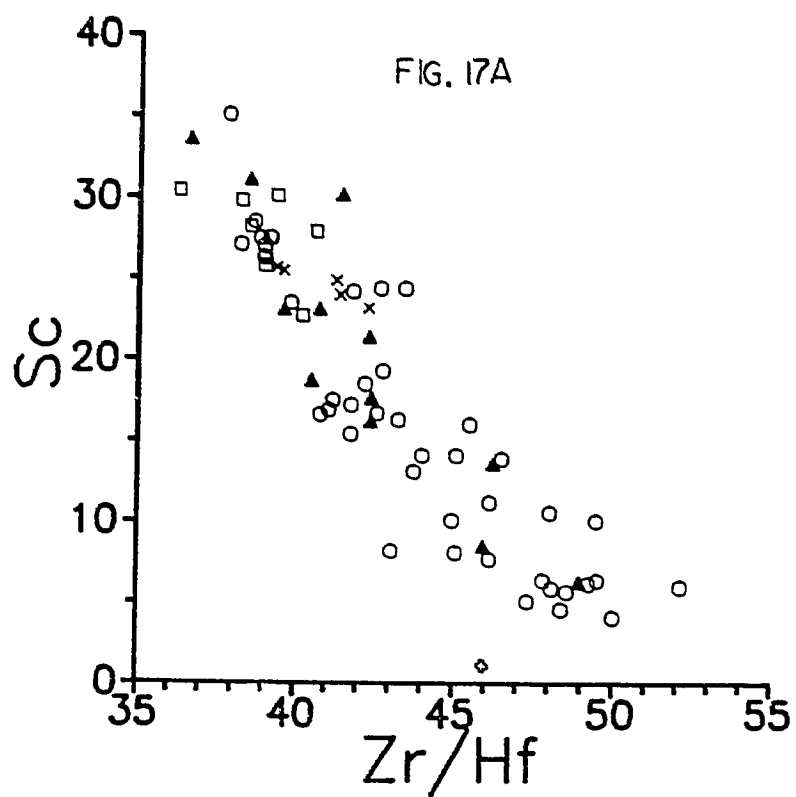
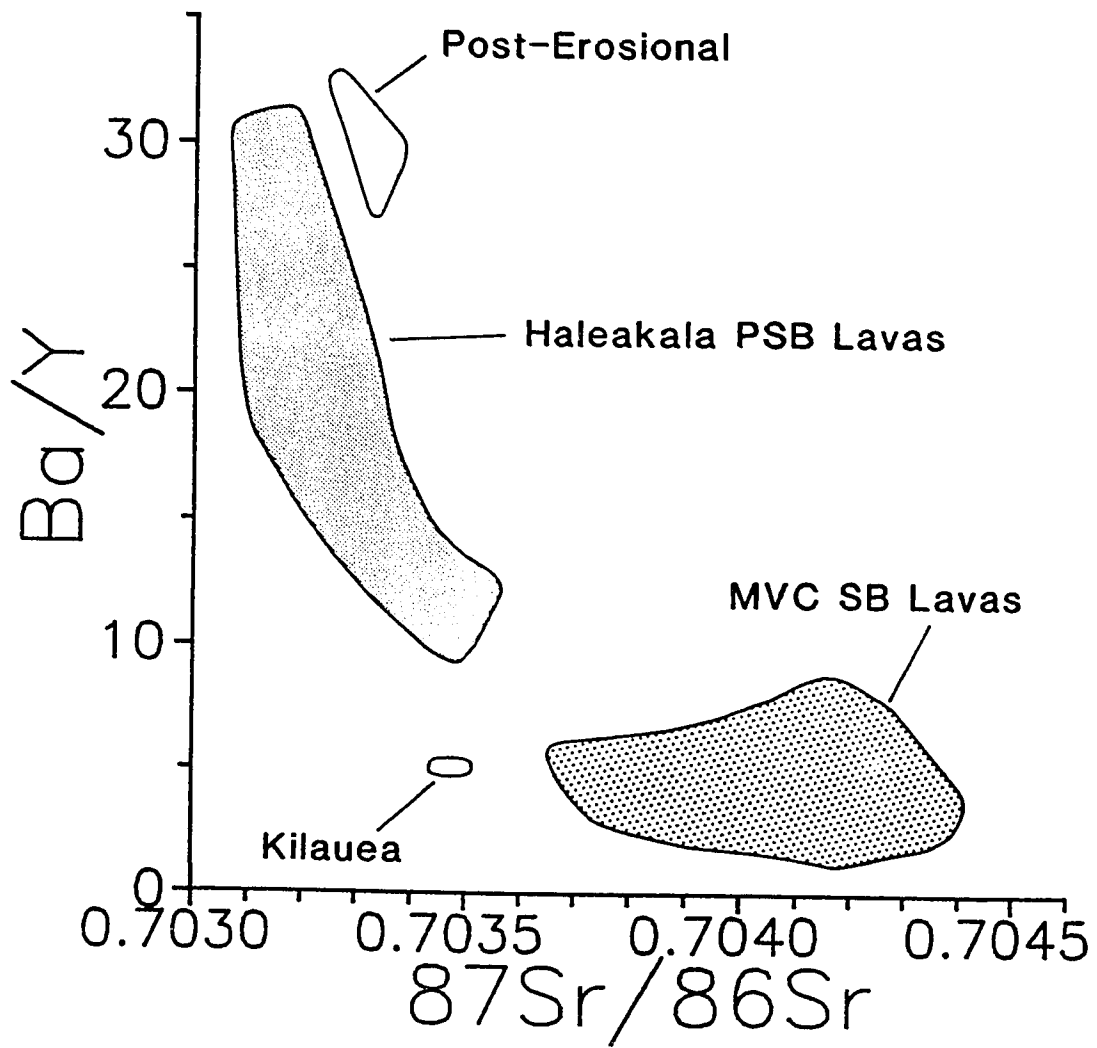
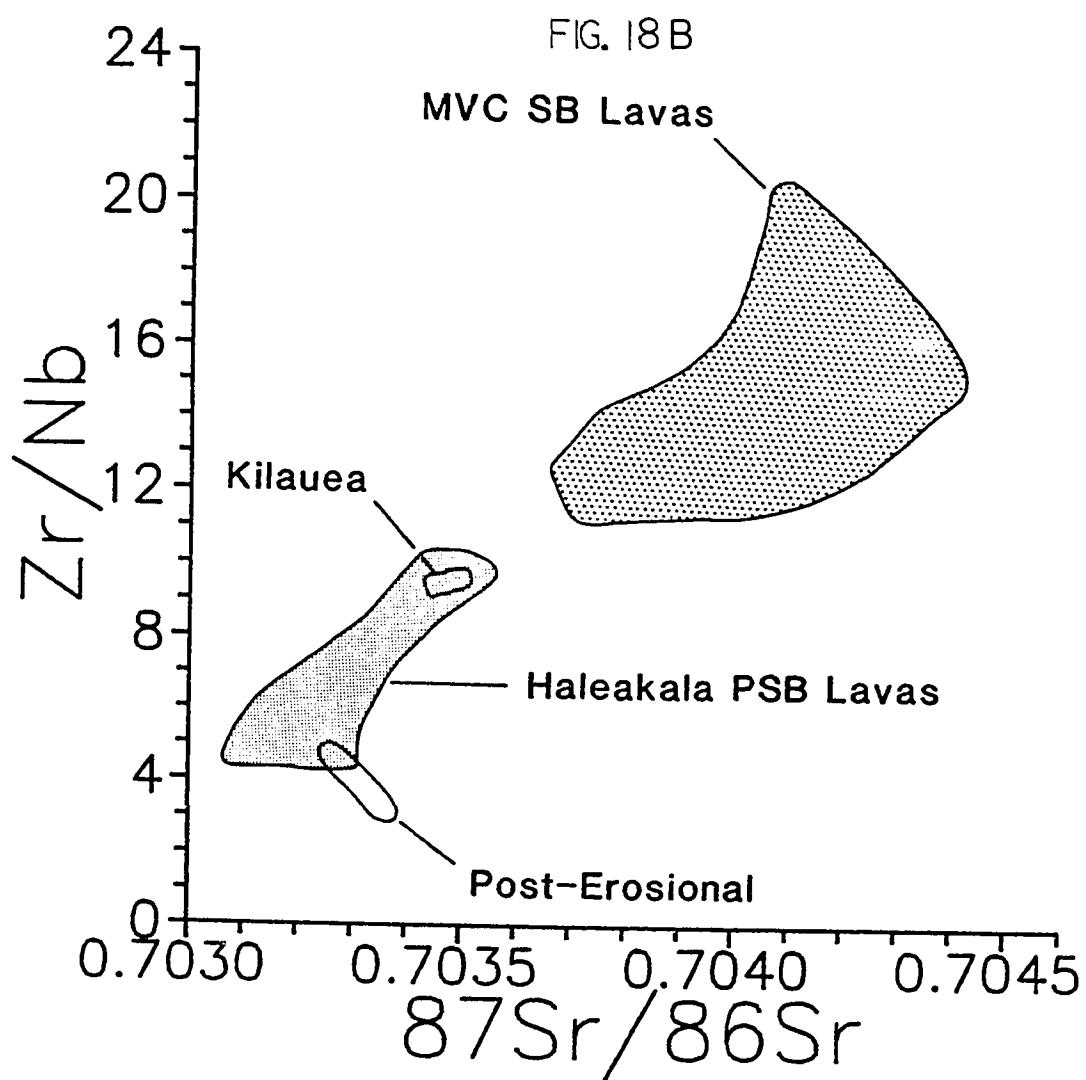


FIG. 18A





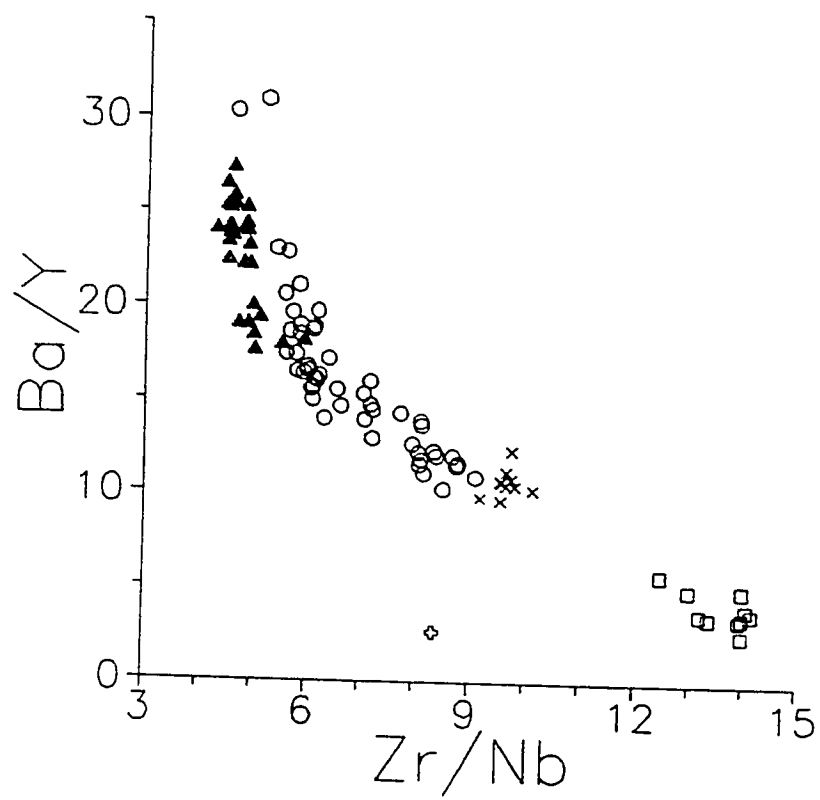
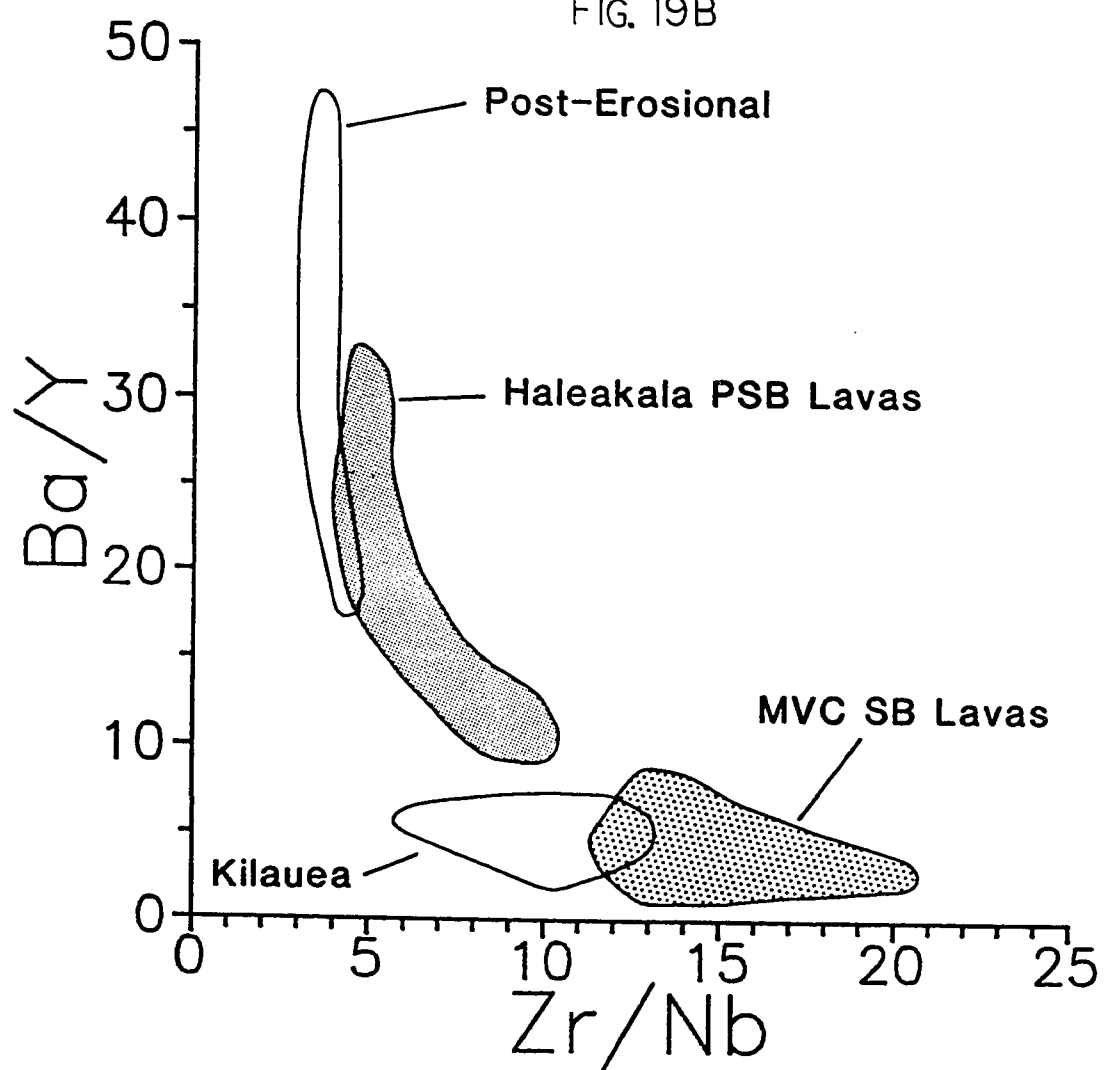
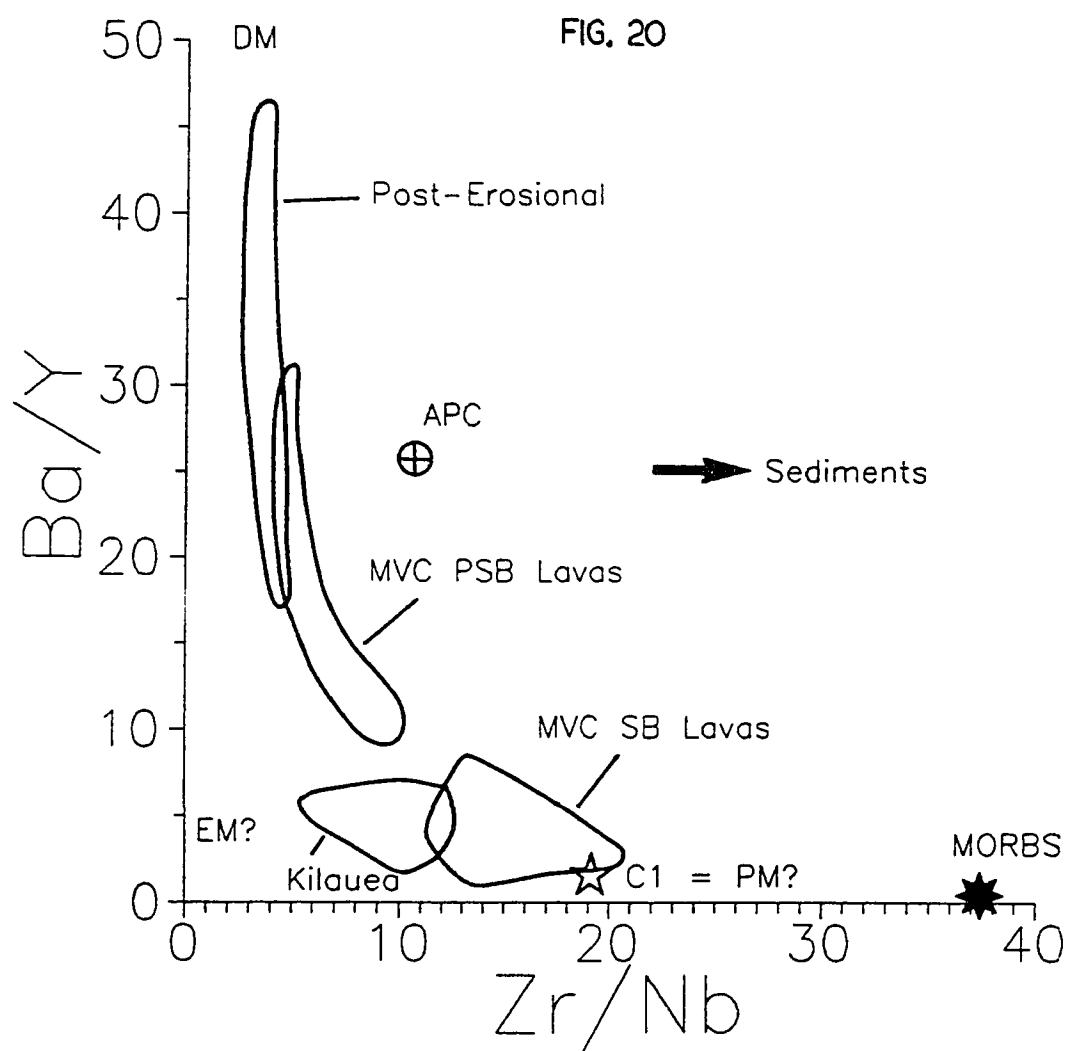


FIG. 19A

FIG. 19B





Chapter 5

**OPEN SYSTEM GEOCHEMICAL EVOLUTION OF ALKALIC CAP LAVAS FROM
HALEAKALA CRATER, HAWAII**

Abstract

50 samples spanning a nearly continuous 1000 foot section of alkalic cap lavas were collected from the northwest wall of Haleakala Crater, located on the island of Maui in the Hawaiian Islands, and analyzed for both major and trace element compositions. These lavas range from alkalic basalt to mugearite and have compositions comparable to those from other Hawaiian alkalic cap suites.

When plotted against relative stratigraphic position, compositional data display cyclic geochemical variations each of which reflects evolution of discrete batches of magma. Magma batches are separated by compositional discontinuities characterized by abrupt upsection *increases* in incompatible element (K_2O , Nb, REE, Th, Ba, Rb) contents, Al_2O_3/CaO ratios, and La/Sm ratios and decreases in compatible element (Ni, Cr, V, Sc) contents. In contrast, within magma batches, systematic compositional variations upsection involve progressive *decreases* in incompatible element contents, Al_2O_3/CaO ratios, and La/Sm ratios and progressive increases in compatible element contents.

The observed geochemical variations are interpreted as resulting from the cyclic operation of a dynamic, evolving, open system magma chamber. Interbatch compositional discontinuities represent periods of low magma flux (or recharge) during which eruption is suppressed and fractionation effects dominate magma mixing (*fractionation cycle*). During periods of high magma flux, the magma chamber is recharged by primitive magmas, causing expulsion of a portion of stored resident magma and mixing with the remaining rest magma. Continued recharge and mixing causes the compositions of lavas erupted during this *eruption cycle* to become progressively more primitive with time. Because lavas erupted at the end of an eruption cycle typically are relatively evolved ($MgO < 7$ wt.%), they may represent either (1) mixed magmas, the implication being that recharge magmas are not erupted and the magma chamber never fully evacuated, or (2) recharge magmas that have undergone fractionation at deeper levels.

Magma batches exposed in the lower half of the section and those from the upper half of the section appear to have been derived from compositionally distinct parental

magmas. This abrupt change in parental magma composition may reflect a change in the source composition of these lavas.

INTRODUCTION

The role of magma chamber processes in controlling the compositions of erupted lavas has been documented for all major tectonic environments, including mid-ocean ridges (Bryan et al., 1979; Rhodes and Dungan, 1979; Elthon, 1984; Karson and Elthon, 1987), volcanic arcs (Reagan et al., 1987), within-plate continental settings (Wörner and Wright, 1984; Leeman and Hawkesworth, 1986), and oceanic islands (e.g. Hawaii: Wright and Fiske, 1971; Wright, 1973; Clague, 1987). Both geochemical and experimental evidence indicate that magma chambers typically behave as open systems. Because open system magma chambers undergo repeated recharge, mixing, and fractional crystallization, magma compositions can potentially be modified to a greater extent than under closed system conditions (O'Hara, 1977; O'Hara and Matthews, 1981). It is therefore important to establish the geochemical evolution of open system magma chambers before lava compositions can be utilized to infer the composition and evolution of their mantle source.

The details of magma migration and storage in magma chambers have been extensively studied at the relatively young and still active shield volcanoes of Kilauea and Mauna Loa, both located on the island of Hawaii. However, lavas erupted from these volcanoes exhibit comparatively little magmatic diversity and consist essentially of compositionally uniform tholeiites. These volcanoes, therefore, provide little insight into the production of evolved lava compositions. Comparable studies of Hawaiian alkalic cap lavas, which display considerably more compositional diversity, are inherently more difficult because there have been no historical eruptions of such lavas, nor are there many thick stratigraphic exposures available for study of the temporal magmatic evolution of prehistoric eruptions. Alkalic series lavas cap the voluminous shields of several Hawaiian volcanoes, but only on Kohala, Haleakala, and West Maui is the full compositional spectrum of alkalic magmatism (i.e. alkalic basalt through trachyte) exposed. Kohala has been the subject of recent investigations (Feigenson et al., 1983; Hofmann et al. 1987; Lanphere and Frey, 1987), but detailed studies of alkalic cap magmatism at

Kohala may never be feasible owing to the thinness of the alkalic cap, poor exposures, and the lack of strong stratigraphic control. Studies of alkalic cap lavas from West Maui are in progress (Sinton et al., 1987) but are at an early stage.

In this paper, we present a geochemical investigation of a nearly continuous stratigraphic section of alkalic cap lavas from Haleakala Crater, located at the summit of Haleakala volcano (Fig. 1). Relatively thick exposures of alkalic cap lavas at Haleakala are particularly well-suited for detailed examination of the geochemical evolution of the Hawaiian alkalic cap stage. Results from this study are interpreted within the framework of an evolving open system magma chamber.

GENERAL GEOLOGIC SETTING AND SAMPLING

Haleakala comprises four recognized formations whose relations and rock-type distribution have been extensively discussed by Stearns and Macdonald (1942), Macdonald and Powers (1946, 1968), and Macdonald (1978). The oldest is the Honomanu Formation (> 0.83 Ma; Naughton et al., 1980) which contains interbedded tholeiitic and alkalic basalts and therefore represents a transitional period between the shield-building (tholeiitic) and alkalic cap stages of Haleakala. Two formations compose the Haleakala alkalic cap stage: the Kumuilihi Formation and the Kula Formation. The Kumuilihi Formation (0.91 to 0.70 Ma; Naughton et al., 1980), presumably the older of the two (Macdonald, 1978), is exposed only in Haleakala Crater and consists of interbedded alkalic basalts and hawaiites (Macdonald, 1978; West and Leeman, 1987). The Kula Formation forms the vast bulk of subaerially exposed lavas at Haleakala and consists of a diverse array of rock types, including alkalic basalts, hawaiites, mugearites, basanitoid, and trachyte. It is separated from the Kumuilihi Formation on the south wall of Haleakala Crater by a profound angular unconformity, possibly representing a fault scarp (Stearns, 1942). Dated lavas range in age from 0.88 Ma (directly overlying Honomanu lavas at Honomanu Valley on the north flank of Haleakala) to 0.36 Ma (McDougall, 1964; Naughton et al., 1980). Unconformably overlying the Kula Formation

is the post-erosional Hana Formation, composed of basanitoids, hawaiiites, and alkalic basalts. The time of inception of Hana volcanism is unknown but one historical eruption has been documented (≈ 1790 ; Oostdam, 1965).

Haleakala Crater is an erosional caldera located at the summit of Haleakala (Stearns, 1942; Macdonald, 1978) [Fig. 1]. Although the floor of the crater is covered with Hana lava flows and cinder cones, with the exception of a relatively small section of the south wall, the walls of Haleakala Crater are composed of interbedded Kula flows. Because the thickness of the Hawaiian alkalic cap thins away from the summit, in part due to shorter distances travelled by more viscous alkalic lavas relative to fluid tholeiitic lavas, lavas collected from the volcano's summit should provide a more continuous record of magmatism than do lavas collected from the distal flanks of the volcano. In addition, lavas exposed in the summit area are fresher than those exposed on the rainy flanks of Haleakala, and are less likely to have had their compositions modified due to migration and storage in rift zones.

PREVIOUS INVESTIGATIONS OF HALEAKALA ALKALIC CAP LAVAS

The petrology of lavas from Haleakala, including representative Kula lavas collected from Haleakala Crater, was presented by Macdonald (1942, 1972) and Macdonald and Powers (1946, 1968). Those authors proposed that Haleakala lavas were tapped from a compositionally zoned magma chamber that was more mafic with depth and in which differentiated magmas (hawaiiites, mugearites, trachytes) collected near the top or in isolated, peripheral pockets. Macdonald and Powers (1946, 1968) further suggested that the post-erosional Hana lavas might have been derived from greater depths than the Kula lavas. The essence of this model is that all Haleakala magma suites (i.e. shield-building, alkalic cap, and post-erosional) were derived from a common parental magma composition by fractional crystallization at various depths in the Haleakala magma chamber. Mineral compositions of lavas studied by Macdonald has been presented by Fodor and others (Fodor et al., 1972, 1975, 1977; Keil et al., 1972; Fodor and Keil, 1979), although

those studies were concerned more with establishing compositional differences between Honomanu, Kula, and Hana Formation lavas rather than deciphering the petrogenesis of these magmas.

Based on trace element and Sr and Nd isotopic studies of drill-core samples collected from the north flank of Haleakala, Chen and Frey (1983, 1985) suggested that shield-building, alkalic cap, and post-erosional lavas possess distinct compositions and represent different degrees of mixing between primitive mantle plume material and small degree melts of depleted material. Helium isotopic studies appear to support a two component mixing hypothesis (Kurz et al., 1985, 1987; Kurz, 1986).

Sr and Pb isotopic systematics of lavas from Haleakala Crater (West and Leeman, 1987) were integrated with isotopic results for other volcanoes of the Maui Volcanic Complex (West et al., 1987) and are consistent with mixing between three components. In those studies, we proposed a model in which Hawaiian shield-building lavas represent relatively uncontaminated melts derived from a Hawaiian mantle plume containing both an isotopically primitive component and an enriched component, whereas post shield-building (alkalic cap and post-erosional) isotopic compositions appear to represent plume melts that underwent increasing amounts of contamination with time by an isotopically depleted component (e.g. depleted upper asthenosphere).

For the study presented here, fifty samples were collected from a continuous 1000 foot section exposed along the northwest wall of Haleakala Crater and traversed by Halemauu Trail. Only fresh flows were collected, and owing to partial coverage of the section by soil zones, vegetation, and talus, not every flow was sampled. However, because the average flow thickness (≈ 19 feet) obtained (excluding ash and soil zones) for 50 samples in 940 feet of section is virtually identical to that estimated by Stearns and Macdonald (1942; 20 feet), our sample suite is probably an accurate representation of the section as a whole.

PETROGRAPHY

The petrography and mineral chemistry of lavas from Haleakala have been discussed in detail by Macdonald (1942, 1978), Macdonald and Powers (1946, 1968), Fodor et al. (1972, 1975, 1977), Keil et al. (1972), and Fodor and Keil (1979). The petrography of samples in our study is essentially equivalent to that of earlier studied rocks and the reader is referred to those studies for more detailed descriptions. Representative mineral modes for some of the lavas from this study are presented in Table 1.

Kula alkalic basalts are fresh and typically contain olivine, clinopyroxene, and plagioclase as their dominant phenocryst/microphenocryst phases with significantly less abundant magnetite microphenocrysts and rare magnetite phenocrysts. Textures range from seriate to strongly porphyritic and in some cases glomeroporphyritic. The groundmass tends to be coarse and weakly trachytic. Plagioclase phenocrysts commonly are zoned and partially resorbed. Olivine phenocrysts commonly contain subgrain boundaries and are also partially resorbed. Some samples contain clinopyroxene-rich crystal clots; these clots typically are monomineralic but may include subordinate magnetite or less commonly olivine.

Kula hawaiites and mugearites are in general nearly aphyric and have strongly trachytic groundmasses. Plagioclase and magnetite are the dominant phenocryst/microphenocryst phases, with less abundant olivine and clinopyroxene. In some of the more evolved samples (e.g. HK-25), clinopyroxene is absent. Commonly, phenocrysts and microphenocrysts are partially resorbed and strongly zoned. Clots of various mineral assemblages are present in some samples and commonly consist of cpx + mt or cpx + ol + mt. Apatite is a common groundmass phase and also occurs as inclusions (typically in plagioclase) in the most evolved lavas, but rarely occurs as a microphenocryst phase (with the exception of sample HK-28). Sample HK-21 contains small phenocrysts of brown amphibole that typically are strongly resorbed, leaving rims of granular magnetite surrounding a fresh core. Commonly, only pseudomorphs of granular magnetite remain to mark former amphibole grains. Two other samples, HK-22 and

HK-23 contain minor groundmass amphibole. As noted by Macdonald (1942), biotite is found rarely in the groundmass of some Kula lavas.

ANALYTICAL TECHNIQUES

Major and trace element data are listed in Table 2. Major oxides were determined by XRF at the University of Massachusetts at Amherst and the University of Houston. Major elements are plotted after setting $\text{Fe}^{2+}/(\text{Fe}^{2+}+\text{Fe}^{3+})$ to 0.90 and recalculating to 100 % on an anhydrous basis. Rb, Sr, Ba, Y, Zr, Nb, Ni, V, Cr, Sc, Cu, and Zn were determined by XRF at the University of Edinburgh. Rare Earth Elements (REE), Th, Ta, Hf, Cr, and Sc were determined by instrumental neutron activation analysis (INAA) at M.I.T. using techniques described by Ila and Frey (1984); additional INAA data was obtained from the University of Oregon using similar methods. Precision, based on six replicate analyses of sample HK-46, is better than 5 % for La, Ce, Nd, Sm, Eu, Yb, Lu, Hf, and Sc, better than 10 % for Th and Ta., and better than 15 % for Tb.

GEOCHEMISTRY

Overall geochemical variations within the Kula Formation and a comparison of those lavas with lavas from the other three Haleakala volcanic formations are described in detail in a companion paper (West and Leeman, in prep.). Lavas of the Kula Formation fall entirely within the alkalic field of the silica-alkalies diagram of Macdonald and Katsura (1964) and form a trend typical of Hawaiian alkalic cap suites (Fig. 2). Relative to the post-erosional Hana Formation, Kula lavas generally are less silica undersaturated (Fig. 2), but the two groups overlap substantially. The compositional diversity of the Kula Formation is large relative that of alkalic cap suites from Hualalai (Clague et al., 1980) which contains few differentiated lavas (i.e. hawaiites), Mauna Kea (Laupahoehoe Group; West et al., 1988) which contains neither basalts nor trachytes and rare mugearite, and Kohala (Hawi Formation; Feigenson et al., 1983; Lanphere and Frey, 1987) and West Maui (Honolua Formation; Macdonald and Katsura, 1964; Macdonald,

1968; Diller, 1982) which contain few basalts in comparison to more evolved rocks (e.g. mugearite, benmoreite, and trachyte).

Major and trace element variations of Kula lavas are described in detail in West and Leeman (in prep.). With increasing incompatible trace element abundance (e.g. Nb), Mg#, CaO, Sc, Cr, and Ni decrease and SiO₂, K₂O, Rb, Ba, Zr, Hf, Y, Th, Ta, and rare-earth elements (REE) increase. P₂O₅ and Sr initially increase with increasing Nb, followed by a decrease at higher Nb concentrations (approximately 70 ppm Nb). Similarly, TiO₂ and V increase at low Nb concentrations but then decrease substantially at Nb abundances greater than 30 ppm.

Magma Batches

In the following sections, we plot geochemical data of the studied samples as a function of relative stratigraphic position, rather than absolute elevation which cannot be determined with sufficient accuracy. Plotted against relative stratigraphic position, geochemical data for Kula Formation lavas from the Halemauu section of Haleakala Crater exhibit distinct compositional breaks that form coherent subsets or batches of lavas (Fig. 3). Admittedly, these subdivisions may be arbitrary owing to incomplete sampling or incomplete deposition of flow units. In eight of the thirteen magma batches identified, the first erupted lavas are hawaiites or mugearites and the final erupted lavas are alkalic basalts, basanitoids, or ankaramites (Table 3). Thus, nearly the entire range of observed rock compositions is successively repeated upsection from batch to batch in the Crater wall section. In the field, the breaks between these batches generally correspond to parts of the section covered by vegetation. These covered areas vary in thickness but are generally thin (< 10 feet). Because extensive vegetative cover is usually confined to soil zones or to ashy or rubbly deposits between lava flows, it is likely that breaks between magma batches represent periods of eruptive quiescence.

The compositional discontinuities separating these magma batches are characterized by significant and abrupt increases in incompatible element contents (e.g. K₂O, Nb, Rb,

Th, LREE) and in some ratios (e.g. $\text{Al}_2\text{O}_3/\text{CaO}$, La/Sm) and complementary decreases in compatible element contents (e.g. Cr, Sc, V) [Fig. 3]. Within batches, incompatible element contents progressively decrease upsection and compatible element contents progressively increase upsection (Fig. 3). The magnitude of interbatch geochemical discontinuities varies from batch to batch, but in some cases (e.g. batch 5 to 6, batch 7 to 8, batch 9 to 10), compositional changes span over half of the entire compositional range of the section. For example, the batch 7 to 8 transition involves an increase in K_2O from 1.01 to 2.21 (equivalent to 63 % of the total compositional range) [Fig. 3]. Intrabatch compositional variations can span even greater ranges: within batch 9, K_2O decreases from 2.67 wt.% to 1.00 wt.% (88 % of the total observed range, excluding the Holua trachyte).

In detail, each batch is characterized by distinctive trace element variations. In figure 4, chondrite-normalized elemental abundances for each batch are plotted separately. Elements are arranged in the order of relative enrichment observed for the typical Kilauea tholeiite, U.S.G.S. standard rock BHVO-1 (see West and Leeman, in prep.). In general, Kula alkalic basalts mimic the BHVO pattern in that from Rb to Ba there is a progressive increase in normalized abundance followed by a progressive decrease from Ba to Lu. Evolved lavas (hawaiites and mugearites) deviate from this pattern by various amounts and commonly show marked negative or even positive anomalies for some elements (e.g. P, Ti, Sr). In addition, interbatch and intrabatch compositional variability appears to be greater for batches in the lower part of the section (batches 1-6) relative to batches in the upper part of the section (batches 7-13) (Figs. 3, 4).

Batch 7 contains a compositional gap and has therefore been further subdivided into two parts, A (four samples, HK-25 to HK-28) and B (eight samples, HK-29 to HK-36). This compositional gap corresponds to a part of the section that was not sampled due to poor exposures. Although geochemical variations within batch 7 follow for the most part those observed in other batches, therefore suggesting it is a single batch, it is possible that batch 7 represents two independent batches that are

incompletely sampled.

Variations in Isotopic Compositions and Trace Element Ratios

Sr, Nd, and Pb isotopic ratios of Kula lavas appear to be correlated with relative stratigraphic position (Chen and Frey, 1985; West and Leeman, 1987) [see Fig. 5], indicating a generally progressive shift in source composition. This shift is also reflected in some incompatible trace element ratios (e.g. Zr/Nb, Ba/Y, La/Yb, La/Hf; see Fig. 5) but not in others (e.g. Ba/Rb, Zr/Hf, La/Ce) (West and Leeman, in prep.). Paradoxically, ratios of highly/moderately incompatible trace elements (H/M ratios; e.g. Zr/Nb, Ba/Y), which are susceptible to change by fractional crystallization, are correlated with stratigraphic position and isotopic composition, whereas ratios of highly incompatible trace elements (H/H ratios; e.g. La/Ce, Ba/Rb) and elements of close geochemical affinity (e.g. Zr/Hf), which should not be affected by magmatic (as opposed to source-related) processes show no such correlation (West and Leeman, in prep.). In contrast to isotopic and trace element ratios, neither major element contents nor trace element abundances change systematically with relative stratigraphic position for the Halemauau section as a whole.

INTERBATCH TRANSITIONS

Half of the interbatch transitions examined in detail are consistent with derivation of evolved, incipient batch lavas from primitive batch-end composition magmas by fractional crystallization. Important fractionating phases include olivine, clinopyroxene, plagioclase, Fe-Ti oxides, apatite, and amphibole. Inconsistencies in the trace element systematics of some interbatch transitions suggest that other processes must have been involved to explain comparable enrichment of variably incompatible elements. Resorption of precipitating mineral phases in an open system magma chamber undergoing infrequent recharge, magma mixing, and fractional crystallization is qualitatively consistent with the observed geochemical variations. Resorption effects are abundantly sup-

ported by petrographic evidence.

General Compositional Variations and Evidence for Crystal Fractionation

Overall geochemical variations and petrographic observations are consistent with fractional crystallization being a dominant process in the evolution of Kula alkalic cap lavas from Haleakala Crater. Fractional crystallization involved olivine, clinopyroxene, plagioclase, and Fe-Ti oxides and, in the most evolved lavas, apatite and amphibole. Interbatch geochemical discontinuities appear to reflect the removal of these phases and in general follow the overall compositional variations observed for Kula lavas.

We propose that interbatch transitions represent periods of relative volcanic quiescence during which magmas undergo protracted differentiation in a magma chamber. There are several indirect lines of evidence to support this contention. (1) Interbatch transitions involve repetitive, consistent, and relatively large changes in composition. (2) Compositions consistently change upsection [i.e. with time] in the sense predicted by fractionation models, i.e. evolved lavas overlie more primitive lavas. (3) Transitions are typically represented in the section by vegetation or ashy and rubbly deposits, which suggests these breaks represent periods of volcanic inactivity.

Interbatch transitions involve decreases in MgO and Ni contents (Fig. 3) which probably reflect olivine fractionation. For most interbatch transitions, Sc abundances increase and $\text{Al}_2\text{O}_3/\text{CaO}$ ratios increase (Fig. 3), suggesting significant clinopyroxene fractionation. However, the relative proportions of fractionating phases appear to differ from case to case. For example, in the transition from batch 1 to batch 2, Sc increases and $\text{Al}_2\text{O}_3/\text{CaO}$ is constant, thereby indicating that clinopyroxene fractionation was probably not important.

Plagioclase phenocrysts and microphenocrysts are found in both evolved and less evolved lavas even though Sr appears to behave for the most part as an incompatible element. Decreased Sr abundances in the most evolved lavas (Nb > 60-70 ppm) indicate that plagioclase fractionation became significant in these magmas. The overall decrease

in Sr/Ba ratios for the Kula Formation indicates that although the bulk partition coefficient for Sr was less than unity in less evolved magmas, plagioclase fractionation was important. However, within batches Sr abundances are not always well correlated with magma chemistry, and for interbatch transitions, Sr may increase, decrease, or remain constant. The apparent buffering of Sr compositions at relatively low (< 700 ppm) and constant abundances and nearly constant $\text{Al}_2\text{O}_3/\text{CaO}$ ratios in the batch 1 to 2 and batch 2 to 3 transitions suggests that even these less evolved lavas have undergone plagioclase fractionation.

Interbatch transitions for batches 5 through 13 involve concurrent drops in TiO_2 , V, and Cr contents and increases in $\text{Al}_2\text{O}_3/\text{TiO}_2$ ratios (Fig. 3). However, for transitions from batch 1 to 2 and 2 to 3, FeO and V increase, and for the first 3 interbatch transitions in the section, TiO_2 contents and $\text{Al}_2\text{O}_3/\text{TiO}_2$ ratios decrease (Fig. 3). These geochemical changes, along with the generally high Ni, Cr, and V and low incompatible trace element abundances of the lavas in batches 1 to 3, suggest that Fe-Ti oxide fractionation was not significant in these magmas.

Although P_2O_5 contents increase for the majority of interbatch transitions, some transitions involve either no change (batches 5 and 6) or an actual drop (e.g. batches 7 and 9) in P_2O_5 (Fig. 3). For those transitions in which P_2O_5 does not increase, $\text{K}_2\text{O}/\text{P}_2\text{O}_5$ ratios increase significantly. These interbatch geochemical changes along with the absolute decrease in P_2O_5 contents at high Nb abundances indicate that the most evolved lavas have undergone significant apatite fractionation.

The role of amphibole in controlling interbatch geochemical variations is uncertain. For the most part, the effects of amphibole fractionation should be comparable to those created by clinopyroxene fractionation, with the possible exception of relative REE abundances. Because amphibole distribution coefficients for the middle REE's [MREE] appear to be higher than those for light or heavy REE's [LREE and HREE, respectively] (Higuchi and Nagasawa, 1968; Irving and Frey, 1984), amphibole fractionation may result in negatively sloped, concave REE patterns.

Detailed Evaluation of Interbatch Transitions

Although the overall geochemical variations exhibited by Kula lavas are indicative of the general role of specific fractionating mineral phases, each individual interbatch transition is unique. It is therefore important to examine these transitions in detail in order to identify possible variations in fractionating mineral assemblage from batch to batch and to better establish the full range of interbatch diversity. In order to further evaluate the viability of fractional crystallization for controlling interbatch transitions, we examine six transitions that span the Haleakala Crater section and that entail relatively large geochemical variations.

In figure 6, trace element abundances of incipient lavas from batches 4, 6, 8, 9, 10, and 13 are normalized to Nb (to adjust lava compositions to comparable differentiation levels) and divided by the Nb-normalized compositions of primitive batch-end lavas from the preceding batch. Nb was chosen because it shows the highest degree of correlation with other highly incompatible elements (e.g. Rb, K, Th, LREE) and is less prone to possible alteration effects than the alkalis (Rb and K). Because Nb is highly incompatible, elements of similar incompatibility should have Nb-normalized enrichment factors of approximately 1.0 on such plots. The deviation of less-incompatible elements from unity will be proportional to their bulk distribution coefficients relative to that for Nb. Fractional crystallization will cause moderately incompatible elements (MREE, Zr, Ba, Hf) to fall slightly below unity and slightly incompatible elements (HREE, Y) to deviate more strongly. Elements whose bulk partition coefficients ≥ 1.0 will have pronounced negative anomalies.

Batch 3 to 4 / Batch 7 to 8

Trace element patterns for interbatch transitions from batch 3 to batch 4 and from batch 7 to batch 8 are broadly consistent with fractional crystallization (Figs. 6a, c). The trace element pattern for the oldest lava from batch 4 (HK-13) has a negative slope with pronounced negative Sr and Ti anomalies consistent with significant plagioclase and Fe-Ti oxide fractionation. Other geochemical evidence (decreased Ni and Sc abundances and increased $\text{Al}_2\text{O}_3/\text{CaO}$; Fig. 3) indicates that significant olivine and clinopyroxene fractionation has also taken place. The only discrepancy is for La, for which there appears to be a negative anomaly. Although apatite has $D^{\text{La}} > 1.0$, neither P_2O_5 nor $\text{P}_2\text{O}_5/\text{K}_2\text{O}$ are anomalously low in this sample, indicating that fractionation of this phase is unlikely to have been significant. The origin of this apparent La anomaly is therefore problematic.

The trace element pattern for the oldest batch 8 lava (HK-37) is similar to that for batch 4, except that it is significantly more fractionated (Fig. 6c). Negative Sr, Eu, and Ti anomalies are consistent with plagioclase and Fe-Ti oxide fractionation, and strong decreases in Ni and Sc abundances along with increased $\text{Al}_2\text{O}_3/\text{CaO}$ indicate olivine and clinopyroxene fractionation. In addition, the slight negative P anomaly, despite an increase in absolute P_2O_5 content (Fig. 3b), indicates apatite fractionation as well. The apparent Sm anomaly could be due to fractionation of apatite, which has relatively high distribution coefficients for MREE compared to LREE and HREE (Watson and Green, 1981).

Batch 5 to 6

The trace element systematics of interbatch transitions other than those just described are more complex and cannot be ascribed solely to fractional crystallization. For example, in the batch 5 to 6 transition (Fig. 6b), negative P, Sm, and Ti anomalies (Fig. 6b) and changes in Ni, Sc, and $\text{Al}_2\text{O}_3/\text{CaO}$ (Fig. 3) are consistent with segregation of apatite, Fe-Ti oxide, olivine, and clinopyroxene; the absolute increase in Sr

abundance (Fig. 3) and lack of negative Sr or Eu anomalies indicates that plagioclase fractionation was not important. However, the similar enrichment in highly (Rb, Th, LREE), moderately (Zr, Ba), and slightly (Y, HREE) incompatible elements is inconsistent with the diverse geochemical behavior typically exhibited by these elements. Based on published partition coefficient data, fractionation of these phases, even if significant apatite and/or amphibole are involved, cannot account for enrichments in Zr, Ba, and Yb over more incompatible elements such as Rb and Th. Although Th partition coefficients for apatite may approach or exceed unity (Irving and Frey, 1984), these values are considerably smaller than Yb partition coefficients. Th partition coefficients for amphibole are also small relative to Yb (Irving and Frey, 1984). Thus, neither apatite nor amphibole fractionation can account for the observed decrease in Th/Yb ratios. Apatite distribution coefficients for Sr are greater than unity and are greater than those for Sm (Watson and Green, 1981), therefore a negative Sr should have been produced especially in light of the negative Sm anomaly. A possible caveat is that amphibole fractionation could conceivably fractionate Sm relative to Sr and thus could have contributed to the Sm anomaly.

Batch 8 to 9

The batch 8 to 9 interbatch transition involves relative depletions in P, Sr, and Ti (Fig. 6d), decreased Ni, Sc, and P_2O_5 contents, and increased Al_2O_3/CaO ratios (Fig. 3). These compositional variations are consistent with fractional crystallization of olivine, clinopyroxene, plagioclase, Fe-Ti oxides, and apatite. However, as in the case for the batch 5 to 6 transition, fractional crystallization cannot account for comparable enrichments in elements possessing geochemically distinct affinities (e.g. LREE, Hf, and Y) and is inconsistent with increased Ba/Nb (10.0–11.7) despite evidence for extensive plagioclase fractionation. A possible explanation for the notably jagged trace element pattern (Fig. 6d) is that HK-40, the batch-end lava of batch 8, is a hawaiite and thus may not be an appropriate parental magma composition for HK-43, the incipient batch 9

lava.

Batch 9 to 10

Negative P, Sr, and Ti anomalies (Fig. 6e) and a decrease in Ni and Sc abundances (Fig. 3) indicate that the batch 9 to 10 transition was accompanied by fractionation of olivine, clinopyroxene, plagioclase, Fe-Ti oxides, and apatite. Fractional crystallization of these phases cannot, however, produce the observed, concave, bow-shaped trace element pattern. As observed for the batch 5 to 6 transition, the slightly incompatible elements Y and especially Yb are relatively more enriched than the moderately incompatible elements. In fact, Yb is enriched relative to even highly incompatible elements such as Nb, La, and Ce, clearly inconsistent with fractional crystallization.

Batch 12 to 13

With the exception of anomalously low Rb and anomalously high Sr, the batch 12 to 13 transition forms a relatively smooth, negative trace element pattern. Negative deviations for P and Ti (Fig. 6f) and drops in both Ni and Sc abundance indicate significant olivine, clinopyroxene, Fe-Ti oxide, and apatite fractionation. The high Sr abundance of HK-59 (1260 ppm Sr) and the pronounced positive Sr anomaly (Fig. 6f) both suggest that this interbatch transition was not accompanied by significant plagioclase fractionation. It is unlikely that the apparent relative depletion in Rb is due to Rb loss from alteration, because, petrographically, sample HK-59 is quite fresh. Instead it appears that HK-58, the primitive batch-end lava of batch 12, contains anomalously high Rb (28 ppm) and plots off the otherwise linear Kula Nb-Rb trend.

Quantitative Evaluation of Fractional Crystallization

In order to quantitatively evaluate the role of fractional crystallization in controlling the compositional changes associated with interbatch transitions, a least-squares approximation method was used. For three transitions (batch 12 to 13, batch 9 to 10, and batch 7 to 8), primitive batch-end lavas were chosen as "parent" magmas and the most evolved (oldest) lavas of each respective overlying batch were chosen as "daughter" magmas. Compositions were first normalized to 100 % on an anhydrous basis with all iron converted to FeO. P_2O_5 was initially excluded from the calculations and then re-included, and a series of models was generated until a best fit was obtained. Models with the lowest sum of squares of residuals (ΣR^2) [and which are geologically reasonable] are presented in Tables 5, 7, and 9. The results of the major element modeling were then used to calculate the predicted trace element composition of the daughter magma, thus both major and trace elements are used to evaluate the consistency of the fractionation models.

Mineral Compositions

Mineral compositions of Haleakala lavas were used in the calculations and were taken from the literature (see Tables 4, 6, and 8 for data sources). Because the compositional range spanned by these interbatch transitions is relatively large, mineral end-member compositions for olivine (Fo and Fa) and plagioclase (An and Ab) were also used. However, in each case, the use of such end-member compositions resulted in either higher residuals or contradictory results (e.g. subtraction of Fo and addition of Fa). Stoichiometric olivine and plagioclase compositions were also tested. It was necessary to use oxide compositions of lavas from other Hawaiian alkalic caps (e.g. Kohala, Mauna Kea, Hualalai) owing to the lack of data for Haleakala lavas.

Results

Batch 12 to 13

Results of the least-squares mixing calculation for deriving the batch 13 hawaiiite [HK-59] from the batch 12 ankaramite [HK-58] are presented in Table 5. Approximately 66 % fractionation of a clinopyroxene (41 %) + olivine (11 %) + plagioclase (8 %) + magnetite (7 %) assemblage is required to produce the best fit. However, the best fit obtained resulted in $\Sigma R^2 \approx 0.467$ which is significantly higher than the generally assumed minimum acceptable value of 0.10 (e.g. LeRoex and Erlank, 1982). The high ΣR^2 is reflected in the poor agreement between the observed and calculated trace element concentrations of the daughter magma. Although apatite fractionation is suggested by the trace element pattern of HK-59 in Fig. 6f, the addition of apatite and P_2O_5 in the modeling produced even larger residuals. The poor results obtained for this model suggest that the batch 12 to 13 transition did not result from simple fractional crystallization alone.

Batch 9 to 10

Table 7 presents the results of modeling for the transition from batch 9 to 10. Again, residuals are relatively high ($\Sigma R^2 \approx 0.333$). Calculations indicate that 57 % crystallization of the batch 9 basanitoid parent magma [HK-50] and removal of a fractionating phase assemblage consisting of clinopyroxene (32 %) + plagioclase (15 %) + magnetite (9 %) + olivine (1 %) + apatite (0.5 %) can produce the batch 10 hawaiiite daughter magma [HK-51]. However, in addition to the poor agreement observed for major elements, calculated trace element concentrations for the daughter magma also differ significantly from observed concentrations. The lack of an acceptable best-fit model and the anomalous enrichment in slightly incompatible trace elements for HK-51 (Fig. 6e) do not support a simple fractional crystallization relationship between HK-50 and HK-51.

Batch 7 to 8

The results of least-squares modeling for the transition from batch 7 to 8 is presented in Table 9. Of the three interbatch transitions modeled, the derivation of the batch 8 mugearite [HK-37] from the batch 7 alkalic basalt [HK-36] produced by far the lowest residuals ($\Sigma R^2 \approx 0.039$) and was thus the only acceptable model. Results indicate that the mugearite can be produced by ≈ 53 % crystallization of the alkalic basalt parent magma and fractionation of clinopyroxene (23 %) + plagioclase (15 %) + magnetite (9 %) + olivine (6 %) + apatite (2 %). This clinopyroxene-dominated phase assemblage is identical to that calculated for the batch 9 to 10 transition but requires a larger role for plagioclase than the batch 12 to 13 transition. In order to produce an acceptable fit, it was necessary to use an olivine composition (Fo 60) more evolved than the calculated equilibrium olivine composition of either the parent (Fo 76) or daughter (Fo 67) magma.

Although the calculated daughter concentrations for some trace elements (e.g. Zr, Nb, Y) agree well with observed concentrations, other elements (e.g. La, Ba) show considerably poorer agreement. The results of trace element modeling for the batch 7 to 8 transition are illustrated in Fig. 7. Also shown are curves representing fractionation of the observed mineral phases. Using the relative phase proportions determined by major element modeling, the calculated degree of crystallization is unable to reproduce the observed increases in both La/Sm and La/Yb ratios (Fig. 7). Because the calculated fractionation curve for clinopyroxene [Cpx] lies either between the calculated [black sun] and observed [filled star] compositions (La/Sm; Fig. 7a) or is nearly coincident with the observed composition (La/Yb; Fig. 7b), it is possible that the relative proportion of clinopyroxene is underestimated by major element modeling.

Evidence for High Pressure Clinopyroxene Fractionation

The results of modeling for the batch 7 to 8 transition appear to require additional amounts of clinopyroxene fractionation beyond that indicated by major element compositional variations. Because the stability field for clinopyroxene expands at higher pressure (e.g. Thompson, 1974; Fujii and Bougault, 1983), it is possible that fractionation may have taken place at moderate to high pressures. This apparent underestimation for the role of clinopyroxene has also been noted for alkalic cap [hawaiite] lavas from Mauna Kea by West et al. (1988) who proposed that those lavas could have formed by moderate pressure ($\geq 2\text{--}5$ kb) fractionation.

Possible Causes for Comparable Enrichments in Highly and Slightly Incompatible Trace Elements

The similar enrichments in highly and slightly incompatible elements observed for three of the six interbatch transitions examined could conceivably have been created by at least three processes. (1) Accumulation of phases containing higher abundances of less incompatible elements relative to highly incompatible elements. (2) Mixing between evolved rest magmas and mafic recharge magmas without accompanying fractionation of mafic phases. (3) Resorption of mafic phases.

Phenocryst Accumulation

Accumulation of mafic phases in the evolved, oldest lavas from each batch can be ruled out because these magmas are essentially aphyric. Most primitive batch-end lavas contain numerous phenocrysts and microphenocrysts and thus may be partly cumulate in origin. The addition of olivine and clinopyroxene to a melt will preferentially enrich magmas in less incompatible elements relative to highly incompatible elements. Normalizing any lava to a such a cumulate magma will therefore result in higher enrichment factors for highly incompatible elements (e.g. Th, La, Ce) and lower enrichment factors for less incompatible elements (e.g. Yb, Y) than would be produced if the

original liquid composition were used for normalization. Because for several interbatch transitions observed enrichment factors for highly incompatible and less incompatible elements are comparable (see Figs. 6b, d, e), accumulation of mafic phases in batch-end lavas is unlikely to have exerted a significant effect on the trace element compositions of these magmas.

Mixing

Mafic magma should contain lower abundances of highly incompatible trace elements relative to less incompatible elements than evolved magmas that have undergone appreciable fractional crystallization. Therefore, mixing of mafic magma into a magma chamber containing evolved magma should produce a mixed magma having a lower highly:less incompatible trace element ratio. In this way, less incompatible elements can be preferentially enriched relative to highly incompatible elements. However, because in mafic magmas less compatible elements are in higher relative [not absolute] abundance than less incompatible elements, a large proportion of mafic magma would be required to enrich highly and less compatible elements to similar extents. Such a large input of mafic magma would also greatly increase the compatible trace element contents of highly fractionated rest magmas. Because the evolved, oldest lavas in each batch lavas contain very low abundances of such elements (e.g. Ni < 10 ppm), it is improbable that these magmas were affected by significant amounts of mixing with mafic magma. In addition, any fractional crystallization of mafic phases will result in preferential enrichment of highly over less incompatible elements, therefore in order to maintain a low highly:less incompatible trace element ratio in the magma, significant crystal fractionation must not occur. However, the low compatible trace element abundances and high incompatible element contents of these evolved lavas indicate that extensive crystal fractionation occurred.

Resorption

Resorption of mafic phenocryst phases (e.g. olivine and clinopyroxene) combined with fractional crystallization of mafic phases would allow compatible trace element contents to decrease while at the same time maintaining relatively high abundances slightly incompatible elements. If this were a continual process, operating in an open system magma chamber undergoing periodic recharge, then the combined affects of recharge, magma mixing, fractional crystallization, and resorption would be similar to that of an evolving magma chamber assimilating small amounts of ultramafic material. Such an effect could also be achieved by resorption of suspended mineral phases present in recharge magmas. There is abundant petrographic evidence to support the role of resorption in these lavas. Where present, phenocrysts and microphenocrysts contained in evolved lavas (mugearites) typically are partially to strongly resorbed. Along with plagioclase, partially resorbed phases include olivine and amphibole. Amphibole may, in fact be a common phase in evolved Haleakala lavas, but not recognized as such due to resorption. Amphibole is present to some extent in all batch 6 lavas. Amphibole phenocrysts, many of them partly to strongly resorbed, are contained in a mugearite flow located on the upper southwest rim of Haleakala Crater (see Macdonald, 1978). Also, a loose rock fragment found on a talus slope below the central west wall of Haleakala Crater contains abundant phenocrysts of brown amphibole.

Besides resorption of amphibole and other mafic phases, resorption of plagioclase may have been important. There is abundant petrographic evidence for strong plagioclase resorption in several evolved Kula lavas. For example, the transition from batch 12 to 13 involves an apparent positive Sr anomaly (Fig. 6f). The evolved, oldest lava from batch 13 [hawaiite HK-59] indeed contains plagioclase microphenocrysts in various stages of resorption and also has the highest Sr concentration of any lava in the Halemauu section.

INTRABATCH VARIATIONS

In contrast to the abrupt compositional discontinuities observed for interbatch transitions, intrabatch variations are gradational and progressively change upsection (Fig. 3). Two possible origins for intrabatch variations will be addressed, corresponding to both open system and closed system magma chamber models.

(1) Successively erupted lavas in a batch may represent evolved magmas resident in a reservoir that has undergone progressively greater amounts of mixing with primitive recharge magma. The composition of the recharge magma is most closely, but not necessarily exactly, approximated by the batch-end lava.

(2) Batches may consist of lavas related to a common parental magma by varying degrees of fractional crystallization. Successively erupted lavas in a batch may represent progressively deeper evacuations of a closed system, compositionally zoned magma chamber. In this model, batch-end lavas could represent magmas parental to other lavas in the same batch, cumulate magmas residing near the bottom of the magma chamber, or recharge magmas unrelated to previously erupted lavas. In the case of the latter two possibilities, parental magmas may not be erupted or may have had their compositions substantially modified (e.g. by crystal accumulation) prior to eruption.

In order to closely evaluate these models, the trace element systematics of three batches (batches 7, 9, and 12) are examined (Figs. 8-10). These batches were chosen because, relative to many of the other batches, they span relatively large compositional ranges and contain batch-end lavas that have relatively primitive compositions. Figures 8-10 present both simple enrichment factors (lava/batch-end lava) for lavas from each batch and also Nb-normalized enrichment factors (as used in figure 6). Simple enrichment factors can be used to illustrate absolute trace element enrichments relative to a either a possible primitive parental magma (model #2 above) or a possible primitive mixing end member [recharge] magma (model #1 above). Nb-normalized enrichment factors illustrate deviation in the behavior of other trace elements from that of a highly incompatible trace element (i.e. Nb).

Batch 7

Inconsistencies in the trace element systematics of batch 7 lavas suggest that the oldest exposed lavas in batch 7 (batch 7A) cannot have evolved by fractional crystallization of an parental magma having the composition of the batch-end alkalic basalt [HK-36]. Batch 7A lavas are highly enriched in incompatible elements relative to those erupted later (batch 7B) [Fig. 8a], and it is apparent from the strong negative anomalies for P, Sr, and Ti (Fig. 8a) and low abundances of Ni and Sc (Fig. 3) that batch 7A lavas have undergone significant apatite, plagioclase, Fe-Ti oxide, olivine, and clinopyroxene fractionation. However, fractionation [in any proportion] of the observed phases cannot explain the comparable or greater enrichment in Yb and Y over Nb (Fig. 8b). In addition, significant Fe-Ti oxide fractionation is indicated by depletions in both TiO_2 and V, yet Zr and Hf are enriched relative to presumably strongly incompatible elements such as Rb, Th, Nb, La, and Ce (Fig. 8b). It is also unlikely that apatite fractionation can explain the apparently excessive enrichments in Zr and Hf. Although data for the partitioning of incompatible elements into apatite are few, there is no obvious reason to believe that apatite partition coefficients for Zr and Hf should be any lower than for highly incompatible elements such as Rb and Nb (c.f. LeRoex and Erlank, 1982).

Batch 7B lavas are only slightly enriched in incompatible elements relative to HK-36 and have nearly flat patterns except for a prominent negative Ti anomaly (Fig. 8a). These lavas also have lower abundances of Sc, Ni, and V and lower $\text{Al}_2\text{O}_3/\text{CaO}$ ratios than HK-36 (Fig. 3). Assuming that HK-36 is indeed parental, then this observation indicates significant clinopyroxene, olivine, and Fe-Ti oxide fractionation. Extensive fractionation of those phases should produce magmas that are enriched in highly relative to moderately and slightly incompatible elements. Because batch 7B lavas are similarly enriched in variably incompatible elements (Fig. 8b) and also display crossing trace element patterns, it is unlikely that these magmas are related to an HK-36 parent by fractional crystallization.

The trace element patterns for batch 7A lavas [HK-26 and HK-28] are crossing and therefore cannot be explained by mixing between magma having a more evolved composition than these two lavas and an HK-36 composition magma. Nb-normalized enrichment factors for batch 7B lavas lie between those for batch 7A lavas and HK-36 (Fig. 7b), and, therefore, are for the most part consistent with derivation of 7B lavas by mixing between 7A and HK-36 magmas. There are, however, inconsistencies for some elements. K, Zr, and Yb, for example, have Nb-normalized enrichment factors of approximately 1.0 which are inconsistent with intermediate batch 7 lavas representing hybrids formed by mixing of evolved batch 7A magma with primitive batch-end alkalic basalt recharge magma (Fig. 8b). Thus, the compositions of batch 7A lavas may only approximate the evolved mixing end member. It is possible that more evolved magmas resided in the magma chamber but that either their compositions were subsequently modified by fractional crystallization or magma mixing, or such evolved magmas were never erupted.

Batch 9

Lavas from batch 9 have comparable enrichment factors for elements of variable incompatibility (e.g. Nb, LREE, Y, HREE) [Fig. 9a]. It is therefore unlikely that any of the evolved batch 9 hawaiites and mugearites could have been produced by fractional crystallization from the observed batch-end basanitoid [HK-50] magma. Relative to HK-50, the most evolved batch 9 lava [mugearite sample HK-43], contains higher incompatible element abundances and has a higher La/Sm ratio, but also has a lower La/Yb ratio. If this mugearite is related to the batch-end basanitoid by fractional crystallization, the relative order of incompatibility for REE observed would require, paradoxically, $D^{Sm} > D^{Yb} > D^{La}$. Although apatite fractionation (as indicated by the strong negative P anomaly) could conceivably decrease Sm/Yb ratios (Watson & Green, 1981), it could not result in enrichment in Yb comparable to that observed for more incompatible elements (e.g. Nb) [Fig. 9b) because D^{Yb} values for apatite are typically

much greater than unity. Similarly, HK-44 is comparably enriched relative to HK-50 in both highly (Rb, K, Th) and slightly (Y, Yb) incompatible elements (enrichment factors of approximately 1.8-2.0), and also has a striking positive P anomaly (Fig. 9a), both of which are inconsistent with fractional crystallization.

Trace element patterns are also inconsistent with derivation of intermediate batch 9 lavas by mixing between the primitive batch-end basanitoid and evolved mugearite composition magmas. For one, intermediate lavas in batch 9 do not have normalized enrichment factors that lie between these two compositional extremes. Secondly, some intermediate batch 9 lavas (e.g. HK-44 and HK-49) are more enriched than HK-43 in LREE, MREE, and HREE, relative to Nb (Fig. 9b), and in fact have Nb normalized enrichment factors greater than unity for these elements.

Batch 12

Batch 12 contains only three lavas, but because batch-end lava, HK-58, is one of the most mafic lavas from the Halemauu section, it is worth evaluating both as a possible parental magma composition and as a primitive mixing end member composition. HK-57 is similar in composition to HK-58, but in a relative sense is enriched in Sr, Ti, Y, and Yb and depleted in Rb and Ba (Fig. 10a). HK-57 has Nb-normalized enrichment factors greater than those for HK-58 for all elements except Rb and Sm (Fig. 10b). Despite having similar incompatible element compositions, HK-57 has significantly lower Sc, Ni, Cr, and MgO contents and higher $\text{Al}_2\text{O}_3/\text{CaO}$ than does HK-58. This contradiction makes it unlikely that these lavas are related by fractional crystallization.

The evolved, oldest lava from batch 9 [hawaiite sample HK-56] is also unlikely to have been produced by fractional crystallization of an HK-58 parent magma. HK-56 appears to be anomalously enriched in K relative to other incompatible elements and, similar to HK-57, appears to be relatively depleted in Rb (Fig. 10a). Yb also appears to be anomalously enriched over more incompatible elements (e.g. Th, LREE, Zr, Ba).

Because HK-56 and HK-57 have Nb-normalized enrichment factors less than and

greater than unity, respectively (Fig. 9b), the intermediate basalt lava [HK-57] cannot have been produced by mixing between the primitive batch-end ankaramite and the evolved batch 12 hawaiite magma compositions. The jagged trace element pattern of the hawaiite further indicates that this lava cannot represent a simple mixed magma involving the primitive batch-end magma and any analyzed lava composition.

MODELING CLOSED AND OPEN SYSTEM FRACTIONATION

Parental Magma Compositions

Intrabatch geochemical variations in each of the three batches examined cannot be explained either by simple mixing of observed primitive and evolved magma compositions, or by fractional crystallization of batch-end composition magmas. A possible explanation is that batch-end lavas may simply be inappropriate parental magma compositions. In order to test the suitability of these lavas for being possible parental magmas, open and closed system magma chamber models were calculated using the phase equilibria-based method of Nielsen (1988). It should be noted that Nielsen's (1988) method is calibrated for low pressure (1 atm), therefore the following calculations can constrain only fractionation occurring in a high-level magma chamber. Four batch-end lavas, representing batches 1, 7, 9, and 12, were chosen as possible parental magma compositions and were used as starting compositions. Results of the computations are listed in Table 4, and selected elements illustrated in Figure 11.

Of the four starting compositions chosen (HK-2, HK-36, HK-50, HK-58), only HK-58 has $\text{MgO} > 7$ wt.% ($\text{MgO} = 11.44$ wt.%) and is therefore the only sample which has olivine as the dominant phase at the initial calculated liquidus temperature (Table 4d). Olivine + spinel follows olivine and is followed by olivine + clinopyroxene + spinel. At lower temperature, clinopyroxene dominates the liquidus phase assemblage which also includes plagioclase + spinel + olivine. HK-2 ($\text{MgO} = 5.96$ wt.%) has spinel, followed by plagioclase, followed by plagioclase + spinel, followed by clinopyroxene + plagioclase, followed by clinopyroxene + plagioclase + spinel (Table 4a). Orthopyroxene appears in

the final calculated assemblage, plagioclase + orthopyroxene + clinopyroxene + spinel. HK-36 (MgO = 6.76 wt.%) has spinel followed by clinopyroxene + plagioclase + olivine + spinel (Table 4b). Olivine falls off the liquidus but reappears at lower temperature in the assemblage plagioclase + clinopyroxene + spinel + olivine. HK-50 (MgO = 6.31 wt.%) has clinopyroxene followed by clinopyroxene + plagioclase followed by clinopyroxene + plagioclase + spinel (Table 4c). At lower temperature, plagioclase becomes dominant over clinopyroxene.

It is clear from the calculated liquidus phase assemblages and low MgO (< 7 wt.%) and Ni (< 100 ppm) contents of HK-2, HK-36, and HK-50 that these lavas are probably not primary liquids and must have been derived from less evolved predecessors. If these lavas represent recharge magma compositions, then it is apparent these melts underwent a previous history of differentiation, either during ascent or deeper-level storage. Because the major and trace element compositions of primitive batch-end lavas are comparable over the scale of the Halemauu section, fractionation during deeper-level storage is probably more likely than ascent-related fractionation. However, even if these magmas were fractionated prior to higher-level emplacement, they may still represent magmas parental to more evolved composition lavas.

Although HK-58 contains high MgO and Ni (217 ppm), it also contains, paradoxically, relatively high incompatible element abundances (e.g. Nb = 31 ppm, Rb = 28 ppm, Ba = 503 ppm) compared to the other batch-end lavas tested (see Table 2). It also contains extremely low Al_2O_3 (11.5 wt.%) relative to other Kula lavas from the Halemauu section (> 14 wt.% Al_2O_3), and geochemically resembles lavas from the post-erosional Hana Formation. It is evaluated as a possible parental magma, but its apparently anomalous composition should be kept in mind.

Results of Calculations

In figure 11, solid curves represent open system evolution in which rates of recharge and fractionation are equal and the system maintains a steady-state mass. This corresponds to the 1-0-0 model of Nielsen (1988), where the three parameters refer to the amounts of recharge, assimilation, and eruption, relative to fractionation. The dashed curves in figure 11 refer to closed system models involving perfect fractional crystallization (the 0-0-0 model of Nielsen, 1988). Inflections in the curves reflect the disappearance and appearance of phases in the calculated equilibrium mineral assemblage. Points where the phase assemblage changes are listed in Table 4.

Open System Recharge Models

It is apparent that, with the exception of Ni, none of the four batch-end compositions follows a liquid line of descent appropriate for a parental magma to the more evolved Kula lavas (Fig. 11). In general, 1-0-0 recharge models predict higher than observed Ni, MgO, and Sc contents lower than observed SiO_2 and Al_2O_3 contents. As predicted by O'Hara (1977) and illustrated by Nielsen (1988), Ni abundances become buffered as fractionation proceeds to higher degrees (Fig. 11a), whereas incompatible element contents (e.g. Nb) continue to increase. The HK-2 starting composition is better able to model Sc (Fig. 11b) and SiO_2 (Fig. 11d) than the other three model parent magma compositions, but the early appearance of spinel on the liquidus and the subsequent dominance of plagioclase (Table 4a) result in initially decreasing Al_2O_3 contents with increasing fractionation, followed by a buffering of Al_2O_3 contents at inappropriately low levels (Fig. 11e).

Closed System Fractionation Models

Closed system fractionation models (0-0-0 models) predict Ni variations adequately (Fig. 11a), but all four starting compositions result in excessively high Sc and MgO and low SiO₂ and Al₂O₃ contents (Figs. 11b-e). As in the recharge models, perfect fractional crystallization of HK-2 results in reasonable Sc contents at lower degrees of fractionation, but fails at higher degrees of fractionation. HK-2 is especially poor for modeling MgO (Fig. 11c) and Al₂O₃ (Fig. 11e). Admittedly, fractionation at higher pressures would most likely produce different results.

Combined Recharge and Mixing with Evolved Liquids

Several workers have speculated that magma chambers may contain highly evolved liquids that either formed in or migrated to boundary layers existing along the sidewalls or at roof of the chamber (see for example, Turner and Gustafson, 1981; Huppert et al., 1986; Langmuir, 1988). If such liquids existed in the Haleakala magma chamber, then they would constitute an additional component in the intrabatch mixing process. Langmuir (1988) proposed that highly differentiated melts could form in isolated boundary layers surrounding the main body of an evolving magma chamber and that these melts could be remixed back into the main convective regime during recharge. In such a boundary layer, considerably more evolved mineral compositions and possibly distinct phase assemblages may precipitate, compared to those that would crystallize in the less evolved interior of the magma chamber, thereby producing a relatively evolved liquid. Such a boundary layer would also probably be relatively volatile-rich. The presence of amphibole in some of the more evolved Kula lavas from Haleakala Crater indicates that a volatile-rich environment did exist.

Batch 9 was chosen to model mixing of evolved liquids with recharge magmas because this batch contains a mafic batch-end lava (HK-50) and the oldest lava is an appreciably evolved mugearite (HK-43). Calculations were performed after the method of Nielsen (1988) with the mugearite used as an assimilant. The results of these com-

putations are presented in Table 5. Assimilation does not change the calculated equilibrium phase assemblage, but it does alter the individual phase proportions and the total amount of crystallization required to achieve a given degree of incompatible element (e.g. Nb) enrichment (Table 5).

Figure 12 illustrates the variation in Sc, MgO, SiO_2 , and Al_2O_3 contents due to combined assimilation, recharge and fractionation. Two assimilation models were investigated (indicated by the long dashed curves in Fig. 12): .5-.5-0 and .25-.75-0, both representing steady-state mass systems in which recharge and assimilation are subordinate to fractionation. These models depict the cases where recharge and assimilation are equal (.5-.5-0) and where assimilation dominates over recharge by a ratio of 3:1 (.25-.75-0). Also illustrated for comparison (Fig. 12), are the previously discussed 1-0-0 and 0-0-0 models (solid and short dashed curves, respectively), and two models depicting very small amounts of recharge with no assimilation (.1-0-0 and .01-0-0 models; solid curves).

No significant deviation from 1-0-0 or 0-0-0 models results from simply lowering the amount of recharge relative to crystallization (.1-0-0 and .01-0-0 models). In comparison, assimilation results in lower Sc and MgO and higher SiO_2 and Al_2O_3 contents of derived liquids, relative to 1-0-0 and 0-0-0 models (Figs. 12b-d). However, calculated liquid compositions are still significantly different from the observed compositions of Kula lavas. The discrepancy in the models may be due to (1) an underestimation of the relative importance of assimilation versus recharge and crystallization, or (2) an incorrect estimation of the composition of the assimilant.

Increasing the ratio of assimilation to recharge to greater than 3:1 would result in further increases in SiO_2 and Al_2O_3 and decreases in Sc and MgO, and thus a better fit to the data. However, a large increase in the relative role of assimilation may not be realistic, because as Nielsen (1988) points out, high assimilation/crystallization rates may be incompatible with heat budget constraints. As an alternative to increased assimilation, it is possible that HK-43 is an inappropriate assimilant composition and is itself a

mixed magma. The evolved liquid assimilated could be considerably more evolved, containing higher SiO_2 and Al_2O_3 and lower compatible element contents (e.g. MgO and Sc) than HK-43.

MAGMA CHAMBER MODEL

The model presented is based on the interbatch and intrabatch variations for Haleakala Crater. Results from the previously discussed trace element systematics and major and trace element modeling are also taken into account. We believe that the available data can best be explained by a dynamic, evolving, unzoned open system magma chamber. The cyclic nature of geochemical variations observed in the Halemau section, and expressed in terms of interbatch geochemical discontinuities and interbatch variations, could represent alternating periods of low and high magma flux. The dynamics of a magma chamber experiencing variations in magma flux regime are illustrated schematically in Figure 13.

Although this model should be applicable to other alkalic cap suites, significant differences in overall magma budget between volcanoes could result in considerable variations in the timing of eruptions and hence in the degree of magmatic differentiation. In addition, there may be subtle differences in the lithology and structure of the crust and lithosphere beneath individual volcanoes that could cause significant variability in the depths of magma chambers. Increased lithostatic pressure experienced by deeper-level chambers could conceivably influence eruptive periodicity.

Low Magma Flux Regime

Because interbatch transitions are characterized geochemically by fractionation-dominated evolution and in the field by apparent gaps in the eruptive record apparently indicating eruptive quiescence, these geochemical discontinuities appear to represent periods of low or negligible magma flux (or recharge). The magma chamber at this point enters the *fractionation cycle* of Fig. 13 (recharge-mixing-fractional crystallization

[FC]-recharge), during which only small volumes of recharge mix with rest magmas. The lack of success of major and trace element modeling indicates that fractional crystallization alone was not sufficient to produce the observed compositional changes, and it is possible that minor recharge combined with resorption of mafic phenocryst phases also occurred. The degree of fractionation experienced by the magma chamber during the fractionation cycle depends on recharge rate and total magma flux into the chamber. Variations in the degree of incompatible element enrichment and compatible element depletion observed for individual batches indicate that both the recharge rate and total magma flux were likely variable throughout the alkalic cap stage.

As long as recharge rates are low enough that the magmatic pressure exerted by the chamber does not exceed lithostatic pressure, the magma chamber will remain in the fractionation cycle. However, even at very low recharge rates, eruption may occur if lithostatic pressure is temporarily exceeded. This could occur if the cumulative mass flux of magma reaches a critical mass, if the buoyancy of rest magma in the chamber has reached some critical point due to decreasing density, or if volatile exsolution during fractional crystallization increased the overall magmatic pressure beyond a critical threshold. It is possible that the presence of amphibole in the mugearites from batch 6 is the result of such volatile build-up. Batch 6 contains only highly evolved lavas that could be the products of volatile-induced eruption. If lithostatic pressure is temporarily exceeded in the low magma flux regime resulting in eruption, the magma chamber will simply follow a path back to the fractionation cycle, i.e. recharge-eruption-mixing-fractional crystallization (Fig. 13).

High Magma Flux Regime

Individual magma batches in the Haleakala Crater section represent eruptive periods separated by periods of quiescence. It is therefore possible that eruptive periods are initiated by a transition from low to high magma flux regime. High magma recharge rates result in the magma chamber entering a complex *eruption cycle* (see Fig. 13) in which geochemical variations are dominated by mixing between primitive recharge magmas [possibly represented by batch-end lavas] and evolved rest magma resident in the chamber. Because batch-end lavas have low MgO and Ni contents (Fig. 3) and therefore appear to have experienced prior fractionation, they may not represent unmodified recharge magmas. Instead, batch-end lavas may simply be the last mixed magmas erupted during a particular eruptive period. Although batch-end lavas may not represent the true compositions of recharge magmas, they are certainly the closest approximation of recharge composition erupted. An important implication of the lack of erupted recharge magmas is that the magma chamber is never completely evacuated.

Following eruption, unexpelled rest magma may mix with the recharge magma and subsequently may undergo fractional crystallization. In fact, trace element systematics (Fig. 8) indicate that lavas at intermediate positions within these batches cannot have been produced by magma mixing alone, but must have been affected by fractional crystallization as well. Recharge and mixing continues until lithostatic pressure is again exceeded and eruption reoccurs. The eruption cycle is thus a period of repeated recharge, eruption, mixing, and fractional crystallization. It is possible that at some critically high recharge rate, fractional crystallization may become insignificant and the eruption cycle could consist of a series of recharge-eruption-mixing events. In addition, open system fractionation modeling suggests that mixing of highly differentiated melts may also have influenced intrabatch geochemical variations.

The above scenario could be further complicated if, during an eruption cycle, magma recharge rate drops to the point where the magma chamber passes into the low magma flux regime for a significant period of time. Such a transition would allow a

series of fractionation cycles to be interspersed. Such detours from one magma flux regime to the other could have profound effects on the compositions of erupted lavas. For example, the small subsections observed within batch 7 (Figs. 3c, d, h, i) may be the result of short periods of low magma flux occurring during an eruption cycle.

Implications for Closed System Magma Chambers

Successively deeper evacuations of a closed system, zoned magma body (as described by Macdonald, 1949) could result in the formation of a compositional sequence in which the most evolved lavas are erupted first, followed progressively by more primitive lavas. There are, however, several lines of evidence which together suggest that a zoned magma chamber did not exist beneath Haleakala, at least not during production of alkalic cap lavas exposed in the walls of Haleakala Crater.

(1) If crystal fractionation occurred primarily by side-wall crystallization, then the composition of magma lowermost in the chamber could be a close approximation of a parental magma. However, trace element systematics are inconsistent with primitive batch-end lavas being parental magmas to lavas from the same batch. In fact, both closed and open system fractionation calculations indicate that, unmodified (e.g. by mixing), batch-end lavas are unlikely parents to any observed lava composition. A possible caveat to those calculations is that they simulate only low pressure fractionation.

(2) Although batch-end lavas contain relatively abundant phenocrysts (see Table 1), these rocks are not picritic. In fact, with exception of HK-58 (batch 12), none of the batch-end lavas in the Halemau section have MgO contents greater than 7 wt.% or more than 100 ppm Ni. These lavas, therefore, cannot represent the highly mafic, cumulate magmas envisioned by Macdonald (1949) as residing at the base of the magma chamber.

(3) If batch-end lavas represent simple cumulates, then their compositions are dependent on the residence times of magma in the magma chamber. Longer periods of residence at the base of the chamber would allow these magmas to accumulate increasingly greater

amounts of phenocrysts. The alkalic cap stage of Hawaiian volcanism is characterized by a progressive decrease in melt production (Wise, 1982; Clague and Dalrymple, 1987). If magma residence times progressively increased in synchronous fashion, the compositions of cumulate magmas should become increasingly more primitive with time, but no such change is observed. For example, batch-end lavas in batches 1-3 range from 0.81-0.96 wt.% K_2O and have Mg#'s from 46-51; batch-end lavas in batches 7, 9, 11, and 12 also have low K_2O contents (0.77-1.05 wt.% K_2O ; Fig. 11) and comparable Mg#'s (Mg# = 42-50, with the exception of HK-58 which has Mg# = 63).

ERUPTION RATE ESTIMATES BASED ON MAGMA BATCHES

Assuming that the 13 magma batches observed in the Halemauu section of Haleakala Crater represent discrete eruptive intervals, a minimum rate of eruption can be calculated if the time span represented by the section as a whole can be estimated. Although no age dates are available for the lower part of the Halemauu section, the maximum age must be less than that of the stratigraphically lower Kumuilahi Formation (i.e. 0.70 ± 0.03 Ma; Naughton et al., 1980). Two estimates of the upper age limit for the section were used: (1) 0.56 ± 0.14 Ma, the age of a lava from the upper rim of the west wall of Haleakala Crater, located at the Kalahaku lookout [Naughton et al., 1980], and (2) 0.49 ± 0.15 Ma, the age of the Holua dike which cuts the Halemauu section on the northwest wall of Haleakala Crater [Naughton et al., 1980].

Based on these K-Ar ages, the Halemauu section could represent as much as 0.14 to 0.21 Ma of eruptive activity. This time interval yields an average of 1 eruption per 10,769-16,154 years, which is significantly greater than estimates made for the alkalic cap stages of Mauna Kea (1 eruption per 1,250-1,500 years; West et al., 1988) and Kohala (1 eruption per 1,900 years; Spengler and Garcia, 1988). An explanation for this discrepancy is that the maximum age used for the base of the Halemauu section is considerably too old. A paleomagnetic survey of the Halemauu section (R. Coe, personal communication) suggests that the time span represented by these lavas is smaller than

that inferred by existing K-Ar data by an order of magnitude. Based on the number of observed reversals in the section and time estimates for changes in the magnetic field, the section spans roughly 26,400 years. The minimum eruption rate based on this estimate is 1 eruption per 2,031 years. This eruption rate is comparable to, although still slightly lower, than those estimated for Mauna Kea and Kohala

Eruption rate estimates for Haleakala, Mauna Kea, and Kohala are all lower than the "alkalic postshield stage" estimate of 1 eruption every 50-1000 years suggested by Clague (1987). These eruption rates are significantly lower than those for early alkalic cap volcanism on Hualalai (1 eruption per 50 years) or for active shield-building volcanism on Kilauea (1 eruption per 1-4 years; Klein, 1982; Dzurisin et al., 1984).

It may be significant that alkalic cap lavas from Haleakala, which span a larger range in composition (alkalic basalt to trachyte) than alkalic cap lavas from either Kohala (mugearite to trachyte; Spengler and Garcia, 1988) or Mauna Kea (hawaiite with very little mugearite), contains the largest proportion of evolved lava compositions also has the lowest eruption rate. In contrast, Mauna Kea, which of the three alkalic caps contains the smallest proportion of evolved lavas, has the highest eruption rate. Thus, the proportion of evolved rock types within a particular alkalic cap sequence is possibly a function of magma supply rate.

CHANGES IN PARENTAL MAGMA COMPOSITION WITH TIME

Systematic temporal variations in Sr and Pb (West and Leeman, 1987) and Nd (Chen and Frey, 1985) isotopic ratios and in several trace element ratios (e.g. Zr/Nb, Ba/Y) indicate that the mantle source composition of Kula lavas progressively changed with time. Therefore, parental (recharge) magma compositions must also have changed, although this variation is not reflected in the major and trace element contents of Kula batch-end lavas or other mafic lavas from the Halemauu section (Fig. 3). Differences in recharge composition between batches are illustrated in Figure 14, where it can be seen that each batch forms a distinct trend. These separate trends may reflect not only dif-

ferent parental (recharge) magma compositions, but may also partly reflect varied magma chamber dynamics.

Changes in Source Mixing Systematics

In addition to the progressive change in the source composition of Kula lavas noted in isotopic and trace element ratios, there appears to have been a relatively abrupt shift in the nature of source mixing systematics within the Kula Formation. Table 6 compares selected geochemical data for all lavas containing MgO > 5 wt.% in batches 1–7A (the older batch group) and in batches 7B–13 (the younger batch group). These two groups possess distinct $^{87}\text{Sr}/^{86}\text{Sr}$, Zr/Nb, and Ba/Y ratios, and, paradoxically, the older batch group tends to contain both higher Zr and lower Nb abundances than the younger batch group, even though average Mg#’s are comparable (46.2 versus 49.3; Table 6). Although mafic lavas from both the older and younger batch groups span comparable ranges in both compatible and incompatible element abundances (Table 6), when these elements are plotted against trace element ratios that reflect changes in source composition (e.g. Zr/Nb), two distinct trends emerge (Fig. 15).

Primitive lavas from the older batches have Zr/Nb and $^{87}\text{Sr}/^{86}\text{Sr}$ ratios close to those for Kumuilihi Formation lavas, but deviate to lower Zr/Nb ratios with increasing Ba and decreasing Sc abundances (Figs. 15a–b). In contrast, younger batch lavas follow trends similar to those for Hana Formation lavas (Figs. 15a–b). Zr/Nb ratios and Ba abundances are negatively correlated for both older and younger batch group lavas (Fig. 15a), suggesting that Zr/Nb ratios are at least partly controlled by fractionation (magma chamber) related processes. For the older batches, Zr/Nb is also positively correlated with Sc abundances (Fig. 15b), although such a correlation does not appear to exist for the younger batch group.

Zr/Nb–Ba–Sc relations suggest that the older batches evolved from parental magmas with Sc contents (and Mg#’s) similar to those in the younger batch parental magmas but with slightly lower Ba abundances and distinct Zr/Nb ratios. Distinct

parental magma compositions and evolutionary trends are supported by variations between Y and Sc abundances (Fig. 15c). For example, older batch lavas probably evolved from parental magmas similar in Y and Sc composition to Kumuilahi lavas but with higher Y abundances than the parental magmas of the younger batches. The younger batches follow an almost identical trend to that for the Hana Formation, except that lavas with higher Y/Sc ratios are produced at higher degrees of fractionation (i.e. Sc < 15 ppm). Although the trends for both groups are consistent, at least in part, with fractionation control, the offset of the two trends requires that distinct parental magma compositions be involved.

The distinct trends displayed by older and younger batches indicate that at some point in the evolution of the Kula Formation, the source composition of these magmas abruptly changed. Because older Kula lavas have $^{87}\text{Sr}/^{86}\text{Sr}$, $^{206}\text{Pb}/^{204}\text{Pb}$, Zr/Nb, and Ba/Y compositions similar to Kumuilahi lavas and fall near the Hawaiian Sr-Pb shield-building array (West and Leeman, 1987; West et al., 1987), these magmas may have been dominated by the Hawaiian plume component. In contrast, the source of younger [less radiogenic Sr and Pb] Kula lavas may have been dominated by a depleted (or DM) component (see West and Leeman, 1987; West et al., 1987). Evidence against a progressive change in the proportions of source components suggests a rather abrupt change in magma supply conditions. It is possible that if multiple plumes are involved in the genesis of Hawaiian lavas (West and Leeman, 1987; West et al., 1987), then the compositional shift might reflect emplacement of magmas derived from a separate plume.

CONCLUSIONS

Alkalic cap lavas from the Halemau section of Haleakala Crater consist of interbedded alkalic basalts, hawaiites, and mugearites. These lavas display upsection, repetitive geochemical variations that define discrete compositional packages which are interpreted to represent distinct magma batches. Cyclic variation in both major and trace element compositions is consistent with a dynamically evolving, open system magma

chamber. This cyclicity may reflect alternating periods of low and high magma flux. Data are inconsistent with periodic evacuations and refillings of an essentially closed system, zoned magma body.

During periods of low magma flux, the magma chamber may enter a fractionation cycle accompanied by limited magma mixing. The observed interbatch geochemical discontinuities and breaks in the section define periods of volcanic quiescence and are a reflection of low magma recharge rates. During periods of high magma flux, increasing recharge results in magmatic pressure exceeding the overburden pressure of the magma chamber and the initiation of an eruption cycle. Recharge magmas may expel only a portion of magma resident in the magma chamber and then mix to some extent with the remaining rest magma. Recharge combined with fractional crystallization continues until eruption again commences. The continuous mixing of recharge magma with progressively more mafic rest magmas followed by eruption could have created the systematic upsection intrabatch compositional variations observed. Ebbs in magma recharge rates may have resulted in increased fractionation effects.

The open system, cyclic behavior inferred for Haleakala alkalic cap lavas is considered to be a natural consequence of a waning magma budget. Decreasing magma supply rates associated with the alkalic cap stage of Hawaiian volcanism result in increased magma chamber residence times and greater magmatic diversity. Alternating periods of low and high magma flux can produce the observed series of geochemically distinct magma batches exposed in Haleakala Crater. This magmatic cyclicity further imposes short-term geochemical imprints over the longer-term geochemical variations produced by changes in source composition.

ACKNOWLEDGEMENTS

Mahalo nui loa to Fred Mullins for invaluable field assistance and to Ron Nagata and Hugo Huntzinger of the Haleakala National Park Service for their warm kokua. We thank Fred Frey, Mike Rhodes, and Don Elthon for access to their laboratories, and especially Godfrey Fitton for providing holistic XRF trace element data. We are indebted to David Gerlach for lab assistance and constructive advice on many disciplinary matters. This work was supported in part through National Science Foundation grants EAR85-12167 and EAR83-20358, G.S.A. Penrose grant 3515-85, and the Rice University Department of Geology and Geophysics.

REFERENCES

- Bryan, W. B., Thompson, G. and Michael, P. J., 1979, Compositional Variation in a Steady-State Zoned Magma Chamber: Mid-Atlantic Ridge at 36°50'N: *Tectonophy.* 55, p. 63-85.
- Chen, C.-Y., 1982, Geochemical and Petrologic Systematics in Lavas from Haleakala Volcano, East Maui: Implications for the Evolution of Hawaiian Mantle: Ph.D. Thesis, M.I.T., 344 p.
- Chen, C.-Y. and Frey, F. A., 1983, Origin of Hawaiian Tholeiites and Alkalic Basalt: *Nature* 302, p. 785-789.
- Chen, C.-Y. and Frey, F. A., 1985, Trace Element and Isotopic Geochemistry of Lavas from Haleakala Volcano, East Maui, Hawaii: Implications for the Origin of Hawaiian Basalts: *J. Geophys. Res.* 90, p. 8743-8768.
- Clague, D. A., 1987, Hawaiian Xenolith Populations, Magma Supply Rates, and Development of Magma Chambers: *Bull. Volcanol.* 49, p. 577-587.
- Clague, D. A. and Dalrymple, G. B., 1987, The Hawaiian-Emperor Volcanic Chain. Part 1. Geologic Evolution: U.S.G.S. Prof. Paper 1350, p. 5-54.
- Clague, D. A., Jackson, E. D. and Wright, T. L., 1980, Petrology of Hualalai Volcano, Hawaii: Implications for Mantle Composition: *Bull. Volcanol.* 43, p. 641-656.
- Diller, D. E., 1982, Contributions to the Geology of West Maui Volcano, Hawaii: M.S. Thesis, University of Hawaii, 237 p.
- Dzurisin, D., Koyanagi, R. Y. and English, T. T., 1984, Magma Supply and Storage at Kilauea Volcano, Hawaii, 1956-1983: *J. Volc. Geoth. Res.* 21, p. 177-206.
- Elthon, D., 1984, Plagioclase Buoyancy in Oceanic Basalts: Chemical Effects: *Geochim. Cosmochim. Acta* 48, p. 753-768.
- Feigenson, M. D., Hofmann, A. W. and Spera, F. J., 1983, Case Studies on the Origin of Basalt II. The Transition from Tholeiitic to Alkalic Volcanism on Kohala Volcano, Hawaii: *Contrib. Mineral. Petrol.* 84, p. 390-405.
- Fodor, R. V. and Keil, K., 1979, Review of the Mineral Chemistry of Volcanic Rocks from Maui, Hawaii: in *Field Trip Guide to the Hawaiian Islands*, H.I.G. Spec. Pub., p. 93-106.
- Fodor, R. V., Keil, K. and Bunch, T. E., 1972, Mineral Chemistry of Volcanic Rocks from Maui, Hawaii: Fe-Ti Oxides: *G.S.A. Abstr. w/Progr.* 4, p. 507.
- Fodor, R. V., Keil, K. and Bunch, T. E. 1975, Contributions to the Mineral Chemistry of Hawaiian Rocks IV. Pyroxenes in Rocks from Haleakala and West Maui Volcanoes, Maui, Hawaii: *Contrib. Mineral. Petrol.* 50, p. 173-195.
- Fodor, R. V., Keil, K. and Bunch, T. E., 1977, Contributions to the Mineral Chemistry of Hawaiian Rocks. VI. Olivines in Rocks from Haleakala and West Maui Volcanoes, Maui, Hawaii: *Pac. Sci.* 31, p. 299-308.
- Fujii, T. and Bougault, H., 1983, Melting Relations of a Magnesian Abyssal Tholeiite

- and the Origin of MORBs: *Earth Planet. Sci. Lett.* 62, p. 283-295.
- Higuchi, H. and Nagasawa, H., 1969, Partition of Trace Elements Between Rock Forming Minerals and the Host Volcanic Rocks: *Earth Planet. Sci. Lett.* 7, p. 281-287.
- Hofmann, A. W., Feigenson, M. D. and Raczek, I., 1987, Kohala Revisited: *Contrib. Mineral. Petrol.* 95, p. 114-122.
- Huppert, H. E., Sparks, R. S. J., Wilson, J. R. and Hallworth, M. A., 1986, Cooling and Crystallization at an Inclined Plane: *Earth Planet. Sci. Lett.* 79, p. 319-328.
- Ila, P. and Frey, F. A., 1984, Utilization of Neutron Activation Analysis in the Study of Geologic Materials: *Atomkernenergie Kerntechnik* 44, p. 710-716.
- Irving, A. J. and Frey, F. A., 1984, Trace Element Abundance in Megacrysts and their Host Basalts: Constraints on Partition Coefficients and Megacryst Genesis: *Geochim. Cosmochim. Acta* 48, p. 1201-1221.
- Karson, J. A. and Elthon, D., 1987, Evidence for Variations in Magma Production Along Oceanic Spreading Centers: A Critical Appraisal: *Geology* 15, p. 127-131.
- Keil, K., Fodor, R. V. and Bunch, T. E., 1972, Contributions to the Mineral Chemistry of Hawaiian Rocks. II. Feldspars and Interstitial Material in Rocks from Haleakala and West Maui Volcanoes, Maui, Hawaii: *Contrib. Mineral. Petrol.* 37, p. 253-275.
- Klein, F. W., 1982, Patterns of Historical Eruptions at Hawaiian Volcanoes: *J. Volc. Geoth. Res.* 12, p. 1-35.
- Kurz, M. D., 1986, Cosmogenic Helium in a Terrestrial Igneous Rock: *Nature* 320, p. 435-439.
- Kurz, M. D., O'Brien, P. A., Garcia, M. O. and Frey, F. A., 1985, Isotopic Evolution of Haleakala Volcano: Primordial, Radiogenic and Cosmogenic Helium: *EOS* 66, p. 1120.
- Kurz, M. D., Garcia, M. O., Frey, F. A. and O'Brien, P. A., 1987, Temporal Helium Isotopic Variations Within Hawaiian Volcanoes: Basalts from Mauna Loa and Haleakala: *Geochim. Cosmochim. Acta* 51, p. 2905-2914.
- Langmuir, C. H., 1988, Geochemical Consequences of the Solidification of Magma Chambers Through "*In Situ*" Fractionation in a Boundary Layer: *Nature*, in press.
- Lanphere, M. A. and Frey, F. A., 1987, Geochemical Evolution of Kohala Volcano, Hawaii: *Contrib. Mineral. Petrol.* 95, p. 100-113.
- Leeman, W. P. and Hawkesworth, C. J., 1986, Open Magma Systems: Trace Element and Isotopic Constraints: *J. Geophys. Res.* 91, p. 5901-5912.
- LeRoex, A. R. and Erlank, A. J., 1982, Quantitative Evaluation of Fractional Crystallization in Bouvet Island Lavas: *J. Volc. Geoth. Res.* 13, p. 309-338.
- Macdonald, G. A., 1942, Petrography of Maui: *Hawaii Div. Hydrogr. Bull.* 7, p. 275-334.
- Macdonald, G. A., 1949, Hawaiian Petrographic Province: *G.S.A. Bull.* 60, p. 1541-

1596.

- Macdonald, G. A., 1968, Composition and Origin of Hawaiian Lavas: G.S.A. Mem. 116, p. 477-522.
- Macdonald, G. A., 1972, Composite Lava Flows on Haleakala Volcano, Hawaii: G.S.A. Bull. 83, p. 2971-2974.
- Macdonald, G. A., 1978, Geologic Map of the Crater Section of Haleakala National Park, Maui, Hawaii: U.S.G.S. Misc. Inv. Ser. Map I-1088.
- Macdonald, G. A. and Katsura, T., 1964, Chemical Composition of Hawaiian Lavas: J. Petrol. 5, p. 82-133.
- Macdonald, G. A. and Powers, H. A., 1946, Contribution to the Petrography of Haleakala Volcano, Hawaii: G.S.A. Bull. 57, p. 115-124.
- Macdonald, G. A. and Powers, H. A., 1968, A Further Contribution to the Petrology of Haleakala Volcano, Hawaii: G.S.A. Bull. 79, p. 877-888.
- McDougall, I., 1964, Potassium-Argon Ages from Lavas of the Hawaiian Islands: G.S.A. Bull. 75, p. 107-128.
- Mo, X., Carmichael, I. S. E., Rivers, M. and Stebbins, J., 1982, The Partial Molar Volume of Fe_2O_3 in Multicomponent Silicate Liquids and the Pressure Dependence of Oxygen Fugacity in Magmas: Min. Mag. 45, p. 237-245.
- Naughton, J. J., Macdonald, G. A. and Greenberg, V. A., 1980, Some Additional Potassium-Argon Ages of Hawaiian Rocks: The Maui Volcanic Complex of Molokai, Maui, Lanai and Kahoolawe: J. Volc. Geoth. Res. 7, p. 339-355.
- Nielsen, R. L., 1988, A Model for the Simulation of Combined Major and Trace Element Liquid Lines of Descent: Geochim. Cosmochim. Acta 52, p. 27-38.
- O'Hara, M. J., 1977, Geochemical Evolution During Fractional Crystallisation of a Periodically Refilled Magma Chamber: Nature 266, p. 503-507.
- Oostdam, B. L., 1965, Age of Lava Flows on Haleakala, Maui, Hawaii: G.S.A. Bull. 76, p. 393-394.
- Rhodes, J. M. and Dungan, M. A., 1979, The Evolution of Ocean-Floor Basaltic Magmas: in *Deep Drilling Results in the Atlantic Ocean: Ocean Crust*, p. 262-272.
- Shaw, H. R., 1972, Viscosities of Magmatic Silicate Liquids: An Empirical Method of Prediction: Am. J. Sci. 272, p. 870-893.
- Sinton, J. M., Diller, D. E. and Chen, C.-Y., 1987, Geology and Petrological Evolution of West Maui Volcano: in *Field Trip Guide to Maui* (J. M. Sinton, ed.), 83rd Ann. G.S.A. Cordilleran Section Meeting, Hilo, Hawaii, p. 13-30.
- Spengler, S. and Garcia, M. O., 1988, Geochemistry of Hawi Lavas, Kohala Volcano, Hawaii: Contrib. Mineral. Petrol., in press.
- Stearns, H. T., 1942, Origin of Haleakala Crater, Island of Maui, Hawaii: G.S.A. Bull. 53, p. 1-14.

- Stearns, H. T. and Macdonald, G. A., 1942, Geology and Ground-Water Resources of the Island of Maui, Hawaii: Hawaii Div. Hydrogr. Bull. 7, 344>p.
- Thompson, R. N., 1974, Primary Basalts and Magma Genesis. I. Skye, North-West Scotland: Contrib. Mineral. Petrol. 45, p. 317-341.
- Turner, J. S. and Gustafson, L. B., 1981, Fluid Motions and Compositional Gradients Produced by Crystallization or Melting at Vertical Boundaries: J. Volc. Geoth. Res. 11, p. 93-125.
- Turner, J. S., Huppert, H. E. and Sparks, R. S. J., 1983, An Experimental Investigation of Volatile Exsolution in Evolving Magma Chambers: J. Volc. Geoth. Res. 16, p. 263-277.
- Watson, E. B. and Green, T. H., 1981, Apatite/Liquid Partition Coefficients for the Rare Earth Elements and Strontium: Earth Planet. Sci. Lett. 56, p. 405-421.
- West, H. B. and Leeman, W. P., 1987, Isotopic Evolution of Lavas from Haleakala Crater, Hawaii: Earth Planet. Sci. Lett. 84, p. 211-225.
- West, H. B., Gerlach, D. C., Leeman, W. P. and Garcia, M. O., 1987, Isotopic Constraints on the Origin of Hawaiian Magmas from the Maui Volcanic Complex, Hawaii: Nature 330, p. 216-220.
- West, H. B., Garcia, M. O., Frey, F. A., and Kennedy, A., 1988, Evolution of Alkalic Cap Lavas: Mauna Kea Volcano, Hawaii: Contrib. Mineral. Petrol., in press.
- Wise, W. S., 1982, A Volume-Time Framework for the Evolution of Mauna Kea Volcano, Hawaii: EOS 62, p. 1137.
- Worner, G. and Wright, T. L., 1984, Evidence for Magma Mixing Within the Laacher See Magma Chamber (East Eifel, Germany): J. Volc. Geoth. Res. 22, p. 301-327.
- Wright, T. L., 1973, Magma Mixing as Illustrated by the 1959 Eruption, Kilauea Volcano, Hawaii: G.S.A. Bull. 84, p. 849-858.
- Wright, T. L. and Fiske, R. S., 1971, Origin of Differentiated and Hybrid Lavas of Kilauea Volcano, Hawaii: J. Petrol. 12, p. 1-56.

Table 1. Mineral modes of representative Kula Formation lavas from the Halemau section of Haleakala Crater. Modes are based on a minimum of 1000 counts.

	<u>Gm</u>	<u>Olivine</u>		<u>Cpx</u>		<u>Plagioclase</u>		<u>Magnetite</u>		<u>Amph</u>	<u>Apat</u>
		<u>ph</u>	<u>mph</u>	<u>ph</u>	<u>mph</u>	<u>ph</u>	<u>mph</u>	<u>ph</u>	<u>mph</u>	<u>ph+mph</u>	<u>mph</u>
HK-1	95.2	0.2	0.2	0.2	0.1	3.1	0.7	-	0.3	-	-
HK-13	97.0	<0.1	0.1	-	-	0.6	-	-	<0.1	-	-
HK-21	99.7	-	-	-	<0.1	0.2	<0.1	-	<0.1	<0.1	-
HK-22	99.3	-	<0.1	-	0.1	-	0.5	-	0.1	#	-
HK-23	99.3	-	0.1	-	-	-	0.4	-	0.2	#	-
HK-25	>99.9	-	<0.1	-	-	<0.1	<0.1	-	<0.1	-	-
HK-26	99.9	-	<0.1	-	<0.1	<0.1	<0.1	-	0.1	-	-
HK-27	99.2	-	0.3	-	<0.1	-	0.1	-	0.4	-	-
HK-28	90.1	<0.1	0.1	0.3	0.6	8.2	-	-	0.7	-	<0.1
HK-29	98.4	-	0.8	-	-	-	0.3	-	0.5	-	-
HK-33	95.1	-	0.5	-	-	1.6	2.2	-	0.6	-	-
HK-36	75.8	0.6	10.0	-	<0.1	0.1	10.6	-	2.9	-	-
HK-37	99.4	-	-	-	<0.1	-	0.5	-	0.1	-	-
HK-39	99.9	-	<0.1	-	<0.1	-	<0.1	-	0.1	-	-
HK-40	99.8	-	-	-	-	-	0.1	-	0.1	-	-
HK-43	99.2	0.15	-	0.1	-	0.3	0.2	-	0.05	-	<0.1
HK-44	94.7	0.1	0.6	-	0.3	1.0	2.3	0.1	0.9	-	-
HK-45	93.0	0.2	0.05	-	0.05	5.75	0.8	0.1	0.05	-	-
HK-49	86.1	0.1	0.5	-	-	6.2	6.5	0.1	0.5	-	-
HK-50	86.0	0.3	3.0	0.3	2.7	-	6.9	-	0.7	-	-
HK-58	68.3	6.4	3.8	20.0	0.7	-	-	-	0.8	-	-

+ phenocryst/microphenocryst distinction not clear.

occurs in groundmass.

* inclusion.

Table 2. Major and trace element data for Kula Formation lavas from the Halemau section of Haleakala Crater.

	Batch 1		Batch 2				Batch 3		
	HK-1	HK-2	HK-5	HK-6	HK-7	HK-8	HK-9	HK-10	HK-11
SiO ₂	46.97	47.15	47.50	47.39	47.15	47.36	47.18	46.32	47.12
Al ₂ O ₃	14.36	16.29	13.97	14.18	14.87	14.97	14.04	14.45	14.31
FeO*	14.02	11.38	13.86	13.70	12.94	12.81	13.77	13.08	12.75
MgO	5.25	5.96	5.20	5.28	5.86	5.54	5.19	6.67	6.55
CaO	10.51	12.20	10.41	10.56	11.46	11.49	10.45	11.10	11.23
Na ₂ O	2.96	2.45	3.13	3.02	2.61	2.73	3.36	3.04	2.79
K ₂ O	1.08	0.81	1.08	1.05	0.87	0.87	1.13	0.96	0.96
P ₂ O ₅	0.47	0.39	0.51	0.52	0.46	0.45	0.54	0.47	0.46
TiO ₂	3.94	3.02	3.90	3.86	3.35	3.36	3.91	3.49	3.43
MnO	0.22	0.16	0.20	0.21	0.19	0.20	0.21	0.21	0.19
B	-	-	-	-	-	-	-	-	-
K	8912	-	-	-	-	-	-	-	-
Cs	0.110	-	-	-	-	-	-	-	-
Rb(ID)	19.48	-	-	-	-	-	-	-	-
Rb(XRF)	19	10	19	17	11	12	19	17	17
Sr(ID)	677	-	-	-	-	-	-	-	-
Sr(XRF)	664	693	618	624	627	641	657	638	657
Ba(ID)	-	-	-	-	-	-	-	-	-
Ba(XRF)	410	312	372	408	347	308	391	350	333
La(XRF)	32	18	26	30	22	28	33	28	30
Ce(XRF)	58	58	63	64	60	65	68	65	61
Nd(XRF)	39	35	46	42	38	36	40	35	35
La	29.6	-	29.7	-	-	25.5	29.7	-	27.1
Ce	73.0	-	69.8	-	-	58.9	71.8	-	63.4
Nd	39.0	-	40.9	-	-	33.9	47.0	-	35.5
Sm	9.13	-	9.83	-	-	8.27	9.33	-	8.38
Eu	3.08	-	3.23	-	-	2.79	3.08	-	2.87
Tb	1.32	-	1.48	-	-	1.15	1.31	-	1.16
Ho	1.40	-	1.46	-	-	1.06	-	-	1.13
Yb	2.49	-	2.63	-	-	2.28	2.10	-	2.12
Lu	0.33	-	0.34	-	-	0.31	0.27	-	0.29
Y	34	27	34	35	30	30	33	29	30
Zr	269	210	282	281	228	230	276	235	237
Hf	6.9	-	7.2	-	-	5.9	6.6	-	6.2
Nb	31	24	31	32	26	27	34	28	29
Ta	2.0	-	2.3	-	-	2.0	2.4	-	2.1
Th	2.3	-	2.0	-	-	1.5	2.6	-	1.9
Ni	38	86	50	48	72	61	40	103	96
V	420	331	397	394	378	387	417	391	389
Cr(INAA)	15	-	31	-	-	96	13	-	178
Cr(XRF)	13	153	26	21	85	73	11	146	151
Sc(INAA)	26.3	-	27.5	-	-	27.0	24.2	-	27.1
Sc(XRF)	22	23	30	30	27	29	23	25	26
Co	61.1	-	57.4	-	-	55.4	56.7	-	59.3
Cu	78	91	68	78	77	89	66	83	86
Zn	119	92	122	117	105	105	119	111	109
Pb(ID)	1.916	-	-	-	-	-	-	-	-

Table 2 (cont). Major and trace element data for Kula Formation lavas from the Halemau section of Haleakala Crater.

	Batch 6		Batch 7A			Batch 7B			
	HK-23	HK-25	HK-26	HK-27	HK-28	HK-29	HK-30	HK-31	HK-32
SiO ₂	52.64	55.37	55.22	54.62	54.39	48.95	48.79	46.60	46.97
Al ₂ O ₃	16.38	17.18	17.14	17.26	15.94	16.14	16.27	15.32	15.32
FeO*	10.20	8.63	8.74	8.58	10.03	12.07	12.08	13.47	13.38
MgO	3.04	2.33	2.36	2.30	3.20	4.82	4.83	4.92	4.66
CaO	6.50	5.25	5.20	5.19	5.26	7.90	7.90	9.82	9.81
Na ₂ O	4.91	5.68	5.78	6.43	5.29	4.12	4.09	3.91	3.93
K ₂ O	2.37	2.58	2.59	2.56	2.50	1.35	1.36	1.28	1.28
P ₂ O ₅	0.94	0.64	0.65	0.70	0.31	0.61	0.61	0.55	0.53
TiO ₂	2.59	1.93	1.92	1.96	2.71	3.62	3.63	3.67	3.67
MnO	0.26	0.27	0.26	0.26	0.22	0.23	0.23	0.24	0.22
B	-	4.9	4.5	4.0	1.8	3.1	2.4	1.9	1.2
K	-	-	-	-	20944	-	-	-	-
Cs	-	-	-	-	1.598	-	-	-	-
Rb(ID)	-	-	-	-	55.85	-	-	-	-
Rb(XRF)	43	48	49	50	55	27	26	26	27
Sr(ID)	-	-	-	-	658	918	-	-	-
Sr(XRF)	955	963	938	931	649	906	918	781	783
Ba(ID)	-	-	-	-	-	-	-	-	-
Ba(XRF)	783	857	818	856	736	546	515	548	527
La(XRF)	61	61	63	64	57	37	34	35	31
Ce(XRF)	139	149	148	145	136	89	92	84	86
Nd(XRF)	79	76	82	75	67	46	47	48	43
La	59.2	-	68.3	-	61.4	38.1	38.0	35.4	35.5
Ce	137.0	-	144.4	-	134.4	87.3	86.6	79.7	80.0
Nd	63.0	-	77.6	-	63.7	45.5	53.0	39.8	46.0
Sm	16.20	-	16.90	-	14.75	9.85	9.78	9.58	9.24
Eu	5.03	-	5.15	-	3.27	3.12	3.24	3.01	2.91
Tb	2.00	-	2.30	-	1.58	1.19	1.26	1.47	1.13
Ho	-	-	2.53	-	1.70	2.30	-	1.90	-
Yb	4.10	-	4.68	-	4.81	2.59	2.60	2.27	3.00
Lu	0.47	-	0.64	-	0.65	0.36	0.29	0.34	0.26
Y	56	58	63	59	58	35	35	33	32
Zr	509	567	563	570	629	308	311	264	261
Hf	10.6	-	12.5	-	14.0	7.0	6.9	6.2	6.4
Nb	72	79	78	79	79	47	47	44	44
Ta	4.2	-	5.0	-	5.1	3.7	3.2	3.4	3.0
Th	4.6	-	4.5	-	6.0	3.2	3.5	3.1	3.0
Ni	3	3	4	4	3	3	2	9	5
V	56	27	25	27	116	177	176	337	340
Cr(INAA)	1	-	1	-	2	-	1	5	1
Cr(XRF)	1	3	-	3	-	1	1	2	-
Sc(INAA)	10.6	-	8.1	-	10.1	14.1	14.1	16.7	16.6
Sc(XRF)	10	8	7	7	9	14	9	13	14
Co	15.3	-	16.1	-	29.0	36.6	34.4	51.5	48.9
Cu	4	2	3	4	4	8	8	14	11
Zn	135	137	140	136	118	101	99	115	114
Pb(ID)	-	-	-	-	4.422	-	-	2.212	-

Table 2 (cont). Major and trace element data for Kula Formation lavas from the Halemau section of Haleakala Crater.

	Batch 7B				Batch 8				Batch 9
	HK-33	HK-34	HK-35	HK-36	HK-37	HK-38	HK-39	HK-40	HK-43
SiO ₂	46.83	44.97	44.82	44.83	52.30	51.68	50.48	50.50	53.86
Al ₂ O ₃	15.36	15.11	14.83	14.85	17.57	17.45	17.24	17.20	17.71
FeO*	13.53	13.98	14.14	14.16	9.24	9.42	10.00	10.09	8.40
MgO	4.82	6.56	6.82	6.76	2.90	3.06	3.78	3.70	2.33
CaO	10.09	10.40	10.65	10.69	6.58	6.85	7.42	7.47	5.35
Na ₂ O	3.49	3.36	3.10	3.09	5.49	5.53	5.11	5.01	6.59
K ₂ O	1.23	1.08	1.02	1.01	2.21	2.12	1.84	1.87	2.67
P ₂ O ₅	0.53	0.47	0.51	0.50	0.97	1.01	0.83	0.82	0.67
TiO ₂	3.67	3.62	3.67	3.67	2.32	2.46	2.88	2.92	2.01
MnO	0.23	0.22	0.21	0.21	0.26	0.25	0.25	0.25	0.26
B	1.6	1.1	2.4	1.8	4.8	-	-	-	-
K	-	-	-	-	18284	-	-	15443	-
Cs	-	-	-	-	0.557	-	-	0.434	-
Rb(ID)	-	-	-	-	50.34	-	-	41.97	-
Rb(XRF)	27	25	21	21	49	46	39	38	60
Sr(ID)	-	-	-	-	1016	-	-	1029	-
Sr(XRF)	815	695	719	760	1013	956	1014	984	740
Ba(ID)	-	-	-	-	-	-	-	-	-
Ba(XRF)	516	407	451	453	849	770	722	664	971
La(XRF)	34	29	35	25	57	59	48	51	66
Ce(XRF)	70	68	71	76	139	139	121	123	144
Nd(XRF)	40	34	36	33	66	64	63	58	64
La	35.2	29.7	29.1	28.9	64.4	59.4	52.5	52.0	62.5
Ce	78.3	68.4	68.2	67.6	141.1	131.0	118.5	113.8	139.6
Nd	40.3	36.0	40.0	35.2	65.0	69.0	56.1	56.0	63.5
Sm	9.08	8.18	8.24	7.92	13.15	12.80	11.82	11.81	13.31
Eu	2.98	2.57	2.72	2.69	3.97	3.83	3.55	3.78	3.93
Tb	1.62	1.12	1.05	0.84	1.37	1.16	1.37	1.59	1.50
Ho	1.60	-	-	1.37	1.50	-	1.80	1.48	2.10
Yb	2.36	1.80	1.60	2.02	3.21	2.20	3.01	2.86	3.75
Lu	0.36	0.33	0.24	0.31	0.45	0.42	0.40	0.41	0.49
Y	31	29	28	28	43	41	38	38	46
Zr	259	227	222	226	445	408	369	353	484
Hf	6.2	5.7	5.2	5.2	9.4	8.4	8.0	8.2	10.0
Nb	43	36	36	37	72	67	63	61	83
Ta	3.2	2.7	2.6	2.6	4.5	4.2	3.7	4.1	4.9
Th	2.6	2.8	2.5	2.6	6.0	5.3	4.8	3.9	6.3
Ni	8	54	57	61	4	4	3	3	4
V	345	407	420	409	58	72	103	105	34
Cr(INAA)	4	42	60	61	-	1	2	1	1
Cr(XRF)	1	34	54	50	2	1	2	2	1
Sc(INAA)	17.2	23.5	24.4	24.4	5.1	5.7	7.7	8.2	4.6
Sc(XRF)	13	20	26	24	3	6	7	7	3
Co	50.8	61.7	62.5	65.5	18.2	19.8	22.8	24.3	15.7
Cu	17	53	51	55	7	4	7	6	5
Zn	116	112	111	111	107	110	110	107	128
Pb(ID)	2.078	-	-	-	4.233	-	-	3.243	4.378

Table 2 (cont). Major and trace element data for Kula Formation lavas from the Halemau section of Haleakala Crater.

	Batch 9				Batch 10			Batch 11	
	HK-44	HK-45	HK-49	HK-50	HK-51	HK-52	HK-53	HK-54	HK-55
SiO ₂	50.08	46.88	46.63	43.70	49.64	49.32	47.45	49.32	46.66
Al ₂ O ₃	16.01	15.23	16.14	14.35	16.79	16.90	16.45	16.04	15.67
FeO*	10.81	13.20	12.67	13.88	10.34	10.40	11.64	11.73	13.83
MgO	3.66	4.92	4.88	6.31	3.44	3.58	4.34	3.54	5.04
CaO	7.81	10.24	10.48	13.25	8.18	8.27	9.92	8.33	10.06
Na ₂ O	5.19	3.65	3.68	2.92	5.32	5.25	4.36	4.96	3.26
K ₂ O	1.85	1.16	1.02	1.00	2.15	2.13	1.53	1.69	1.05
P ₂ O ₅	1.01	0.51	0.51	0.41	0.72	0.71	0.63	0.77	0.49
TiO ₂	3.15	3.75	3.58	3.76	3.02	3.04	3.18	3.18	3.48
MnO	0.25	0.23	0.22	0.18	0.24	0.25	0.22	0.25	0.23
B	-	-	-	1.8	-	-	-	-	-
K	-	-	-	8415	-	-	-	-	-
Cs	-	-	-	0.242	-	-	-	-	-
Rb(ID)	-	-	-	22.69	-	-	-	-	-
Rb(XRF)	39	24	20	21	47	48	34	37	21
Sr(ID)	-	-	-	719	-	-	-	-	-
Sr(XRF)	846	787	853	697	886	939	876	734	744
Ba(ID)	-	-	-	-	-	-	-	-	-
Ba(XRF)	729	535	437	454	747	805	611	673	474
La(XRF)	53	31	26	22	53	51	39	45	32
Ce(XRF)	125	82	72	60	119	129	95	108	74
Nd(XRF)	62	42	36	31	56	63	47	54	38
La	52.5	33.3	29.6	27.4	52.8	52.5	40.6	48.2	30.7
Ce	121.0	74.8	67.5	63.5	116.0	113.0	93.2	104.0	70.5
Nd	67.0	38.8	38.0	32.9	-	-	43.0	-	43.0
Sm	13.20	9.21	8.15	7.66	11.90	12.00	9.93	12.00	8.23
Eu	4.02	2.86	2.64	2.49	3.58	3.62	3.09	3.69	2.74
Tb	1.45	0.88	0.99	0.91	1.16	1.42	1.15	1.52	1.21
Ho	-	1.20	-	1.06	-	-	-	-	-
Yb	2.70	2.39	2.40	1.50	3.10	3.70	2.40	3.00	1.60
Lu	0.46	0.31	0.31	0.21	0.36	0.35	0.25	0.43	0.27
Y	44	31	29	24	40	39	33	43	29
Zr	366	243	213	202	380	384	293	346	230
Hf	7.4	5.9	5.1	5.2	7.9	7.8	6.3	7.5	5.6
Nb	63	38	35	33	67	69	50	57	37
Ta	3.9	2.6	2.6	2.3	4.3	4.3	3.5	3.9	2.6
Th	4.5	2.8	2.7	2.3	5.4	4.8	3.8	4.6	2.5
Ni	4	11	7	64	4	3	7	4	12
V	133	334	286	548	174	179	264	166	319
Cr(INAA)	1	8	13	30	2	2	9	2	9
Cr(XRF)	1	4	13	25	-	2	5	1	9
Sc(INAA)	10.1	17.5	15.4	27.5	5.9	6.2	13.9	11.2	16.9
Sc(XRF)	12	15	15	24	5	5	15	11	15
Co	28.7	48.3	44.7	66.4	29.8	27.9	41.6	34.0	53.6
Cu	12	18	12	120	4	8	18	10	21
Zn	125	124	102	110	126	126	111	122	113
Pb(ID)	-	-	-	1.800	3.302	-	-	-	-

Table 2 (cont). Major and trace element data for Kula Formation lavas from the Halemauu section of Haleakala Crater.

	Batch 12			Batch 13	
	HK-56	HK-57	HK-58	HK-59	HK-60
SiO ₂	50.36	43.54	44.22	49.53	45.41
Al ₂ O ₃	17.46	14.64	11.51	18.07	15.09
FeO*	10.43	14.85	13.33	10.42	13.82
MgO	3.54	7.13	11.44	2.79	6.32
CaO	7.21	12.12	12.65	7.59	10.23
Na ₂ O	5.14	2.57	2.16	5.89	3.53
K ₂ O	1.89	0.81	0.77	2.02	1.19
P ₂ O ₅	0.74	0.43	0.44	0.82	0.53
TiO ₂	2.82	3.48	3.07	2.45	3.43
MnO	0.25	0.20	0.19	0.25	0.21
B	-	-	-	-	-
K	-	-	-	1284	-
Cs	-	-	-	0.573	-
Rb(ID)	-	-	-	52.20	-
Rb(XRF)	42	18	28	50	28
Sr(ID)	-	-	-	1284	-
Sr(XRF)	1092	665	580	1260	747
Ba(ID)	-	-	-	865	-
Ba(XRF)	829	437	503	941	531
La(XRF)	49	19	22	47	25
Ce(XRF)	117	73	49	125	75
Nd(XRF)	55	36	28	55	34
La	48.1	26.1	25.8	55.9	-
Ce	104.0	60.1	58.5	126.2	-
Nd	47.0	33.0	29.8	55.2	-
Sm	10.90	7.37	6.81	11.36	-
Eu	3.42	2.46	2.38	3.36	-
Tb	1.18	1.28	0.66	1.28	-
Ho	-	-	0.96	1.00	-
Yb	2.70	1.80	1.34	2.09	-
Lu	0.28	0.27	0.17	0.30	-
Y	36	26	22	31	27
Zr	330	174	174	325	223
Hf	6.9	4.5	4.6	6.5	-
Nb	61	29	31	70	39
Ta	3.9	2.3	2.3	4.5	-
Th	4.6	2.5	2.5	5.9	-
Ni	3	59	217	9	60
V	70	503	408	66	373
Cr(INAA)	4	76	610	18	-
Cr(XRF)	1	67	552	9	63
Sc(INAA)	6.4	28.5	35.1	4.1	-
Sc(XRF)	4	26	32	5	19
Co	22.1	73.2	82.3	28.4	-
Cu	7	58	102	14	65
Zn	114	105	96	124	111
Pb(ID)	-	-	2.054	3.296	-

Table 3. Range in rock compositions in magma batches from the Halemauu section of Haleakala Crater. Initial rock refers to initial rock type in the magma batch (lowermost, stratigraphically) and final rock refers to the final rock type in the magma batch (uppermost, stratigraphically).

<u>Batch</u>	<u># Samples</u>	<u>Initial rock</u>	<u>Final rock</u>
1	2	mafic hawaiite	alkalic basalt
2	4	mafic hawaiite	alkalic basalt
3	3	mafic hawaiite	alkalic basalt
4	1	hawaiite	-
5	6	hawaiite	hawaiite
6	3	mugearite	mugearite
7	12	mugearite	alkalic basalt
8	4	mugearite	hawaiite
9	5	mugearite	basanitoid
10	3	hawaiite	hawaiite
11	2	hawaiite	alkalic basalt
12	3	hawaiite	ankaramite
13	2	nepheline hawaiite	basanitoid

Summary of total number of batches exhibiting the observed variations in rock type for the Halemauu section.

<u># batches</u>	<u>Rock Type Variation</u>
6	hawaiite - alkalic basalt/basanitoid/ankaramite
2	mugearite - alkalic basalt/basanitoid/ankaramite
1	mugearite - hawaiite
2	hawaiite - hawaiite
1	mugearite - mugearite

Table 4. Parent-daughter lava compositions and mineral compositions used in least-squares calculation for the transition from batch 12 to 13, given in Table 5.

	HK-58	Ol	Plag	Cpx	Mt	HK-59
SiO ₂	43.61	40.01	46.80	47.70	-	48.99
Al ₂ O ₃	11.35	-	32.50	6.82	1.56	17.87
FeO	13.33	14.36	0.66	7.45	72.80	10.42
MgO	11.28	45.63	-	13.34	1.40	2.76
CaO	12.47	-	17.50	21.35	-	7.51
Na ₂ O	2.13	-	1.70	0.65	-	5.83
K ₂ O	0.76	-	0.10	0.03	-	2.00
P ₂ O ₅	0.43	-	-	-	-	0.81
TiO ₂	3.03	-	-	1.89	19.90	2.42
MnO	0.19	-	-	0.16	1.50	0.25
Cr ₂ O ₃	-	-	-	0.23	0.01	-

-
- Ol Calculated composition of olivine in equilibrium with HK-58 (Fo 85).
 KD(Fe-Mg) = 0.30 (Roeder and Emslie, 1970).
- Plag Plagioclase phenocryst in alkalic basalt from the Halemau section of
 Haleakala Crater (sample C-140; Macdonald and Powers, 1968).
- Cpx Clinopyroxene phenocryst in picritic basalt from upper west wall of
 Haleakala Crater (sample 7; Macdonald and Powers, 1946; table 1).
- Mt Magnetite from Kohala benmoreite (sample 62-1; Macdonald and Katsura,
 1964; analysis from BVSP volume).
-

Table 5. Results of major element least-squares modeling for the transition from batch 12 to 13. Parental magma = HK-58, daughter = HK-59. Also shown are observed and calculated concentrations for selected trace elements. Trace element mineral partition coefficients are taken from LeRoex and Erlank (1982). Compositions of subtracted mineral phases are given in Table 4.

	<u>Obs</u>	<u>Calc</u>	<u>Residuals</u>	<u>Component</u>	<u>Propor.</u>
SiO ₂	48.99	49.08	-0.08936	HK-58	1.00000
Al ₂ O ₃	17.87	17.84	0.02904	<i>Olivine</i>	0.10691
FeO	10.42	10.41	0.01190	<i>Plag</i>	0.07775
MgO	2.76	2.68	0.07462	<i>Cpx</i>	0.40532
CaO	7.51	7.38	0.12551	<i>Mt</i>	0.07220
Na ₂ O	5.83	5.20	-0.62117	HK-59	0.33782
K ₂ O	2.00	2.22	-0.22078		
TiO ₂	2.42	2.47	-0.05106	$\Sigma R^2 = 0.46749$	
La	55.9	69.8			
Sm	11.36	15.34			
Yb	2.09	2.61			
Ba	941	1473			
Zr	325	431			
Nb	70	82			
Y	31	38			
Sc	4.1	2.5			

Table 6. Parent-daughter lava compositions and mineral compositions used in least-squares calculation for the transition from batch 9 to 10, given in Table 7.

	HK-50	Ol	Plag	Cpx	Mt	Ap	HK-51
SiO ₂	43.07	38.74	46.80	47.70	-	-	49.10
Al ₂ O ₃	14.14	-	32.50	6.82	1.56	-	16.61
FeO	13.88	21.15	0.66	7.45	72.80	0.21	10.34
MgO	6.22	40.10	-	13.34	1.40	0.54	3.40
CaO	13.06	-	17.50	21.35	-	52.40	8.09
Na ₂ O	2.88	-	1.70	0.65	-	-	5.26
K ₂ O	0.99	-	0.10	0.03	-	-	2.13
P ₂ O ₅	0.40	-	-	-	-	40.98	0.71
TiO ₂	3.71	-	-	1.89	19.90	-	2.99
MnO	0.18	-	-	0.16	1.50	1.52	0.24
Cr ₂ O ₃	-	-	-	0.23	0.01	-	-

Ol Olivine Fo 70.

Plag Plagioclase phenocryst in alkalic basalt from the Halemau section of Haleakala Crater (sample C-140; Macdonald and Powers, 1968).

Cpx Clinopyroxene phenocryst in picritic basalt from upper west wall of Haleakala Crater (sample 7; Macdonald and Powers, 1946; table 1).

Mt Magnetite from Kohala benmoreite (sample 62-1; Macdonald and Katsura, 1964; analysis from BVSP volume).

Ap Apatite (Deer et al., 1966).

Table 7. Results of major element least-squares modeling for the transition from batch 9 to 10. Parental magma = HK-50, daughter = HK-51. Also shown are observed and calculated concentrations for selected trace elements. Trace element mineral partition coefficients are taken from LeRoex and Erlank (1982). Compositions of subtracted mineral phases are given in Table 6.

	<u>Obs</u>	<u>Calc</u>	<u>Residuals</u>	<u>Component</u>	<u>Propor.</u>
SiO ₂	49.10	49.08	0.10848	HK-50	1.00000
Al ₂ O ₃	16.61	16.66	-0.04918	<i>Olivine</i>	0.00966
FeO	10.34	10.35	-0.01343	<i>Plag</i>	0.14787
MgO	3.40	3.50	-0.09772	<i>Cpx</i>	0.31632
CaO	8.09	8.24	-0.15166	<i>Mt</i>	0.09407
Na ₂ O	5.26	5.73	-0.47082	<i>Apatite</i>	0.00453
K ₂ O	2.13	2.28	-0.14983	HK-51	0.42755
P ₂ O ₅	0.71	0.52	0.19528		
TiO ₂	2.99	2.93	0.05984	$\Sigma R^2 = 0.33275$	
La	52.8	53.8			
Sm	11.90	12.64			
Yb	3.10	2.41			
Ba	747	1053			
Zr	380	418			
Nb	67	70			
Y	40	33			
Sc	5.9	3.9			

Table 8. Parent-daughter lava compositions and mineral compositions used in least-squares calculation for the transition from batch 7 to 8, given in Table 9.

	HK-36	Ol	Plag	Cpx	Mt	Ap	HK-37
SiO ₂	44.17	37.42	47.40	47.70	-	-	51.80
Al ₂ O ₃	14.63	-	32.80	6.82	1.44	-	17.40
FeO	14.16	28.20	0.59	7.45	68.30	0.21	9.24
MgO	6.66	34.37	-	13.34	3.18	0.54	2.87
CaO	10.53	-	16.50	21.35	-	52.40	6.52
Na ₂ O	3.04	-	2.10	0.65	-	-	5.44
K ₂ O	1.00	-	0.10	0.03	-	-	2.19
P ₂ O ₅	0.49	-	-	-	-	40.98	0.96
TiO ₂	3.62	-	-	1.89	22.70	-	2.30
MnO	0.21	-	-	0.16	0.76	1.52	0.26
Cr ₂ O ₃	-	-	-	0.23	1.56	-	-

Ol Olivine Fo 60.

Plag Plagioclase phenocryst in hawaiiite from the Halemau section of Haleakala Crater (sample C-137; Macdonald and Powers, 1968).

Cpx Clinopyroxene phenocryst in picritic basalt from upper west wall of Haleakala Crater (sample 7; Macdonald and Powers, 1946; table 1).

Mt Magnetite from Hualalai alkalic basalt (sample HAW-11; analysis from BVSP volume).

Ap Apatite (Deer et al., 1966).

Table 9. Results of major element least-squares modeling for the transition from batch 7 to 8. Parental magma = HK-36, daughter = HK-37. Also shown are observed and calculated concentrations for selected trace elements. Trace element mineral partition coefficients are taken from LeRoex and Erlank (1982). Compositions of subtracted mineral phases are given in Table 8.

	<u>Obs</u>	<u>Calc</u>	<u>Residuals</u>	<u>Component</u>	<u>Propor.</u>
SiO ₂	51.80	51.78	0.01603	HK-36	1.00000
Al ₂ O ₃	17.40	17.40	0.00327	<i>Olivine</i>	0.05607
FeO	9.24	9.27	-0.02740	<i>Plag</i>	0.14830
MgO	2.87	2.87	0.00504	<i>Cpx</i>	0.23279
CaO	6.52	6.55	-0.03328	<i>Mt</i>	0.09477
Na ₂ O	5.44	5.58	-0.14761	<i>Apatite</i>	0.00167
K ₂ O	2.19	2.11	0.08327	HK-37	0.46641
P ₂ O ₅	0.96	0.92	0.04262		
TiO ₂	2.30	2.22	0.08154	$\Sigma R^2 = 0.03934$	
La	64.4	56.1			
Sm	13.15	13.81			
Yb	3.21	3.37			
Ba	849	964			
Zr	445	434			
Nb	72	73			
Y	43	42			
Sc	5.1	6.3			

Table 10a. Parameters for open and closed system models for batch-end lava HK-2 (batch 1), calculated after the method of Nielsen (1988). 0-0-0 models represent perfect fractional crystallization of a closed system magma chamber. 1-0-0 models represent a steady-state mass, open system magma chamber undergoing continual recharge and fractional crystallization of the calculated liquidus phase assemblage. Listed are liquidus temperatures and corresponding fractionating phase assemblages and phase proportions for each change in phase assemblage. Cryst = degree of crystallization of the system. Final temperature and phase assemblage listed for each model corresponds to liquid compositions with ~ 90 ppm Nb.

Model	T (C)	Phase	Propor	Cryst	Nb (ppm)
<u>HK-2:</u>					
0-0-0	1209.5	Sp	0.0003	0.0003	24.0
	1185.5	Plag	0.0400	0.0403	25.0
	1171.9	Plag	0.0400	0.0806	26.0
		Sp	0.0003		
	1153.3	Cpx	0.0220	0.1606	28.3
		Plag	0.0180		
	1145.0	Cpx	0.0220	0.2408	31.1
		Plag	0.0180		
		Sp	0.0002		
	1108.4	Opx	0.0100	0.7339	85.3
		Cpx	0.0080		
		Plag	0.0180		
		Sp	0.0056		
1-0-0	1209.5	Sp	0.0003	0.0003	24.0
	1186.0	Plag	0.0400	0.0403	24.9
	1174.0	Plag	0.0400	0.0806	25.8
		Sp	0.0003		
	1153.0	Cpx	0.0120	0.1606	27.7
		Plag	0.0280		
	1147.6	Cpx	0.0180	0.2808	30.3
		Plag	0.0220		
		Sp	0.0002		
	*1120.2	Opx	0.0020	2.0309	65.8
		Cpx	0.0140		
		Plag	0.0200		
		Sp	0.0041		
	*1106.8	Opx	0.0040	3.4442	90.2
		Cpx	0.0140		
		Plag	0.0200		
		Sp	0.0038		

* From 1120.2 C to 1106.8 C, Opx + Cpx + Plag + Sp is the dominant phase assemblage but periodic transitions to a Cpx + Plag + Sp also occur.

Table 10b. Parameters for open and closed system models for batch-end lava HK-36 (batch 7), calculated after the method of Nielsen (1988). See table 4a for explanation of headings.

Model	T (C)	Phase	Proport	Cryst	Nb (ppm)
<u>HK-36:</u>					
0-0-0	1200	Sp	0.0003	0.0003	37.0
		Oliv	0.0080	0.0410	38.5
	1140.1	Cpx	0.0140		
		Plag	0.0140		
		Sp	0.0047		
		Cpx	0.0180	0.1235	42.0
	1138.4	Plag	0.0160		
		Sp	0.0072		
		Oliv	0.0020	0.6167	94.2
		Cpx	0.0160		
		Plag	0.0180		
		Sp	0.0056		
1-0-0	1200	Sp	0.0003	0.0003	37.0
		Oliv	0.0100	0.0410	38.4
	*1140.5	Cpx	0.0100		
		Plag	0.0160		
		Sp	0.0047		
		Cpx	0.0180	0.0815	39.8
	*1139.3	Plag	0.0160		
		Sp	0.0065		
		Cpx	0.0180	1.7048	90.2
		Plag	0.0160		
		Sp	0.0057		

* From 1140.5 C to the final liquidus temperature listed (1111.8 C), the equilibrium phase assemblage alternates between Oliv + Cpx + Plag + Sp and Cpx + Plag + Sp.

Table 10c. Parameters for open and closed system models for batch-end lava HK-50 (batch 9), calculated after the method of Nielsen (1988). See table 4a for explanation of headings.

Model	T (C)	Phase	Propor	Cryst	Nb (ppm)
<u>HK-50:</u>					
0-0-0	1150	Cpx	0.0020	0.0020	33.1
	1143.8	Cpx	0.0280	0.0420	34.4
		Plag	0.0120		
	1136.9	Cpx	0.0220	0.1228	37.3
		Plag	0.0180		
		Sp	0.0008		
	1103.4	Cpx	0.0160	0.6535	92.7
		Plag	0.0180		
		Sp	0.0064		
1-0-0	1150	Cpx	0.0020	0.0020	33.1
	1145.3	Cpx	0.0180	0.0220	33.7
		Plag	0.0020		
	1137.9	Cpx	0.0100	0.1222	36.8
		Plag	0.0100		
		Sp	0.0002		
	1103.9	Cpx	0.0080	2.0303	90.4
		Plag	0.0100		
		Sp	0.0027		

Table 10d. Parameters for open and closed system models for batch-end lava HK-58 (batch 12), calculated after the method of Nielsen (1988). See table 4a for explanation of headings.

Model	T (C)	Phase	Proport	Cryst	Nb (ppm)
<u>HK-58:</u>					
0-0-0	1300	Oliv	0.0020	0.0020	31.0
	1237.6	Oliv	0.0400	0.0424	32.2
		Sp	0.0004		
	1199.2	Oliv	0.0380	0.0831	33.5
		Cpx	0.0020		
		Sp	0.0007		
	1189.5	Cpx	0.0400	0.1233	34.9
		Sp	0.0003		
	1154.9	Cpx	0.0400	0.2436	40.0
	1142.5	Cpx	0.0380	0.2838	42.1
		Plag	0.0020		
		Sp	0.0002		
	1127.5	Oliv	0.0020	0.5730	69.7
		Cpx	0.0160		
		Plag	0.0160		
		Sp	0.0072		
	1123.6	Cpx	0.0180	0.6150	77.1
		Plag	0.0180		
		Sp	0.0060		
	1114.1	Oliv	0.0020	0.6958	97.2
		Cpx	0.0140		
		Plag	0.0180		
		Sp	0.0064		
1-0-0	1300	Oliv	0.0020	0.0020	31.0
	1239.0	Oliv	0.0400	0.0424	32.2
		Sp	0.0004		
	1192.6	Oliv	0.0080	0.1234	34.4
		Cpx	0.0320		
		Sp	0.0003		
	1142.8	Oliv	0.0020	0.4059	42.6
		Cpx	0.0360		
		Plag	0.0020		
		Sp	0.0009		
	1119.6	Oliv	0.0040	2.2255	90.5
		Cpx	0.0220		
		Plag	0.0100		
		Sp	0.0041		

Table 11. Parameters for open system models for batch-end lava HK-50 from batch 9 undergoing periodic recharge combined with assimilation of HK-43 composition material. Calculations were made using the method of Nielsen (1988). Models represent the case of a steady-state mass magma chamber undergoing both recharge and assimilation, combined with continuous fractional crystallization of the calculated liquidus phase assemblage. The .5-.5-0 model is for equal amounts of recharge and assimilation, and the .25-.75-0 model is for a 3:1 dominance of assimilation over recharge rate. Listed are liquidus temperatures and corresponding fractionating phase assemblages and phase proportions for each change in phase assemblage. Cryst = degree of crystallization of the system. Final temperature and phase assemblage listed for each model corresponds to liquid compositions with ~ 90 ppm Nb.

<u>Model</u>	<u>T (C)</u>	<u>Phase</u>	<u>Propor</u>	<u>Cryst</u>	<u>Nb (ppm)</u>
<u>.5-.5-0:</u>					
	1150	Cpx	0.0020	0.0020	33.1
	1143.3	Cpx	0.0260	0.0420	35.3
		Plag	0.0140		
	1136.5	Cpx	0.0180	0.1221	39.7
		Plag	0.0200		
		Sp	0.0021		
	1106.4	Cpx	0.0160	1.1054	90.4
		Plag	0.0180		
		Sp	0.0060		
<u>.25-.75-0:</u>					
	1150	Cpx	0.0020	0.0020	33.1
	1142.8	Cpx	0.0260	0.0420	35.8
		Plag	0.0140		
	1135.6	Cpx	0.0200	0.1239	41.3
		Plag	0.0180		
		Sp	0.0039		
	1106.4	Cpx	0.0160	0.9052	91.0
		Plag	0.0180		
		Sp	0.0069		

Table 12. Comparison of selected major and trace element ranges and averages for lavas from magma batches 1-7A and magma batches 7B-13 containing greater than 5 wt.% MgO. All lavas are from the Halemauu section of Haleakala Crater.

	<i>Batches 1 to 7A</i>		<i>Batches 7B to 13</i>	
	<u>range</u>	<u>avg.</u>	<u>range</u>	<u>avg.</u>
Mg#	42.6-50.9	46.2	47.4-63.0	49.3
Al ₂ O ₃	13.97-16.29	14.60	11.51-15.67	14.51
Sc	22-30	26.1	19-32	23.3
Nb	24-34	29.1	29-39	34.8
Zr	210-282	229	174-230	210
Zr/Nb	8.12-9.10	8.59	5.61-6.31	6.03
Ba/Y	10.27-12.07	11.45	14.03-22.86	17.62
⁸⁷ Sr/ ⁸⁶ Sr*	0.70334-0.70340	0.70337	0.70308-0.70334	0.70322

* Range and average refer to all lavas from the Halemauu section of Haleakala Crater, not just those with greater than 5 wt.% MgO.

FIGURE CAPTIONS

Figure 1. Simplified Map of Haleakala Crater and position relative to the island of Maui (taken from West and Leeman, 1987; after Macdonald (1978). Shaded areas represent Kula Formation lavas. Solid areas represent Kumuiliahi Formation lavas. hachured areas represent Hana Formation lava flows and cinder cones. Halemauu Trail section is indicated by solid line located at the northwest wall of Haleakala Crater.

Figure 2. Silica-alkalies diagram for Kula Formation lavas from Haleakala Crater. Diagonal line represents the division between alkalic and tholeiitic lavas (Macdonald and Katsura, 1964). Shown for comparison are fields for Honomanu, Kumuiliahi, and Hana Formation lavas from Haleakala. Open cross represents the Holua trachyte, exposed at the base of the northwest wall of Haleakala Crater and mapped as part of the Kula Formation (Macdonald, 1978). Hana, Kumuiliahi, and Honomanu data from West and Leeman (in prep.). Additional Honomanu data from Macdonald and Powers (1968) and Chen (1982).

Figure 3. Major and trace element compositions and ratios versus relative stratigraphic position for Kula Formation lavas from the Halemauu section of Haleakala Crater. (a) K_2O , (b) P_2O_5 , (c) SiO_2 , (d) MgO , (e) Nb, (f) Sc [XRF data], (g) Ni, (h) V, (i) Al_2O_3/CaO , (j) Al_2O_3/TiO_2 , (k) La/Sm. Vertical lines delineate geochemical discontinuities that define individual magma batches. Within batches (intrabatch), incompatible element abundances progressively decrease upsection, whereas compatible element abundances progressively increase upsection. Between batches (interbatch), there are abrupt increases in incompatible elements and abrupt decreases in compatible elements.

Figure 4. (a) to (m) Mo'o (Mantle Overview Order) diagrams for lavas from individual magma batches from the Halemauu section of Haleakala Crater. (n) Mo'o diagram for

samples HK-46, the stratigraphically lowermost exposed lava in Haleakala Crater [south wall], and HK-48, an amphibole-bearing mugearite collected from Pakaoao on the top of the southwest wall of Haleakala Crater. Range for Haleakala Crater Halemauu section lavas shown for comparison. Data for HK-46 and HK-48 from West and Leeman (in prep.). Elements are normalized to CI chondrite abundances with the exception of Rb, K, and P which are normalized to estimated primitive mantle abundances. The relative order of elements corresponds to the order of enrichment observed for a typical Kilauea tholeiite (U.S.G.S. Rock Standard, BHVO-1; see West and Leeman, in prep.). The relative trace element compositions for individual batches varies significantly. Batches from the upper part of the section (batches 7 to 13) tend to span larger ranges than those from the lower part of the section (batches 1 to 6).

Figure 5. (a) $^{87}\text{Sr}/^{86}\text{Sr}$, (b) $^{206}\text{Pb}/^{204}\text{Pb}$, and Zr/Nb ratios versus relative stratigraphic position for Kula Formation lavas from the Halemauu section of Haleakala Crater. Isotopic data from West and Leeman (1987). Although Sr and Pb isotopic compositions and Zr/Nb ratios (which correlate with isotope ratios; West and Leeman, in prep.) are correlated with relative stratigraphic position, interbatch compositional differences are generally within analytical error. Intrabatch variations are generally not systematic nor are they consistent from batch to batch. Thus, compositional variations associated with magma batches are not controlled by source processes but rather are magmatic in origin.

Figure 6. Nb normalized enrichment factors for six interbatch transitions from the Halemauu section of Haleakala Crater. Compositions of incipient batch lavas are normalized to Nb and divided by Nb normalized compositions of primitive batch-end lavas of the previous batch. Fractional crystallization should produce enrichment factors of approximately 1.0 for highly incompatible trace elements (Rb, K, Th, La, Ce). The degree of negative deviation from unity reflects the bulk partition coefficient of the particular element relative to Nb. Moderately incompatible elements that are slightly

more compatible than Nb will fall just below unity (Zr, Sm, Ba, Hf), whereas elements that are only slightly compatible (Y, Yb) will deviate more strongly. Elements whose bulk partition coefficients are relatively high (> 1.0) will exhibit strong negative deviations from unity. For interbatch transitions to be consistent with an origin by fractional crystallization, the trace element patterns of incipient batch lavas should have overall negative slopes, enrichment factors < 1.0 for most incompatible elements, and negative deviations for more compatible elements residing in the fractionating phase assemblage. See text for discussion of individual interbatch transitions.

Figure 7. Nb versus (a) La/Sm and (b) La/Yb for calculated [black sun = Calc] and observed [filled star = HK-37] daughter magma compositions, based on least-squares major element modeling for the transition from batch 7 to 8. The large open star symbol represents the batch 7 alkalic basalt parent magma [HK-36]. Results are given in Table 9. Also shown are fractionation trends for the observed mineral phases; small dots on the curves refer to values of $(1 - F)$ [0.01, 0.05, 0.10, 0.20,.....]

Figure 8. (a) Enrichment factors and (b) Nb normalized enrichment factors for selected batch 7 lavas normalized to HK-36, the primitive batch-end lava from batch 7. Symbols as follows: five-pointed star - HK-26, six-pointed star - HK-28, square - HK-29, triangle - HK-31, circle - HK-33. HK-26 and HK-28 belong to batch 7A and are considerably more evolved than overlying batch 7B lavas. Crossing patterns for batch 7A lavas in (a) indicates that these magmas could not have been produced by mixing of an HK-36 composition parental magma with a more evolved composition. Similarly, batch 7B lavas could not have been produced by mixing of HK-36 magma with batch 7A composition magmas. (b) illustrates the anomalous enrichments in Rb, K, Zr, Hf, and Yb over Nb for batch 7A lavas, inconsistent with either a mixing or fractionation origin for these magmas. Trace element patterns for batch 7B lavas are also incompatible both with mixing between batch 7A and HK-36 composition magmas and with fractional

crystallization from an HK-36 parental magma.

Figure 9. (a) Enrichment Factors and (b) Nb normalized enrichment factors for lavas from batch 9 normalized to HK-50, the primitive batch-end lavas from batch 9. Symbols as follows: star - HK-43, square - HK-44, triangle - HK-45, circle - HK-49. Anomalously high absolute (a) and relative [to Nb] (b) enrichments in elements that are only slightly compatible (e.g. Y, HREE) are inconsistent with derivation of any batch 9 lava by fractional crystallization involving any observed phase of an HK-50 composition parental magma. Trace element patterns (b) suggest that simple mixing between HK-43 and HK-50 composition magmas could not have produced the compositions observed for other batch 9 lavas.

Figure 10. (a) Enrichment Factors and (b) Nb normalized enrichment factors for lavas from batch 12 normalized to HK-58, the primitive batch-end lavas from batch 12. Symbols as follows: triangle - HK-56, circle - HK-57. Trace element systematics are inconsistent with derivation of batch 12 lavas from an HK-58 parent magma composition by fractional crystallization. Similarly, it is unlikely that either HK-56 or HK-57 represent simple mixes between HK-58 mafic magma and evolved magma.

Figure 11. Nb versus (a) Ni, (b) Sc, (c) MgO, (d) SiO₂, and (e) Al₂O₃ for open and closed system fractionation models for lavas from Haleakala Crater. Four parental magma starting compositions were used, representing primitive batch-end lava compositions from batches 1 (HK-2), 7 (HK-36), 9 (HK-50), and 12 (HK-58). Equilibrium phase assemblages and liquid lines of descent were calculated using the method of Nielsen (1988). Solid curves represent steady-state models (the 1-0-0 model of Nielsen, 1988) in which recharge is equal to fractionation. Dashed curves represent perfect fractional crystallization (the 0-0-0 model of Nielsen, 1988).

Figure 12. Nb versus (a) Sc, (b) MgO, (c) SiO₂, and (d) Al₂O₃ for open and closed system fractionation models for HK-50, the primitive batch-end lava of batch 9. Solid curves depict three recharge models, 1-0-0 (see Fig. 11), .1-0-0, and .01-0-0, representing decreasing amounts of recharge relative to fractionation. Small dashed curve depicts perfect fractional crystallization (see Fig. 11). Long dashed curves depict recharge and fractionation combined with assimilation of the incipient batch 9 lava composition, HK-43. The two assimilation models correspond to steady-state mass models, .5-.5-0 and .25-.75-0, where assimilation is equal to recharge and dominates recharge 3:1, respectively.

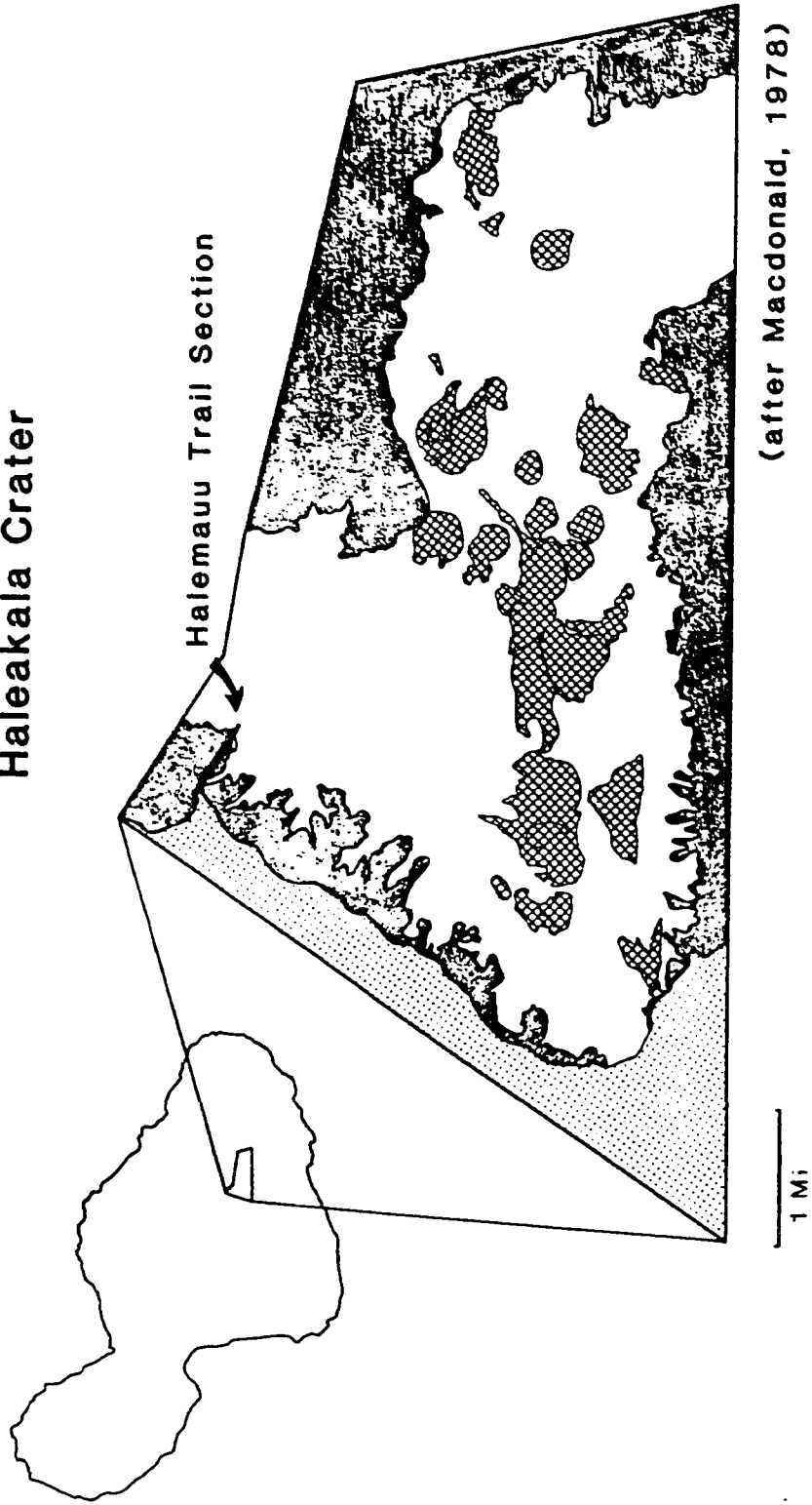
Figure 13. Schematic diagram illustrating the cyclic interaction between low and high magma flux regimes. Within the low magma flux regime, recharge rates are low and fractional crystallization dominates over magma mixing. During this *fractionation cycle*, magma resident in the magma chamber may undergo prolonged fractional crystallization in the absence of recharge, or may undergo a series of mixing-fractionation events if recharge rates are too low to exceed the overburden pressure. Recharge events involving small volumes of recharge magma may result in the expulsion of minor amounts of magma without producing a major eruptive period. Volatile exsolution after prolonged magma storage may also produce spurious eruptions within the low magma flux regime. Within the high magma flux regime, recharge rates are high and an *eruption cycle* is initiated. Magma mixing dominates over fractional crystallization, and during prolonged recharge, a series of recharge - eruption - mixing events may occur. If magma recharge temporarily ebbs, fractional crystallization will become more significant. Prolonged excursions into the low magma flux regime may result in strong fractionation effects due to lack of eruption.

Figure 14. Zr versus Nb for lavas from ten selected magma batches from the Halemau section of Haleakala Crater that display relatively large compositional variations. With

the exception of batch 13, only batches with three or more samples are plotted. Symbols as follows: solid stars - batch 1, triangles - batch 2, X's - batch 5, squares - batch 6, open crosses - batch 7, crosses - batch 8, diamonds - batch 9, open stars - batch 10, six-pointed stars - batch 12, solid circles - batch 13. Lines connect individual batches, with arrows indicating upsection geochemical variations. Distinct trends for batches indicate these lavas were derived from parental magmas having variable Zr/Nb ratios and that subsequent intrabatch evolution was unique for each batch.

Figure 15. (a) Ba vs. Zr/Nb, (b) Sc vs. Zr/Nb, and (c) Y versus Sc for Kula lavas from Haleakala Crater. Shown for comparison are fields for early post shield-building (PSB) lavas from the Kumuilihi Formation (light stippled field) and post-erosional lavas from the Hana Formation (darker shading) [data from West and Leeman, in prep.]. Essentially discrete fields for batches from the lower part of the Haleakala Crater section (batches 1 to 7a; the older batch group) and batches from the upper part of the section (batches 7b to 13; the younger batch group) indicate that these two groups were derived from compositionally distinct parental magmas. Covariations between Zr/Nb ratios and Ba and Sc abundances suggests that this ratio is influenced by magmatic (magma chamber) processes as well as changes in source composition. The shift in source composition resulted in separate evolutionary paths for older batch group and younger batch group lavas. The older batch group derives from parental magmas having compositions similar to early PSB (Kumuilihi) lavas, whereas the younger batch group follows a path similar to post-erosional (Hana) lavas.

Haleakala Crater



(after Macdonald, 1978)

FIG. 1

FIG.2

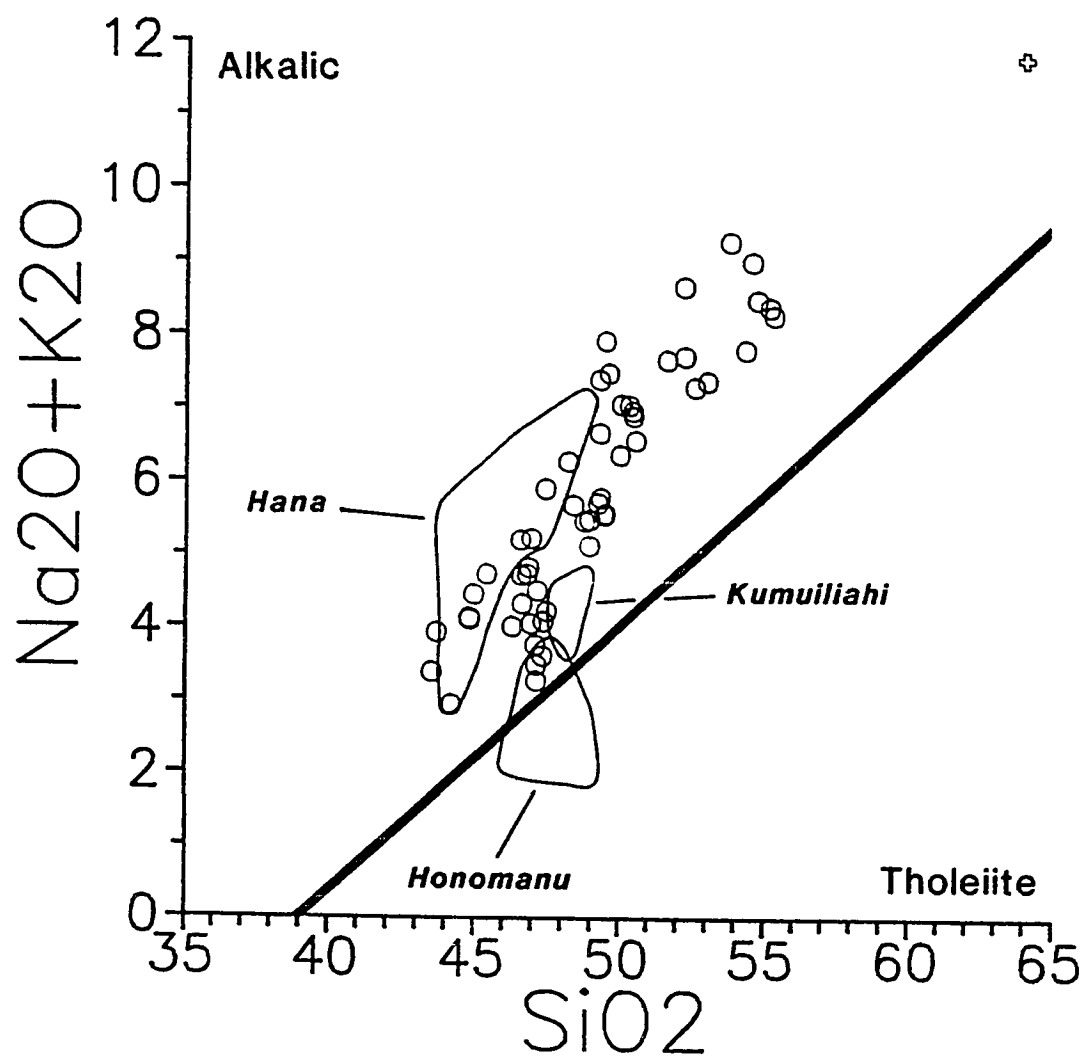


FIG. 3A

284

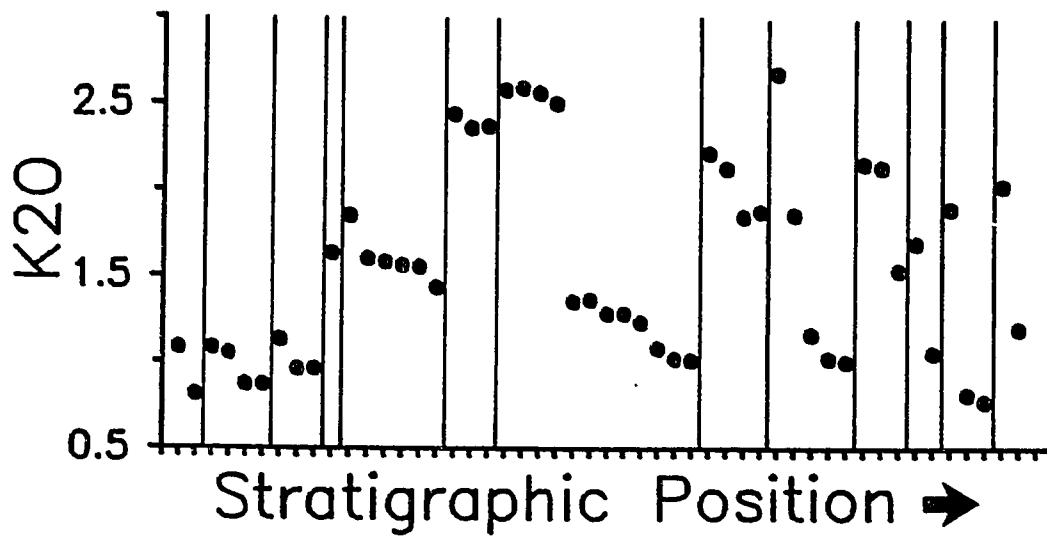


FIG. 3B

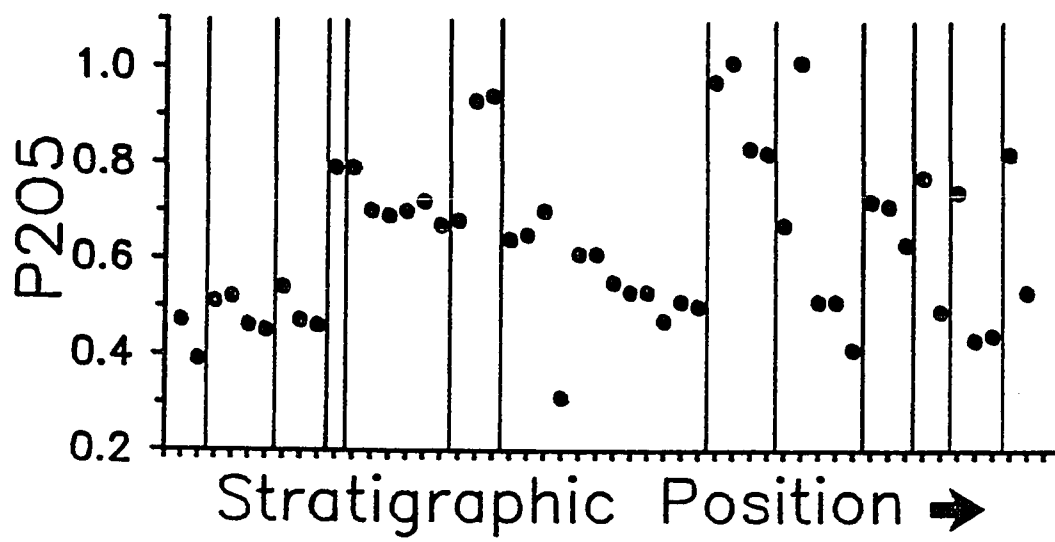


FIG. 3C

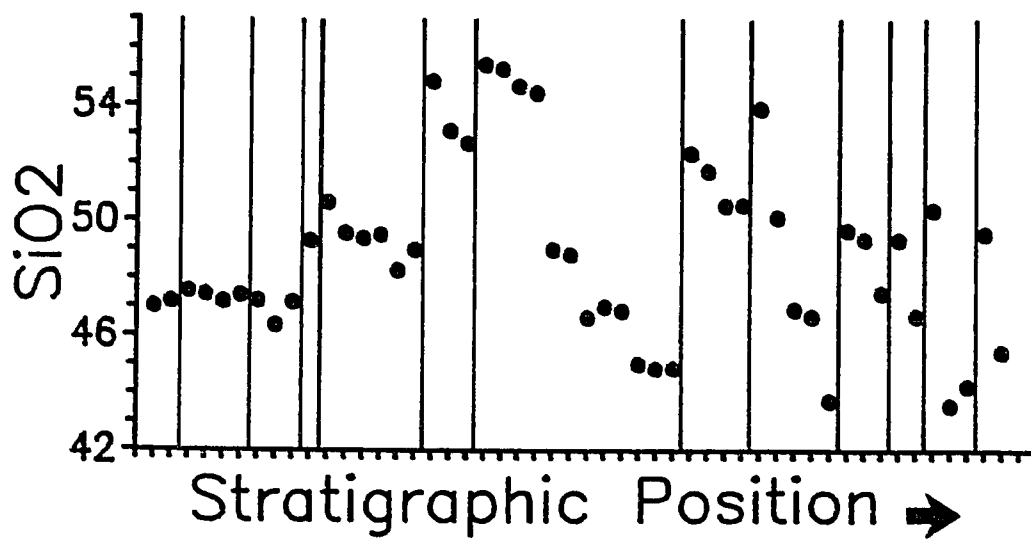


FIG. 3D

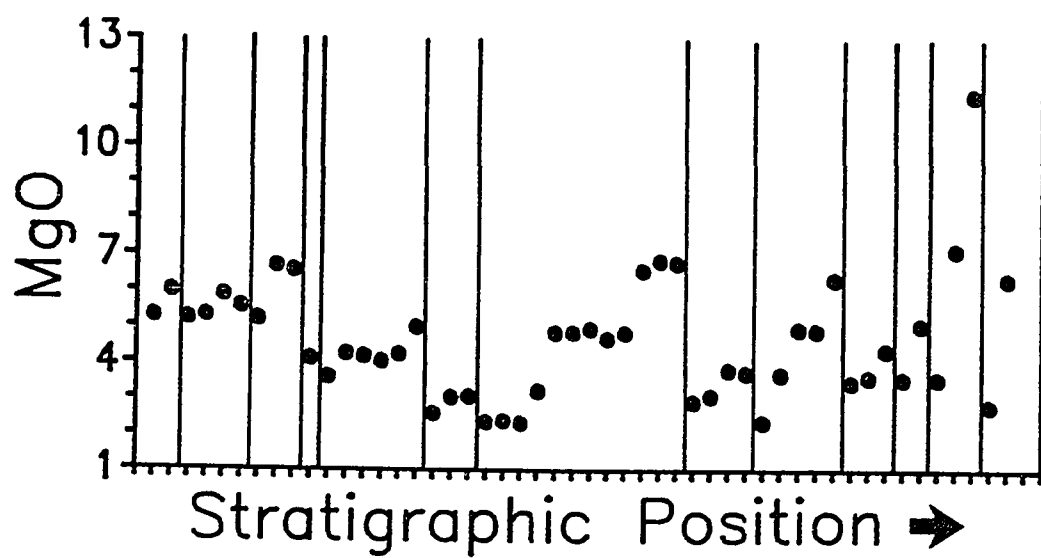


FIG. 3E

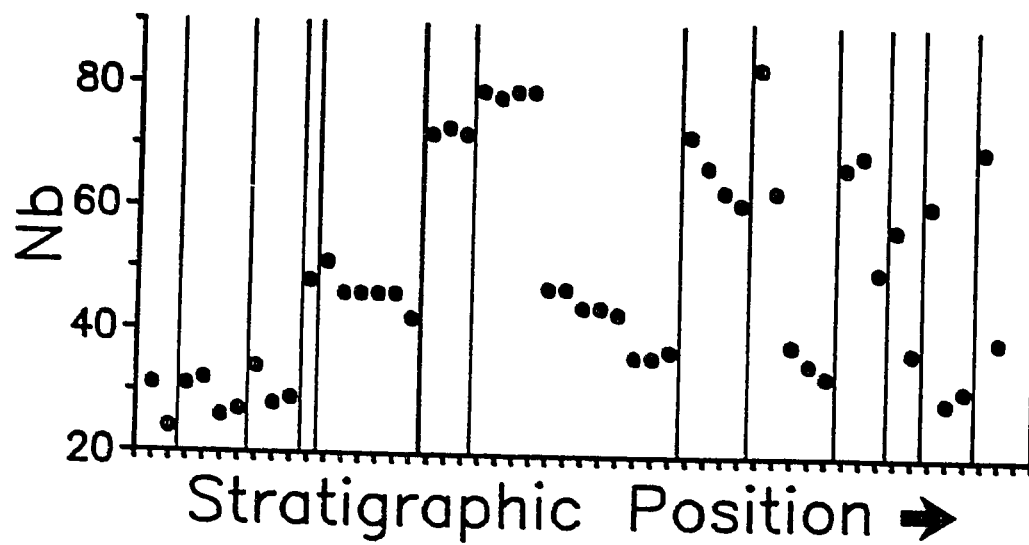


FIG. 3F

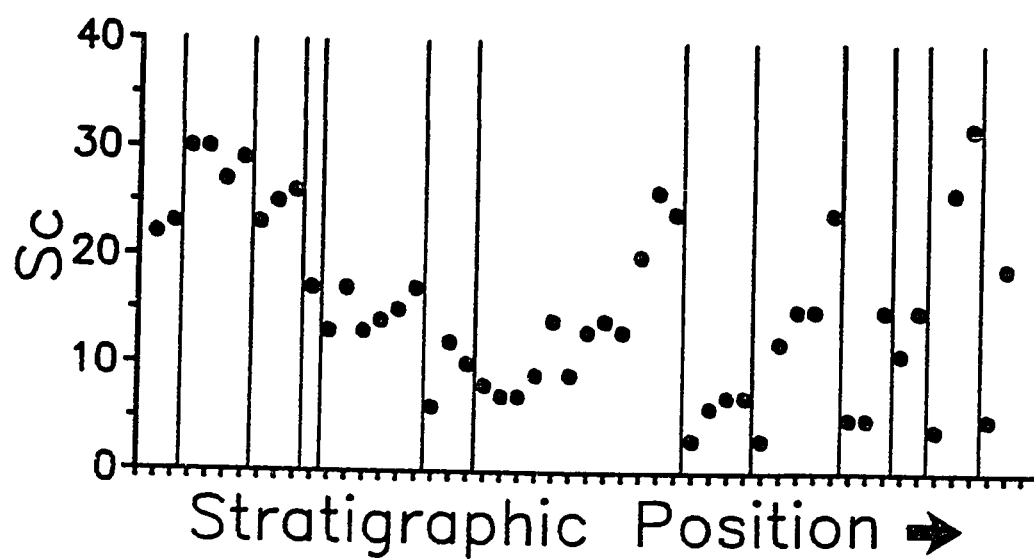


FIG. 3G

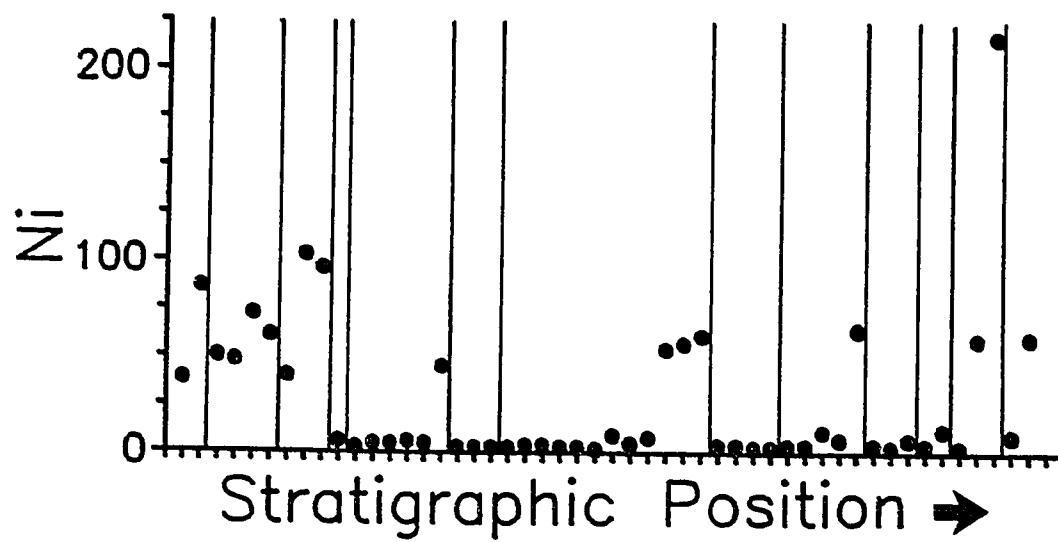
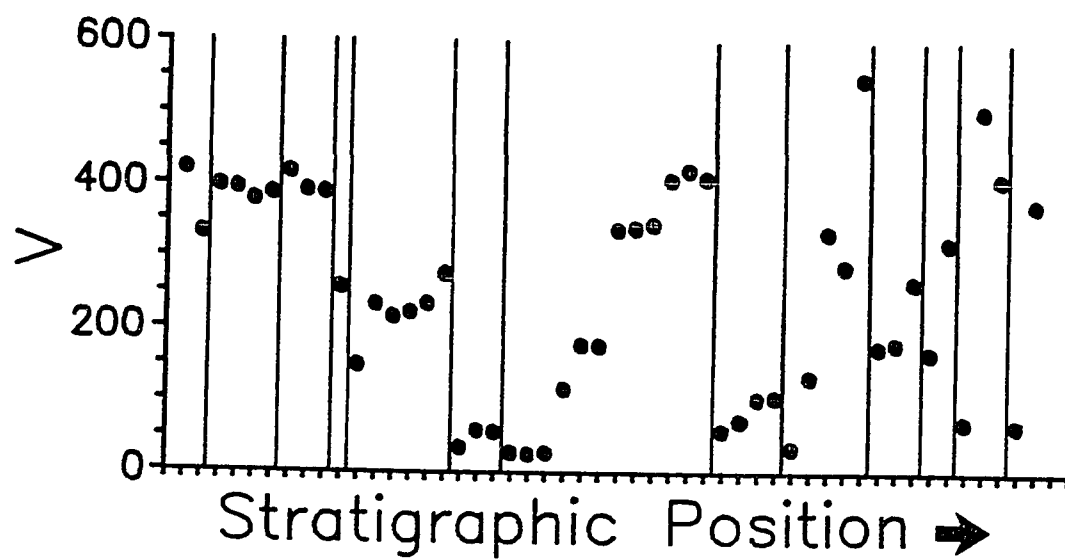


FIG. 3H



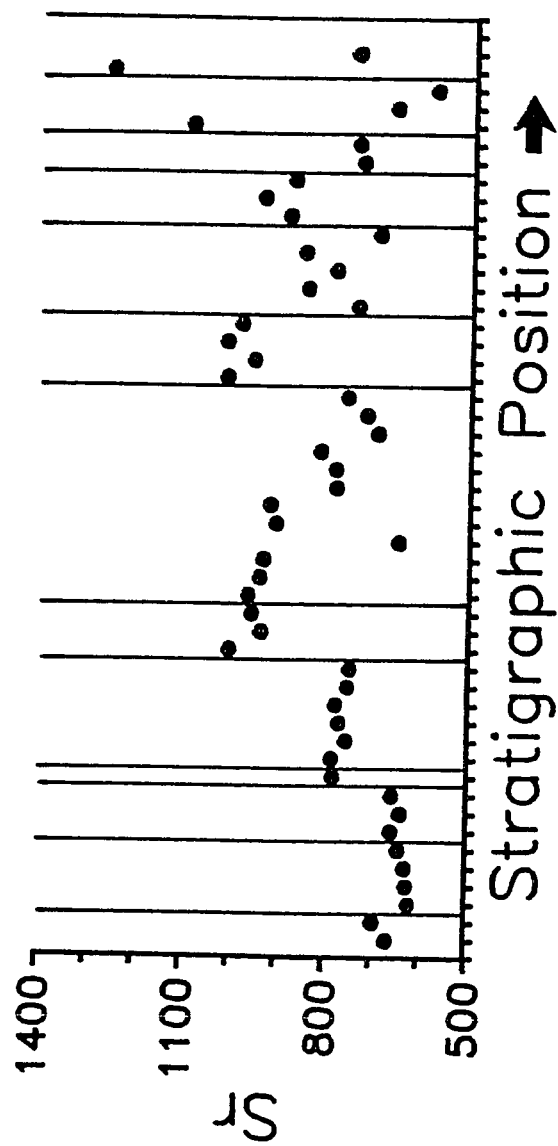


FIG. 31

FIG. 3J

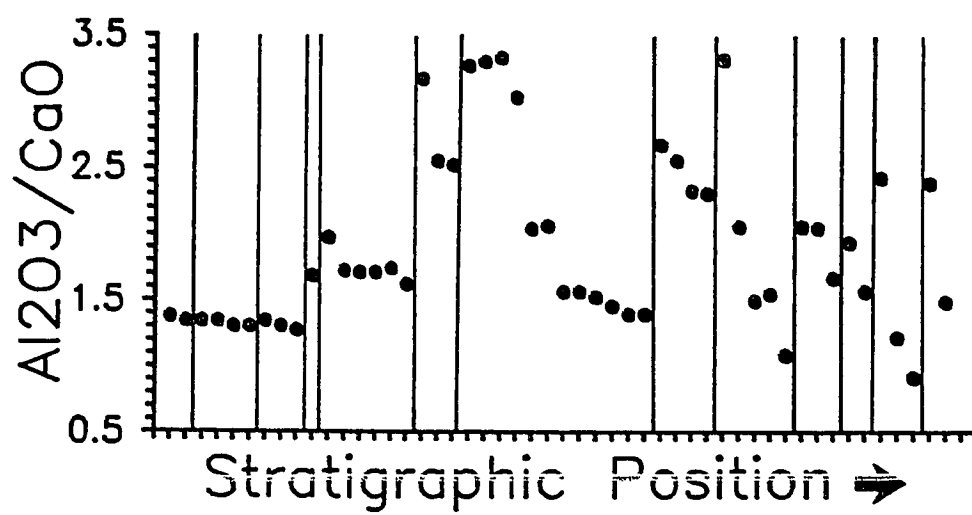
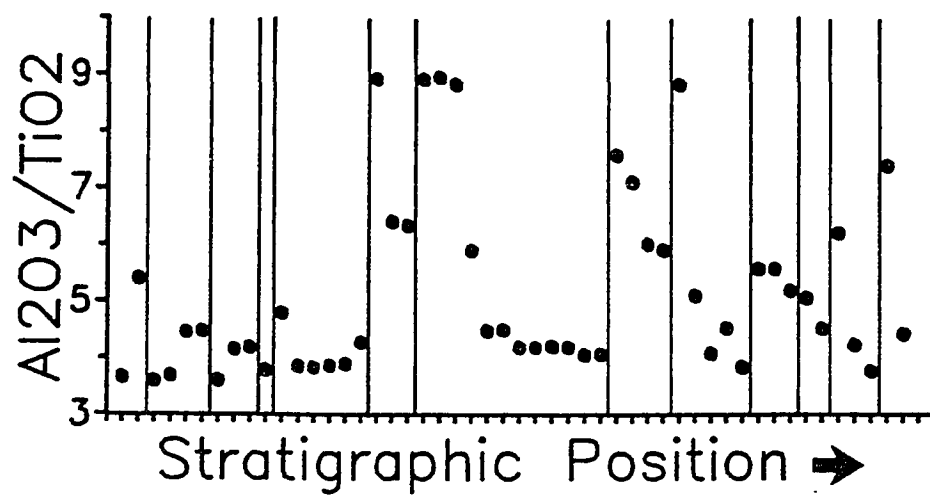


FIG. 3K



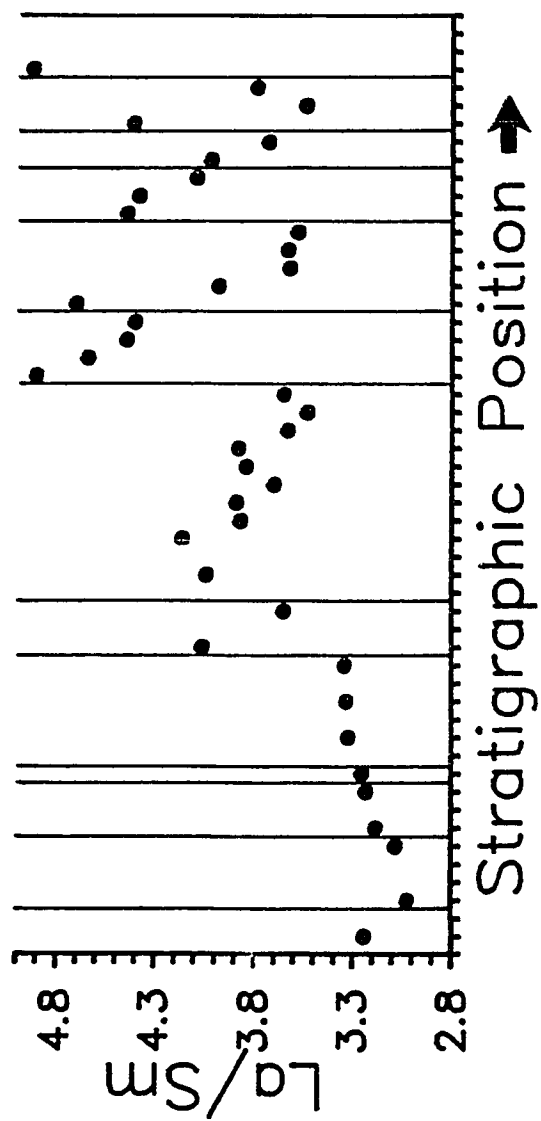


FIG. 3L

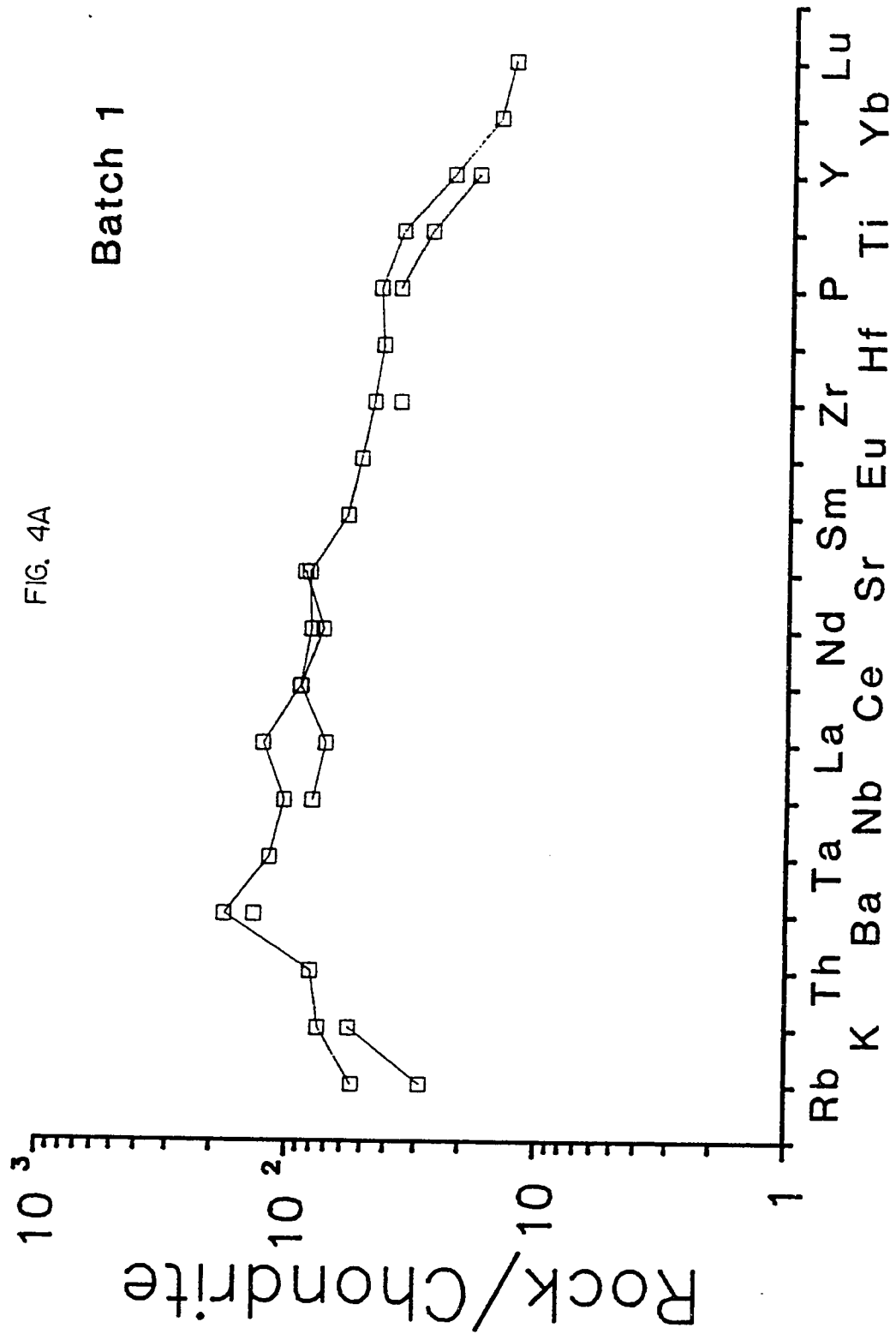
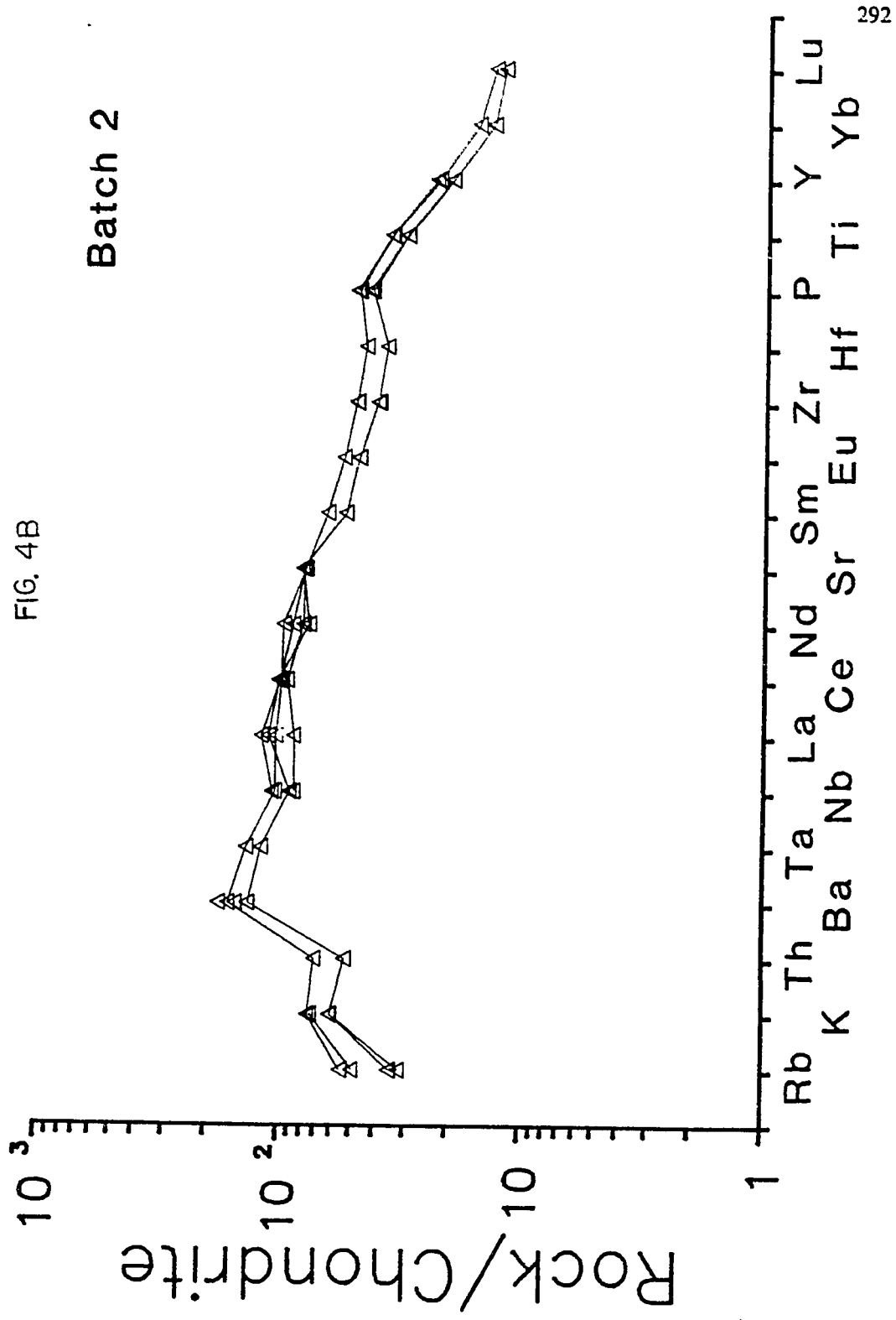
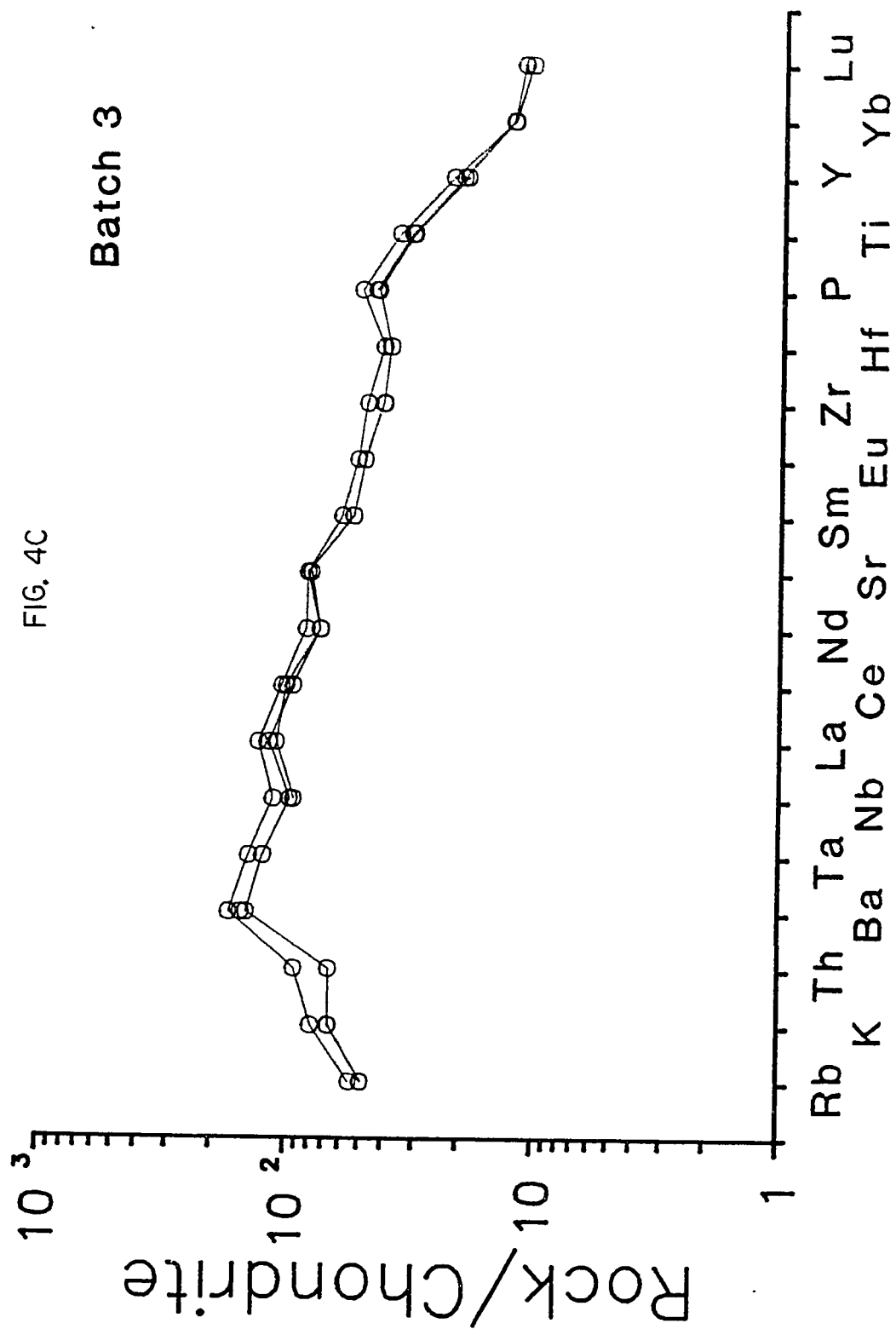
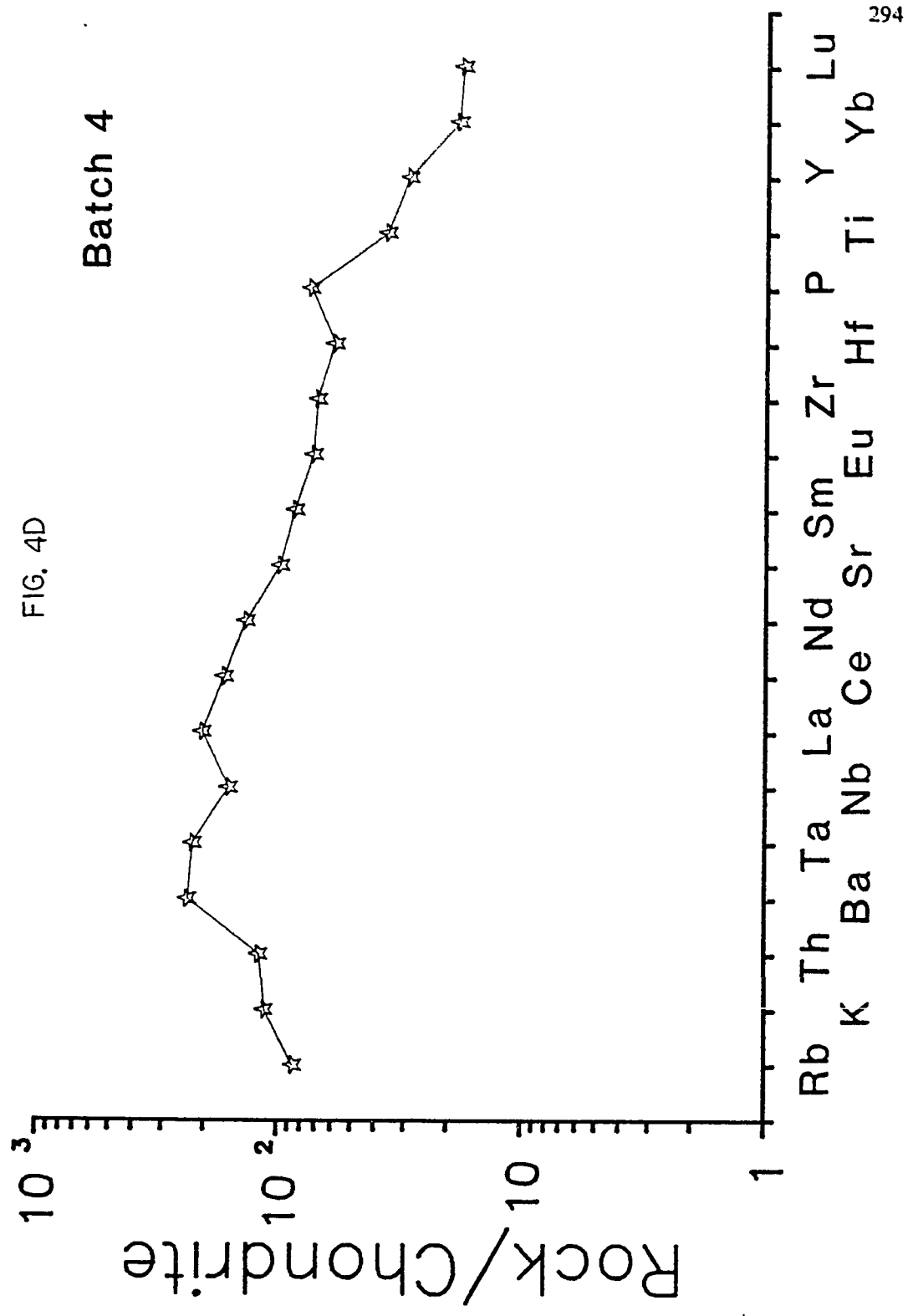
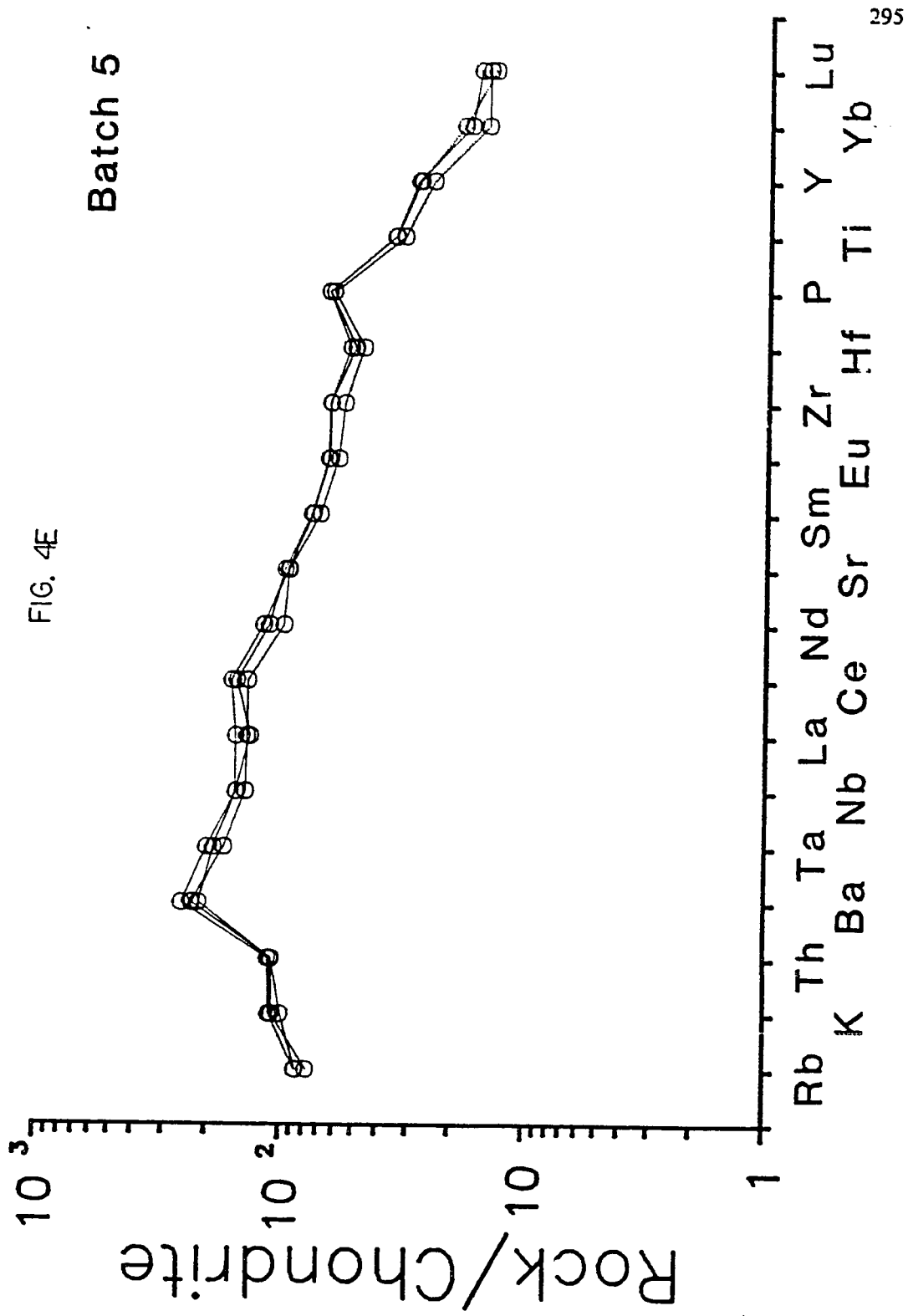


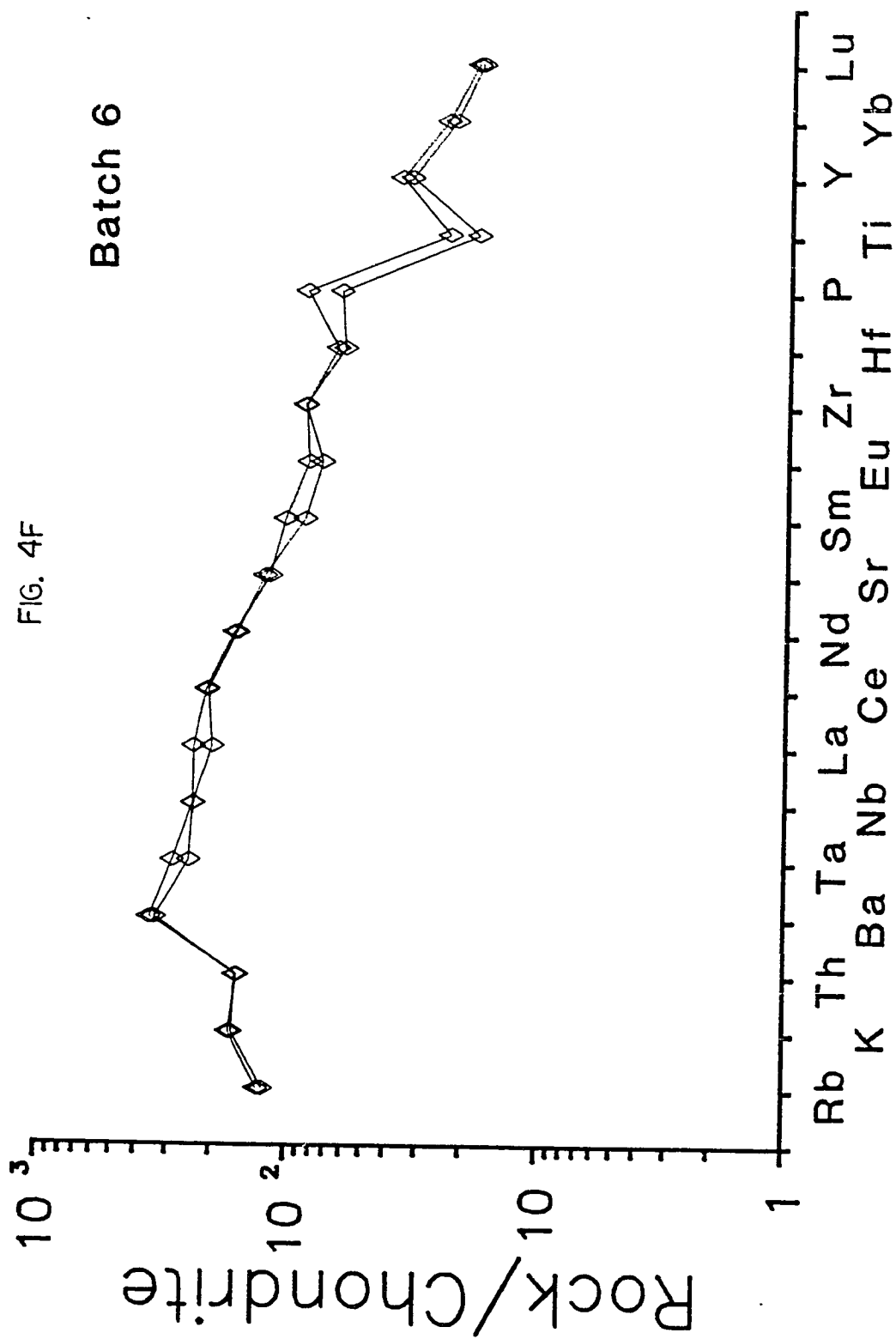
FIG. 4A

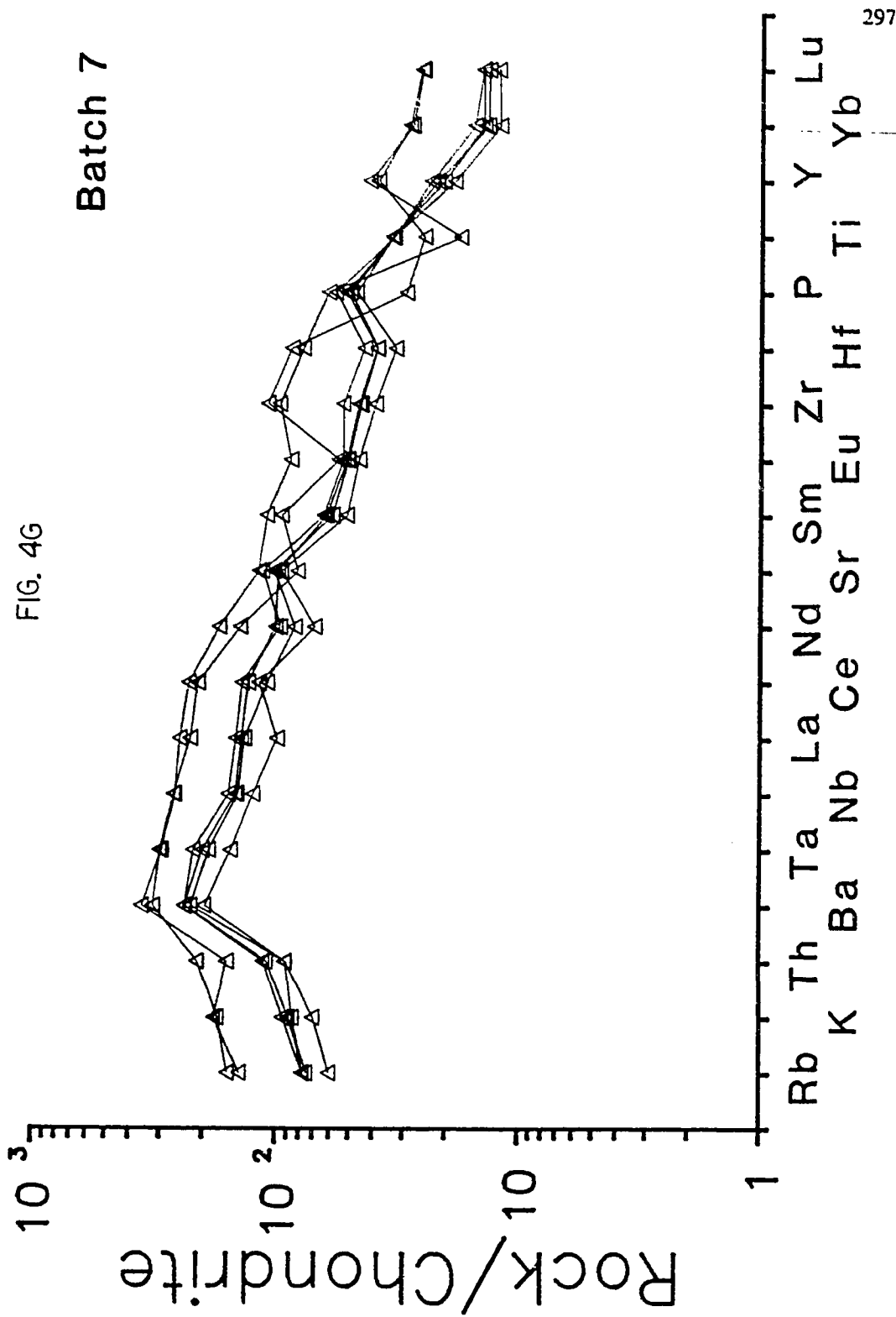


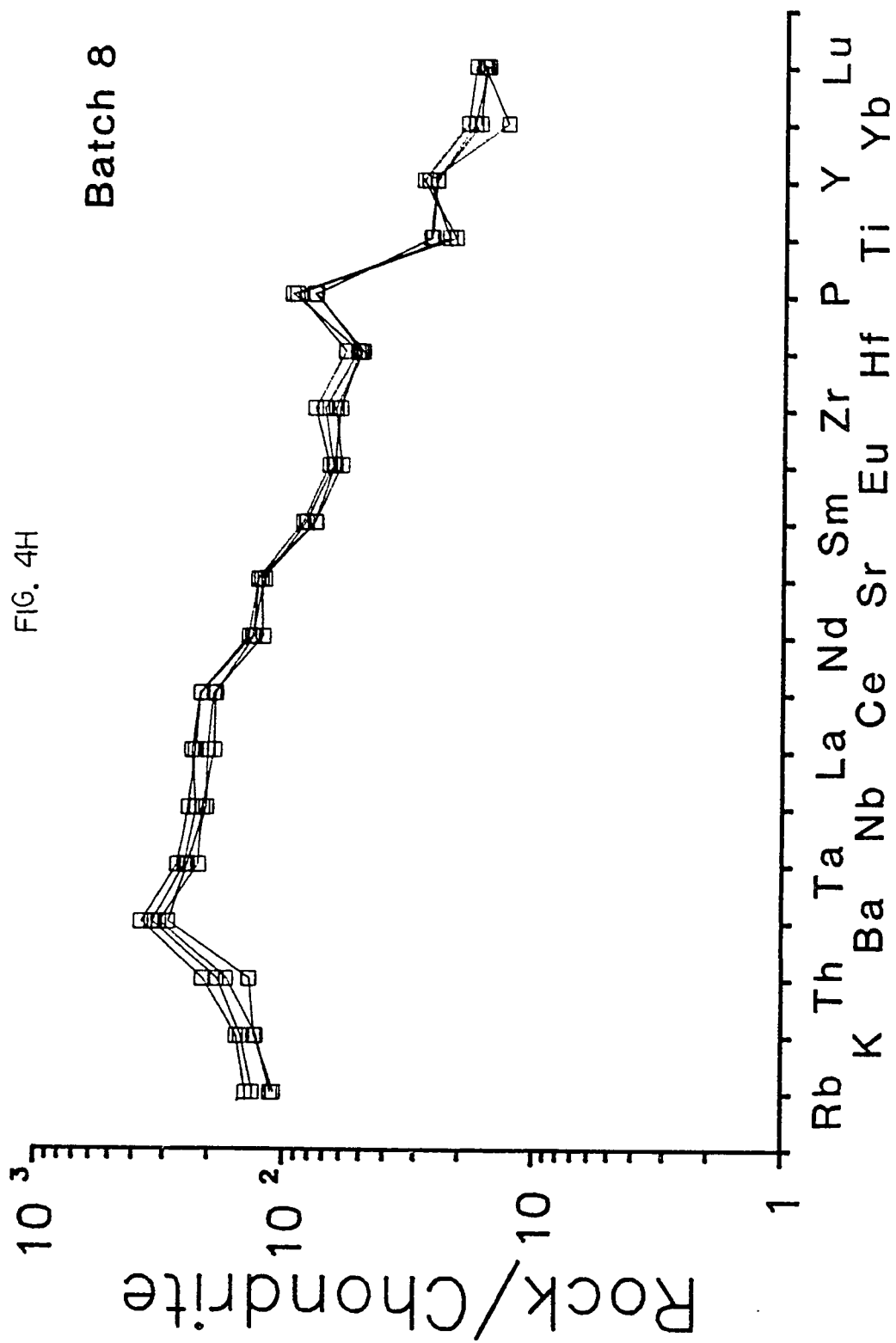


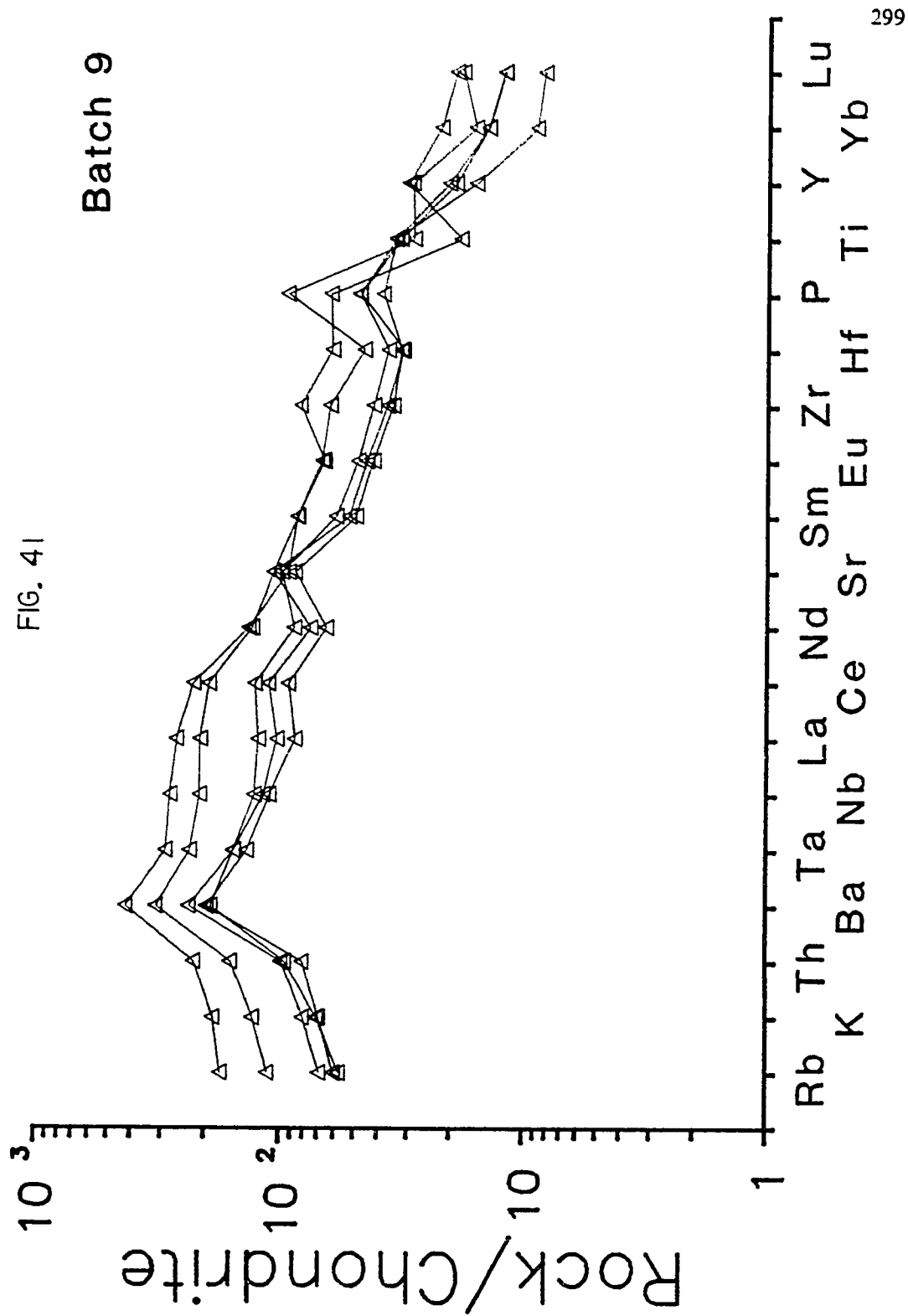


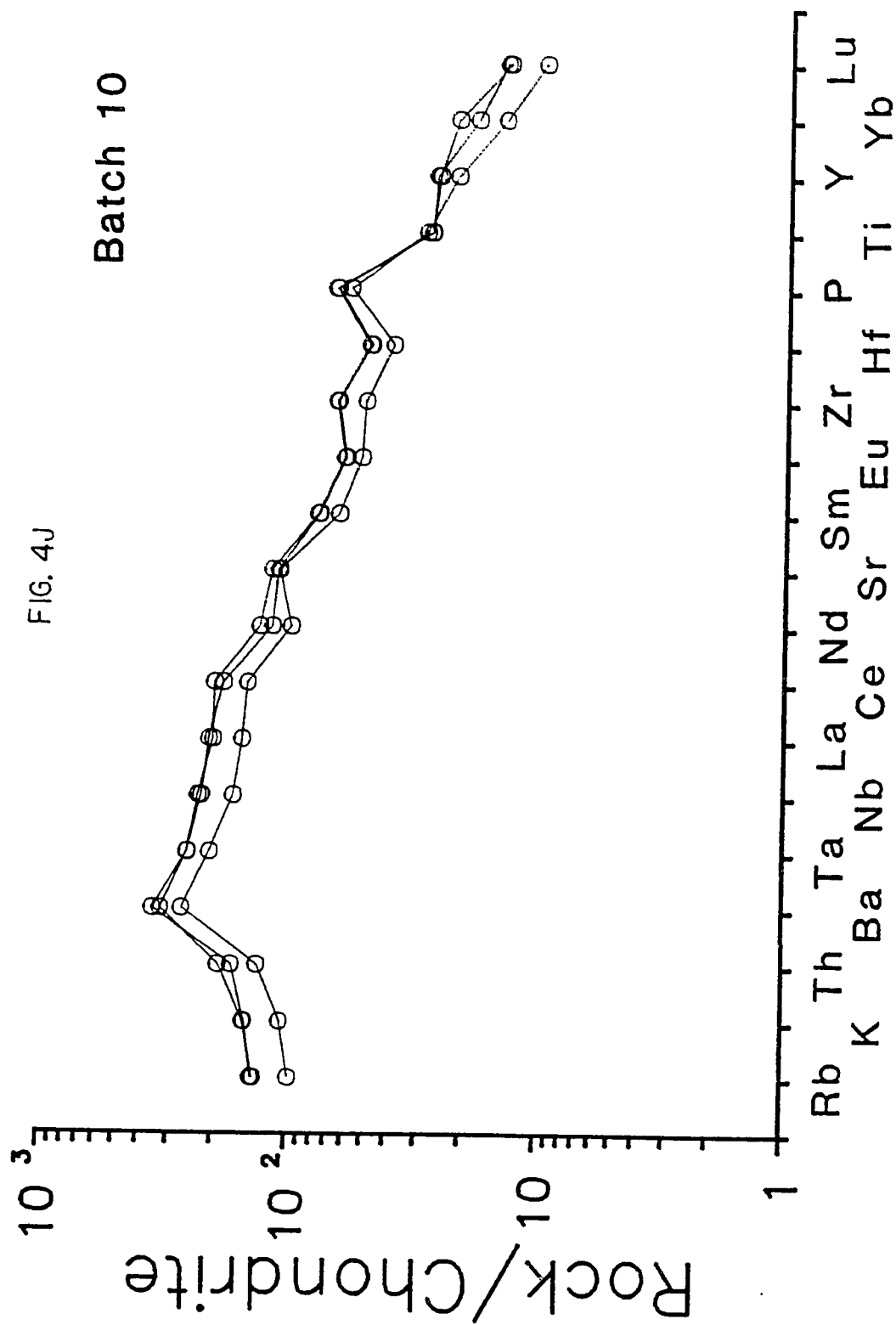


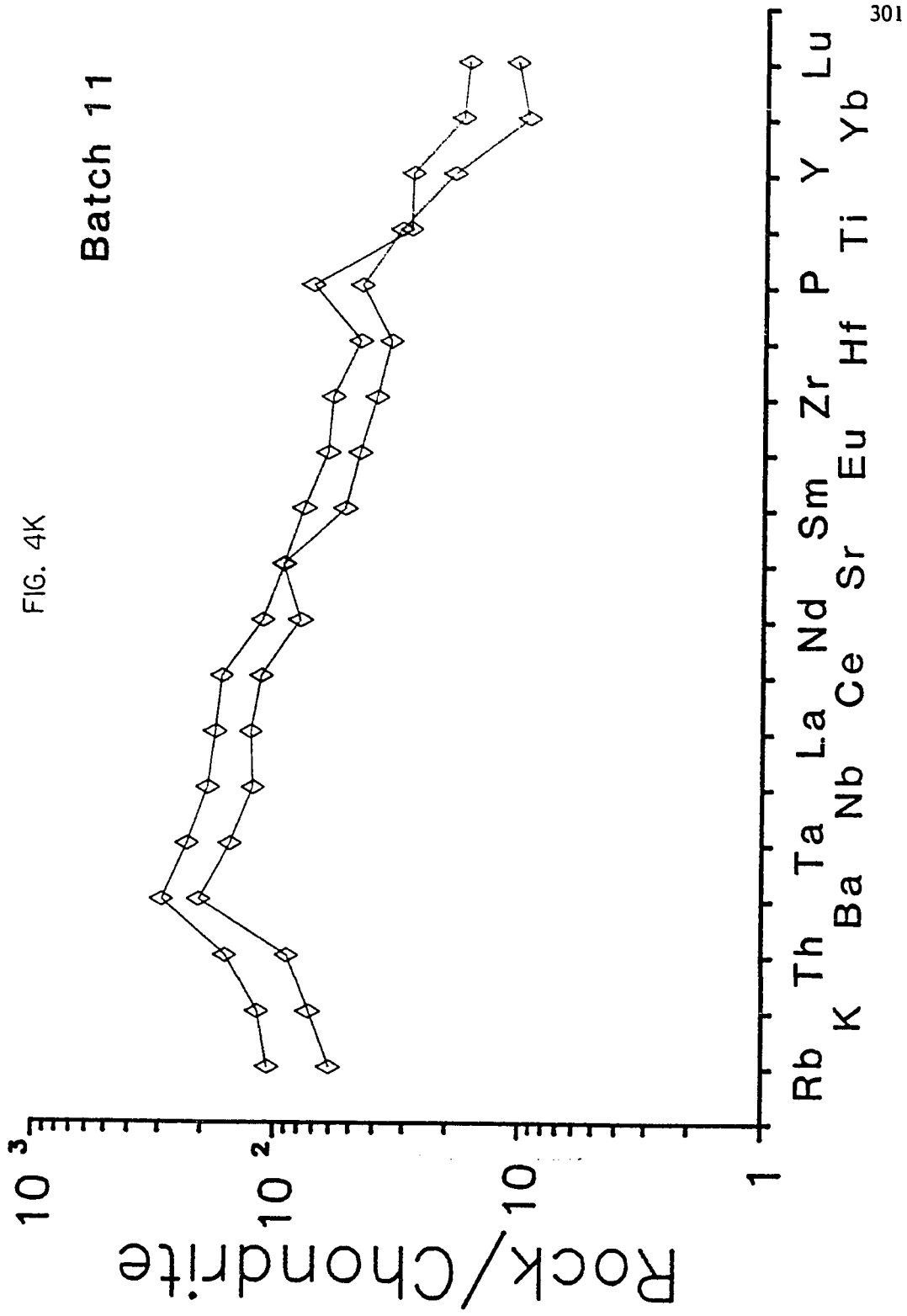


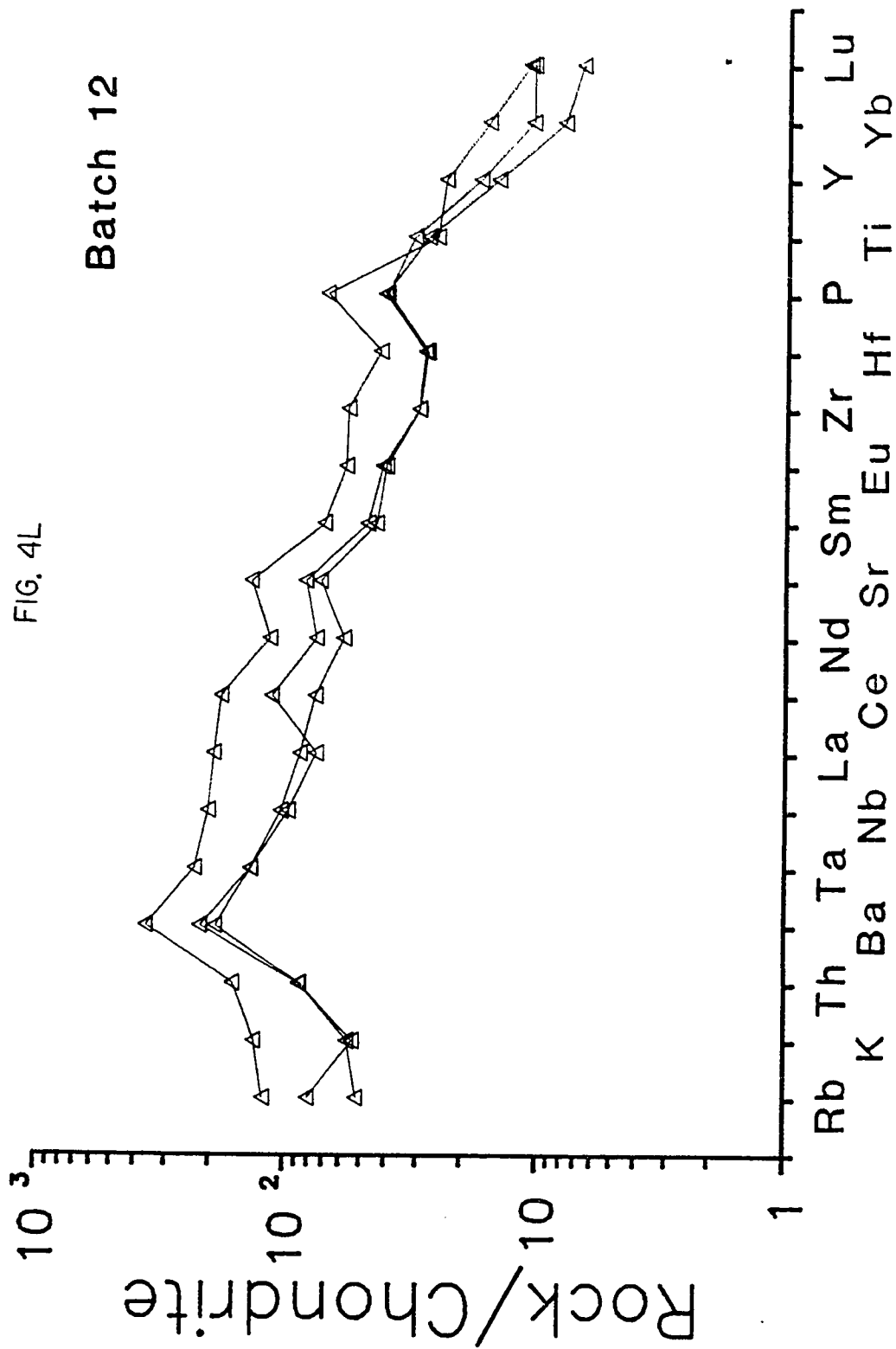


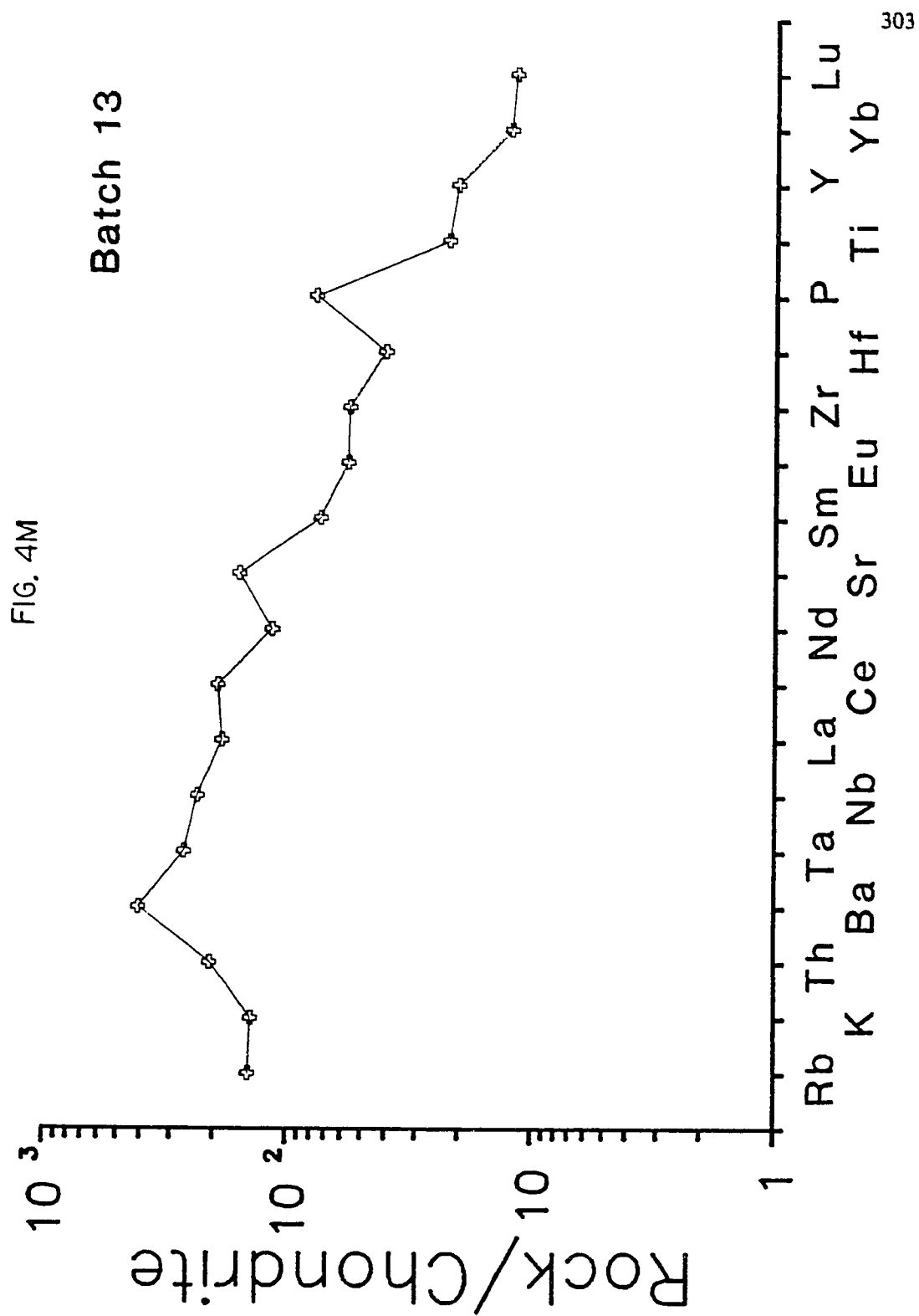












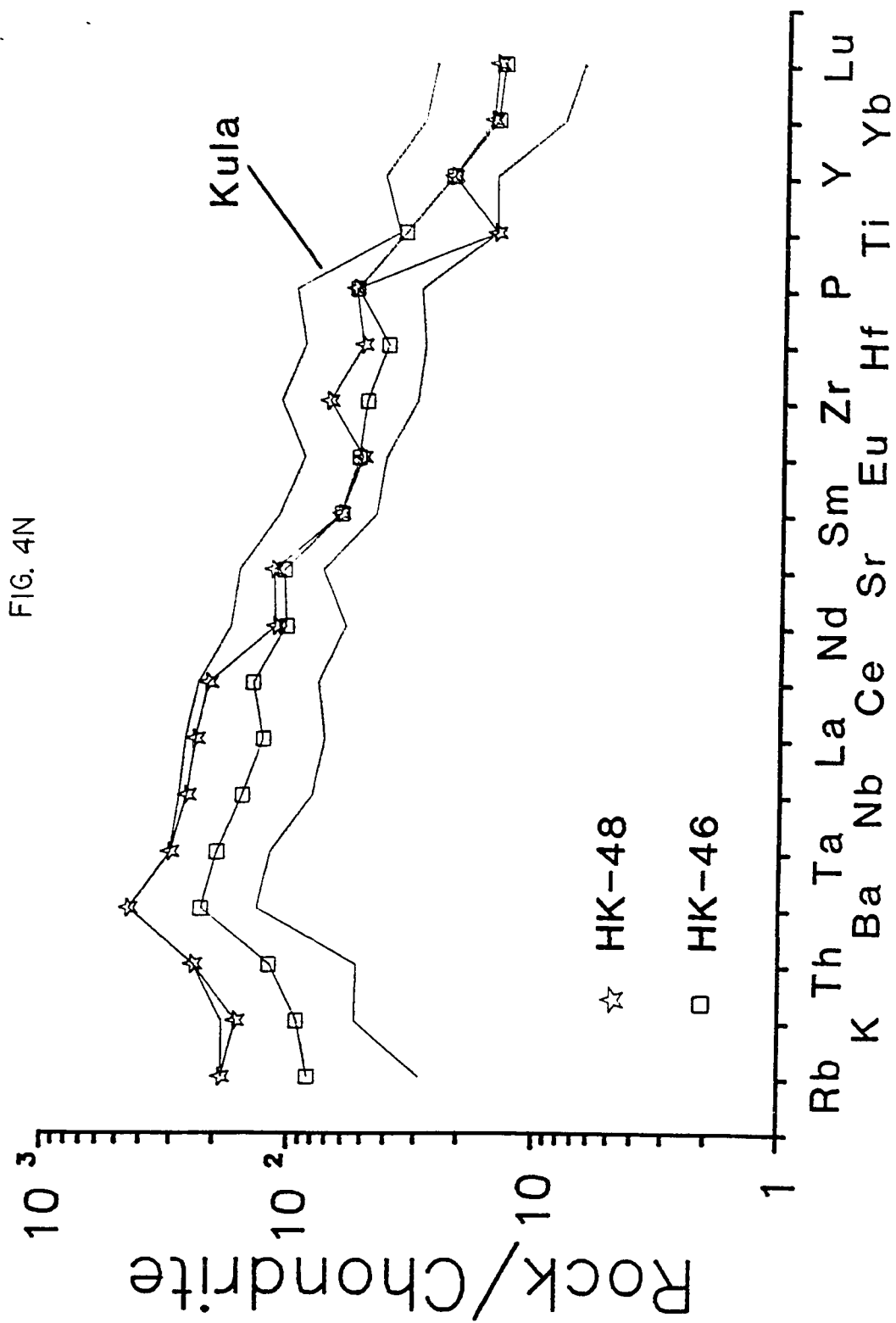


FIG. 5A

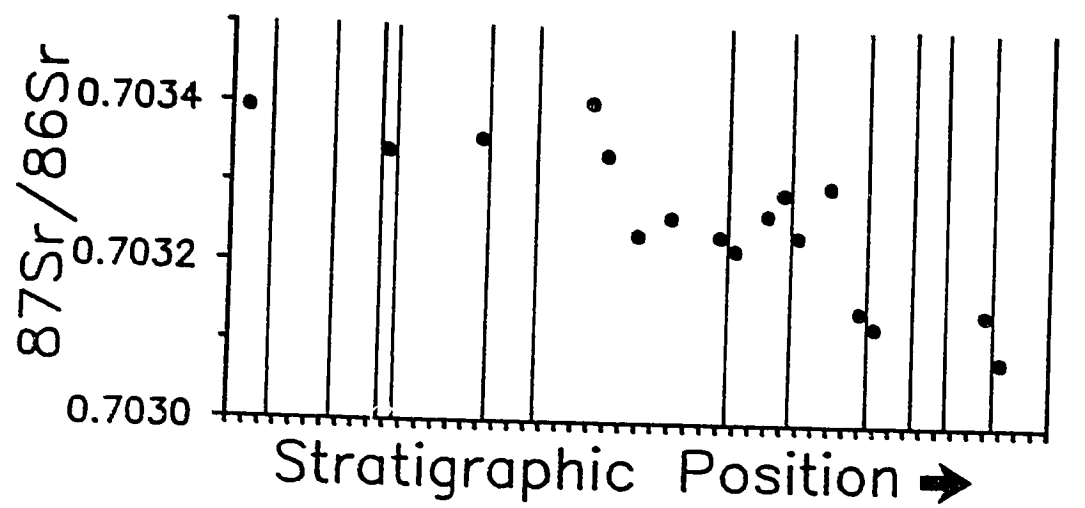


FIG. 5B

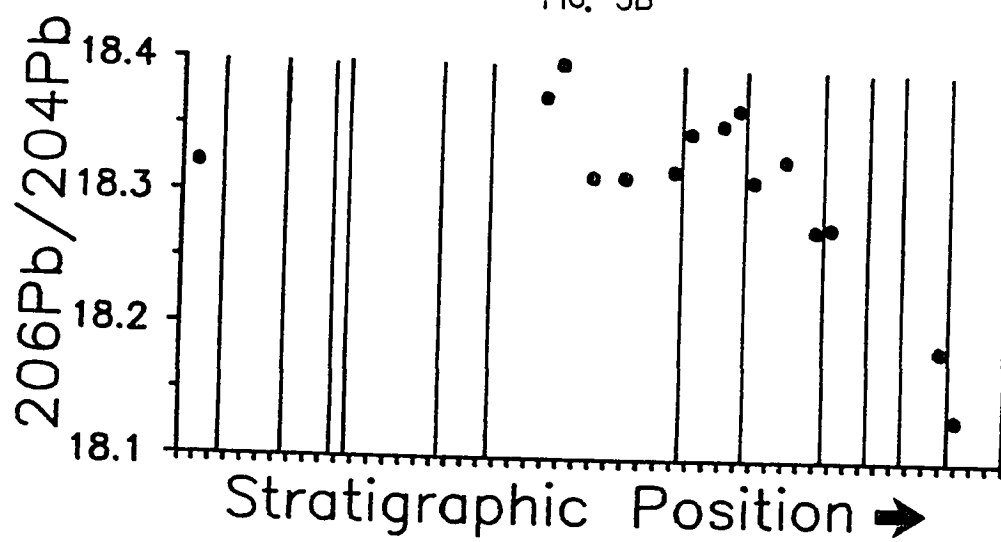


FIG. 5C

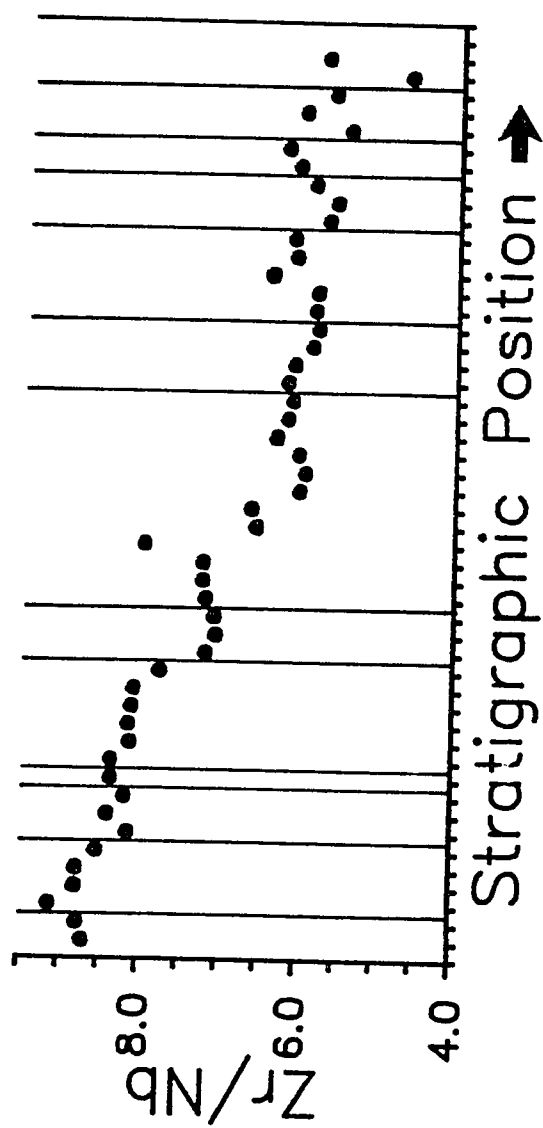


FIG. 6A

Batch 3 → Batch 4

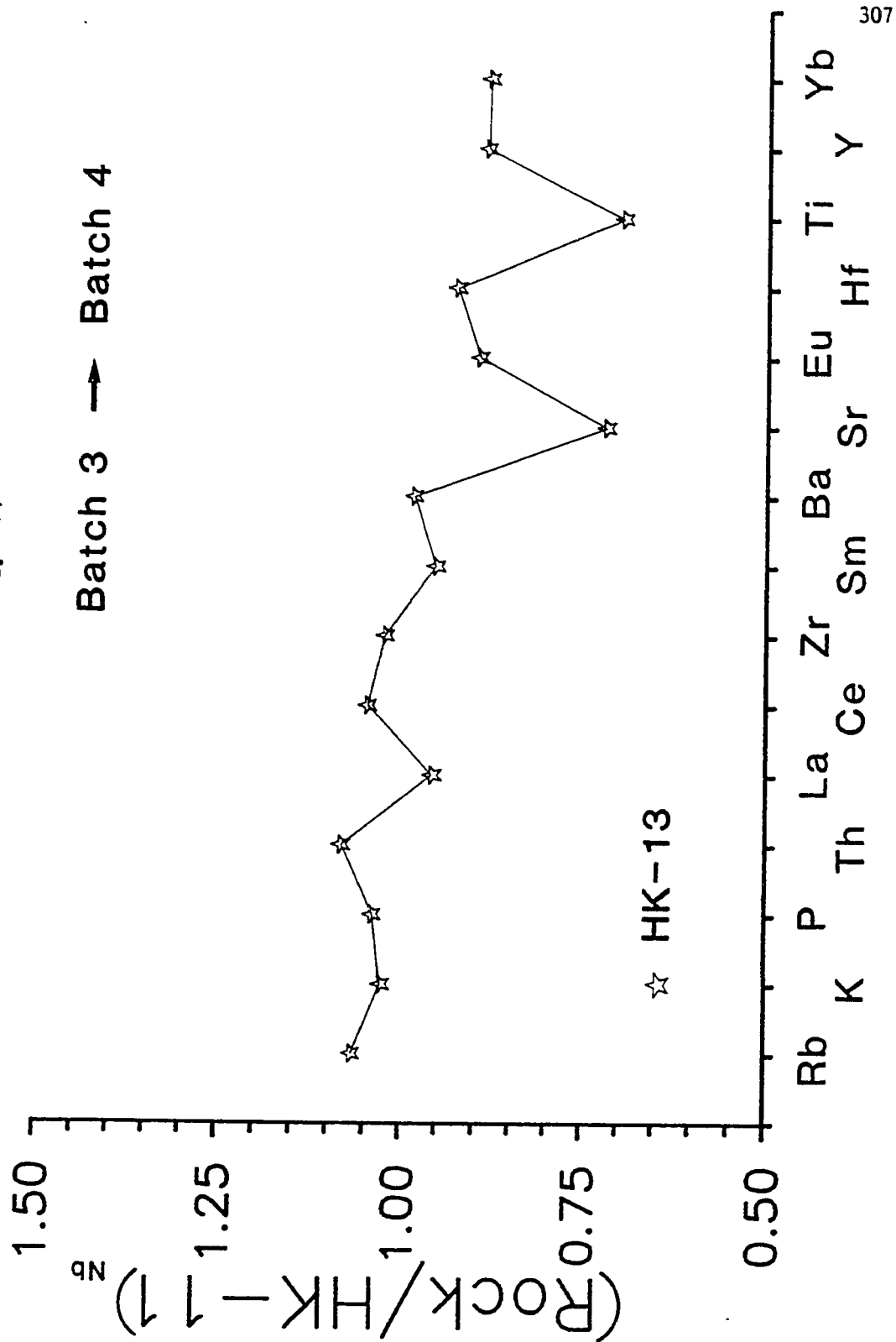


FIG. 6B

Batch 5 → Batch 6

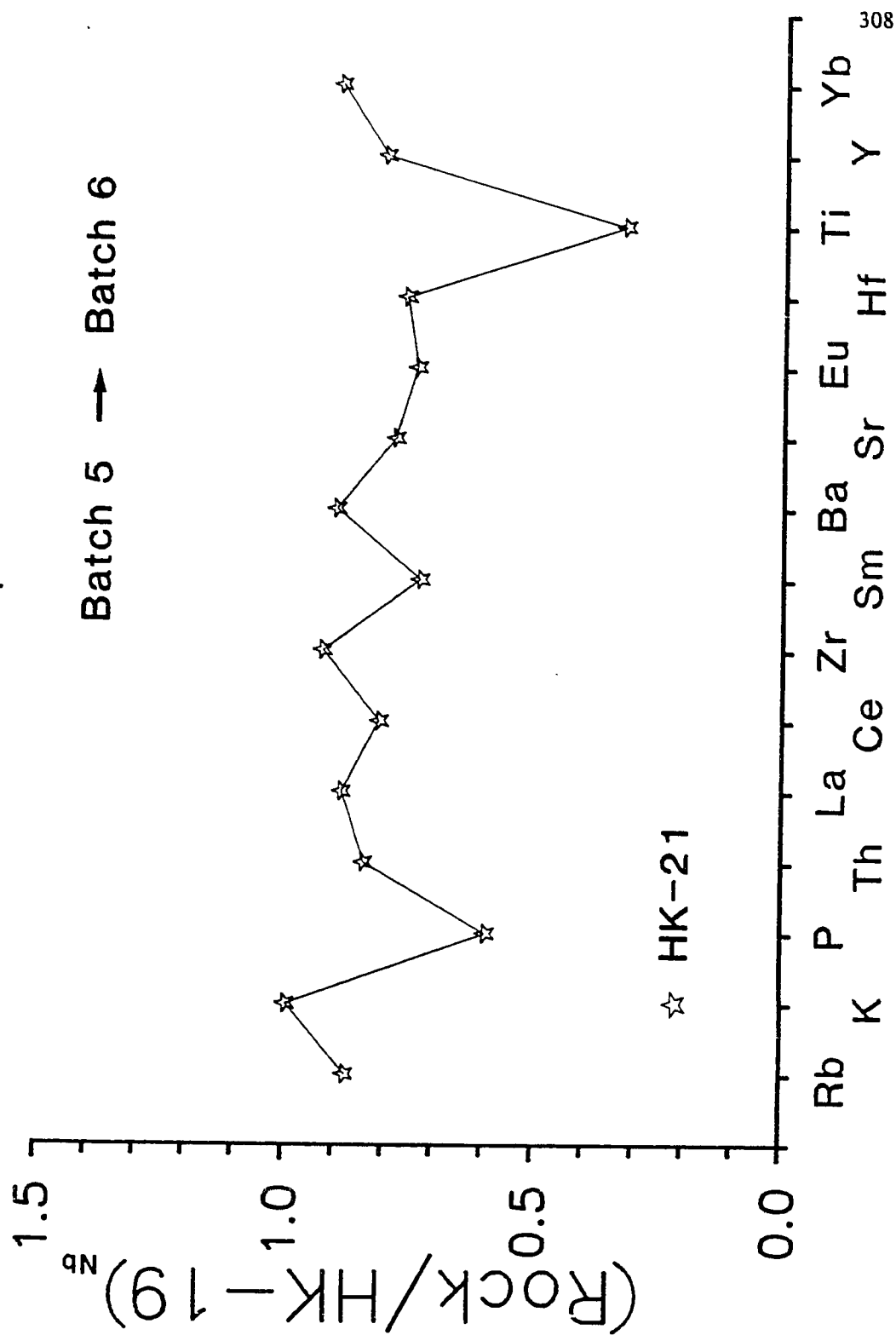
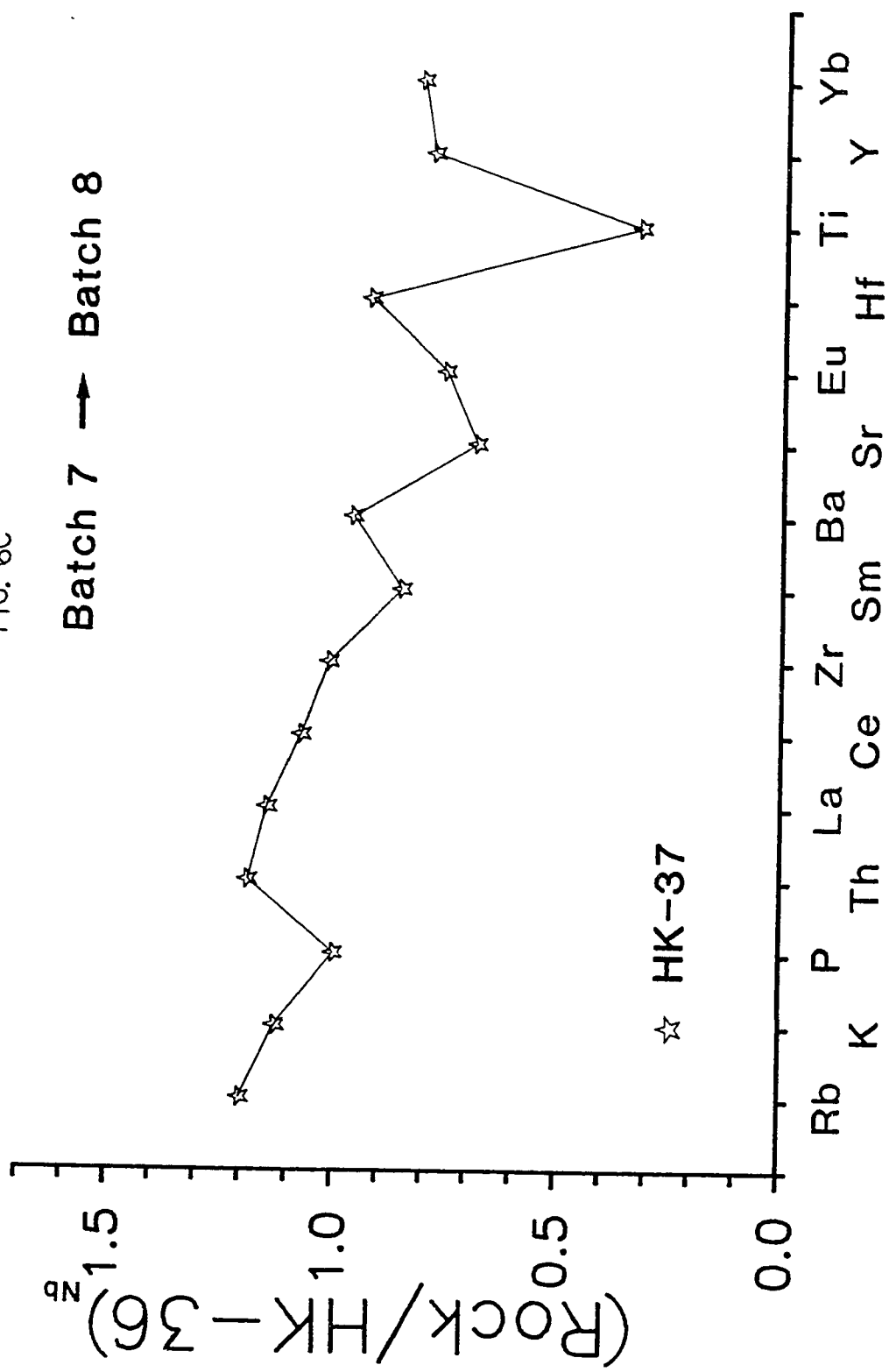


FIG. 6C

Batch 7 → Batch 8



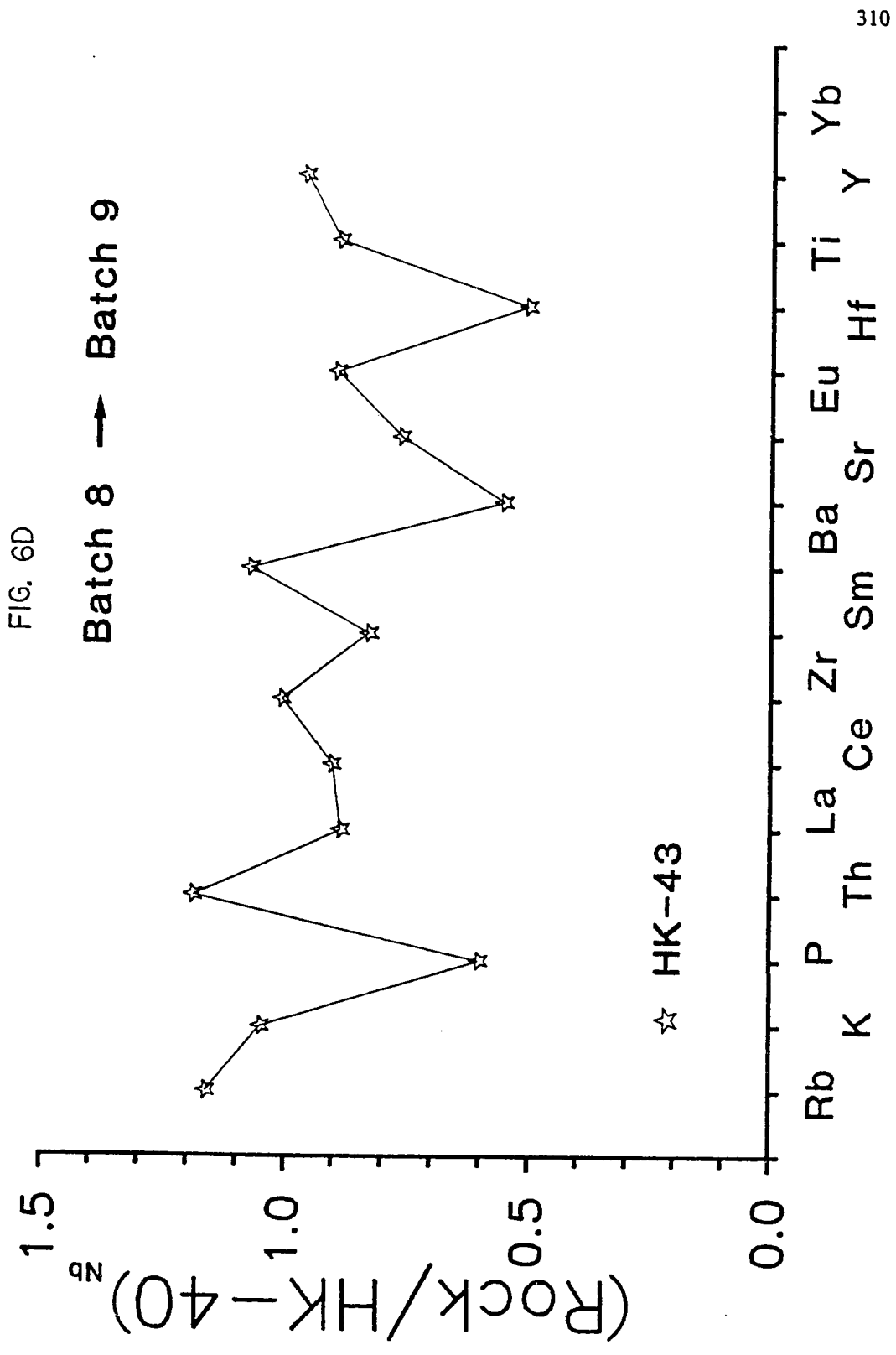


FIG. 6E

Batch 9 → Batch 10

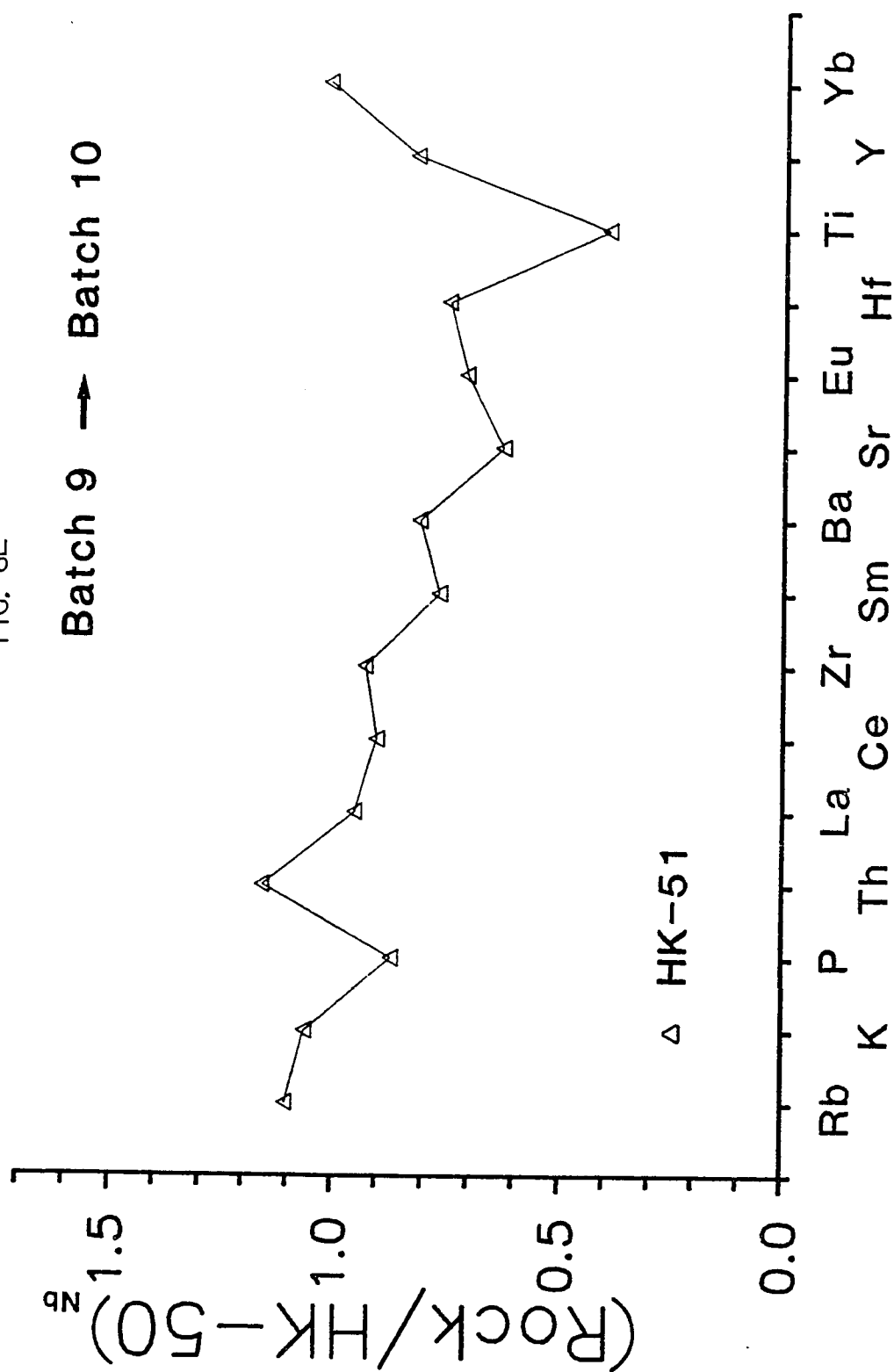


FIG. 6F

Batch 12 → Batch 13

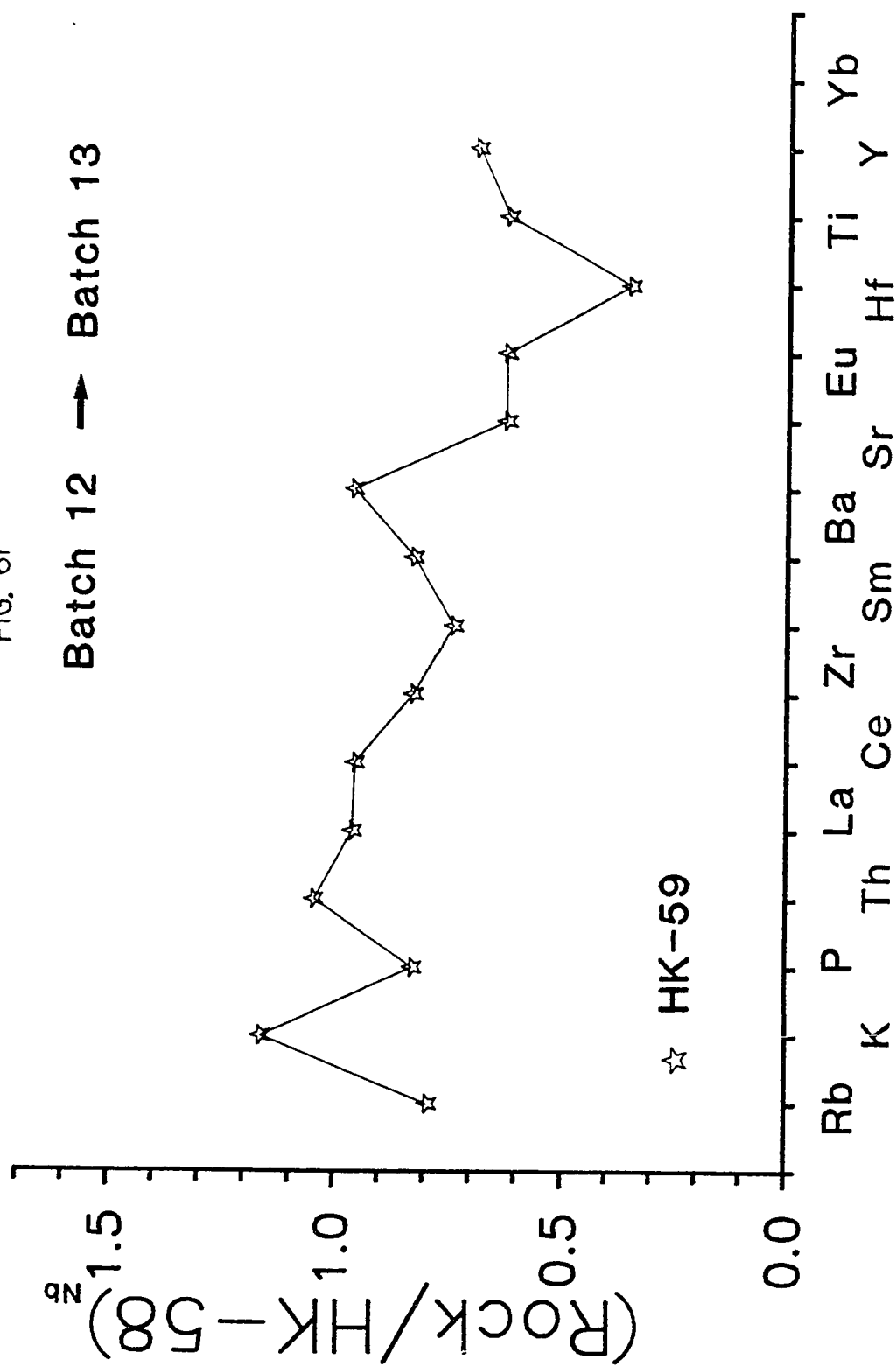


FIG. 7A

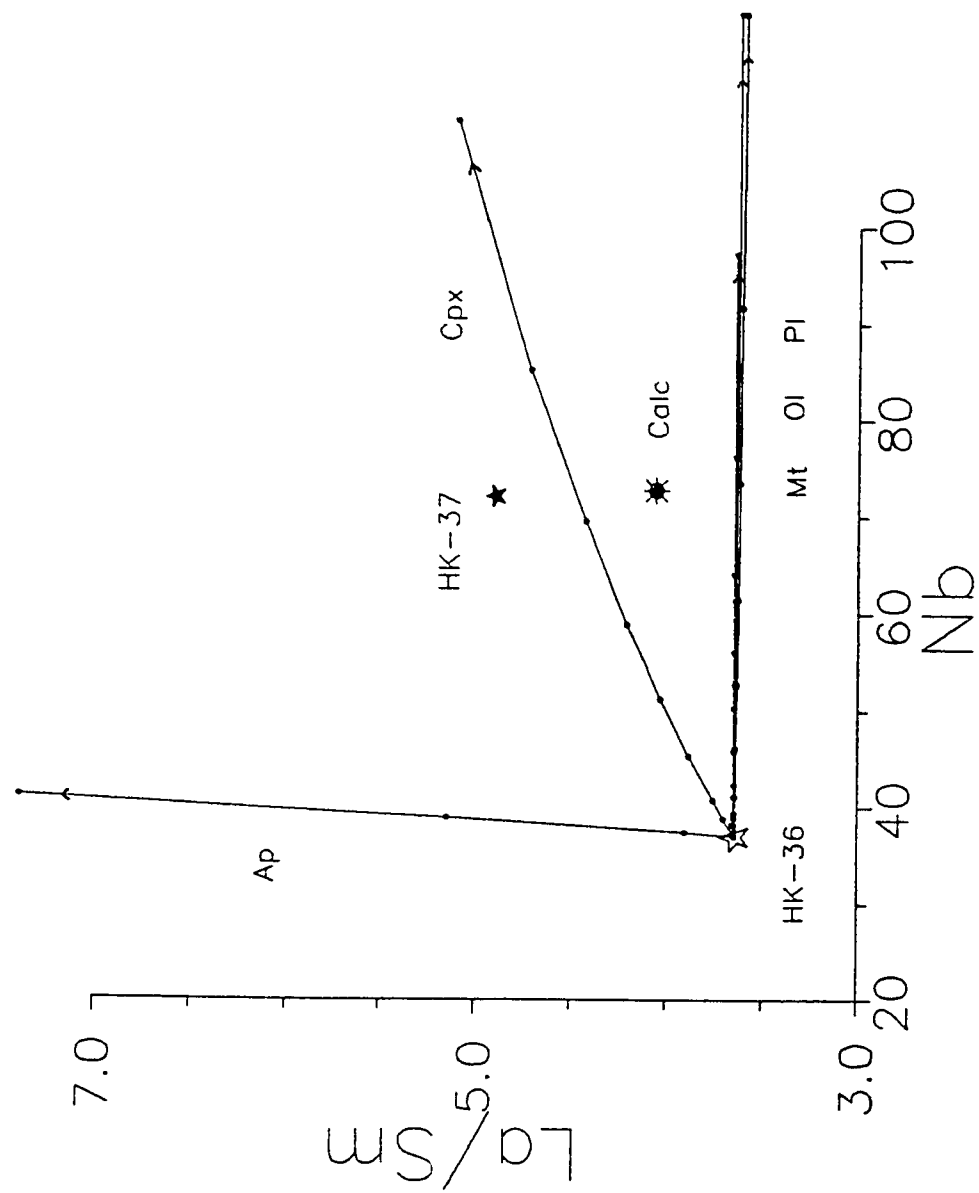
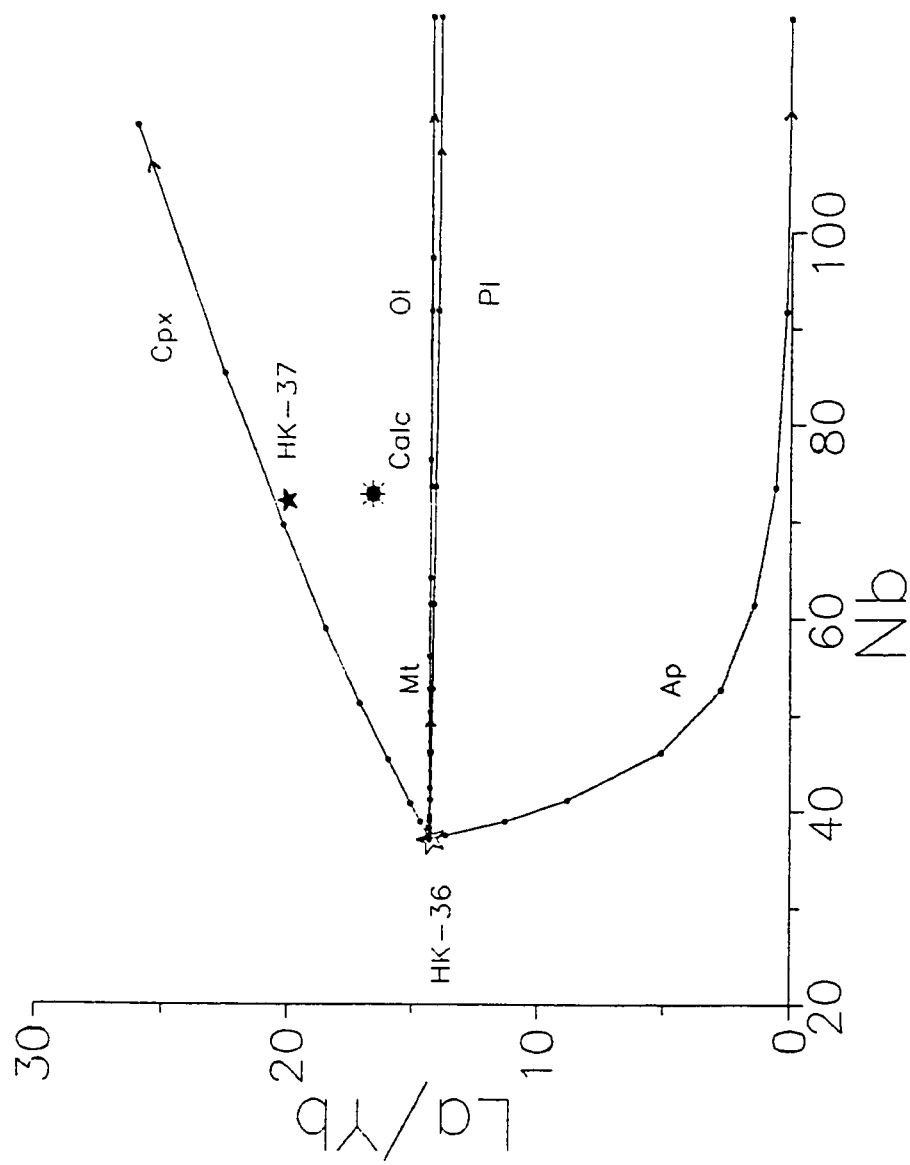


FIG. 7B



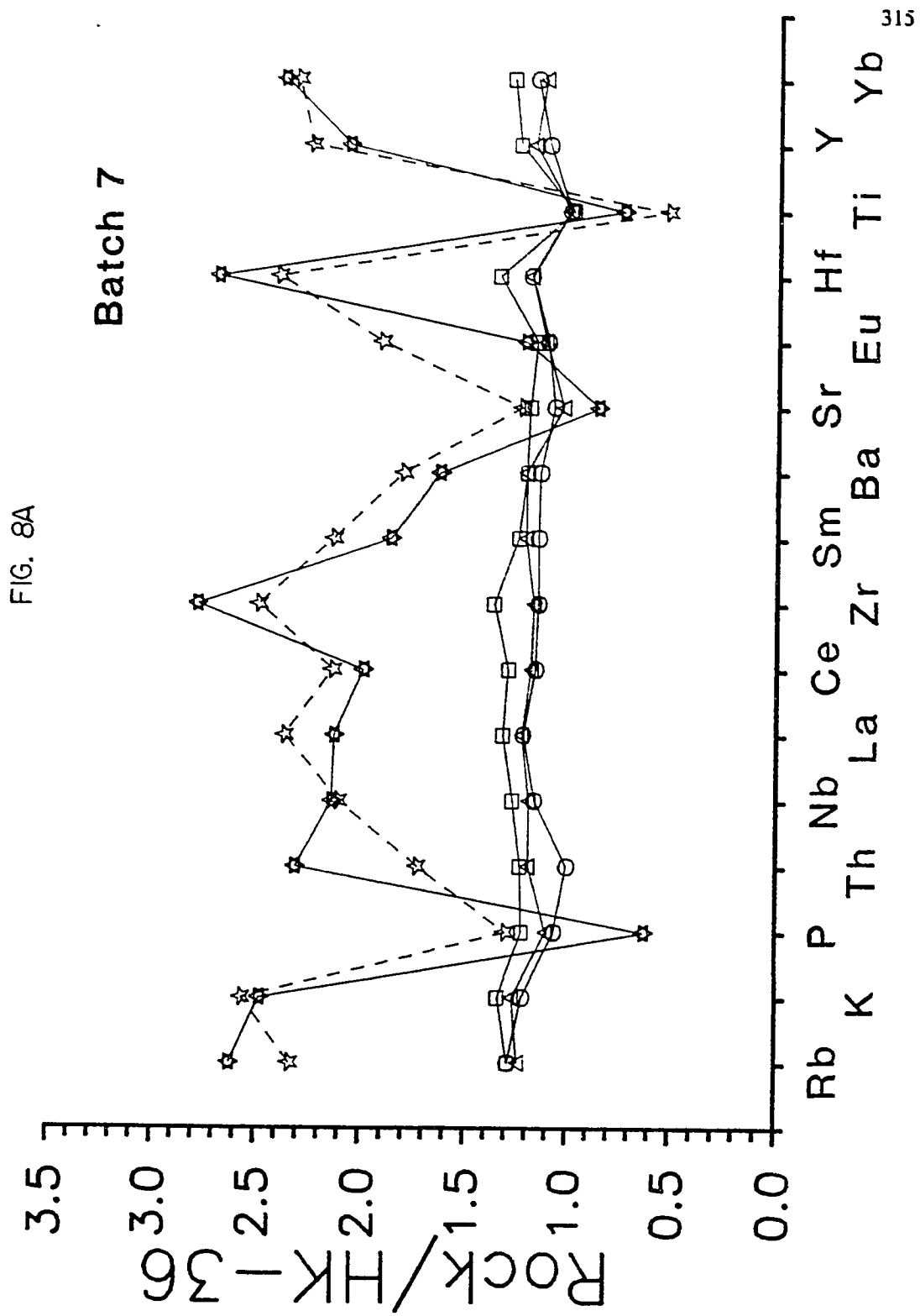
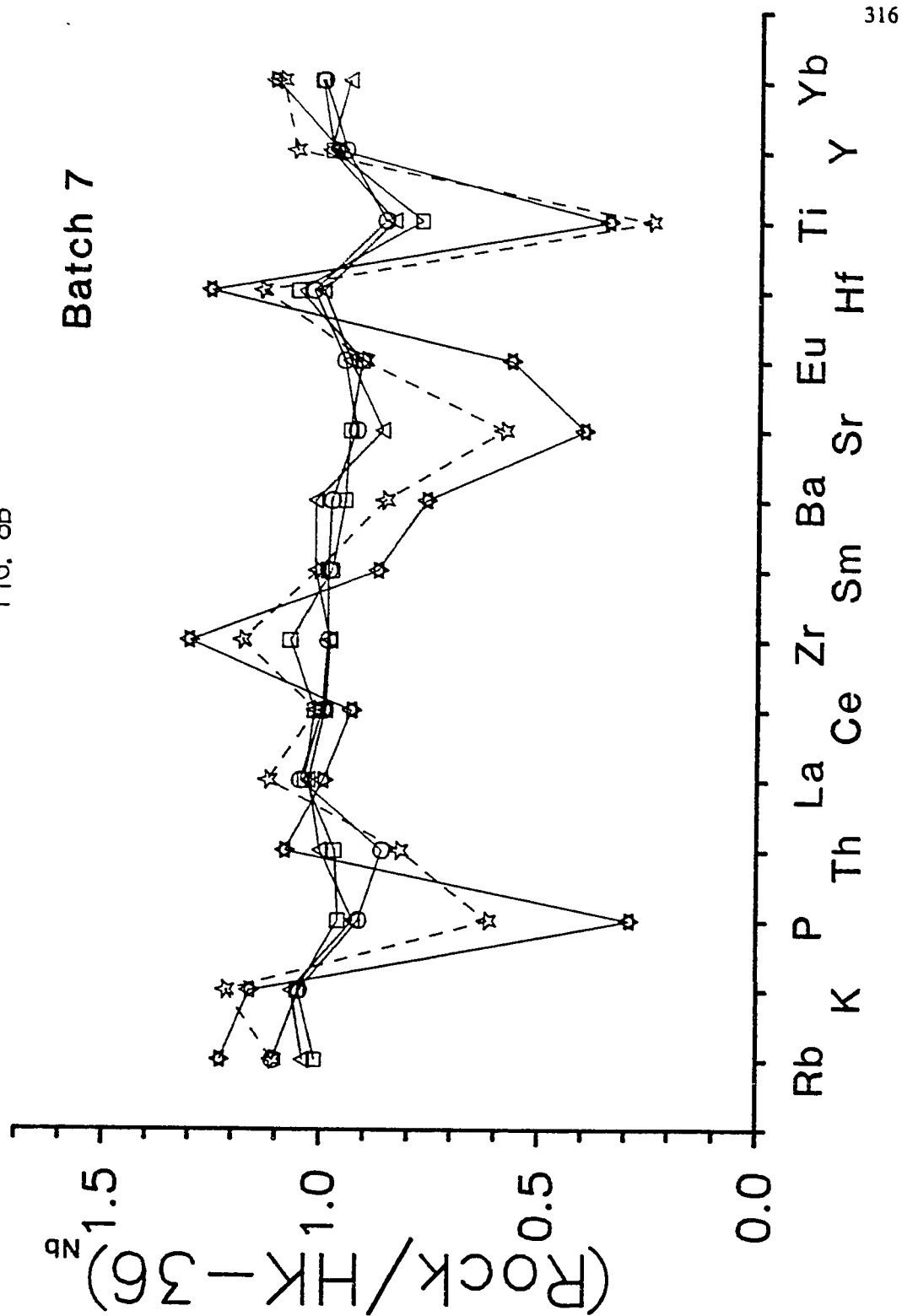


FIG. 8B

Batch 7



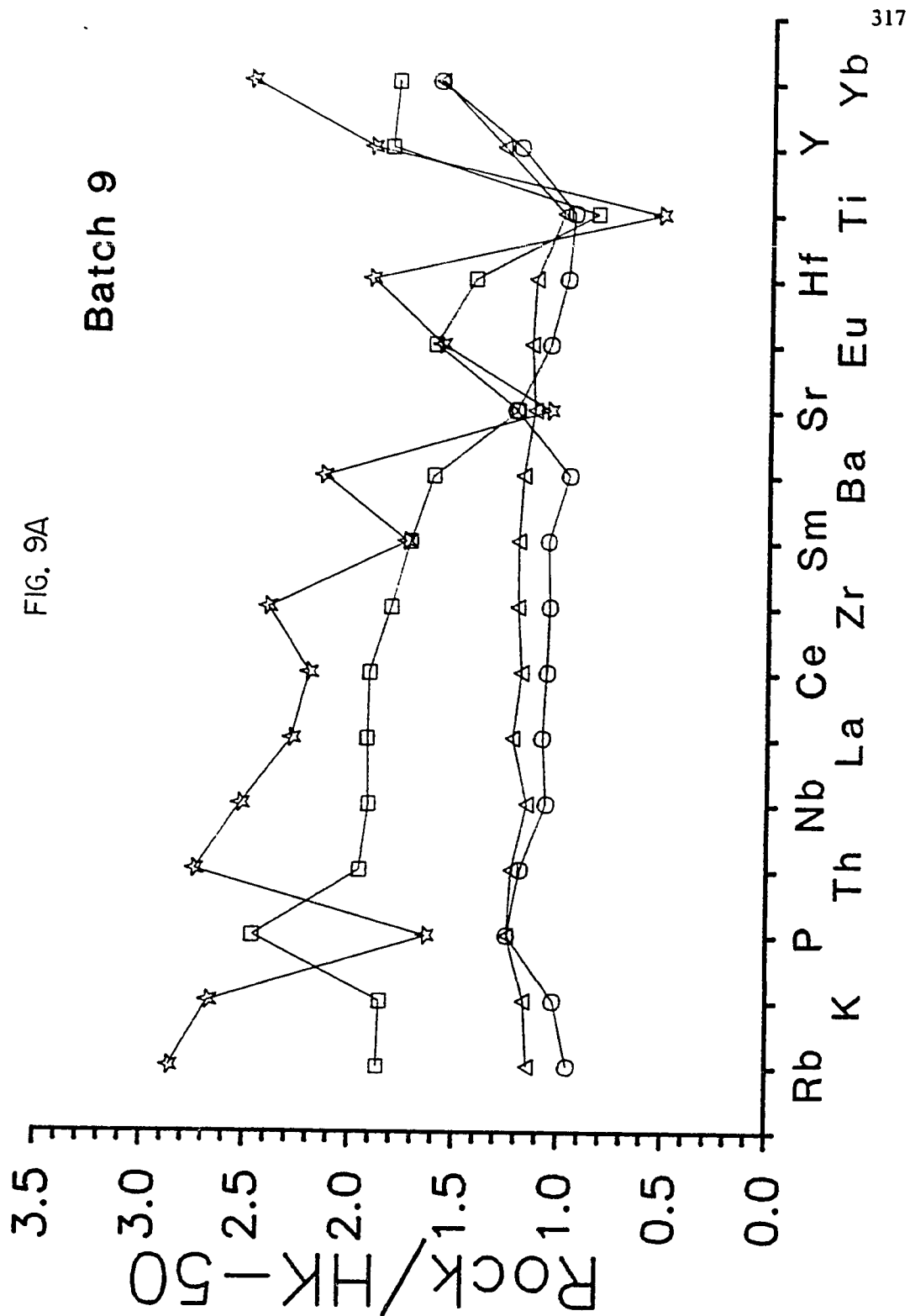
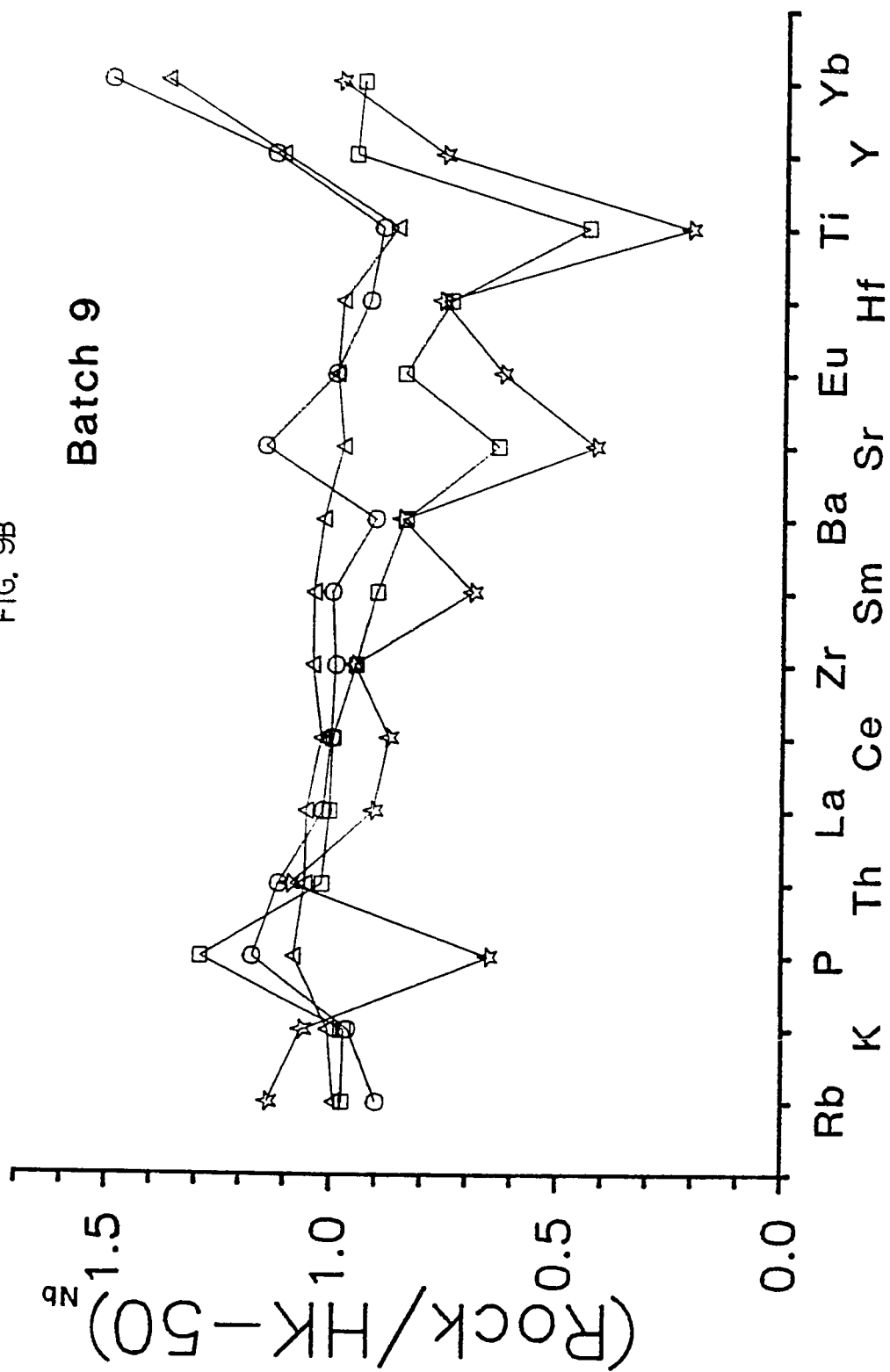


FIG. 9B

Batch 9



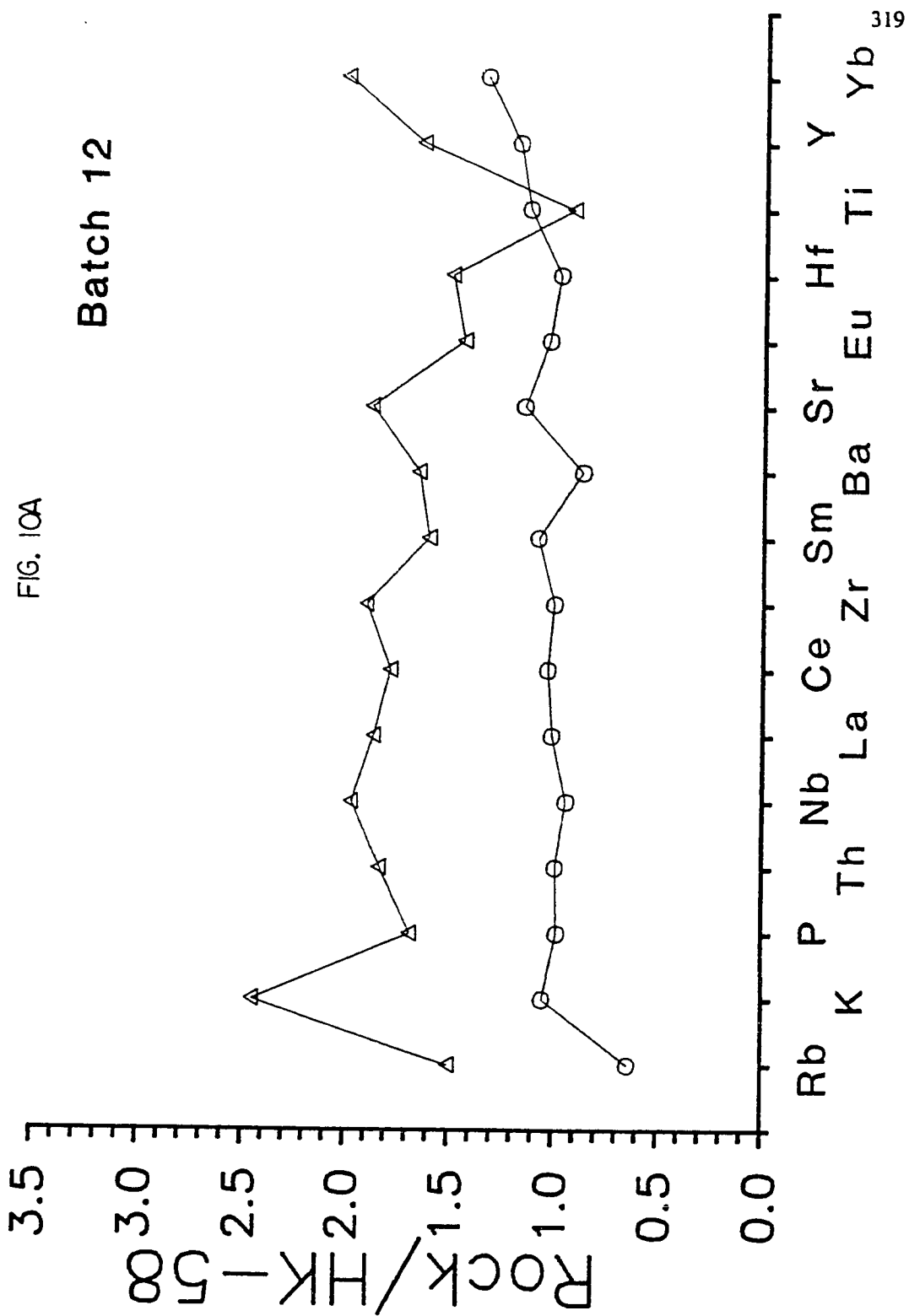
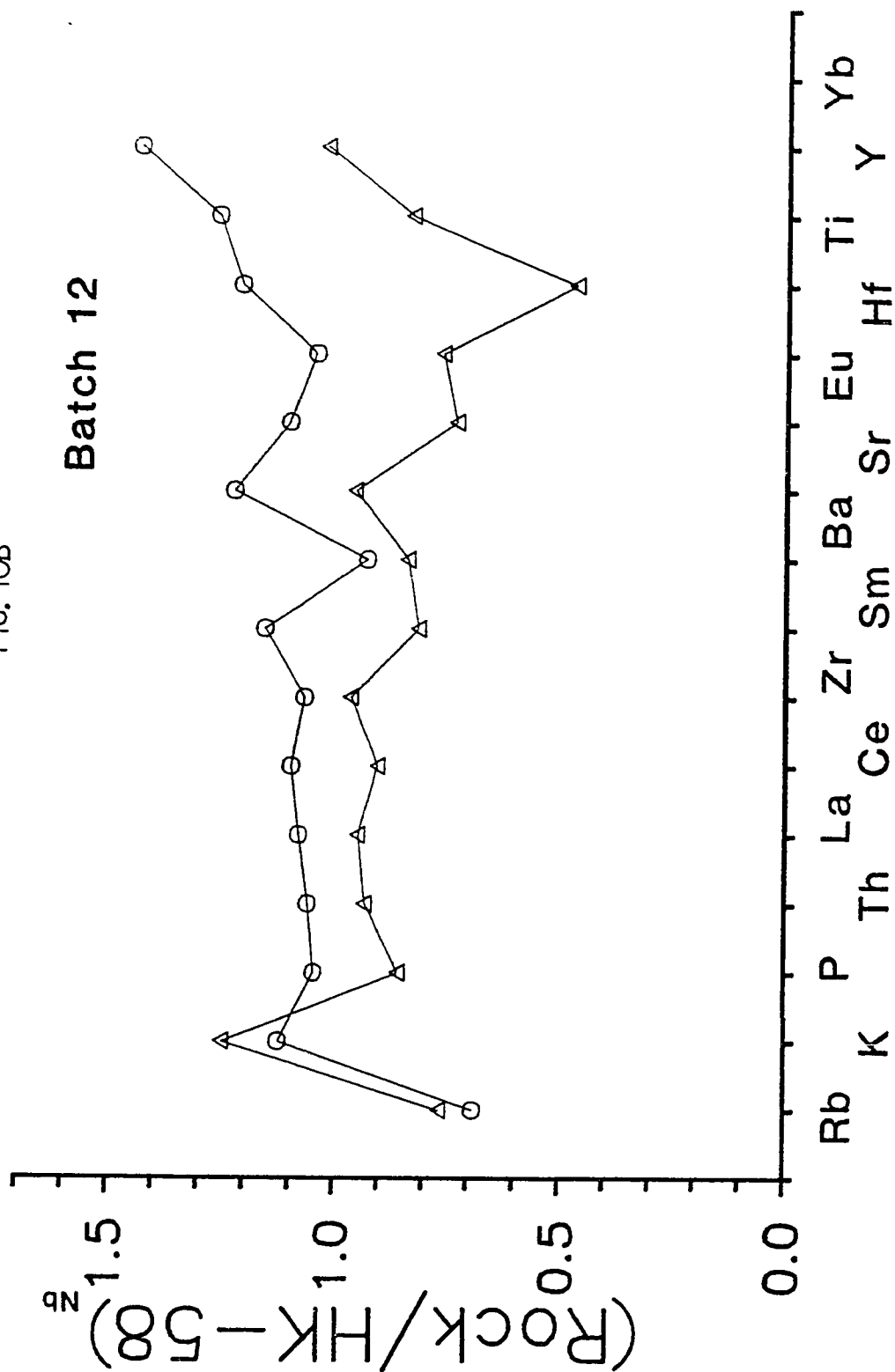


FIG. 10B

Batch 12



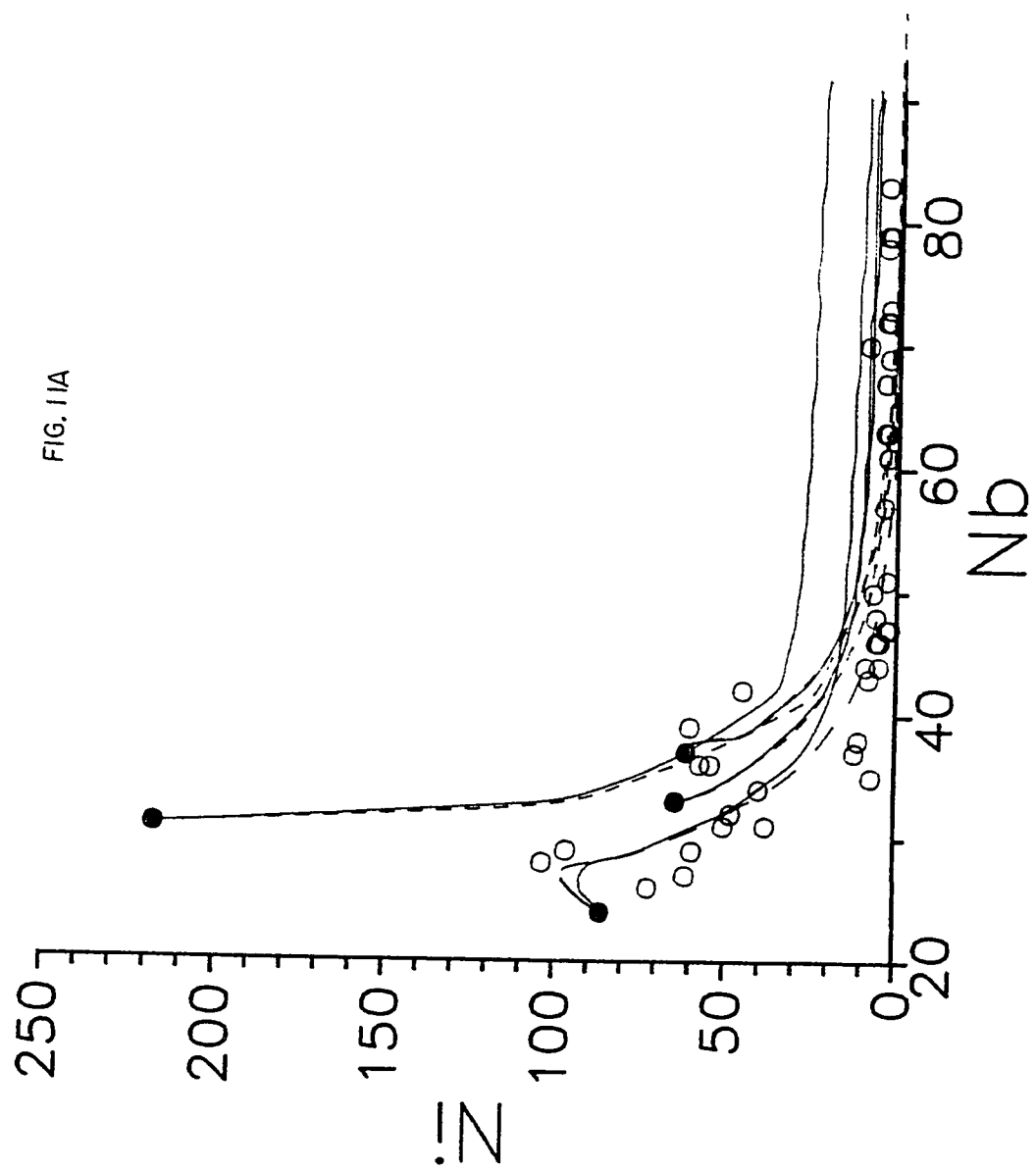


FIG. 11B

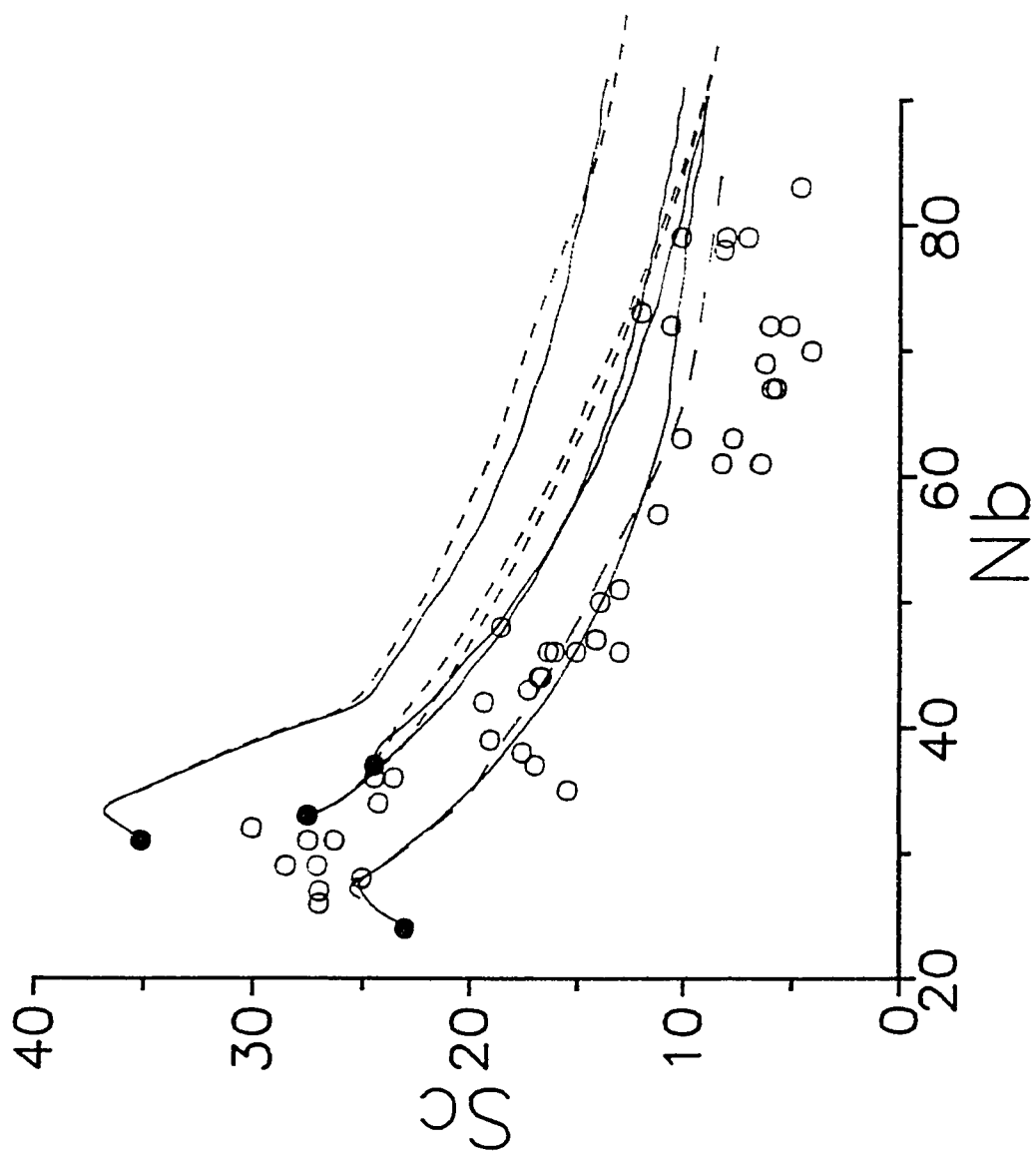
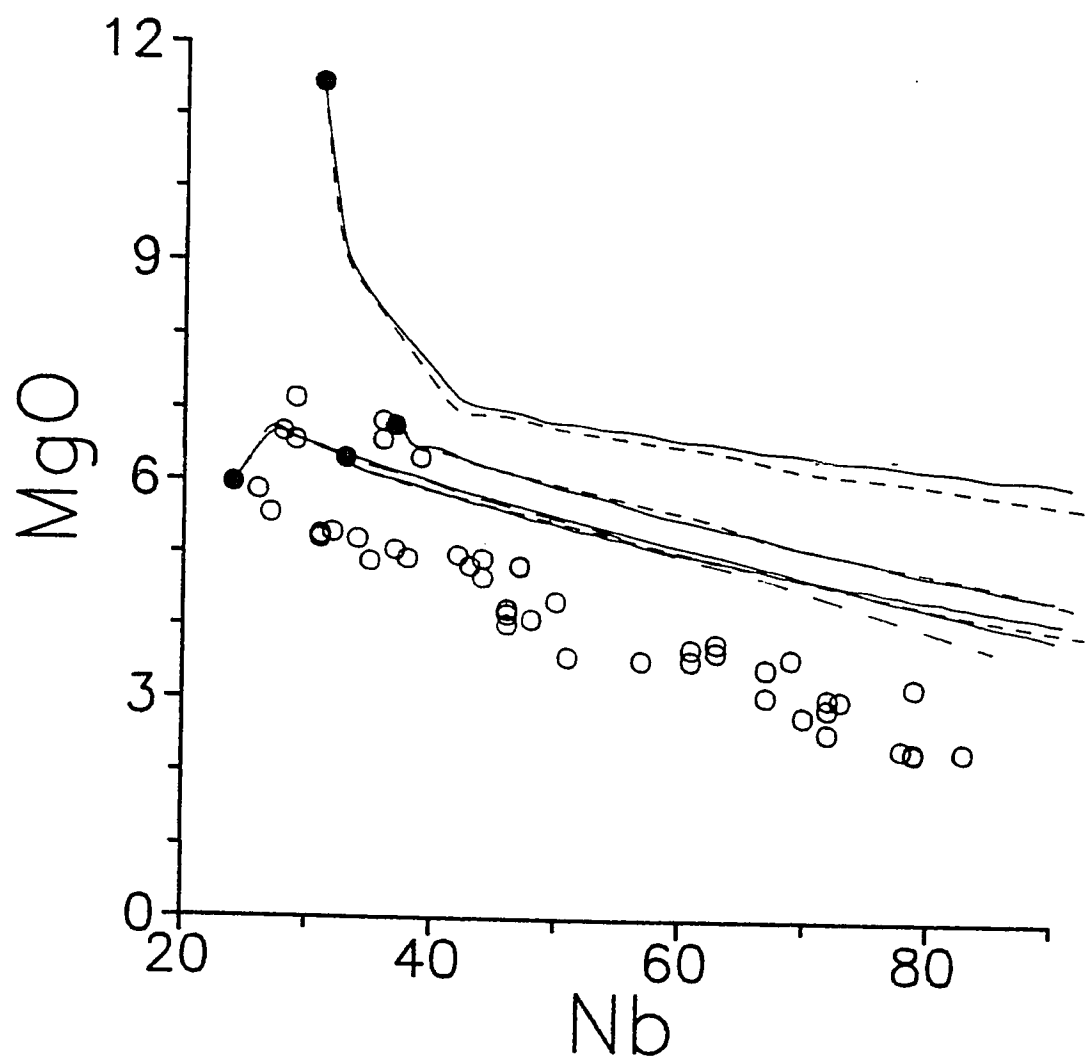


FIG. 11C



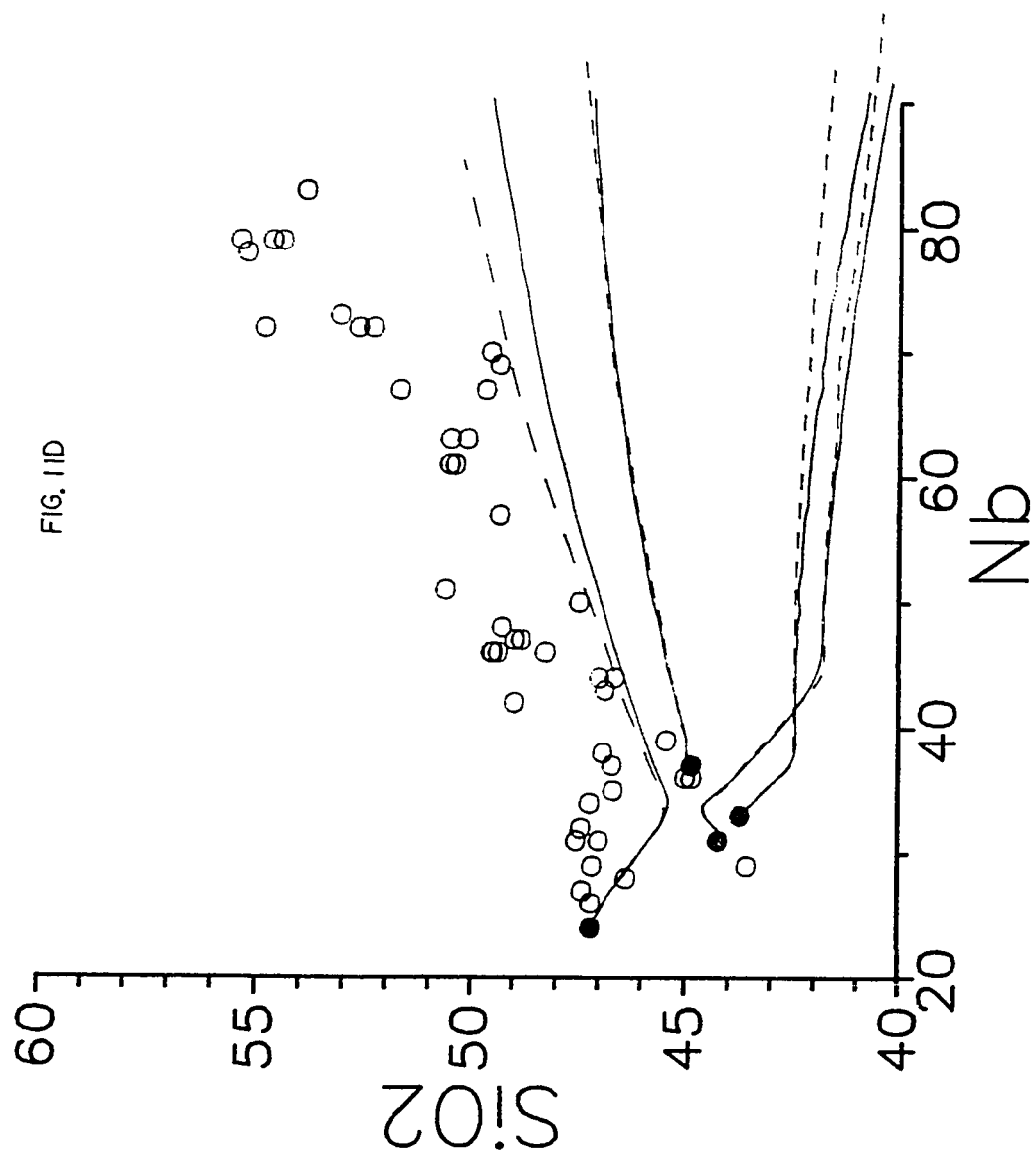


FIG. 11E

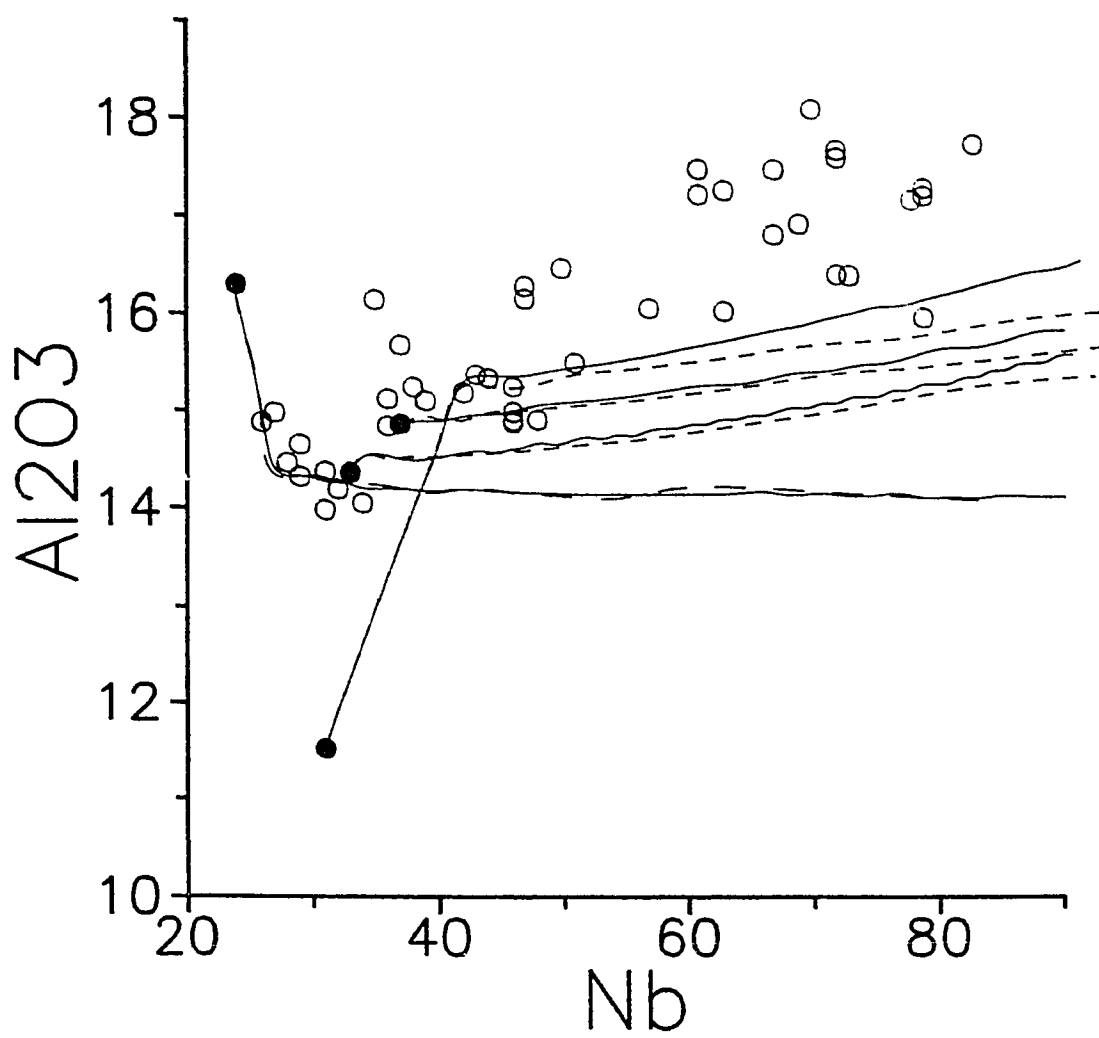


FIG. 12A

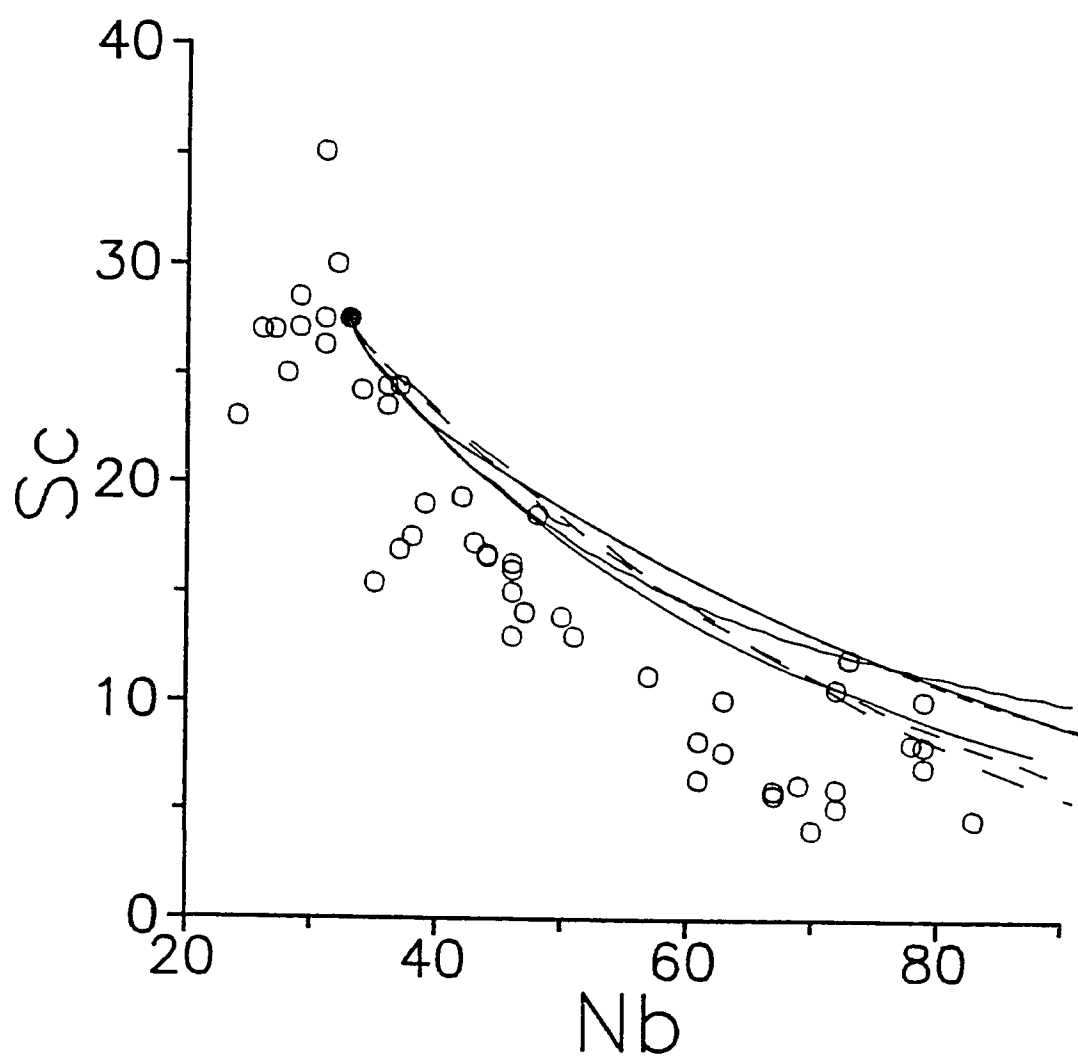


FIG. 12B

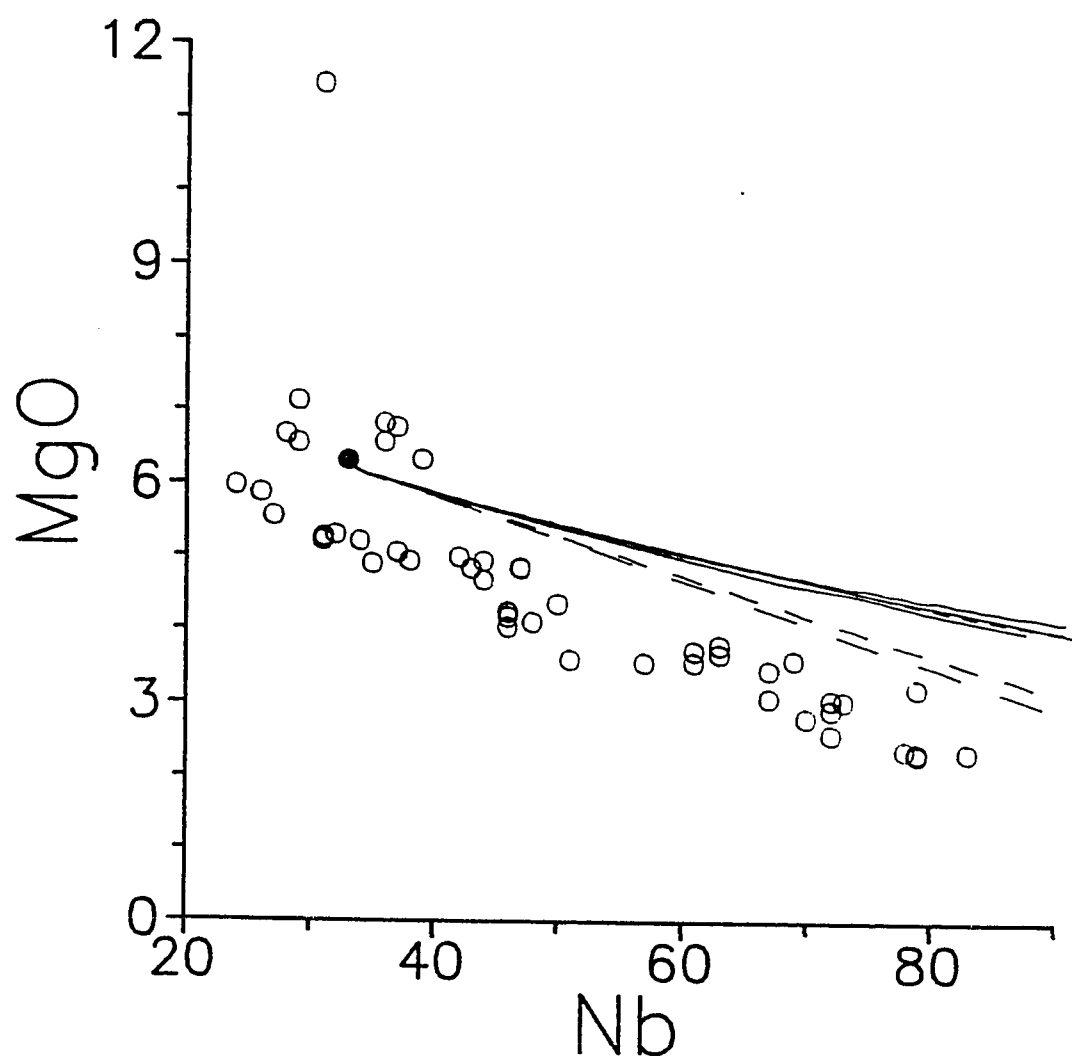


FIG. 12C

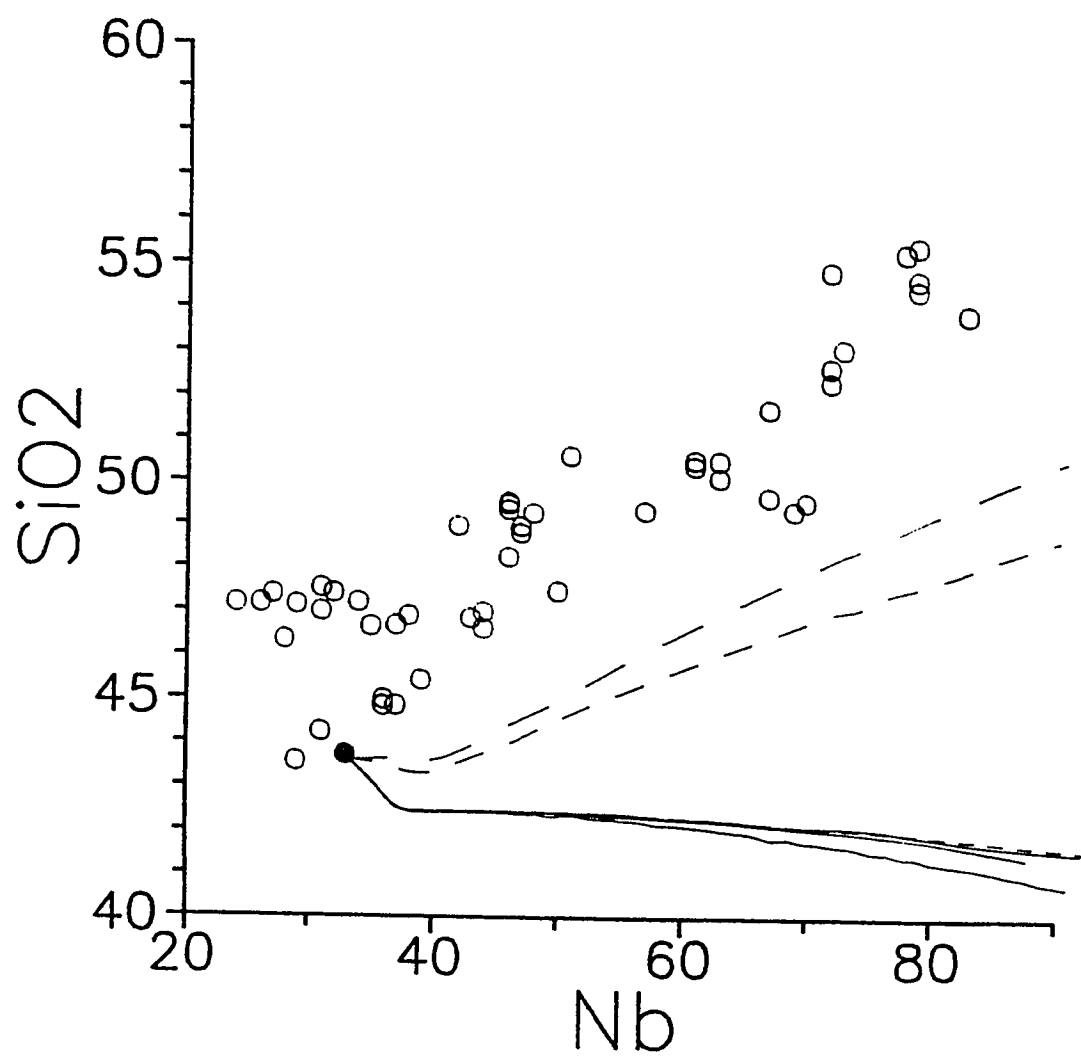
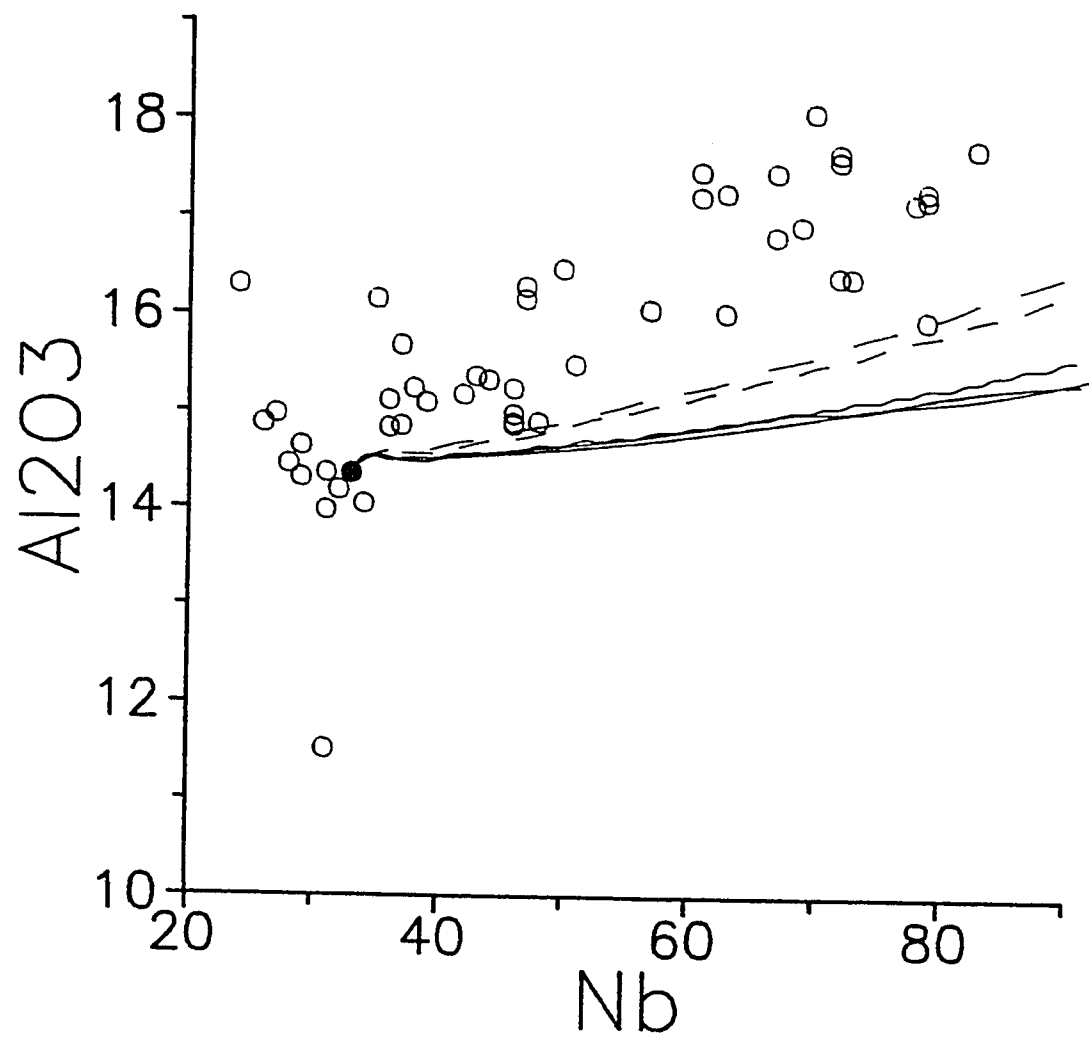


FIG. 12D



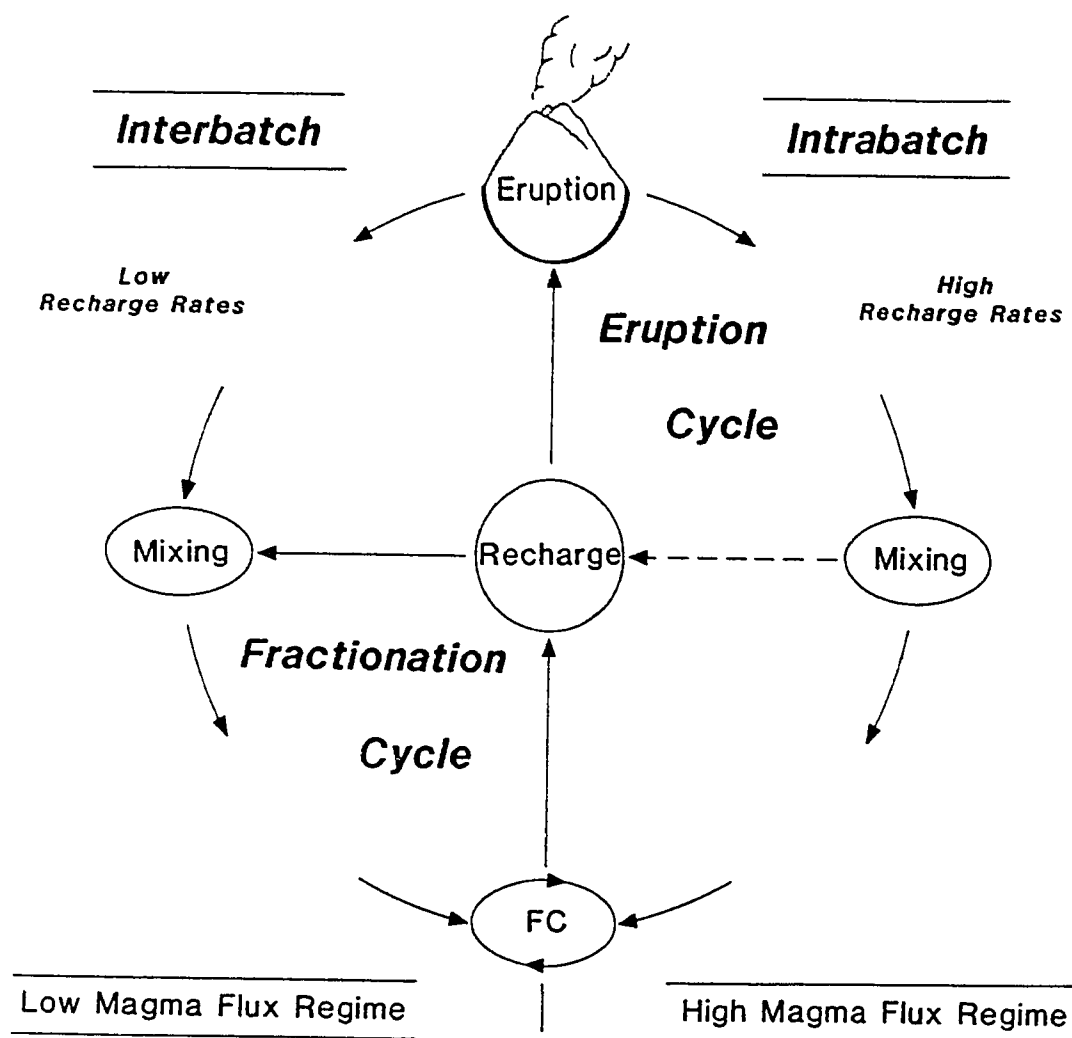


FIG. 13

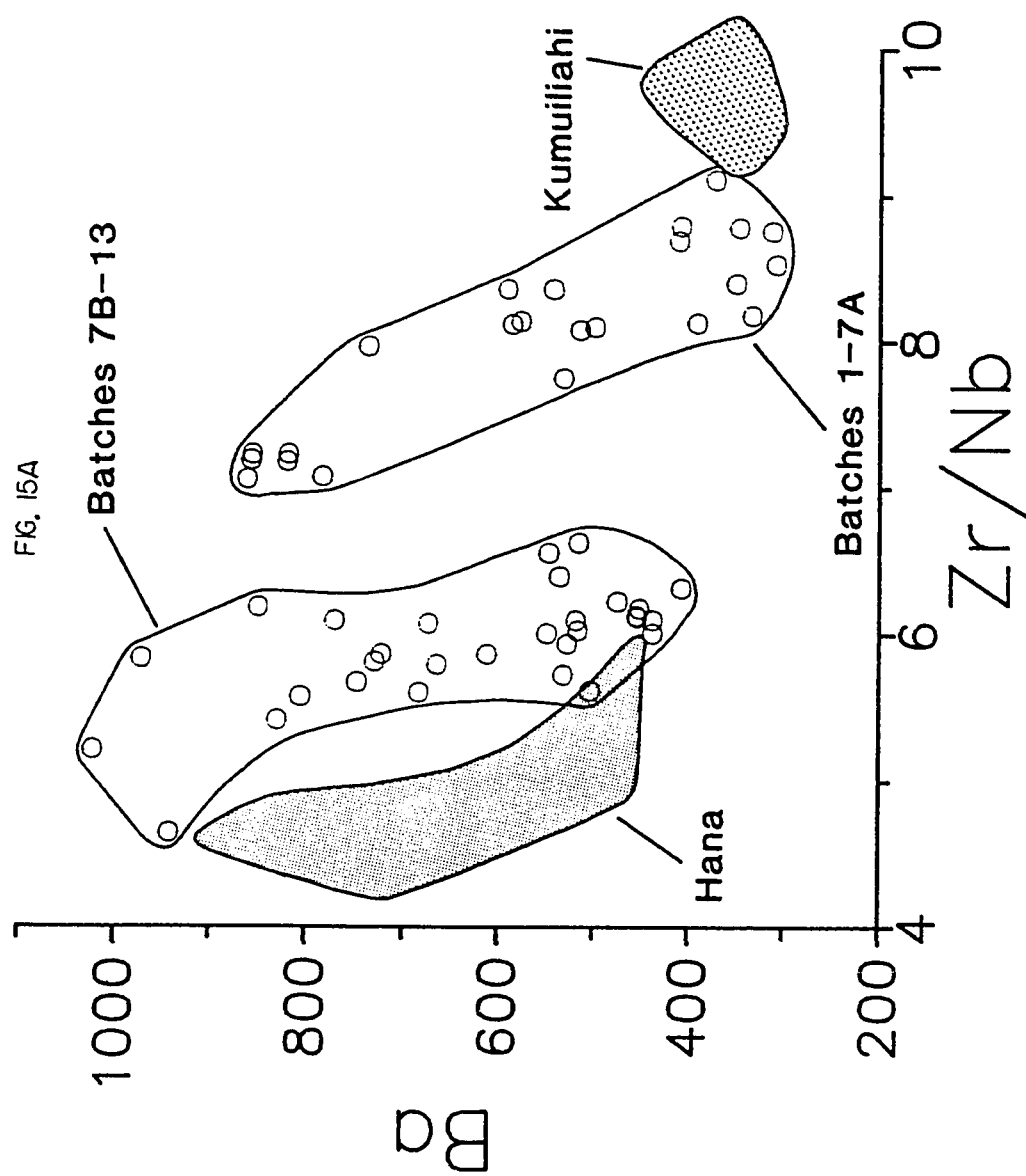


FIG. 15B

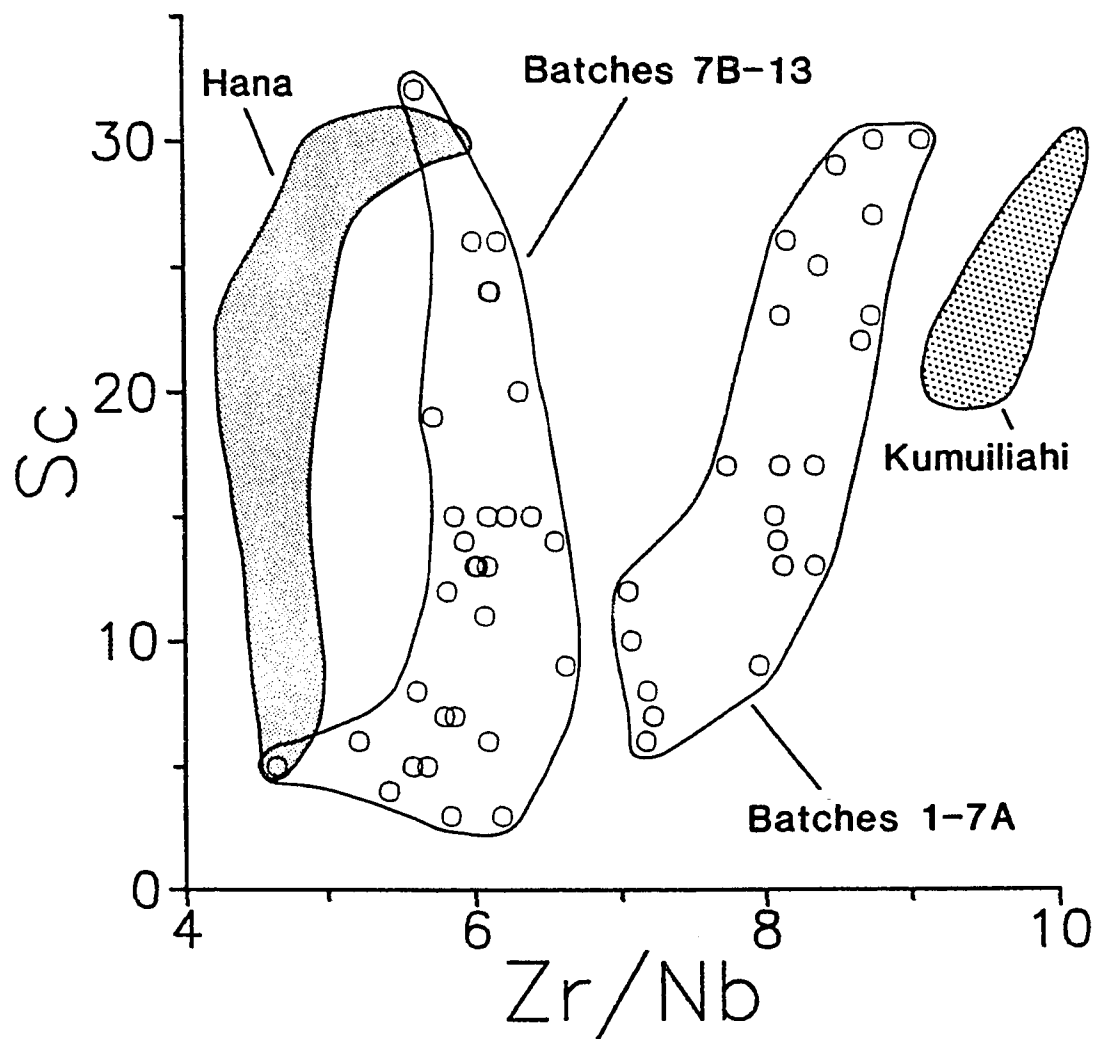
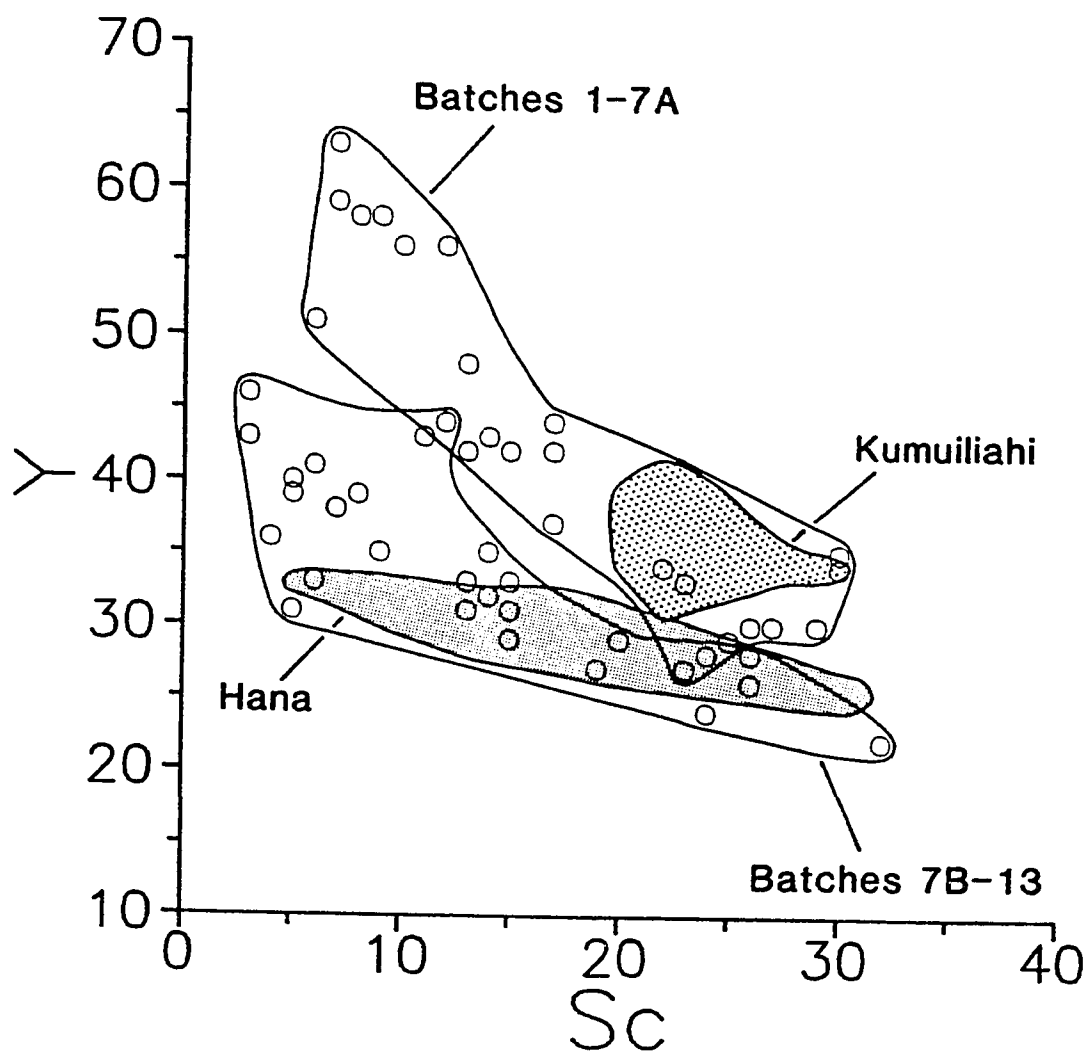


FIG. 15C



Appendix 1a. XRF Major element data for Kula Formation lavas from Haleakala Crater. All data obtained at the University of Houston. 335

	HK-1	HK-2	HK-5	HK-6	HK-7	HK-8	HK-9	HK-10	HK-11
SiO ₂	45.73	46.05	46.38	46.78	45.99	46.05	46.39	42.71	46.53
Al ₂ O ₃	13.98	15.91	13.64	14.00	14.50	14.56	13.81	12.01	14.13
Fe ₂ O ₃	15.19	12.36	15.05	15.04	14.05	13.84	15.05	12.06	14.00
MgO	5.11	5.82	5.08	5.21	5.72	5.39	5.10	5.71	6.47
CaO	10.23	11.92	10.16	10.42	11.18	11.17	10.28	8.89	11.09
Na ₂ O	2.88	2.39	3.06	2.98	2.55	2.65	3.30	2.10	2.76
K ₂ O	1.05	0.79	1.05	1.04	0.85	0.85	1.11	0.83	0.95
P ₂ O ₅	0.46	0.38	0.50	0.51	0.45	0.44	0.53	0.39	0.45
TiO ₂	3.84	2.95	3.81	3.81	3.27	3.27	3.84	2.76	3.39
MnO	0.21	0.21	0.20	0.21	0.19	0.19	0.21	0.14	0.19
LOI	0.32	0.15	0.37	0.63	0.51	0.68	0.93	0.83	0.41
Total	99.00	98.93	99.30	100.63	99.26	99.09	100.55	88.40	100.37

	HK-13	HK-14	HK-15	HK-16	HK-17	HK-18	HK-19	HK-21	HK-22
SiO ₂	48.02	49.60	48.36	48.04	48.03	39.75	47.48	53.65	51.33
Al ₂ O ₃	14.52	15.18	14.53	14.47	14.53	13.59	14.72	17.28	15.83
Fe ₂ O ₃	13.04	12.53	13.19	13.19	13.19	11.09	12.72	8.61	10.75
MgO	3.99	3.51	4.13	4.05	3.90	3.85	4.82	2.52	2.92
CaO	8.64	7.69	8.47	8.45	8.50	6.79	9.08	5.44	6.22
Na ₂ O	3.97	4.61	3.86	4.08	3.86	3.71	3.57	5.90	4.84
K ₂ O	1.59	1.81	1.56	1.54	1.51	1.31	1.39	2.39	2.28
P ₂ O ₅	0.77	0.77	0.68	0.67	0.68	0.60	0.65	0.67	0.90
TiO ₂	3.85	3.18	3.78	3.79	3.78	3.25	3.45	1.94	2.48
MnO	0.22	0.24	0.23	0.22	0.23	0.20	0.21	0.24	0.25
LOI	0.52	0.39	0.09	0.63	0.99	-	0.54	0.71	0.69
Total	99.13	99.51	98.88	99.13	99.20	84.14	98.63	99.35	98.49

	HK-23	HK-25	HK-26	HK-27	HK-28	HK-29	HK-30	HK-31	HK-32
SiO ₂	50.06	53.64	53.40	50.03	52.88	48.33	48.04	45.47	45.93
Al ₂ O ₃	15.58	16.64	16.58	16.33	15.50	15.94	16.02	14.95	14.98
Fe ₂ O ₃	10.78	9.43	9.39	8.59	10.84	13.25	13.23	14.61	14.54
MgO	2.89	2.26	2.28	2.26	3.11	4.76	4.76	4.80	4.56
CaO	6.18	5.09	5.03	4.64	5.11	7.80	7.78	9.58	9.59
Na ₂ O	4.67	5.50	5.59	5.84	5.14	4.07	4.03	3.82	3.84
K ₂ O	2.25	2.50	2.50	2.28	2.43	1.33	1.34	1.25	1.25
P ₂ O ₅	0.89	0.62	0.63	0.51	0.30	0.60	0.60	0.54	0.52
TiO ₂	2.46	1.87	1.86	1.70	2.63	3.57	3.57	3.58	3.59
MnO	0.25	0.26	0.25	0.21	0.21	0.23	0.23	0.23	0.22
LOI	-	0.15	0.94	-	-	0.21	0.41	0.56	0.59
Total	96.01	97.96	98.45	92.39	98.15	100.01	100.01	99.39	99.61

	HK-33	HK-34	HK-35	HK-36	HK-37	HK-38	HK-39	HK-40	HK-43
SiO ₂	45.40	44.15	44.01	43.83	49.94	49.63	48.70	48.61	52.67
Al ₂ O ₃	14.89	14.83	14.56	14.52	16.78	16.76	16.63	16.56	17.32
Fe ₂ O ₃	14.58	15.26	15.43	15.39	9.80	10.05	10.72	10.79	9.28
MgO	4.67	6.44	6.70	6.61	2.77	2.94	3.65	3.56	2.28
CaO	9.78	10.21	10.46	10.45	6.28	6.58	7.16	7.19	5.23
Na ₂ O	3.38	3.30	3.04	3.02	5.24	5.31	4.93	4.82	6.44
K ₂ O	1.19	1.06	1.00	0.99	2.11	2.04	1.78	1.80	2.61
P ₂ O ₅	0.51	0.46	0.50	0.49	0.93	0.97	0.80	0.79	0.66
TiO ₂	3.56	3.55	3.60	3.59	2.22	2.36	2.78	2.81	1.97
MnO	0.22	0.22	0.21	0.21	0.25	0.24	0.24	0.24	0.25
LOI	-	0.03	0.56	0.35	0.36	0.43	0.23	0.29	0.13
Total	98.18	99.51	100.07	99.45	96.68	97.31	97.62	97.46	98.84

	HK-44	HK-45	HK-46	HK-47	HK-48	HK-49	HK-50	HK-51	HK-52
SiO ₂	48.26	46.04	47.52	48.57	50.76	45.22	42.81	47.81	48.25
Al ₂ O ₃	15.43	14.96	15.92	15.89	17.02	15.65	14.06	16.17	16.53
Fe ₂ O ₃	11.58	14.42	13.06	11.74	9.84	13.65	15.36	11.25	11.49
MgO	3.53	4.83	4.62	3.74	3.48	4.73	6.18	3.31	3.50
CaO	7.53	10.06	8.16	7.71	6.08	10.16	12.98	7.78	8.09
Na ₂ O	5.00	3.58	4.26	4.55	6.13	3.57	2.86	5.12	5.14
K ₂ O	1.78	1.14	1.31	1.61	2.27	0.99	0.98	2.07	2.08
P ₂ O ₅	0.97	0.50	0.56	0.77	0.56	0.49	0.40	0.69	0.69
TiO ₂	3.00	3.68	3.66	3.23	1.55	3.47	3.68	2.91	2.97
MnO	0.24	0.23	0.22	0.25	0.23	0.21	0.18	0.23	0.24
LOI	0.35	0.23	0.79	1.05	0.29	0.15	0.40	0.23	0.16
Total	97.71	99.67	100.08	99.11	98.19	98.29	99.89	97.57	99.14

	HK-53	HK-54	HK-55	HK-56	HK-57	HK-58	HK-59	HK-60	HK-61
SiO ₂	46.12	47.65	44.69	49.03	42.09	43.01	48.03	43.75	47.92
Al ₂ O ₃	16.08	15.50	15.01	17.00	14.15	11.20	17.52	14.54	13.57
Fe ₂ O ₃	12.57	12.59	14.72	11.46	15.95	14.41	11.41	14.80	13.55
MgO	4.22	3.42	4.83	3.45	6.89	11.13	2.71	6.09	5.12
CaO	9.64	8.05	9.64	7.02	11.72	12.30	7.36	9.86	9.75
Na ₂ O	4.24	4.79	3.12	5.00	2.48	2.10	5.71	3.40	2.70
K ₂ O	1.49	1.63	1.01	1.84	0.78	0.75	1.96	1.15	0.73
P ₂ O ₅	0.61	0.74	0.47	0.72	0.42	0.43	0.80	0.51	0.42
TiO ₂	3.09	3.07	3.33	2.75	3.36	2.99	2.38	3.30	3.53
MnO	0.21	0.24	0.22	0.24	0.19	0.18	0.24	0.20	0.17
LOI	0.42	0.35	0.41	0.18	0.15	-	0.39	0.03	0.91
Total	98.69	98.03	97.45	98.69	98.18	98.50	98.51	97.63	98.37

Appendix 1a (cont). XRF Major element data for Kula Formation lavas from Haleakala Crater.
All data obtained at the University of Houston.

337

	HK-62	HOLUA
SiO ₂	47.15	62.07
Al ₂ O ₃	13.64	16.04
Fe ₂ O ₃	13.54	6.26
MgO	5.17	0.21
CaO	9.87	0.84
Na ₂ O	2.60	6.47
K ₂ O	0.67	4.92
P ₂ O ₅	0.42	0.02
TiO ₂	3.54	0.33
MnO	0.17	0.12
LOI	-	0.35
Total	96.77	97.63

Appendix 1b. XRF Major element data for Hana Formation lavas from Haleakala Crater. All data obtained at the University of Houston. 338

	HH-1	HH-2	HH-3	HH-4	HH-5	HH-6	HH-7	HH-8	HH-9
SiO ₂	43.34	45.53	44.12	45.49	43.87	43.76	43.35	43.10	43.09
Al ₂ O ₃	12.37	15.21	13.98	15.36	12.83	12.65	12.59	13.58	13.41
Fe ₂ O ₃	14.66	12.93	13.63	13.07	14.38	14.32	14.89	14.64	15.00
MgO	9.48	5.56	7.09	5.73	9.06	9.42	8.79	6.40	6.54
CaO	11.62	9.17	10.46	9.28	11.53	11.60	11.64	11.12	11.02
Na ₂ O	2.71	4.08	3.60	3.91	2.86	2.61	2.84	3.56	3.74
K ₂ O	0.97	1.53	1.31	1.40	0.94	0.92	0.96	1.44	1.47
P ₂ O ₅	0.40	0.64	0.56	0.57	0.45	0.42	0.48	0.55	0.57
TiO ₂	3.25	3.05	3.13	3.03	3.00	2.94	3.15	3.75	3.83
MnO	0.20	0.21	0.20	0.57	0.20	0.20	0.20	0.20	0.21
LOI	0.21	0.01	-	0.10	-	0.52	0.63	-	0.24
Total	99.21	97.92	98.08	98.51	99.12	99.36	99.52	98.34	99.12

	HH-10	HH-11	HH-12	HH-13	HH-14	HH-15	HH-16	HH-17	HH-18
SiO ₂	48.55	42.68	43.08	43.12	47.03	45.08	45.87	45.72	45.15
Al ₂ O ₃	17.46	11.29	13.49	13.60	16.86	16.24	16.53	16.29	16.45
Fe ₂ O ₃	11.79	14.80	14.73	14.68	11.48	13.05	13.08	13.31	12.17
MgO	3.64	10.89	6.52	6.36	3.49	5.05	5.13	4.93	4.25
CaO	7.97	11.96	10.72	10.86	7.73	8.62	8.47	8.34	8.29
Na ₂ O	5.13	2.13	3.57	3.62	5.01	4.05	4.56	3.97	4.51
K ₂ O	1.93	0.76	1.44	1.44	1.88	1.50	1.57	1.84	1.96
P ₂ O ₅	0.77	0.34	0.57	0.59	0.78	0.55	0.56	0.57	0.76
TiO ₂	2.86	2.96	3.70	3.68	2.75	3.39	3.40	3.23	3.21
MnO	0.24	0.19	0.20	0.21	0.22	0.20	0.20	0.21	0.23
LOI	0.40	-	0.01	0.02	0.03	0.32	0.69	2.00	0.15
Total	100.74	98.00	98.03	98.18	97.26	98.05	100.06	100.41	97.13

	HH-19	HH-20	HH-21	HH-22	HH-23	HH-24	HH-25	HH-26	HH-27
SiO ₂	42.43	44.79	45.40	48.31	43.29	45.60	44.23	44.26	43.96
Al ₂ O ₃	14.10	14.40	15.88	15.56	12.63	15.29	15.13	14.66	14.94
Fe ₂ O ₃	15.24	16.29	13.20	14.34	14.86	13.89	13.90	13.85	14.83
MgO	5.64	6.55	5.10	6.10	9.59	7.01	5.76	5.67	7.40
CaO	9.89	11.02	8.82	9.85	11.94	10.44	9.65	9.58	11.65
Na ₂ O	3.91	2.93	3.52	3.83	2.37	4.01	3.73	3.33	2.97
K ₂ O	1.58	1.04	1.59	1.51	1.12	1.38	1.46	1.48	1.04
P ₂ O ₅	0.60	0.46	0.56	0.55	0.37	0.53	0.53	0.58	0.48
TiO ₂	3.89	3.69	3.31	3.33	3.08	3.26	3.23	3.43	3.23
MnO	0.22	0.22	0.20	0.21	0.20	0.21	0.20	0.20	0.20
LOI	-	0.23	1.88	0.01	1.44	0.57	0.08	0.40	0.81
Total	97.50	101.62	99.46	103.60	100.89	102.19	97.90	97.44	101.51

Appendix 1b (cont). XRF Major element data for Hana Formation lavas from Haleakala Crater.
All data obtained at the University of Houston.

339

	HH-28	HH-29
SiO ₂	42.67	44.59
Al ₂ O ₃	13.31	15.57
Fe ₂ O ₃	14.88	13.96
MgO	6.52	5.41
CaO	10.93	9.16
Na ₂ O	3.51	3.87
K ₂ O	1.45	1.40
P ₂ O ₅	0.57	0.49
TiO ₂	3.80	3.46
MnO	0.21	0.20
LOI	0.15	-
Total	98.00	98.11

Appendix 1c. XRF Major element data for Kumuilihi Formation lavas from Haleakala Crater. All data obtained at the University of Houston.

	HKU-1	HKU-2	HKU-3	HKU-4	HKU-5	HKU-6	HKU-7	HKU-8	HKU-9
SiO ₂	46.42	46.78	47.43	46.30	47.02	47.00	46.13	46.86	47.29
Al ₂ O ₃	16.49	16.67	14.20	14.70	14.99	15.99	14.07	16.23	14.03
Fe ₂ O ₃	12.37	12.21	14.81	13.61	13.58	12.76	14.35	12.36	13.58
MgO	3.89	4.08	4.52	4.30	4.33	3.88	3.90	3.87	4.41
CaO	10.37	10.68	10.15	10.44	10.45	10.26	9.53	10.15	9.49
Na ₂ O	2.84	2.67	3.04	2.85	2.92	3.03	3.14	3.01	3.39
K ₂ O	0.92	0.89	1.12	0.98	1.01	1.00	1.21	1.06	1.18
P ₂ O ₅	0.47	0.46	0.58	0.52	0.54	0.56	0.64	0.54	0.61
TiO ₂	3.38	3.34	4.24	3.81	3.84	3.77	4.37	3.60	3.86
MnO	0.16	0.16	0.20	0.18	0.19	0.17	0.19	0.16	0.19
LOI	0.97	0.52	0.02	0.55	0.25	0.40	0.78	0.79	-
Total	98.28	98.46	100.31	98.24	99.12	98.82	98.31	98.63	98.03

HKU-10

SiO ₂	47.06
Al ₂ O ₃	15.39
Fe ₂ O ₃	13.47
MgO	4.45
CaO	10.52
Na ₂ O	3.06
K ₂ O	0.98
P ₂ O ₅	0.55
TiO ₂	3.82
MnO	0.17
LOI	0.53
Total	100.00

Appendix 1d. XRF Major element data for Honomanu Formation lavas from Haleakala Crater. All data obtained at the University of Houston.

	HHM-1	HHM-2	HHM-3	HHM-4A	HHM-4B	HHM-5	HHM-6	HHM-7	HHM-8
SiO ₂	47.04	47.40	46.43	47.97	47.38	46.85	48.80	47.37	48.39
Al ₂ O ₃	14.60	14.73	14.70	13.56	14.37	14.50	13.98	13.98	15.44
Fe ₂ O ₃	13.36	13.37	13.59	14.85	13.67	13.28	14.83	13.72	13.64
MgO	7.97	7.21	7.88	6.30	7.60	7.85	10.14	7.92	6.78
CaO	10.33	10.23	9.90	10.60	9.98	10.24	9.03	10.40	10.34
Na ₂ O	2.45	2.28	2.37	2.07	1.98	2.49	2.09	2.51	2.56
K ₂ O	0.31	0.14	0.39	0.39	0.32	0.36	0.16	0.32	0.28
P ₂ O ₅	0.37	0.31	0.36	0.38	0.31	0.38	0.27	0.33	0.31
TiO ₂	3.12	2.84	3.13	3.42	2.69	3.08	2.61	2.94	2.72
MnO	0.17	0.17	0.17	0.20	0.18	0.17	0.21	0.18	0.18
LOI	1.17	1.96	1.62	1.36	1.87	0.66	1.87	0.57	1.48
Total	100.89	100.64	100.54	101.10	100.35	99.86	103.99	100.24	102.12

	HHM-9
SiO ₂	47.21
Al ₂ O ₃	14.98
Fe ₂ O ₃	13.34
MgO	6.56
CaO	10.35
Na ₂ O	2.37
K ₂ O	0.28
P ₂ O ₅	0.27
TiO ₂	2.59
MnO	0.18
LOI	1.03
Total	99.16

Appendix 2a. XRF Major element data for Kula Formation lavas from Haleakala Crater. All data obtained at the University of Massachusetts at Amherst.

	HK-1	HK-10	HK-18	HK-27	HK-28	HK-29	HK-31	HK-33	HK-36
SiO ₂	45.54	45.56	47.43	54.02	52.76	47.02	45.02	45.04	42.82
Al ₂ O ₃	14.47	14.21	14.98	17.07	15.90	16.19	15.63	15.79	15.18
Fe ₂ O ₃	15.59	14.30	13.37	9.43	10.90	13.27	14.86	15.02	15.64
MgO	5.16	6.56	4.15	2.27	3.09	4.68	4.82	4.84	6.76
CaO	10.38	10.92	8.59	5.13	5.25	7.85	9.66	9.93	10.39
Na ₂ O	3.23	2.99	4.63	6.36	5.54	4.57	4.23	3.92	3.40
K ₂ O	1.04	0.94	1.52	2.53	2.44	1.32	1.23	1.20	0.99
P ₂ O ₅	0.48	0.46	0.71	0.69	0.34	0.60	0.54	0.54	0.50
TiO ₂	3.94	3.43	3.87	1.94	2.72	3.59	3.68	3.68	3.68
MnO	0.21	0.21	0.24	0.26	0.22	0.22	0.22	0.21	0.22
Total	100.04	99.58	99.49	99.70	99.16	99.31	99.89	100.17	99.58

	HK-37	HK-39	HK-43	HK-44	HK-46	HK-47	HK-48	HK-50	HK-56
SiO ₂	51.19	49.05	52.52	48.46	46.56	48.12	51.08	41.68	48.71
Al ₂ O ₃	17.67	17.33	17.83	16.36	16.43	16.66	17.71	14.63	17.42
Fe ₂ O ₃	10.11	11.04	9.31	11.86	13.29	11.94	10.03	15.77	11.51
MgO	2.84	3.70	2.24	3.55	4.69	3.92	3.47	6.16	3.47
CaO	6.57	7.43	5.38	7.73	8.28	7.84	6.39	12.90	7.18
Na ₂ O	5.73	5.56	7.05	5.44	4.38	5.21	6.61	3.08	5.35
K ₂ O	2.17	1.81	2.64	1.80	1.32	1.62	2.31	0.96	1.86
P ₂ O ₅	0.99	0.82	0.72	1.05	0.58	0.79	0.59	0.43	0.80
TiO ₂	2.31	2.87	2.01	3.14	3.74	3.33	1.62	3.82	2.82
MnO	0.25	0.24	0.24	0.25	0.24	0.26	0.23	0.20	0.24
Total	99.83	99.85	99.94	99.64	99.51	99.69	100.04	99.63	99.36

	HK-59	HK-61	HOLUA
SiO ₂	47.64	48.16	62.99
Al ₂ O ₃	17.96	14.54	16.44
Fe ₂ O ₃	11.64	14.07	6.19
MgO	2.71	5.47	-
CaO	7.62	10.01	0.79
Na ₂ O	6.17	3.19	7.45
K ₂ O	1.98	0.74	5.01
P ₂ O ₅	0.89	0.44	0.05
TiO ₂	2.47	3.71	0.32
MnO	0.22	0.16	0.21
Total	99.30	100.49	99.45

Appendix 2b. XRF Major element data for Hana Formation lavas from Haleakala Crater. All data obtained at the University of Massachusetts at Amherst.

	HH-1	HH-3	HH-6	HH-7	HH-11	HH-14	HH-16	HH-17	HH-18
SiO ₂	42.54	43.68	42.71	42.49	42.10	46.94	44.99	45.29	45.27
Al ₂ O ₃	12.95	14.66	13.29	13.55	12.05	17.91	16.96	17.06	17.09
Fe ₂ O ₃	15.05	14.13	14.72	15.37	15.43	11.84	13.24	13.61	12.56
MgO	9.62	7.46	9.54	9.09	11.24	3.52	5.06	4.91	4.22
CaO	11.61	10.67	11.66	11.77	12.17	7.99	8.60	8.45	8.56
Na ₂ O	3.00	4.12	2.82	3.19	2.53	5.65	4.74	4.30	5.42
K ₂ O	0.94	1.32	0.90	0.96	0.77	1.90	1.55	1.82	1.98
P ₂ O ₅	0.37	0.55	0.43	0.45	0.34	0.79	0.59	0.61	0.81
TiO ₂	3.33	3.26	3.05	3.28	3.10	2.86	3.49	3.31	3.32
MnO	0.20	0.20	0.19	0.19	0.17	0.22	0.20	0.22	0.23
Total	99.61	100.05	99.31	100.34	99.90	99.62	99.42	99.58	99.46

	HH-19	HH-20	HH-21	HH-23	HH-26	HH-28
SiO ₂	41.92	41.64	45.02	42.41	43.67	42.05
Al ₂ O ₃	15.14	14.82	16.79	12.91	15.68	14.07
Fe ₂ O ₃	15.73	16.52	13.80	15.20	14.38	15.47
MgO	5.88	6.63	5.27	9.62	5.97	6.71
CaO	10.09	10.94	9.07	11.95	9.75	11.07
Na ₂ O	4.26	3.12	3.95	2.70	3.86	4.19
K ₂ O	1.59	1.02	1.60	1.12	1.49	1.47
P ₂ O ₅	0.67	0.48	0.55	0.40	0.63	0.62
TiO ₂	4.04	3.75	3.46	3.16	3.60	3.96
MnO	0.22	0.23	0.21	0.20	0.22	0.23
Total	99.54	99.15	99.72	99.67	99.25	99.84

Appendix 2c. XRF Major element data for Kumuilihi Formation lavas from Haleakala Crater. All data obtained at the University of Massachusetts at Amherst.

	HKU-1	HKU-2	HKU-5	HKU-7	HKU-9	HKU-10
SiO ₂	46.72	46.71	46.13	46.34	47.08	46.30
Al ₂ O ₃	17.38	17.33	15.57	14.64	14.88	15.76
Fe ₂ O ₃	12.83	12.45	13.89	14.87	14.01	13.78
MgO	4.00	4.11	4.44	4.13	4.61	4.43
CaO	10.66	10.85	10.46	9.78	9.70	10.56
Na ₂ O	3.12	3.27	3.17	3.57	3.77	3.39
K ₂ O	0.94	0.91	1.01	1.22	1.20	0.98
P ₂ O ₅	0.50	0.48	0.58	0.66	0.68	0.59
TiO ₂	3.54	3.46	3.89	4.52	3.98	3.90
MnO	0.16	0.16	0.19	0.20	0.20	0.19
Total	99.85	99.73	99.33	99.93	100.11	99.88

Appendix 2d. XRF Major element data for Honomanu Formation lavas from Haleakala Crater. All data obtained at the University of Massachusetts.

	HHM-1
SiO ₂	45.95
Al ₂ O ₃	15.04
Fe ₂ O ₃	13.50
MgO	7.86
CaO	10.29
Na ₂ O	2.69
K ₂ O	0.31
P ₂ O ₅	0.39
TiO ₂	3.23
MnO	0.19
Total	99.45

Appendix 3. Normalizing values used for mo'o diagrams.

<u>Element</u>	<u>Chondrite</u>	<u>Mantle</u>	<u>Ref.</u>
SiO ₂	-	46.2	10
Al ₂ O ₃	-	4.75	10
FeO	-	7.70	10
MgO	-	35.5	10
CaO	-	4.36	10
Na ₂ O	-	0.40	10
K ₂ O	-	0.014455	8
P ₂ O ₅	-	0.01054	8
TiO ₂	0.0727	0.10909	9
MnO	-	0.13	10
U	0.0081	-	5
Th	0.0286	-	5
Pb	2.77	0.12	3,8
Cs	0.186	0.012	5,8
Rb	2.30	0.35	5,8
K	509	120	1,8
P	1180	46	5,8
Sr	7.92	-	3
Ba	2.31	-	3
La	0.253	-	1
Ce	0.645	-	1
Pr	0.0965	-	2
Nd	0.476	-	1
Sm	0.154	-	1
Eu	0.0587	-	1
Gd	0.204	-	1
Tb	0.0397	-	2
Dy	0.252	-	1
Ho	0.0606	-	2
Er	0.166	-	1
Tm	0.0260	-	2
Yb	0.168	-	1
Lu	0.0253	-	1
Y	1.50	-	5
Hf	0.124	0.160	3
Zr	3.87	5.75	3
Nb	0.3	-	4
Ta	0.017	-	5
Ni	1060	-	7
Cr	2650	-	7
Sc	5.81	-	7
V	57	-	7
Ti	436	654	5,9
Li	1.57	-	6

Reference:

- 1 Nakamura (1974)
- 2 Davis & Grossman (1979)
- 3 Knab (1981)
- 4 Graham & Mason (1972)

Type:

- Orgueil C1 Chondrite
 C1 Chondrite
 Orgueil C1 Chondrite
 Ivuna C1 Chondrite

5 Anders & Ebihara (1981)	Orgueil C1 Chondrite
6 Nichiporuk & Moore (1974)	Ivuna & Orgueil C1 Chondrites
7 Kellemeyn & Wasson (1981)	Orgueil C1 Chondrite
8 Sun (1980)	Undepleted Mantle
9 Taylor & McLennan (1985)	C1 Compilation
10 Palme & Nickel (1985)	Primitive Mantle

Full References:

- Anders, E. and Ebihara, M., 1982, Solar-System Abundances of the Elements: *Geochim. Cosmochim. Acta* 46, p. 2363-2380.
- Davis, A. M. and Grossman, L., 1979, Condensation and Fractionation of Rare Earths in the Solar Nebula: *Geochim. Cosmochim. Acta* 43, p. 1611-1632.
- Graham, A. L. and Mason, B., 1972, Niobium in Meteorites: *Geochim. Cosmochim. Acta* 36, p. 917-922.
- Kallemeyn, G. W. and Wasson, J. T., 1981, The Compositional Classification of Chondrites - I. The Carbonaceous Chondrite Groups: *Geochim. Cosmochim. Acta* 45, p. 1217-1230.
- Knab, H.-J., 1981, The Distribution of Trace Elements in Carbonaceous Chondrites: *Geochim. Cosmochim. Acta* 45, p. 1563-1572.
- Nakamura, H., 1974, Distribution of REE, Ba, Fe, Mg, Na and K in Carbonaceous and Ordinary Chondrites: *Geochim. Cosmochim. Acta* 38, p. 757-775.
- Nichiporuk, W. and Moore, C. B., 1974, Lithium, Sodium and Potassium Abundances in Carbonaceous Chondrites: *Geochim. Cosmochim. Acta* 38, p. 1691-1701.
- Palme, H. and Nickel, K. G., 1985, Ca/Al Ratios and Composition of the Earth's Upper Mantle: *Geochim. Cosmochim. Acta* 59, p. 2123-2132.
- Sun, S.-S., 1980, Lead Isotope Study of Young Volcanic Rocks from Mid-Ocean Ridges, Ocean Islands and Island Arcs: *Phil. Trans. R. Soc. London A*-297, p. 409-445.
- Taylor, S. R. and McLennan, S. M., 1985, *The Continental Crust: Its Composition and Evolution*, Blackwell Scientific, 312 p.

Appendix 4. List of samples and sample locations. Kula Formation lavas from the Halemau trail section are listed in order of *increasing* stratigraphic height. Other Kula lavas are listed according to sample number. Hana Formation lavas are listed by sample number; hc, hco, hs, hka, hmh, and hb designations refer map units given by Macdonald (1978). Kumulihi and Honomanu Formation lavas are listed in order of *decreasing* stratigraphic height.

Kula Formation

(with increasing stratigraphic height)

HK-1	Mafic Hawaiiite	Base of Halemau Trail.
HK-2	Alkalic Basalt	Halemau Trail.
HK-5	Mafic Hawaiiite	Halemau Trail.
HK-6	Mafic Hawaiiite	Halemau Trail.
HK-7	Alkalic Basalt	Halemau Trail.
HK-8	Alkalic Basalt	Halemau Trail.
HK-9	Mafic Hawaiiite	Halemau Trail.
HK-10	Alkalic Basalt	Halemau Trail.
HK-11	Alkalic Basalt	Halemau Trail.
HK-12	dike	Halemau Trail.
HK-13	Hawaiiite	Halemau Trail.
HK-14	Hawaiiite	Halemau Trail.
HK-15	Hawaiiite	Halemau Trail.
HK-16	Hawaiiite	Halemau Trail.
HK-17	Hawaiiite	Halemau Trail.
HK-18	Hawaiiite	Halemau Trail.
HK-19	Hawaiiite	Halemau Trail.
HK-21	Mugearite	Halemau Trail.
HK-22	Hawaiiite	Halemau Trail.
HK-23	Mugearite	Halemau Trail.
HK-25	Mugearite	Halemau Trail.
HK-26	Mugearite	Halemau Trail.
HK-27	Mugearite	Halemau Trail.
HK-28	Mugearite	Halemau Trail.
HK-29	Hawaiiite	Halemau Trail.
HK-30	Hawaiiite	Halemau Trail.
HK-31	Hawaiiite	Halemau Trail.
HK-32	Hawaiiite	Halemau Trail.
HK-33	Mafic Hawaiiite	Halemau Trail.
HK-34	Basanitoid	Halemau Trail.
HK-35	Alkalic Basalt	Halemau Trail.
HK-36	Alkalic Basalt	Halemau Trail.
HK-37	Mugearite	Halemau Trail.
HK-38	Hawaiiite	Halemau Trail.
HK-39	Hawaiiite	Halemau Trail.
HK-40	Hawaiiite	Halemau Trail.
HK-43	Mugearite	Halemau Trail.
HK-44	Hawaiiite	Halemau Trail.
HK-45	Mafic Hawaiiite	Halemau Trail.
HK-46	Hawaiiite	South wall, Haleakala Crater, flow directly over- lying Kumulihi Formation beneath Kumulihi Peak.
HK-47	Hawaiiite	South wall, Haleakala Crater, flow directly over- lying HK-46.
HK-48	Nepheline Mugearite	Halemau Trail.
HK-49	Alkalic Basalt	Halemau Trail.

HK-50	Basanitoid	Halemauu Trail.
HK-51	Hawaiite	Halemauu Trail.
HK-52	Hawaiite	Halemauu Trail.
HK-53	Hawaiite	Halemauu Trail.
HK-54	Hawaiite	Halemauu Trail.
HK-55	Alkalic Basalt	Halemauu Trail.
HK-56	Hawaiite	Halemauu Trail.
HK-57	Basanitoid	Halemauu Trail.
HK-58	Ankaramite	Halemauu Trail.
HK-59	Nepheline Hawaiite	Halemauu Trail.
HK-60	Basanitoid	Halemauu Trail.
HK-61	Mafic Hawaiite	Honomanu Valley, flow directly above soil zone at Honomanu-Kula transition.
HK-62	Alkalic Basalt	Halemauu Trail.

Hana Formation

HH-1	Basanitoid	Halalii (hc).
HH-2	Hawaiite	Ka Moa O Pele (hc).
HH-3	Basanitoid	Cone north of Ka Moa O Pele (hco).
HH-4	Hawaiite	Puu O Pele (hc).
HH-5	Basanitoid	Puu O Maui (hc).
HH-6	Basanitoid	Cone located between Puu O Maui and Kamaolii (hco).
HH-7	Basanitoid	Kamaolii (hc).
HH-8	Basanitoid	Kalua O Ka Oo (hc).
HH-10	Hawaiite	Spatter cone, northeast of Halalii (hs).
HH-11	Basanitoid	Puu Naue (hc).
HH-12	Basanitoid	Cone northwest of Puu Mamane, mapped by Macdonald (1978) as part of Puu Mamane.
HH-13	Basanitoid	Puu Kumu (hc).
HH-14	Hawaiite	Puu Nole (hc).
HH-15	Hawaiite	Kaluaiki (hc).
HH-16	Hawaiite	Laie Puu (hco).
HH-17	Hawaiite	Oili Puu (hc).
HH-18	Hawaiite	Kalua Awa (hka).
HH-19	Basanitoid	Aa flow from vents north of Mauna Hina (hnh).
HH-20	Alkalic Basalt	Cone southeast of Puu Maile (hc).
HH-21	Hawaiite	Puu Maile (hc).
HH-22	Hawaiite	Cone south of Puu Nole (hco).
HH-23	Basanitoid	Cone south of Puu Naue (hs).
HH-24	Basanitoid	Puu Kauaia (hco).
HH-25	Basanitoid	Flow, south side of Namana O Ke Akua (hb).
HH-26	Basanitoid	Honokahua (hco).
HH-27	Basanitoid	Mauna Hina (hco).
HH-28	Basanitoid	Cone north of Kaluu O Ka Oo (hco).
HH-29	Basanitoid	Cone east of Magnetic Peak (hc).

Kumuilihi Formation

HKU-1	Alkalic Basalt	South wall, Haleakala Crater, uppermost Kumuilihi flow.
HKU-2	Alkalic Basalt	South wall, Haleakala Crater.
HKU-3	Mafic Hawaiite	South wall, Haleakala Crater.
HKU-4	Alkalic Basalt	South wall, Haleakala Crater.
HKU-5	Alkalic Basalt	South wall, Haleakala Crater.
HKU-6	Alkalic Basalt	South wall, Haleakala Crater.
HKU-7	Hawaiite	South wall, Haleakala Crater.
HKU-8	Alkalic Basalt	South wall, Haleakala Crater.
HKU-9	Hawaiite	South wall, Haleakala Crater.
HKU-10	Mafic Hawaiite	South wall, Haleakala Crater.

Honomanu Formation

HHM-1	Tholeiite	Honomanu Valley, uppermost exposed Honomanu lava, directly underlying the Honomanu-Kula transition.
HHM-2	Tholeiite	Honomanu Valley.
HHM-3	Tholeiite	Honomanu Valley.
HHM-4a	Tholeiite	Honomanu Valley.
HHM-4b	Tholeiite	Honomanu Valley.
HHM-5	Tholeiite	Honomanu Valley.
HHM-6	Tholeiite	Honomanu Valley.
HHM-7	Tholeiite	Honomanu Valley.
HHM-8	Tholeiite	Honomanu Valley.
HHM-9	Tholeiite	Honomanu Valley.

Appendix 5. Trace element abundances of standard rock BHVO-1 and sample HK-46.

	<u>BHVO-1</u>			<u>HK-46</u>	
	<u>(1)</u>	<u>(2)</u>	<u>Avg.</u>	<u>±</u>	<u>% σ</u>
La	15.40	16.7	36.9	0.5	1.36
Ce	40.6	41	85.8	1.8	2.14
Nd	24.7	24	43.4	1.4	3.11
Sm	6.27	6.1	9.52	0.15	1.59
Eu	2.19	2.0	3.09	0.10	3.13
Tb	0.78	1.0	1.08	0.15	13.89
Ho	0.93	0.94	1.69	0.48	28.34
Yb	1.87	2.1	2.47	0.11	4.45
Lu	0.305	0.320	0.350	0.017	4.86
Th	1.65	1.1	3.33	0.33	9.91
Ta	1.01	1.1	3.33	0.25	7.36
Hf	4.4	4.2	6.44	0.26	4.04
Sc	32.98	30	13.09	0.15	1.13
Cr	298	300	1.5	*	*

(1) This study. Elemental abundances determined by instrumental neutron activation analysis.

(2) Compilation by Gladney and Goode (1981).

(3) Average and standard deviation (σ) for HK-46 based on six replicate analyses.

* Measured abundances of Cr for HK-46 are low and comparable to the analytical uncertainty.
